

## INFORMATION TO USERS

This manuscript has been reproduced from the microfilm master. UMI films the text directly from the original or copy submitted. Thus, some thesis and dissertation copies are in typewriter face, while others may be from any type of computer printer.

**The quality of this reproduction is dependent upon the quality of the copy submitted.** Broken or indistinct print, colored or poor quality illustrations and photographs, print bleedthrough, substandard margins, and improper alignment can adversely affect reproduction.

In the unlikely event that the author did not send UMI a complete manuscript and there are missing pages, these will be noted. Also, if unauthorized copyright material had to be removed, a note will indicate the deletion.

Oversize materials (e.g., maps, drawings, charts) are reproduced by sectioning the original, beginning at the upper left-hand corner and continuing from left to right in equal sections with small overlaps.

ProQuest Information and Learning  
300 North Zeeb Road, Ann Arbor, MI 48106-1346 USA  
800-521-0600

UMI<sup>®</sup>



**GEOLOGY OF THE UPPER CRETACEOUS NANAIMO  
GROUP, SOUTHERNMOST GULF ISLANDS AND  
ADJACENT SAANICH PENINSULA, SOUTHWESTERN  
BRITISH COLUMBIA.**

by

Patrick D. Johnstone  
B.Sc., Simon Fraser University, 1997.

THESIS SUBMITTED IN PARTIAL FULFILLMENT OF  
THE REQUIREMENTS FOR THE DEGREE OF

MASTER OF SCIENCE

In the  
Department of  
Earth Sciences

© Patrick D. Johnstone 2006

SIMON FRASER UNIVERSITY

Fall 2006

All rights reserved. This work may not be  
reproduced in whole or in part, by photocopy  
or other means, without permission of the author.



Library and  
Archives Canada

Bibliothèque et  
Archives Canada

978-0-494-29461-1

Published Heritage  
Branch

Direction du  
Patrimoine de l'édition

395 Wellington Street  
Ottawa ON K1A 0N4  
Canada

395, rue Wellington  
Ottawa ON K1A 0N4  
Canada

*Your file* *Votre référence*

*ISBN:*

*Our file* *Notre référence*

*ISBN:*

#### NOTICE:

The author has granted a non-exclusive license allowing Library and Archives Canada to reproduce, publish, archive, preserve, conserve, communicate to the public by telecommunication or on the Internet, loan, distribute and sell theses worldwide, for commercial or non-commercial purposes, in microform, paper, electronic and/or any other formats.

The author retains copyright ownership and moral rights in this thesis. Neither the thesis nor substantial extracts from it may be printed or otherwise reproduced without the author's permission.

#### AVIS:

L'auteur a accordé une licence non exclusive permettant à la Bibliothèque et Archives Canada de reproduire, publier, archiver, sauvegarder, conserver, transmettre au public par télécommunication ou par l'Internet, prêter, distribuer et vendre des thèses partout dans le monde, à des fins commerciales ou autres, sur support microforme, papier, électronique et/ou autres formats.

L'auteur conserve la propriété du droit d'auteur et des droits moraux qui protègent cette thèse. Ni la thèse ni des extraits substantiels de celle-ci ne doivent être imprimés ou autrement reproduits sans son autorisation.

---

In compliance with the Canadian Privacy Act some supporting forms may have been removed from this thesis.

Conformément à la loi canadienne sur la protection de la vie privée, quelques formulaires secondaires ont été enlevés de cette thèse.

While these forms may be included in the document page count, their removal does not represent any loss of content from the thesis.

Bien que ces formulaires aient inclus dans la pagination, il n'y aura aucun contenu manquant.

  
**Canada**



# APPROVAL

**Name:** Patrick Johnstone

**Degree:** Master of Science

**Title of Thesis:** Geology of the Upper Cretaceous Nanaimo Group,  
Southernmost Gulf Islands and adjacent Saanich  
Peninsula, Southwestern British Columbia

**Examining Committee:**

**Chair:** **Dr. Dan Gibson**  
Assistant Professor, Department of Earth Sciences

---

**Dr. Peter Mustard**  
Senior Supervisor  
Associate Professor, Department of Earth Sciences

---

**Dr. James MacEachern**  
Supervisor  
Associate Professor, Department of Earth Sciences

---

**Dr. Stuart Sutherland**  
External Examiner  
EOS, University of British Columbia

**Date Defended/Approved:** November 28, 2006



**SIMON FRASER  
UNIVERSITY library**

## **DECLARATION OF PARTIAL COPYRIGHT LICENCE**

The author, whose copyright is declared on the title page of this work, has granted to Simon Fraser University the right to lend this thesis, project or extended essay to users of the Simon Fraser University Library, and to make partial or single copies only for such users or in response to a request from the library of any other university, or other educational institution, on its own behalf or for one of its users.

The author has further granted permission to Simon Fraser University to keep or make a digital copy for use in its circulating collection (currently available to the public at the "Institutional Repository" link of the SFU Library website <[www.lib.sfu.ca](http://www.lib.sfu.ca)> at: <<http://ir.lib.sfu.ca/handle/1892/112>>) and, without changing the content, to translate the thesis/project or extended essays, if technically possible, to any medium or format for the purpose of preservation of the digital work.

The author has further agreed that permission for multiple copying of this work for scholarly purposes may be granted by either the author or the Dean of Graduate Studies.

It is understood that copying or publication of this work for financial gain shall not be allowed without the author's written permission.

Permission for public performance, or limited permission for private scholarly use, of any multimedia materials forming part of this work, may have been granted by the author. This information may be found on the separately catalogued multimedia material and in the signed Partial Copyright Licence.

The original Partial Copyright Licence attesting to these terms, and signed by this author, may be found in the original bound copy of this work, retained in the Simon Fraser University Archive.

Simon Fraser University Library  
Burnaby, BC, Canada

## **ABSTRACT**

The Upper Cretaceous Nanaimo Group is a succession of siliciclastic marginal-marine and marine sediments in southwestern British Columbia. On the north tip of the Saanich Peninsula and several small, adjacent islands, the lowest three formations of the Nanaimo group are exposed. The basal unconformity is overlain by Comox Formation conglomerates and sandstones representing deposition along a high-relief, storm-swept shoreline open to the proto-Pacific Ocean. Fan-delta, strandplain-shoreface, and barrier-island complex deposits are preserved within this formation. The Haslam and Extension formations, representing mudstone-sandstone turbidites and conglomerate-sandstone submarine channel fills respectively, overlay the Comox Formation. The depositional history suggests slow, persistent transgression within a peripheral foreland basin, with sediment supplied by contemporaneous thrusts to the east.

Nanaimo Group strata has been affected by at least two major deformation events. Evidence from the Eocene Cowichan Fold and Thrust System and the Neogene Gulf Island Thrust System is preserved within the study area.

**Keywords: Nanaimo Group, Upper Cretaceous, Comox Formation, Haslam Formation, Extension Formation.**

## ACKNOWLEDGEMENTS

I was very fortunate to be able to complete a project under the supervision of Peter Mustard and James MacEachern. Dr. Mustard introduced me to the Nanaimo Group, guided this project, and provided all the financial, logistical and scientific support that one student could consume. Dr. MacEachern provided extensive scientific advice, and somehow made long strings of criticism sound constructive. They are exceptional professors, supervisors, and friends, and were fundamental to my development as a geologist (although I absolve them of all blame for the results of that development).

The greatest field season ever was made so by the expert boatsmanship, superb photo-scalability, and excellent field assistancy of Jeremy Major. Dr. Steve Phillips captained the good ship Morena, provided logistics, and imparted a small percentage of his great knowledge of the Gulf Islands. Pierre Nadeau provided essential structural advice while displaying suspect kayak skills. Emily Gonzales and the random groups of UBC Ecologists always made a field day (or camp evening) better when our paths crossed. The numerous island owners and caretakers were tolerant of, and usually welcoming of, a couple of guys with hammers wandering their beaches.

Back in reality, my knowledge of geology (and the quality of my life) was improved through interactions with unlistable numbers of Grad-Crew and assorted SFU-EASC hangers-on. Special thanks go to Cindy Hansen, John Lerette, and Dr. Kerrie Bann for occasionally lending me small portions of their ample brain supplies at times when I was lacking. Dr. Stuart Sutherland took the time to read this weighty tome, provided useful critical review, and improved the final product.

Finally, I have to thank Antigone Dixon-Warren for immeasurable patience and tolerance as I gradually sauntered towards completing this project. In a life full of lucky events, ending up in your sphere of influence was the luckiest.

# TABLE OF CONTENTS

<b>Approval .....</b>	<b>ii</b>
<b>Abstract .....</b>	<b>iii</b>
<b>Acknowledgements .....</b>	<b>iv</b>
<b>Table of Contents .....</b>	<b>v</b>
<b>List of Figures .....</b>	<b>vii</b>
<b>List of Tables .....</b>	<b>x</b>
<b>Chapter 1: Introduction .....</b>	<b>1</b>
Purpose.. .....	1
Study Area .....	1
Regional Geology .....	3
Previous Work.....	8
Nanaimo Group Stratigraphy .....	10
Lithostratigraphy .....	10
Biostratigraphy .....	11
Nanaimo Group Structure .....	12
Thesis Objectives.....	18
Methods.....	19
<b>Chapter 2: Sedimentology and Stratigraphy .....</b>	<b>24</b>
Facies Descriptions.....	24
Conglomerate facies:.....	24
Sandstone Facies.....	31
Muddy Facies .....	38
Heterolithic Facies .....	41
Substrate-Controlled Ichnofacies.....	46
Stratigraphy .....	51
Basal Unconformity.....	51
Comox Formation .....	52
Benson Member .....	53
Saanich Member .....	54
Haslam Formation.....	58
Extension Formation .....	61
Pender and Protection Formations .....	63
<b>Chapter 3: Depositional Environments .....</b>	<b>66</b>
Rocky Shoreline.....	67

Fan Delta Complex .....	68
Fan-Delta Facies Models.....	74
Facies Association 1: Fan-Delta Complex.....	76
Storm-Dominated Shoreline.....	78
Shoreface Facies Models .....	82
Facies Association 2: Storm-Dominated Shoreface. ....	87
Barrier-Barred Coastline. ....	92
Facies models .....	94
Facies Association 3: Barrier-Island Complex. ....	99
Submarine Fan. ....	104
Facies Models. ....	111
Facies Association 4: Submarine Fan. ....	116
Synthesis .....	120
<b>Chapter 4: Sediment Provenance .....</b>	<b>126</b>
Sandstone Composition.....	127
Conglomerate Clast Lithology.....	131
Paleocurrent Analysis .....	139
Provenance.....	149
<b>Chapter 5: Structural Geology .....</b>	<b>153</b>
Overview.....	153
Bedding Orientation .....	153
Brittle Structures .....	155
Folding and Foliation.....	167
Structural Synthesis .....	177
<b>Chapter 6: Summary and Conclusions .....</b>	<b>186</b>
<b>References .....</b>	<b>193</b>
<b>Appendices.....</b>	<b>205</b>
Appendix A: Vertical Stratigraphic Sections.....	206
Appendix B: Structural Data.....	269
Appendix C: Thin Section Petrography. ....	301
Appendix D: Conglomerate Clast Lithologies.....	314
Appendix E: Paleocurrent data. ....	316
Appendix F: GIS Techniques. ....	324

## LIST OF FIGURES

Figure 1: Map of study location. ....	2
Figure 2: Geography of study.....	4
Figure 3: Regional geology of the Nanaimo Group. ....	5
Figure 4: Stratigraphy of the Nanaimo Group. ....	11
Figure 5: Selected structural geology of the southern Nanaimo Group.....	13
Figure 6: Facies C1 Basal Conglomerate.. ....	25
Figure 7: Facies C2 Conglomerates.....	27
Figure 9: Facies P1 Pebbly Sandstones.. ....	30
Figure 10: Facies S1 Coarse-Grained Sandstones.....	32
Figure 11: Facies S2 Medium-Grained Sandstones.....	34
Figure 12: Facies S3 Cross-Bedded Sandstones.. ....	35
Figure 13: Facies S4 Bioturbated Sandstone.....	37
Figure 14: Facies M1 Bioturbated Muddy Sandstone. ....	39
Figure 15: Facies M2 Carbonaceous Shale.. ....	40
Figure 16: Facies H1 Intercalated Mudstone-Sandstone.. ....	42
Figure 17: Facies H2 Heterolithic Sandstone-Mudstone.....	43
Figure 18: Facies H3 Graded Sandstone-Mudstone couplets.....	45
Figure 19: <i>Glossifungites</i> Ichnofacies-demarcated discontinuities.....	48
Figure 20: Juxtaposed <i>Glossifungites</i> Ichnofacies and <i>Teredolites</i> Ichnofacies associated with discontinuities.. ....	50
Figure 21: Comox Formation exposures.....	56
Figure 22: Haslam Formation exposures.. ....	59
Figure 23: Extension Formation exposures.....	62
Figure 24: Model fan-delta complex,.....	72
Figure 25: Typical expressions of Facies Association 1.....	77
Figure 26: Shoreface models.. ....	79
Figure 27: Cross-section of model shoreface,.....	81
Figure 28: Typical expressions of Facies Association 2.....	89
Figure 29: Comparative morphology of barrier island complex and wave dominated estuaries. ....	95
Figure 30: Ravinement of transgressive barrier island complex models. ....	95
Figure 31: Typical expressions of Facies Association 3.....	100

Figure 32: Submarine fan types .....	107
Figure 33: Typical expressions of Facies Association 4.....	117
Figure 34: Exposures of the Comox Formation - Haslam Formation transition.. .....	118
Figure 35: Ternary diagrams.....	132
Figure 36: Conglomerate clast counts, locations and gross clast lithology. ....	134
Figure 37: Conglomerate clast count results, Comox Formation. ....	135
Figure 38: Conglomerate Clast count results, Extension Formation. ....	137
Figure 39: Rotated paleocurrent trends from the Comox Formation: Facies Association 1.....	144
Figure 40: Rotated paleocurrent trends from the Comox Formation: Facies Association 2.....	145
Figure 41: Rotated paleocurrent trends from the Comox Formation: Facies Association 3.....	146
Figure 42: Rotated paleocurrent trends from the Haslam Formation. ....	147
Figure 43: Rotated paleocurrent trends from the Extension Formation.....	148
Figure 44: Poles to bedding planes, by domain. ....	154
Figure 45: Poles to planes of brittle structures. ....	157
Figure 46: Poles to planes of joints. ....	159
Figure 47: Joints exposed on Pym Island and Piers Island.....	160
Figure 48: Faults measured in study area.....	163
Figure 49: Faults by domain.....	164
Figure 50: Shear zone on Coal Island.....	165
Figure 51: Large rotated block within Coal Island shear zone.....	166
Figure 52: Folds in turbidites on Domville Island.....	169
Figure 53: Measurements of folds on Domville Island.....	169
Figure 54: Folds in Haslam Formation turbidites, Piers Island.. ..	170
Figure 55: Folds on Portland Island .....	172
Figure 56: Inferred fault in Iroquois Channel. ....	172
Figure 57: Folds in Deep Cove.....	174
Figure 58: Beta diagram of folding in Towner Bay. ....	174
Figure 59: Measurements of fold between Gooch and Domville domains. ....	175
Figure 60: Foliation measurements by domain. ....	175
Figure 61: Inferred fault between Domville and Brethour Islands.....	179
Figure 62: Inferred fault orientations, Colburne Passage. ....	179
Figure 63: Overturning of the Gooch Island - Comet Island stratigraphy. ....	182
Figure 64: Block model showing model paleogeography of study area, .....	187
 Figure A 1: Locations of Measured Sections.....	 207



Figure A 2: Measured Section symbology legend .....	208
Figure A 3: Location Map, MS001 and MS004. ....	209
Figure A 4: Location Map, MS002.....	217
Figure A 5: Location Map, MS003.....	221
Figure A 6: Location Map, MS005 and MS006 .....	226
Figure A 7: Location Map, MS007 and MS012.. ....	233
Figure A 8: Location Map, MS008.....	237
Figure A 9: Location Map, MS009.....	243
Figure A 10: Location Map, MS010.....	247
Figure A 11: Location Map, MS011.....	255
Figure C 1: Geographic distribution of thin section samples. ....	302
Figure BP-1: Geology of the Upper Cretaceous Nanaimo Group, Southernmost Gulf Islands and Adjacent Saanich Peninsula, southwestern British Columbia.....	Back Pocket

## LIST OF TABLES

Table 1: Bioturbation Index .....	20
Table 2: Flow types typical of submarine fan settings. ....	109
Table 3: Generalized facies associated with submarine fans.....	113
Table 4: Modal Lithology of sandstone framework grains. ....	129
Table 5: Clast count data for Comox Formation conglomerates.. ....	133
Table 6: Clast count data for Extension Formation conglomerates.....	136
Table 7: Clast count data from this study compared to those of earlier studies.....	138
Table 8: Summary of rotated paleocurrent data .....	142
Table B 1: Structural trends and eigenvalues. ....	269
Table B 2: Bedding measurements and eigenvalues. ....	270
Table B 3: Brittle structure measurements and eigenvalues .....	270
Table B 4: Bedding Data. ....	271
Table B 5: Brittle Fracture Data.....	286
Table B 6: Foliation Data.....	294
Table B 7: Fault Data. ....	296
Table B 8: Folds on Domville Island.....	299
Table B 9: Folds on Piers Island.....	300
Table D 1: Conglomerate Clast Lithologies, Comox Formation. ....	314
Table D 2: Conglomerate Clast Lithologies, Extension Formation. ....	315
Table D 3: Conglomerate Clast Lithologies, all data .....	315
Table D 4: Paleocurrent Data.....	317

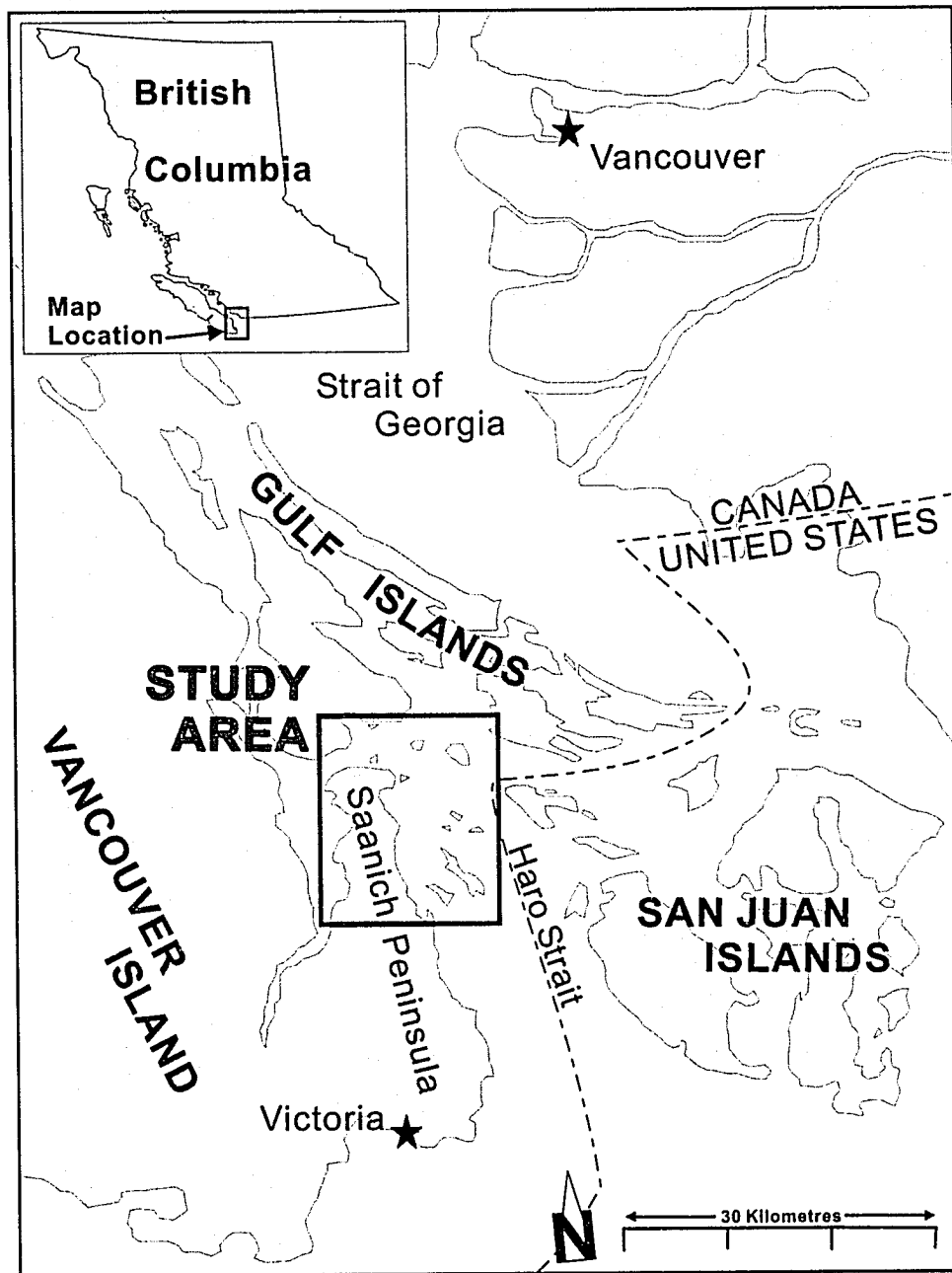
# **CHAPTER 1: INTRODUCTION**

## **Purpose**

The purpose of this research project is to improve the understanding of the geology of the Upper Cretaceous strata that comprise the north end of the Saanich Peninsula and numerous small islands adjacent to the peninsula and south of Salt Spring Island. This research adds to the existing database on the Nanaimo Group through large-scale mapping in an area previously understudied by the numerous workers who have studied the Nanaimo Group. Through sedimentological descriptions and interpretations, petrologic studies, and structural analysis, this research provides a better understanding of the depositional setting and evolution of the Nanaimo Basin during Late Cretaceous time. Further, this work outlines a sequence of structural events that have influenced the southwestern corner of British Columbia from the Cretaceous to the present, and also provides a new 1:20,000-scale geologic map of the study area.

## **Study Area**

The study area is situated within the Strait of Georgia in southwestern British Columbia, between the major cities of Vancouver and Victoria (Figure 1). The study area includes the north part of the Saanich Peninsula of Vancouver



**Figure 1: Map of study location.**

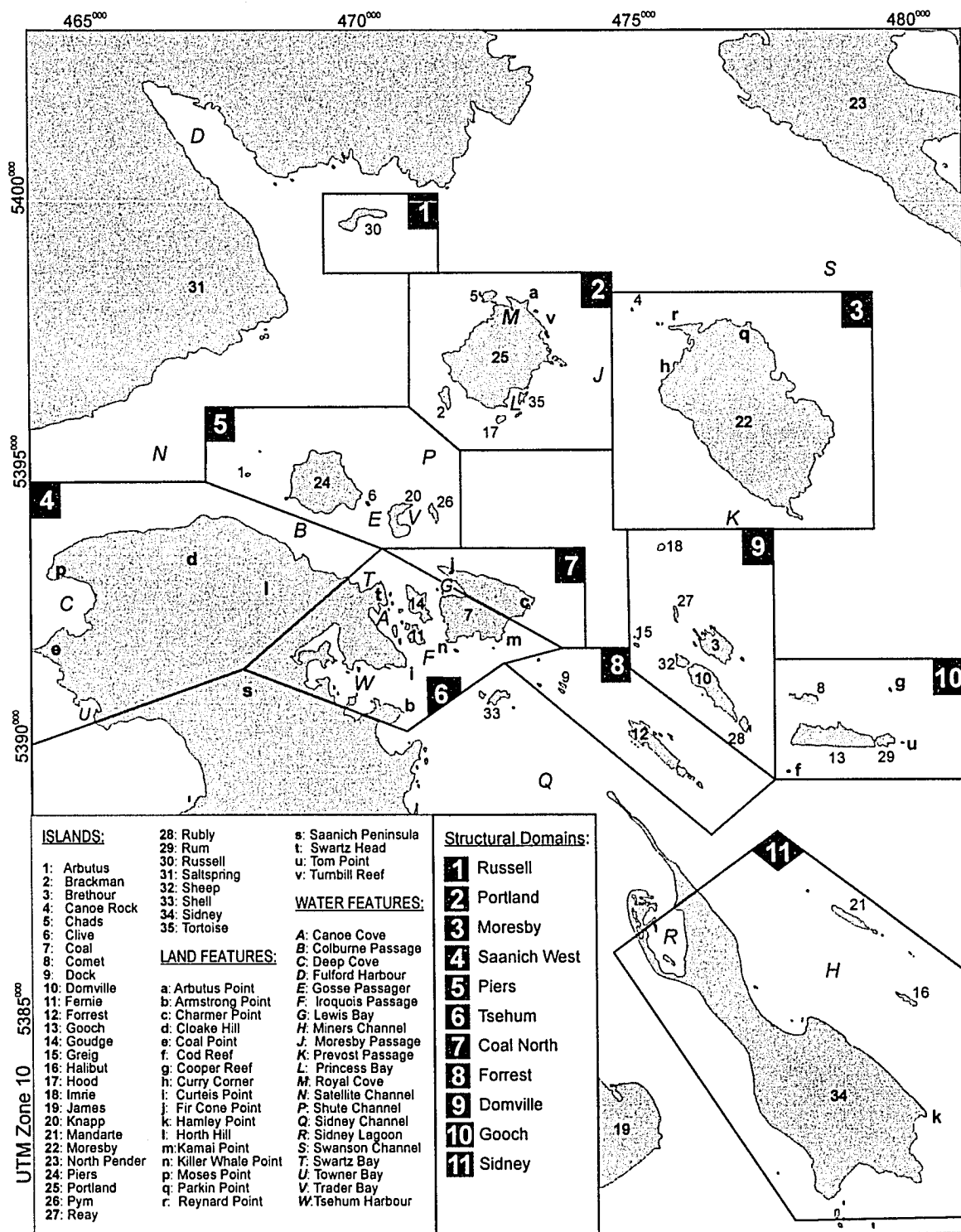
Island, and several dozen small islands between the Peninsula and Haro Strait to the east (Figure 2; see also Backpocket Map). These islands range in size from 570-hectare Sidney Island to small islets exposed only at low tide. All islands are in Canadian waters, with Russell Island at the north of the study area, and

Sidney Island at the south. The highest elevations are 148 metres on Moresby Island and 141 metres at Horth Hill on the Saanich Peninsula, although most islands have an exposed relief of only a few tens of metres. Ocean depths between islands rarely exceed 100 metres, and the spring tide range is approximately 3.3 metres.

The north end of the Saanich Peninsula is moderately developed, with a mixture of forests, rural and suburban property. Most of the adjacent islands are forested, sparsely developed, and most are privately owned. All islands have excellent outcrop exposed in and above the modern intertidal zone, commonly extending several metres above highest tide line. Within the study area, the Saanich Peninsula has similar coastline outcrops, as well as limited interior outcrops, mostly comprising road cuts and bluffs.

## **Regional Geology**

The study area is part of the southwestern Canadian Cordillera, and is underlain by, or is proximal to, several allochthonous terranes, which represent a complex tectonic history (Figure 3). Wrangellia Terrane or the Coast Belt serve as the immediate substrate to the Nanaimo Group (Monger and Journeay, 1994). On the San Juan Islands to the southeast, the North Cascades – San Juan Complex is in fault contact with the Nanaimo Group across thrust faults interpreted to be syn-depositional (Brandon *et al.*, 1988), and may also act as local basement. The Pacific Rim and Crescent terranes occur outside the field area to the west, however their geologic history may be important to the post-depositional deformation of the Nanaimo Group.



**Figure 2: Geography of study area with structural domains outlined. See also Backpocket Map.**

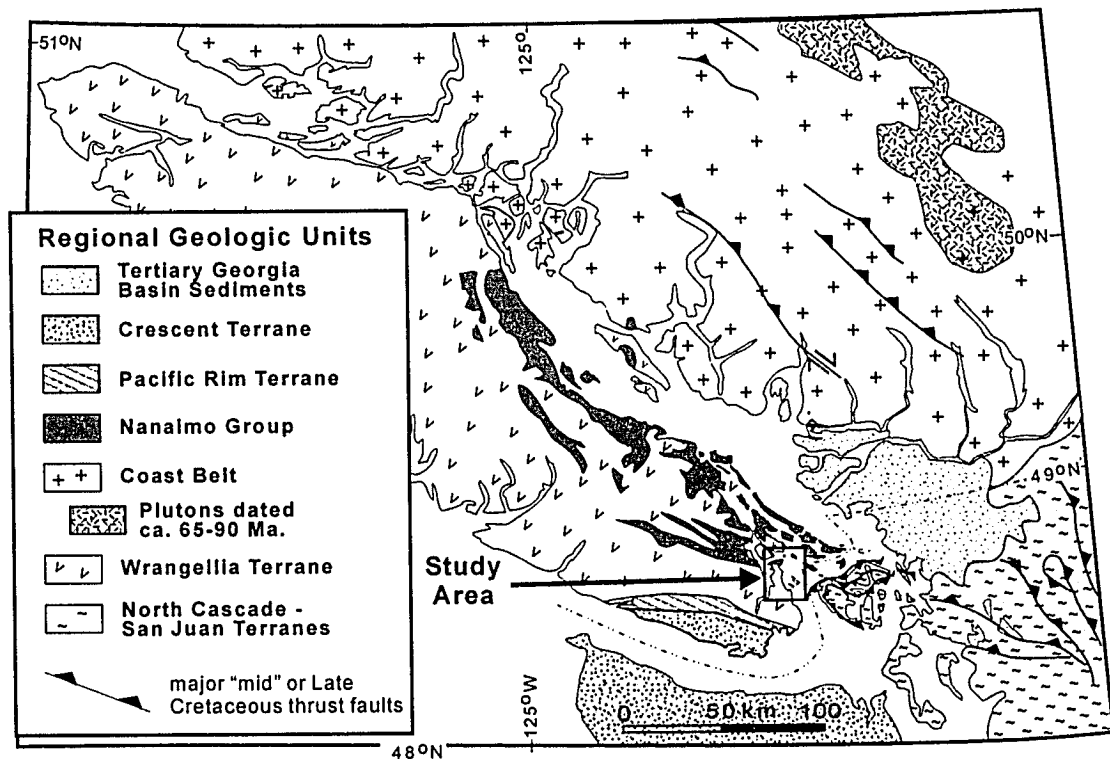


Figure 3: Regional geology of the Nanaimo Group (modified from Mustard, 1994).

Vancouver Island is composed almost entirely of rocks of the Wrangellia Terrane, an amalgam of Devonian arc-related volcanic and sedimentary rocks (Sicker Group), Late Carboniferous and Permian sedimentary strata (Buttle Lake Group), Upper Triassic basalt and carbonates (Vancouver Group), and Lower Jurassic arc volcanics (Bonanza Group), which record a history of arc volcanism, ocean plateau formation, and marine carbonate and clastic deposition (Yorath *et al.*, 1999). At the latitude of the study area, Wrangellia accreted to the North American continental margin in Late Jurassic or Early Cretaceous time (Monger and Journeay, 1994). Beyond forming the bulk of Vancouver Island, Wrangellian rocks are also found on the Gulf Islands and along the coast of the mainland

north of the study area, where they are intruded by plutonic rocks of the Coast Belt (Friedman *et al.*, 1995).

The southern extent of the Coast Belt is approximately 75 kilometres to the east of the study area, although Nanaimo Group rocks unconformably overlie Coast Belt rocks in the Lower Mainland area of British Columbia, and at Lang Bay farther to the north (Mustard and Rouse, 1991). The southern Coast Belt is dominantly (~85%) plutons of Middle Jurassic to Tertiary ages, with minor Paleozoic and Eocene components. Contained within this plutonic amalgamation are commonly fault-bounded slivers of various Paleozoic to Mesozoic terranes, including the Bridge River (a Mississippian to Jurassic accretionary complex), and the Cadwallader, Methow, Chilliwack and Harrison terranes (island arcs and associated sedimentary rocks, ranging from the Devonian to the Lower Cretaceous). In the southern Coast Belt, local occurrences of Cretaceous volcanics and sedimentary rocks are variously metamorphosed, and assigned to the Gambier Group. Eocene to Holocene plutonic, volcanic and sedimentary rocks overlap the southern Coast Belt. Most notably, components of the Cascade magmatic arc are expressed as widely dispersed Oligocene to Miocene intrusive rocks, and the modern arc magmatism of several stratovolcanoes including Mount Baker and Mount Garibaldi (Monger and Journeay, 1994).

The southern locus of Late Cretaceous magmatism is offset towards the eastern margin of the complex (Friedman *et al.*, 1995). Thus, magmatism coeval with Nanaimo Group deposition occurred several hundred kilometres east of the



depocentre of the study area, even without taking substantial post-Cretaceous shortening into account.

The Coast Belt west of this Late Cretaceous plutonic locus, and the Cascades core south of it, are cross-cut by a series of Late Cretaceous thrust faults. The faults are margin-parallel, and are dominantly southwest-vergent with low to moderate dips to the east, although with some late-stage, northeast-vergent, high-angle, out-of-sequence back thrusts. The thrusting in the Coast Belt occurred from 100 to at least 80 Ma, with a migration towards the northeast around 90 Ma (Journeay and Friedman, 1993; Umhoefer and Miller, 1996). Thrusting in the Cascades occurred from at least 96 Ma to 70 Ma (Paterson *et al.*, 2004; Matzel *et al.*, 2004).

Southeast of the study area, the San Juan – Cascades complex is an amalgamation of several small, far-travelled terranes, with ages ranging from the early Paleozoic Era to the middle of the Cretaceous Period (Brandon *et al.*, 1988). These terranes began to amalgamate sometime during the Jurassic Period, and underwent extensive thrusting in the Late Cretaceous (Bergh, 2002). This thrusting is recorded in the southern Nanaimo Group, which contains detrital rocks from the San Juan nappes, presumably related to thrust thickening and unroofing.

Farther to the west and southwest, the Pacific Rim and Crescent terranes are accretionary complexes that underplated the southwestern margin of Wrangellia Terrane during the Paleogene (Rushmore and Cowan, 1985; Clowes *et al.*, 1987). The Pacific Rim Terrane is a meta-sedimentary and meta-igneous

assemblage that formed in the Cretaceous. It has a complex accretionary history, but may have been in place by the early Eocene (Yorath *et al.*, 1999). The Crescent Terrane of southern Vancouver Island consists of Paleocene-Eocene volcanics that accreted to, and underplated, the Pacific Rim Terrane in the late Eocene (Groome *et al.*, 2003).

This tectonic history of the region places Nanaimo Group sedimentation in the forearc position, within a very broad Late Cretaceous continental margin arc–trench gap. The arc massif (represented by coeval plutonism in the southeastern Coast Belt) and the accretionary complex (presumed to be emplaced under the western edge of Wrangellia) were separated by several hundred kilometres. The width of this arc-trench gap, coupled with the complete lack of direct arc volcanic input into the basin suggest that a traditional forearc model is a poor fit for the basin. The abundant evidence of coeval thrusting in the arc and adjacent San Juan – Cascades indicate the Nanaimo Group was deposited into a collision-related peripheral foreland basin (Mustard 1994).

## **Previous Work**

The Nanaimo Group was named by G.M. Dawson (1890), who applied the term to the Cretaceous sedimentary rocks of eastern Vancouver Island. Extensive mapping and local study has been conducted since coal mining of terrestrial units began in the mid-1800s. The first detailed stratigraphic sections produced from the northern “Comox” section of the basin were published by Richardson (1872), and the first complete subdivision of the stratigraphy of the

southern "Nanaimo" successions was completed by Clapp (1913) and Clapp and Cooke (1917).

Local and regional lithostratigraphic and biostratigraphic correlations have been attempted by several workers. Muller and Jeletzky (1970) summarized these efforts and established a unified lithostratigraphic succession for the entire basin, integrating nomenclature from the two main outcrop areas. This stratigraphy was further refined by Ward (1978) and in a basin synthesis by Mustard (1994).

Numerous student theses have been completed on various aspects of the Nanaimo Group (earlier work summarized in Mustard, 1994), including important basin-wide syntheses by Pacht (1980) and England (1990). Further studies have explored the structural history of the basin (England and Calon, 1991; England and Bustin, 1998; Journeay and Morrisson, 1999), biochronology of the basin (Haggart, 1994; Haggart *et al.*, 2005), provenance of Nanaimo Group sediments (Mahoney *et al.*, 1999), paleomagnetic analysis of the sediments (Enkin *et al.*, 2001), and the relation of Upper Cretaceous sediments to overlying Paleogene sedimentary units (Mustard and Rouse, 1994). However, the majority of recent studies are large-scale, local analyses of particular locations or units (*e.g.* Treptau, 2002; Katnick and Mustard, 2003). The area of this study has, up to now, been largely overlooked for detailed stratigraphic study, although Muller and Jeletzky (1970), England (1990), Haggart (1994), and Haggart *et al.* (2005) examined some parts of the study area during their research.

## Nanaimo Group Stratigraphy

### Lithostratigraphy

Several workers dating back to Richardson (1872) and Clapp (1914) established local stratigraphies for the numerous units of the Nanaimo Group. Early studies were dominated by the interpretation that the northern "Comox" and southern "Nanaimo" basins were coincident, but not correlated, being separated by a paleo-highground named the Nanoose Arch. The unified single-basin stratigraphy established by Muller and Jeletzky (1970) and summarised in Mustard (1994) is preferred by most workers, although not all (see England, 1989). The general single-basin stratigraphy established by Muller and Jeletzky (1970) integrated nomenclature from both main depocentres. They named nine formations representing five fining-upwards depositional cycles, each recording a transgression from a fluvial or deltaic setting to a deep marine one. Further refinement of this stratigraphy continued with important contributions by Ward (1978), Pacht (1984), and Haggart (1994). The history of two-basin *versus* one-basin stratigraphy is well summarized in Mustard (1994).

Currently, the Nanaimo Group is divided into 11 lithostratigraphic formations (Figure 4), integrating biostratigraphically defined zones from the Turonian to the Maastrichtian stages, while also recognizing the laterally diachronous nature of some formations. The units are entirely siliciclastic, and range from cobble conglomerate to mudstone, although sandstone is the dominant exposed lithology. Depositional environments range from alluvial to "deep" marine with submarine fan successions dominating the

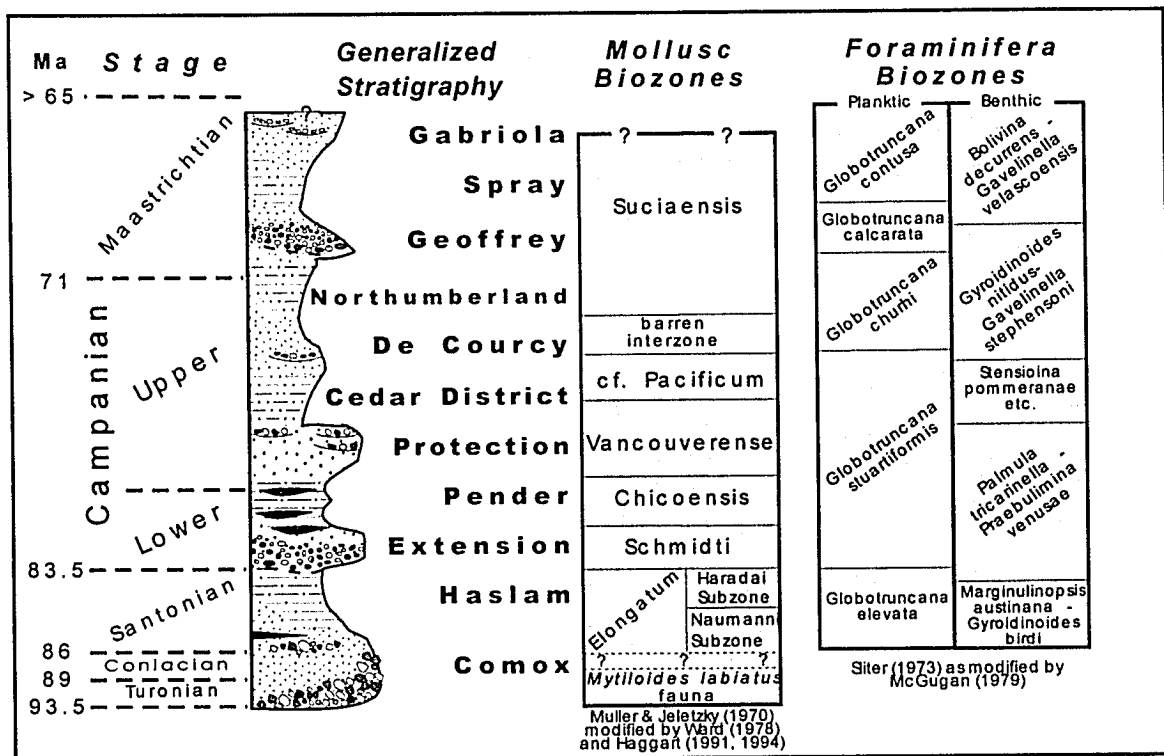


Figure 4: Stratigraphy of the Nanaimo Group (modified from Mustard, 1994).

upper units, and lower units characterized by nearshore marine to non-marine settings. Economic coal measures within these basal units have been mined since the 1850's, and consequently, the terrestrial parts of these basal units have been most thoroughly studied.

### Biostratigraphy

Extensive biostratigraphic studies of the Nanaimo Group have established molluscan and foraminiferal biozones for the basin (Figure 4), and provide an

age range of early Turonian to Maastrichtian with no significant identified age gaps (Mustard, 1994).

Early molluscan stratigraphic studies are summarized by Muller and Jeletzky (1970), who also established a biozonation based on widespread ammonites and inoceramid bivalves. Ward (1978) and Haggart (1994) have refined this scheme to include nine biozones from the lower Turonian to the Maastrichtian. Only the top of the Nanaimo Group succession is poorly constrained, because the Gabriola Formation has not yielded age-diagnostic fossils.

Microfossil studies established foraminifera biozones (refined by McGugan 1979), which span the basin from the lower Santonian to the Maastrichtian, and palynological suites which also establish Late Cretaceous ages for several outlier parts of the basin (summarized in Mustard, 1994).

### **Nanaimo Group Structure**

Most of the Nanaimo Group has been structurally deformed by several Cenozoic events, including folding and thrust-thickening. The present exposed extent (approximately 240 by 90 kilometres) is only partially representative of what must have been a much larger depositional basin prior to tectonic shortening and extensive unroofing (England and Calon, 1991). In the Gulf Islands region, the Nanaimo Group generally dips moderately to the northeast, probably as a response to the tilting of Wrangellia by the underthrusting of young Juan de Fuca Plate crust under the western edge of North America (Mustard,

1994). This general trend is augmented by and overprints two major Tertiary deformation events: the Cowichan Fold and Thrust System, and the Gulf Islands Thrust System (Figure 5).

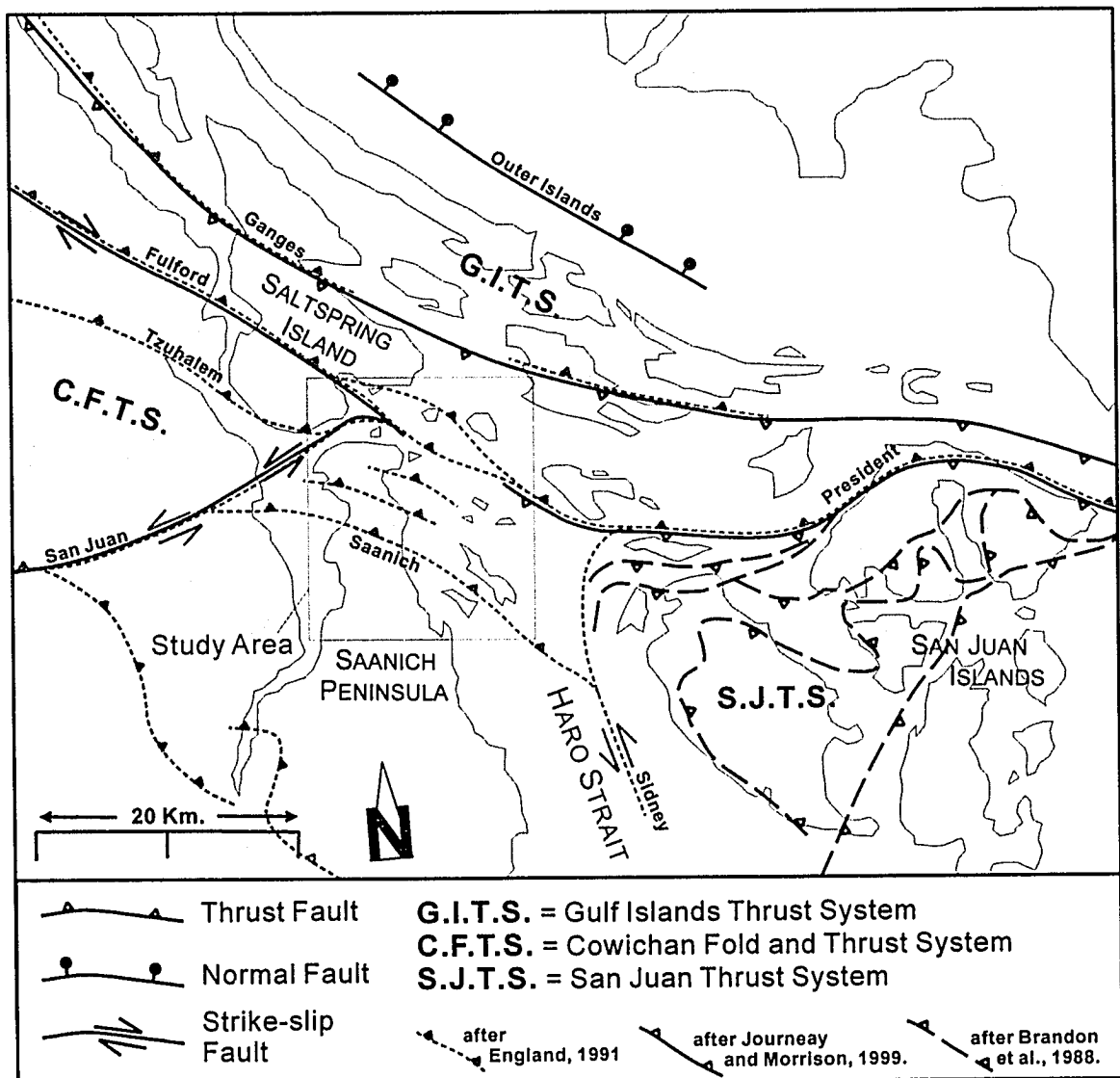


Figure 5: Selected structural geology of the southern Nanaimo Group, as interpreted in previous regional studies.

The Cowichan Fold and Thrust System (CFTS) deforms all of southeastern Vancouver Island and the Canadian Gulf Islands, including Paleozoic Wrangellian rocks and overlying Cretaceous to Eocene sedimentary rocks (England and Calon, 1991). This is interpreted as a southwest verging, thick-skinned thrust system. High-angle, northwest-southeast trending faults and generally broad fault-bend folding of the CFTS control the topography of the Gulf Islands (Mustard, 1994). This thrust system was divided into "Northern" and "Southern" belts by England and Calon (1991). The northern belt was interpreted as a partially exhumed leading imbricate fan with the leading thrust being the Fulford Fault. The southern belt (including the majority of the study area) represents a thrust duplex with an inferred, and completely blind, southeast striking sole thrust named the Saanich Fault (Figure 5).

The timing of thrusting within the CFTS is constrained to the middle Eocene (ca. 45-50 Ma). This timing is bounded by the deformation of Paleocene- to early Eocene-aged units on the outer Gulf Islands (Mustard and Rouse, 1994), dating of dykes in the northern part of the fold belt inferred to post-date deformation (Massey, 1995), and fission track dating of thrust sheets within the southern belt (Johnson *et al.*, 1986, England *et al.*, 1997).

More recent work has identified a younger, northeast verging fold and thrust system that partly cross-cuts the CFTS, named the Gulf Island Thrust System (GITS) by Journey and Morrison (1999). Folds are broad and open in the outer Gulf Islands, but become tight with steep, southwest dipping overturned limbs, and west-northwest trending hinge lines near the Ganges Fault zone.



Journeay and Morrison (1999) suggest the GITS represents a change from compressional to transtensional tectonics in the Neogene, with late dextral shear and margin-parallel extension along the forearc margin. A similar transition from contractional to transtensional strain is recorded in the Cascades core to the southwest, although here the transition is interpreted to be an Eocene-aged event (Paterson *et al.*, 2004).

The boundary between the GITS and the CFTS is represented by the Fulford Fault, one of several major regional faults that previous studies have inferred to pass through the study area. The Fulford Fault is a steeply dipping, northwest-southeast trending anastomosing shear zone that cuts across southern Saltspring Island and Fulford Harbour, passing through the field area and into Haro Strait. The fault was originally interpreted to be a northeast-dipping, southwest-verging thrust fault that roots in the sole thrust of the CFTS and extends into the President Fault zone in the San Juan Islands (England and Calon, 1991). This is at odds with most other interpretations of the President Fault as a southward-dipping, north-verging thrust (Johnson, 1981; Brandon *et al.*, 1988).

Journeay and Morrison (1999) reinterpreted the Fulford Fault as a high-angle, southwest-dipping shear zone with oblique top-to-the-northeast dextral movement on the north part of Saltspring Island. Along the west coast of Fulford Harbour, shear fabrics indicate dextral displacement, and offsets of high-angle normal faults suggest late-stage displacement of at least 6 kilometres. The fault

is projected through the study area, where it merges with the north-verging President Fault (Figure 5).

Other major regional faults that have been drawn through the study area include the Tzuhalem and Saanich faults. The Tzuhalem is a steeply dipping southwest vergent thrust that cuts the southwestern tip of Saltspring Island roughly parallel to the Fulford fault zone. The Tzuhalem has been interpreted to bring Paleozoic Wrangellian rocks on the north into contact with Nanaimo Group rocks in the south (Muller, 1980), although the fault may be coincident with a Cretaceous unconformity, making interpretation of displacement by relative ages of these rocks problematic (England, 1990). The Saanich Fault has no surface expression, but has been inferred to be the sole thrust of the southern CFTS and to pass southeastward under thick Quaternary cover from the central Saanich Peninsula, through Sidney Channel, and into Haro Strait (England, 1990).

The San Juan Fault is a major structural feature on southern Vancouver Island, which on the west half of the island forms the boundary between Wrangellian volcanic rocks to the north and accretionary complex rocks of the Pacific Rim Terrane to the south (Clowes *et al.*, 1987). To the east, this fault offsets Wrangellian rocks with apparent sinistral offset exceeding 30 kilometres, before passing into Satellite Channel between Saltspring Island and the Saanich Peninsula (DeBari *et al.*, 1999; Journeay *et al.*, 2000). The relationship between this fault and the Fulford Fault, which should cross-cut in the middle of the study area, is uncertain.

Johnston and Acton (2003) have developed a model of the Cenozoic deformation of southern Vancouver Island, which they describe as a counter-clockwise rotating orocline. This observation is based on the comparison of (dominantly Nanaimo Group) bedding inclinations across southern Vancouver Island, a southward increase in contraction, a north-to-south transition from minor deformation through conical folds to cylindrical folds, along with interpreted coeval extension in the Barkley Sound area of Vancouver Island (Johnston and Acton, 2003). The area of this study is located near the southern edge of this inferred orocline, where fold-and thrust contraction would be at its maximum, and shearing related to oroclinal bending (northeast-trending sinistral faults, northwest-trending dextral faults) should be most apparent.

Finally, the study area represents the Canadian islands closest to the San Juan Thrust System (SJTS) of the San Juan Islands of Washington State. The SJTS is a Late Cretaceous sequence of southward-dipping thrust faults that juxtaposes several Paleozoic to Cretaceous terranes (Brandon *et al.*, 1988). The thrusting is at least partially coeval with Nanaimo Group sedimentation, and clasts derived from San Juan nappes are common in conglomerates of the Nanaimo Group on the northern San Juan Islands (Mustard, 1994). The Nanaimo Group rocks are in fault contact with the leading edge of the San Juan nappes along the President Fault. This fault is interpreted to be a southward-dipping thrust based on stratigraphic relationships with the Nanaimo Group and the sharp contrast of metamorphic grade between the Nanaimo Group rocks and the adjacent San Juan nappes (Brandon *et al.*, 1988).

## **Thesis Objectives**

One of the main objectives of this study was to prepare a geologic map of the Canadian Gulf Islands between the south end of Saltspring Island and the south end of Sidney Island, and the adjacent northern end of the Saanich Peninsula, at a scale of 1:20:000 (see Backpocket Map). The map displays lithologic units exposed at the surface and the relationships between the Nanaimo Group sedimentary succession and pre-Cretaceous basement rocks. The map is supported by cross sections, measured sections (see Appendix A), a structural synthesis of the study area (Chapter 5 and Appendix B), and detailed lithologic and stratigraphic descriptions of the Nanaimo Group units of the study area (Chapters 2 and 3, and Appendix A).

Geologic units are assigned to formations and (where appropriate) members that reflect their lithostratigraphic relationship to the existing stratigraphy of the Gulf Islands preserved to the north and east as described in other studies. Major facies are described, supported by representative measured sections in select locations (Appendix A). Facies associations are constructed in order to assist with the interpretation of depositional environments and Late Cretaceous paleoenvironmental description of this part of the southern Canadian Cordillera (Chapter 3).

The study area includes the southernmost Nanaimo Group outcrops within Canada and some of the oldest units in the succession, which makes the provenance of local Nanaimo Group sediments worthy of analysis. Provenance study includes thin section petrology of sandstones (Appendix C), clast counts of

conglomerates (Appendix D), and paleocurrent measurement (Appendix E), as discussed in Chapter 4.

Finally, the study area is adjacent to, or cross-cut by, major deformation events of the Cowichan Fold and Thrust System, the Gulf Island Thrust System and the San Juan Thrust System. Further detailed analysis of the structures exposed at the surface, integrated with a better understanding of the local and regional stratigraphy, improves the understanding of the structural history of the basin since the Cretaceous, and the regional geology of the southern Canadian Cordillera (see Chapter 5).

## **Methods**

Field mapping of the study area was performed during the summer of 2003, augmented by a week in 2004. Field work included the northern tip of the Saanich Peninsula, including all areas north of the city of Sidney on the east and north of Princess Bay on the west. A small boat was used to access the islands of the field area, bounded by Russell Island to the north, Haro Strait to the east, Sidney Island to the south, and Saanich Peninsula to the west.

Field mapping was performed using 1:20,000 scale basemaps prepared previously from various digital map sources, including British Columbia TRIM maps, digitized Canadian Hydrographic Service nautical charts, and digitized Canadian NTS topographic maps. Aerial photographs were used for navigation and outcrop identification. UTM locations of stations were recorded digitally using

a hand-held Global Positioning System unit, augmented by map and aerial photograph references.

Fieldwork involved description of lithologic units, including grain size (using a Wentworth-scale grain card), measurement and description of sedimentary structures, sediment maturity, and fossil content. Trace fossils were identified and photographed, and Bioturbation Index (BI) was estimated, based on the classification scheme of Reineck (1963) as modified by Bann *et al.* (2004), outlined below in Table 1.

**Table 1: Bioturbation Index (adapted from Reineck, 1963, as modified by Bann *et al.*, 2004)**

Index	Bioturbation	Bedding structures	Trace density	Trace overlap
0	absent	undisturbed	none	n/a
1	sparse	distinct	sparse	none
2	uncommon	distinct	low	rare
3	moderate	boundaries sharp	moderate	rare
4	common	boundaries indistinct	high	common
5	abundant	just visible	abundant	abundant
6	complete	completely disrupted	abundant	homogenous

Lithologic contacts were described. Bedding plane orientation, fractures, and minor faults were identified and measured using a geologic compass. Hand samples were collected and returned to the laboratory where appropriate. Photographs were taken of both representative structures and unique structures in order to augment descriptions. Field units were described at the facies level,

with facies associations assembled to assist with the interpretation of depositional environments (Chapter 3).

Measured sections were hand drafted at 1:100 scale. Measured section locations were chosen in areas where continuous sections could be confidently measured, while attempting to measure a representative sample of lithologic units and facies associations of the field area. Further, measured sections were collected as correlation tools where along-strike relationships are unclear. A total of 12 sections were measured, representing more than 1200 metres of stratigraphic thickness. Measured sections were collected using a cm-scale measure tape (with ground distances converted to formation thickness based on local bedding dip), and a 1.5 metre Jacob Staff with an inclinometer, augmented by photographs and sample collection (Appendix A).

Twenty one sandstone hand samples were cut for thin sections, representing all three of the Nanaimo Group formations mapped in the field area, and sample sites were well dispersed geographically (see Appendix C). Thin sections were prepared by Vancouver Petrographics and stained with sodium cobaltinitrite to aid in the identification of K-feldspars. Thin sections allowed improved description of lithology by qualitative analysis of clast composition, cement types and diagenesis, and textures. Eleven of the thin sections were coarse-grained enough and fresh enough for detailed framework grain composition analysis. Modal analysis used a random search pattern, and counts were performed until 100 grains were been counted (stops on matrix, pore space, or cement were counted in order to estimate proportions of each, but

were not included in the minimum 100 points required for framework modal analysis). These samples were plotted on QFL and associated ternary diagrams (Chapter 4).

Clast counts were performed at 5 locations where conglomerates outcropped (see Appendix D). Sampling was randomized by stretching a string across the outcrop at various angles relative to bedding, and identifying the first 20-30 clasts of a size large enough to macroscopically identify with aid of a 10x hand lens (1.5 – 2 cm minimum). The process was repeated with a new string orientation until 100 clasts were counted at each station. Clasts were characterized by gross lithologic character (Chapter 4).

Paleocurrent measurements were taken at any opportunity, for a total of 907 measurements from 79 separate beds, representing 51 station locations. The majority of these measures are cross bedded sandstones or conglomerates, and the strike and dip of identified foreset planes were measured. On several sandstone beds, there were surface exposures of asymmetric ripples and the paleocurrent direction was measured as a trend and plunge along the bedding surface. Finally, three thick conglomerate beds were measured for imbrication of clasts. The orientation of the apparent a-b plane of non-spherical clasts was measured for dip and dip direction, with the paleocurrent azimuth interpreted to be 180 degrees from the average dip direction (Appendix E).

For each station, the paleocurrent dip direction lineations were plotted on a Schmidt stereonet along with the measured bedding plane. The lineations were digitally rotated about strike of bedding using stereonet-plotting software to bring



the bedding plane to horizontal. If bedding was interpreted to be folded, stereonet rotation was about identified fold axis including correction for fold plunge. The rotated paleocurrent vectors were plotted on a rose diagram to show mean paleocurrent direction and distribution for each geologic unit and structural domain (Chapter 4).

More than 3500 structural measurements were taken during field mapping. To simplify data management and to aid with structural interpretation, the data were separated into 11 structural domains (Figure 2). The delineation of domains was based upon geographic locations of islands, dominant geologic units, and common bedding aspects within domains. Data was digitized and plotted as stereonets of bedding, fractures, foliations, and folds. Large fold features were interpreted by plotting bedding orientations of fold limbs and creating  $\beta$ - and  $\pi$ -diagrams. Density contouring of structural data on Schmidt stereonets was used to identify trends within and between structural domains. Contouring was performed digitally using a Gaussian counting method, with the stereonet divided into a 36x36 counting grid and kurtosis = 100, with contour levels adjusted according to the data set (see Chapter 5 and Appendix B).

Data collected in the field was later digitized into a Geographic Information Systems (GIS) database. Basemap production, structural data processing, and digital elevation modelling were performed using the GIS software. Specific GIS techniques used are outlined in Appendix F.

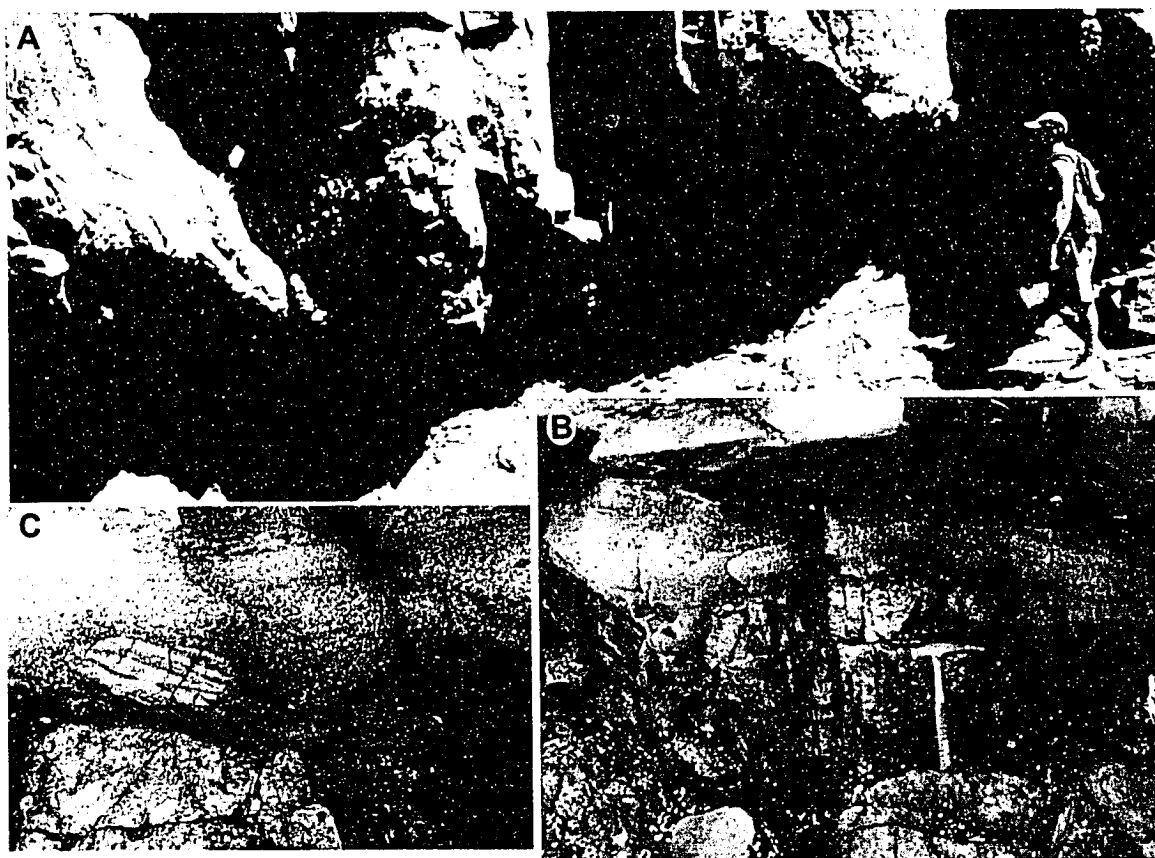
## CHAPTER 2: SEDIMENTOLOGY AND STRATIGRAPHY

### Facies Descriptions

The Upper Cretaceous sedimentary rocks of the study area are represented by 13 distinct lithofacies, ranging from cobble conglomerates to silty mudstones. Lithofacies descriptions are based on detailed analysis during 1:20,000-scale geologic mapping (see Backpocket Map), and 12 measured sections totalling more than 1300m measured at 1:100 scale (see Appendix A). Lithofacies are described by lithology, grain size, textural maturity, primary sedimentary bedding structures, fabrics, the presence or absence of body fossils, and trace fossils.

#### **Conglomerate facies:**

*Facies C1: Basal Conglomerate.* A pebble to boulder conglomerate is commonly deposited upon the basal unconformity (Figure 6). Clasts are dominantly well-rounded, although some are angular to subrounded. Clast lithologies reflect local basement lithologies, and may vary in their degree of weathering, juxtaposing well weathered clasts against relatively fresh-looking clasts. Clast size varies widely, ranging from pebbles to large boulders. The conglomerate is typically clast supported, with a coarse-grained, moderate- to well-sorted sandstone matrix. The matrix is generally volcanic litharenite (*cf.* Folk, 1974), and the local lithology and colour commonly reflect that of the framework

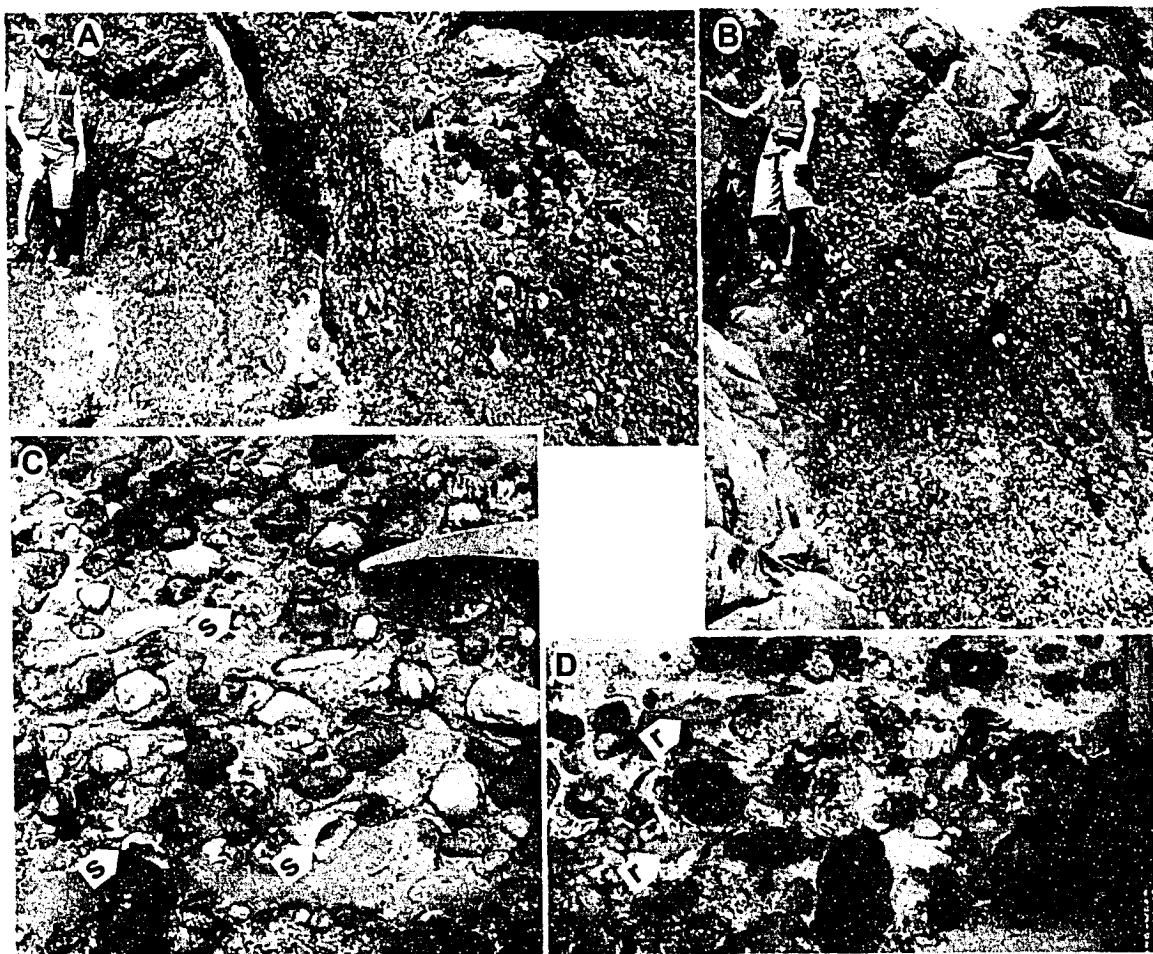


**Figure 6: Facies C1 Basal Conglomerate. A: Two-metre-thick basal conglomerate on Russell Island with large, subangular to rounded clasts of local basement rock entrained in well-sorted sandstone. B: Thin basal conglomerate on Moresby Island, with unsorted boulder- to pebble-sized basement clasts and parallel stratification in overlying sandstones. C: Moresby Island; note subangular local basement clasts adjacent to well rounded exotic clast. Rounded clast is approximately 25 cm long.**

clasts. The conglomerates vary in thickness from single clasts up to 4 metres thick, and commonly grade upwards into pebbly sandstones. Bedding is generally poorly defined, although some parallel stratification is apparent in sandy, matrix-rich portions, with laminations deformed around the larger clasts. Fossils in the conglomerates are limited to very rare, largely pulverised shell fragments entrained in the matrix. No trace fossils were identified.

*Facies C2: Conglomerate, sandy matrix.* Well-sorted, pebble to cobble conglomerates with a sandstone matrix occur in the Comox and Extension formations (Figure 7). Clasts are subrounded to rounded, range from large pebbles to large cobbles, and are poorly to well sorted. The conglomerate is clast supported and polymictic (see Chapter 4 for detailed clast compositions). Locally, clasts include large mudstone rip-up clasts, robust bivalve shells, and assorted shell fragments. The matrix comprises a well sorted, medium- to coarse-grained volcanic litharenite (*cf.* Folk, 1974). Conglomerates either form thick beds exceeding one metre with intercalated sandstone lenses (most common in Extension Formation), or medium to thick beds contained within thick pebbly sandstone packages (most common in Comox Formation). Thick beds have poorly defined top and basal contacts, with normal and reverse grading into pebbly sandstone, planar stratification, and crude clast imbrication. Medium-scale beds have erosive bases and commonly grade upwards, with bed thicknesses pinching and swelling laterally. Common thicknesses are between 30 and 150 centimetres in contiguous beds extending over 100 metres. Trough cross bedding and planar stratification are locally well developed. Carbonaceous detritus is also locally common, as are robust shell fragments, both dispersed and in stringers. No ichnofossils were identified in these conglomeratic units.

*Facies C3: Conglomerate, mixed matrix.* A poorly sorted pebble to cobble conglomerate with a mixed muddy sandstone matrix is locally deposited proximal to the basal unconformity of the Nanaimo Group (Figure 8). Clasts range from pebbles to cobbles with rare boulders, showing highly variable degrees of



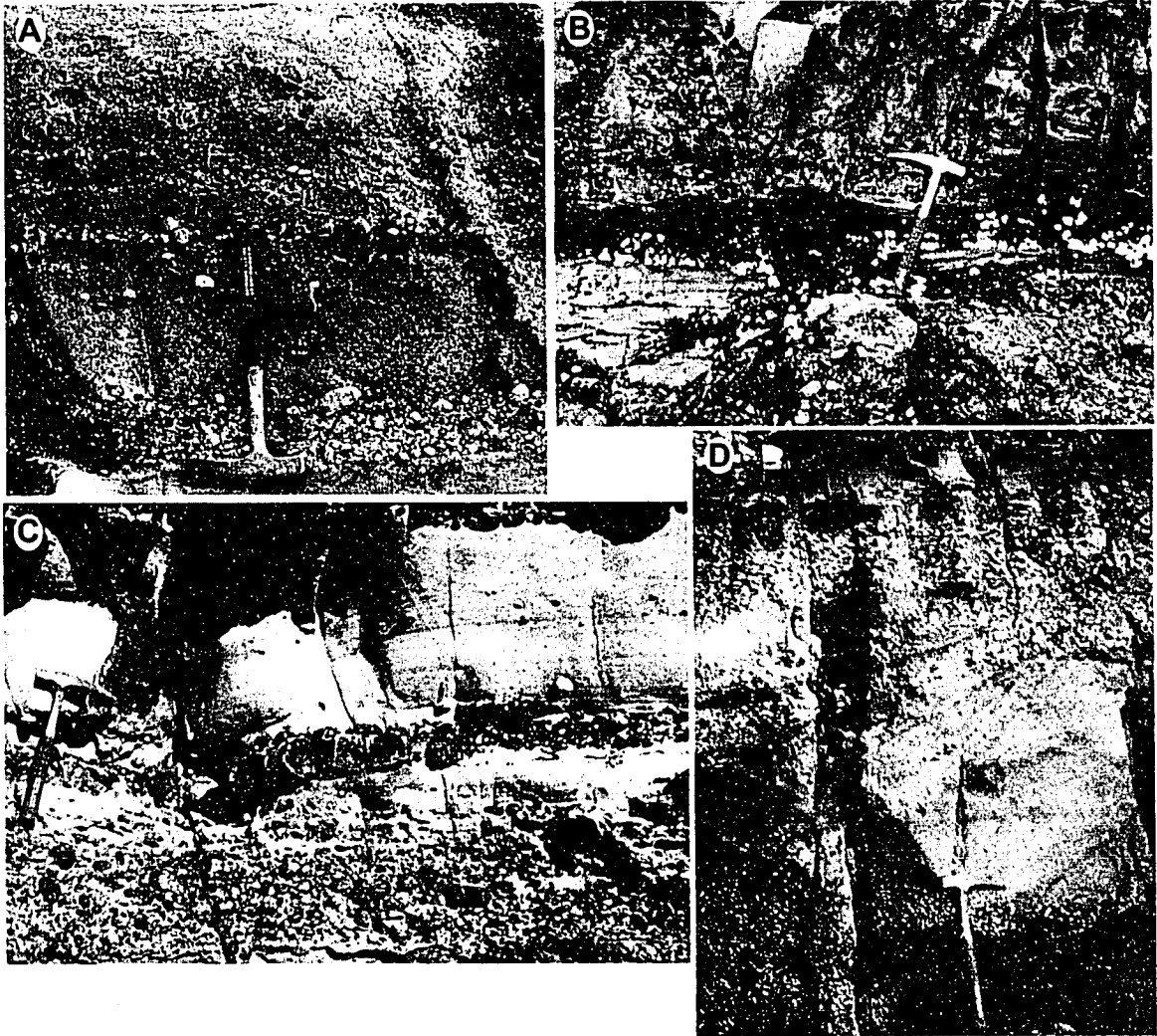
**Figure 7: Facies C2 Conglomerates.** A: Thick-bedded pebble conglomerate with sandy matrix on Piers Island. B: Single thick bed of the conglomerate between coarse-grained sandstone beds, Domville Island. C: Polymictic pebble conglomerate on Halibut Island includes robust bivalve shells as clasts (s), Piers Island. D: A different bed of the same unit featuring large, silty mudstone rip-up clasts (r).



**Figure 8: Facies C3 Conglomerates. A: Poorly sorted, medium-bedded pebble to boulder conglomerate on Moresby Island. Note unsorted muddy sandstone matrix. B: Same unit on Portland Island, where highly weathered clasts are juxtaposed with relatively fresh-looking clasts of same lithology C: Cross-bedding in pebbly, clast-poor bed of same unit, Moresby Island. D: Matrix-depleted bed displays a fabric approaching open-framework conglomerate, Moresby Island. E: Crude normal and reverse grading, Moresby Island.**

roundness, sphericity, and weathering. Clasts are generally monomictic and closely reflect local basement lithologies. The matrix is a moderately to poorly sorted mix of granule- to fine-grained sandstone and muddy siltstone. The sandstone matrix closely reflects the colour and lithology of the dominant local clasts, and is compositionally very immature. Crude grading is common, with some beds ranging from open-framework, clast-supported cobble conglomerate to matrix-supported "diamictite" over 30 to 100 centimetres. Where clast contents are high, lobe-shaped plugs of clasts fill erosional scours developed on underlying beds. Where clast contents are lower, beds are of medium thickness (10-30 cm), normally graded, and parallel stratified or locally tabular cross bedded. Thin carbonaceous siltstone drapes are locally present. Body fossils are limited to a single location containing bivalve shell fragments. No definitive ichnofossils were identified. Small clastic dykes, dewatering and larger fluid escape structures (*cf.* Postma, 1983), and slump structures commonly disrupt bedding.

*Facies P1: Pebbly sandstone.* Matrix-supported pebble conglomerates to pebbly sandstones are present in all formations excepting the Haslam, commonly as a transitional unit between lower conglomeratic facies and overlying sandstones (Figure 9). Pebbly sandstones are moderately sorted but bimodal, with well-rounded pebble clasts, rarely up to cobble size. Sandstone compositions range from volcanic litharenite to feldspathic litharenite (*cf.* Folk, 1974), and commonly reflect the lithology of local basement (or lower conglomerates where the conglomerates are polymictic). Pebbles are commonly



**Figure 9: Facies P1 Pebbly Sandstones. A: Pebbly, coarse-grained sandstone with pebbles dispersed and in stringers, Sidney Island. B: Trough cross-bedded pebbly sandstone on top of a thick pebble conglomerate lens, Domville Island. C: Pebbly sandstone grades out of pebble conglomerates and shows planar parallel stratification, Mandarte Island. D: Pebbly sandstone overlying better sorted sandstone. Note trough-shaped erosive base of pebbly unit with pebble lag, Russell Island.**

dispersed or concentrated in stringers or as lags. Moderately sorted sandstone matrix varies from medium-grained to granular, and is modally coarse-grained. Some carbonaceous detritus, coal fragments, and muddy rip-up clasts are locally present. Beds range from 10 to 30 centimetres thick, with erosive bases and

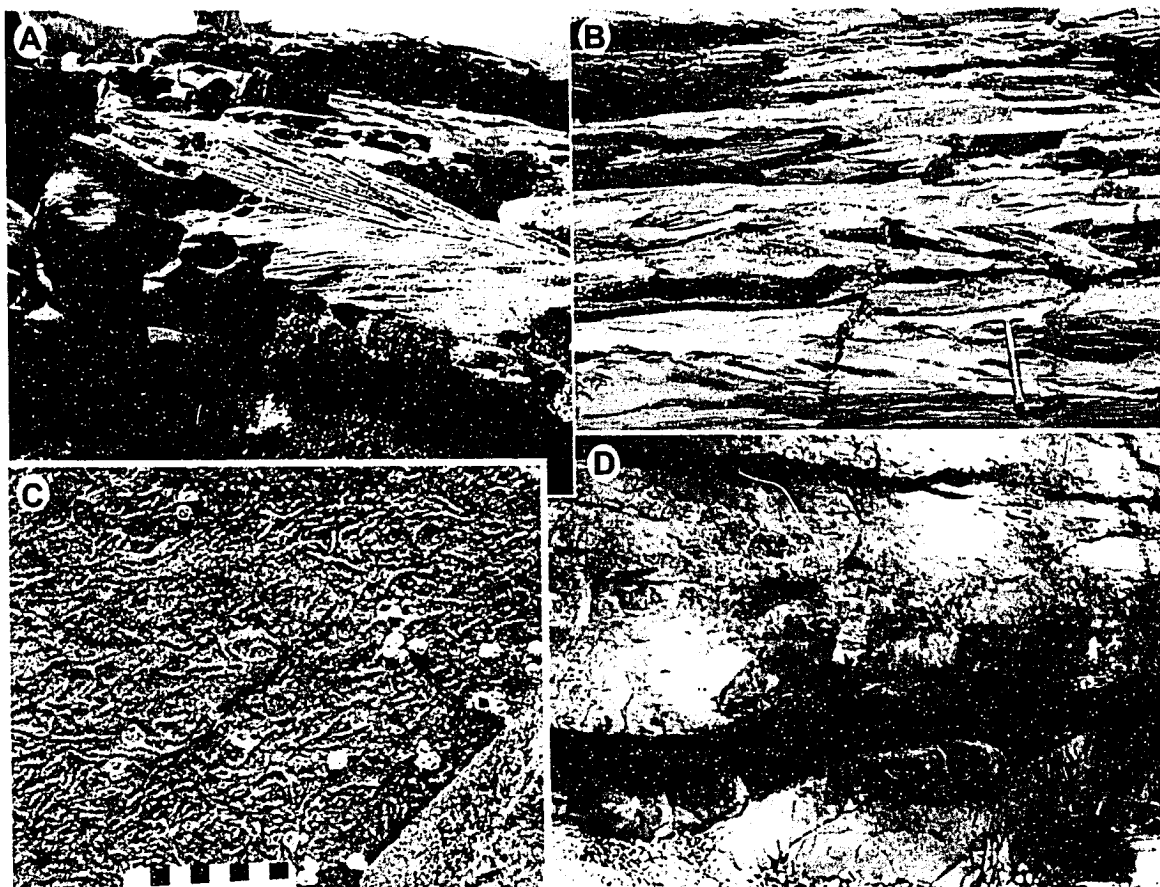


local thin, hematite-stained siltstone drapes. Bedding is dominated by planar parallel stratification or is apparently massive, with rare, local trough cross-beds typically associated with coarser-grained sections. Body fossils are limited to uncommon shell fragments, generally robust bivalve shells, with rare gastropod and cephalopod material. Fossils are dispersed, with some concordant stringers of bivalve shells, commonly aligned in a convex-upward arrangement.

Ichnofossils are sporadically distributed with a bioturbation index (BI) of 0 to 1 (see Table 1). Ichnogenera identified include *Ophiomorpha*, *Schaubcylindrichnus*, and *Palaeophycus*.

### **Sandstone Facies**

*Facies S1: Coarse-Grained Sandstone.* Coarse-grained sandstone is common throughout the middle and upper parts of the Comox Formation (Figure 10). These sandstones are moderately sorted, with grain sizes generally ranging from upper medium to lower very coarse; modal grain size is lower coarse. Lithology is generally feldspathic litharenite (*cf.* Folk, 1974). Dispersed, solitary, well-rounded pebbles and thin granule lags are common. Pebble lags and silty fine-grained sandstone drapes are rare. Beds are generally sharp-based, and of thin to medium thicknesses (5 -30 cm), typically erosionally amalgamated into 60-100 cm-thick bedsets. Bedding is dominated by low-angle planar to low angle undulatory parallel stratification with swale-shaped bases, interpreted to represent swaley cross-stratification (SCS). Planar parallel stratification and trough cross bedding are locally developed, commonly associated with coarser-



**Figure 10: Facies S1 Coarse-Grained Sandstones. A:** Coarse-grained sandstone with low angle parallel stratification (swaley cross stratification), Coal Point, Saanich Peninsula. **B:** Coarse-grained sandstone showing trough cross-bedding and planar parallel stratification, Reynard Point, Moresby Island. **C:** *Macaronichnus segregatis* well preserved in lower coarse-grained sandstones, Moresby Island. **D:** Facies S1 coarse-grained sandstones deposited directly on the basal unconformity, with no basal conglomerate present. Basement rocks are smoothly polished at unconformity. Overlying sandstone is parallel stratified and undulations likely resulted from differential compaction.

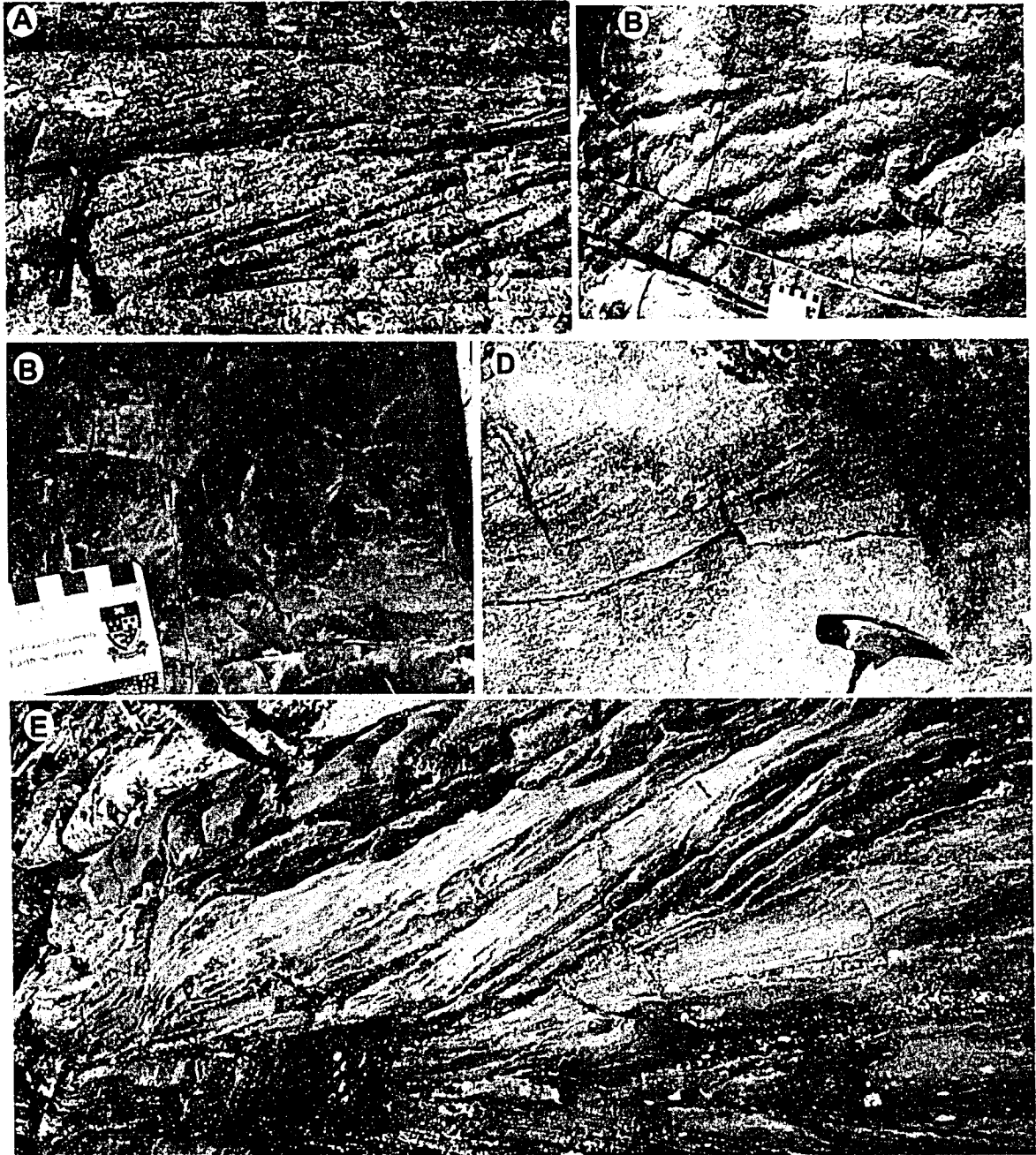
grained lags. Rare, robust bivalve fragments are individually dispersed or concentrated as thin lags, and are commonly oriented with convex surfaces upwards. Bioturbation is rare and sporadically distributed (BI 0-1), although *Ophiomorpha* is well represented in most locations. Locally, mono-generic assemblages of *Macaronichnus* (*M. segregatis* and *M. isp.*) are very well preserved.

*Facies S2: Medium-grained Sandstone.* Moderately sorted, upper medium-grained sandstones are common throughout the study area (Figure 11). These sandstones are predominantly feldspathic litharenites (*cf.* Folk, 1974), tan to medium grey in colour, and range from medium- to lower coarse- grained (modally upper medium-grained). Solitary dispersed pebbles and very thin granule stringers are locally common, as are silty mudstone rip-up clasts, very thin silty drapes, and carbonaceous detritus. Pebbly lags and organic muddy interlaminae are rare. Bed thicknesses range from medium to thick, and beds are locally amalgamated into bedsets several metres thick. Parallel stratification, planar cross beds or apparently massive beds are most common. Low-angle parallel stratification is locally common, with sharp, swale-shaped bases and some convex-upwards lamination, interpreted to represent swaley cross-stratification (SCS) and hummocky cross stratification (HCS). Graded beds, symmetrical ripples, and loading structures are locally present. Robust shell fragments are rarely dispersed, and commonly concentrated into coquina-like lags or stringers up to 10 centimetres thick. Bioturbation is of low intensity (BI 1-2) and sporadically distributed. *Ophiomorpha*, *Planolites*, *Palaeophycus*, *Schaubcylichnus freyi*, *Diplocraterion*, *Thalassinoides*, and *Macaronichnus* are present, representing a low-diversity expression of the *Skolithos* Ichnofacies.

*Facies S3: Cross-Bedded Sandstone.* Cross-bedded, upper medium-to lower coarse-grained sandstone is most common in the Comox Formation (Figure 12), although it is also present in the upper Extension Formation. The sandstone is well sorted, with rare fine-grained partings. Lithology is modally



Figure 11: Facies S2 Medium-Grained Sandstones. A: Upper medium-grained sandstone, displaying a succession from with low-angle parallel stratification (SCS), into convex upwards parallel stratification (HCS), a thin bioturbated bed (BI 2), and an apparently massive thicker bed at top, Swartz Head, Saanich Peninsula. B: Apparently massive, medium-grained sandstone displays low-angle parallel lamination where lightly weathered (right). Note burrowed contact with lower mudstones at base of bed, Forrest Island; C: Combined-flow ripples in medium-grained sandstone containing some coarse-grained lags, faint *Macaronichnus* isp. (m) and dispersed very small pebbles, Pellow Islets. D: Medium-bedded, upper medium-grained sandstone. Very thin carbonaceous laminae mark faint trough-cross bedding, with most beds parallel stratified or apparently massive. Very sparsely distributed *Ophiomorpha* (o) present, Forrest Island. E: Hummocky cross-stratified, upper medium-grained sandstone, western Saanich Peninsula.

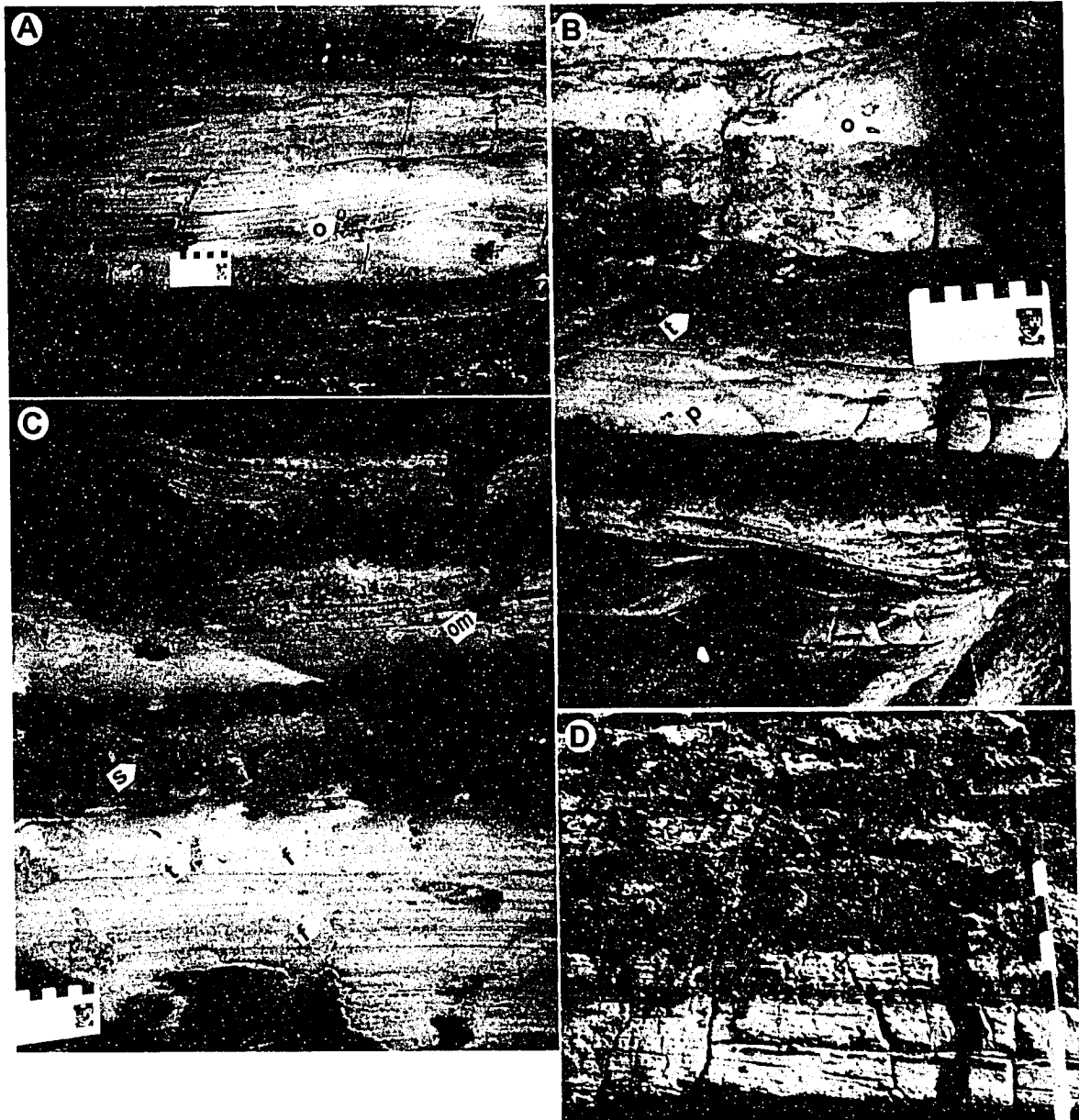


**Figure 12: Facies S3 Cross-Bedded Sandstones. A: Tabular cross beds at medium scale, well expressed in well-weathered, medium-grained sandstone, Fernie Island. B: Current ripples exposed on upper surface of medium-thickness trough cross-bedded sandstones, near Coal Point, Saanich Peninsula; C: Bedding plane of cross-bedded sandstone with abundant deciduous leaf impressions, Brethour Island; D: Trough cross beds overlying apparently massive bed of medium-grained sandstone with thin carbonaceous partings, near Coal Point, Saanich Peninsula; E: Large-scale trough cross-beds and low-angle parallel stratification in moderately sorted, lower coarse-grained sandstones, western Saanich Peninsula.**

feldspathic litharenite (*cf.* Folk, 1974). Medium-thickness beds are trough cross-stratified, with some planar cross-stratification or low-angle parallel stratification. Current ripples occur locally. No body fossils or ichnofossils are identified in this facies, although localized carbonaceous detritus include leaf impressions and coal fragments up to 5 centimetres long.

*Facies S4: Bioturbated Sandstone.* Bioturbated sandstones are common in the upper parts of Comox Formation (Figure 13). These sandstones are moderately to well sorted, medium to lower coarse-grained, tan to medium grey feldspathic litharenites (*cf.* Folk, 1974). Some small, dispersed pebbles or thin lags are present, as are thin siltstone or mudstone interlaminae and carbonaceous detritus. Two distinct bedding types are repeated over 1- to 10-metre thick cycles. Parallel stratified sands with swale-shaped bases and common upward-convex parallel lamination are widespread, and are interpreted to represent hummocky cross-stratification (HCS) and swaley cross-stratification (SCS). These HSC/SCS beds range in thickness from 10 to 100 centimetres, erosionally amalgamated into bedsets up to 7 metres thick. The second bedding form comprises apparently massive sandstones up to 1 m thick, with only intermittent and faint parallel laminations. Dark grey mottling is apparent on weathered surfaces. These mottled beds are interpreted to represent intervals where bioturbation has almost completely destroyed original bedding.

*Ophiomorpha*, *Palaeophycus*, and *Thalassinoides* occur in the stratified bedsets, where bioturbation is low intensity (BI 0-1), whereas the apparently high-intensity zones (BI 5-6) generally lack identifiable ichnogenera. Molluscan shell fragments



**Figure 13: Facies S4 Bioturbated Sandstone.** A: Alternating high- and low-intensity bioturbation with well stratified SCS sandstone. Note the solitary *Ophiomorpha* (o) where bioturbation is sparse, Coal Island; B: Alternating parallel laminated and bioturbated sandstone. Note abundant *Ophiomorpha* (o), *Palaeophycus* (p), *Thalassinoides* (t), and carbonaceous content of highly bioturbated beds. C: Similar alternating laminated and bioturbated sandstone units with large *Ophiomorpha* containing meniscae (om), *Teichichnus* (t), *Skolithos* (s), and fugichnia (f), Mandarte Island. D: Similar unit, where alternating beds are thicker, and surface is weathered, showing strong contrast between laminated and bioturbated sandstones (divisions on scale bar are 10cm each), Sidney Lagoon.

are commonly dispersed in sandstones, and rarely form coquina-like lags or lenses within beds.

### **Muddy Facies**

*Facies M1: Bioturbated Muddy Sandstone.* These muddy sandstones have abundant bioturbation, commonly disrupting primary sedimentary structures (Figure 14). Units are moderately sorted, with grain sizes ranging from lower medium-grained sand to silty mud, and are mottled grey in colour. Mudstones and sandstones are interbedded, with beds up to 10 cm thick. Sandstone beds display thick parallel laminations, and abundant interstitial clay and silt. Overall, however, laminations and interbeds are poorly defined, as beds are amalgamated and disrupted by moderate to high degrees of bioturbation (BI 2-4), as well as loading and dewatering structures. Ichnogenera include *Ophiomorpha*, *Planolites*, *Palaeophycus*, *Zoophycos*, *Skolithos*, *Teichichnus*, *Chondrites*, and *Helminthopsis*, possibly representing a proximal expression of the *Cruziana* Ichnofacies. Carbonaceous and woody detritus are locally common, as are bivalve and gastropod shells and dispersed shell fragments.

*Facies M2: Carbonaceous shale.* Dark-coloured silty shales are common in the upper Comox Formation (Figure 15). These shales are dark grey to black, weathering to a hematite-stained, lighter tan-grey, especially where sandy. Mudstones are very silt rich, locally with thin, fine- to medium-grained sandstone interbeds. Parallel stratification at the very thin bed to lamination scale is generally poorly expressed, as the unit is commonly sheared or displays



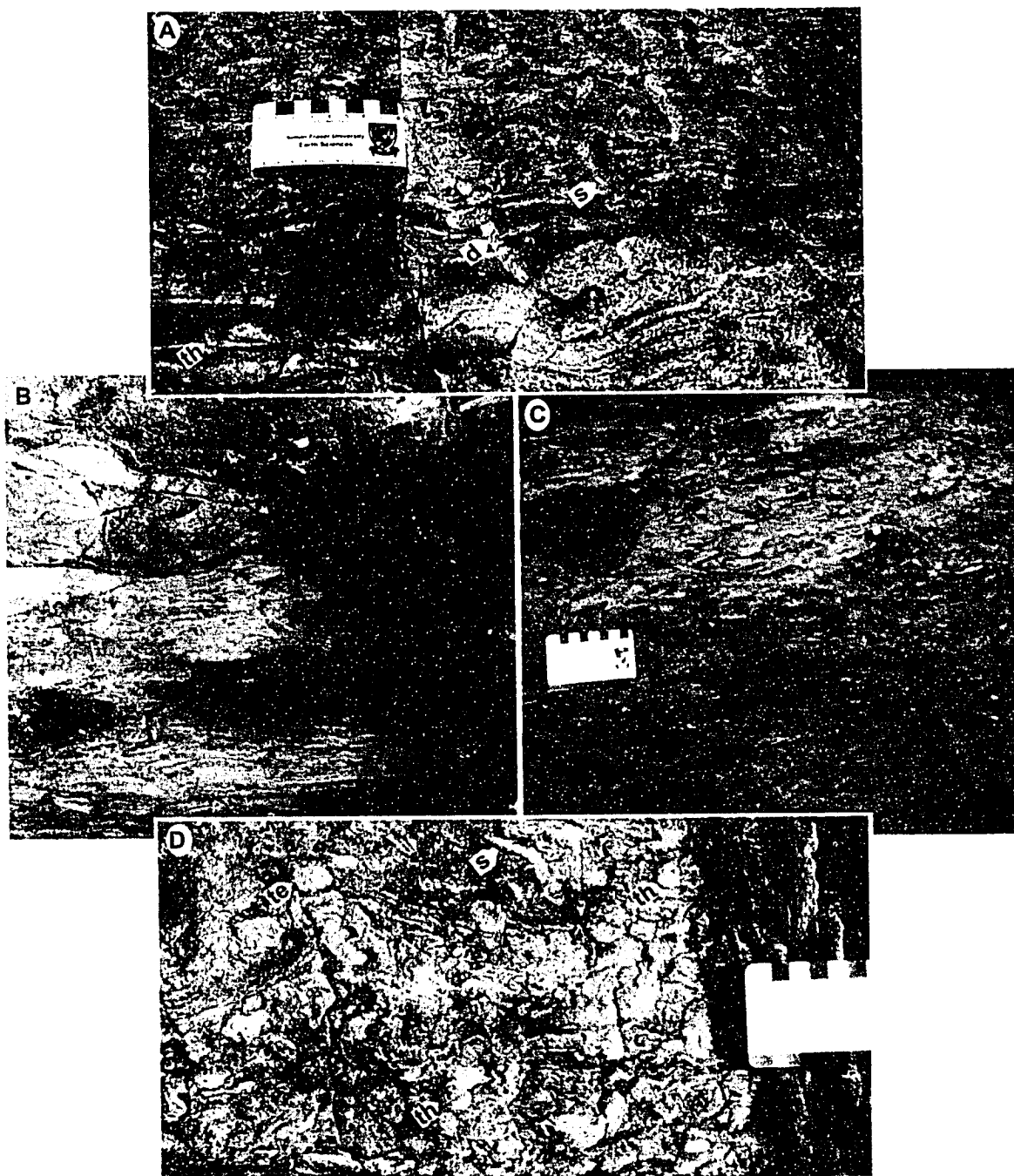


Figure 14: Facies M1 Bioturbated Muddy Sandstone. A: Laminated sandstones and silty mudstones, pervasively bioturbated (BI 4-5). Ichnogenera include vertical structures (*Diplo craterion* [d], *Skolithos* [s]) and horizontal structures (*Teichichnus* [te], *Thalassinoides* [th]). Coal Point, Saanich Peninsula; B: Similar unit, with BI 3, more preserved laminations, lower abundance of same ichnogenera, large carbonaceous fragments, and loaded contact with overlying massive sandstone. Comet Island; C: Unit showing BI 5. Small concretions at top are small, lined burrows of *Ophiomorpha*. Russell Island; D: Unit on Comet Island with BI ~5 and the similar ichnogenera as "A".



**Figure 15: Facies M2 Carbonaceous Shale.** A: Typical appearance of carbonaceous shale facies, with bedding completely disrupted by spheroidal weathering and hematite-stained weathered surfaces, Gooch Island; B: Large exposure of carbonaceous shales with bedding almost completely disrupted. Pale-coloured lenses are sandy concretions, likely boudinaged remains of thin interbeds. Brethour Island; C: Root-like coal fragments dispersed in sandy shale with possible *Teredolites* (t), Forrest Island; D: At the same location as "B", numerous logs and root mounds are located in apparent life position (parallel to one another and normal to bedding), Brethour Island; E: Very carbonaceous shale, with large burrows (*Thalassinoides*) passively filled by coarse sands from unit above, representing the *Glossifungites* Ichnofacies. Tsehum Harbour, Saanich Peninsula.

spheroidal weathering. Bedding structures are also disrupted by apparent dewatering and loading structures, locally abundant bioturbation, and local *in situ* rootlets. Current ripples and parallel lamination are present locally. Bioturbation varies from completely absent (BI 0) to medium-intensity (BI 2-3), with localized burrows subtending from coarser-grained overlying units. Ichnogenera include *Ophiomorpha*, *Thalassinoides*, *Diplocraterion*, *Teichichnus*, and *Skolithos*. Carbonaceous detritus ranging from thin films to large woody debris and logs (commonly burrowed with *Teredolites*), or thin coal beds (up to 20 cm) are locally common.

### **Heterolithic Facies**

*Facies H1: Intercalated Mudstone-Sandstone.* Interbedded sandstone and mudstone intervals are common throughout the Comox Formation (Figure 16). The sandstone interbeds are 10-50 cm thick, well sorted, medium-grained, and rarely fining upwards. The intercalated mudstones are dark, silty, and commonly very carbonaceous, and rarely exceed 5 cm thick. Bedding thicknesses are thin to medium-scale, and show planar parallel stratification or undulatory parallel stratification. Trough cross-bedding and ripple cross-lamination are locally developed, including rare combined flow ripples. Bioturbation is of low to moderate intensity (BI 1-3), with *Ophiomorpha*, *Thalassinoides*, *Diplocraterion*, and *Palaeophycus* extending between beds, and rare local *Chondrites* and *Cylindrichnus*. Fossil shell fragments and woody debris are rare and widely dispersed throughout the facies.

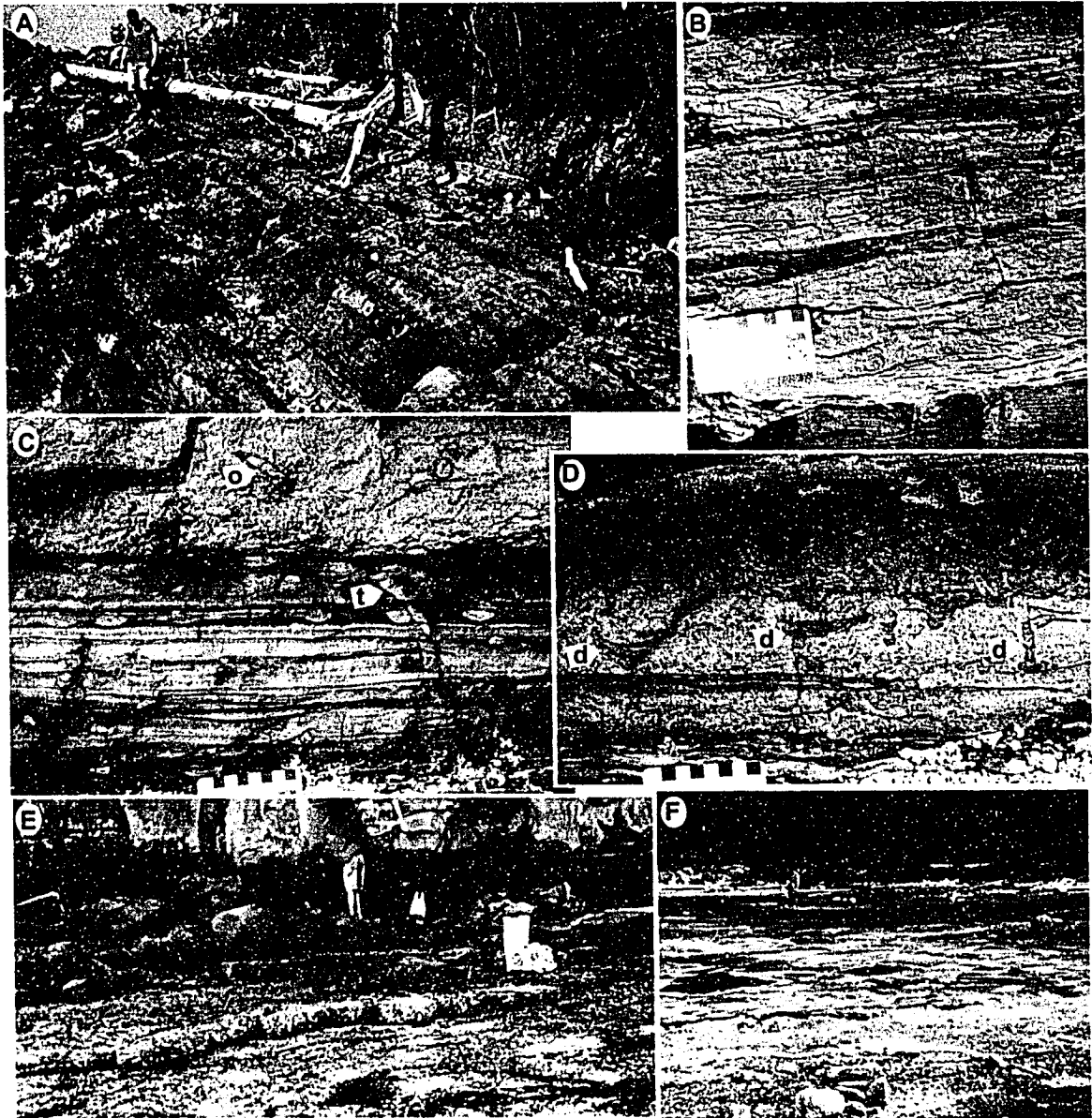
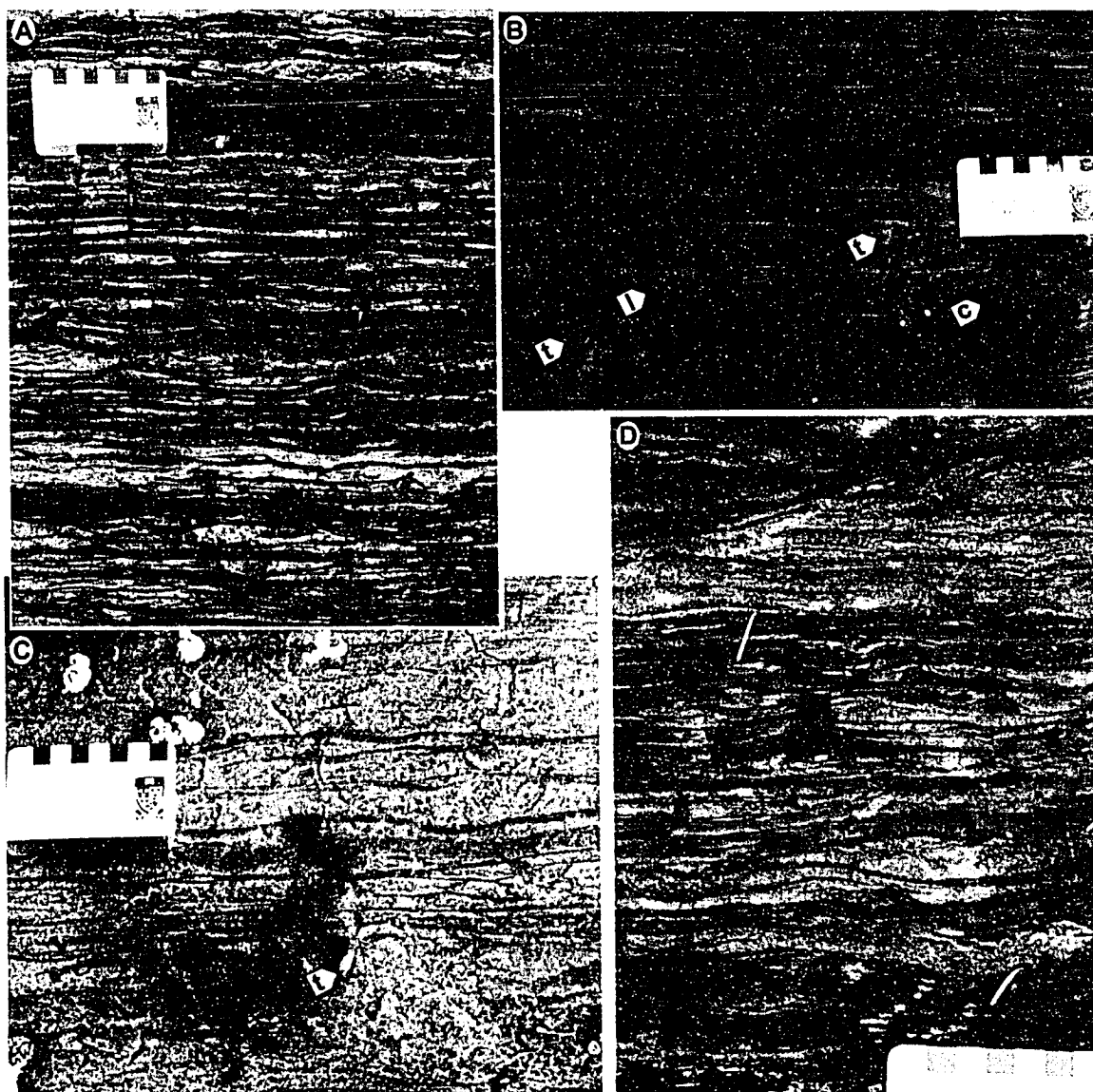


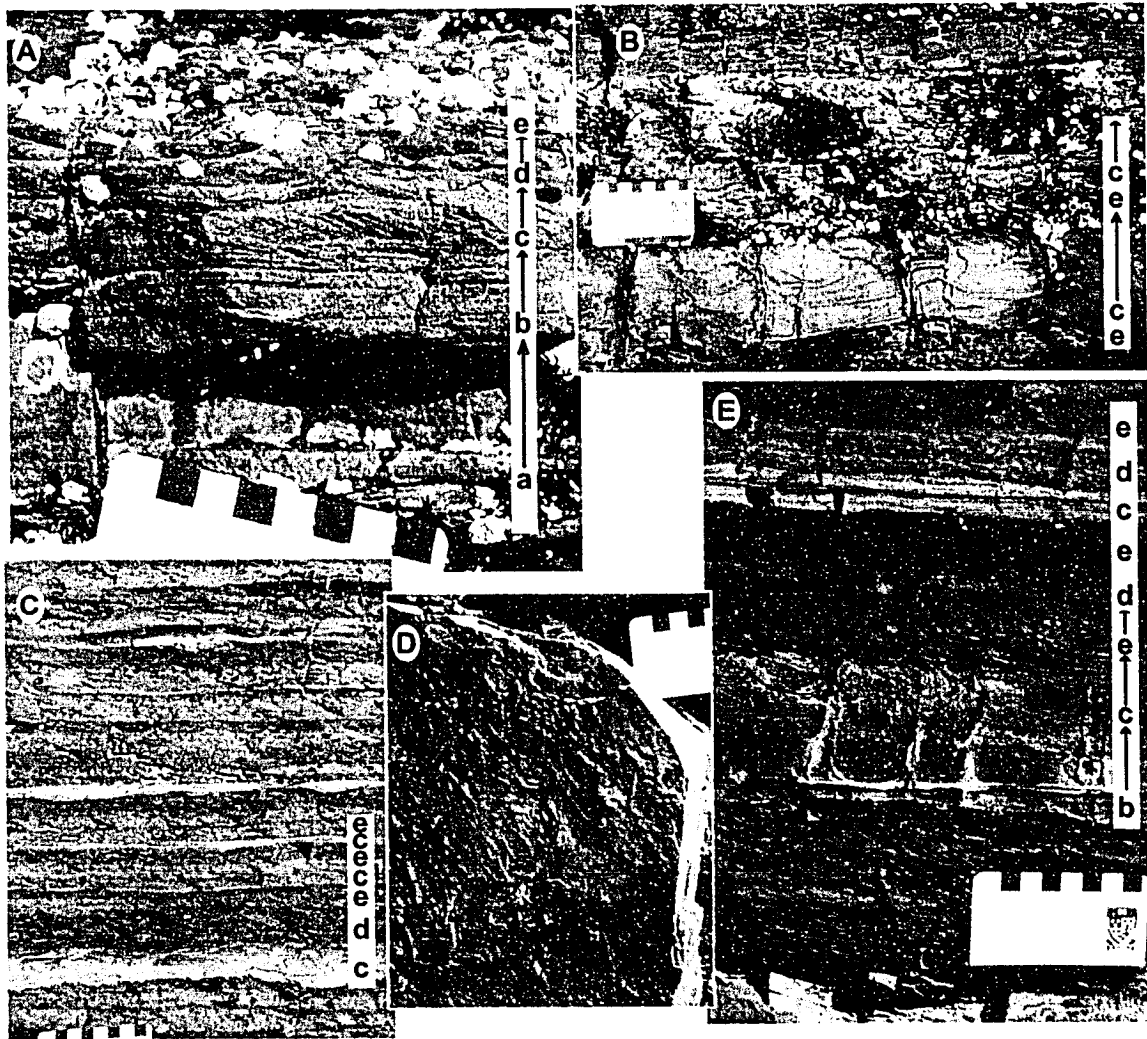
Figure 16: Facies H1 Intercalated Mudstone-Sandstone. A: Steep-dipping exposure of intercalated sandstones and mudstones, Moses Point, Saanich Peninsula. B: Interbedded sandstones and mudstones, with an overall fining-upward succession and lacking graded beds. Combined-flow ripples and parallel lamination in sandstones, Forrest Island; C: Repeated fining-upward heterolithic successions ranging from sandstone dominated to mudstone dominated. Mudstone at base is carbonaceous. The expression of burrows changes from *Thalassinoides* (t) in mudstone substrates to *Ophiomorpha* (o) in sandstones, Brackman Island; D: Similar units with a largely mono-specific assemblage of *Diplocraterion* (d), locally truncated by coarser-grained cross-bedded sandstone above. Goudge Island; E: Flat-lying Facies H1 recessive mudstones and resistant sandstone interbeds (foreground). Unit becomes muddier and more carbonaceous below erosive, loaded contact with overlying massive sandstones. Arbutus Point, Portland Island; F: Similar, flat-lying exposure on Moresby Island.



**Figure 17: Facies H2 Heterolithic Sandstone-Mudstone. A: Wavy bedding, with medium-grained sandstone and silty mudstone beds (BI 0-1), Coal Island; B: Lenticular bedding, comprising silty mudstone with few preserved current ripple cross laminated sandstones and some parallel lamination. Sparse bioturbation includes *Thalassinoides* (t), *Chondrites* (c) and possible *Lockeia* (l). Forrest Island; C: Flaser to wavy bedding, *Thalassinoides* (t) at the base. Forrest Island; D: Wavy to lenticular bedding with upper medium-grained sandstone, Brethour Island.**

Facies H2: Heterolithic Sandstone-Mudstone. At several locations within the Comox Formation, interbeds of mudstone and sandstone display distinct lenticular, wavy, and flaser bedding (Figure 17). The tan grey sandstone interbeds are well sorted, medium to upper fine-grained, very thin to thin bedded, and current ripple laminated. Interstitial mudstones are darker coloured and silty. Bedding is generally well preserved, and typically comprises subequal proportions of continuous sandstone and mudstone beds (wavy bedding), although units locally grade to lenticular or flaser bedding. Coarsening- or fining-upward successions over several metres are common. Bioturbation is of low intensity (BI 1-2) with *Diplocraterion*, *Teichichnus*, *Planolites*, *Skolithos*, and *Taenidium*. No body fossils or carbonaceous detritus were observed in these beds.

Facies H3: Graded Couplets. The Haslam Formation is dominated by graded sandstone-mudstone couplets (Figure 18). Sandstone beds are contiguous over 10s to 100s of metres with sharp erosive bases, are invariably normally graded, and range in thickness from very thin (where sandstones are lower fine-grained), to thick (up to 50 cm thick where sandstones are coarse-grained). These beds grade upward into dark silty mudstone beds. The unit ranges from 80% sandstone to 80% silty mudstone, commonly over 5-20 metre intervals. Bedforms follow typical waning-flow patterns from massive sandstone through parallel laminated, current ripple and convolute laminated sandstones, capped by parallel laminated sandy siltstones, and draped by silty mudstones. Parting lineation, tool marks, loading and dewatering structures are locally



**Figure 18: Facies H3 Graded Sandstone-Mudstone couplets. A:** Sandstone-mudstone couplet, reflecting waning flow conditions, grading from massive sandstone ("Bouma"  $T_A$ ) through upper plane bed laminated ( $T_B$ ), current ripple cross-laminated sandstones ( $T_C$ ), and planar laminated silty mudstone ( $T_D$ ). Swartz Bay, Saanich Peninsula; **B:** Couplet of similar scale, although  $T_C$  unit is convolute bedded, Knapp Island; **C:** Thin, discontinuous  $T_C$  sandstones within  $T_D$  and  $T_E$  siltstones and mudstones, north tip of Saanich Peninsula; **D:** Bottom surface of  $T_B$  sandstone bed within  $T_{BCD}$  couplets display groove and load casts. Pym Island; **E:** Thick  $T_{BCE}$  with convolute beds overlain by several  $T_{DE}$  beds, and a very thin  $T_{CDE}$  bed. Piers Island.

present. Body fossils are limited to rare single shells or fragments. Bioturbation is generally of low intensity (BI 1), with few distinct ichnogenera. Recognizable traces include *Scolicia*, *Chondrites*, rare *Thalassinoides*, and *Zoophycos*. All ichnogenera are diminutive, and there is a distinct paucity of vertical structures.

## **Substrate-Controlled Ichnofacies.**

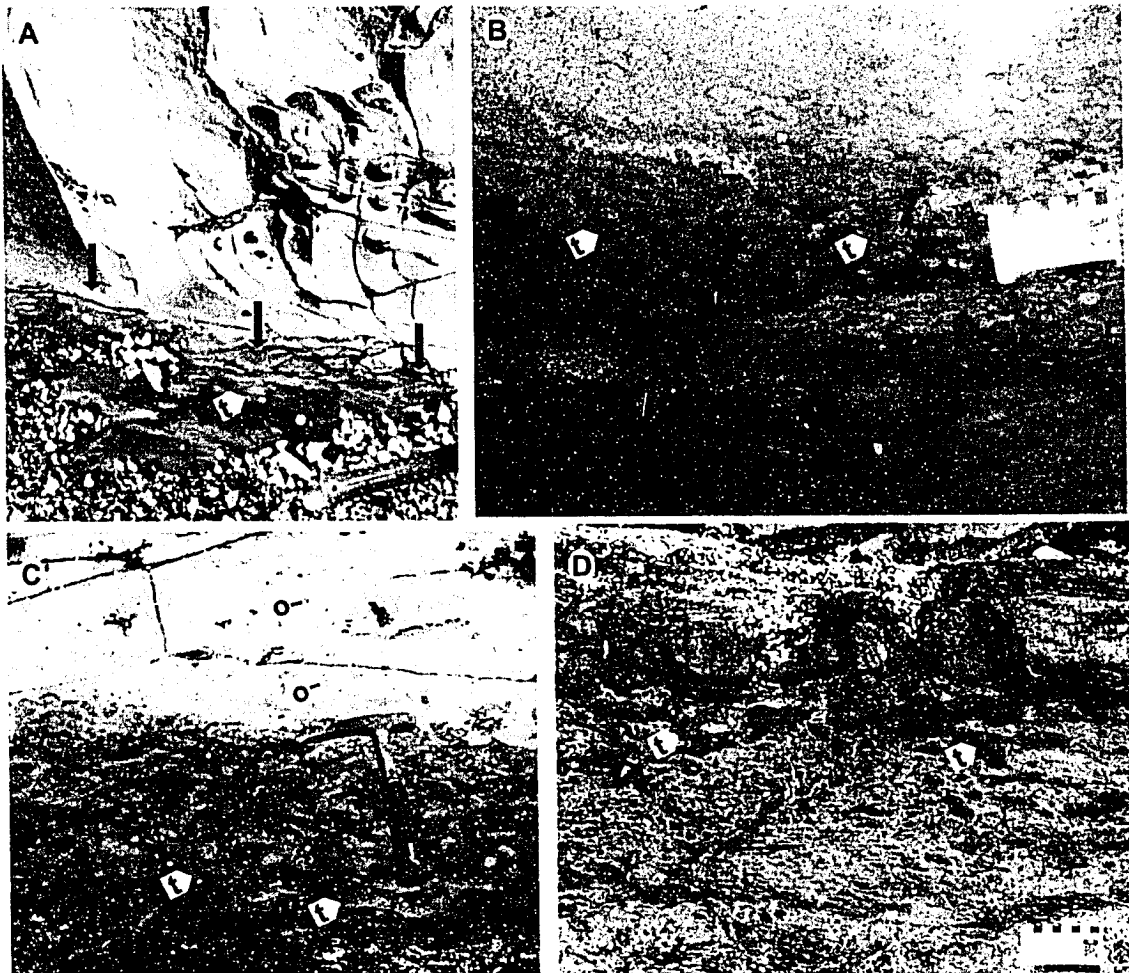
The study area includes several examples of the substrate-specific ichnofacies. Substrate types including stiffground, firmground, and woodground (*cf.* Pemberton *et al.*, 1992; 2004) are present, with complex ichnofacies relationships between them and the adjacent softgrounds.

The *Glossifungites* Ichnofacies is normally defined by predominately vertical to subvertical, sharp-walled and unlined dwelling burrows in a firm (typically compacted, dewatered mud) substrate. Dwelling structures are commonly passively infilled with contrasting sediment. Burrows are typically abundant, with a low diversity of large dwelling structures (*e.g.*, Pemberton and Frey, 1985). The conditions for stability of large, unlined burrow systems are only met by partially dewatered and compacted shales. Uncompacted shales will tend to flow and slump, leading to burrow collapse and precluding robust vertical dwellings. The *Glossifungites* Ichnofacies may be interpreted to reflect a shallowly buried and partially exhumed substrate, and therefore represent a stratigraphic break (MacEachern *et al.*, 1992; Pemberton and MacEachern, 1995; Pemberton *et al.*, 2004), although there are additional processes other than burial-exhumation which may cause a muddy substrate to become firm. The degree of "firmness" required for a substrate to host the *Glossifungites* Ichnofacies varies from nearly lithified firmgrounds to cohesive stiffgrounds. In the latter case, significant post-boring deformation may compact or otherwise modify the burrows (Gingras *et al.*, 2000).



The *Teredolites* Ichnofacies is defined by borings excavated into wood or highly carbonaceous substrates, passively filled by overlying sediments (Bromley *et al.*, 1984). The namesake ichnogenus *Teredolites* are clustered, cylindrical or pouch-shaped borings made by marine bivalves. It is important to differentiate *in situ* plants (stumps, roots) and xylic substrates from accumulations of allochthonous wood material, as it may be impossible to recognize where or when the wood was bored (Savrda, 1991; Savrda *et al.*, 1993). The *Teredolites* Ichnofacies should only be applied to continuous xylic substrates reflecting an environment conducive to original boring. (Pemberton *et al.*, 2004; Gingras *et al.*, 2004).

*Glossifungites* Ichnofacies are encountered at several locations within the study area, generally within silty mudstones of Facies M2 where it is overlain by sandstones of Facies S2 or S3 (Figure 19). The traces are predominantly firmground *Thalassinoides* that extend downwards as much as 30 cm from the mudstone/sandstone facies contact. The nature of that contact varies, at some localities, the contact is sharp and (less commonly) passes laterally into sharp, unburrowed contacts, suggesting a stratigraphic break concurrent with the *Glossifungites* Ichnofacies-demarcated discontinuity (Figure 19a). More commonly, the contact between mudstone facies featuring the firmground suites and the overlying sandstone is diffuse (Figure 19b, c). In these occurrences, the *Glossifungites* Ichnofacies is dominated by firmground *Thalassinoides*, and the overlying softground suite features *Ophiomorpha*. Although the firmground



**Figure 19: *Glossifungites* ichnofacies-delineated discontinuities. A: passively infilled *Thalassinoides* (t) in upper 30 cm of Facies M2 mudstones, erosively overlain by Facies S2 coarse-grained sandstones (arrows at contact), Forrest Island; B: Diffuse contact with firmground *Thalassinoides* (t), passively filled by overlying sandstone Forrest Island; C: *Glossifungites* ichnofacies-delineated discontinuity. Exposed surface is close to bedding plane orientation, exaggerating the diffuseness of the contact. *Ophiomorpha* (o) in upper unit reflect softground burrowing, and are similar in size and orientation to the firmground *Thalassinoides* (t) in the lower unit. Moresby Island. D: Very large *Thalassinoides* (t) in carbonaceous mudstone substrate are passively filled by coarse sandstone from relatively thin overlying sandstone lens. This contact is within an intertonguing sandstone-mudstone sequence. Tsehum Harbour, Saanich Peninsula.**

substrate is commonly much more pervasively burrowed than the overlying softground, in some instances the firmground *Thalassinoides* appear to pass upward into softground *Ophiomorpha*. Finally, *Glossifungites* Ichnofacies-

demarcated discontinuities exist between tongues at some intertonguing contacts (Figure 19d).

*In situ Teredolites*-bored wood and xylic substrates within the study area are commonly related along strike with *Glossifungites* Ichnofacies-demarcated discontinuities, a scenario identified in the modern by Gingras *et al.* (2004). In several locations, root mounds and tree stems bored with *Teredolites* occur in apparent life position, rooted within a mudstone substrate. The muddy substrate itself displays firmground *Thalassinoides* passively infilled with overlying coarse-grained sandstone, interpreted to represent the *Glossifungites* Ichnofacies (Figure 20a,b). Although the substrate was firm enough to support large-diameter unlined burrows, post-depositional deformation of the underlying unit is locally present (suggesting stiffground as opposed to firmground conditions). In other locations, a burrowed muddy substrate is highly carbonaceous, blurring the distinction between a firmground and a truly xylic substrate (Figure 20c). This distinction is further complicated by lateral transitions in substrate consistency from sharp softground contacts to firmground contacts and into xylic contacts. Classification of suites consisting of passively infilled *Thalassinoides* or *Gastrochaenolites* strictly to *Glossifungites* Ichnofacies versus *Teredolites* Ichnofacies is problematic, as the ichnogenera may occur in both, and differentiation relies on the determination of the xylic nature of the substrate, a difficult parameter to quantify in peaty substrates.

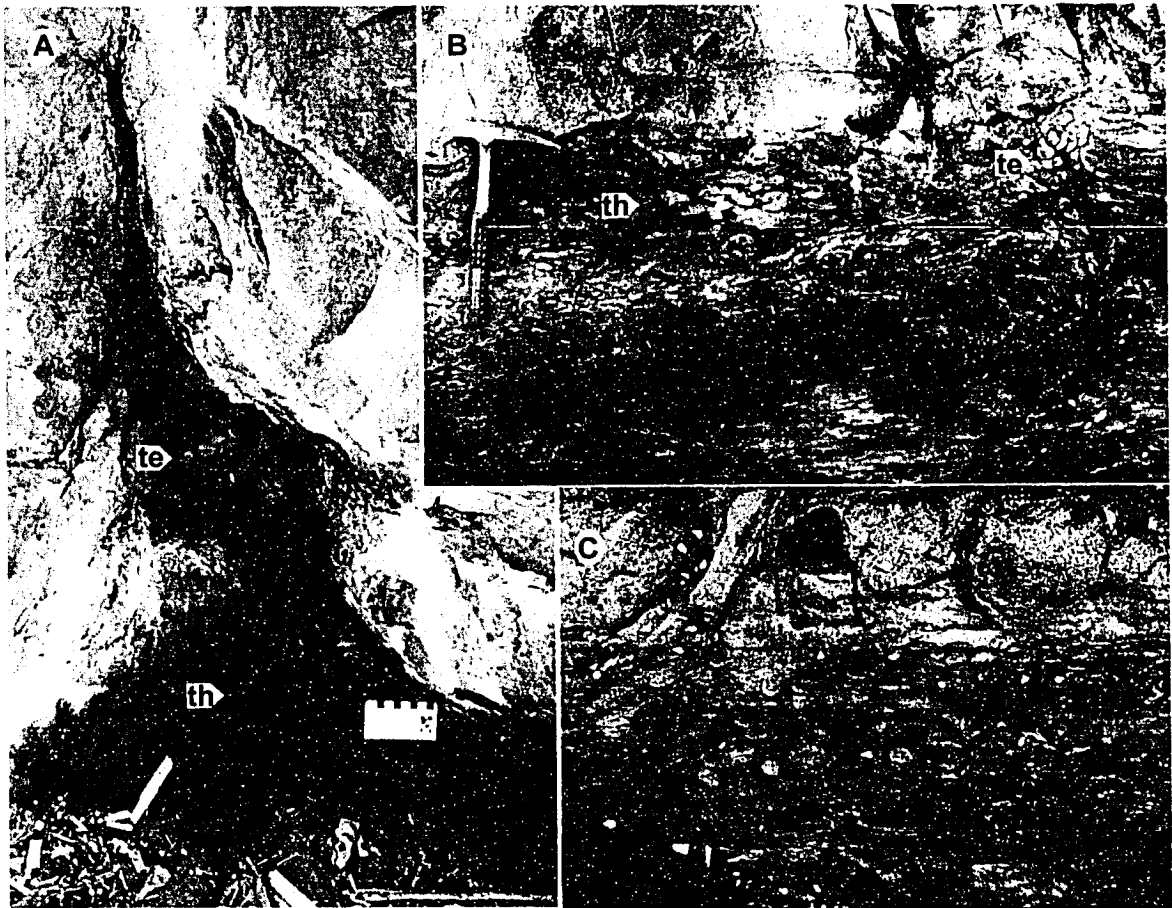


Figure 20: Juxtaposed *Glossifungites* Ichnofacies and *Teredolites* Ichnofacies associated with discontinuities. A: Root mound and stem anchored in silty mudstone, cross-cutting discontinuity and extending into overlying coarse-grained sandstone. Lower unit has firmground *Thalassinoides* (th) passively filled by the coarse-grained sandstone from above, and has been deformed by loading of the overlying sandstone, Brethour Island; B: Similar contact on Forrest Island, where mudstone is very carbonaceous. Both *Thalassinoides* (th) in lower substrate and *Teredolites* (te) in root mound are passively filled with coarse-grained sandstone from above. Branch-like structures in the overlying sandstone may be connected to the root mound. C: Transition from very carbonaceous mudstone below to upper medium-grained sandstone above is cross-cut by passively filled *Thalassinoides* and *Gastrochaenolites*. Swartz Head, Saanich Peninsula.

## **Stratigraphy**

The Nanaimo Group within the study area is divided into 3 formations: the basal Comox Formation, the Haslam Formation, and the Extension Formation (see Backpocket Map). These formations reflect the lowest three units of the Upper Cretaceous succession in the Nanaimo Basin, as described by previous workers (Ward, 1978; Mustard, 1994). Some previous studies have assigned some rock assemblages in the study area to an "Extension-Protection Formation" (Muller and Jeletzky, 1970), to the younger Protection Formation (England, 1990), or to an older "Sidney Formation" (Haggart *et al.*, 2005), but data collected during this study do not support these interpretations. The general stratigraphy of the formations present in the study area is provided below, from the basal unconformity upward, relating lithologic character to representative facies as described previously.

---

## **Basal Unconformity**

The basal unconformity is well exposed at several locations in the field area. Where exposed, the contact is sharp and erosive, and undulates over several metres (Figure 6). Basin-wide, the paleorelief of this unconformity has been demonstrated to exceed 100m in broad east-west trending valleys that account for some of the varying thickness of the Comox Formation (Atchison, 1968; Kenyon *et al.*, 1992; Mustard, 1994). Identification of these valleys is complicated by Tertiary deformation of the basin, just as inferring major fault

structures between islands in the study area is complicated by the unpredictability of this potential stratigraphic marker. The basal unconformity is an angular unconformity in most localities, where rocks below this unconformity are stratified meta-volcanics. Locally, this discontinuity is a nonconformity over unstratified plutonic rocks.

In some locations a basal conglomerate (Facies C1) is present, composed entirely of local basement materials, although this conglomerate is rarely more than a few metres thick (Figure 6b,c). In many locations, there is a juxtaposition of highly weathered local basement clasts and largely unaltered clasts. This suggests *in situ* weathering and some level of regolith development, although no regolith or paleosol is preserved. In locations where the basement conglomerate is absent, the unconformity is smooth and displays no weathering, although it is commonly intensely fractured (Figure 10d). *Trypanites* Ichnofacies hardground suites have not been identified in the underlying units, and clasts lack evidence of limpet, barnacle, or bivalve attachment.

## **Comox Formation**

The name Comox Formation was introduced by Clapp (1912) for coal-bearing units in the Comox area of Vancouver Island. Muller and Jeletzky (1970) recognized the correlation between the basal units of the Comox area ("Comox Formation") and the basal conglomerate of the Nanaimo area ("Benson Formation"). They defined the Comox Formation as the basal unit of the Nanaimo Group, and in the southern basin delineated a basal conglomeratic unit within the formation, termed the Benson Member.

## **Benson Member**

Although the "Benson Formation" is used by some workers for the basal unit south of Nanaimo (see Pacht, 1984; England, 1990), the correlation of the basal units across the entire Nanaimo Basin as the Comox Formation, suggested by Muller and Jeletzky and others is preferred (*cf.*, Mustard, 1994). The Benson Member is generally a poorly sorted conglomerate and rarely breccia with a coarse-grained sandstone matrix, deposited directly upon the basal unconformity. It gradationally passes upward into the Saanich Member of the Comox Formation, which is a predominantly sandstone unit with significant heterolithic and mudstone successions. Within the study area, it is exposed on Saanich Peninsula and Sidney, Portland, Moresby, and Russell Islands (see measured sections MS002 and MS008, Appendix A).

The Benson Member is dominated by the conglomeratic facies, C1 and C3. Where C1 constitutes the basal conglomerate, it varies from a single clast thick to several metres thick, occurs directly on the basal unconformity, and invariably grades vertically over a few metres into a well-sorted sandstone or pebbly sandstone of the Saanich Member (Figure 6a). Where C3 comprises the basal conglomerate, the unit is generally thicker (up to several tens of metres). The top is generally gradational into a moderately- or well-sorted sandstone of the Saanich Member, although the gradation may extend over 10's of metres. In some localities, or there is an intertonguing relationship with the upper unit.

The thickest contiguous packages of Benson Member conglomerates identified in the field area occur on Moresby Island (Figure 8d,e). Although the

basal and top contacts are nowhere identified from the same package, there are two locations where Facies C3 conglomerate is greater than 50m thick. On the west coast of Moresby Island, this thickness appears to exceed 100 metres with a diffuse gradational top.

### **Saanich Member**

The Saanich Member of the Comox Formation is only defined in the southern Nanaimo Group, and is correlated with the coal-bearing Dunsmuir and Cumberland members of the northern outcrop area (Mustard, 1994). Basin-wide, the Saanich Member generally comprises medium-bedded, coarse-grained sandstones with minor interbeds of fine-grained sandstone and mudstone. This member gradationally overlies the Benson Member or locally directly overlies the basal unconformity where the Benson Member is not present. It grades upward into thin-bedded sandstone and mudstone of the Haslam Formation.

In the study area, the Saanich Member represents all of the stratigraphy of Coal, Brethour, Comet, and Forrest islands, and the majority of the Nanaimo Group units on the Saanich Peninsula, Sidney, Moresby, Portland, and Russell islands (see measured sections MS001, MS002, MS003, MS004, MS007, MS008, MS009, MS011, and MS012, Appendix A).

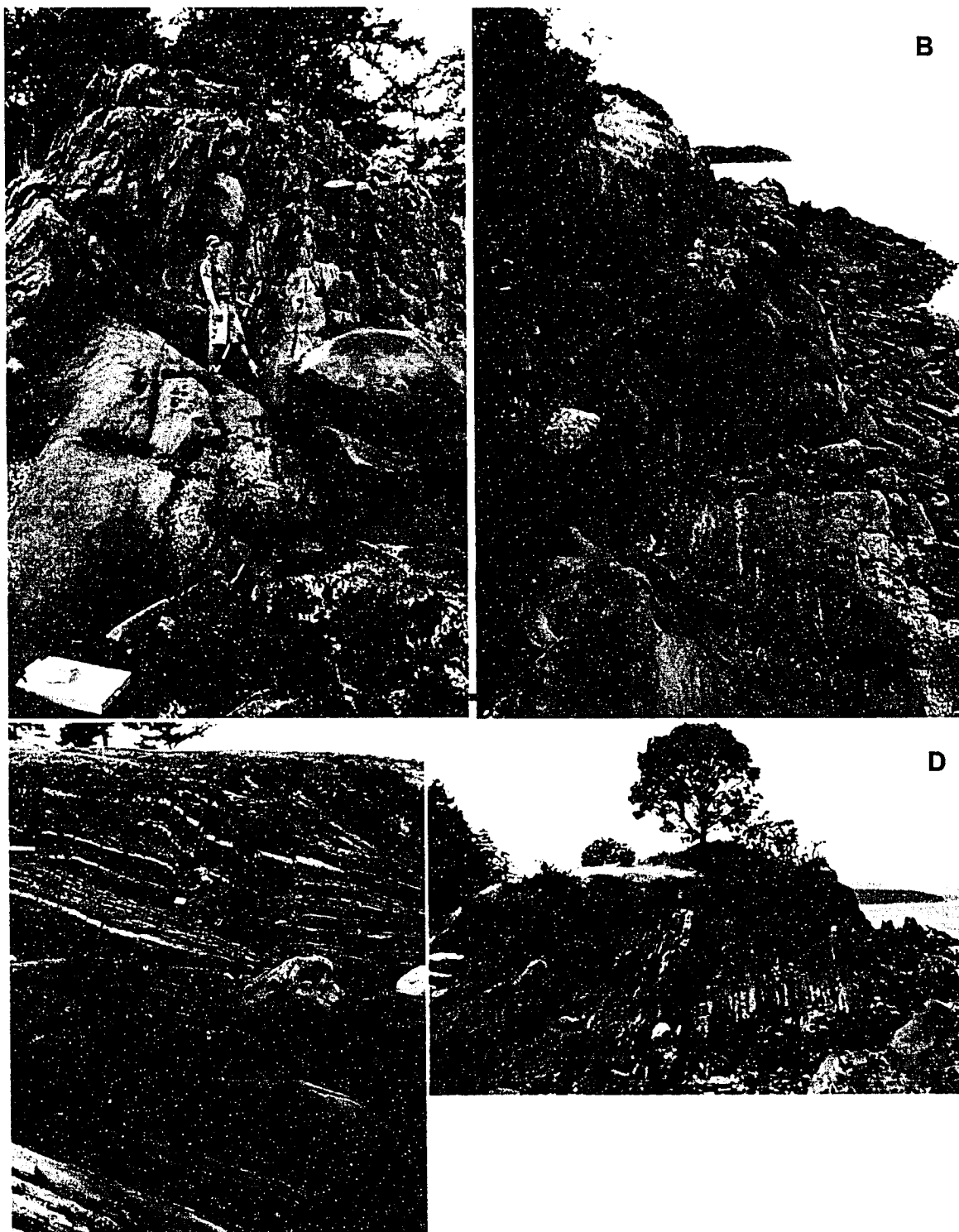
The Saanich Member is dominated by sandstone facies, although there are extensive muddy and heterolithic areas, as well as some thin conglomeratic exposures. All sandstone facies are represented, with Facies S1 most common near the basal conglomerate, locally intercalated with Facies P1 pebbly



sandstones. Facies S2 and S3 are most commonly distributed in 10- to 50- m thick packages, separating finer-grained and heterolithic units (Figure 21 a, b). Facies S4 is more common towards the top of the Saanich Member, and commonly fines upward, grading into the Haslam Formation at several locations.

Muddy and heterolithic facies are also well represented in the Saanich Member. Commonly, Facies M1 and M2 form recessive packages 10-50 m thick which are separated by equally thick sandstone packages. An exception to this rule is seen on Russell Island, where the entire west coast of the island is composed of Facies M1 muddy sandstone. Facies H2 has a similar distribution pattern and may, in places, represent a similar lithology to Facies M1 and M2, although it is better preserved with original bedding less disrupted by bioturbation (as in Facies M1) or dewatering and weathering (as in Facies M2). Facies H1, however, is more extensive (Figure 21c,d), and can form units more than 50m thick, as occurs on Moresby and Portland Islands, and in the deep cove area of the Saanich Peninsula.

The base of the Saanich Member either grades out of Benson Member conglomerates, or is in erosional contact with the basal unconformity where the Benson Member is absent. The top of the Saanich Member is gradational with the overlying, finer-grained Haslam Formation. The total thickness of the Saanich Member within the study area is difficult to estimate, as no complete section from the Benson Member to the Haslam Formation is exposed. The basal unconformity and the transition into Haslam Formation are both exposed along the shorelines of the Saanich Peninsula, however previous workers have



**Figure 21: Comox Formation exposures. A: Thick bedded massive and cross bedded sandstones, Saanich Member, Comet Island. B: Thick- to medium-bedded cross-bedded, coarse- and medium-grained sandstones, Saanich Member, Dock Island. C: Several metres of heterolithic sandstones with intercalated mudstones, upper Saanich Member, Sidney Island D: Thin bedded medium-grained sandstones, Forrest Island.**

interpreted a considerable amount of thrust thickening of this succession (e.g., England, 1990; England and Calon, 1991). Although large-scale thrust structures are not identified in this study, some minor faulting and folding along both east and west coasts (see Chapter 5) do make correlation challenging.

The best estimate for the thickness of the Saanich Member on the Saanich Peninsula may be from the intermittent outcrops in the interior of the peninsula. A coarse-grained outcrop on Tatlow Road near Gardiner Pond lies along strike of an exposure of the basal unconformity in Tsehum Harbour, and there are no large structures interpreted between this outcrop and the Comox-Haslam transition on the north shore of the peninsula. Tracing outcrops along dip over Horth Hill, this leads to an interpreted thickness of approximately 1000m. This is almost twice the estimated thickness for the Comox Formation identified in other studies (*cf.* England, 1990; Mustard, 1994), and definitively measured within the study area (such as on Brethour or Moresby Islands), although not out of scale with other seemingly contiguous successions of the Saanich Member, such as on the islands of Iroquois Channel.

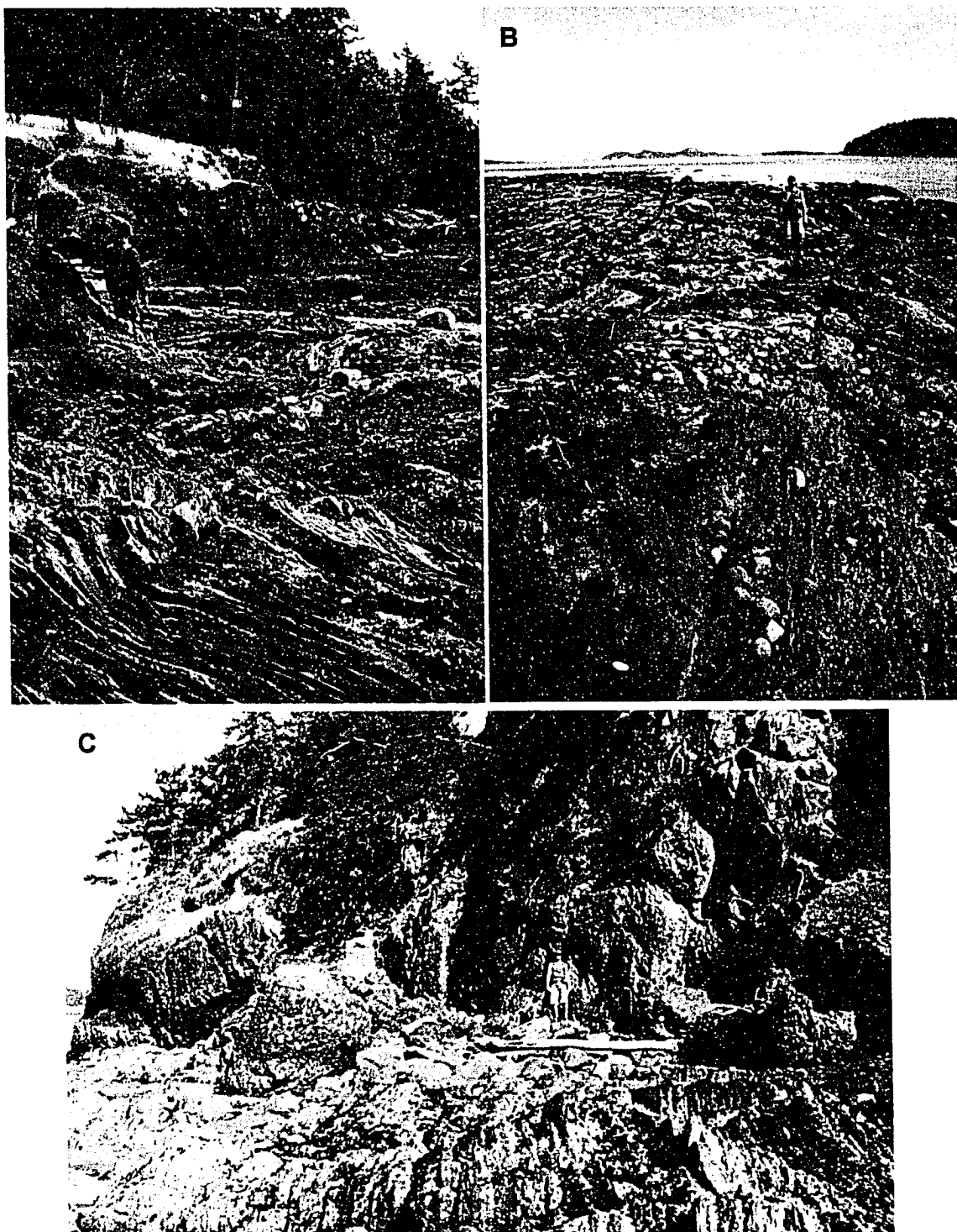
The base of the Saanich Member is identified on top of a thin Benson Member conglomerate on Sidney Island, with the succession repeated on Halibut Island. Saanich Member sandstones make up the bedrock of Mandarte and Forrest islands to the northeast. This repeated succession is interpreted to be the result of a thrust fault that passes through Miners Channel (see Backpocket Map).

## **Haslam Formation**

The Haslam Formation was also introduced by Clapp (1912) as the lowest mudstone-dominant unit in the Nanaimo succession, and was described in detail by Ward and Stanley (1982). This intercalated thin-bedded sandstone and mudstone unit gradationally overlies the Comox Formation and is gradationally (or rarely erosively) overlain by, or locally intertongues with, Extension Formation conglomerates and sandstones. In the southern outcrop areas, the Haslam Formation likely exceeds the 200 metres of thickness commonly observed in northern areas, although the recessive nature of the unit and inferred structural thickening make true stratigraphic thicknesses uncertain (Mustard, 1994).

Within the study area, the Haslam Formation represents the majority of the strata on Pym, Knapp and Piers islands, and along the southwestern coast of Domville Island (Figure 22). Smaller, disconnected exposures of shales along the north shores of the Saanich Peninsula and Coal Island are interpreted to represent a transition from lower Comox Formation sandstones into Haslam Formation. All exposures of Haslam Formation within the study area are of Facies H3 graded sandstone-mudstone couplets (see measured sections MS005 and MS006, Appendix A).

Where exposed on the Saanich Peninsula and Coal Island, the base of the Haslam Formation is gradational with the underlying Comox Formation sandstones. The top of the unit is exposed on Domville Island, where Extension Formation conglomerates and sandstones sharply and erosionally overly Haslam Formation mudstones. The same contact is exposed on nearby Sheep Island,



**Figure 22: Haslam Formation exposures. A: complexly folded sandstone-mudstone turbidites on west shore of Domville Island. Bluffs in background are overlying Extension Formation conglomerates. B: Mudstone dominated turbidites on south shore of Pym Island. Deformation in this unit is soft-sediment and constrained to specific bedsets. C: Sandstone-mudstone turbidites (foreground) are in fault contact with Extension Formation conglomerates (background) on Sheep Island.**

although a bedding-parallel fault disrupts the contact (Figure 22c). On Piers Island, there is an intertonguing relationship between the Haslam and Extension formations. Here, Extension Formation conglomerates erosively overlie Haslam Formation mudstones along sharp contacts (very well exposed on Piers and Clive Islands). These Extension Formation units grade upward over a few metres back into Haslam Formation mudstones before the sequence is repeated again.

Much like the Comox Formation below, an absolute measurement of Haslam Formation thickness is difficult because the base and top are not exposed in the same area. A minimum thickness is estimated at 300m, based on the successions on southern Knapp and Piers Islands, both of which contain exposures of the Haslam-Extension transition. Although the exposures on Piers Island are fold-thickened, these folds are not obviously present on Knapp Island. The base of the Haslam Formation is exposed only a few hundred metres to the south on Saanich Peninsula, however significant faults have been interpreted to cut the passage between these outcrops (see Chapter 5).

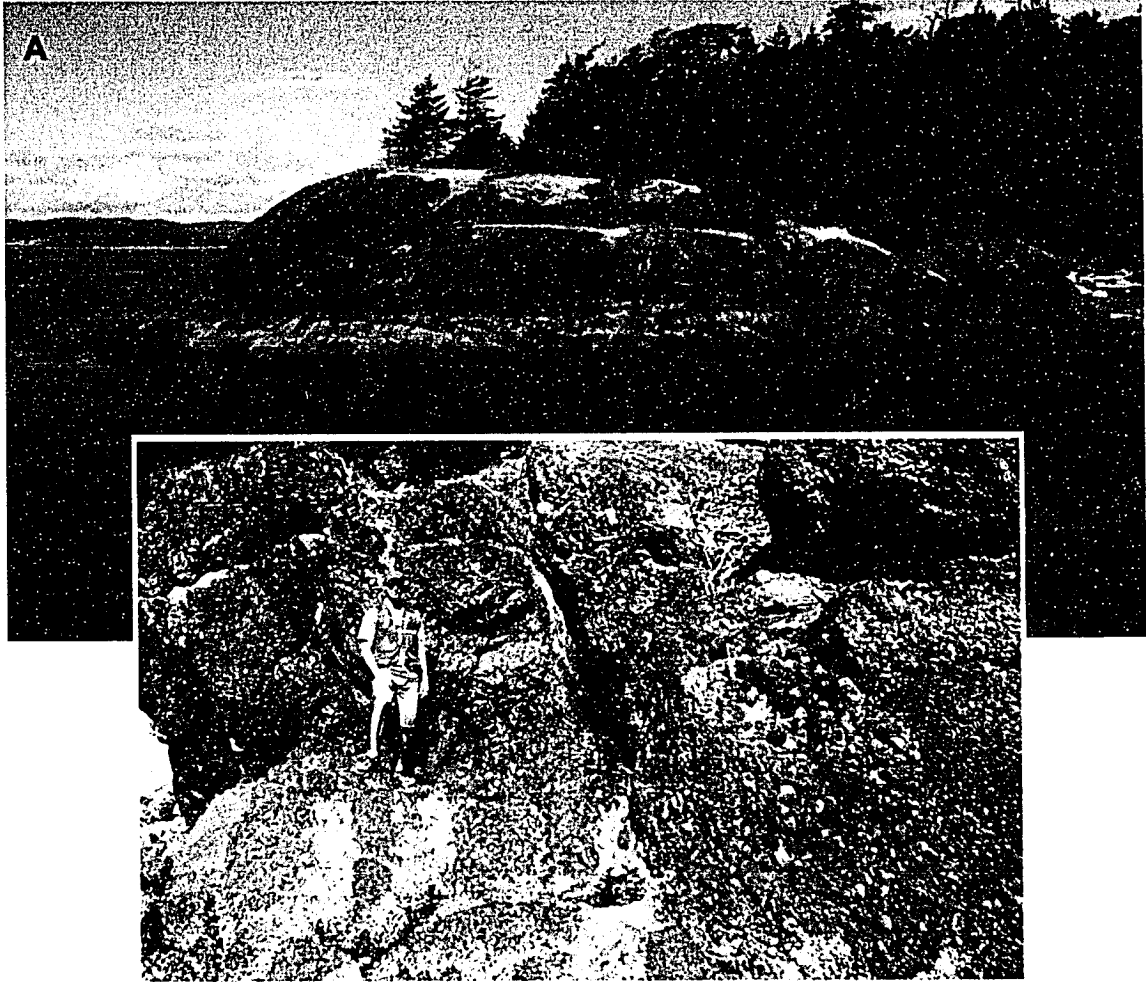
Earlier studies have suggested the mudstone-conglomerate-mudstone sequences on Piers Island represent Haslam-Extension or even Comox-Haslam sequences stacked by a series of near-bedding-parallel thrust faults (*cf.* England, 1990), or an intertonguing between the Haslam Formation and the "Extension-Protection Formation" (Muller, 1980). These interpretations are not supported by data collected during the course of this study. Although minor shear structures are locally present on Piers Island, there is no evidence of significant, formation-scale thrust faulting on the island. Sandstone units on northern Piers Island and

Knapp Island better match Extension Formation pebbly sandstones than Comox Formation sandstones. Furthermore, abundant exposures of conformable and erosive contacts between Haslam and Extension Formation units suggest autocyclic deposition.

## **Extension Formation**

The name Extension Formation was originally applied by Clapp (1912) to a conglomerate unit overlying the Wellington coal seam in the coal mining region of Nanaimo. Muller and Jeletzky (1970) reduced the Extension to the level of a member of their Extension-Protection Formation, however, more recent studies have reinstated the formation status of the Extension (Ward, 1978, England, 1990, Mustard, 1994). The Extension Formation is typically a thick-bedded, poorly to moderately sorted, pebble to cobble conglomerate with a coarse-grained sandstone matrix (Figure 23). Commonly, the unit fines upward into a pebbly, coarse-grained sandstone. It has an erosive, or locally gradational to intertonguing lower contact with Haslam Formation sandstones and mudstones, and a gradational upper contact into the mudstone-dominated Pender Formation. The Extension Formation is typically more than 200 metres thick in the southern part of the basin, and thins to the north (Mustard, 1994).

Within the study area, the Extension Formation consists of thick-bedded conglomerates of Facies C2, and thick-bedded pebbly sandstones of Facies P1 (see measured sections MS006 and MS010, Appendix A). The unit also includes cross-bedded sandstones of Facies S3, although these are only exposed on



**Figure 23: Extension Formation exposures. A: South shore of Gooch Island. Thick conglomerate and minor sandstone beds are overturned to the north (picture right). B: Thick, graded pebble to cobble conglomerate beds and minor sandstone interbeds, Rum Island.**

Gooch Island. The unit generally fines upward with Facies C2 common at the base, passing upward to Facies P1 and Facies S3. The base is generally sharp and erosive into the Haslam Formation, and is well exposed on Domville Island. On Piers Clive and Knapp Islands, however, several thick tongues of Extension Formation conglomerates and sandstones partially cross-cut the islands, enveloped in Haslam Formation sandstone and mudstones. The lower contacts of the intertongues are erosive. The Facies S3 exposures on northern Gooch



Island may represent a gradational transition into the overlying Pender Formation, although no Pender Formation units were identified in the field area.

The thickness of the Extension Formation within the study area can only be estimated. The base of the unit is not exposed on Gooch Island, the top is not exposed on Domville Island, and correlation between the two islands is complicated by a large fold structure separating them (see Chapter 5). The thickest continuous succession exposed is from the south coast of Gooch Island to the transitional Facies S3 sandstones on the north shore. This indicates a minimum measured thickness of the Extension Formation of approximately 350 metres.

## **Pender and Protection Formations**

Previous workers assigned several units in the study area to the Pender Formation (*e.g.*, England, 1990) or to the now-disused "Extension-Protection Formation" (*e.g.*, Muller and Jeletzky, 1970). Data collected during this study do not support either of these correlations, and these units are described here only to clarify the reasons for this re-interpretation.

The "Extension-Protection Formation" of Muller and Jeletzky (1970) was defined stratigraphically in the coal mining region around Nanaimo, more than 50 kilometres north of the study area. It was correlated with conglomerates and sandstones exposed on Saltspring and Pender islands (north and northeast of the study area, respectively), and with similar units in the study area on Piers, Domville, and Gooch islands. The reasons for assigning the sandstone and

mudstone units of Piers, Knapp, northern Coal, Brethour and Comet islands to this formation are not explicit. It is presumed that the finer-grained units stratigraphically above the distinct conglomerates were correlated with the sandstone-dominated "Protection Member" of the upper "Extension-Protection Formation", as seen farther north in the basin.

Ward (1978) differentiated the Extension, Pender, and Protection formations. At the southern end of the basin on Pender Island, the Pender Formation was described as fine-grained sandstones and mudstones above the Extension Formation, and approximately 100 m thick. The Protection Formation was described as a distinctively white, well-sorted sandstone with local shale interbeds, comprising a total thickness of nearly 400 m. Ward also recognized that the fine-grained units on the north shore of Piers Island are a repeated stratigraphy of the Haslam Formation, and that the sandstones on the north shore of Coal Island correlate best with the Comox Formation. Following the revised stratigraphy of Ward (1978), England (1990) assigned the sandstone units on Comet and Brethour Islands to the Protection Formation, based on their stratigraphic position overlying Extension Formation conglomerates. The Pender Formation is assumed to be covered by the sea in the channels between islands in this scenario.

The sandstones on Brethour and Comet islands are here assigned to the Comox Formation, based on the consistency in lithology and sedimentary features to other Comox Formation units, and the interpreted deposition environment of the formation. Supporting paleoenvironmental arguments for this

re-interpretation are outlined in the following chapter. These arguments favour the location of a fault between Domville and Brethour islands that has brought older Comox Formation rocks into a stratigraphic position above the Extension Formation rocks on Domville Island. The same fault is interpreted to pass between Gooch and Comet Islands, causing a similar juxtaposition, although the fault is here overturned by the same large fold which has overturned the strata of Gooch and Comet islands (see Chapter 5). It is possible, however, that the finer-grained units at the north end of Gooch Island may represent a transition from Extension Formation into Pender Formation. These finer-grained outcrops are limited to the northernmost shore, are minor compared to surrounding sandstone facies, and are not of mappable scale. Their identification here only serves to locate the approximate top of the Extension Formation on Gooch Island.

## CHAPTER 3: DEPOSITIONAL ENVIRONMENTS

The depositional environments of the Upper Cretaceous Nanaimo Group have been assessed in several previous studies. Earlier work recognized coal-bearing strata of Vancouver Island and marine ammonites and molluscs throughout the basin. Muller and Jeletzky (1970) summarised this earlier work, and proposed a depositional history. In their model, sandstone-conglomerate dominated units (including the lower Comox Formation and the Extension Formation) are interpreted to represent fluvial and deltaic deposits. Mudstone-sandstone coal-bearing strata (including the upper Comox Formation) are interpreted to represent deltaic or lagoonal settings, and mudstone-dominated strata (including the Haslam Formation) are interpreted to represent shallow marine to shelf settings. Five transgressive-regressive cycles are described, each with a conglomerate-sandstone or heterolithic, fluvial or deltaic basal unit grading upward into fully marine basinal mudstones. Only the uppermost fifth cycle lacks an upper marine unit (Muller and Jeletzky, 1970).

Ward and Stanley (1982) and Pacht (1984) recognised that conglomerate and sandstone facies in the Extension Formation, and indeed in most parts of the southern Nanaimo Basin, did not represent fluvial or deltaic deposition. They interpreted large channels, commonly with single-channel fills and diffuse internal structures, to represent sediment gravity flow deposits. They further interpreted a deep marine depositional setting and submarine fan complexes for these units in

general. Consequently, non-marine deposition in the basin was deemed to be limited to the coal-bearing units on Vancouver Island. This model of a gradual single transgressive succession, from non-marine through marginal to fully marine settings has been expanded upon by subsequent research (e.g. England, 1990; Mustard, 1994; Johnstone *et al.*, 2006).

This chapter presents interpretations of the depositional history of the Nanaimo Group strata of the study area. These interpretations are based on facies descriptions from the previous chapter, organized into facies associations. Through the description of facies associations and the relationships between these associations, facies models are developed, which in turn allow the interpretation of the paleogeographic history of the study area during the Late Cretaceous. The depositional settings are discussed in stratigraphic order starting at the basal unconformity, through several shallow marine settings (fan delta, shoreface, barrier island complex) into a slope-margin submarine fan complex.

## **Rocky Shoreline**

The basal unconformity of the Nanaimo Group strata of the study area is described in the previous chapter. Where a basal conglomerate is present, a juxtaposition of fresh-looking and well-weathered clasts suggests *in situ* weathering and some level of regolith development (Figure 8b). In all localities, this basal conglomerate fines upward within only a few metres into sandstone units with sedimentary structures, shells and ichnofossils suggesting marine depositional environments. Where the conglomerate is absent, the unconformity

appears polished, with paleo-weathering evidence limited to locally intense fracturing, and is overlain well-sorted sandstones (Figure 10d). Although the underlying volcanic rocks lack boring attributable to the *Trypanites* Ichnofacies or evidence of limpet, barnacle, or bivalve attachment, the units immediately overlying the unconformity contain locally abundant bivalve shell fragments and marine ichnological suites.

The nature of the unconformity and the overlying sediments suggest that it represents erosion along a rocky marine shoreline (Johnstone *et al.*, 2006). The high relief of this paleo-shoreline is typical of the basal unconformity of the Nanaimo Group (Atchison, 1968; Mustard, 1994). The paleotopography creates the opportunity for the preservation of a diverse suite of depositional environments, although published facies models of such are largely lacking due to the common impression that rocky shorelines are erosive settings with little preservation potential for their deposits (Felton, 2002). Detailed below are three depositional environments preserved along this Late Cretaceous shoreline as observed in the study area: fan-delta complexes, storm-dominated open shorelines, and embayed shorelines. Finally, data are presented supporting a deeper-water setting for some of the upper units in the study area.

### **Fan Delta Complex**

The terms “alluvial fan” and “fan delta” can be somewhat ambiguous in much of the literature. An alluvial fan is here considered a distributary fluvial system formed where streams emerge from a confined valley onto a basin floor (*cf.* Miall, 1992). The most common definition of a fan delta is an alluvial fan

which progrades directly into a standing body of water (e.g. McPherson *et al.*, 1987, 1988; Miall, 1992), although the term is probably best reserved for that part of the alluvial fan which is subaqueous, with the entire fan and delta system collectively termed the “fan-delta complex” (cf. Nemec and Steel, 1988).

Generally, alluvial fans are thought to best develop in areas of active tectonics (uplifting a headland above the basin floor), infrequent but intense precipitation (commonly associated with desert climates), and/or recently deglaciated settings where there is abundant loose sediment stored on steep slopes (e.g., Blair and McPherson, 1994; Postma, 1990). There are several examples, however, of mass-flow type fans and fan deltas forming in areas unrelated to either glacial activity or active tectonics (Nemec and Steel, 1988). Similarly, such fan delta complexes occur in climate types ranging from deserts to rainforests (Blair and McPherson, 1994). In addition, though fan deltas are widely considered characteristic of regressive coasts, there is significant potential for progradation and preservation of fan delta deposits even along transgressive coasts.

Alluvial fans are depositional bodies generated on the steep edges of basins, where feeder channels braid and a large volume of coarse sediment is deposited. This places the resultant fan deltas at one of the extreme ends of most delta classification systems, particularly as most of these schemes are based on studies of low-gradient fluvial systems for which fan deltas are a poor fit (Nemec, 1990). For example, in the traditional tripartite river-, wave-, and tide-dominated delta classification of Galloway (1975), fan deltas should comprise the

most fluvial of the river-dominated deltas, in that their morphology is almost entirely controlled by the feeder system. Nevertheless, the predicted “birds-foot” morphologies are not apparent in fan deltas. In the more robust classification system proposed by Postma (1990), the nature of the feeder system, gradient, and depth of basin are fundamental, and fan deltas correspondingly represent a Type-A Gilbert-style delta in which transport energy is provided by inertia from the feeder stream.

Alluvial fans and fan delta complexes typically have semi-conical shapes with a plano-convex profile and steep slopes (Blair and McPherson, 1994). Alluvial fans have slopes that may exceed 30° where gravelly, and up to 20° if sand-dominated (Reading and Collinson, 1996). In contrast, fan delta slopes range from 1.5° to 25° (Blair and McPherson, 1994). These gross morphologic characteristics are rarely exposed in the rock record, however, and identification of fan delta deposits relies on understanding of the depositional processes responsible for their creation.

Fan deltas form in settings where mass wasting and sediment gravity flows provide the sediment, and wave and/or tidal action re-works the sediment. The typical location of a fan delta system at the base of a steep slope, combined with an abundance of sediment coming out of suspension due to suddenly unconfined stream flow, typically results in a large supply of mixed-grade sediments. Although a great variety of depositional processes are active in any alluvial fan setting, most of these processes have short travel lengths, allowing limited time for sediment sorting. This is somewhat mitigated in the fan-delta



complex by the opportunity for extensive marine reworking, and the variety of depositional processes increases in the subaqueous part of the complex (Nemec and Steel, 1984). The principal sediment transport and deposit mechanisms can be generalized into three groups: mass wasting events, sediment gravity flows, and fluvial processes (Figure 24).

Mass wasting processes include rock falls, slides and avalanches, along with colluvial slides (Blair and McPherson, 1994). Rock falls involve gravel and larger clasts bouncing and rolling down the slope after cliff failure. With sufficient fall distance and rock mass, energy may be high enough to pulverise rock into sands and silts, resulting in a massive, dry grain-flow typically termed a rock avalanche. A slide, in contrast, may be rapid or very slow, and involves movement of a large intact block of rock ("rock slide") or amalgamated colluvium ("colluvial slide") along a glide plane. Although deposits from these processes may be important in some fan-delta systems, they are not evident in the study area and are not dealt with further.

Sediment gravity flows that are common to fan-delta systems include grain flows, debris flows, and turbidity currents (Blair and McPherson, 1994). Grain flows (sometimes termed "non-cohesive debris flows") are plastic, laminar flows of sediment where suspension is maintained only by the dispersive pressures of inter-grain collisions. This type of flow is more common in well-sorted sediments, especially sands, and only possible on steep slopes ( $>18^\circ$  in subaqueous sand) such that shear stress is not quickly overwhelmed by friction generated from grain collisions (Lowe, 1976). True debris flows, in contrast, commonly involve

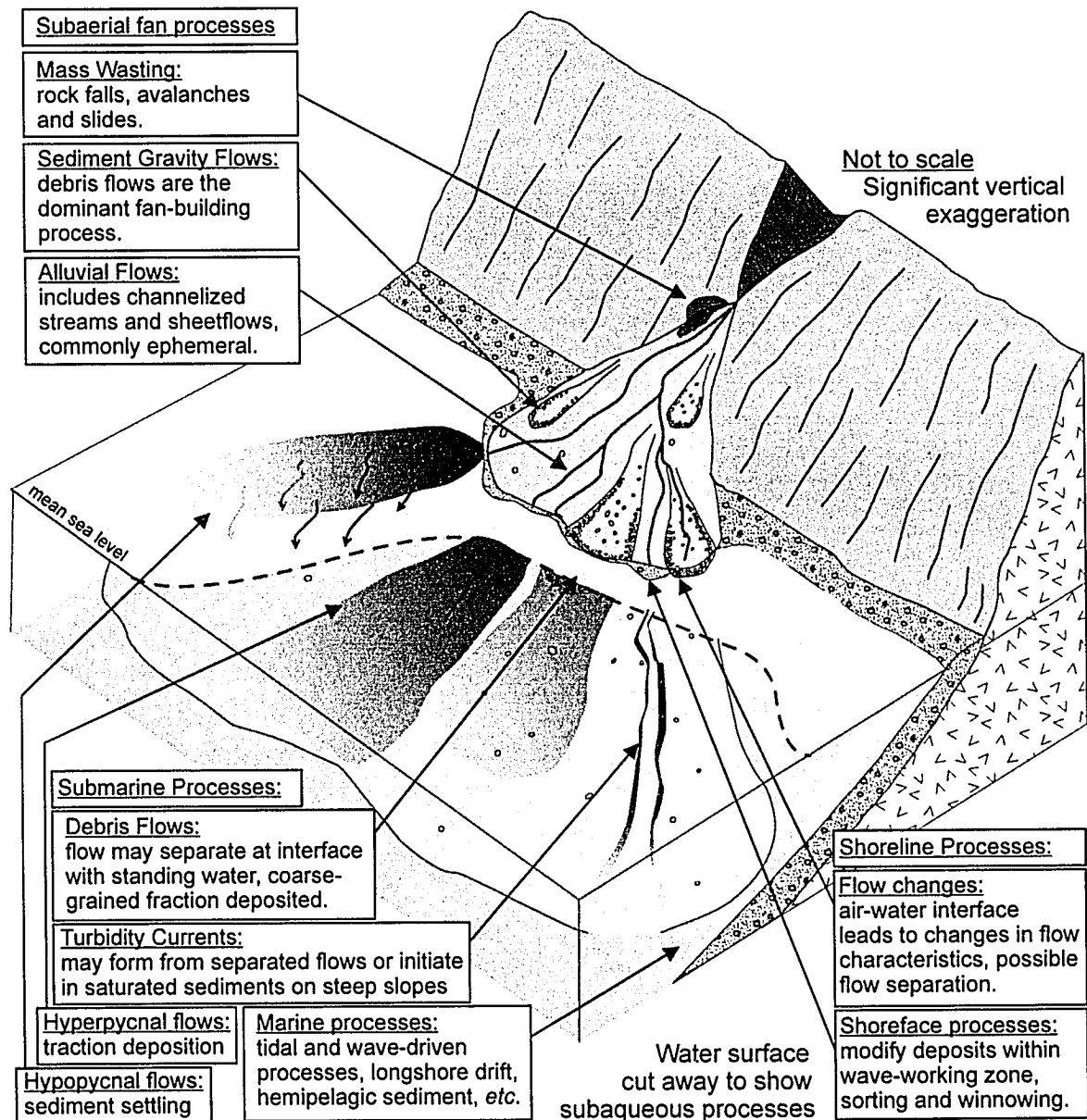


Figure 24: Model fan-delta complex, showing typical sediment transport and depositional processes as outlined by Nemec and Steel (1984), Postma (1990), Miall (1992), and Blair and McPherson (1994).

poorly sorted materials, and may move on very gentle slopes once movement is initiated (Rodine and Johnson, 1976). Debris flows of this type involve the plastic, laminar flow of a saturated, muddy matrix mixed with larger clasts. The clasts are supported by the cohesive strength of the matrix, along with some dispersive pressures and the relative buoyancy of some clasts over the mixed water-and-mud matrix (Hampton, 1975; Lowe, 1982). Turbidity currents involve turbid flows of low-density water and sediment mixtures. Their flow characteristics and deposits are discussed in detail below in the section on submarine fans (see Table 2).

Streams on most alluvial fans are ephemeral, or have large flood-discharge to base-discharge ratios (Miall, 1992). As a result, non-flood-stage fluvial processes rarely leave preserveable deposits, and are not major elements in alluvial fan growth. Fluvial processes active during flood stage flows, however, are important in building alluvial fans, including both sheet floods and incised channel floods. The former are rare, catastrophic events causing unconfined supercritical water flow to expand rapidly across the fan surface. The latter are generally erosive, but leave channel forms that are commonly lined by cobbles and boulders (Blair and McPherson, 1994). It is important to note that both flood and non-flood fluvial processes transport significant sediment to the subaqueous portion of the fan delta complex.

Blair and McPherson (1994) identify two distinct types of alluvial fans based on dominant transport mechanisms: Type-I fans, dominated by debris-flow processes; and Type-II fans, dominated by sheet flood deposition. Type-II fans

are more common where there is a paucity of clay material in the source rock. Compared to Type-I fans, sheetflood-dominated Type-II fans tend to form much gentler slopes, and to fine distally. Facies representing Type-II fans were not recognized in the study area, and are not discussed further.

### **Fan-Delta Facies Models.**

The combination of ephemeral unconfined flows, steep slopes, abundance of sediment of all calibres, and combination of subaerial and subaqueous flows can lead to an almost unlimited variety of mass flow deposits in the fan delta system (Nemec and Steel, 1984). Generalized models that outline a conglomeratic "proximal fan", a pebbly sandstone "middle fan", and a sandstone "distal fan" (e.g. McGowan and Groat, 1971), are at best sorely inadequate, and at worst entirely inaccurate (Blair and McPherson, 1994). Models that are constructed with a comprehension of sediment flow mechanisms tend to be more robust, especially those which recognize how fan slopes coupled with sediment and water supply interact to create predictable progressions of transport mechanisms, from the fan apex to the subaqueous fan-delta.

One such scheme is outlined by Postma (1990). Here, the upper reaches of the fan-delta system are dominated by debris flows, resulting in the deposition of massive, clast-supported gravels, with some horizontally stratified gravel and sand from grain flows (where slopes are adequate) and minor sheet flows. Minor trough- and planar-cross bedded sandstones also occur, related to scour fills and surficial reworking by fluvial processes. The delta front is dominated by processes that carry sediment from the upper fan by inertia, which is quickly

dissipated in the subaqueous environment, resulting in increased sediment sorting and bedload deposition. Deposits trend towards matrix-supported gravels, with a predominance of horizontal lamination within the finer-grained component. Processes on the lower delta front include continuations of the subaerial flows, although turbid density currents tend to replace debris flows as the primary depositional mechanism, owing to increased water mixing and a loss of cohesive strength in the matrix (Nemec and Steel, 1984). The resulting deposits are laminated and current-rippled sands. Finally, marine processes, including hemipelagic sedimentation, will be increasingly preserved with depth (Figure 24).

Debris flow deposits on the subaerial Type-I fans form sheet-like beds with little basal erosion. They may be ungraded or well graded, with inversely graded bases common, and grading may change along slope within the same bedsets. Bedding is commonly crudely developed, although buoyantly supported large clasts may become concentrated at the tops and sides of "plug-shaped" flows. Such clasts are rarely imbricated. Beds range from polymodal to bimodal, and from clast supported to matrix supported (Nemec and Steel, 1984).

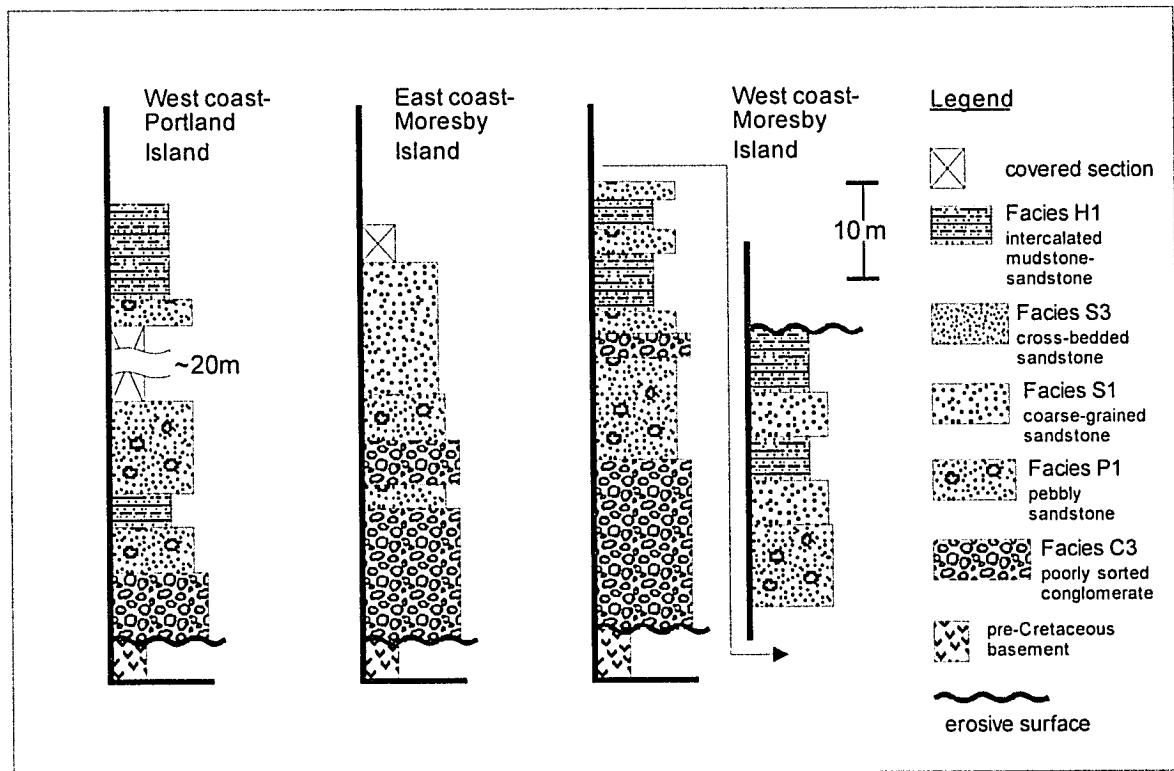
These flows become more organized internally as they enter the subaqueous portion of the fan. Some clast alignment or imbrication may occur in hydrodynamically stable positions, and units generally increase in matrix content. As flows enter standing water they may split, depositing thin, scourless gravel lenses encased in muds (Nemec and Steel 1984). Subaqueous deposition may further be inferred from the presence of marine fossils and bioturbation (*cf.* Soegaard and MacEachern, 2003), or the presence of wave-generated features

(e.g. HCS, SCS; Bann *et al.*, 2004). Large fluid-escape structures are common where large masses of saturated sediment are rapidly deposited into a subaqueous setting (Postma, 1983). Finally, bedding angles along the fan-delta complex may change significantly and form clinoforms. Bedding in the upper delta slope may be inclined up to 25° relative to horizontal, with the slope closer to 5° for the lower delta (Postma, 1984).

### **Facies Association 1: Fan-Delta Complex**

In several locations within the study area, the basal unconformity is overlain by a thick (several metres) package of conglomerates with a poorly sorted matrix (Facies C3). At three locations, a succession overlying the basal unconformity comprising unsorted conglomerates passing into well-organized sandstones is preserved (Figure 25). The conglomerates are characteristic of debris flow deposition. They become finer-grained, better organized, and richer in matrix up section, consistent with the interpretation of a Type-I alluvial fan delta complex.

At all localities, these conglomerates are overlain by better stratified sandstones and pebbly sandstones (Facies P1 and S1), which are commonly trough cross bedded or planar parallel laminated, and normally graded. Low-intensity bioturbation by a low diversity suite of the *Skolithos* Ichnofacies, the presence of bivalve molds, and of large fluid escape structures suggest a subaqueous marine setting. These deposits likely represent the subaqueous deposition of bedload sediment derived from sheetfloods, channel floods, or ephemeral stream flow in the upper alluvial system.



**Figure 25: Typical expressions of Facies Association 1.**

At each location, these sandstones are overlain by heterolithic sandstone-mudstone units (Facies H1) with abundant evidence of upper to lower shoreface deposition (see Storm Dominated Shoreface facies models, below). Such characteristic features include the presence of marine bivalve fossils, marine ichnologic assemblages (e.g. suites attributable to the *Cruziana* Ichnofacies), and primary sedimentary structures suggesting fully marine processes. At the Moresby Island locality, these overlying marine units have bedding angles up to 20° shallower than the underlying poorly sorted conglomerates, suggesting a steep angle of repose for the conglomerate beds, as may be expected for coarse-grained debris flow deposits in the subaerial portion of a Type-I alluvial fan-delta.

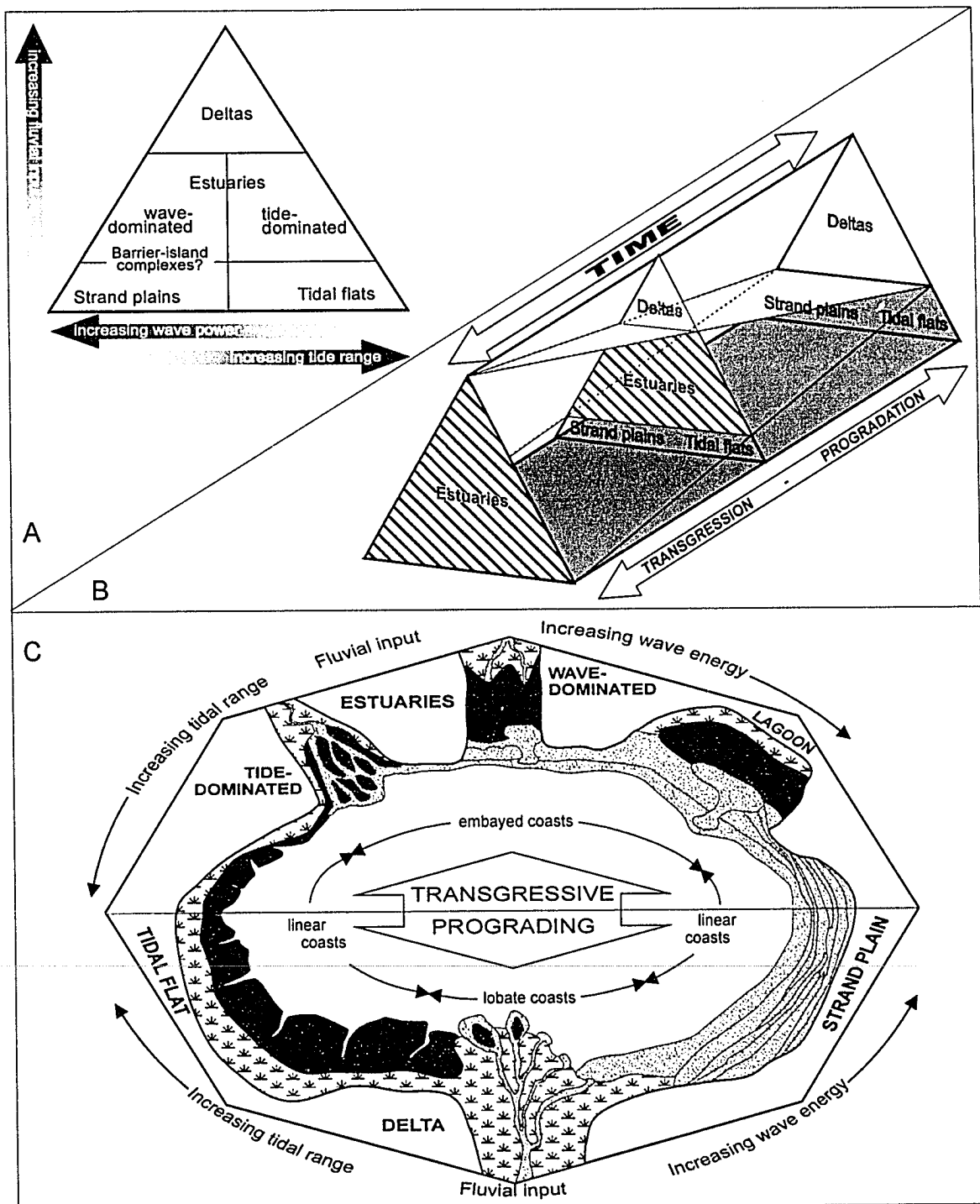
The emphasis on progradation of fans into standing water downplays the role of transgression in the preservation of fan-delta units in areas other than “traditional” settings (e.g. recently deglaciated environments or along active fault scarps). On an eroding, rocky shoreline, small fans should be expected to form, and with continued transgression, these fans have a high preservation potential as fan deltas.

### **Storm-Dominated Shoreline.**

A common expression of the basal Comox Formation in the study area is that of a rocky, storm-swept shoreline, which was drowned by gradual but persistent transgression (Johnstone *et al.*, 2006). The shoreface system comprises the entire region of a marine coast where tides and waves are the primary sediment dispersal system. Components of the shoreface system, from the swash zone to the offshore transition, are preserved within the study area.

Coastal systems have been classified on the basis of the dominant processes which shape them, with a traditional ternary classification of river-dominated (primarily deltas), tide-dominated, and wave-dominated (Figure 26a). Although this classification scheme does not consider the effects of grain size on coastal morphology, it does effectively outline the conditions under which different shoreline types form. When the effects of sea level change are added to the classification (Figure 26b), the evolutionary changes of shorelines types can be predicted. A more diagrammatic model can be drawn (similar to Boyd *et al.*, 1992), with the major coastline types positioned in relation to their dominant processes (Figure 26c). Typical transgressive shoreline types (e.g., tidal flats,



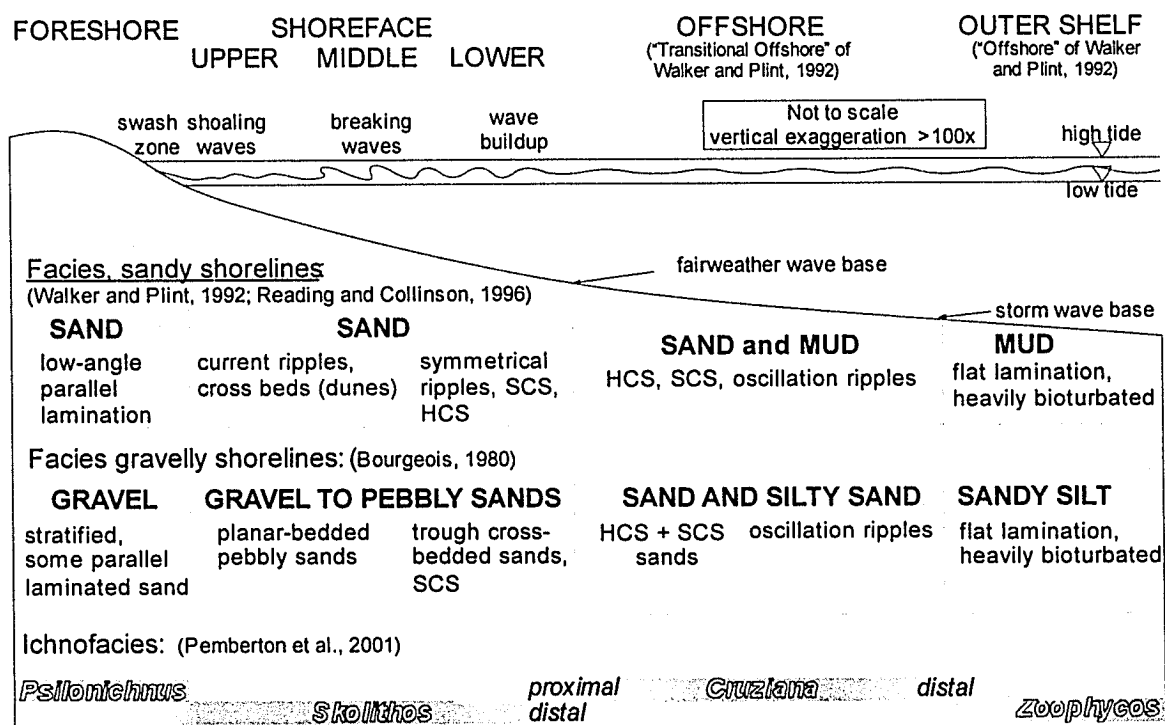


**Figure 26: Shoreface models. A: Traditional tripartite classification scheme (after Dalrymple *et al.*, 1992); B: Triangular model modified to show genetic changes in environments relative to changing sea levels (after Boyd *et al.*, 1992); C: Plan view of coastal environments distributed relative to major influences on coastal morphology; sea level change, sediment input, wave and tidal energy (modified from Boyd *et al.*, 1992).**

estuaries, barrier-lagoon systems) can be displayed opposite their typical regressive/prograding shoreline corollaries (e.g., tidal flats, deltas, and strandplains).

By these classifications, the coastal system represented by the Comox Formation units in the study area is a transgressive strandplain type (Johnstone *et al.* 2006). Although typically associated with regressive coasts, strandplains can form in transgressive settings if there is an abundant sediment supply (Reading and Collinson, 1996). Further, strandplain-type shorelines can develop adjacent to more traditional barrier-lagoon type transgressive shorelines, and may be difficult to distinguish from the marine component of barrier islands. In actuality, thick transgressive shoreface deposits are commonplace along tectonically active margins (Bourgeois, 1980).

Morphologically, strandplain coasts are linear and generally exhibit low gradients. Sandy shoreface systems may have near-horizontal platforms above sea level, steepening towards the beach where gradients are typically in the range of 1:8. Upper shoreface gradients are generally quite low, in the magnitude of 1:200, shallowing with depth to gradients as low as 1:2000 (Walker and Plint, 1992). Generally, the deposits of these shorelines fine distally, although several exceptions to this rule are outlined below. The shoreline system has been divided into subenvironments based on tide range and wave influence (Figure 27; after Walker and Plint, 1992; Reading and Collinson, 1996). The backshore is the area above the mean high water line, and is only marine influenced during storm



**Figure 27: Cross-section of model shoreface, displaying partitions defined by differing wave energy conditions, facies typical of sandy and gravelly coasts, and typical ichnofacies (in non-gravelly substrates). Based on the models described by Bourgeois (1980), Walker and Plint (1992), Reading and Collinson (1996), with ichnofacies ranges after Pemberton et al. (2001)**

events or very large spring tides. The foreshore is the area between mean high and mean low tide levels (*i.e.* the “intertidal” region). The shoreface is the region between the foreshore and the deepest level influenced by “fair-weather” waves, typically 5-15 m (up to 25m in open oceans) and is where most day-to-day sediment transport takes place (Komar, 1976). The offshore (or “transitional offshore” of Walker and Plint, 1992) is a region defined by suspension settling during fair-weather conditions, although intermittent storm wave activity modifies or may completely erode, fair-weather deposits. The outer shelf (or “offshore” of Walker and Plint, 1992) begins below the mean storm wavebase.

## Shoreface Facies Models

The main agents of sediment transport for strandplain type coasts are longshore drift or coastal current drift. For this type of coastline to form in a transgressive setting, there generally must be a large sediment supply that is constantly renewed (Reading and Collinson, 1996). The sediment budget is one where sediment is constantly supplied to the shoreface laterally along the beach by longshore drift, with net sediment transport in an onshore direction during fair-weather conditions. During storm events, the same sediment is removed from the shoreface and foreshore, and is transported towards the offshore transition and shelf areas (Walker and Plint, 1992).

Facies typical of the foreshore reflect the constant reworking of the beach sediment by wave swash. Deposition is largely restricted to fair-weather conditions, as storms lead to significant foreshore erosion (Komar, 1976). On sandy beaches, these deposits are characterized by well-sorted sands that are low-angle parallel laminated, with a shallow dip seaward reflecting the slope of the beach (Reading and Collinson, 1996). Local cross-lamination may also be present, as a result of lateral migration of beach structures. These will typically dip seaward, but may have varying longshore components (Komar, 1976). The very high energy conditions and loose, constantly reworked substrate tend to make preservation of biogenic structures very rare. However, the trace *Macaronichnus segregatis* may form dense mono-specific suites in this setting (Saunders and Pemberton, 1986; Saunders *et al.*, 1994).

The shoreface can be subdivided into upper, middle, and lower parts, on the basis of the prevalent type of wave action that typically takes place (Figure 27). The lower shoreface is where fair-weather waves begin to influence the sediment-water interface, and oscillatory wave action leads to symmetrical ripples. The middle shoreface is the zone of breaking waves, and the upper shoreface the zone of shoaling waves, resulting in wave-forced currents and a high-energy environment, with sediment calibres the largest of the entire shoreline (Komar, 1976). The shoreface is also a zone where conditions vary considerably between storm and fair-weather conditions. Although it is the fair-weather deposits which define the subenvironment, very little of these fair-weather deposits may be preserved in a storm-dominated environment. Recognition of fair-weather deposits and storm-condition overprints is fundamental to building a shoreface facies model (MacEachern and Pemberton, 1992; Pemberton and MacEachern, 1997; Bann and Fielding, 2004).

Within the upper shoreface, translatory wave motion during fair-weather conditions result in seaward-dipping low-angle parallel lamination and multi-directional high-angle trough cross-lamination formed by dunes, commonly mantled by asymmetrical ripples indicating on-shore and longshore current directions (Reading and Collinson, 1996). Trace fossils are rarely abundant in this setting, and diversity is commonly low. The constant shifting of sediment leads to poor preservation of any but the most deeply penetrating structures, (*e.g. Ophiomorpha, Conichnus, Diplocraterion*) typically corresponding to the *Skolithos* ichnofacies (Pemberton *et al.*, 2001). These fair-weather deposits are

commonly scoured and largely removed by storm processes. Storm events are primarily erosive, and re-initiation of deposition during subsequent fair-weather conditions results in amalgamated beds that commonly feature coarse-grained basal lags (Niedoroda *et al.*, 1985).

The middle shoreface is a zone where fair-weather waves build up to breaking, and wave orbits become progressively more elliptical near the base, with nearly horizontal to-and-fro action. As a result, high-angle cross lamination becomes less common with depth, to be replaced with small-scale, oscillation ripples (Komar, 1976). Ichnology of the middle shoreface is dominated by the archetypal *Skolithos* Ichnofacies, representing mostly vertical to subvertical dwelling burrows of suspension feeders and passive carnivores, and although diversity is typically low, burrow intensity may be high (MacEachern and Pemberton, 1992). In the lower shoreface, oscillatory ripples are of lower energy and larger wavelength, and deposits generally fine seaward as material transported landward by higher energy waves are returned by lower-energy rip currents which allow differential settling from the sediment cloud (Niedoroda, 1985). The ichnology in these fair-weather deposits is typically of high intensity, and transitional between a distal expression of the *Skolithos* Ichnofacies and a proximal expression of the *Cruziana* Ichnofacies, with increasing numbers of suspension feeding and grazing structures concomitant with a general reduction in wave energy and sediment grain size (MacEachern and Pemberton, 1992; Pemberton and MacEachern, 1997; Pemberton *et al.*, 2001; Bann *et al.*, 2004).

Depending on the frequency and intensity of storm events, fair-weather deposits of the shoreface may be partially or completely scoured and removed by high-energy storm waves, and tempestite deposits may dominate the middle and lower shoreface (Pemberton and MacEachern, 1997; Bann and Fielding, 2004). Although these storm deposits may represent the majority or all of the succession in a storm-dominated setting, they may be highly variable due to varying storm intensities (Pemberton and MacEachern, 1997). In the middle shoreface, these deposits are predominantly swaley cross-stratified (SCS) well-sorted sands, with lesser hummocky cross-stratification (HCS). In the lower shoreface, HCS becomes more common, as the net movement of sediment during storm events is toward the lower shoreface, and preservation of hummocks is favoured (Dott and Bourgeois, 1982). Thin, coarse-grained lags are common, as are oscillation ripples at the top of bedsets representing waning-flow conditions. Ichnology is generally of lower intensity and diversity than in fair-weather suites, although post-storm opportunistic colonization of the storm beds may lead to higher intensities near the tops of amalgamated bedsets.

The transition zone between the shoreface and the offshore is a region which may experience alternation from high energy storm waves and very low energy suspension settling during fair-weather conditions. With significant storm influence, the resulting deposits typically consist of alternating fine-grained sandy muds with intense bioturbation and upward-fining beds of parallel laminated fine-grained sands, representing the waning conditions of storm events (Komar, 1976). Structures include oscillation and combined-flow ripples, ripple cross-

lamination, and small-scale HCS (Walker and Plint, 1992; Bann and Fielding, 2004). The ichnology of this transition zone is dominated by deposit feeding and grazing structures characteristic of the *Cruziana* Ichnofacies, although some suspension-feeding structures of the *Skolithos* Ichnofacies may also be present, particularly in better sorted sandy units, reflecting opportunistic colonization of tempestites (MacEachern and Pemberton, 1992; Pemberton and MacEachern, 1997). Fugichnia may also be common in the storm-related beds. The intensity of bioturbation and diversity of ichnofossils generally increases along with the dominance of muddy substrates seaward, with the gradual transition into shelf conditions.

The offshore is characterized by reduced storm energy, and storm events become increasingly less erosional and more depositional with depth. The substrate is mud-dominated, with distally fining and thinning sandy interbeds (representing distal tempestites). Structures are largely limited to wave ripples and flat lamination, although rare, very large storm events can introduce well-sorted, small scale HCS sands (Komar, 1976; Reading and Collinson, 1992; Bann and Fielding, 2004). With increasing depth, deposit-feeding structures are gradually replaced by grazing and foraging structures, represented by a transition from the *Cruziana* Ichnofacies to the *Zoophycos* Ichnofacies (Pemberton and MacEachern, 1997; Bann and Fielding, 2004).

These typical facies are most commonly preserved as a sanding-upward succession related to the progradation of the shoreface during sea level highstands, or as isolated sand bodies enclosed by marine mudstones, if



preserved during lowstand progradation (*cf.* Walker and Plint, 1992).

Nevertheless, preservation during transgression is also possible, with a basal sand layer (representing the high-energy upper shoreface) advancing landward and passing upward into progressively more distal and muddier facies (Niedoroda *et al.*, 1985). Bourgeois (1980) describes a 200m thick sequence from the Upper Cretaceous of southern California that follows this pattern. From the shoreface upward, grain sizes, abundance of pebble lenses and thicknesses of hummocky cross-stratification all decrease. Concurrently, burrowing intensity and trace fossil diversity, symmetrical-ripple lamination, and intercalated plant debris all increase upward.

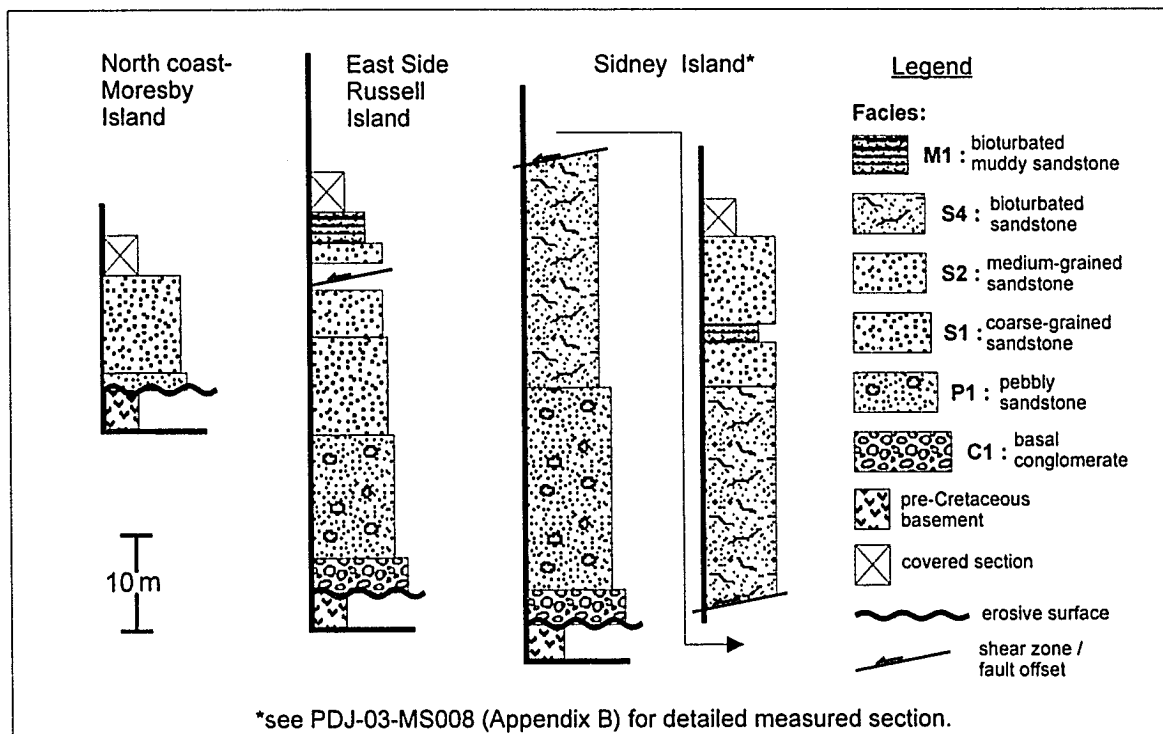
### **Facies Association 2: Storm-Dominated Shoreface.**

There are several locations within the field area where the entire Comox Formation succession displays upward fining from a conglomerate or coarse sandstone basal layer overlying the unconformity through to finer-grained sandstone and into heterolithic sandstone-mudstone units toward the top (Figure 28). Where coarse-grained basal units exist, they have been assigned to the Benson Member of the Comox Formation, although the majority of the deposits are assigned to the Saanich Member.

The simplest succession is exposed on the north shore of Moresby Island, where a discontinuous basal conglomerate less than 1m thick passes into approximately 10 m of parallel laminated, coarse-grained sandstone of Facies S1 with a well-preserved monospecific assemblage of *Macaronichnus segregatis*. Such trace fossil suites are distinctive of the foreshore-upper shoreface transition

(*cf.* Saunders and Pemberton, 1986; Saunders *et al.*, 1994). The top of this succession is not exposed.

Russell Island displays a continuous transgressive succession from the basal unconformity to offshore-transition deposits (Figure 28). Less complete successions are also exposed along the east coast of Portland Island, on the northeast shore of Brethour Island, on the Saanich Peninsula, the north half of Coal Island, and the Sidney-Halibut-Mandarte island group. Although local variations exist, the succession is similar between these locations, and is comparable to the basal Comox Formation successions described from nearby Saltspring Island (Johnstone *et al.*, 2006).



**Figure 28: Typical expressions of Facies Association 2.**

On Russell Island, the basal conglomerate (Facies C1), ranges from less than 1m to approximately 4m in thickness, passing upward into several metres of pebbly sandstone (Facies P1). In turn, this fines upward into coarse- or medium-grained sandstones with varying levels of bioturbation. On Russell Island and the Saanich Peninsula, this sandstone is coarser-grained and displays both trough cross-beds and parallel lamination (Facies S1), before passing into medium-grained sandstone with moderate intensity bioturbation representing a low-diversity expression of the *Skolithos* Ichnofacies (Facies S2). On Sidney and Brethour Island, the lowermost sandstone is medium-grained with thin silty laminae, and alternates between low-angle parallel lamination in the better-sorted sandstones and more intensely bioturbated siltier sandstones (Facies S4). This facies occurs above the Facies S2 sandstones in the other localities. In all localities, Facies S4 fines upwards gradually into muddier facies (*i.e.*, Facies M1 or M2), with the proportion of bioturbated silty mudstones increasing relative to the well-stratified sandstone interbeds.

This succession is interpreted to represent deposition on a storm-dominated, rocky shoreline that was drowned by transgression. The basal conglomerate represents a lag on a ravinement surface that either amalgamated with or incised through an earlier sequence boundary. This ravinement surface migrated landward during transgression. The coarser sandstone and pebbly sandstone above this discontinuity represents high-energy foreshore settings, as indicated by the large grain sizes, presence of pebbles and granules on lag surfaces, and the monospecific *Macaronichnus segregatis* suites. The continued

upward fining, increase of silty and muddy interlaminae, increasing HCS preservation, and progressively more diverse and intense bioturbation all support gradual continued deepening to an offshore setting.

At most localities, the top of this succession is not exposed, being covered by the present day sea. Exceptions to this occur on the north shore of the Saanich Peninsula and the north shore of Coal Island. In both of these locations, Facies S4 bioturbated sandstone continues to fine upwards into mud-dominated Facies H2. The thin-bedded heterolithic units exposed on the very top of this succession are assigned to Facies H3 and designated as Haslam Formation (and are described in more detail below in the section on submarine fan facies).

The amalgamated storm deposits on the Saanich Peninsula, Sidney Island, and nearby Saltspring Island are thick and generally coarse-grained. Bedset and bed thicknesses are similar to those described from the Eocene shoreface deposits of Oregon (Chan and Dott, 1986), and the Upper Cretaceous of California (Bourgeois, 1980), whereas they are several times thicker than is typical of the Western Interior Seaway (Frey and Howard, 1990; Duke *et al.*, 1991). The preservation of these thick successions also suggests a long, persistent transgression coupled with abundant supply of sediment. Johnstone *et al.* (2006) describe a storm-swept shoreline open to the full force of proto-Pacific storms, and a steadily increasing accommodation space.

## **Barrier-Barred Coastline.**

Several localities within the study area assigned to the Saanich Member of the Comox Formation contain alternating sandstone-dominated and heterolithic sandstone-mudstone successions with a combination of sedimentary and fossil characteristics suggesting deposition along a barrier-barred coastline. This comprises a suite of environments most common in transgressive settings, and in settings where wave processes dominate over tidal processes (Heward, 1981; Boyd *et al.*, 1992; see Figure 26).

The two expressions of this coastline type are wave-dominated estuaries and barrier island complexes. An estuary is a semi-enclosed coastal environment where fluvial and marine depositional systems interact. They are generally the seaward portion of a drowned fluvial valley system (Boyd *et al.*, 1992), where progradation of the fluvial delta has not kept pace with transgression, and a sediment sink has formed between the fully marine and fluvial settings (Dalrymple, 1992). In contrast, barrier island complexes do not have significant direct fluvial input, and are instead defined by linear, coast-parallel, shifting sand bodies that separate muddy lagoonal sediments landward from muddy offshore sediments lying basinward (Reinson, 1992). Both wave-dominated estuaries and barrier island complexes rely on micro- to meso tidal conditions (generally less than 4 metres), and an abundance of longshore sediment supply in order to form (Kraft and Chrzastowski, 1985). The primary morphologic difference between the two coastal embayment types is the shoreline-parallel nature of the lagoons behind the barrier island system, whereas central basins of estuaries are

generally oriented perpendicular to the shoreline and display bayhead delta deposition into them from river-sediment discharge into the system..

Both depositional systems feature some type of shore-parallel sediment body (*i.e.* the barrier), which includes: a seaward-facing beach and shoreface system; a sediment platform that is at least partially exposed and may feature sand dunes; washover fans and tidal deltas that cross-cut the barrier; and embayed water bodies with varying water levels and salinities (Boyd *et al.*, 1992). Oertel (1985) defined the six elements of the barrier island system that influence the morphology of the barrier island system (Figure 29). These are the mainland, the backbarrier lagoon, the inlets and inlet deltas, the barrier island, the barrier platform, and the shoreface.

The backbarrier lagoon may be an open-water lagoon (which maintains a constant water surface through tidal cycles) or an expandable lagoon (which may expand or contract significantly during tidal cycles). Such settings have a significant effect on the growth of lagoon-bordering marshes and mangroves. Most sedimentation within the lagoon centre is muddy, although significant volumes of sand can be introduced by inlet channels and deltas, and by fluvial systems in the estuary setting. Wave reworking along the shallow lagoon margins may also concentrate sand. The barrier island itself commonly contains sand dunes, washover deposits, and locally salt marshes. The seaward face of the barrier has the same morphology from the foreshore to the offshore as a strandplain shoreline, as previously described in the Storm-Dominated Shoreline section above.

## **Facies models**

Facies models described here represent the mainland outward towards the seaward face of the barrier. Facies typical of barrier island systems are described, with reference made to estuaries only as to how they compare with lagoonal facies. Within the study area, no definitive evidence of estuarine influence (*e.g.* fluvial channels, bay-head delta deposits) was identified. Nonetheless, this lack of preserved evidence does not eliminate an estuary as a possible setting.

Sediments within back-barrier lagoons are dominated by muds and sandy muds, are generally bioturbated, and commonly feature symmetrical ripples (Oertel, 1985). These muds may contain varying amounts of intercalated marine sand from washovers or inlet deltas, and fluvial sands in the case of estuaries. Discrete beds of sand result in heterolithic intervals characterized by lenticular, wavy or flaser bedding. Marshes may form along the margins of lagoons, especially in expandable lagoons, resulting in rootlets and the formation of thin peats within the muds (Oertel, 1985; Boothroyd, 1985). Regardless of marsh formation, the muds deposited in lagoons associated with humid or temperate climates are commonly rich in organic matter (Reading and Collinson, 1996). In addition to this, restricted seawater mixing, and intermittent precipitation and fluvial input lead to markedly fluctuating salinities. For these reasons, trace fossils suites are typically of low-diversity, with bioturbation of varying intensities, and feature morphologically simple ichnogenera and diminished trace sizes (Beynon *et al.*, 1988; MacEachern and Pemberton, 1994; Bann *et al.*, 2004).



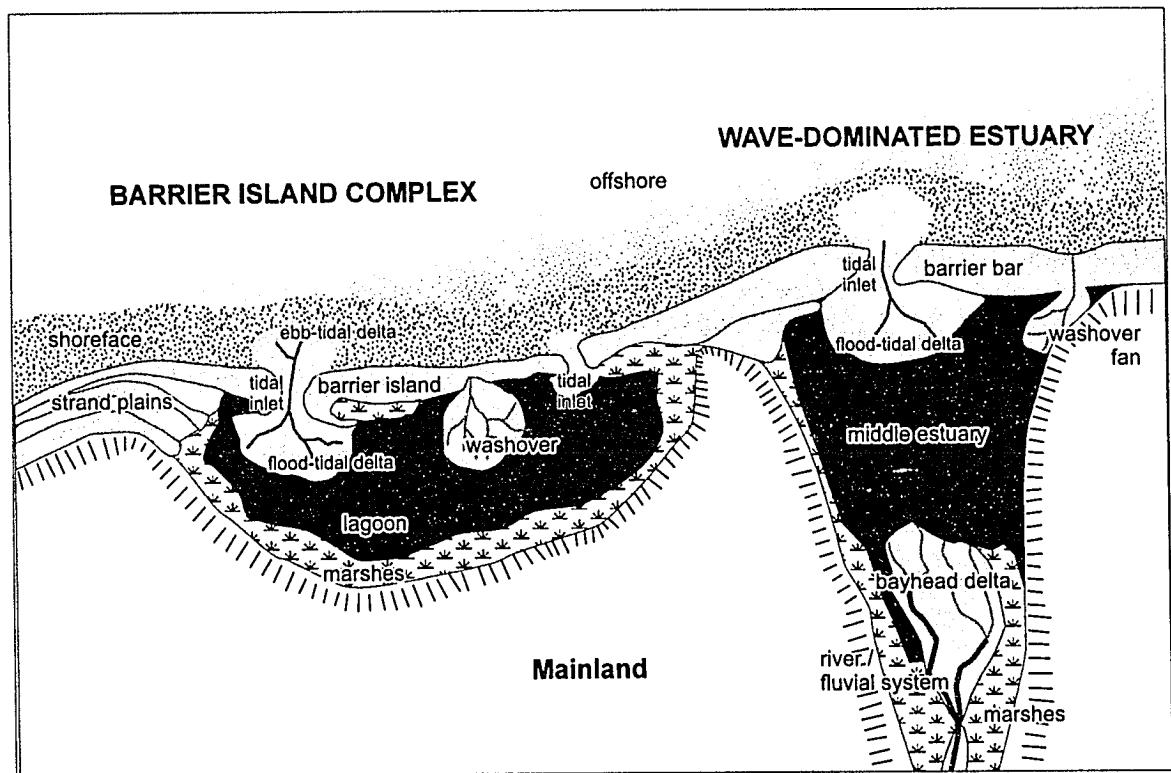


Figure 29: Comparative morphology of barrier island complex and wave dominated estuaries, and major components of each system as described by Oertel (1985) and Reinson (1992), and Boyd et al. (1992).

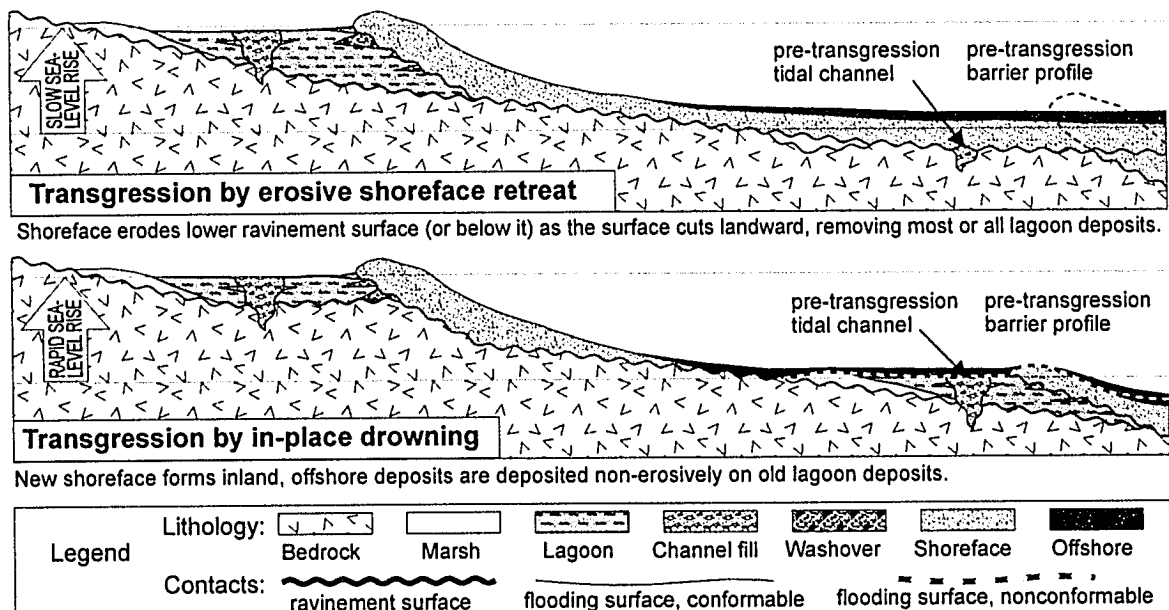


Figure 30: Ravinement of transgressive barrier island complex and effect of relative rate of sea level rise as interpreted by Kraft and Chrzastowski (1985) and Reading and Collinson (1986). The two models displayed represent end-members in a continuum which exists along irregular transgressive shorelines.

Tidal inlet channels and flood tidal deltas form within lagoons, where breaches in the barrier island complex allow wave- or tide-driven water and shoreface-derived sands to be transported into the lagoon. Such channels are erosive features, and once a channel system is established, it may act to transport water both into and out of the lagoon, depending on tide and wave conditions. As a result, current-generated structures produced within the channel-delta system may display bimodal flow patterns (Boothroyd, 1985). Facies common to the channels record waning energy flows, commonly with a coarse basal lag (possibly with angular rip-up clasts) and landward-directed trough cross-bedding, passing upward into bi-directional cross-bedding with or without preserved ripples and mud drapes at the top (Oertel, 1985; Reinson, 1992). The channels lead to deltas draping over and interfingering with the lagoonal muds, with thin sheet sands or current ripple laminated sands thinning and fining landward, leading to flaser and wavy heterolithic bedding (Oertel, 1985).

In microtidal settings, inlet channels and deltas may be sporadically distributed, with open water only entering the lagoon during large storm events. During these events, waves may breach the barrier for the duration of the storm (and for some time after until the beach is healed), resulting in a washover fan (Reading and Collinson, 1996). Washover fans are relatively thin and lobe-shaped, with planar erosive bases, subhorizontal planar stratification, and small to medium-scale cross-bedding, although the top may be re-worked into oscillation ripples (Reinsen, 1992). The same breach may be used by several

washover events though flow is almost exclusively land-ward, and washovers generally lack the bimodal cross bedding of inlet deltas.

The barrier island is a complex system with a seaward facing beach-shoreface system similar to a strandplain beach, eolian dunes and washover deposits variously affected by vegetation, and a landward facing beach-marsh system (Oertel, 1985). The deposits of the seaward-facing beach system are the same as those seen in a strandplain beach (see Storm-Dominated Shoreline section above), and it is the shoreward transport of sands that is responsible for the growth of the barrier island (Reading and Collinson, 1996). The beach commonly sits on a ravinement surface, with barrier island and washover sands eroding lagoonal muds and marsh deposits (Boothroyd, 1985).

Wave-dominated estuaries comprise three distinct depositional zones: an inner (landward), high-energy fluvial zone (bay-head delts); a low-energy central zone; and a high-energy outer zone (estuary mouth/barrier) where wave-driven processes dominate. The two most seaward zones of such estuaries are similar to barrier island-lagoon complexes, as they are formed by similar processes (Boyd *et al.*, 1992). The effects of fluvial input may be preserved in deposits of all three zones however, leading to more complex facies associations. This is particularly true in the central basin or "lagoonal" zone. Features may include thick, coarsening-upward sand bodies, with seaward directed cross-bedding reflecting flood events, or ichnology displaying increased biotic stress caused by rapidly changing salinities and water oxygen levels, related to marine-fluvial mixing (Beynon *et al.*, 1988; Reinsen, 1992; MacEachern and Pemberton, 1994).

Most barred shorelines form during marine transgressions, and the rate of transgression along with the sediment supply at the shoreface influences the amount of preservation displayed in the rock record (Figure 30). This is partially the result of the two ravinement surfaces that are formed as the barrier island system migrates landward; one on the mainland at the base of the fringing marsh or landward edge of the lagoon, and the other at the landward edge of the barrier island itself (Kraft and Chrzastowski, 1985). Transgressive styles can be described in relation to two end-member types: in place drowning and shoreface retreat (Reading and Collinson, 1996). A continuum exists between these end members, and both end-member types may exist along the same shoreline, as varying shoreline topographies and sediment supplies affect the local transgression rate (Kraft and Chrzastowski, 1985).

If transgression is slow, the barrier island slowly migrates across the lagoon, with the lagoon, in turn, migrating inland (Figure 30a). During this form of erosive shoreface retreat, the ravinement surface created at the landward edge of the shoreface may erode through backbarrier deposits. If the migration is slow enough, all evidence of a lagoonal system may be removed by this erosion (Heward, 1981; Reading and Collinson, 1996). The basal deposits of the succession will comprise upper shoreface coarse clastics, possibly with a thin gravel lag, and these deposits may be indistinguishable from those of a transgressive strandplain shoreline.

During rapid transgression, a barrier complex may be preserved place, with the coastline rapidly displaced landward and a new shoreface forming at the

lagoon/mainland interface (Figure 30 b). This “in place drowning” of the entire complex results in a high preservation potential for all facies. A typical sequence would have a basal ravinement surface draped by marsh or muddy lagoonal deposits, with varying amounts of intercalated sandstone. This surface may be cross-cut by tidal channels and draped with tidal deltas or washover deposits. A ravinement surface above this lagoonal deposit would be covered by foreshore to upper shoreface deposits, which fine upwards through shoreface to offshore deposits, reflecting a gradational deepening (Boothroyd, 1985; Pemberton *et al.*, 2001).

### **Facies Association 3: Barrier-Island Complex.**

There are several locations within the study area where the Saanich Member of the Comox Formation comprises thick, amalgamated sandstone packages, interspersed with finer-grained units of varying thickness and character. The most contiguous sections of this type are exposed on Brethour Island, Comet Island, the area around Tsehum Harbour from Armstrong Point to southern Coal Island, and on Forrest Island. Each succession is discrete (with only vague correlation possible between the islands), but the overall pattern is distinct. The sandstone units are largely erosively based, and finer-grained units are either muddy and carbonaceous, or comprise thin-bedded heterolithic sandstone-mudstone packages with minor internal gradations (Figure 31).

The succession on Forrest Island is complex. There Facies S2 sandstones at the base of the exposed section have medium-scale thicknesses of graded bedding. This unit grades into Facies H1 sandstone and mudstone,

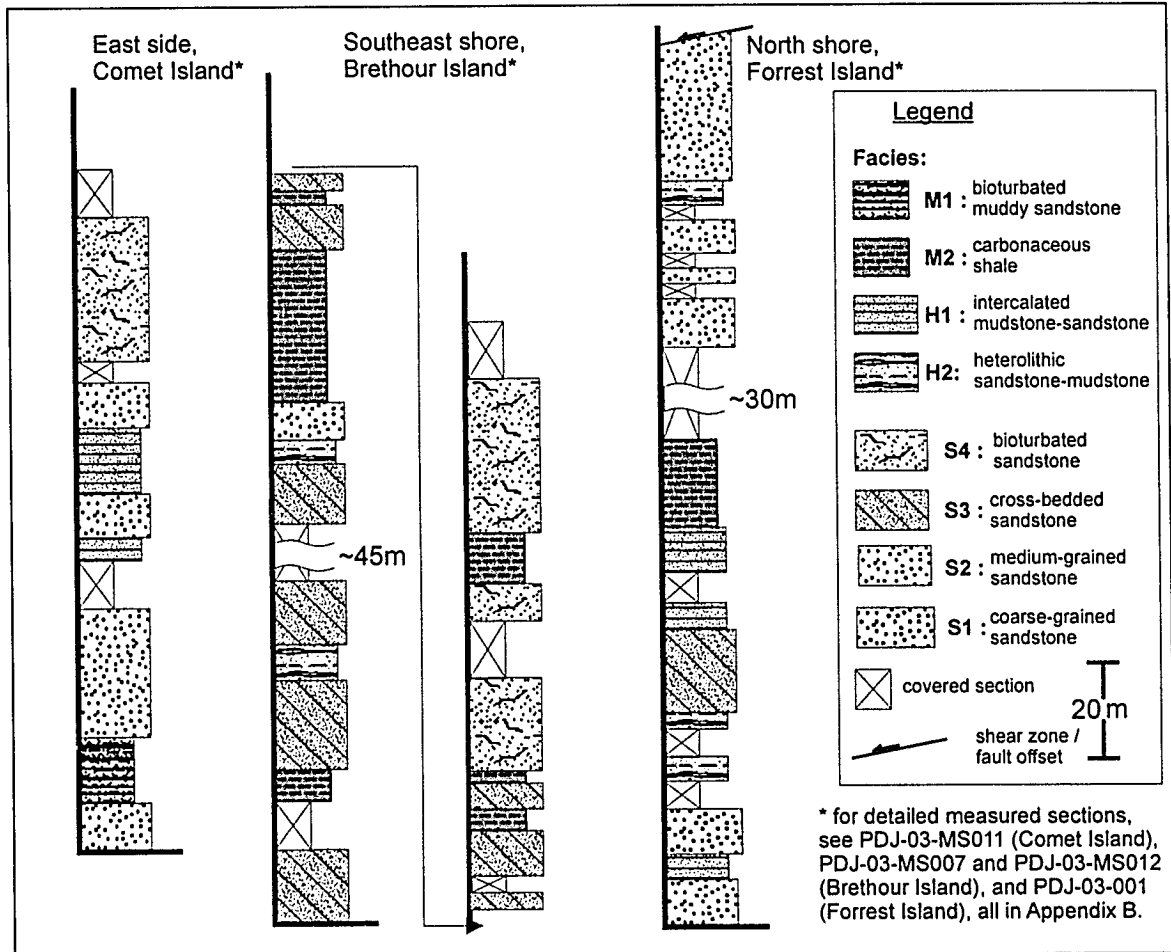


Figure 31: Typical expressions of Facies Association 3.

which in turn fines and becomes increasingly carbonaceous upsection. An eight-metre thick sandstone unit erosively overlies this carbonaceous mudstone, with a pebble lag at the base. The sandstone also contains several pebbly internal erosion surfaces and grades to fine-grained sandstone (Facies S1). The next units exposed above this are heterolithic sandstone-mudstone, with wavy to flaser bedding (Facies H2), and sections which appear to represent tidal cycles. These in turn are erosively overlain by another succession of thickly cross-bedded sandstones (Facies S3).

This cycle of fining upwards into carbonaceous mudstones, only to be overlain by thick sandstone successions with erosive bases is repeated 3 more times over 130 m of section. Bioturbation increases with the proportion of mudstone, although overall it is rather sparse, and limited to a few simple ichnogenera, generally *Thalassinoides* in mudstones, and *Ophiomorpha* in sandier substrates. Larger fragments of wood debris and rhizoliths contain *Teredolites*. Finally, at several sandstone-over-mudstone interfaces, the upper sandstone appears to passively infill firmground *Thalassinoides* in the lower unit.

This succession may represent a deepening lagoonal setting, with deposits becoming finer-grained and more carbonaceous with increasing water depth. Alternately, barrier development may have served to reduce the amount of sand introduced during tidal cycles. Generally low biodiversity due to stresses imposed by salinity fluctuations and/or reduced oxygen is consistent with restricted lagoons (Beynon *et al.*, 1988; MacEachern and Pemberton, 1994; Bann *et al.*, 2004). These muddy units are cross-cut by several tidal channel

and/or washover deposits, represented by well-sorted coarse-grained sandstones with local gravelly lags, and by the passively infilled burrows in the muddy substrate. The presence of *Teredolites* in xylic substrates and woody debris suggest deposition in a saline setting (Savrda, 1991; Savrda *et al.*, 1993). Upward-coarsening successions suggesting bay-head delta progradation were not identified, further making the interpretation of an estuarine setting less favourable.

The well-exposed succession on Brethour Island is similar to that on Forrest Island. The lowest sandstone-over-mudstone interface in the succession contains firmground *Thalassinoides* in the lower unit (Facies M2), passively infilled with the sandstone of the overlying sandstone unit (Facies S3), as well as abundant mudstone and coal rip-up clasts in the base of the sandstone. At one location, a root mound crosses this interface, and is bored with *Teredolites*, which are in turn filled by the sandstone (Figure 20a). Farther up section, a thin sandy section has abundant leaf fragments, and the muddy unit above this (Facies M2) features several dozen root mounds with attached tree stems, that are parallel to one another and cross-cut mudstone-sandstone interbeds, indicating apparent life position (Figure 15d). This wood material is not bored with *Teredolites*. Several cycles of heterolithic mudstone-sandstone (facies M2 or H2), each tens of metres thick, erosively capped by "clean" well-sorted sandstone (Facies S3), comprise the section on Brethour Island, much like that on Forrest Island. Near the top of the section, the uppermost heterolithic unit (Facies H2) coarsens upward for several metres, becoming sand-dominated



relative to the predominantly muddy character displayed lower in the section. This is truncated by a loaded, erosive contact with the overlying sandstone. This sandstone (Facies S4) contains granules and small pebbles concentrated near the base, as well as mudstone and carbonaceous mudstone rip-up clasts. This unit contains bivalve shell fragments, varying levels of bioturbation, and low-angle planar lamination.

This section is interpreted to represent a setting similar to that described on Forrest Island. The fine-grained and heterolithic units represent low-energy lagoonal settings, with abundant organic detritus introduced. Locally, the lagoon was marshy, with several *in situ* tree stumps preserved. The thick sandstone successions are invariably erosively based and well sorted, and include sedimentary structures that suggest tidal delta or washover deposits. The top of this section, however, may represent transgression of the barrier island over the lagoonal deposits. The increase in sand content in the heterolithic unit may represent the approaching barrier, which introduced more washover, flood-tidal delta, or wind-blown sand into the lagoon at the shoreward-facing barrier beach, forming a type of "wind tidal flat" (*cf.* Davis, 1996). The bioturbated, well-sorted sandstone above this is interpreted to represent the shoreface component of the barrier island itself. The upper portion of this succession, coupled with a thick preserved section of shoreface and transitional-offshore deposits, is preserved along strike on Comet Island.

## **Submarine Fan.**

Submarine fans are large, positive-relief features found on the sea bed adjacent to continental shelves, and represent the primary coarse-siliciclastic depositional system of the deep ocean (Stow *et al.*, 1996). They are formed by cyclic sediment-gravity flows, which transport large amounts of mixed sediment from shelf or delta settings towards the basin, generally along submarine canyons or channel systems.

Fans can be formed, and their deposits preserved, in ocean depths from storm wave-base to the abyssal depths (Walker, 1992). Although their name implies a generic morphology, submarine fans rarely form true conical fans (Shanmugam and Moiola, 1988). Their shape is largely affected by basin topography, geography of source areas, and even Coriolis forces, resulting in geometries almost as varied as those of fluvial deltas (Clark and Pickering, 1996). Submarine fans range from small, local systems of a few square kilometres, to tens of thousands of square kilometres. The massive scales of some fans make recognition of their features in the ancient record (*e.g.*, from outcrops and drill core) challenging.

Although it is compelling to compare submarine fans and channel systems to their subaerial counterparts (deltas and rivers, respectively), there are significant differences between the systems (in addition to the aforementioned scale issue), as outlined by Clark and Pickering (1996). Rivers only exceed bankfull discharge during floods, whereas submarine flows commonly exceed their banks, resulting the phenomenon of flow-stripping (discussed below).

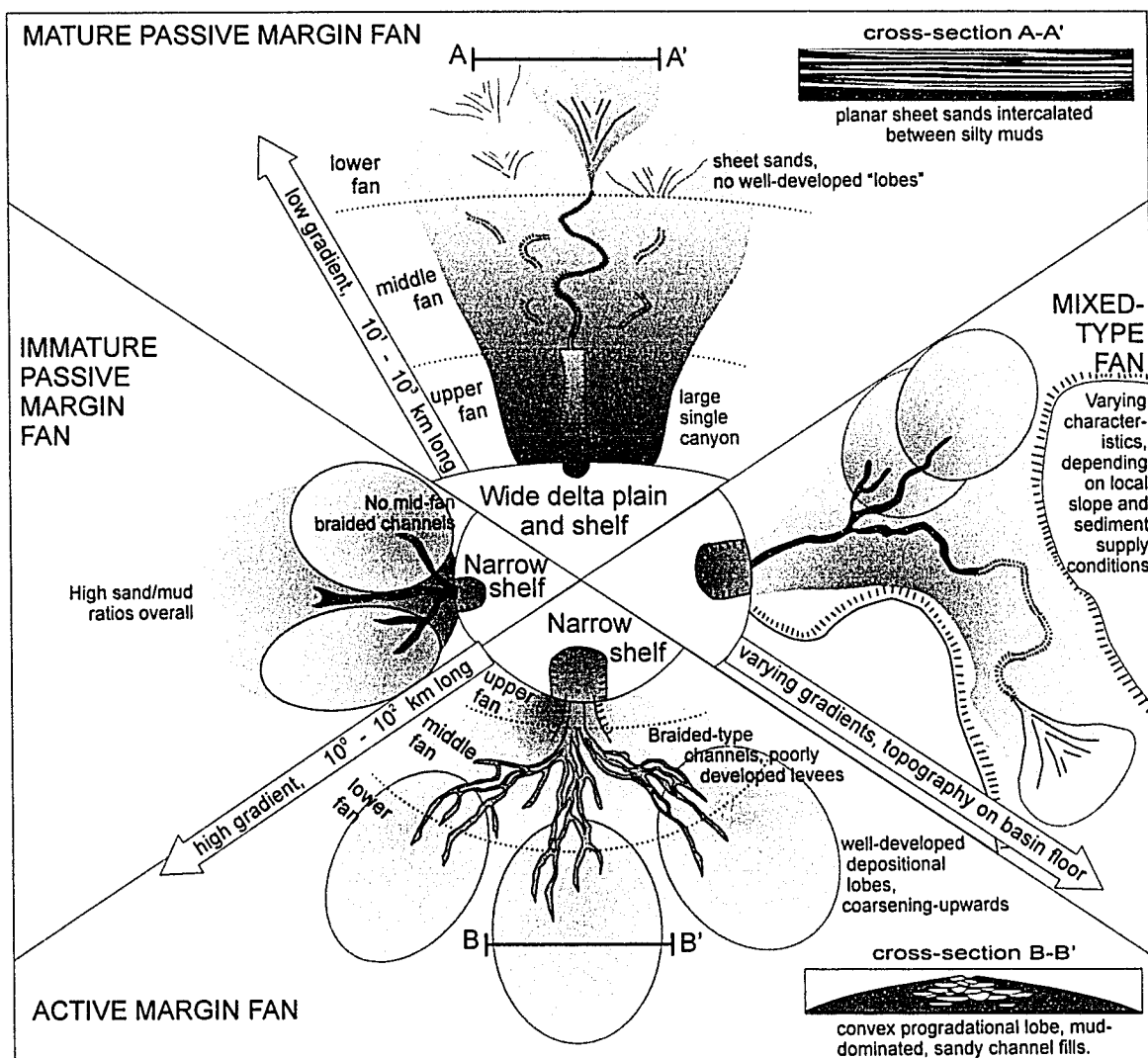
Fluvial flows also do not entrain the overlying medium (air), and are generally in constant flow, whereas entrained media (water) is an important component of most submarine sediment gravity flows, and these flows are highly ephemeral in character.

Morphologically, submarine fans are typically divided into a tripartite scheme of an upper, middle and lower fan. Generally, these correspond to an upper fan containing canyon-like feeder systems, a middle fan consisting mainly of channel-levee complexes, and a lower fan comprising progradational lobes or sheet sands; although these terms are used differently by different workers (Shanmugam and Moiola, 1988). Submarine fans have been classified by various workers using combinations of morphology and dominant sediment type, as well as by tectonic setting (Reading and Richards, 1994).

Reading and Richards (1994; see also Stow *et al.*, 1996, for additional examples and references) used numerous observations of modern systems to erect a "unifying" classification scheme, wherein fan systems with single, multiple, or apron-style "linear" source areas are further delineated by their modal sediment grain sizes. "Mud-rich" fan systems are generally large and elongate, and form on low gradient slopes. They have a valley-type upper fan, a middle fan of channel-levee complexes with very high levees, and a lower fan dominated by sheet sands. "Mud/sand-rich" fans tend to be of a more intermediate size, and are commonly found on steeper slopes below narrow shelves. Their upper fans are typically made up of single feeder channel filled with sand. This divides into distributaries in the middle fan where aggradation over lower lobes strips the

deposits of sand, resulting in muddier prograding lobes in the lower fan. "Sand-rich" fans are intermediate to small in size and are dominated by sand. These rely on a sand-rich shelf with significant sedimentation rates (typically related to deltas). The dominance of sand-sized sediment calibres results in weak levees, leading to braided-channel morphologies in the middle fan, and rapid aggradation that limits the growth of progradational lobes in the comparatively diminutive lower fan. Finally, "gravel-rich" fans are generally associated with coarse-grained fan-delta systems whose morphology they mimic (with diminutive size and high gradients), although they fine distally into fine-grained, prograding lobes typical of other submarine fans.

Shanmugam and Moiola (1988) modified the scheme introduced by Bouma *et al.* (1985), which classifies fans by tectonic setting. The scheme also somewhat simplifies the tripartite division of the fan components (Figure 32). Fans developing on mature passive margins tend to be mud-rich with low gradients, and lack well-developed prograding depositional lobes. They feature an upper fan with a large, single canyon; a middle fan with well-developed channel-levee complexes (due to the high stability of the fine-grained levee banks), and commonly with a single sinuous active channel; and a lower fan composed of extensive sheet sand deposits and lacking in discrete depositional lobes. Fans on active margins, by contrast, tend to be more compact, with short, steep upper fans, middle fans with braided channel systems, and lower fans comprising numerous coarsening-upward depositional lobes. Transitional between these end-member types are those fans developed on immature



**Figure 32: Submarine fan types, classified based on tectonic setting of basin margin. Ideal models, modified from classification introduced by Bouma et al. (1985), as modified by Shanmugam and Moiola (1988).**

passive margins that have a high gradient and a high sand/mud ratio. Such fans have well-developed lobes similar to active margin fans, but lack the extensive mid-fan braided channels. Finally, mixed-setting fans include those developed where restrictive basin geometry or complex basin-edge tectonics strongly influence fan development. Fans in these scenarios defy simplified classifications (Shanmugam and Moiola, 1988).

Regardless of fan morphology, the dominant sedimentary process operating on submarine fans are sediment gravity flows, with channelized turbidity currents and debris flows constituting the two dominant flow types (Shanmugam and Moiola, 1988). The low-density turbidity current (and resultant deposition of "Bouma-type" turbidites) is almost universally associated with submarine fans, although this represents only one end-member of a variety of potential flow types in the setting (see Table 2). The other flow type end member is represented by cohesive debris flows. Other mass-wasting processes such as debris avalanches and slumps are locally represented in submarine fans, and have been covered in more detail in the Fan Delta section.

Debris flows are plastic flows of mixed sediment and water, where flow is generally laminar and supported by a combination of dispersive pressures, matrix strength, and buoyancy of clasts within a dense, saturated matrix. They are generally divided into cohesive and non-cohesive flows, the former relying on a muddy matrix with high cohesive strength to maintain the flow, whereas the latter is sandier, and dispersive forces caused by intraclast collisions constitute the primary support mechanism. The non-cohesive type of debris flow requires high

**Table 2: Flow types typical of submarine fan settings.**

	Debris Flows		Sandy Debris Flows	Turbidity Currents	
	cohesive (mud flows)	non-cohesive (grain flows)		"high-density"	"low-density"
<b>Flow Type</b>	Laminar	Laminar	Laminar	Turbid	Turbid
<b>Rheology</b>	Plastic (Bingham)	Plastic (Bingham)	Plastic (Bingham)	Fluid (Newtonian)	Fluid (Newtonian)
<b>Clast Support Mechanisms</b>	Cohesive strength of matrix; some buoyancy	dispersive pressures; some buoyant lift	matrix strength; dispersive pressure; buoyant lift	fluid turbulence	fluid turbulence
<b>Typical Content</b>	Fine-grained, clay-rich matrix; floating larger clasts	well-sorted sand and gravel	low concentration of mud; some grains; may or may not be large clasts	sand and gravel	medium-grained sand and/or finer
<b>Depositional Model</b>	cohesive freezing	frictional freezing	traction and frictional freezing	collapse fallout, basal freezing, aggradation, then traction, (in that order)	traction followed by suspension settling
<b>Deposits</b>	poorly sorted matrix supporting "plugs" of floating clasts	well-sorted, massive sand and gravel; inverse grading at base	rafted sediments above sandstone; inverse grading of clasts; floating granules in fine-grained sandstone; planar fabrics.	inverse grading to massive sandstone, plane-bed / cross-bedded sands, fluid escape structures (Lowe S <sub>1</sub> -S <sub>3</sub> )	continuous, normally graded sandstone/mudstone beds, Bouma T <sub>A</sub> - T <sub>E</sub> .

Condensed from Lowe (1982), Shanmugam (1996) and Stow *et al.* (1996).

gradients to maintain the flow, and are, therefore, not common in submarine fan settings (Shanmugam and Moiola, 1988). They may be more common in the upper fan on steep canyon walls and shelf edges, especially on active margins where slopes are highest.

Turbidity currents have similarly been divided into two end-member types, termed "high-density" and "low-density" (Lowe, 1982). All turbidity flows involve liquid flow of sediment-water mixtures that are supported by fluid turbulence. The "low-density" end-member involves sand and mud, and through autosuspension, may travel great distances along gentle slopes with very little loss of momentum. The "high-density" end-member on the other hand contains more sand and gravel, and is commonly capped by a "low-density" turbidity current. Lowe (1982) suggested the "high-density" end member may represent a transitional flow type between debris flows and "low-density" turbidity flows (Lowe, 1982).

This classification of low-density *versus* high-density turbidity currents has been challenged in a multi-faceted criticism (Shanmugam, 1996). Concerns include the use of a physical property which cannot be practically measured (density of the flow) as the dividing line; the confusion inherent in modifying the name of one end member to describe a transitional form; the questionable validity of describing a "transitional" state between a Newtonian fluid and a Bingham plastic; and several problems related to the description of transport mechanisms by the relating them to depositional mechanisms nearby, particularly when the relationship between the two mechanisms are poorly understood. Shanmugam (1996) prefers the term "sandy debris flows" for the



transitional flow type between debris flows and turbidity currents, and outlines the properties of these flows and their expected deposit types. Both terminologies are outlined in Table 2, as they both commonly appear in the literature, especially where they are related to facies models for submarine fans.

### **Facies Models.**

The typical sequence of depositional structures developed in submarine fans were described in detail by Bouma (1962) and Bouma *et al.* (1985), and are applied almost universally, although they only truly apply to low-density turbidity currents and their deposits: mud-sand turbidites (Stow *et al.*, 1992). Subsequent models have been developed for coarser-grained turbidites (Lowe, 1982), and mud-dominated turbidites (Stow and Shanmugam, 1980).

The classic “Bouma sequence” involves sediment fully entrained by fluid turbulence that begins to collide and settle as flow energy begins to wane. At some point, shear stress is no longer able to overcome friction between the colliding grains, and the lower part of a flow, where coarser sediment has settled, “freezes” in place, depositing “massive” sand (unit T<sub>A</sub>). The reworking of this massive sand and traction deposition at the base of the overlying flow results in upper flow regime planar bed lamination of sands (unit T<sub>B</sub>), which may, in turn, be reworked or draped by ripple cross-laminated sands (T<sub>C</sub>). If significant new sediment is introduced at this stage, climbing ripples may form, and rapid deposition may trap considerable water, leading to soft sediment deformation of bedding due to dewatering (*e.g.* convolute bedding). As waning of flow continues, silts are deposited largely out of suspension and form thin laminations that drape

the ripple ( $T_D$ ). Finally, silts and clays entrained by the turbidity current settle from the turbid sediment cloud ( $T_{Et}$ ), to be eventually replaced by normal marine hemipelagic deposition ( $T_{Eh}$ ) that caps the entire succession.

The resulting "classic turbidite" facies comprises thick successions of medium- to thin-bedded, but laterally extensive, sand-mud couplets (Walker, 1992). Beds generally have sharp, commonly non-erosive bases, although with abundant tool marks and scours reflecting the high energy conditions present at the base of an auto-suspended flow and the softness of the underlying muddy substrate.

Lowe (1982) developed a new classification of coarse-grained deposits resulting from turbidity currents, which compliments the Bouma sequence valid for fine-grained deposition. These are divided by grain size, with gravel-dominated deposits characterized by inversely-graded traction carpet gravels (R2) and suspension-deposited massive and normally graded gravels (R3). Sand-dominated deposits comprise: sand and pebbly sand containing traction-generated structures with plane lamination or cross-stratification (S1); thin, inverse-graded layers deposited from traction carpets (S2); and structureless or normally graded sands (S3) that correlate with Bouma  $T_A$  sands (Lowe, 1982). These correspond roughly with the four coarse-grained turbidite deposits suggested by Walker (1975), although there is significant overlap between the facies in the two models. These also correlate with the four coarsest-grained facies types identified by Mutti and Ricci Lucchi (1972) for the deep sea. The relationships between these three models and the facies described in Chapter 2

of this study are outlined in Table 3. Walker (1975) and Mutti and Ricci Lucchi (1972) also recognized the importance of pebbly mudstone facies, as well as slump and slide deposits, in the submarine fan setting. Although these facies types were not recognized in a submarine fan setting during this study, their characteristics are described the section covering fan deltas.

**Table 3: Generalized facies associated with submarine fans.**

Dominant Grain Size	Structure	Grading	Bouma (1962)	Walker (1975)	Lowe (1982)	Mutti & Ricci Lucci (1972)	This study
clay/silt	planar lamination	N	T <sub>E</sub>			C, D	H3
silt	planar lamination		T <sub>D</sub>				
sand	current ripple laminated		T <sub>C</sub>				
sand	planar lamination		T <sub>B</sub>				
sand	massive		T <sub>A</sub>				
sand	thin parallel-laminated	I			S2	B	P1
pebbly sand	plane or cross stratified	N		P1	S1		
				C1			
gravel	none - imbricated	N		C2	R3	A	C2
gravel	poorly developed	I		C3	R2		
gravel	none	none		C4			

The end-member submarine fan types suggested by Shanmugam and Moiola (1988) imply a predictable facies succession for each of the three major partitions of the typical fan types, developed as a consequence of fan progradation. Although a useful framework for characterization of fans based on deposits in the rock record, these models are somewhat limited by their simplicity. The models are based on single, point-source fans (e.g. those forming

below a delta front) and not multiple overlapping fans with varying sources and multiple active lobes.

The ideal passive-margin submarine fan deposits should be floored by basin plain deposits of pelagic and/or hemipelagic muds. The lower fan will be dominated by thin but areally extensive sheet sand deposits, represented by the Bouma  $T_C$ - $T_E$  units, with less common thicker sand deposits associated with distal channel fills (Bouma  $T_A$ - $T_C$ , and Lowe S1-S3), which are locally intercalated with thin hemipelagic muds. The middle fan will be dominated by well-developed channel-levee systems. The levees will consist of sand-mud couplets ( $T_A$ - $T_E$ ), whereas channel fills will range from massive conglomerates to well stratified sands, commonly in stacked fining-upwards successions (S1-R3). Stacked classical turbidites will form fining-upward successions with progradation because the toe of the fan is sand-rich compared to the levee complexes. The channels in these complexes are typically in excess of 1000m wide and 100m deep, with levees that extend a further 10km from the channel (Winn and Dott, 1978; Walker, 1985; Clark and Pickering, 1996). In the "upper" middle fan, large flow volumes and generally high energy should result in a concentration of "CCC"-type turbidites, where rapid deposition leads to increased proportions of rip-up clasts, climbing ripples, and/or convolute bedding (Walker, 1985). The upper fan will be dominated by channels filled with coarse clastics, coupled with slump and slide features due to canyon erosion.

In contrast, a submarine fan in an active basin margin should have a similar basin plain, covered by upward-coarsening sequences of sand-mud

turbidites ( $T_A$ - $T_E$ ), representing prograding depositional lobes of the lower fan. These would be overlain by middle fan deposits dominated by gravel- and sand-filled channel complexes (Lowe R2, R3, S3-S1), with mud deposition limited to thin hemipelagic drapes, which would be rarely preserved due to erosive amalgamation.

The existence of upward-coarsening and upward-fining sequences in turbidites, particularly those documented by Mutti and Ricci Lucchi (1972), have been challenged as simplistic and too susceptible to observer bias at the outcrop scale. However, this does not discount the general observation that the lower fan in mud-rich fans is typically sandier than the middle fan (Walker, 1992). Numerous case studies have reported that channel migration in the middle fan appears to have been rather sudden, likely the result of avulsion, as there is no progressive increase in sand content in the levee systems below channel erosion surfaces (Walker, 1985).

In a sequence stratigraphic framework, rapid submarine fan development is commonly linked to lowered sea levels (Shanmugam and Moiola, 1988). Generally, transgressive conditions lead to fan abandonment and resumed pelagic deposition, whereas falling stage leads to new fan development as sediment stored in shoreline systems is re-mobilized towards the basin. Lowstand leads to growth of channel-levee complexes and gradual fining. Such construction stops with rising sea level (Walker, 1992). Eustacy is less effective in active margins, as steeper slopes and narrow shelves mean that fluvial systems may continue to supply sediment directly to the fan in any stage of sea

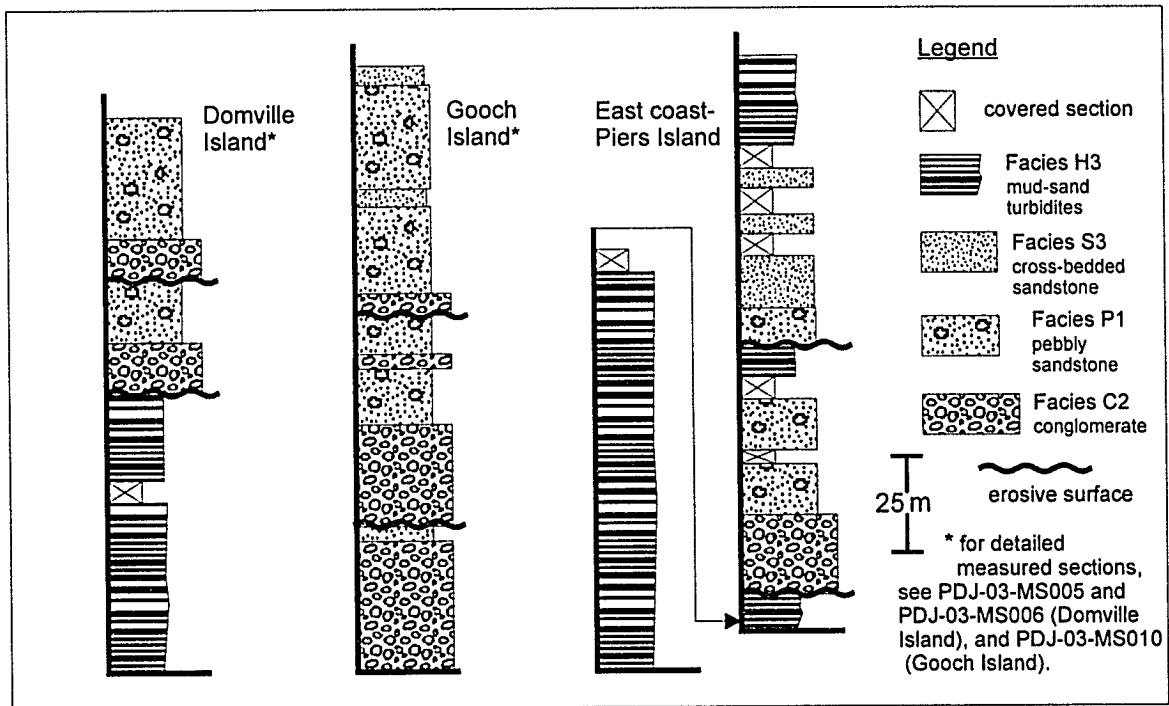
level change (Shanmugam and Moiola, 1988), and earthquakes along tectonically active margins may increase the propensity for turbidity currents to form, as observed in modern fans (Walker, 1992).

#### **Facies Association 4: Submarine Fan.**

Within the study area, facies interpreted to represent submarine fan deposition are expressed within the Haslam and Extension formations. These outcrop in the Piers-Pym-Knapp island group, the Sheep-Domville-Rubly island group, and the Gooch-Rum island group. The general trend is one of thin-bedded, mud-sand turbidites, cut by one or more large gravel-sand channel systems (Figure 33). In the Swartz Bay region on the north edge of the Saanich Peninsula and on the north side of Coal Island, outcrops of silty mudstones with thin sandstone interbeds pass gradationally out of coarser sandstone units of the Comox Formation. At each of these localities, the upper mudstone units display current-generated turbidite-type deposits (with well developed current ripples and convolute bedding) similar to those exposed on adjacent Pym and Knapp Islands. There is also evidence of significant soft-sediment deformation including bed-parallel slump and slide features within these mudstone units (Figure 34).

##### **FA 4a: Distal / Peripheral Fan Deposits.**

The Haslam Formation within the study area comprises thin to medium-bedded, sand-mud turbidites assigned to Facies H3. Bouma sequences in these thin beds are dominated by  $T_{CE}$  and  $T_{CDE}$ , which pass into sandier  $T_{ACE}$  and



**Figure 33: Typical expressions of Facies Association 4.**

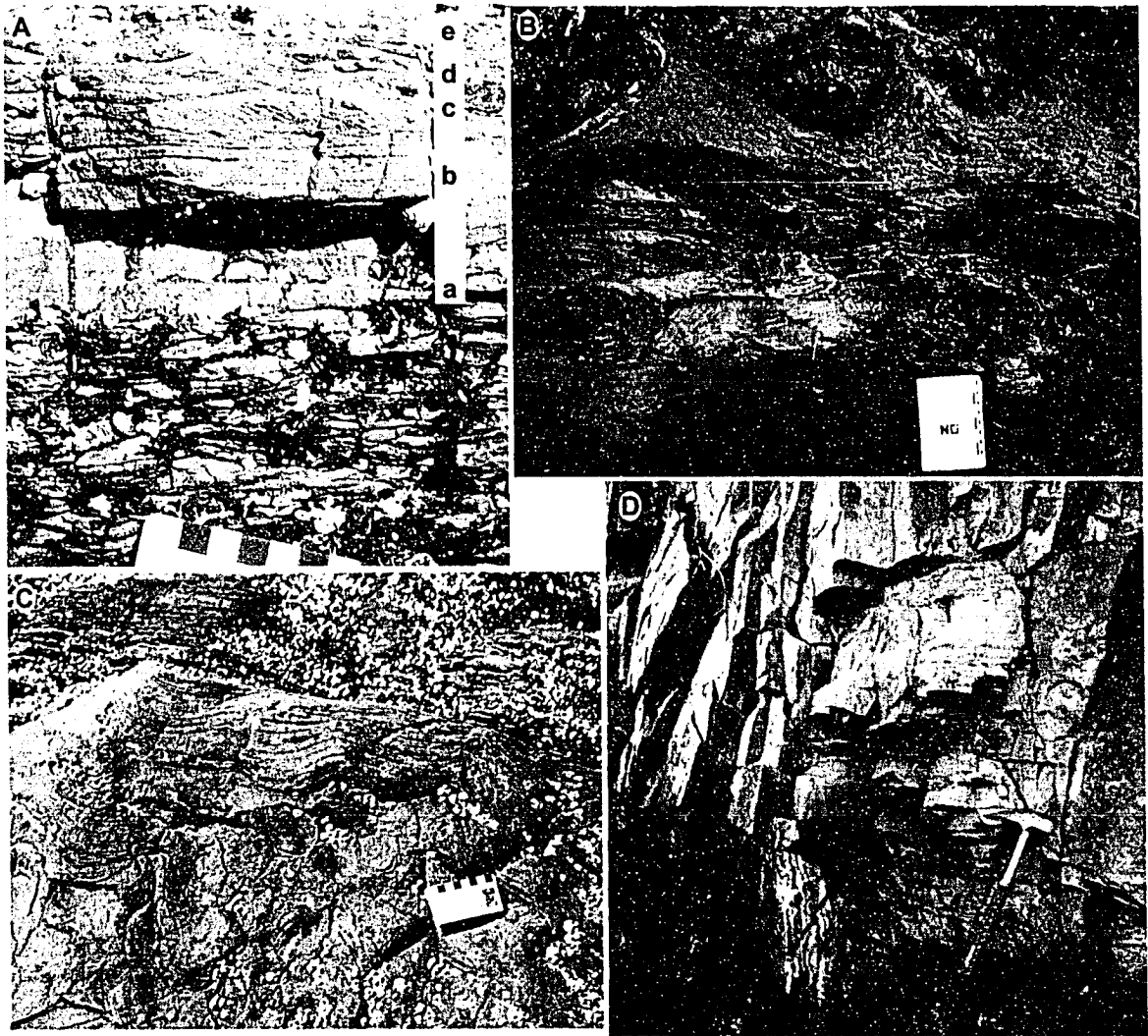


Figure 34: Exposures of the Comox Formation - Haslam Formation transition. (clockwise from top left) A: 10 cm-thick T<sub>ABCDE</sub> "Bouma" sequence (labelled) from medium-grained sandstone into silty muds, Saanich Peninsula; B: Soft sediment deformation of muddy deposits, Saanich Peninsula; C: Slump deposits in sandstone, horizontally laminated blocks in center of photograph are constrained between steeply dipping upper and lower beds, north shore Coal Island; D: Soft sediment deformation in silty mudstones, north Coal Island.



T<sub>ABCD</sub> over 5-20m thick, fining- and coarsening-upward sequences. These turbidites tend to be thicker and sandier on Piers Island in comparison to those on Domville Island, although the Domville Island exposures tend to vary more in overall grain size. Both current-ripple lamination and convolute bedding/climbing ripples are common in T<sub>c</sub> units, with the latter manifestation more common on Piers Island. Bioturbation is of low intensity (BI 1-2), with a low diversity of diminutive ichnogenera, possibly representing a distal expression of the *Cruziana* Ichnofacies.

These deposits are interpreted to represent turbidite deposition within a submarine fan complex. The lack of wave or tidal re-working, the presence of large slump-related soft sediment deformation structures, and the trace fossil assemblage, suggest deposition on the slope-apron. Two possible settings are along the periphery of the middle fan in a typical active margin fan, or at the "toe" of a mixed-type submarine fan prograding along the slope apron. In either instance, proximity to primary sediment sources (channels) and position relative to the varying direction of fan propagation result in the fluctuating mud-sand ratios.

The units exposed on the north shore of Coal Island and in Swartz Bay also represent Facies Association 4a. It is interpreted that these units were deposited by turbidity flows in a relatively high-gradient shelf or shelf-apron setting (as indicated by abundant slump and slide evidence). They may represent initial submarine fan growth along a transgressive shoreline, or the distal deposits of fan deltas forming at the shoreline.

#### **FA 4b: Channel Deposits.**

Extension Formation deposits in the field area comprise several thick fining-upward successions of pebble to cobble conglomerate (Facies C2), through pebbly sandstones (P1), to cross-bedded, medium-grained sandstones (S3). The conglomerates sit erosively on thin-bedded turbidites wherever the base is exposed, and on Piers Island the sandstones at the top of the succession fine into more thin-bedded mud-sand turbidites. The total thickness of channel fills exceeds 150m on Gooch Island, however several conglomerate-to-sandstone 25-50m thick upward-fining successions appear to be amalgamated, with little or no mudstone preserved between intervals.

The conglomerate-to-sandstone successions are interpreted to represent the fills of submarine channels that are eroding into more "distal" lower fan deposits. The shift from FA 4a sand-mud turbidite deposition to FA 4b conglomerate deposition may be the result of fan progradation, or channel avulsion across the fan apron. This reinforces the interpretation of braided-channel type deposition in the middle fan of an active-margin or mixed type submarine fan.

### **Synthesis**

The combination of sedimentary environments preserved in the Nanaimo Group rocks of the study area agree with previous interpretations of a single transgressive sequence in the Late Cretaceous. Transgression took place over a rocky, storm-swept shoreline that was open to the high-energy events of a "proto-Pacific" Ocean, and with high and varying relief along the coastline, resulting in a

variety of marginal marine sedimentary environments. Deepening continued for a time sufficient to permit the highest units in the study area to be deposited well below storm wave base in a slope-margin submarine fan setting.

The first three identified facies associations may correlate with one another along depositional strike along a high-relief and diachronous basal unconformity. Alluvial debris fans depositing mixed sediment directly into the ocean (Facies Association 1) may have supplied sufficient coarse sediment to allow preservation of strandplain-type shorelines (Facies Association 2) in a transgressive setting. The presence of these gravelly fan deltas suggest an abundant supply of coarse sediment at the shoreface, whereas the relatively thin deposits of shoreface gravel, preserved only as lag or thin shore-normal interbeds near gravel source areas, suggest a small tidal range (Dashtgard *et al.*, 2006).

The relationship between Facies Association 2 and Facies Association 3 shoreline types likely relates only to the rate of local transgression, as controlled by local topography. Where bedrock slopes are steeper, the rate of shoreward inundation will be much lower than in localities where slopes are gentle. With the slower inundation rate, shoreface deposits will erode through backshore and foreshore deposits due to the ravinement surface, leading to succession similar to Facies Association 2 (Bourgeois and Leithold, 1984). Gentle slopes, however, may result in more rapid inundation, and barrier-island bypass, promoting Facies Association 3-type deposits.

All the shoreface deposits, whether preserved as the bulk of Facies Association 2, or as the capping units of facies associations 1 and 3, have common characteristics. Sandstones tend to be thick bedded and of medium grain size. They feature hummocky cross-stratification and bedsets of the scale observed on open shorelines along active marine margins (Chan and Dott 1986), which are considerably larger than those described from the Western Interior Seaway (Frey and Howard 1990; Duke *et al.* 1991). This scale difference implies that the Comox shoreline was exposed to the full force of large proto-Pacific storms, and not protected by an embayment or large island (Johnstone *et al.*, 2006). The preservation of almost 1000m of barrier complex, shoreface, and transitional offshore deposits along the Saanich Peninsula and Coal Island suggest a long period of persistent transgression with ample and consistent sediment input to limit the rate of transgression.

Ultimately, the transgression was able to overrun the study area and allow deposition of "deep-water" submarine fan deposits (Facies Association 4). Although traditional models suggest that submarine fans do not grow during transgression (c.f. Walker, 1992), ample opportunity exists for sediment delivery into the deep ocean during rising sea level, especially in restricted basins and along active margins where shelf slopes are high and earthquakes are common (Shanmugam and Moiola, 1988; Walker, 1992). One interpretation would have the Haslam Formation muddy turbidites of Facies Association 4a deposited during the rising sea level stage, and the coarser conglomerate and sandstone of the Extension Formation (Facies Association 4b) deposited as fan growth began

in earnest during a highstand but stable period of sea level. However, the timing of sea level rise and fall along this active margin during Nanaimo Group time is speculative, and variations in tectonic activity could strongly influence both local sea levels and sediment influx patterns.

The fan delta complexes that have been identified in the Comox Formation (FA 1) represent a significant potential source of the large quantities of mixed sediment necessary for submarine fan growth. Debris flows and large flood events can transport large quantities of mixed, saturated sediment to the submarine parts of the fan delta complex (Figure 24). Turbidity currents may form in the subaqueous portion of the fan delta complex from separation of subaerial debris flows, or be initiated in the lower fan delta from failure of saturated sediments (Nemec and Steel, 1984; Postma, 1990).

The tectonic setting of the Nanaimo Group most closely approximates the active margin end-member of the submarine fan classification scheme of Shanmugam and Moiola (1988). However, the complex peripheral foreland setting within a forearc, with a basin forming upon a recently docked and partially emergent Wrangellia, may better correspond to the 4<sup>th</sup>, "mixed type" margin setting. It may be expected that the basin slope and floor topography was irregular with significant impediments to fan development, including an (inferred) foreland bulge. Notably, the submarine fan deposits preserved in the study area were likely deposited at shelf depth, relatively proximal to the high-relief coastline that is the source of fan sediments. As such, tectonic setting models such as those of Shanmugam and Moiola may not be well represented.

The lack of upward-coarsening sequences in the mud-sand turbidites of the Haslam Formation within the study area suggest channel avulsion eroding into levee deposits as opposed to gradual progradation of the middle fan. This does differ from some Haslam Formation units described in localities to the north (Ward and Stanley, 1982; England, 1990; Mustard, 1994), where the Haslam units coarsen and thicken upward into the Extension Formation.

The single-transgression model for the study area also leads to a re-interpretation of the stratigraphy of the study area. The sandstone-mudstone units on Brethour and Comet islands have been previously assigned to a now-disused "Extension-Protection Formation" (e.g., Muller and Jeletzky, 1970), or to the Protection Formation (e.g., England, 1990). However, the Protection Formation outside of the Nanaimo coal mining region consists entirely of thick successions of submarine grain flow deposits or turbidites, interpreted to represent large overlapping submarine fan complexes. On Saltspring, Pender, and other islands surrounding the study area, the Protection Formation was deposited below storm wave base, on the lower shelf (Mustard, 1994). In contrast, the sedimentary facies on Brethour and Comet Islands suggest marginal marine deposition, including the incontrovertible presence of fossilized *in situ* tree stumps on the south shore of Brethour Island. A significant marine regression in the Campanian would be required for these marginal marine units to be deposited stratigraphically above the lower shelf Haslam and Extension Formations, as suggested by these earlier interpretations. The extensive study of the Nanaimo Group by numerous workers has never identified any evidence of

regression between Extension and Protection formation deposition (Mustard, 1994). Thus, the more likely interpretation is that Brethour and Comet islands comprise Comox Formation units which have been structurally emplaced the Extension Formation strata on Domville and Gooch islands by an inferred fault (Figure 61, Chapter 5).

## CHAPTER 4: SEDIMENT PROVENANCE

Numerous previous studies of sediment provenance trends have been performed on the various parts of the Nanaimo Group (e.g., Pacht, 1984; England, 1990; Mustard, 1994; Mustard *et al.*, 1995; Mahoney *et al.*, 1999; Katnick and Mustard, 2003). Earlier models suggested that the major source of Nanaimo Group sediment was the Wrangellia Terrane to the west, with only minor contributions from the Coast Mountains to the east (*cf.* Muller and Jeletzky, 1970). However, more recent studies using sediment composition and paleocurrent analyses have concluded that Wrangellia was a major source only to local basal units, with the exception of the slightly higher coal-bearing units in the vicinity of the city of Nanaimo (Ward and Stanley, 1982; Pacht, 1984). Instead, the main sediment source for lower units of the Nanaimo Group are inferred to be the San Juan thrust nappes to the south, and concurrently thrust areas in adjacent Washington State. The Coast Belt became a major source of detritus during deposition of the upper part of Nanaimo Group stratigraphy (Pacht, 1984; England and Hiscott, 1992). More recent detrital zircon studies have further diminished the role of Wrangellia as a sediment source, by showing that the Coast Belt may have been a significant source for much of the basin as early as the early Campanian Epoch, and that at least some sediment was arriving at the basin from cratonic sources farther to the east (Mustard *et al.*, 1995; Mahoney *et al.*, 1999).



The locality selected for this study may be significant for provenance analysis, as it represents both the oldest Nanaimo Group deposits and those closest to the San Juan nappes, while the sediments rest directly upon Wrangellian basement rocks. Provenance of Nanaimo Group sediments of the study area were interpreted through analysis of paleocurrent trends and compositional studies of sandstone framework grains and conglomerate clasts. The complete set of collected data is presented in appendices C (thin section analyses of sandstone), D (conglomerate clast lithologies), and E (paleocurrent analyses). Summaries of individual and comprehensive data trends are described here.

## **Sandstone Composition**

Detailed analyses of sandstone compositions from the Nanaimo Group have been performed in numerous previous studies (e.g., Pacht, 1984; Ward and Stanley, 1982; England, 1990; Mustard, 1994; Katnick and Mustard, 2003). Through these studies, a comprehensive database of sandstone petrographic information has been developed, with significant contributions from localities in the vicinity of this study area (see Mustard, 1994 for a summary of earlier data).

These previous studies have described the Comox Formation sandstones within the study area as arkosic to lithic arenites (e.g., England, 1990; Mustard, 1994). Pacht (1980) described a "high plagioclase arkose" from the Tsehum Harbour area of the Saanich Peninsula, an area mapped here as Comox Formation; however his sample was collected close to the basal unconformity

where the basement rock comprises Jurassic granodiorites, and it is likely not typical of Comox Formation sandstones from the region.

In a comprehensive study of the Haslam Formation, Ward and Stanley (1982) described Haslam sandstones from the study area as chert lithic arenites, with significant volcanic grain contents. Haslam Formation sandstones have also been described from throughout the Nanaimo Group as arkosic arenite, although this study area represents a portion of the Nanaimo Group where Haslam and Comox formation sandstones are locally enriched in chert and other lithic fragments (Mustard, 1994).

Extension Formation sandstones have been found to be richer in chert than lower units, and are generally described as lithic arenites (England, 1990; Mustard, 1994). This is generally compatible with "chert-rich lithic arenites" described by Pacht (1980) from the Extension Formation in areas along strike to the west (Cowichan Lake) and east (Stuart Island) of the study area.

Post-deposition alteration of Nanaimo Group sediments is limited to compaction, cementation, and minor diagenetic alteration (Mustard, 1994). Stewart and Page (1973) recognized very low-temperature metamorphic products, including laumontite and heulandite, along with alteration of plagioclase and biotite and the development of a phyllosilicate matrix within Nanaimo Group sandstones. They further recognized a depth-zonation of metamorphism, with a minor increase in the grade of zeolite assemblages below the top 1000m of section. However, their analysis of metamorphism within the Nanaimo Group was

limited in extent and hampered by a poor understanding of the provenance of Nanaimo Group sediments over time and over the extent of the basin.

Eleven hand samples collected during this study were analysed using thin section petrography, with specific analysis techniques outlined in Chapter 1 and Appendix C. Results of modal analysis of framework grains are presented in Table 4, with complete thin section descriptions and photomicrographs in Appendix C.

**Table 4: Modal Lithology of sandstone framework grains, counts for each sample (n=100). Qm: monocrystalline quartz grains; Qp: polycrystalline quartz grains; P: plagioclase (including microcline); K: potassium feldspars; Lm: lithic fragments displaying metamorphic texture; Lv: volcanic lithic fragment (including plutonic); Ls: sedimentary lithic fragment (excepting chert); cht: chert.**

Sample	Formation	Location	Qm	Qp	P	K	Lm	Lv	Ls	cht	Folk (1974) Classification
138a	Comox	Moresby I.	16	32	14	0	12	14	5	7	Feldspathic Litharenite
14a		Sidney I.	17	19	10	2	0	28	15	9	Volcanic Litharenite
04a		Coal Point	16	13	12	4	1	27	16	11	Volcanic Litharenite
116b		Hood I.	10	20	21	5	4	31	4	5	Feldspathic Litharenite
37a		Forrest I.	19	16	11	6	3	29	5	11	Volcanic Litharenite
126a		Coal I.	21	4	28	0	0	24	14	9	Feldspathic Litharenite
72b		Comet I.	8	31	13	4	1	29	8	6	Feldspathic Litharenite
111b		Imrie I.	20	14	17	5	4	33	5	2	Feldspathic Litharenite
128a		Piers I.	20	11	8	7	12	26	4	12	Volcanic Litharenite
56b	Extension	Gooch I.	22	18	11	4	9	21	5	10	Volcanic Litharenite
135a		Arbutus I.	19	16	7	6	14	19	5	14	Volcanic Litharenite

The sandstones analysed are dominantly feldspathic litharenites, with some volcanic litharenites. Sandstones are textually submature, with generally subangular grains and moderate degrees of sorting. Quartz grains comprise both mono- and poly-crystalline forms, with generally straight extinction and little suturing of grain contacts, and represent only 35% of framework grains.

Feldspars constitute 15-20% of all grains, of which approximately 75% are plagioclase with only a small proportion of microcline. Lithic fragments are dominated by volcanic grains, both as aphanitic mafic types and as more intermediate types, commonly displaying feldspar laths in an aphanitic groundmass. Very few phaneritic or extrusive igneous fragments are identified, likely due to the medium-grained character of the sandstones analysed.

Recycled sedimentary fragments are also common, with chert representing more than half of all sedimentary fragments, and minor amounts of mudstones, recycled sandstones, and (calcareous or carbonaceous) fossil fragments. Rock fragments displaying metamorphic textures are less common. Accessory minerals include detrital micas, locally abundant opaque grains, chlorite, and glauconite.

Proportion of primary matrix ranges from less than 1% to almost 5% in the most poorly sorted samples, and mainly comprises silt-sized particles that reflect the lithology of the surrounding framework grains. Secondary chlorite, sericite and other alteration minerals appear in varying proportions in the matrix. Cement is dominated by clay minerals and hematite, with only small amounts of non-detrital calcite.

Evidence of diagenesis includes mechanical compaction (deformation of ductile grains), and minor chemical compaction (dissolution at contacts). There is no evidence of quartz overgrowths. There is abundant chloritization of micas, and most feldspars appear "dusty", due to alteration to sericite or illite. Hematite staining of clay cement is pervasive. Porosity is generally very low (commonly

~2%, and never exceeding 5%) with secondary clay, hematite and rare calcite filling the pore spaces.

There are some differences between sandstone samples collected from the Comox Formation and those collected from the Extension Formation. The average Extension Formation sample plots as a volcanic litharenite on the Folk (1974) ternary diagram, whereas most Comox Formation samples plot as feldspathic litharenite, although there is a considerable amount of overlap (Figure 35). This reflects several differences in the composition of the framework grains. Although Comox Formation samples have typically more feldspar and volcanic rock fragments than Extension Formation samples, each population is within a standard deviation of the other. There are, however, significantly more chert grains and lithic fragments that display metamorphic textures in the Extension Formation samples.

### **Conglomerate Clast Lithology**

Conglomerate facies are exposed in several locations across the study area, however many locations do not lend themselves to meaningful clast lithology counts. The basal conglomerates of the Comox Formation as exposed on northern Moresby Island or Russell Island are clast-poor and monomictic. Clasts nearly always share lithology with the immediately subjacent basement. Conglomerate within unconformity-proximal facies associations that are interpreted to represent deposition in fan delta settings, such as those exposed on western Portland or eastern Moresby Island, are similarly monomictic, although they commonly display varying weathering or

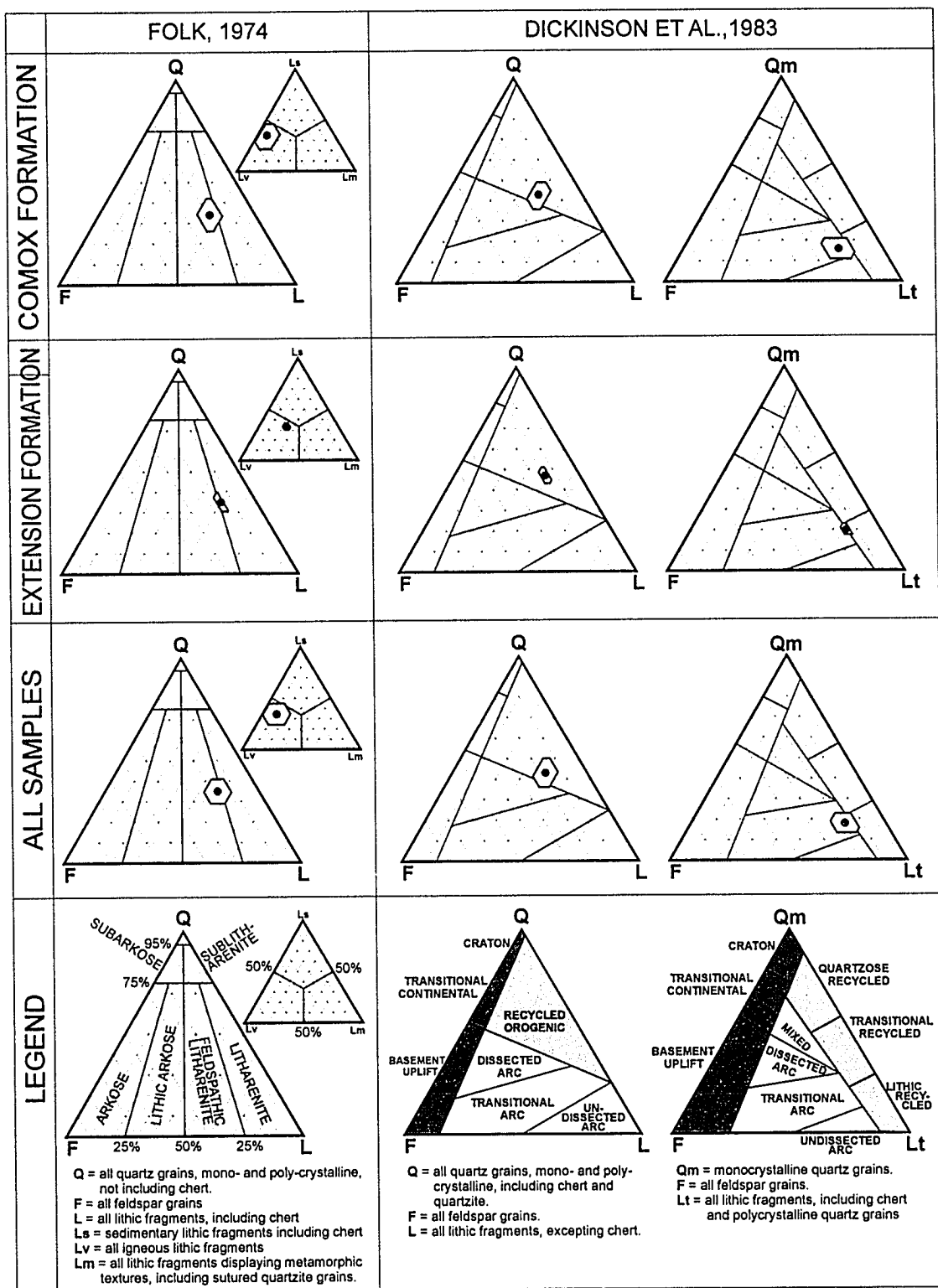


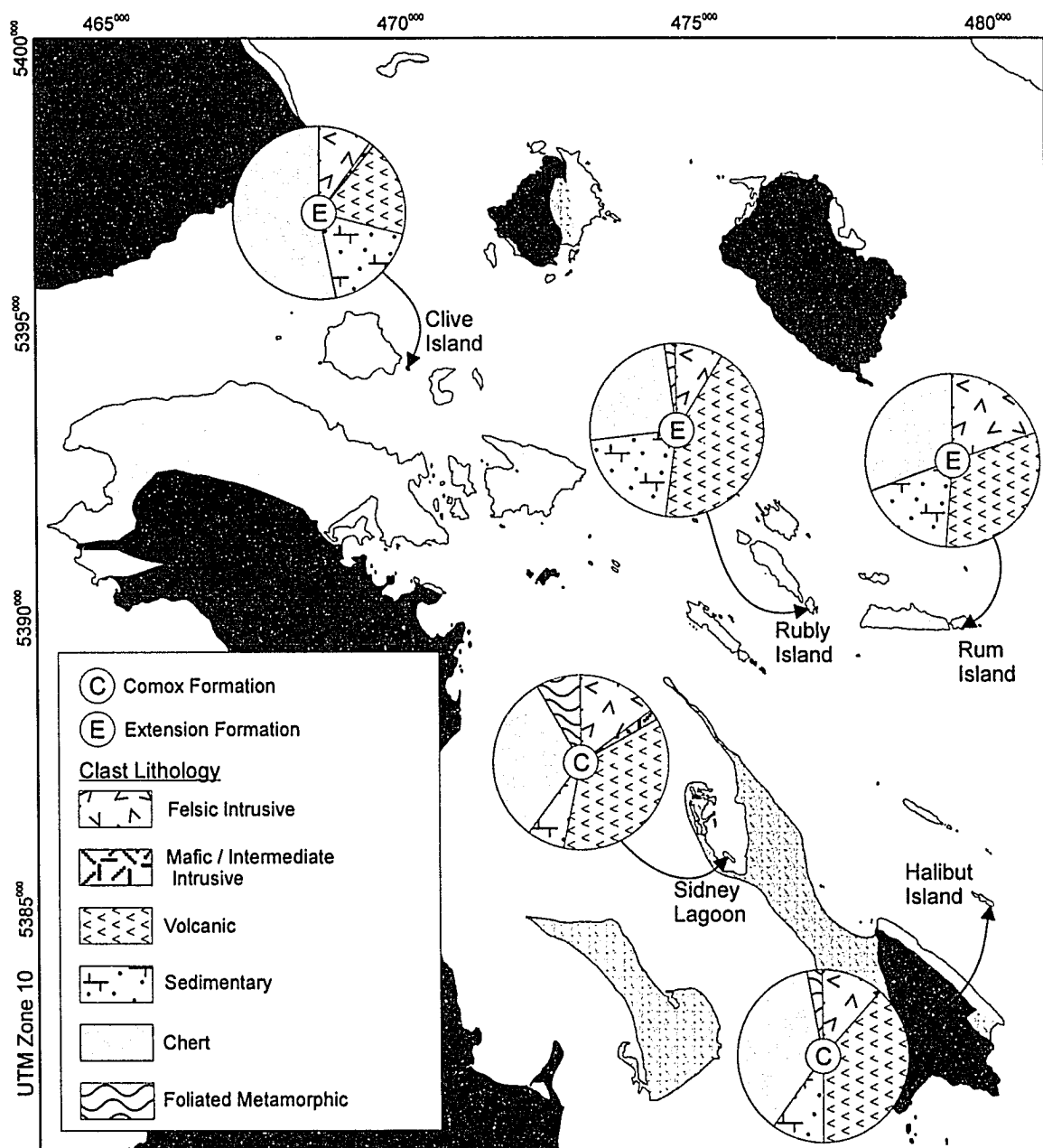
Figure 35: Ternary diagrams: results from thin section sandstone framework grain modal analysis.

homogeneous local lithology shifts that reflect local changes in basement materials.

Comox Formation pebble conglomerates exposed as interbeds within dominantly sandstone facies on Halibut Island and on the island within Sidney Lagoon were analysed for clast lithology patterns (Figure 36; see Appendix D for all data). At both locations, clasts are small to large pebbles and moderately to well rounded. Conglomerates are clast-supported with an upper medium- to coarse-grained sandstone matrix. Clast lithologies are similar between the two stations (Table 5; Figure 37), with counts of each population lying within the 95% confidence intervals of the other population. The most common clasts are dark grey and dark green volcanics, and green and white chert, with lesser intrusive, sedimentary and metamorphic clasts. One notable contrast is the local abundance of large, robust shell fragments entrained as clasts in the Halibut Island example, which accounts for the larger proportion of sedimentary clasts.

**Table 5: Clast count data for Comox Formation conglomerates. See Appendix D for complete data and confidence intervals.**

Lithology of clast	Clast Counts		
	Sidney Lagoon	Halibut Island	all Comox
Felsic intrusive	15	12	27
Mafic intrusive	2	0	2
Volcanic	36	38	74
Sedimentary	7	10	17
Chert	32	37	69
Foliated metamorphic	8	3	11
Total	100	100	200



**Figure 36: Conglomerate clast counts, locations and gross clast lithology.**



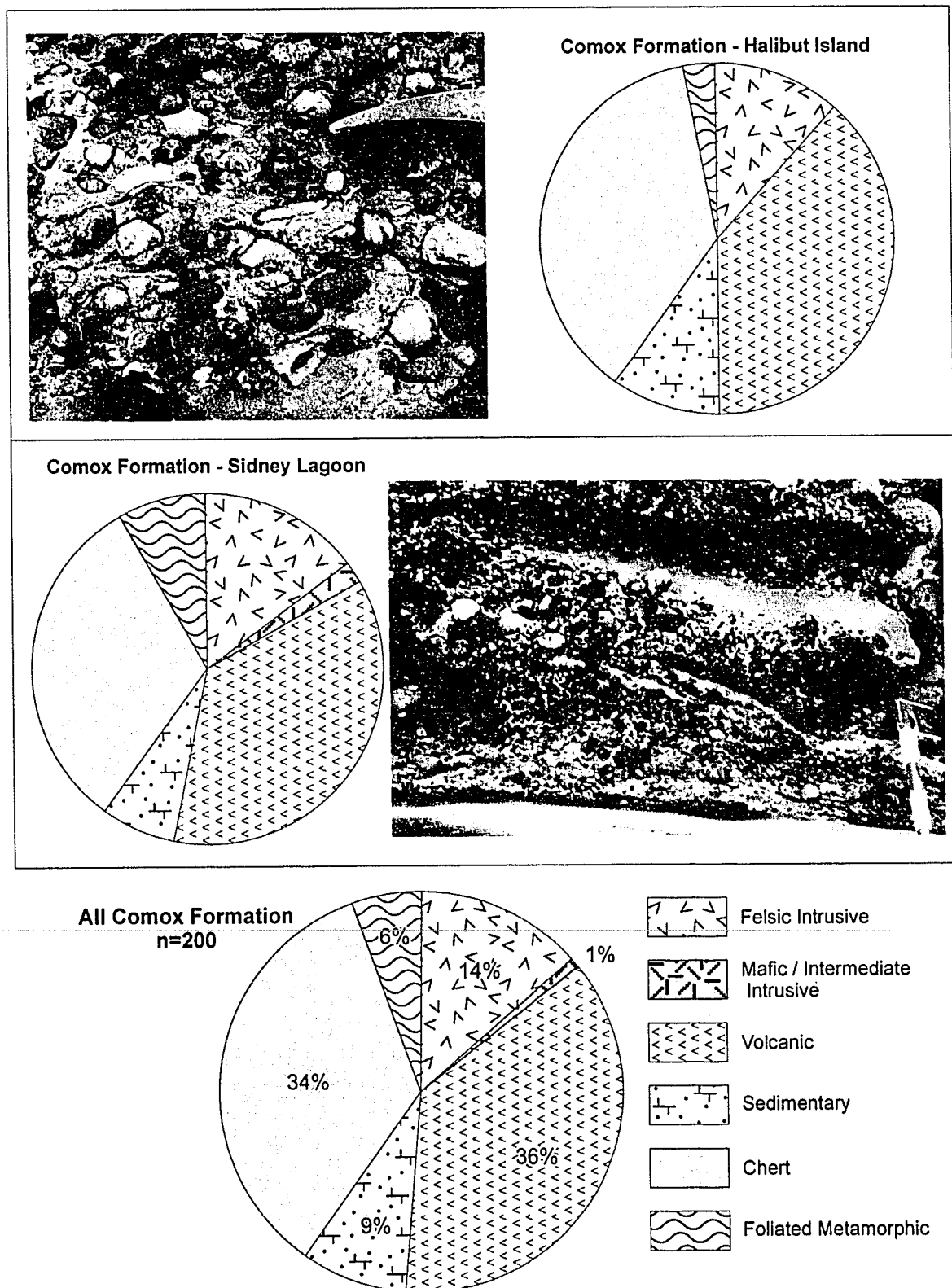


Figure 37: Conglomerate clast count results, Comox Formation.

Clasts of Extension Formation pebble and cobble conglomerates were counted on Clive, Rubly, and Rum islands (Figure 36; see Appendix D for all data). These conglomerates are generally very thick bedded, crudely graded and locally imbricated, with rounded pebble- to cobble-sized clasts, and a well sorted, coarse-grained sandstone matrix. Clasts have a lithologic distribution similar to the Comox Formation, except for significantly greater proportions of sedimentary clasts, and less metamorphic clasts that display foliation (Table 6; Figure 38). Clast lithologies vary somewhat within the Extension Formation population, with the Rum Island sample containing significantly more intrusive clasts, and the Clive Island sample enriched in chert and with fewer volcanic clasts. Chert clasts are black, green and yellow; volcanics are dark green or lesser dark grey; and intrusive clasts are generally felsic and light in colour.

**Table 6: Clast count data for Extension Formation conglomerates. See Appendix D for complete data and confidence intervals.**

Lithology of clast	Clast Counts			
	Clive Islet	Rum Island	Rubly Island	all Extension
Felsic intrusive	10	20	9	27
Mafic intrusive	1	0	0	2
Volcanic	18	31	43	74
Sedimentary	18	18	21	17
Chert	53	31	25	69
Foliated metamorphic	0	0	2	11
Total	100	100	100	300

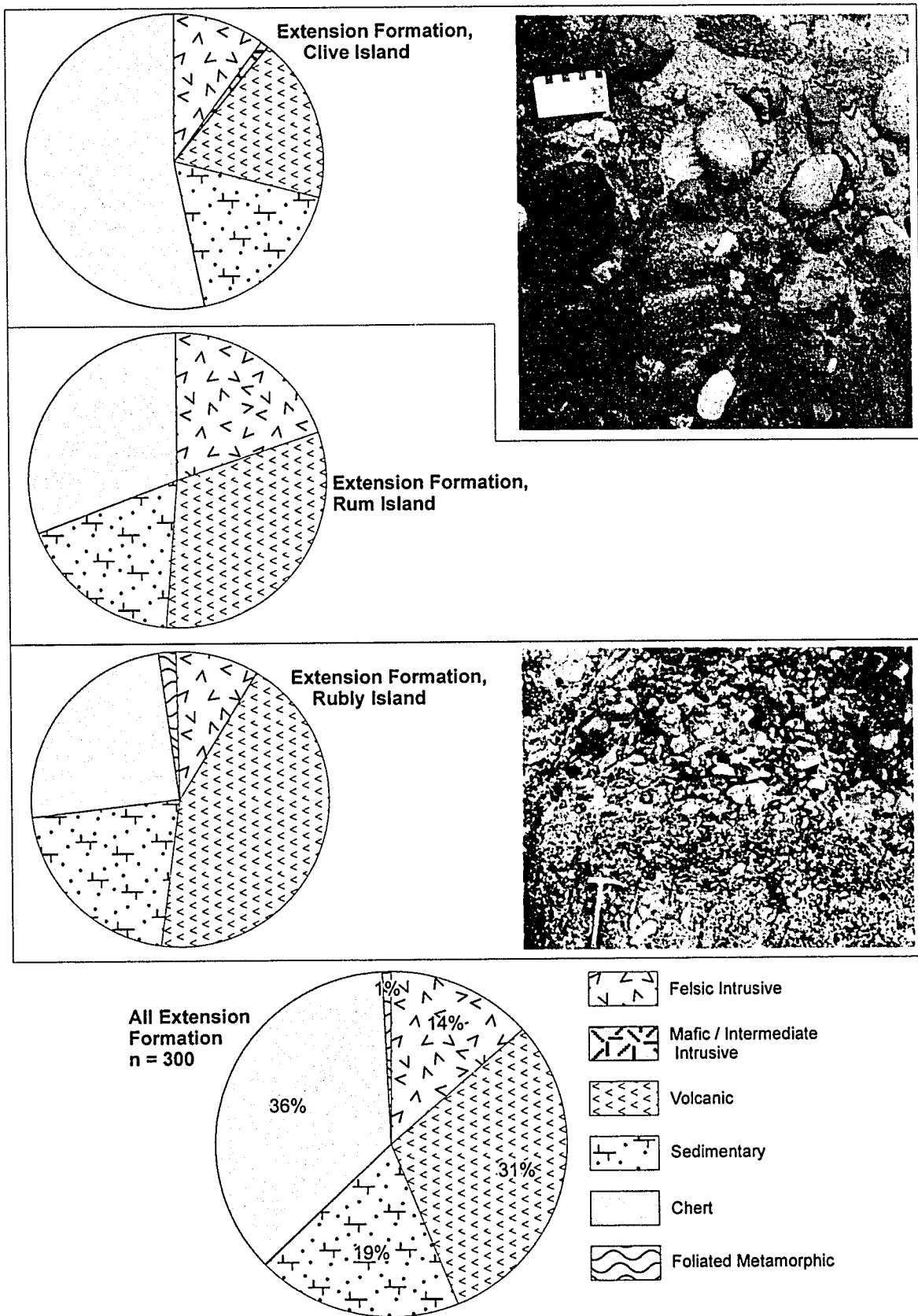


Figure 38: Conglomerate Clast count results, Extension Formation.

The clast compositions detailed here agree well with those from previous basin-wide studies of the Nanaimo Group (see Mustard, 1994 for summary), although some significant differences exist (see Table 7). Notably, this study found the proportion of chert clasts in the Comox and Extension formations to be similar, whereas earlier studies suggested that the Extension is much richer in chert. Similarly, earlier studies showed enrichment in intrusive clasts in the Comox Formation, which is not reflected by data collected in this study.

**Table 7: Clast count data from this study compared to those of earlier studies as compiled by Mustard (1994). All figures are percentages of total clasts. For complete count data and confidence intervals, see Appendix D.**

Clast Lithology (% of total counts)	Comox		Extension		All data, this study	Basin-wide, earlier studies
	This study	Earlier studies	This study	Earlier studies		
Felsic intrusive	14	32	13	9	13	17
Mafic intrusive	1	8	0	1	1	7
Volcanic	37	37	31	16	33	30
Sedimentary	9	5	19	7	15	4
Chert	35	10	36	67	36	35
Foliated metamorphic	6	8	1	1	3	8

Both of these discrepancies may be explained by the location of this study area at the extreme southern end of the exposed Nanaimo Group. Earlier studies of Extension Formation conglomerates show that the proportion of chert clasts decreases markedly in the north and central parts of the basin (Mustard, 1994). Similarly, relative proximity to the plutonic rocks of the Coast Belt leads to local enrichment in felsic intrusive clasts in the more northern parts of the basin.

## Paleocurrent Analysis

A total of 907 paleocurrent measurements were taken from 79 separate beds, representing 51 station locations (see Appendix E for all data). The majority of these measures (69 beds) are cross-bedded sandstones or conglomerates, and the strike and dip of identified foreset planes (average of 9 measurements per bed) were recorded. On seven sandstone beds there were surface exposures of asymmetric ripples. The paleocurrent direction was measured as a trend and plunge along the bedding surface, with an average of 5 measurements per exposure (less for straight crested ripple sets, more for those with undulating crests). Finally, clast imbrication was measured from three thick conglomerate beds. The orientations of the apparent a-b plane of non-spherical clasts (100 each from two beds, 55 from the third) were measured, with the paleocurrent azimuth interpreted to be  $180^\circ$  from the average dip direction.

In all cases, the strike and dip of the bedding plane was also measured, and this plane was used as a reference for the rotation of the paleocurrent data to original horizontal. Paleocurrents measured in the overturned beds of the Gooch Domain, however, were rotated first about the axis of the fold interpreted to have overturned that domain (see Chapter 5), after the plunge of the fold was corrected to horizontal. The paleocurrent azimuth was then rotated again to bring the resultant position of the rotated bedding plane to horizontal. This technique was applied wherever beds were interpreted to have been folded and the fold axis could be estimated or measured.

The general trend for all paleocurrents indicate that paleoflow was towards the northwest, although there is considerable variation (see Table 8). This trend is strongest in samples from the Extension Formation, and generally weak in the Comox and Haslam formations, reflecting the paleoenvironmental settings of the measured strata.

Paleocurrent results from the Comox Formation have an overall weak trend towards the west in a general sense, although populations for individual beds show much more complex patterns (Figures 39, 40, and 41). Populations from sandstone units assigned to Facies Association 2 are dominated by north-western flow directions, for both cross-bedded and current rippled sandstones. Locally, more eastern flow is indicated, most notably on Portland Island and Mandarte Island (Figure 40d,e,f, and J). Populations from sandstones and heterolithic units assigned to Facies Association 3 form a weaker trend towards a westward flow direction (Figure 41). The varying flow directions indicated within these units likely reflects the various sediment dispersal processes at work within the interpreted barrier-island complex depositional environment. Onshore and longshore-directed processes at the shoreface operate in close proximity to tidal channels, washover fans, and wind-forced currents within the lagoonal setting. Higher-resolution, dedicated paleocurrent studies of Comox Formation units on Brethour or Forrest islands would be required to clarify these trends.

Haslam Formation examples are scarce, due to the lack of extensive outcrop, the predominantly silty mudstone lithology of the formation, and local structural deformation of much of the bedding (Figure 42). Further, the data

collected from Sheep Island (Domville domain) gives an opposing trend to all other data, possibly as a result of being collected in a highly folded area (see Chapter 5). The deformation history in the area is likely complex, and paleocurrents cannot confidently be resolved using a single fold correction to horizontal around strike.

The Extension Formation trends in both sandstones and conglomerates strongly suggest an overall northwestern flow direction (Figure 43). Imbrications of a-b planes of non-spherical conglomerate clasts were diffuse where clasts were small and more equant (*i.e.* Rubly Island), but were strongly bimodal for other locations. The bimodal distribution probably indicates deposition by traction, with elongate clasts rotating about their a-axis during flow (*cf.* Potter and Pettijohn, 1977; Miall, 1999).

**Table 8: Summary of rotated paleocurrent data with statistical analysis, including reference to rose diagrams in following figures. Type of paleocurrent measurement is indicated, where "x" = cross-bedding foresets ; "cr" = current ripple lineations ; "Cl" = Imbrication of conglomerate clasts .**

Form- ation	FA	Domain	Rose Diagram	Beds	Type	N	Direction (azimuth)	Raleigh %	Circular Variance	CSD (+/- Degrees)	95% CI
Comox	FA 1	Moresby	Fig. 39a	1	x	8	140	98.6	0.014	9.6	6.3
	FA 2	Moresby	Fig. 40a	3	x	29	355	67.9	0.321	50.4	18.7
		Portland (A)	Fig. 40b	1	x	16	166	89.0	0.110	27.6	13.6
		Portland (B)	Fig. 40c	1	x	11	298	99.3	0.007	7.0	0.0
		Portland (C)	Fig. 40d	3	x	23	083	85.1	0.149	32.5	13.3
		Portland (D)	Fig. 40e	4	x	34	042	91.3	0.087	24.4	8.2
		Portland (E)	Fig. 40f	2	x	17	302	87.6	0.124	29.5	14.1
		Portland (F)	Fig. 40g	1	cr	3	013	100.0	0.000	0.0	0.0
		Sidney (A)	Fig. 40h	3	x	24	244	74.0	0.260	44.4	17.9
		Sidney (B)	Fig. 40i	1	x	10	074	97.8	0.022	12.1	7.4
		Sidney (C)	Fig. 40j	1	x	6	295	93.7	0.063	20.6	16.7
		Coal North (A)	Fig. 40k	2	cr	15	321	99.0	0.010	8.0	0.0
		Coal North (B)	Fig. 40l	1	cr	5	113	99.8	0.002	3.5	0.0
		Coal North (C)	Fig. 40m	1	x	8	341	99.2	0.008	7.5	0.0
		Coal North (D)	Fig. 40n	2	x	16	272	98.5	0.015	10.0	4.6
		Coal North (E)	Fig. 40o	1	cr	3	313	100.0	0.000	0.0	0.0
		Saanich W (A)	Fig. 40p	1	x	8	307	83.1	0.169	34.9	24.7
		SaanichW (B)	Fig. 40q	2	cr	6	003	99.0	0.010	8.1	0.0
	FA 3	Tsehum (A)	Fig. 41a	2	x	17	uniform	17.6	0.824	106.8	uniform
		Tsehum (B)	Fig 41b	2	x	18	248	99.1	0.009	7.6	0.0
		Tsehum (C)	Fig 41c	2	x	21	205	97.9	0.021	11.8	5.0
		Tsehum (D)	Fig 41d	1	x	10	008	98.3	0.017	10.5	6.2
		Domville (A)	Fig 41e	1	x	11	234	98.2	0.018	10.8	6.1
		Domville (B)	Fig 41f	2	x	17	uniform	27.0	0.730	92.7	uniform
		Domville (C)	Fig 41g	3	x	27	232	91.4	0.086	24.2	9.1
		Domville (D)	Fig 41h	1	x	13	261	95.2	0.048	17.9	9.7
		Forrest (A)	Fig 41i	1	x	9	290	99.2	0.008	7.2	0.0
		Forrest (B)	Fig 41j	2	x	21	154	95.4	0.046	17.6	7.5
		Forrest (C)	Fig 41k	2	x	18	uniform	35.0	0.650	83.0	uniform
		Forrest (D)	Fig 41l	1	x	10	344	98.7	0.013	9.1	5.4
		Forrest (E)	Fig 41m	2	x	18	117	77.2	0.228	41.3	19.2
		Forrest (F)	Fig 41n	2	x	18	340	91.8	0.082	23.7	11.0
		Gooch	Fig 41o	1	x	9	181	98.5	0.015	10.1	6.2
All Comox				56		479	281	16.8	.832	108.3	22.1



Table 8 Cont'd

Form- ation	FA	Domain	Rose Diagram	Beds	Type	N	Direction (azimuth)	Raleig h %	Circular Variance	CSD (+/- Degrees)	95% CI
Haslam	FA 4a	Domville	Fig. 42a	3	x	23	141	87.4	0.126	30.0	12.2
		Piers (A)	Fig. 42b	1	x	8	323	98.6	0.014	9.5	6.2
		Piers (B)	Fig. 42c	1	x	9	268	99.1	0.009	7.5	0.0
	All Haslam			5		40	uniform	24.4	0.756	96.3	uniform
Extension	FA 4b	Domville (A)	Fig. 43a	1	x	9	081	96.7	0.033	14.9	9.7
		Domville (B)	Fig 43b	1	x	8	334	95.5	0.045	17.3	12.0
		Domville (C)	Fig 43c	4	x	39	300	89.6	0.104	26.9	8.4
		Domville (IMB)	Fig 43d	1	CI	55	009	46.4	0.536	71.0	22.2
		Gooch (A)	Fig 43e	1	x	10	006	98.4	0.016	10.4	6.1
		Gooch (B)	Fig 43f	1	x	10	350	98.8	0.012	9.0	5.4
		Gooch (C)	Fig 43g	1	x	8	306	97.7	0.023	12.3	8.4
		Gooch (D)	Fig 43h	3	x	24	336	82.9	0.171	35.0	14.3
		Gooch (E)	Fig 43i	2	x	19	029	85.0	0.147	32.0	14.6
		Gooch (F)	Fig 43j	1	x	8	279	98.8	0.011	8.4	5.7
		Gooch (IMB)	Fig 43k	1	CI	100	331	40.4	0.596	77.1	19.1
		Piers (IMB)	Fig 43l	1	CI	100	279	24.3	0.757	96.3	34.1
	All Extension			18		390	331	42.7	0.573	74.7	9.0

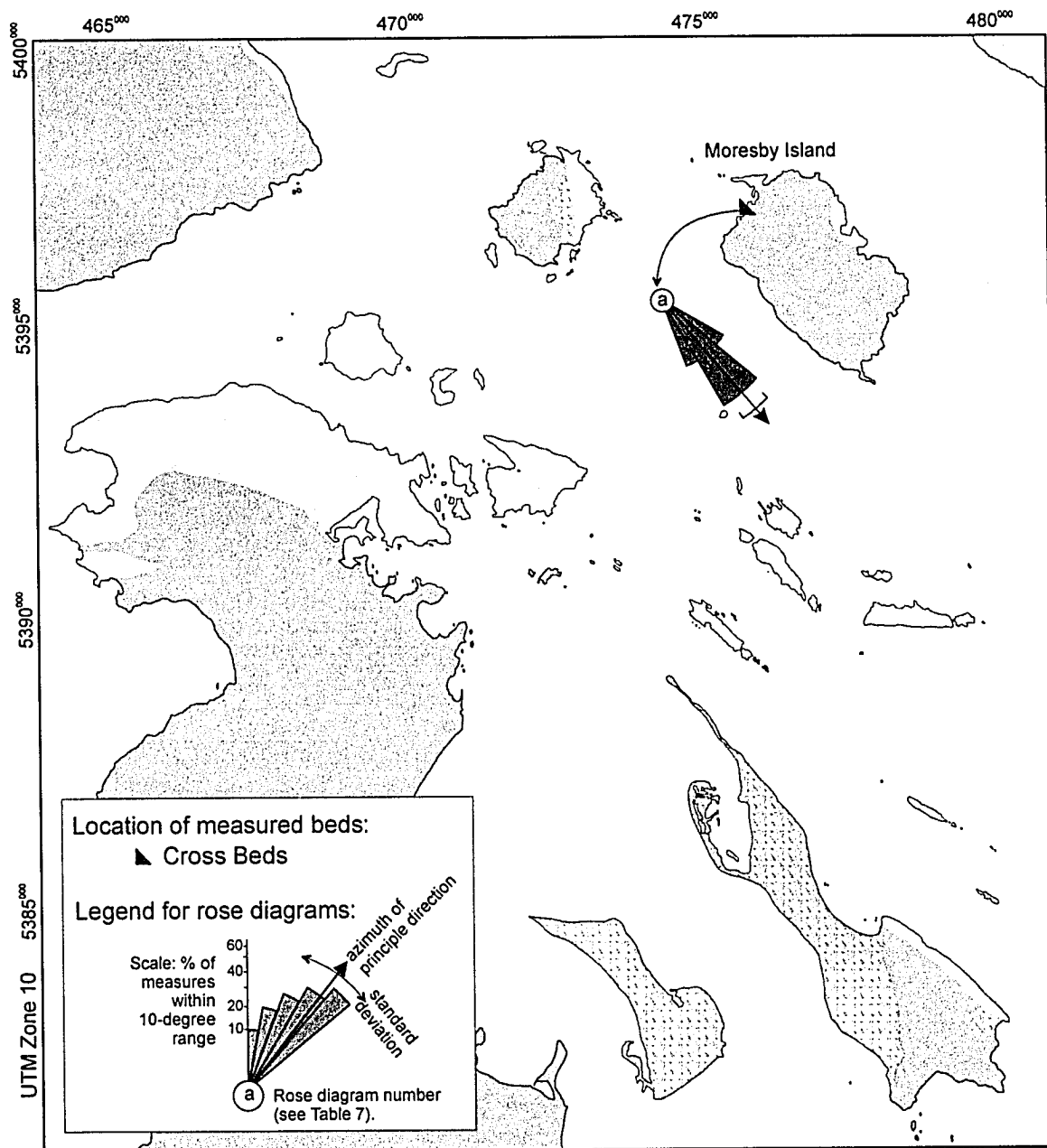


Figure 39: Rotated Paleocurrent trends form the Comox Formation: Facies Association 1.

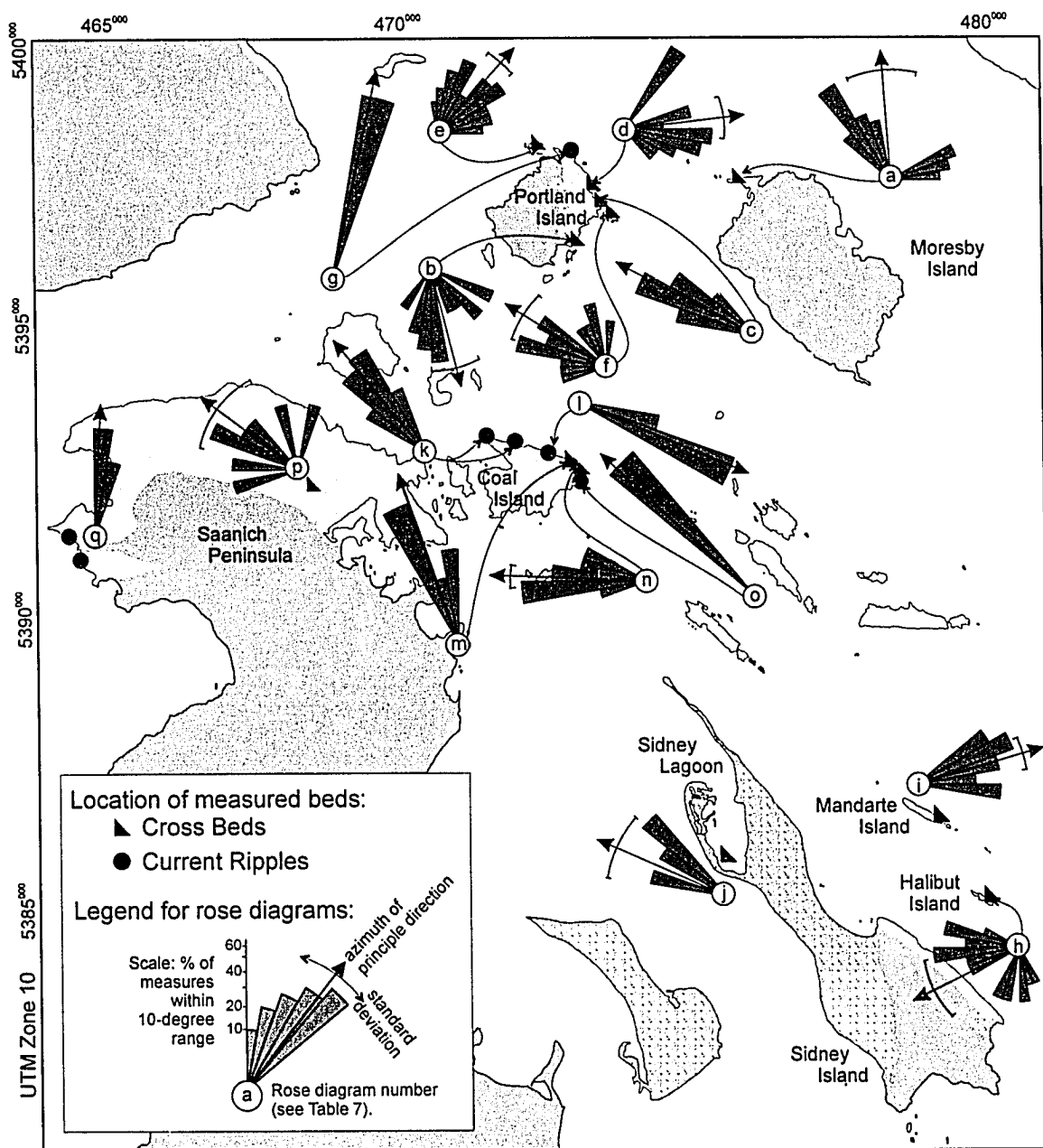


Figure 40: Rotated Paleocurrent trends from the Comox Formation: Facies Association 2.

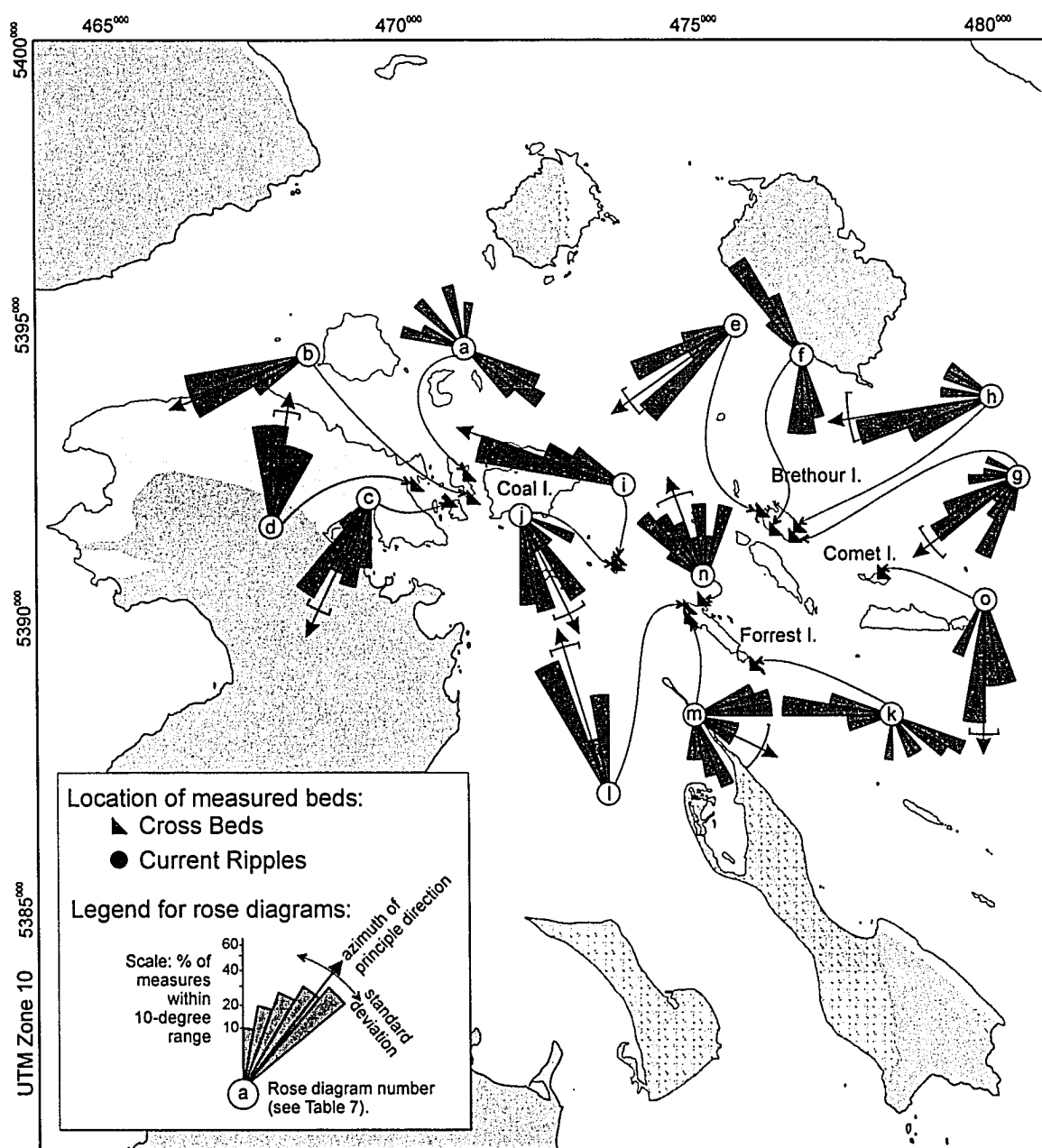


Figure 41: Rotated Paleocurrent trends from the Comox Formation: Facies Association 3.

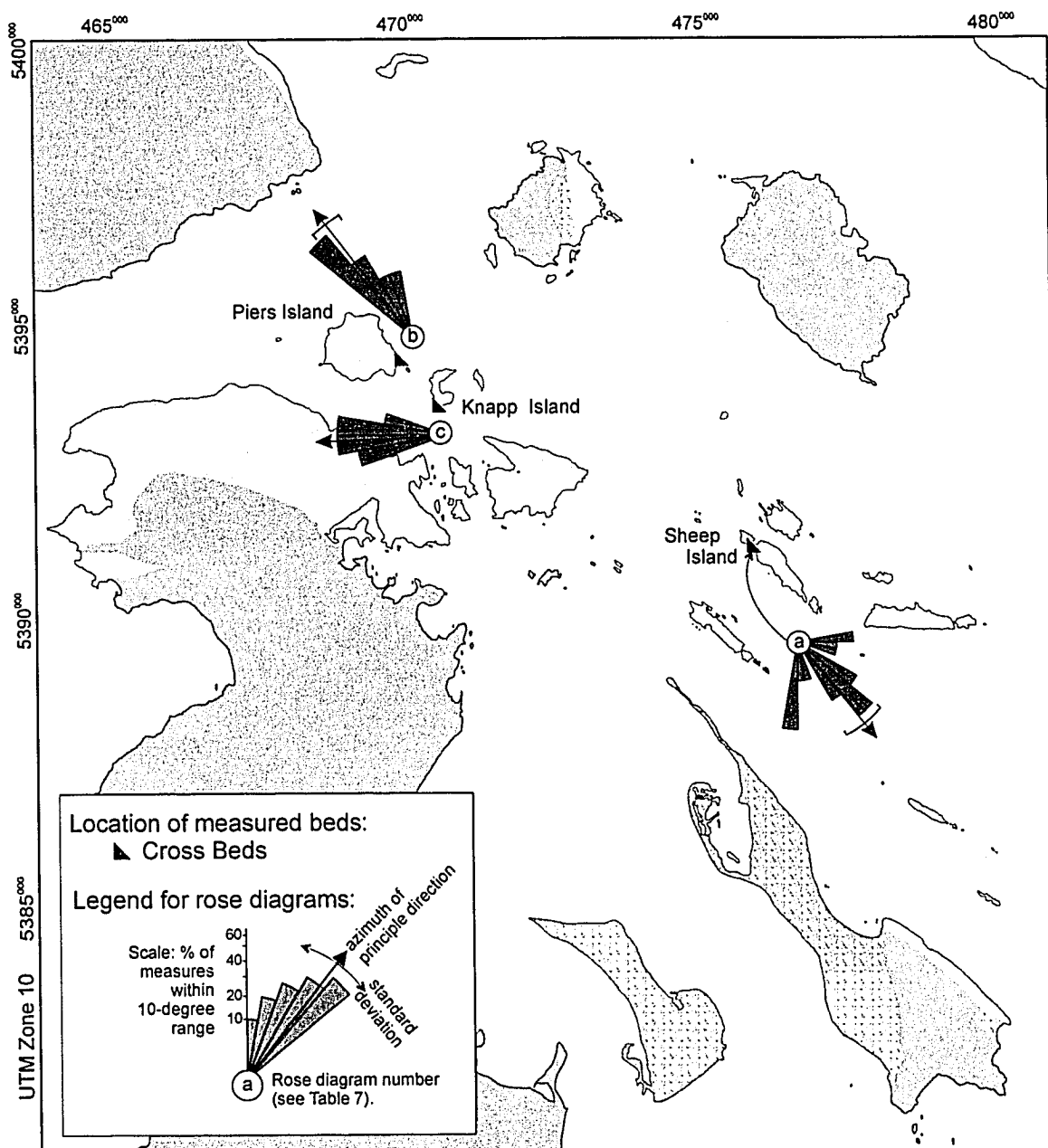


Figure 42: Rotated Paleocurrent trends form the Haslam Formation.

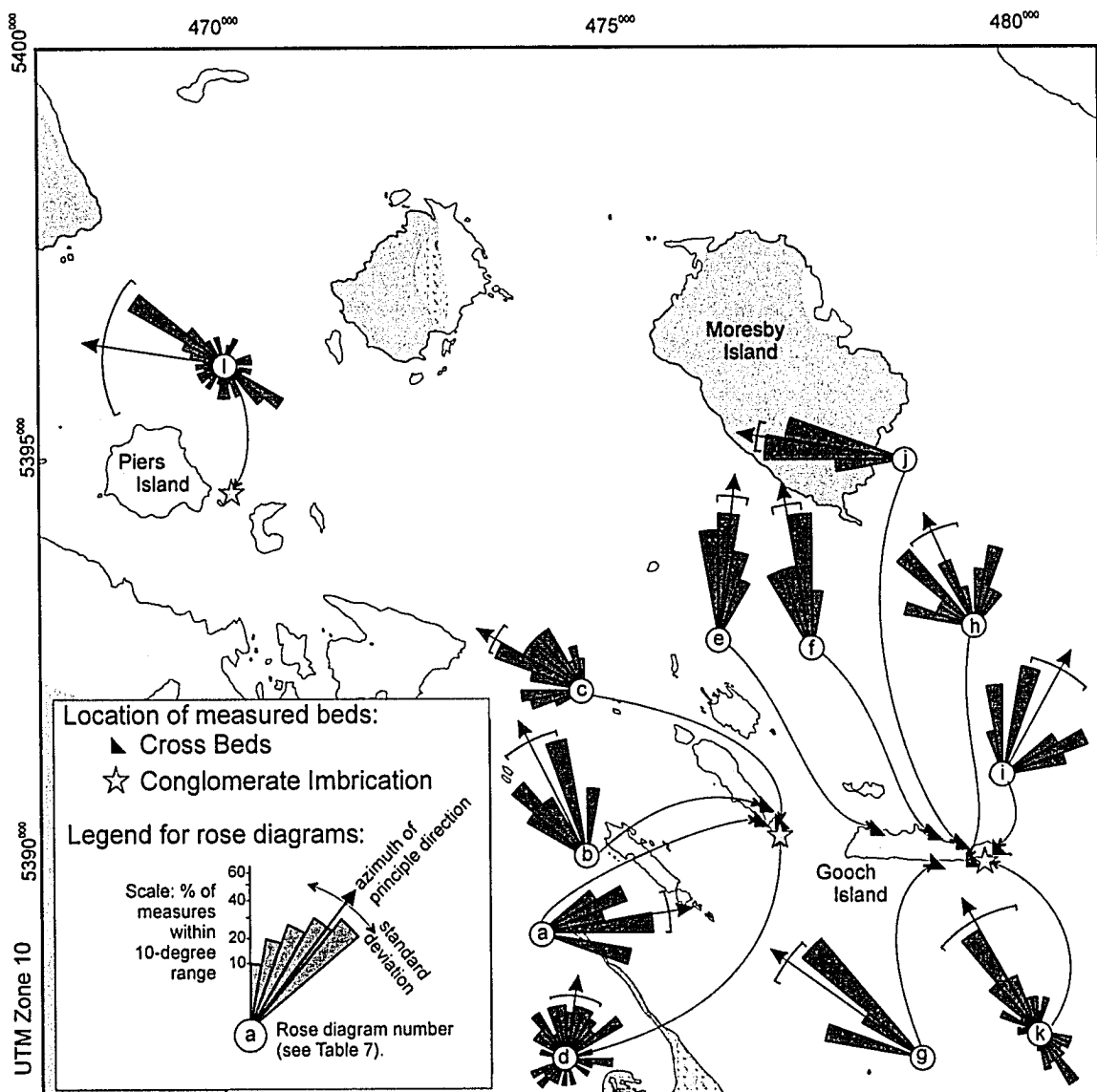


Figure 43: rotated Paleocurrent trends from the Extension Formation.

## **Provenance**

The combination of paleocurrent, sandstone and conglomerate lithology trends evaluated suggest a two-phase provenance history for the study area. Trends for the Comox Formation appear to be overwhelmingly influenced by local basement conditions, including both paleotopography and local changes in basement lithology. In contrast, the Extension Formation shows more consistent trend with respect to both lithologies and paleocurrents.

The Comox Formation is interpreted to represent shoreface and barrier-island type depositional settings (see Chapter 3), and, as a result, has rather mixed paleocurrent trends. A weak westward overall trend likely represents net movement of sediment in the offshore direction, although there is considerable shore-parallel and onshore flow preserved. These patterns are further complicated by the irregular topography of the basal unconformity, with orientations of reflective shorelines varying over time and along depositional strike. The resultant paleocurrents probably define local headland-cove relationships than overall net-sediment transport.

Sediment lithologies also vary in the Comox Formation and commonly reflect local basement lithology; a trend observable in both outcrop and thin section analysis. The overall immaturity of the sandstones (with a lack of rounding, and abundant unaltered feldspar and volcanic lithic fragments relative to quartz grains), reinforces the interpretation of a predominantly local source for these sediments. This becomes more evident with increasing sample proximity to the basal unconformity (see Moresby and Sydney Island samples, Table 4).

Higher-resolution dedicated paleocurrent studies of the upper Comox Formation units may clarify some of the uncertainties about the paleoenvironmental conditions of this unit.

In comparison, trends observed in the Extension Formation are more consistent, indicating a sediment provenance to the southeast. Imbrication of non-equant clasts and cross-bedding in conglomerates and sandstone strongly indicate a northwestward flow direction. A reduction in unaltered feldspars and an increase in metamorphic and chert lithic fragments (compared with samples from the Comox Formation) in the sandstones indicate slightly more mature sediments, possibly from a more distal source than local Wrangellian basement. Conglomerate clast lithologies also reflect less clearly the local basement conditions, and include clast types not seen in local Wrangellian basement.

Paleocurrent data from the Haslam Formation is limited, due to the recessive nature of the Haslam Formation units, the lack of well preserved and exposed current ripple horizons in the turbidites, and the significant post-depositional deformation of the beds. Results for the two main outcrop areas presented contradictory paleoflow directions, possibly reflecting the difficulty in estimating original bedding orientation in poly-deformed strata.

Overall trends suggest deposition on a north-south oriented coastline, open to the west. There is a transition from an irregular coastline to submarine channels with northeast directed flow. This is in agreement with much of the paleocurrent data previously collected from the lower Nanaimo Group along the southern part of the basin (Pacht, 1984; Mustard, 1994), but contrasts with some



interpretations of paleoenvironmental shorelines as suggested by England (1990).

The immature sandstones that are prevalent in the lower Nanaimo Group indicate a proximal sediment source. The use of QFL and QmFLt ternary diagrams (*cf.* Dickinson *et al.*, 1983; see Appendix C for analysis techniques) suggests a source area that includes both transitional arc and lithic to transitional recycled orogen settings (Figure 35). There are several sediment sources to the east of the study area that may provide the relatively fresh volcanic rock fragments that dominate these samples. Along with acting as local basement, Wrangellian rocks likely existed to the east of the basin, where they were being intruded by Coast Belt plutons (Friedman *et al.*, 1995). The San Juan nappes to the southeast include several units of Late Jurassic and/or Early Cretaceous age (Brandon *et al.*, 1988), along with sources of sedimentary and metamorphic lithic fragments that become more prevalent in the Extension Formation. It is possible that the subtle shift in lithology from Comox Formation to Extension Formation reflects increased sourcing of “recycled orogen” type sediments from the San Juan nappes, as suggested by Mustard *et al.* (1995). This change in source may also account for the increase in recycled sedimentary clasts found in Extension Formation conglomerates.

This study is located at the southern extremity of the preserved Nanaimo Basin, and the lithologies observed contrast somewhat from typical Nanaimo Group deposits. Sandstones from the study area are relatively quartz-poor and richer in volcanic rock fragments than typical Nanaimo Group sandstones, which

are typically lithic to arkosic arenites (Mustard, 1994). Contrasts between conglomerate clast counts from the study area and “typical” Nanaimo Group deposits have already been noted (see Table 7). These contrasts suggest that sediment provenance differs along the north-south extent of the Nanaimo Group, and changed over time. It is likely that in the southern end of the basin, the San Juan nappes and Cascades became the principal source of detritus after initial dominance of local Wrangellian basement. Farther north, the emergent, then dissected, Coast Belt arc was the most significant source of sediment to the basin, particularly for younger units (Mustard, 1994; Katnick and Mustard, 2003).

The atypical provenance of the study area may also be a result of earlier deposition, following a sequence suggested by Mustard *et al.* (1995). Turonian units in the study area predate the bulk of Nanaimo Group sedimentation, but are concurrent to the most significant thrusting in the Cascades and San Juan nappes (Brandon *et al.*, 1988; Matzel *et al.*, 2004; Paterson *et al.*, 2004). Concurrent and later thrusting in the southwestern Coast Belt (Journeay *et al.*, 1992; Umhoefer and Miller, 1996) may have become a more significant source over time, as Nanaimo Group sedimentation spread into regions more proximal to the Coast Belt. As such, variations in clastic composition may in part also be a reflection of lithostratigraphic diachroneity.

## **CHAPTER 5: STRUCTURAL GEOLOGY**

### **Overview**

More than 3000 measurements of bedding aspect, brittle fractures, folds, foliations, and faults were collected from the study area. Appendix B contains all structural data in tabular form, separated in terms of measurement type and structural domain. This chapter provides a summary of trends observed, utilizing stereonet projection of data, and compares the structural data to regional structural systems as described in Chapter 1. All measurements are reported using the “right-hand rule”, where the strike azimuth is 90 degrees counter-clockwise from the direction of maximum dip.

### **Bedding Orientation**

Almost 1500 measurements were recorded of primary bedding structures (see Appendix B for all tabulated data), not including 900+ paleocurrent measurements recorded (see Chapter 4). The dominant trend observed is of a shallow to steep dip towards the northeast, best displayed in the Sidney, Forrest, Domville and Coal North domains, where strong clusters of bedding planes strike around azimuth 290, with dips ranging from 55 to 75 degrees to the north (Figure 44). The mean bedding orientation is 290/53N, with the distribution of poles to bedding slightly girdled along a great circle with an orientation of 017/87NW. However, there are both subtle and obvious variations within and across domains.

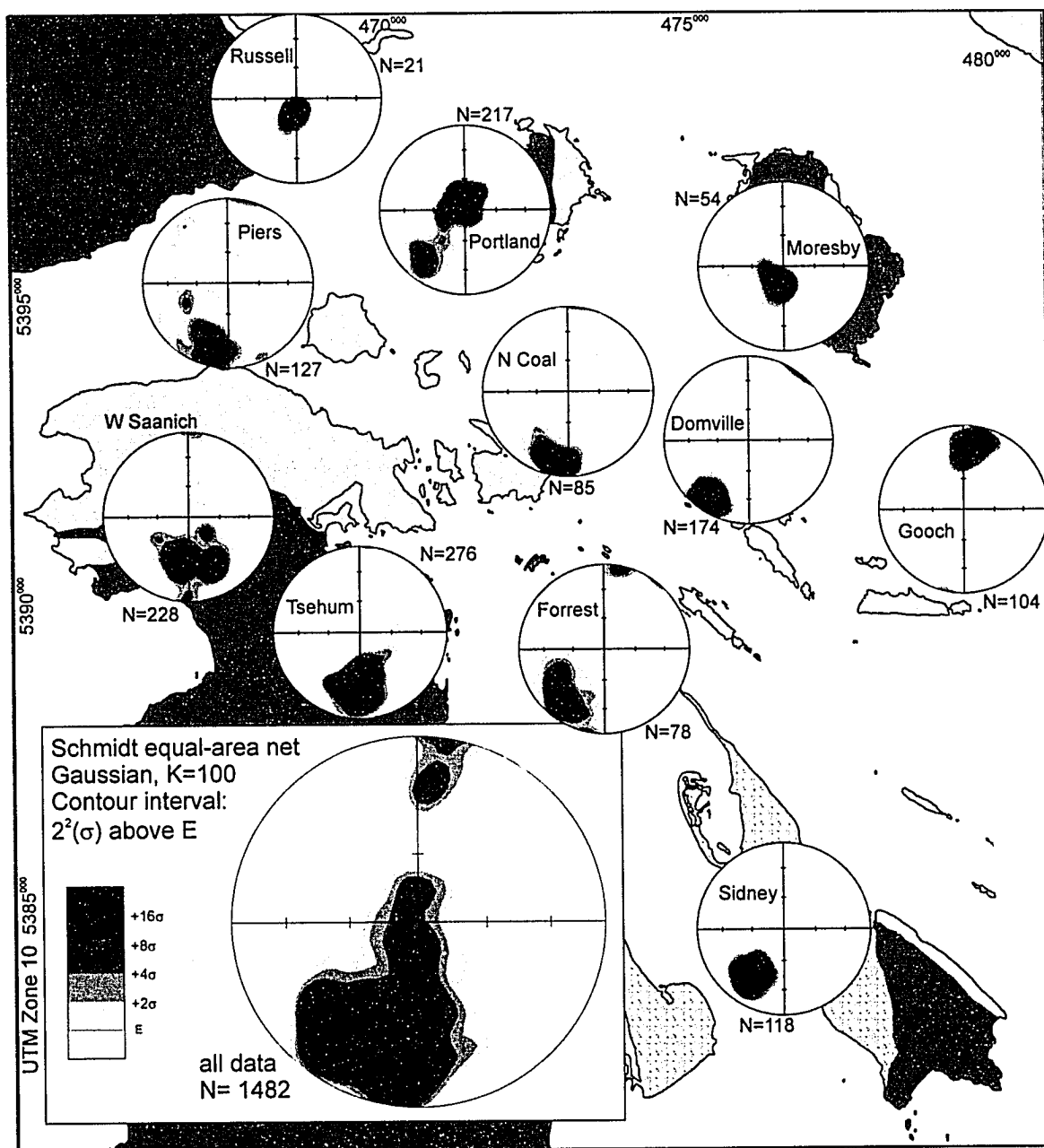


Figure 44: Poles to bedding planes, by domain.

As apparent on Figure 44, bedding dips are shallower in the north of the study area (Russell, Moresby, and most of Portland domains) with the poles to bedding tightly clustered, whereas domains to the west have steeper bedding dips (Tsehum and Piers), and display less tightly clustered poles. The poles to bedding planes in Portland, Piers, and Saanich domains have slightly girdled distributions. On Portland Island, this girdling can be attributed to several NW-SE trending tight folds along the east coast of the island. On Piers Island, small folds in fine-grained units along the south shore affect the bedding average. The combination of a very broad antiform along the spine of the Saanich Peninsula and some small fault-related structures in Towner Bay similarly affect the Saanich domain distributions.

Bedding in the Gooch domain sharply contrasts with the rest of the study area. Strata on Gooch, Rum, and Comet Islands is overturned to the north, and strikes almost east-west with a moderate to steep southward dip. Within the Gooch domain, bedding dips become steeper to the north but strike varies little across the domain. This is interpreted to represent the overturned limb of a large fold, as discussed below along with the other fold structures interpreted from bedding data.

## **Brittle Structures**

Brittle structures are defined herein as joints, shear fractures, and fractures of indeterminate movement. Of the approximately 1100 brittle structures measured (data tabulated in Appendix B), the vast majority are of the indeterminate offset type, at least partially due to the poor preservation potential

of slickenlines, slickenfibers, or plumose structures in the modern intertidal region where most of the fractures are measured. For this reason, all brittle fractures are first treated as a single population, then specific analysis is performed of identified joints and shear fractures/minor faults.

Brittle structures show strong trends generally perpendicular to those of bedding orientation (compare Figures 44 and 45). The overall trend is towards near vertical fractures which strike NE-SW, with a mean plane oriented at 031/89SE (Figure 45). A similar trend is well displayed on the stereonets of most domains with subtle variations (*e.g.* Tsehum and Saanich domains, which show more north-south oriented mean planes compared to the Portland or Sidney domains). Major deviations from this trend are apparent in the Piers and Gooch domains.

The Gooch domain has a girdled distribution of poles to fracture planes, with the girdle forming along a great circle with a pole oriented at 42→001. Much like the bedding distribution, Gooch domain stands apart as it is dominated by a large fold structure as described below.

The distribution of poles to fracture planes in the Piers domain is more uniform than in other domains, although the mean value does not vary from that in nearby domains. It is possible that this uniformity displays a sampling bias in other domains. Most islands in the study area are elongate along a northwest-southeast axis. As a result, considerably more outcrop is exposed on the longer southwest and northeast shores of the islands. Fractures normal to these

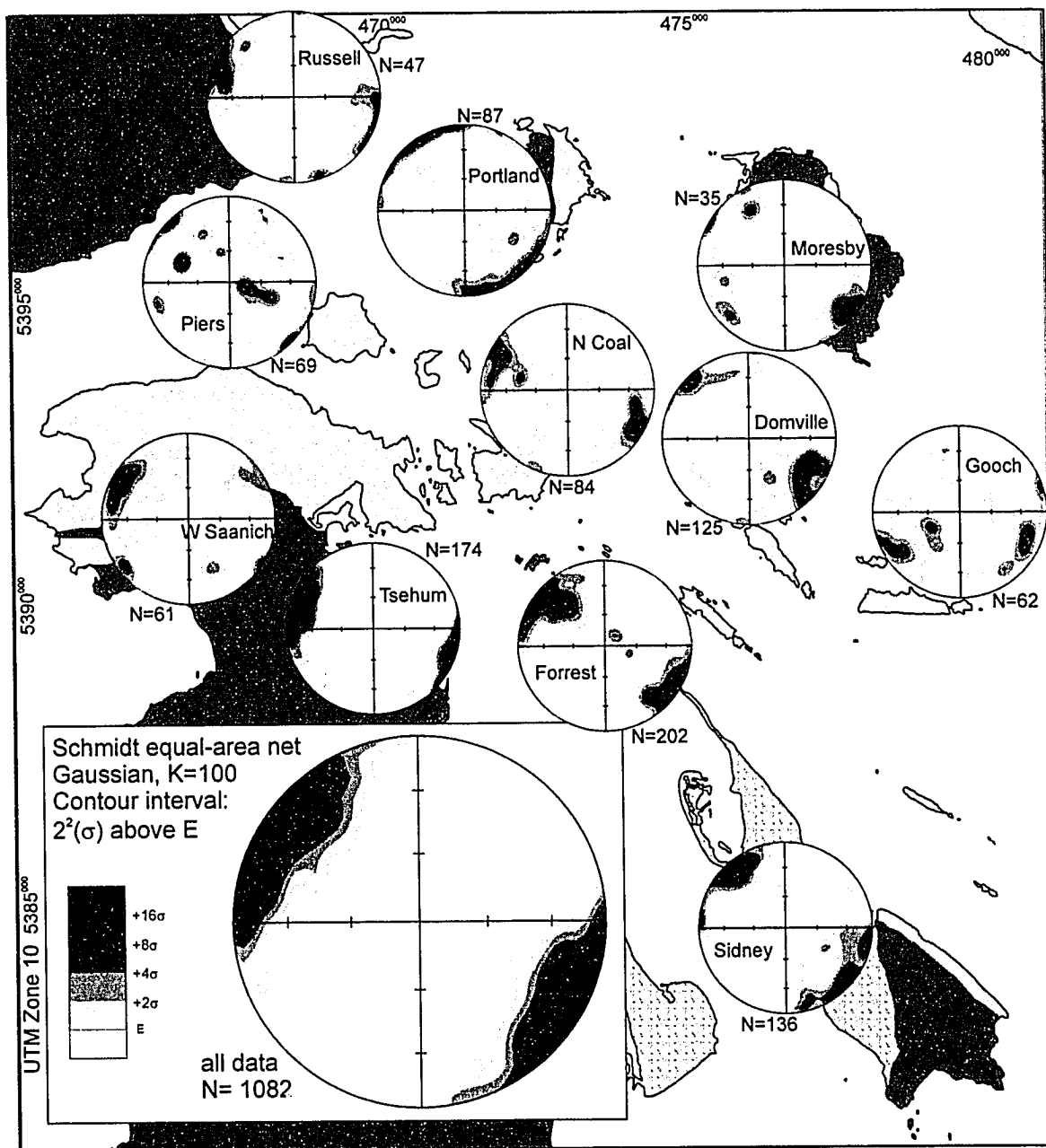


Figure 45: Poles to planes of brittle structures.

shorelines may be preferentially exposed relative to fractures parallel to the shorelines, leading to a biased sampling of the population. Piers Island is more equant than other islands, with shoreline outcrop on all sides. If the relative uniformity of measures in Piers Domain does reflect sampling bias in other domains, it is important to note that the mean plane of fractures from Piers Domain is close to the mean value for all domains combined, and the Tsehum and Saanich domains (which also include coastlines of varying orientation) do not show a diffuse a distribution. In addition, the distribution becomes more “typical” if the large number of joint measures from Piers Island is removed from the sample.

Joints were identified as extension-caused brittle fractures, on the basis of either visible plumose structures, or where parallel, systematic mineral veins suggest dilation along fracture surfaces. There are 10 locations in three domains where jointing was identified and measured, with a total of 65 measurements (Figure 46; see Appendix B for all data).

Within the Piers domain, the majority of measures are thin, parallel calcite veins with a regular spacing frequency of approximately 10 per metre, within thin-bedded sandstone-mudstone couplets (Figure 47). Commonly, the calcite-filled joints are visible in the sandstone beds with alternating mudstone layers not similarly jointed, and in some locations the joints are cross-cut by shear fabrics. In other localities, joints have the same spacing frequency and similar orientations, but no calcite fill was identified (Figure 47b). The distribution of



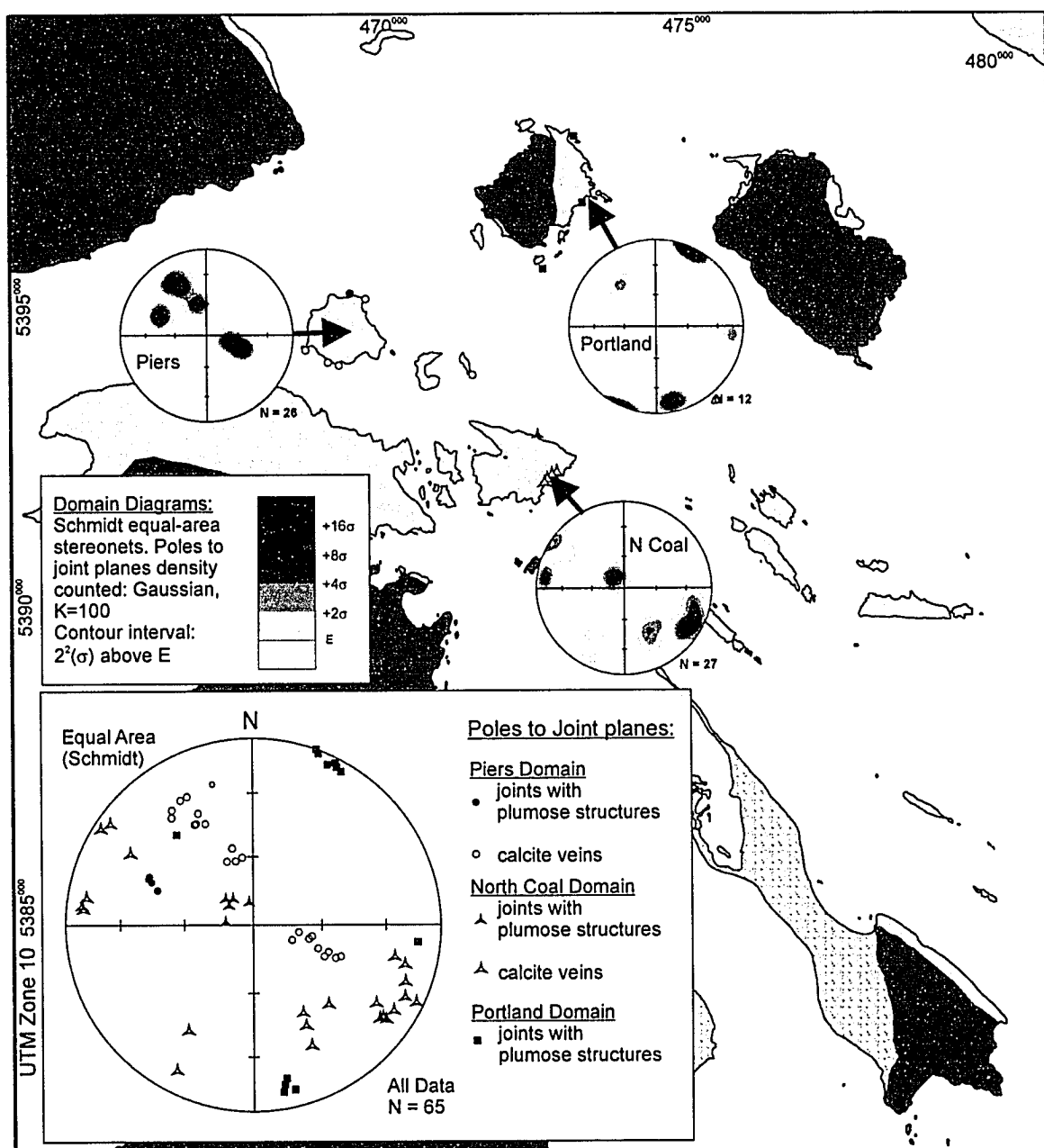
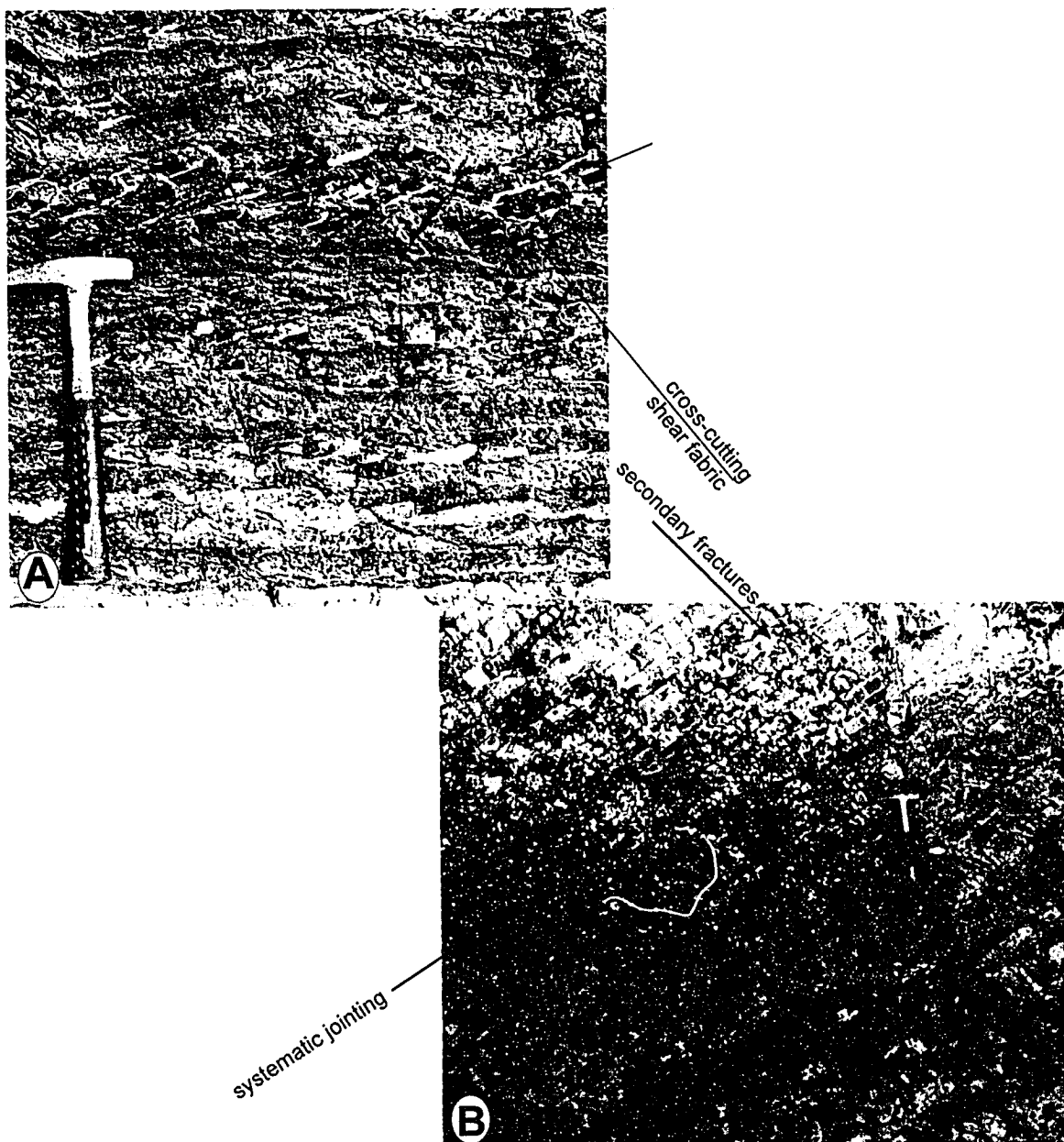


Figure 46: Poles to planes of joints.



**Figure 47: Joints exposed on Pym Island (A), where they are filled with calcite and cross-cut by a shear fabric, and on western Piers Island (B), where they are systematic and occur at regular spacing, but are not filled.**

poles to joint planes is girdled along a plane at 310/78NE, with the median plane around 060/32SE. Where shear fabrics are associated with the joints, the foliation has an average orientation of 307/83NE, and shearing is apparently sinistral, as suggested by offset and edge-deflection of joints.

A large number of calcite-filled joints were identified in the muddy sandstone just north of the large shear zone cross-cutting Coal Island. The veins are less than 1 centimetre thick, with regular spacing from 5 to 20 centimetres. They are intermittently exposed over several dozen metres north of the main shear zone. The median plane of these joints is oriented at 120/76NW, although the distribution of poles to the planes is girdled along a plane oriented at 105/43SW (see also Figure 50).

On the north shore of Coal Island, and in several locations in the Portland domain, local non-systematic jointing was identified, although no obvious domain-wide trends were observed. On Hood Island at the south end of the Portland domain, joints identified as gash fractures associated with local small shear zones were observed in sandstone beds.

Brittle fractures were identified as shear structures if there was visible offset of marker beds, slickenlines or slickenfibers on the fracture surface, or if there were associated structures (such as en echelon fracture systems) identifying that there was a displacement along the fracture plane. There are 245 measurements of brittle fractures that meet these criteria, representing 121 individual structures. Only the average orientation of each individual structure was used for analysis below (see Appendix B for all data).

Of the 121 individual structures, 42 structures were of uncertain offset, where marker beds are only seen on one side of the structure, or slickensides are bi-directional. The other 79 structures were dominantly strike-slip, with 34 dextral, 27 sinistral, 10 normal, and 8 reverse offsets indicated (Figure 48). Populations of shear fractures with identified offsets were small for most domains (Figure 49), with data density ranging from 7 to 19 structures per domain, and no inter-domain trends were identified. Significant individual structures were added to the geological map.

Shear fractures with identified strike-slip movement are separated into dextral and sinistral populations, each of which have strongly clustered trends. The median plane of each population is plotted on a stereonet, and the two populations are interpreted to represent a conjugate pair (Figure 48).

One large fault structure is partially exposed on Coal Island, and forms the boundary between the North Coal and Tsehum domains. This shear zone is exposed on the southeast shore of Coal Island as a ~100 metre wide area of sheared Comox Formation rocks, with the intensity of deformation increasing to the west, to a point where the shear zone is covered by more than 10 metres of Quaternary sediments (Figure 50). The shear zone is interpreted to trace northwest (~azimuth 300), following the low ground through the middle of Coal Island and through Lewis Bay. The shear zone is a brittle-ductile type, probably reflecting the variable rheology of the alternating silty-mudstone and sandstone facies of the Comox Formation, although multiple re-activations of the shear zone is also a possibility (Davis and Reynolds, 1996). Shear indicators such as

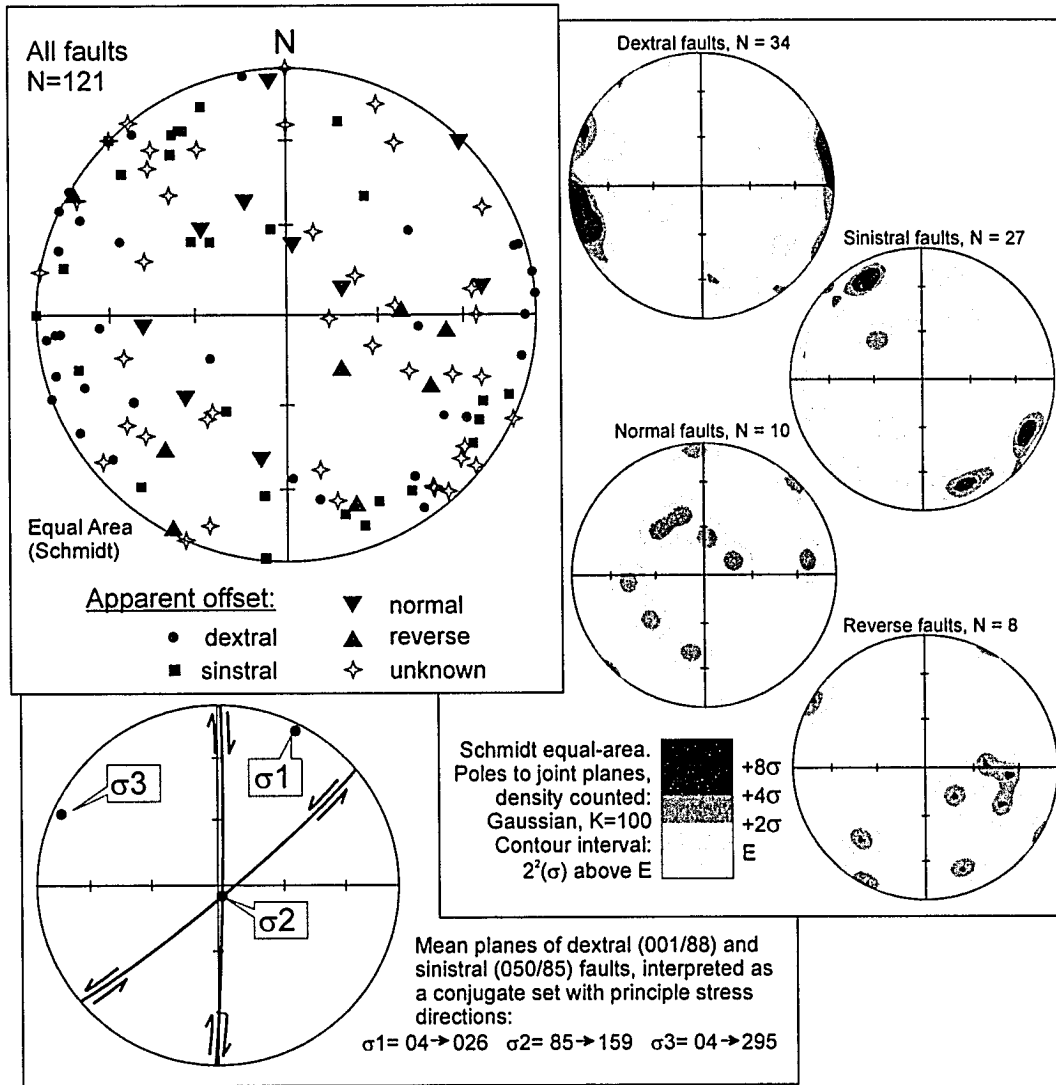


Figure 48: Faults measured in study area.

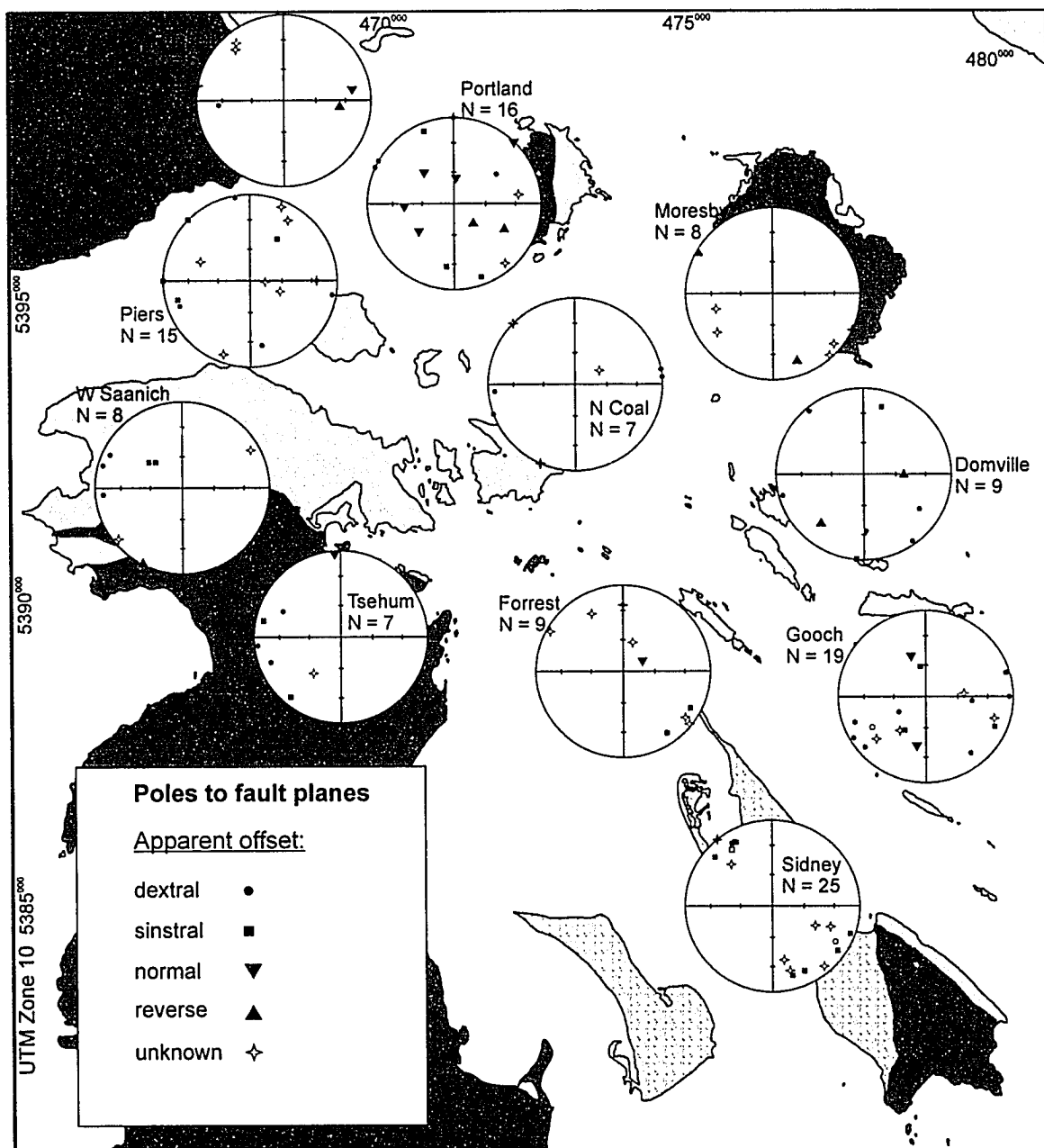


Figure 49: Faults distributed by domain.

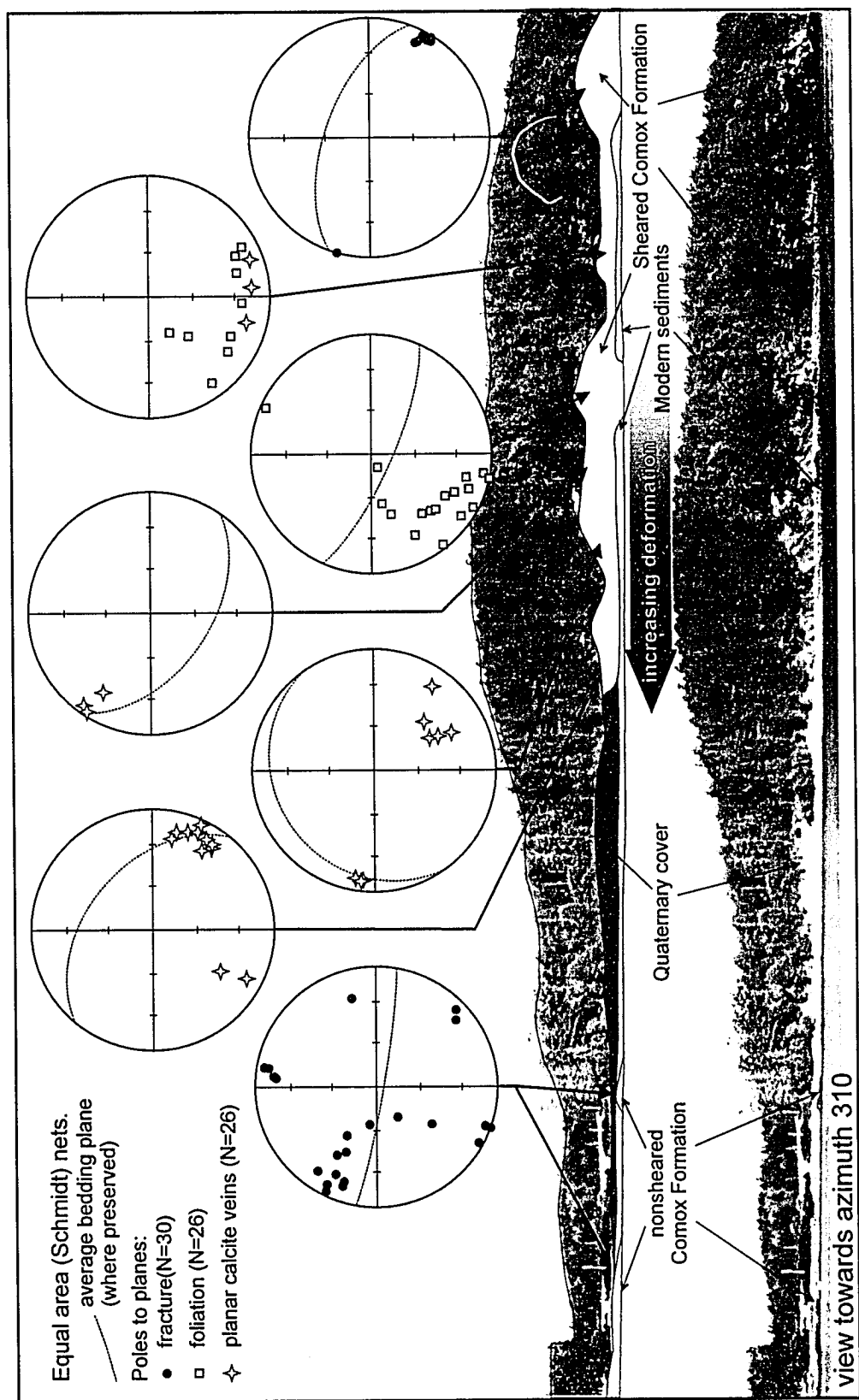


Figure 50: Shear zone on Coal Island

foliation, fractures, and aligned mineral veins are intermittently present (Figure 50, see Appendix B for all data). Foliation planes average around 300/64NE, and steepen slightly to the west, although there is a wide dispersal of measured values. En echelon calcite veins towards the centre of the shear zone are oriented along 210/76MW, which is approximately normal to the main shear plane. Interpretation of sense of shear is further complicated by the anastomosing character of the shear zone and the presence of large blocks of undeformed rock entrained within the shear zone, with the rotation direction of the blocks poorly defined (Figure 51).



**Figure 51: Large rotated block within Coal Island shear zone.**



Larger fault structures are interpreted to pass between some of the islands of the field area, or through areas where outcrop is limited (see Backpocket Map). These interpretations are either based on changes in bedding orientations between islands, formation and facies changes between islands compared to interpreted stratigraphy, or the presence of local drag-fold structures. Faults connected to drag fold structures are discussed in the next section under folds. The larger, regional faults are discussed below as part of the regional structural synthesis.

## **Folding and Foliation**

Folding is apparent at several scales within the field area. Fine-grained units of the Haslam Formation within the Piers and Domville domains contain small folds that can be measured directly, because the fold wavelength is generally less than 10 metres. In several places, medium-scale folds are indicated by changes in bedding orientations over tens of metres, with  $\pi$ - and  $\beta$ -diagrams required to calculate the orientation of the fold axis (*cf.* Davis and Reynolds, 1996). The largest folds are indicated by examining orientations of all measures between domains which reflect folds with limbs of hundreds of metres or more, such as the overturned units of the Gooch domain.

Domville and Piers domains both contain extensive outcrops of Haslam Formation sandstone-mudstone couplets interpreted to represent turbidite successions (see Chapter 2). On Domville and Piers Islands, these turbidites are complexly folded with fold heights and widths of less than 10 metres. The folds are interpreted to be tectonic, not penedepositional structures related to slumping

of unconsolidated sediments (*cf.* Maltman, 1994). This interpretation is based on the extensive area of similar folding (Figure 52), the lack of bounding non-folded sediments, the lack of fluid escape or liquefaction structures, and the general appearance of the folds which suggests a higher rheology contrast between sandy and muddy layers than would be expected for unconsolidated sediments (Ramsay and Huber, 1987).

The folds on Domville Island are apparently near cylindrical, with chevron, elliptical, and some conjugate shapes (Figure 52b-d). Fold limb angles range from open to tight, with no isoclinal folds observed. Axial-planar cleavage is poorly developed absent or. Hinge lines and axial surfaces were measured from 14 separate hinge zones along the 800-metre long stretch of the southwest coast of Domville Island. The folds are moderately plunging and moderately inclined in terms of the Fleuty classification (Fleuty, 1964), with the mean axial surface of 344/55NE, and the mean fold axis of 42→127 (Figure 53).

Folds in the same Haslam Formation units are also exposed on the south coast of Piers Island. These folds are similarly chevron- or elliptical-shaped, and open, although generally larger than those seen on Domville Island with wider hinge zones. The fold trends were calculated by producing  $\beta$ -diagrams from limb orientations (Figure 54). The resolved mean axis of folds moderately plunges around 53→066, and the mean axial surface (as an average of resolved bisecting surfaces) is upright, with an average orientation of 059/81SE (See Appendix B for all data).

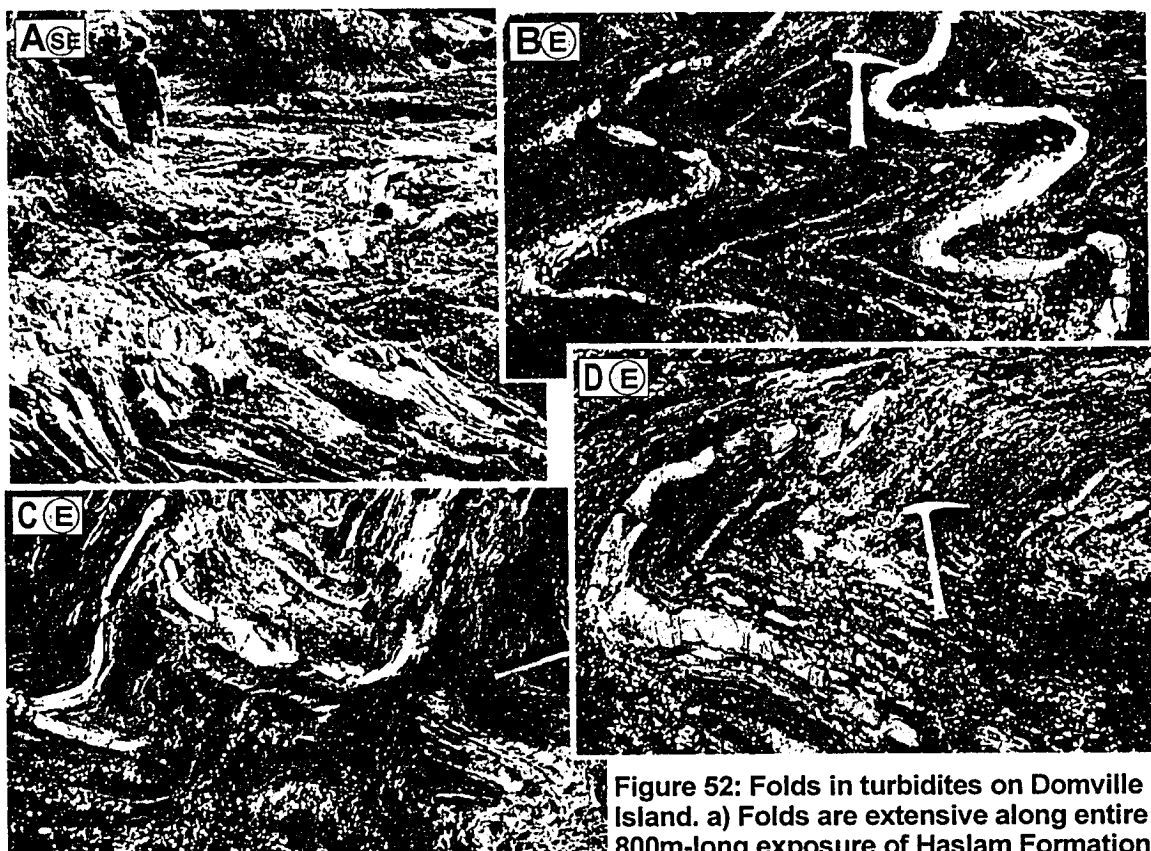


Figure 52: Folds in turbidites on Domville Island. a) Folds are extensive along entire 800m-long exposure of Haslam Formation. b) Ellipsoidal and chevron fold shapes. c) Conjugate folds. d) large cylindrical folds with amplitudes of several metres.

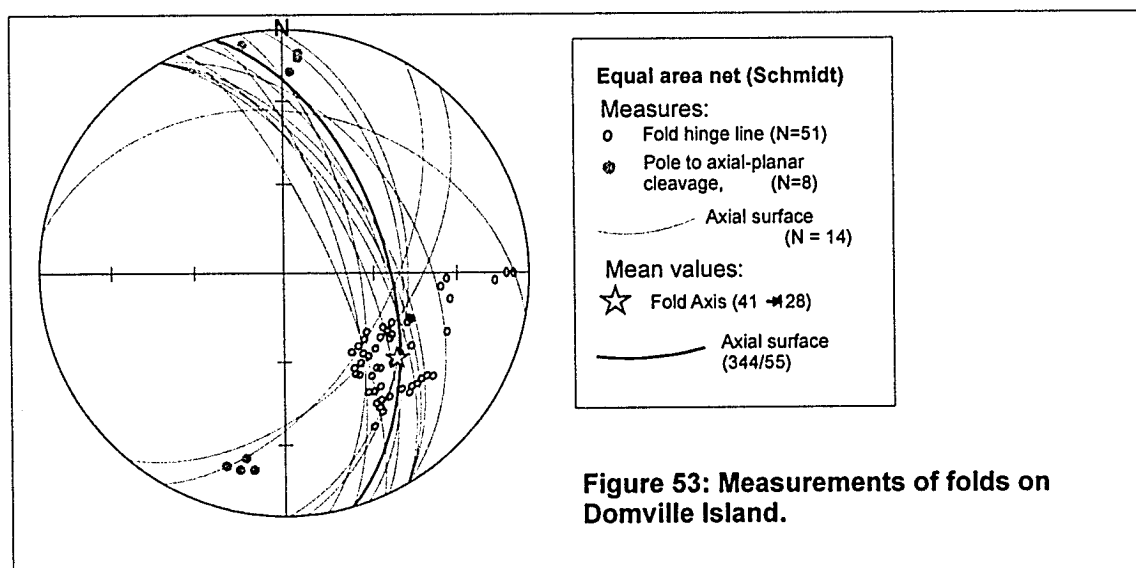


Figure 53: Measurements of folds on Domville Island.

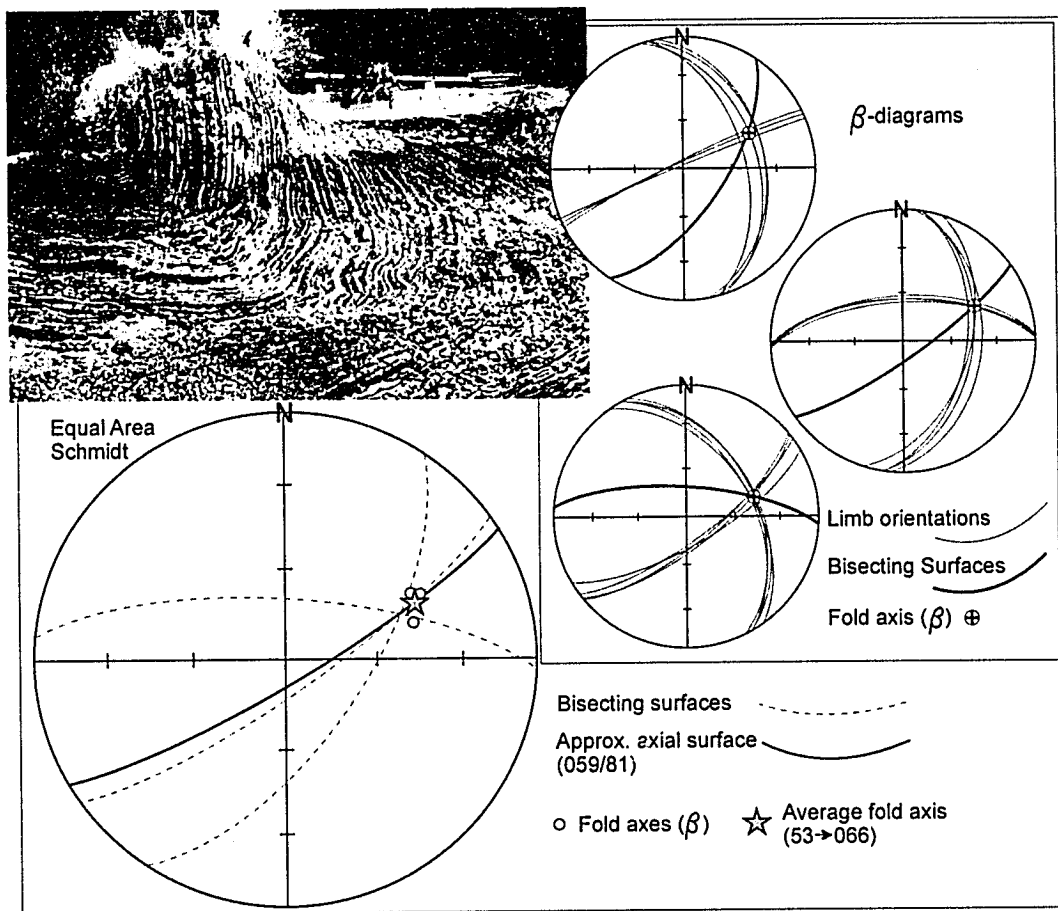


Figure 54: Folds on Piers Island.

Larger folds are apparent in Comox Formation rocks on the east side of Portland Island, between Arbutus Point and the Pellow Islets (see Backpocket Map and cross section A-A'). Although hinge zones are not well exposed along this coast, a  $\pi$ -diagram of poles to the bedding orientations along the coast indicates a large (wavelength ~100 m), sub-horizontal, moderately inclined, open fold with a hinge line of approximately 06→126 and an axial surface near 121/53SW, with the fold very near cylindrical (Figure 55a). Near the hinge zone just south of Arbutus Point, finer-grained units have a pronounced cleavage, interpreted to be axial-planar cleavage to this fold, with the average plane orientation of 113/64SW. Two other broad folds are recognized on the eastern half of Portland Island (Figure 55 b and c), and have similar orientations.

A fold of similar scale occurs as a broad structure in Iroquois Channel, just north of Tsehum Harbour, and is readily apparent in aerial photography of the area (Figure 56). This is interpreted to be a drag fold along a fault that passes through Canoe Cove and underneath the Swartz Bay ferry terminal to the northwest, although the fault itself is not exposed. With the hinge line of the fold plunging moderately (~22°) towards azimuth 306, and the fault trace interpreted to run through the channel between Kolb Islets and the Saanich Peninsula, the sense of vergence of the drag fold indicates that the NE side of the fault moved upward relative to the SW side. The direction and magnitude of any oblique offset on this fault is unknown, as is the orientation of the fault below the surface trace.

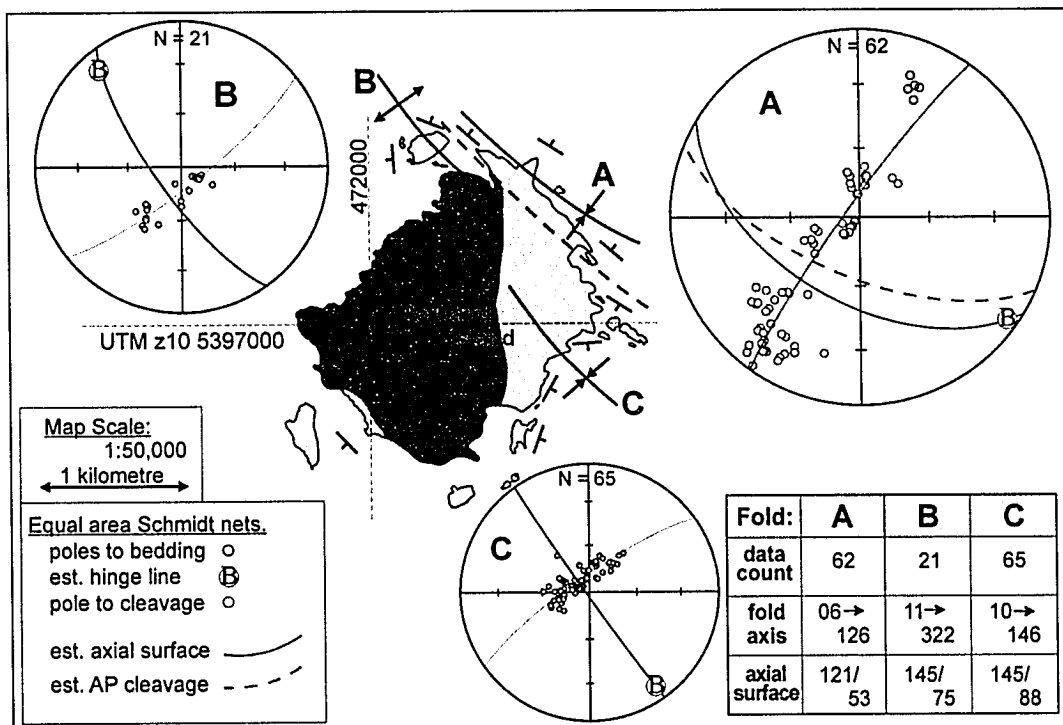


Figure 55: Folds on Portland Island.

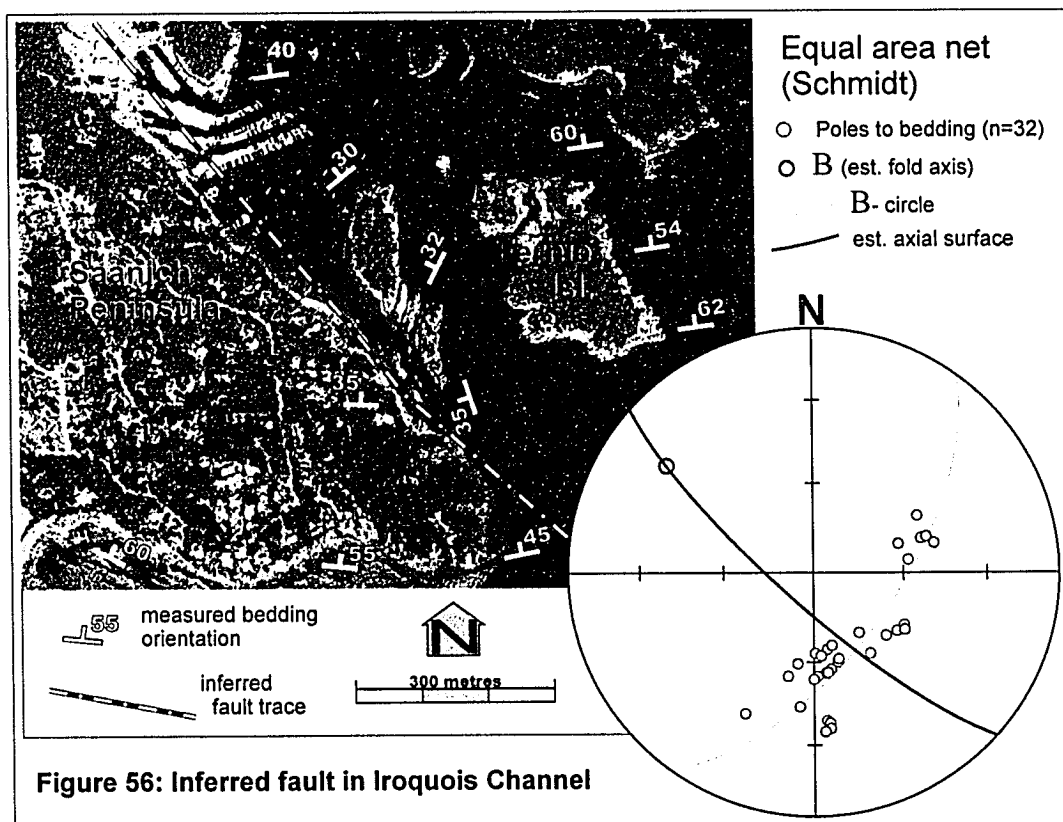


Figure 56: Inferred fault in Iroquois Channel

Folds of similar scale are also interpreted on the west coast of the Saanich Peninsula between Coal Point and Deep Cove, based on bedding orientation changes (Figure 57; see Backpack Map and cross section B-B'). These folds are broad, open, and near cylindrical, with hinge lines plunging moderately to the northwest (~azimuth 290), and a fold wavelength of more than 500m. Just over one kilometre south at Towner Bay, at least two much smaller folds (with widths of approximately 10 metres) are exposed. These folds have similar hinge orientations and poorly developed axial-planar cleavage (Figure 58), and may be related to near-vertical reverse faults interpreted from stratigraphy in the Warrior Point area to the south (see Backpack Map and cross section B-B').

Finally, a large fold is interpreted in the eastern margin of the study area, spanning the Domville and Gooch domains. The stratigraphy of the two domains are well correlated (see chapter 2), and the bedding orientation within the Domville domain matches that of most nearby domains, with beds dipping moderately to the northeast. In contrast, strata of the Gooch domain are overturned to the north, with moderate to steep dips to the south. The cause of this disparity is interpreted as a large fold, with all of the Gooch domain within one large, overturned limb (Figure 59). This overturned syncline has a hinge line that plunges moderately towards the southeast, and if the bisecting surface of the fold is interpreted to approximate the axial surface, the fold is reclined.

A well developed regional foliation is not present in the study area, although local cleavage and shear-type fabrics occur. As described above, there is an axial-planar cleavage identified in direct association with several folds,

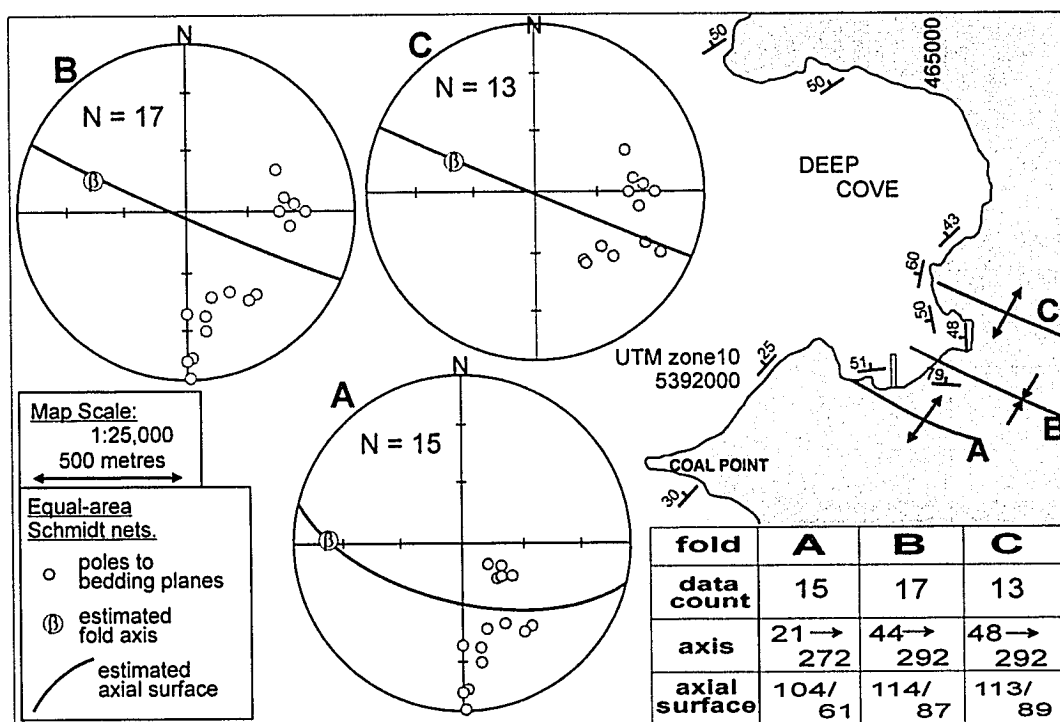


Figure 57: Folding around Deep Cove.

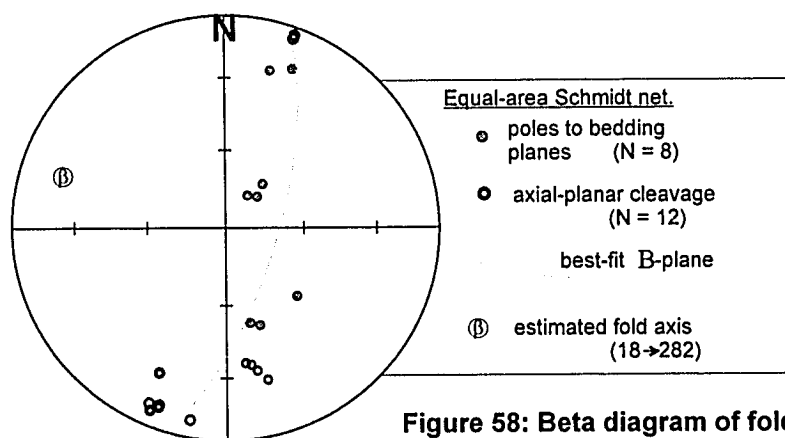
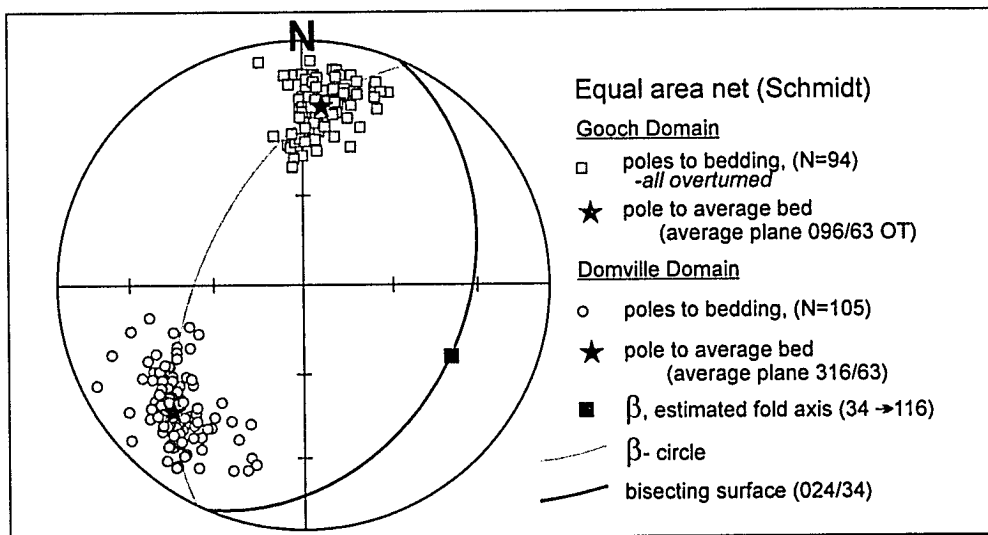
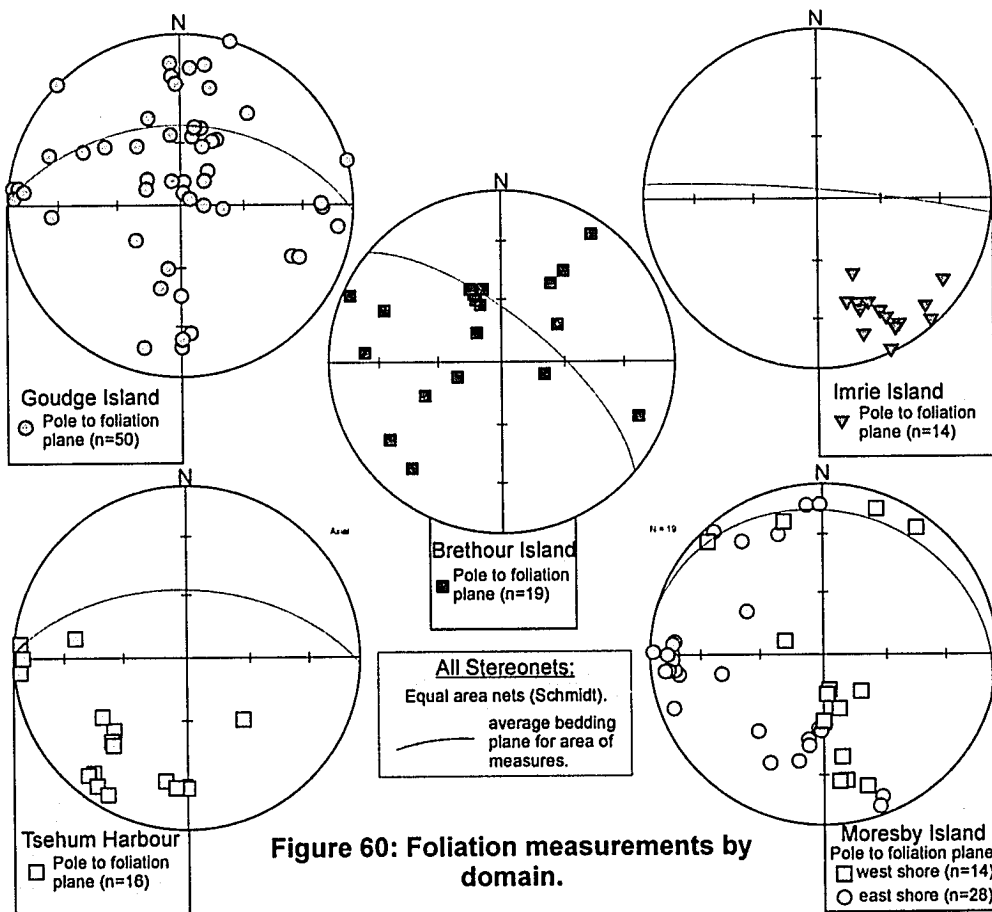


Figure 58: Beta diagram of folding around Towner Bay.





**Figure 59: Measurements of fold between Gooch and Domville domains.**



**Figure 60: Foliation measurements by domain.**

shear fabrics are associated with joint sets in the Piers Domain, and foliations occur within the large shear zone on Coal Island. There are also several locations where foliation fabrics are present but are not obviously associated with other local structures and are described below (all data are listed in Appendix C).

Goudge Island within the Tsehum domain is composed of alternating sandstone and silty mudstone packages of the upper Comox Formation (see Chapter 2). Several of the mudstone units display foliations, although sense of shear indicators were not recognized. The foliations generally dip moderately to the south (where local bedding dips steeply to the north), although the clustering of data is weak, and there is no recognizable trend across the island (Figure 60). Just to the west, near the northernmost extension of Tsehum Harbour, shear fabrics are exposed in roadcuts. The foliations cluster around 312/65NE and a few local deformed coal spars suggest counter-clockwise (sinistral) shear.

Similar strong foliation fabrics in mudstones were observed and measured on Moresby, Brethour, and Imrie Islands (Figure 60), but true sense-of-shear indicators were not observed in any of these locations. Some of these fabrics are only very locally developed, in some examples limited to single bedsets, and are likely pene-depositional fabrics related to soft sediment slumps or related to burial compaction. Significantly, in none of these locations is cleavage near parallel to bedding. Pervasive bedding-parallel cleavage is nowhere observed in the study area, arguing against the layer-parallel shortening suggested by England and Calon (1991).

## Structural synthesis

Many of the structural trends observed in the field area allow general interpretation of regional stress during deformation events. The dominant trend for the field area has the direction of highest principal stress oriented towards the northeast (azimuth ~030), and the least principle stress axes oriented towards the northwest (azimuth ~300). This is reflected in the data for regional jointing and shear fractures, and is consistent with previously described southwest-vergent shortening along the Cowichan Fold and Thrust System (England and Calon, 1991) and northeast-vergent shortening along the Gulf Islands Thrust System (Journey and Morrison, 1999).

Variations on this single stress regime are expressed on westernmost Saanich Peninsula, where reverse faults strike east-west. The large, reclined fold between the Gooch and Domville domains has a southeast plunging hinge line which may not be related to this NW-SE compression.

The folding of Haslam Formation turbidites on Piers and Domville Islands are similar in scale and form, but are inferred to have resulted from separate events. The fold axes of both fold sets plunge moderately to the east, although the trend on Domville is rotated approximately 60 degrees clockwise relative to that on Piers (the average bedding orientation on Domville is similarly rotated clockwise relative to Piers, although the difference is closer to 20 degrees). The folds on Domville are interpreted to represent deformation related to oblique-reverse movement on a fault located within the channel between Domville and Brethour Islands. The location of a fault in this channel is required by contrasting

the stratigraphy on the two islands. Comox Formation rocks on Brethour Island occur stratigraphically above the younger Haslam and Extension Formation rocks on Domville Island (see Chapter 2). This is easiest to explain as a structural superposition due to the presence of a fault in the channel between the islands. The channel (and presumed fault trace) is oriented along a strike of azimuth 130, and is aligned with the Fulford Fault system. The amount of oblique offset recorded by the folds on Domville Island varies according to the inferred dip of the fault plane. A near-vertical fault would have more dextral-reverse movement, with the lower block moving northeast (relative to a fixed upper block), where a shallower fault dip to the northwest would resolve to less dextral offset, with the lower block moving northwest (Figure 61).

The folds on Piers Island are more likely associated with the shear zone that passes through the centre of Coal Island, the fault that passes under Swartz Bay, or a combination of both. These faults both appear to be high angle (by following traces on Coal Island and in Iroquois Channel), oblique reverse with possible sinistral offset, and are inferred to pass through Colburne Passage between Piers Island and the Saanich Peninsula (Figure 62). To the northwest, these faults are likely connected to the Tzuhalem Fault on Saltspring Island, or to a distal extension of the San Juan Fault. To the southeast, these faults trace through the study area. The Swartz Bay fault passes south of the Little Group islands (and may be responsible for the relative uplift of basement rocks on Shell and Little Shell islands), and through Miners Channel (where it may be responsible for uplift of Benson Member conglomerates on Halibut Island). The

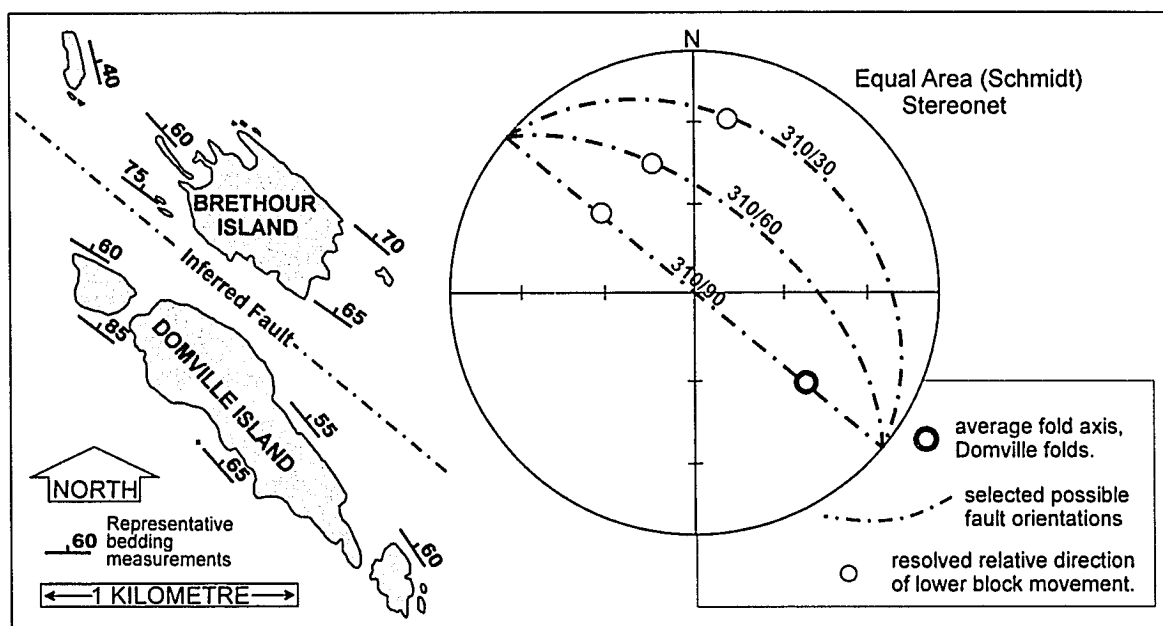


Figure 61: Inferred fault between Domville and Brethour Islands

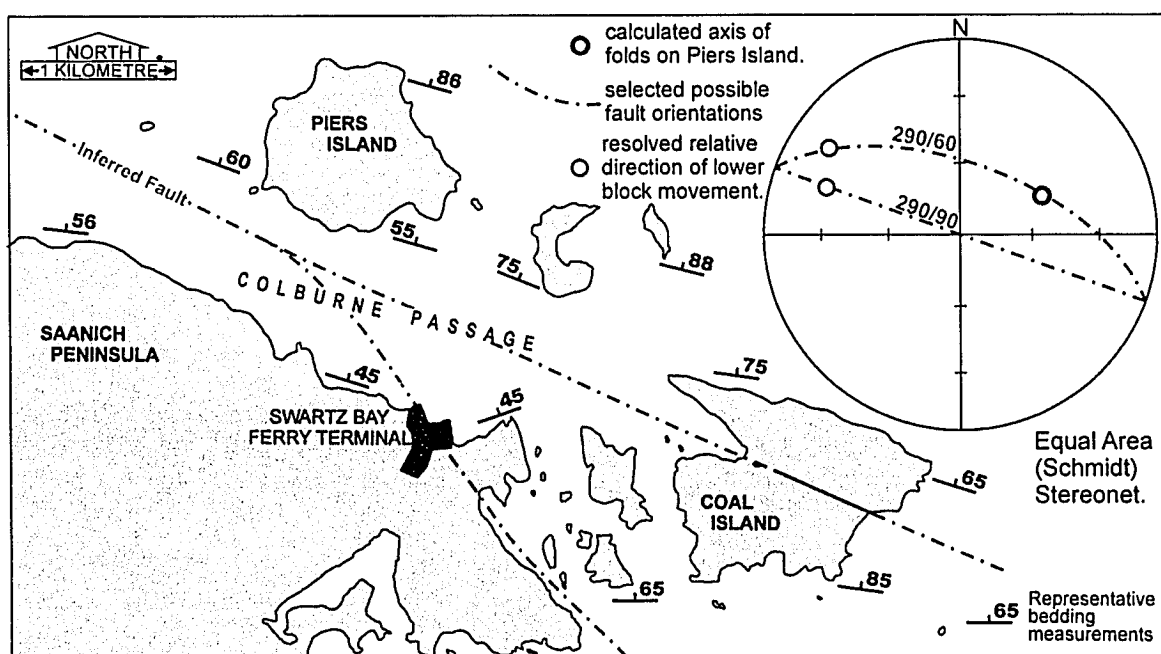


Figure 62: Inferred fault orientations, Colburne Passage.

Coal Island fault appears to pass through the channel between Domville and Forrest Islands.

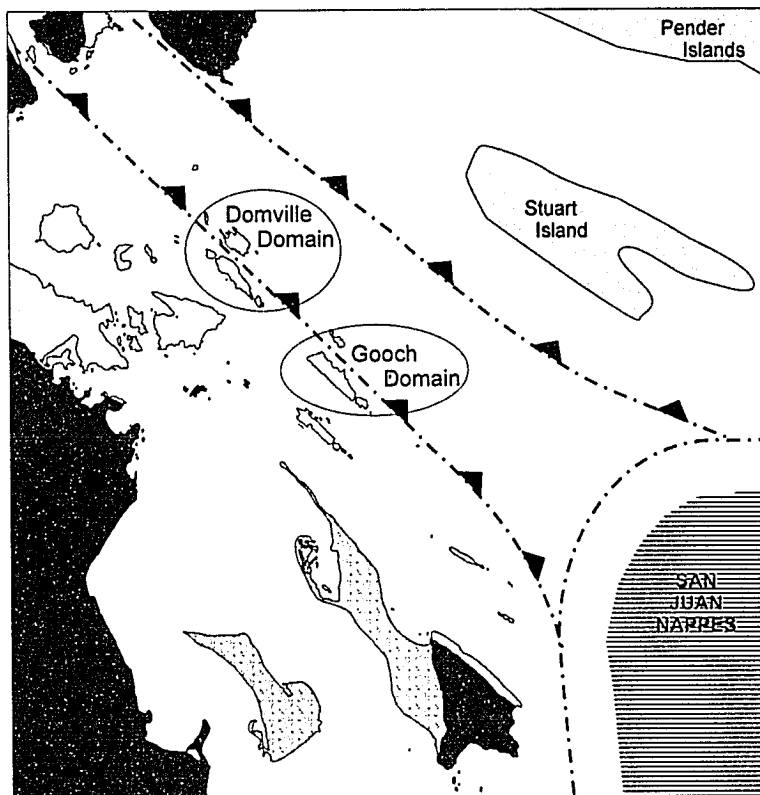
Several other faults have been located from changes in bedding orientations, including east-west striking high-angle reverse faults on the north side of Towner Bay on Saanich Peninsula, and a near-vertical dextral fault cutting the northwest shore of Portland Island. However, a number of faults which have been inferred to cross-cut the study area by previous studies (see Muller, 1980 and England, 1990) have now been removed due to a lack of evidence for their existence. This is most apparent on Piers Island.

Previous studies have drawn multiple thrust faults through Piers Island in order to explain repeated cycles of alternating sandy mudstones and sandy conglomerates (England, 1990; England and Calon, 1991). No actual large fault structures were observed as part of this study, nor any minor structures that might indicate any cryptic faults. However, erosional and conformal contacts are abundant. The repeated mudstone-conglomerate cycles are here reinterpreted to represent several partially overlapping conglomeratic channels eroding into a muddy submarine fan. This results in an intertonguing relationship between the Haslam and Extension Formation (see Chapter 2). Similarly, on Moresby Island, recognition of significant and irregular paleorelief of the Late Cretaceous unconformity surface results in a similar re-interpretation of complex original sedimentary patterns that were formerly mapped as thrust-caused repetitions.

One large anomalous structure in the study area is the large fold resulting in the overturned bedding in Gooch Domain. The fold is an overturned syncline

which is reclined to the southeast. The west limb of the fold has bedding orientations approximately parallel to surrounding domains, leading to the interpretation that the east limb has been overturned towards the north. The rock units on Gooch and Comet Islands are correlated to similar units on Domville and Brethour Islands respectively. This requires that the previously discussed thrust fault separating Domville and Brethour must also pass between Gooch and Comet Islands. Furthermore, the brittle fracture patterns on Gooch have a modal plane orientation normal to bedding, similar to other outcrop areas. Therefore, the event leading to the overturning of Gooch Domain must post-date the thrusting of Brethour Island and the major fracturing event. The northeast orientation of the fold trace is also problematic, as it aligns with no other structures in the study area, nor with structures on the adjacent San Juan Islands.

One possible solution to this enigma may be in the two-phase movement history of the Fulford Fault as suggested by Journeay and Morrison (1999). The Fulford Fault is a leading thrust in the Eocene Cowichan Fold and Thrust System (CFTS). A splay of the Fulford Fault with high angle reverse slip moved Comox Formation rocks of Brethour Island up in relation to Extension Formation units in the Domville domain (Figure 63). During the Neogene, the Fulford Fault system was reactivated by dextral transtension as part of the Gulf Islands Thrust System (GITS). At this time, movement along the Fulford Fault System in the field area stepped down to a splay which is now in the channel between Domville and Forrest Islands, before joining the Sydney Fault in Haro Strait. The block north of



Eocene Cowichan Fold and Thrust System

# Neogene Gulf Islands Thrust System

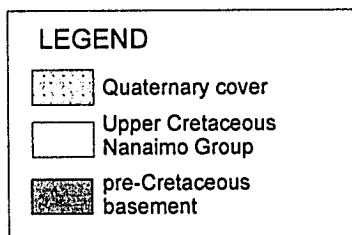
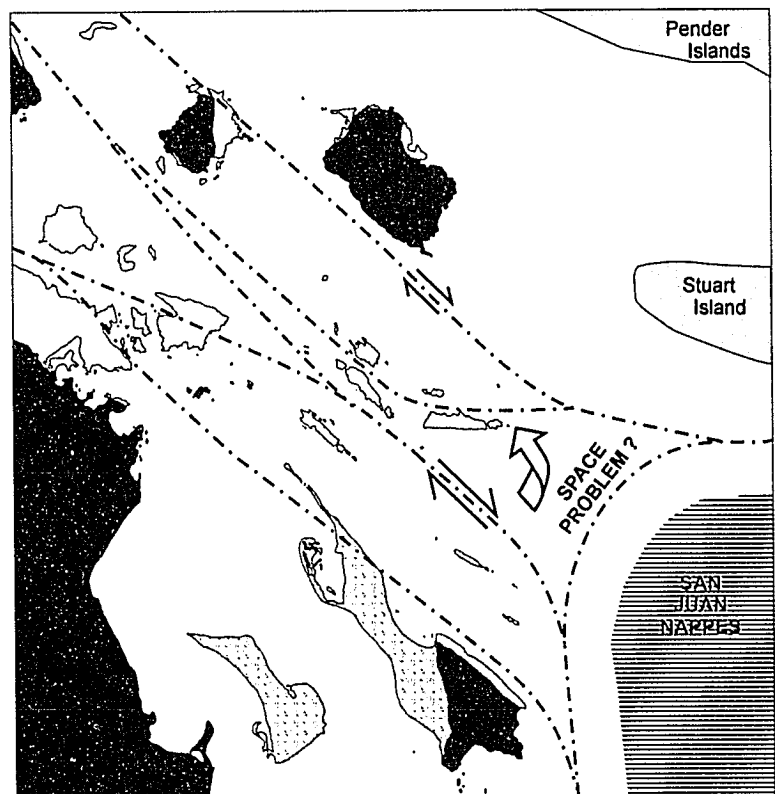


Figure 63: Two-phase movement interpreted to be responsible for the thrust repeating then overturning of the Gooch Island - Comet Island stratigraphy.





this fault may have developed a space problem with dextral movement pushing it into the San Juan nappes. It is this space problem which could have caused overturning of Gooch Domain rocks (Figure 63). The strike of the interpreted axial surface of the fold is approximately orthogonal to the Fulford Fault, and near normal to the nearest boundary with the San Juan nappes to the southeast. This space accommodation solution also explains why this block is overturned, although the Sidney Domain to the south and Stuart Island to the east are not.

Structures observed in the study area can be associated with the CFTS and the GITS. The aforementioned southwest vergent thrusts between Domville and Brethour Islands, the thrusting north of Towner Bay, and the overall northeast dip of bedding are all interpreted to be a result of Eocene shortening in an overall NE-SW direction. Although the bulk of the study area is southeast of the GITS as described by Journeay and Morrison (1999), some dextral transtensional structures interpreted as post-Eocene are apparent, such as the large dextral-normal fault observed on Portland Island, and the overturned Gooch Domain fold.

Although the study area contains some of the oldest deposits of the Nanaimo Group (Haggart, 1991; Haggart, 2005; see Chapter 1), and is proximal to pene-depositional thrusting of the San Juan nappes, no systematic soft sediment deformation related to the San Juan thrusting was observed. This may be because the rocks of the study area were deposited well west of the San Juan nappes and the separation of the nappes from the Nanaimo Group rocks of the

study area may have been even greater before Eocene margin-parallel shortening and Neogene dextral movement.

The study area location is at the southern extremity of a large orocline structure postulated by Johnston and Acton (2003). According to their model, the study location is where shear strain is highest during an earlier bending phase of rotation, and then becomes a zone of contraction during a later block-rotation phase. This model predicts several deformation events should be evident within the study area: northwest trending dextral shear (along azimuth ~290); northeast trending sinistral shear (along azimuth ~045); and fold and thrust shortening which increased in extent over time, with folds axes trending towards azimuth ~298. The model also suggests that the Cowichan Fold and Thrust belt shortening must exceed the 15 kilometres interpreted by England and Calon (1991).

The results of this study do not support this bend-then-rotate orocline model for southern Vancouver Island. Although sinistral shear measured in the study area trends close to the predicted value (azimuth 050 vs. 045), numerous dextral shear measures are almost normal to predicted values (azimuth 001 vs. 295), even if the values were reduced to accommodate late block rotation. The interpreted offsets of the Fulford Fault Zone through the field area is at odds with the predicted shear-then-thrust timing required by the orocline model. Finally, numerous thrust faults interpreted by earlier studies to cross-cut the field area do not exist, nor does evidence of significant bedding-parallel shortening along less competent layers, making it difficult to support a hypothesis of increased

shortening (although the study area represents only part of the modelled zone of compression). Southward-verging reverse faults and large northeast trending fold structures identified in the field area point to a tectonic history more complex than that of a single oroclinal event.

## **CHAPTER 6: SUMMARY AND CONCLUSIONS**

The Upper Cretaceous strata of the study area represent the lowest three formations of the Nanaimo Group, and were deposited in marginal marine to fully marine settings along a storm-swept coastline open to the west, within a peripheral foreland basin. This conclusion is supported by sedimentological descriptions and interpretations based on facies descriptions assembled into facies associations, and is reinforced by provenance and structural data. These findings update the stratigraphy of the study area and improve integration with previous studies from other parts of the basin. Further, the results of this study allow comparison of several existing models for the depositional and structural history of the study area.

The Nanaimo Group strata of the study are assigned to the Comox, Halsam and Extension formations, the three lowest units in the Nanaimo Group stratigraphy. Previous studies that have assigned units in the study area to the Protection, "Extension-Protection", or "Sidney" formations are not supported by this study.

The sedimentary environments represented by these deposits include a rocky, storm-swept coastline; alluvial fans and fan deltas developing along this high-relief coastline; a transgressive sandy shoreline where shoreface and barrier-island shoreline types are preserved from the beach to the transitional offshore; and submarine fans developing on the shelf or slope apron (Figure 64).

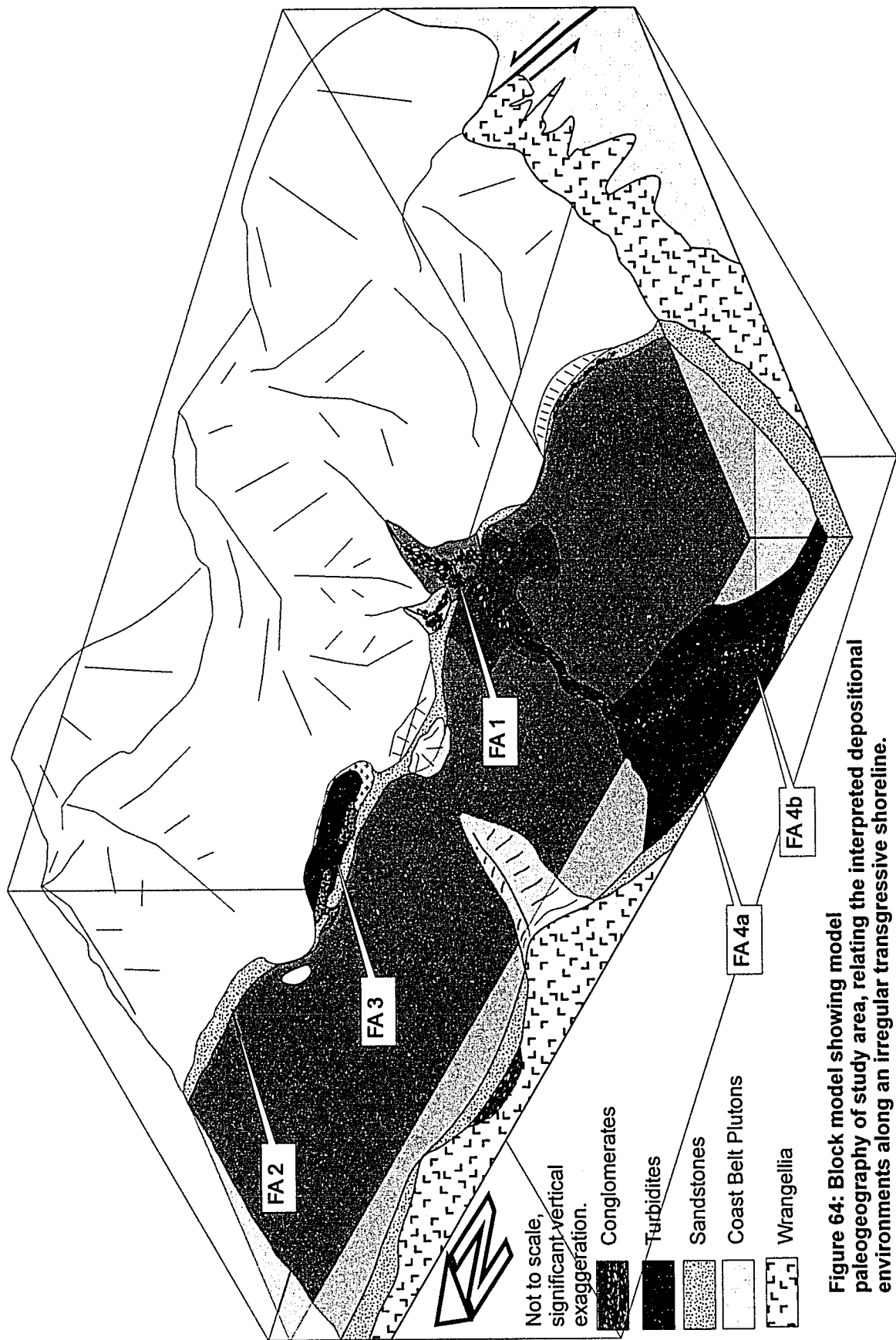


Figure 64: Block model showing model paleogeography of study area, relating the interpreted depositional environments along an irregular transgressive shoreline.

The development of submarine fans in a transgressive setting may be linked to the abundant supply of mixed sediment delivered to the shoreline by the fan deltas. The succession of deposits from these settings indicates a single transgressive sequence for the early Late Cretaceous within the study area. The coarseness and immaturity of sediments along this shoreline, combined with the thickness of preservation along a transgressing shoreline, further suggest an abundant sediment supply at the shoreface, and a long period of persistent transgression.

Provenance data suggest net sediment flow initially controlled by local irregular topography, gradually becoming westward-directed with transgression. Sediment composition follows a similar trend, being initially dominated by local basement lithology, with a gradual increase in more distal sources. These sources likely include the San Juan nappes and Cascades to the east and southeast, with less influence from the Coast Belt arc than seen in other parts of the Nanaimo Basin.

Structural data collected during this study confirm the local strain directions present during the formation of the Cowichan Fold and Thrust System and Gulf Islands Thrust System. Direct and indirect evidence of several large structures was collected, and though this evidence, improved inferences are made of the location and nature of major unexposed structures through the study. Several previously interpreted major faults have either been re-interpreted or removed completely due to lack of evidence. Evidence was also found that may supported the two-phase movement history of the Fulford Fault as proposed

by Journeay and Morrison (1999). No evidence was found in the study area of soft-sediment deformation related to the contemporaneous San Juan Thrust System, nor did the findings of this study support the "fold-then-bend" orocline model of Johnston and Acton (2003).

Although a barrier-island complex is the sedimentary environment that best fits the heterogeneous units of the upper Comox Formation, an estuarine environment can not be discounted as another possible interpretation. No evidence of direct fluvial input or units interpreted as deposits of bay-head deltas were identified. However, dedicated paleocurrent analysis and higher resolution ichnological-sedimentological study of the deposits in the Tsehum Harbour region of Saanich Peninsula or the successions on Forrest and Brethour islands may improve the certainty of these interpretations by delineating units with shore-parallel, offshore and on-shore directed flow.

Finally, the sedimentological and structural data collected during this study have tectonic implications. Although variously described as a forearc basin (England, 1990; England and Bustin, 1998) and a peripheral foreland basin (Journeay and Friedman, 1993; Mustard, 1994), the setting of the Upper Cretaceous Nanaimo Basin does not definitively fit into the "traditional" definition of either category.

Although strictly located in a forearc setting (between a subduction zone and the resultant arc massif), none of the characteristics traditionally associated with a forearc basin apply to the Nanaimo Basin. Forearc basins are the result of sediment trapping between the relative uplifts of a subduction complex and an

arc massif (Dickinson, 1995). However, the Nanaimo Basin was near the centre of a very wide (>300 km) arc-trench gap, with active thrust sheets separating the basin from the contemporaneously active portions of the arc (Journeay and Friedman, 1993; Friedman *et al.*, 1995; Umhoefer and Miller, 1996; Matzel *et al.*, 2004). The sedimentary fill of the Nanaimo Basin, particularly in the study area, stands in contrast to the traditional fill of forearc basins. These basins commonly lack a distinct basal unconformity, and are filled with deep marine pelagic or turbidite sediments that gradually shoal upward, through coarser turbidite facies, into marginal- or non-marine coarse clastics (Dickinson and Seely, 1979; Blatt, 1992). Volcaniclastic sediments dominate, and ash layers or intercalated lava flows are common (Dickinson, 1995). No direct evidence of contemporaneous volcanic activity has ever been identified in the Nanaimo Group, nor is there evidence of significant Late Cretaceous thrusting or uplift in Wrangellia to the west of the basin. Furthermore, the pattern of sedimentation observed in the study area (persistent transgression from marginal marine to deeper marine settings) does not match the expected pattern presented by the forearc basin model.

Peripheral foreland basins form where collision related to the attempted subduction of a passive continental margin, island arc, or oceanic platform causes margin-directed thrusting in the overriding plate. The formation of a fold- and thrust belt in the overlying crust results in lithospheric loading and subsidence of the foreland region, forming a sedimentary basin (Miall, 1995). Peripheral forelands commonly feature a basal unconformity related to erosion



over a topographic high, presumed to be a forebulge resulting from basement loading (Sinclair, 1997). The sediments overlying this basal unconformity traditionally include a basal shallow marine coarse clastic unit, overlain by progressively deeper-water deposits, then deep marine turbidite facies (Miall, 1995; Sinclair, 1997). The sedimentological evidence from the study area and the Nanaimo Group in general, agree very well with this model, and there is abundant evidence of contemporaneous thrusting to the east of the basin, from where the sediment was sourced.

However, there remain significant flaws with the traditional peripheral foreland basin model when applied to the Nanaimo Basin. Most models of peripheral foreland basins show the locus of deposition upon the downgoing plate in the collision zone (c.f. Pfiffner, 1986; Ricci Lucchi, 1986; Miall, 1995; Sinclair, 1997; Lallemand *et al.*, 2001), which is not the case in the Nanaimo Basin. Peripheral foreland models were developed with a passive margin being subducted and normal faults causing weaknesses in the basin floor, leading to basin collapse and accelerated subsidence required for the conventional "underfilled" basin sedimentology (Royden and Karner, 1984; Miall, 1995). The Nanaimo Group was not deposited upon the rifted, collapsing basement of a passive margin, but upon the westward (inactive) margins of an arc and the Wrangellia Terrane, which had long accreted to the continental margin (Yorath, 1991). This relatively rigid basement would presumably resist collapse, resulting in a wide, shallow basin when compared to "normal" peripheral foreland basins. Notwithstanding these deviations from the traditional model, the provenance

evidence and characteristics of the basin fill within the study area reinforce the interpretation that foreland thrust stacking was the primary mechanism of basin formation for the Upper Cretaceous Nanaimo Group.

## REFERENCES

- Atchison, M.E., 1968. Stratigraphy and depositional environments of the Comox Formation (Upper Cretaceous), Vancouver Island, British Columbia; M.Sc. thesis, Northwestern University, De Kalb, Illinois. 139p.
- Bann, K.L., and Fielding, C.R., 2004. An integrated ichnological and sedimentological comparison of non-deltaic shoreface and subaqueous delta deposits in Permian reservoir units of Australia. *in* The Application of Ichnology to Palaeoenvironmental and Stratigraphic Analysis, *edited by* D. McIlroy. Geological Society, London, Special Publications v. 228, pp. 273-310.
- Bann, K.L., Fielding, C.R., MacEachern, J.A., and Tye, S.C., 2004. Differentiation of estuarine and offshore marine deposits using integrated ichnology and sedimentology: Permian Pebbly Beach Formation, Sydney Basin, Australia. *in* The Application of Ichnology to Palaeoenvironmental and Stratigraphic Analysis, *edited by* D. McIlroy. Geological Society, London, Special Publications v. 228, pp. 179-212.
- Blair, T.C., and McPherson, J.G., 1994. Alluvial fans and their natural distinction from rivers based on morphology, hydraulic processes, sedimentary processes, and facies assemblages. *Journal of Sedimentary Research*, Vol. A64, No. 3. pp.450-489.
- Blatt, H., 1992. *Sedimentary Petrology*, second edition. W.H. Freeman, New York.
- Bergh, S.G., 2002. Linked thrust and strike-slip faulting during the Late Cretaceous terrane accretion in the San Juan thrust system, Northwest Cascades orogen, Washington. *Geological Society of America Bulletin*, v. 114, no. 8; pp. 934-949.
- Beynon, B.M., Pemberton, S.G., Bell, D.A., and Logan, C.A., 1988. Environmental implications of ichnofossils from the Lower Cretaceous Grand Rapids Formation, Cold Lake Oil Sands Deposit. *in* Sequences, Stratigraphy, Sedimentology: Surface and Subsurface. *edited by* D.P. James and D.A. Leckie. Canadian Society of Petroleum Geologists, Memoir 15. pp.275-290.
- Boothroyd, J.C., 1985. Tidal Inlets and Tidal Deltas. *in* Coastal Sedimentary Environments, 2<sup>nd</sup> edition, *edited by* R.A. Davis. Springer-Verlag, New York. pp.445-532.
- Bouma, A.H., 1962. *Sedimentology of some flysch deposits*, Elsevier, Amsterdam. 168p.

- Bouma, A.H., Normark, W.R., and Barnes, N.E., (eds) 1985. Submarine fans and related turbidite systems. Springer-Verlag, New York. 351p.
- Bourgeois, J. 1980. A transgressive shelf sequence exhibiting hummocky stratification: the Cape Sebastian Sandstone (Upper Cretaceous), southwestern Oregon. *Journal of Sedimentary Petrology*, vol. 50, pp 681-702.
- Bourgeois, J. and Leithold, E.L., 1984. Wave-worked conglomerates, depositional processes and criteria for recognition. *in* *Sedimentology of Gravels and Conglomerates*, edited by E.H. Koster and R.J. Steel. Canadian Society of Petroleum Geologists, Memoir 10, pp. 331-343.
- Boyd, R., Dalrymple, R., and Zaitlin, B.A., 1992. Classification of clastic coastal depositional environments. *Sedimentary Geology*, Vol. 80, pp139-150.
- Brandon, M.T., Cowan, D.S., and Vance, J.A., 1988. The Late Cretaceous San Juan Thrust System, San Juan Islands, Washington. Geological Society of America Special Paper 221. 81 p.
- Bromley, R.G., Pemberton, S.G., and Rahmani, R.A., 1984. A Cretaceous woodground: the *Teredolites* ichnofacies: *Journal of Paleontology*, V.58, pp. 488-498.
- Cathyl-Bickford, C.G., and Hoffman, G.L., 1991. Geology of coal resources of the Nanaimo Group in the Alberni, Ash River, Cowie Creek, and Parksville areas, Vancouver Island. *In* Paper 1991-1, Geological Fieldwork 1990: British Columbia Ministry of Mines and Petroleum Resources. pp.381-385.
- Chan, M.A., and Dott, R.H. 1986. Depositional facies and progradational sequences in Eocene wave-dominated deltaic complexes, southwestern Oregon. *American Association of Petroleum Geologists Bulletin*, vol. 70, pp. 415-429.
- Cheaney, R.F. 1983. *Statistical Methods in Geology for field and lab decisions*. George Allen & Unwin, London. 169p.
- Clarke, J.D., and Pickering, K.T., 1996. *Submarine Channels: processes and architecture*. Vallis Press, London.
- Clapp, C.H., 1912. Note on the geology of the Comox and Suquash Coal Fields. Geological Survey of Canada Summary Report 1911. pp.105-107.
- Clapp, C.H., 1914. Geology of the Nanaimo map-area. Geological Survey of Canada Memoir 51.
- Clapp, C.H., and Cooke, H.C., 1917. Sooke and Duncan map-areas, Vancouver. Geological Survey of Canada Memoir 96.
- Clowes, R.M., Brandon, M.T., Green, A.G., Yorath, C.J., Sutherland Brown, A., Kanasewich, E.R., and Spencer, C., 1987. Lithoprobe – southern Vancouver Island: Cenozoic subduction complex imaged by deep seismic reflections. *Canadian Journal of Earth Sciences*, v.24; pp. 31-51.

- Dalrymple, R.W., Zaitlin, B.A., and Boyd, R., 1992. Estuarine facies models: conceptual basis and stratigraphic implications. *Journal of Sedimentary Petrology*, vol. 62, pp.1130-1146.
- Dashtgard, S.E., Gingras, M.K., and Butler, K.E., 2006. Sedimentology and stratigraphy of a transgressive, muddy gravel beach: Waterside Beach, Bay of Fundy, Canada. *Sedimentology*, vol. 53. pp. 279-296.
- Dawson, G.M., 1890. Notes on the Cretaceous of the British Columbia Region: The Nanaimo Group. *American Journal of Science*, V.39, pp. 180-183.
- Davis, G.H, and Reynolds, S.J., 1996. Structural geology of rocks and regions. John Wiley & Sons, Inc., New York. 776p.
- DeBari, S.M., Anderson, R.G., and Mortensen, J.K., 1999. Correlation among lower to upper crustal components in an island arc: the Jurassic Bonanza arc, Vancouver Island, Canada. *Canadian Journal of Earth Sciences* v.36; pp.1371-1413.
- Dickinson, W.R., 1985. Interpreting provenance relations from detrital modes of sandstones. *in Provenance of Arenites, edited by G. G. Zuffa*, Reidel Publishing, pp.333-361.
- Dickinson, W.R., 1995. Forearc Basins. *in Tectonics of Sedimentary Basins, edited by C.J. Busby and R.V. Ingersoll*. Blackwell Scientific Publications, Cambridge. pp.221-262.
- Dickinson, W.R., and Seely, D.R., 1979. Structure and Stratigraphy of Forearc Regions. *American Association of Petroleum Geologists Bulletin*, v. 63. pp.2-31.
- Dott, R.H., and Bourgeois, J., 1982. Hummocky stratification: Significance of its variable bedding sequences: *Geological Society of America Bulletin* 93: pp663-680.
- Duke, W.L., Arnott, R.W.C., and Cheel, R.L. 1991. Shelf sandstones and hummocky cross-stratification; new insights on a stormy debate. *Geology*, vol. 19. pp.625-628.
- England, T.D.J., 1989. Lithostratigraphy of the Nanaimo Group, Georgia Basin, southwestern British Columbia; *in Current Research, Part E*, Geological Survey of Canada Paper 89-1E, p.103-108.
- England, T.D.J., 1990. Late Cretaceous to Paleogene evolution of the Georgia Basin, southwestern British Columbia; Ph.D. thesis, Memorial University of Newfoundland, St. John's, Newfoundland, 481p.
- England, T.D.J., and Bustin, R.M. 1998. Architecture of the Georgia Basin southwestern British Columbia. *Bulletin of Canadian Petroleum Geology* 46 (2): 288-320.
- England, T.D.J., and Calon, T.J. 1991. The Cowichan Fold and thrust system, Vancouver Island, southwestern British Columbia. *Geological Society of America Bulletin* 103: 336-362.

- England, T.D.J., and Hiscott, R.N., 1992. Lithostratigraphy and deep-water setting of the upper Nanaimo Group (upper Cretaceous), outer Gulf Islands of southwestern British Columbia. *Canadian Journal of Earth Sciences* v.29; pp.574-595.
- England, T.D.J., Currie, L.D., Massey, N.W.D., Roden-Tice, M.K., and Miller, D.S., 1997. Apatite fission-track dating of the Cowichan fold and thrust system, southern Vancouver Island, British Columbia. *Canadian Journal of Earth Sciences* v.34; pp.635-645.
- Enkin, R.J., Baker, J., and Mustard, P.S., 2001. Paleomagnetism of the Upper Cretaceous Nanaimo group, southwestern Canadian Cordillera. *Canadian Journal of Earth Sciences*, v. 38, pp.1403-1422.
- Felton, E.A., Sedimentology of rocky shorelines: 1. A review of the problem, with analytical methods, and insights gained from the Hulopoe Gravel and the modern rocky shoreline of Lanai, Hawaii. *Sedimentary Geology* v. 152. pp.221-245.
- Fleuty, M.J., 1964. The description of folds. *Geological Association Proceedings*, V. 75; pp. 461-492.
- Friedman, R.M., Mahoney, J.B., and Cui, Y., 1995. Magmatic evolution of the southern Coast Belt: constraints from Nd-Sr isotopic systematics and geochronology of the southern Coast Plutonic Complex. *Canadian Journal of Earth Sciences* V.32; pp.1681-1698.
- Frey, R.W., and Howard, J.D. 1990. Trace fossils and depositional sequences in a clastic shelf setting, Upper Cretaceous of Utah. *Journal of Paleontology*, Vol. 64. pp.803-820.
- Galloway, W.E., 1975. Process framework for describing the morphologic and stratigraphic evolution of deltaic depositional systems. *In Deltas, models for exploration, edited by M.L. Broussard*. Houston Geological Society, Houston, Texas. pp.87-98.
- Gingras, M.K., Pemberton, S.G., and Saunders, T.D.A., 2000. Firmness profiles associated with tidal creek deposits: the temporal significance of *Glossifungites* assemblages. *Journal Of Sedimentary Research*, vol. 70, pp.1017-1025.
- Gingras, M.K., MacEachern, J.A., and Pickerill, R.K., 2004. Modern perspectives on the *Teredolites* Ichnofacies: observations from Willapa Bay, Washington. *Palaos*, v.19, p.79-88.
- Groome, W.G., Thorkelson, D.J., Friedman, R.M., Mortensen, J.K., Massey, N.W.D., Marshall, D.D., and Layer, P.W., 2003. Magmatic and tectonic history of the Leech River Complex, Vancouver Island, British Columbia: Evidence for ridge-trench intersection and accretion of the Crescent Terrane; *in Geology of a transpressional orogen developed during ridge-trench interaction along the North Pacific margin, edited by V.B. Sisson*,

- S.M. Roeske, and T.L. Pavlis. Geological Society of America Special Paper 371. pp. 327-353.
- Haggart, J.W. 1994. Turonian (Upper Cretaceous) strata and biochronology of southern Gulf Islands, British Columbia. *In* Paper 94-A. Geological Survey of Canada, pp. 159-164.
- Haggart, J.W., Ward, P.D., and Orr, W., 2005. Turonian (Upper Cretaceous) lithostratigraphy and biochronology, southern Gulf Islands, British Columbia, and northern San Juan Islands, Washington State. *Canadian Journal of Earth Sciences*, v. 42; pp.2001-2020.
- Hampton, M.A., 1975. Competence of fine-grained debris flows. *Journal of Sedimentary Petrology*, v. 45. pp.834-844.
- Heward, A.P., 1981. A review of wave-dominated clastic shoreline deposits. *Earth-Science Reviews*, v. 17, pp. 223-276.
- Johnson, S.Y., 1981. The Spieden Group: an anomalous piece of the Cordilleran paleogeographic puzzle. *Canadian Journal of Earth Sciences*, v.18; pp.1694-1707.
- Johnson, S.Y., Zimmermann, R.A., Naeser, C.W., and Whetten, J.T., 1996. Fission-track dating of the tectonic development of the San Juan Islands, Washington. *Canadian Journal of Earth Sciences* v.23, pp.1777-1802.
- Johnston, S.T., and Acton, S., 2003. The Eocene Southern Vancouver Island Orocline – A response to seamount accretion and the cause of fold-and-thrust belt and extensional basin formation. *Tectonophysics* v.365, pp.165-183.
- Johnstone, P.D., Mustard, P.S., and MacEachern, J.A., 2006. The basal unconformity of the Nanaimo Group, southwestern British Columbia: a Late Cretaceous storm-swept rocky shoreline. *Canadian Journal of Earth Sciences* (in press).
- Journey, J.M., and Friedman, R.M., 1993. The Coast Belt Thrust System: Evidence of Late Cretaceous shortening in southwest British Columbia. *Tectonics*, V.12, No.3, pp.756-775.
- Journey, J.M., and Morrison, J. 1999. Field investigation of Cenozoic structures in the northern Cascadia forearc, southwestern British Columbia. *In* Paper 99-1A. Geological Survey of Canada, pp. 239-250.
- Journey, J.M., Saunders, C., Van Konijnenburg, J.H., and Jaasma, M., 1992. Fault systems of the Eastern Coast Belt, southwest British Columbia. *Canadian Journal of Earth Sciences*, v.22, pp.154-174.
- Journey, J.M., Williams, S.P., and Wheeler, J.O., 2000. Tectonic Assemblage Map, Vancouver, British Columbia –USA. Geological Survey of Canada Open File 2948a, scale 1:1,000,000.
- Katnick, D.C., and Mustard, P.S. 2003. Geology of Denman and Hornby Islands, British Columbia: implications for Nanaimo Basin evolution and formal

- definition of the Geoffrey and Spray formations, upper Cretaceous Nanaimo Group. *Canadian Journal of Earth Sciences* v.40, pp.375-393.
- Kenyon, C., Bickford, C.G.C., and Hoffman, G., 1992. Quinsam and Chute Creek coal deposits (NTS 92F/13,14); British Columbia Ministry of Mines and Petroleum Resources Paper 1991-3, 90p.
- Komar, P.D., 1976. *Beach Processes and Sedimentation*. Prentice-Hall, Inc., Englewood Cliffs, New Jersey. 429p.
- Kraft, J.C., and Chrzastowski, M.J., 1985. Coastal Stratigraphic Sequences. *in* *Coastal Sedimentary Environments*, 2<sup>nd</sup> edition, *edited by* R.A. Davis. Springer-Verlag, New York. pp.533-624.
- Lallemand, S., Liu, C.S., Angelier, J, and Tsai, Y.B., 2001. Active subduction and collision in Southeast Asia. *Tectonophysics*, vol. 333. pp.1-7.
- Lowe, D.R., 1976. Grain flow and grain flow deposits. *Journal of Sedimentary Petrology*, v.46, pp.188-189.
- Lowe, D.R., 1982. Sediment gravity flows: II. Depositional models with special reference to the deposits of high-density turbidity currents. *Journal of Sedimentary Petrology*, V. 52, No. 1 pp.279-297.
- MacEachern, J.A., and Pemberton, S.G., 1992. Ichnological aspects of Cretaceous shoreface successions and shoreface variability in the Western Interior Seaway of North America. *in* *Applications of Ichnology to Petroleum Exploration: A Core Workshop*. *edited by* S.G. Pemberton. Society of Economic Paleontologists and Mineralogists, Tulsa, Oklahoma, vol. 17, pp. 54-84.
- MacEachern, J.A., Raychaudhuri, I., and Pemberton, S.G., 1992. Stratigraphic application of the *Glossifungites* ichnofacies: delineating discontinuities in the rock record. *in* *Application of Ichnology to Petroleum Exploration: A Core Workshop*. *edited by* S.G. Pemberton. Society of Economic Paleontologists and Mineralogists, Core Workshop Notes, Tulsa, Oklahoma. vol. 17, pp.169-198.
- Mahoney, J.B., Mustard, P.S., Haggart, J.W., Friedman, R.M., Fanning, C.M., and McNicoll, V.J. 1999. Archean zircons in the Cretaceous Strata of the western Canadian Cordillera: the "Baja B.C." hypothesis fails a "crucial test". *Geology* v.27, pp.195-198.
- Maltman, A., 1994. Deformation structures preserved in rocks. *in* *The geological deformation of sediments*: *edited by* A. Maltman, Chapman and Hall, Leeds, U.K., pp.261-307.
- Massey, N.W.D., 1995. Geology of the Alberni-Nanaimo Lakes Area (92 F/1W, 92 F/2E), British Columbia Ministry of Energy, Mines and Petroleum Resources Paper 1992-2.
- Matzel, J.E.P., Bowring, S.A., and Miller, R.B., 2004. Protolith age of the Swakane Gneiss, North Cascades, Washington: Evidence of rapid



- underthrusting of sediments beneath and arc. *Tectonics*, v.23, TC6009; 18p.
- McGugan, A., 1979. Biostratigraphy and Paleoecology of Upper Cretaceous (Campanian and Maastrichtian) foraminifera from the upper Lambert, Northumberland, and Spray formations. *Canadian Journal of earth Sciences*, V.16, pp.2263-2274.
- McPherson, J.G., Shanmugam, G., and Moiola, R.J., 1987. Fan deltas and braid deltas: varieties of coarse-grained deltas. *American Association of Petroleum Geologists Bulletin* 99, pp.331-340.
- McPherson, J.G., Shanmugam, G., and Moiola, R.J., 1988. Fan deltas and braid deltas: conceptual problems. *in Fan Deltas: Sedimentology and Tectonic Settings*, edited by W. Nemec and R.J. Steel. Blackie and Son, Glasgow. pp.14-22.
- Miall, A.D., 1992. Alluvial Deposits. *in Facies Models: response to sea level change*. edited by R.G. Walker and N.P. James. Geological Association of Canada, St. John's.
- Miall, A.D., 1995. Collision-related Foreland Basins. *in Tectonics of Sedimentary Basins*, edited by C.J. Busby and R.V. Ingersoll. Blackwell Scientific Publications, Cambridge. pp.393-424.
- Miall, A.D., 1999. *Principles of Sedimentary Basin Analysis* (3<sup>rd</sup> edition). Springer-Verlag, New York, 616 p.
- Monger, J.W.H., and Journeay, J.M., 1994. Guide to the Geology and Tectonic Evolution of the Southern Coast Mountains. Geological Survey of Canada Open File 2490; 77 p.
- Muller, J.E., 1980. Geology: Victoria map area, British Columbia (Map 1553A). Geological Survey of Canada scale 1:100,000.
- Muller, J.E., and Jeletzky, J.A., 1970. Geology of the Upper Cretaceous Nanaimo Group, Vancouver Island and Gulf Islands, British Columbia; Geological Survey of Canada Paper 69-25, 77p.
- Mustard, P.S., 1994. The Upper Cretaceous Nanaimo Group, Georgia Basin; *in Geology and Geologic Hazards of the Vancouver Region, Southwestern British Columbia*, edited by J.W.H. Monger. Geological Survey of Canada Bulletin 481, p.27-95.
- Mustard, P.S., and Rouse, G.E., 1991. Sedimentary outliers of the eastern Georgia Basin margin, British Columbia; *in Current Research, Part A*, Geological Survey of Canada Paper 91-1A, p.229-240.
- Mustard, P.S., and Rouse, G.E., 1994. Stratigraphy and evolution of Tertiary Georgia basin and subjacent Upper Cretaceous sedimentary rocks, southwestern British Columbia and northwestern Washington State; *in Geology and Geologic Hazards of the Vancouver Region, Southwestern*

- British Columbia, *edited by* J.W.H. Monger. Geological Survey of Canada Bulletin 481, p.97-169.
- Mustard, P.S., Parrish, R.R., and McNicoll, V., 1995. Provenance of the Upper Cretaceous Nanaimo Group, British Columbia: Evidence from U-Pb analyses of detrital zircons, *in* Stratigraphic Evolution of Foreland Basins, *edited by* S.L. Dorobek and G.M. Ross. Society of Economic Paleontologists and Mineralogists Special Publication 52, pp.65-75.
- Mutti, E., and Ricci Lucchi, F., 1972. Turbidites of the Northern Apennines: introduction to facies analysis. *International Geology Review*, v.20, p.125-166.
- Nemec, W., 1990. Deltas – remarks on terminology and classification. *in* Coarse-grained Deltas, *edited by* A. Colella and D.B. Prior. International Association of Sedimentologists Special Publication 10. pp3-12.
- Nemec, W., and Steel, R.J., 1984. Alluvial and coastal conglomerates: their significant features and some comments on gravely mass-flow deposits. *in* Sedimentology of Gravels and Conglomerates, *edited by* E.H. Koster and R.J. Steel. Canadian Society of Petroleum Geologists, Memoir 10, pp.1-31.
- Nemec, W., and Steel, R.J., 1988. What is a fan delta and how do we recognize it? *in* Fan Deltas: Sedimentology and Tectonic Settings, *edited by* W. Nemec and R.J. Steel. Blackie and Son, Glasgow.
- Niedoroda, A.W., Swift, D.J.P., and Hopkins, T.S., 1985. The Shoreface, *in* Coastal Sedimentary Environments, 2<sup>nd</sup> edition, *edited by* R.A. Davis. Springer-Verlag, New York. pp.533-624.
- Oertel, G.F., 1985. The barrier island system. *in* Barrier Islands, *edited by* G.F. Oertel and S.P. Leatherman. Marine Geology vol. 63. pp.1-18.
- Pacht, J.A., 1980. Sedimentology and petrology of the Late Cretaceous Nanaimo Group in the Nanaimo Basin, Washington and British Columbia: implications for Late Cretaceous tectonics; Ph.D. thesis, Ohio State University, Columbus, Ohio, 368p.
- Pacht, J.A., 1984. Petrologic evolution and Paleogeography of the Late Cretaceous Nanaimo Basin, Washington and British Columbia: implications for Cretaceous tectonics. *Geological Society of America Bulletin* v.95, pp.766-778.
- Paterson, S.R., Miller, R.B., Alsleben, H., Whitney, D.L., Valley, P.M., and Hurlow, H., 2004. Driving mechanisms for >40 km of exhumation during contraction and extension in a continental arc, Cascades core, Washington. *Tectonics*, v.23, TC3005; 30p.
- Pemberton, S.G., and Frey, R.W., 1985. The *Glossifungites* ichnofacies: modern examples from the Georgia coast, U.S.A., *in* Biogenic Structures: Their use in interpreting depositional environments, *edited by* H.A. Curran.

Society of Economic Paleontologists and Mineralogists Special Publication 35, pp.237-259.

- Pemberton, S.G., and MacEachern, J.A., 1997. The ichnological signature of storm deposits: the use of trace fossils in event stratigraphy. *in* Paleontological Event Horizons: Ecological and Evolutionary Implications. *edited by* C.E. Brett. Columbia University Press, New York, pp.73-109.
- Pemberton, S.G., Spila, M., Pulham, A.J., Saunders, T., MacEachern, J.A., Robbins, D., and Sinclair, I.K., 2001. Ichnology & Sedimentology of Shallow to Marginal Marine Systems, Ben Nevis & Avalon Reservoirs, Jeanne d'Arc Basin. Short Course Volume 15, Geological Association of Canada. St. John's Newfoundland. 343p.
- Pemberton, S.G., MacEachern, J.A., and Saunders, T., 2004. Stratigraphic application of substrate-specific ichnofacies: delineating discontinuities in the rock record. *in* The Application of Ichnology to Palaeoenvironmental and Stratigraphic Analysis, *edited by* D. McIlroy. Geological Society, London, Special Publications v. 228, pp. 29-62.
- Pfiffner, O.A., 1986. Evolution of the north Alpine foreland basin in the Central Alps. *in* Foreland Basins *edited by* P.A. Allen and P. Harwood. International Association of Sedimentologists, Special Publication 8. pp 105-139.
- Postma, G., 1983. Water escape structures in the context of a depositional model of a mass-flow dominated conglomeratic fan-delta (Abrioja Formation, Pliocene, Almeria Basin, SE Spain). *Sedimentology*, v. 30. pp.91-103.
- Postma, G., 1984. Mass-flow conglomerates in a submarine canyon: Abrioja fan-delta, Pliocene, southeast Spain. *in* Sedimentology of Gravels and Conglomerates, *edited by* E.H. Koster and R.J. Steel. Canadian Society of Petroleum Geologists, Memoir 10, pp.237-258.
- Postma, G., 1990. Depositional architecture and facies of river and fan deltas: a synthesis. *in* Coarse-grained Deltas, *edited by* A. Colella and D.B. Prior., International Association of Sedimentologists Special Publication 10. pp13-27.
- Potter, P.E., and Pettijohn, F.J., 1977. Paleocurrent and Basin Analysis (2<sup>nd</sup> edition). Springer-Verlag, New York, 420p.
- Ramsay, J.G., and Huber, M.I., 1987. The techniques of modern structural geology, vol. 2: Folds and Fractures. Academic Press, London, 307p.
- Reading, H.G. and Collinson, J.D., 1996. Clastic coasts. *in* Sedimentary Environments: Processes, Facies and Stratigraphy, 3<sup>rd</sup> edition. *edited by* H.G. Reading. Blackwell Science, Oxford.
- Reading, H.G., and Richards, M., 1994. Turbidite systems in deep-water basin margins classified by grain size and feeder system. AAPG Bulletin, v. 78, pp792-822.

- Reineck, H. E. 1963. Sedimentgefüge im Bereich der südlichen Nordsee. *Abhandlungen der Senckenbergische Naturforschische Gesellschaft*, V.505. pp. 1-38.
- Reinson, G.E., 1992. Transgressive barrier island and estuarine systems. *in* *Facies Models: response to sea level change. edited by R.G. Walker and N.P. James. Geological Association of Canada, St. John's.*
- Ricci Lucchi, F. 1986. The Oligocene to Recent foreland basins of the northern Apennines. *in* *Foreland Basins edited by P.A. Allen and P. Harwood. International Association of Sedimentologists, Special Publication 8. pp 105-139.*
- Richardson, J., 1872. Coal Fields of the east coast of Vancouver Island; Geological Survey of Canada, Report of Progress, 1871-1872, pt.3. pp.73-100.
- Rodine, J.D., and Johnson, A.M., 1976. The ability of debris, heavily freighted with coarse clastic materials, to flow on gentle slopes. *Sedimentology*, v.23 pp. 213-224.
- Royden, L., and Karner, G.D., 1984. Flexure of lithosphere beneath Apennine and Carpathian foredeep basins: evidence for an insufficient topographic load. *American Association of Petroleum Geologists Bulletin*, v.68. pp.704-712.
- Rushmore, M.E., and Cowan, D.S., 1985. Jurassic-Cretaceous rock units along the southern edge of the Wrangellia terrane on Vancouver Island. *Canadian Journal of Earth Sciences*, V.22, pp.1223-1232.
- Saunders, T., and Pemberton, S.G., 1986. Trace fossils and sedimentology of the Appaloosa Sandstone: Bearpaw-Horseshoe Canyon Formation transition, Dorthy, Alberta: Canadian Society of Petroleum Geologists Field Trip Guide Book, 117p.
- Saunders, T.D.A., MacEachern, J.A., and Pemberton, S.G., 1994. Cadotte Member Sandstone: progradation in a boreal basin prone to winter storms. *in* *Mannville Core Conference, edited by S.G. Pemberton, D.P. James, and M. Wrightman. Canadian Society of Petroleum Geologists, Calgary, Alberta. pp.331-349.*
- Savrda, C.E., 1991. *Teredolites*, wood substrates, and sea-level dynamics. *Geology*, vol. 19, pp.905-908.
- Savrda, C.E., Ozalas, K., Demko, T.H., Hutchinson, R.A., and Scheiwe, T.D., 1993. Log grounds and the ichnofossil *Teredolites* in transgressive deposits of the Clayton Formation (Lower Paleocene), western Alabama. *Palaos*, v.8, p311-324.
- Shanmugam, G., 1996. High-density turbidity currents: are they sandy debris flows? *Journal of Sedimentary Research*, V. 66 no. 1, pp.2-10.

- Shanmugam, G., and Moiola, R.J., 1988. Submarine fans: characteristics, models, classification, and reservoir potential. *Earth-Science Reviews*, v. 24, pp.383-428.
- Sinclair, H.D., 1997. Tectonostratigraphic model for underfilled peripheral foreland basins: an Alpine perspective. *Geological Society of America Bulletin*, v.109. pp.324-346.
- Soegaard, K., and MacEachern, J.A., 2003. Integrated sedimentological, ichnological, and sequence stratigraphic model of a coarse clastic fan delta reservoir: Middle Jurassic Oseberg Formation, North Sea, Norway. *American Association of Petroleum Geologists Annual Convention Abstracts Volume*, Salt Lake City, Utah, May, 2003, p. A160.
- Stewart, R.J., and Page, R.J., 1973. Zeolite Facies Metamorphism of the Late Cretaceous Nanaimo Group, Vancouver Island and Gulf Islands, British Columbia. *Canadian Journal of Earth Sciences*, v.11, pp.280-284.
- Stow, D.A.V., and Shanmugam, G., 1980. Sequence of structures in fine-grained turbidites; comparison of recent deep-sea and ancient flysch sediment. *Sedimentary geology*, v. 25, pp.23-42.
- Stow, D.A.V., Reading, H.G., and Collinson, J.D., 1996. Deep seas. *in* *Sedimentary Environments: Processes, Facies and Stratigraphy*, 3<sup>rd</sup> edition. *edited by* H.G. Reading. Blackwell Science, Oxford.
- Treptau, K., 2002. An Integrated Sedimentological-Ichnological Paleoecological Assessment of the Upper Campanian Cedar District Formation, Upper Cretaceous Nanaimo Group, Southwest British Columbia. M.Sc Thesis, Simon Fraser University, Burnaby, Canada.
- Umhoefer, P.J., and Miller, R.B., 1996. Mid-Cretaceous thrusting in the southern Coast Belt, British Columbia and Washington, after strike-slip reconstruction. *Tectonics*, V.15, No. 2, pp. 545-565.
- Walker, R.G., 1975. Generalized facies models for resedimented conglomerates of turbidite association. *Geological Society of America Bulletin*, V.86, pp737-748.
- Walker, R.G., 1985. Mudstones and thin-bedded turbidites associated with the Upper Cretaceous Wheeler Gorge Conglomerates, California: a possible channel-levee complex. *Journal of Sedimentary Petrology*, V. 55, pp.279-290.
- Walker, R.G., 1992. Turbidites and submarine fans. *in* *Facies Models: response to sea level change*. *edited by* R.G. Walker and N.P. James. Geological Association of Canada, St. John's.
- Walker, R.G. and Plint, A.G., 1992. Wave- and Storm-Dominated Shallow Marine Systems. *in* *Facies Models: response to sea level change*. *edited by* R.G. Walker and N.P. James. Geological Association of Canada, St. John's.

- Ward, P.D., 1978. Revisions to the stratigraphy and biochronology of the Upper Cretaceous Nanaimo Group, British Columbia and Washington State; Canadian journal of Earth Sciences, V.15, pp.405-423.
- Ward, P.D., and Stanley, K.O., 1982. The Haslam Formation: a Late Santonian-Early Campanian forearc basin deposit in the Insular Belt of southwestern British Columbia and adjacent Washington. Journal of Sedimentary Petrology, v.52, No. 3., pp 975-990.
- Winn, R.D., and Dott, R.H., 1978. Submarine-fan turbidities and resedimented conglomerates in a Mesozoic arc-rear marginal basin in southern South America. *In: Sedimentation in submarine canyons, fans, and trenches. Edited by D.J. Stanley and G. Kelling: Dowden, Hutchinson and Ross, Stroudsburg, PA. pp.362-373.*
- Yorath, C.J., 1991. Upper Jurassic to Paleogene assemblages. *in Geology of the Cordilleran Orogen in Canada. edited by H. Gabrielse and C.J. Yorath. Geological Survey of Canada Geology of Canada no.4. pp.329-371.*
- Yorath, C.J., Sutherland Brown, A., and Massey, N.W.D., 1999. Lithoprobe, Southern Vancouver Island, British Columbia: Geology. Geological Survey of Canada Bulletin 498; 145 p.

## APPENDICES

## **Appendix A: Vertical Stratigraphic Sections.**

Twelve vertical stratigraphic sections were measured, representing more than 1300 m of total measured stratigraphy. Measured section locations were chosen in areas where continuous sections could be confidently measured, while attempting to measure a representative sample of lithologic units and facies associations of the field area. Sections were measured using a cm-scale measured tape and a 1.5 m Jacob staff with an inclinometer, depending upon inclination of bedding. A field transit was used to confirm bedding measurement and for scaling offsets. Sections were hand drafted at 1:100 scale, with photographs and samples collected to augment data.

The following 12 measured sections describe basic lithologic character, presence of primary bedding structures, biogenic structures, and fossils. Sections are divided into facies as described in Chapter 2. The distribution of measured sections is shown on Figure A 1, and each individual section is preceded by a detailed location map displaying the section starting and end points, and offsets utilized. Figure A 2 provides a legend of symbols common to all sections.



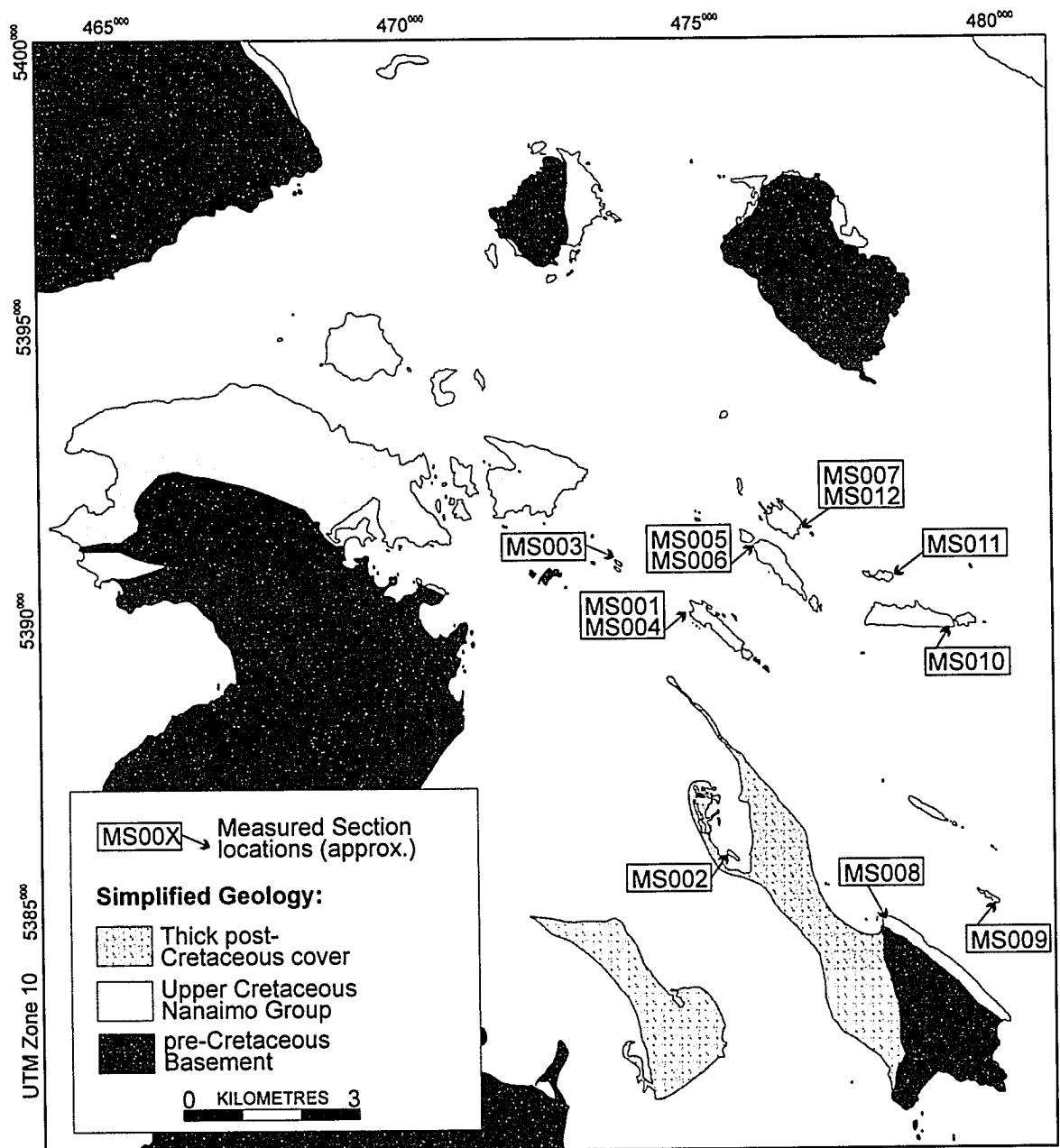



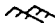








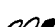


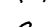











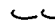



Figure A 1: Locations of measured sections.

## Measured Sections Legend.














### Physical Structures

-  Planar cross stratification
-  Trough cross stratification
-  Current ripples
-  Aggradational current ripples
-  Combined flow ripples
-  Hummocky cross stratification
-  Swaley cross stratification
-  Wavy parallel stratification
-  Planar parallel stratification
-  Low-angle parallel stratification
-  Discontinuous mud drapes
-  Dispersed pebbles
-  Clast imbrication
-  Convolute strata
-  Dewatering structures
-  Flame structures
-  Loading structures
-  Synsedimentary folds
-  Concretions
-  Rip-up clasts
-  Syneresis cracks
-  Calcite veins
-  Carbonaceous detritus
-  Firmground







### Fossil Materials


-  Body fossil
-  Fossil fragments
-  Plant fossil
-  Large coal fragments (>1cm.)
-  Coal bed

### Ichnofossils

-  Bioturbate mottling
-  Chondrites
-  Diplocraterion
-  Glossifungites
-  Macaronichnus
-  Ophiomorpha
-  Palaeophycus
-  Planolites
-  Skolithos
-  Teichichnus
-  Terbellina
-  Teredolites
-  Thalassinoides

### Lithology

-  Conglomerate
-  Pebbly Sandstone
-  Sandstone
-  Silty Sandstone
-  Silty Mudstone
-  Volcanic Basement

 Coarsening  
upward  
succession


 Fining  
upward  
succession

Figure A 2: Measured section symbology legend.

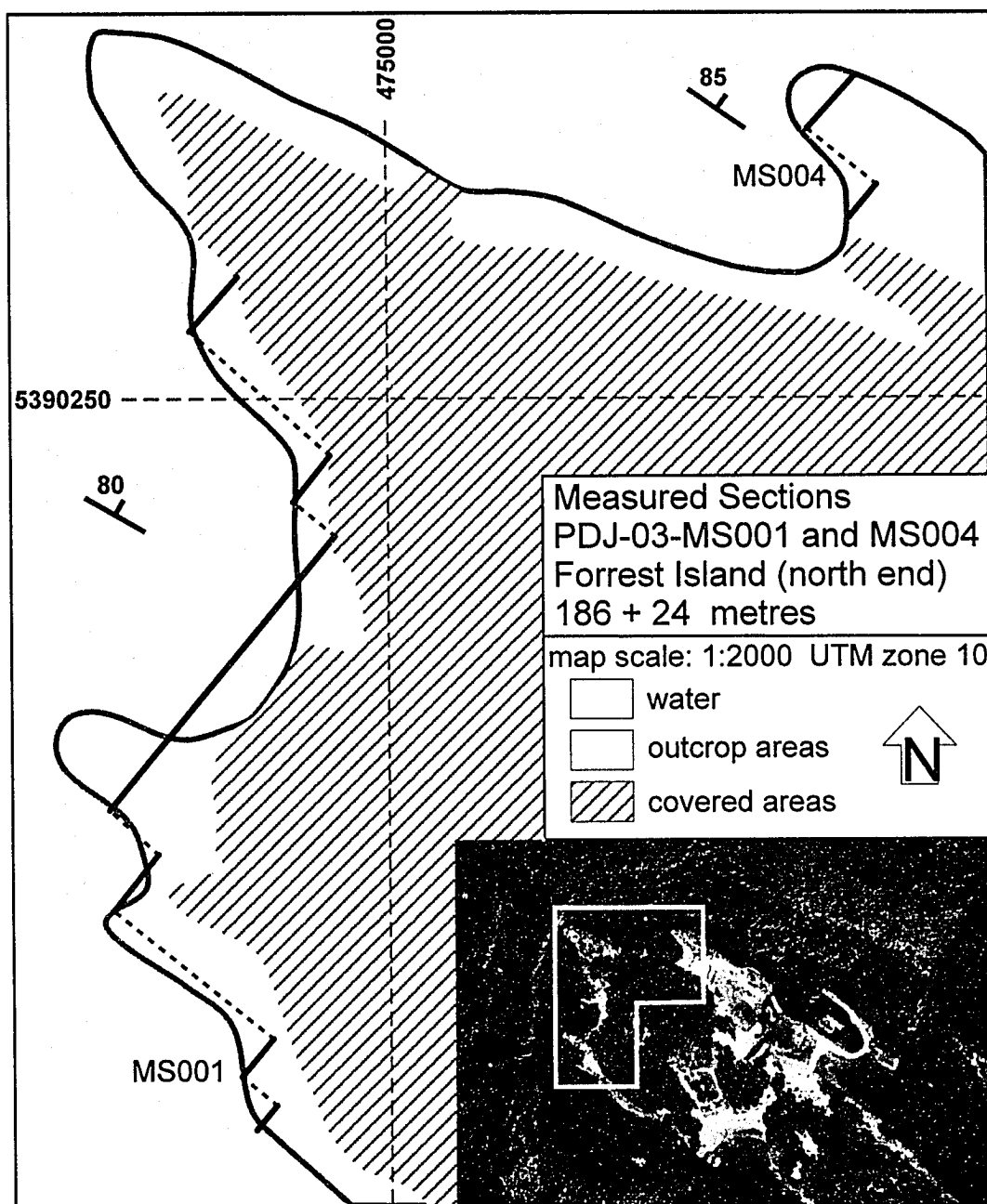


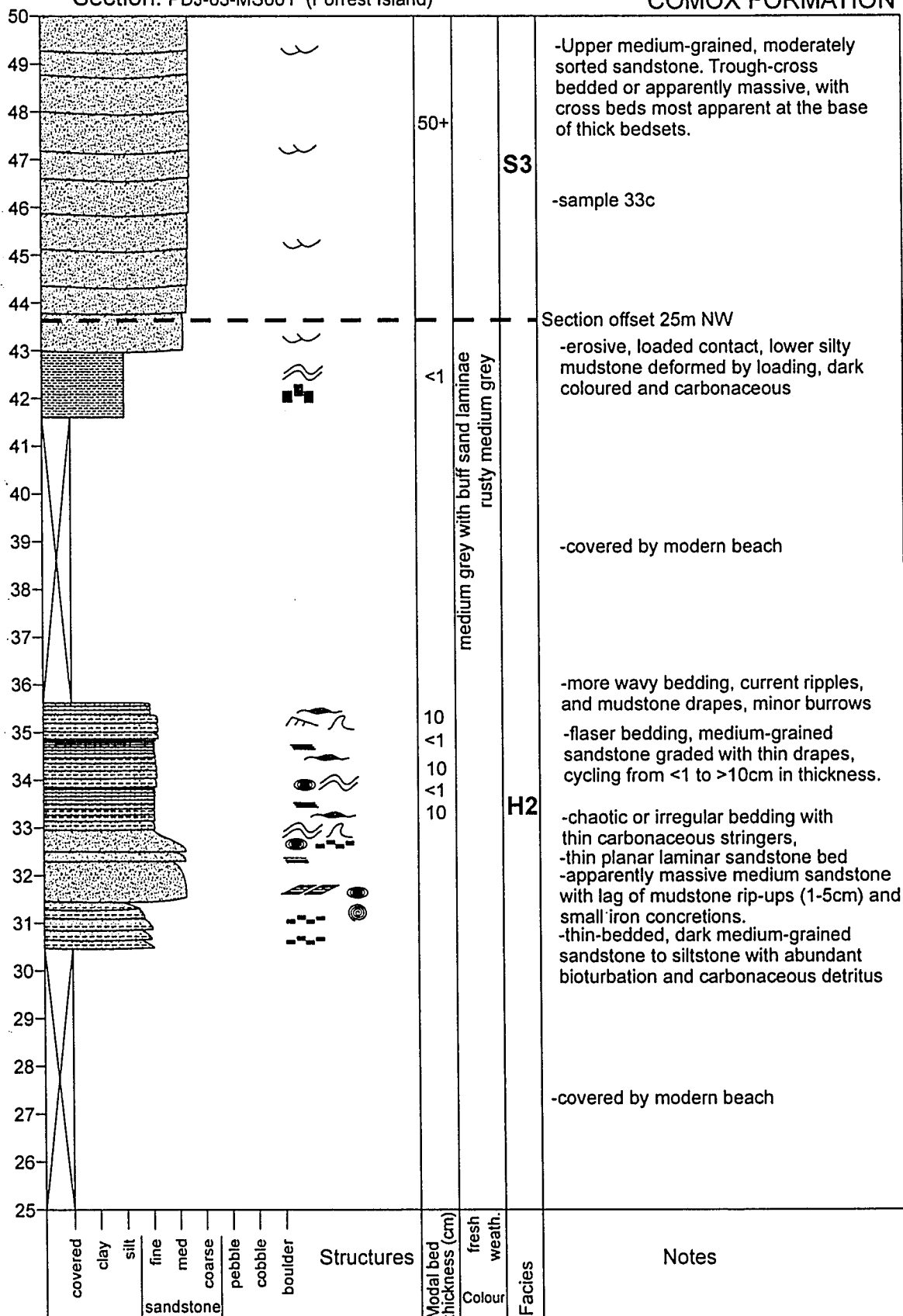
Figure A 3: Location Map, measured section MS001 and MS004.

## COMOX FORMATION



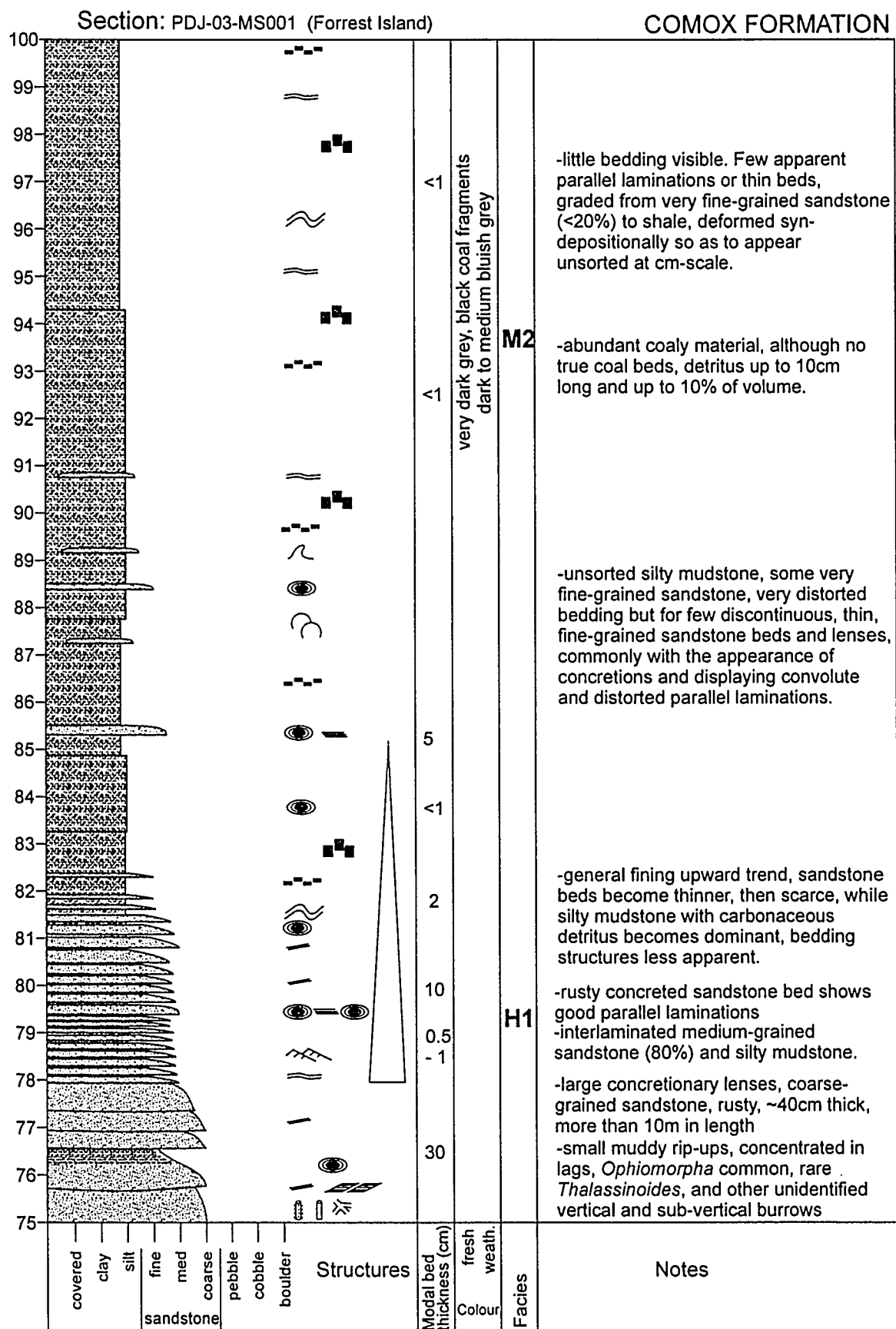
## Section: PDJ-03-MS001 (Forrest Island)

## COMOX FORMATION



## COMOX FORMATION





## COMOX FORMATION



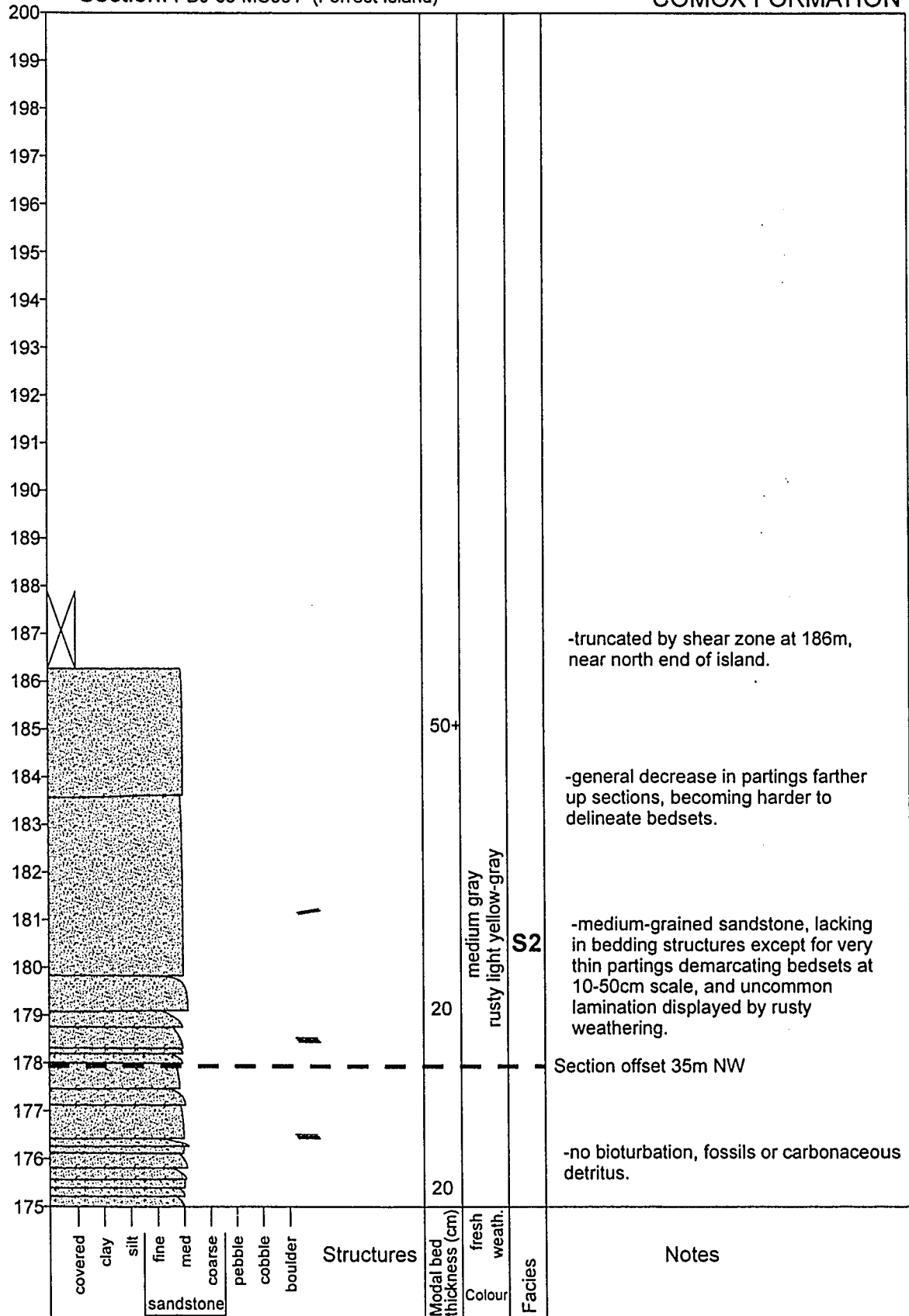


## COMOX FORMATION



## Section: PDJ-03-MS001 (Forrest Island)

## COMOX FORMATION



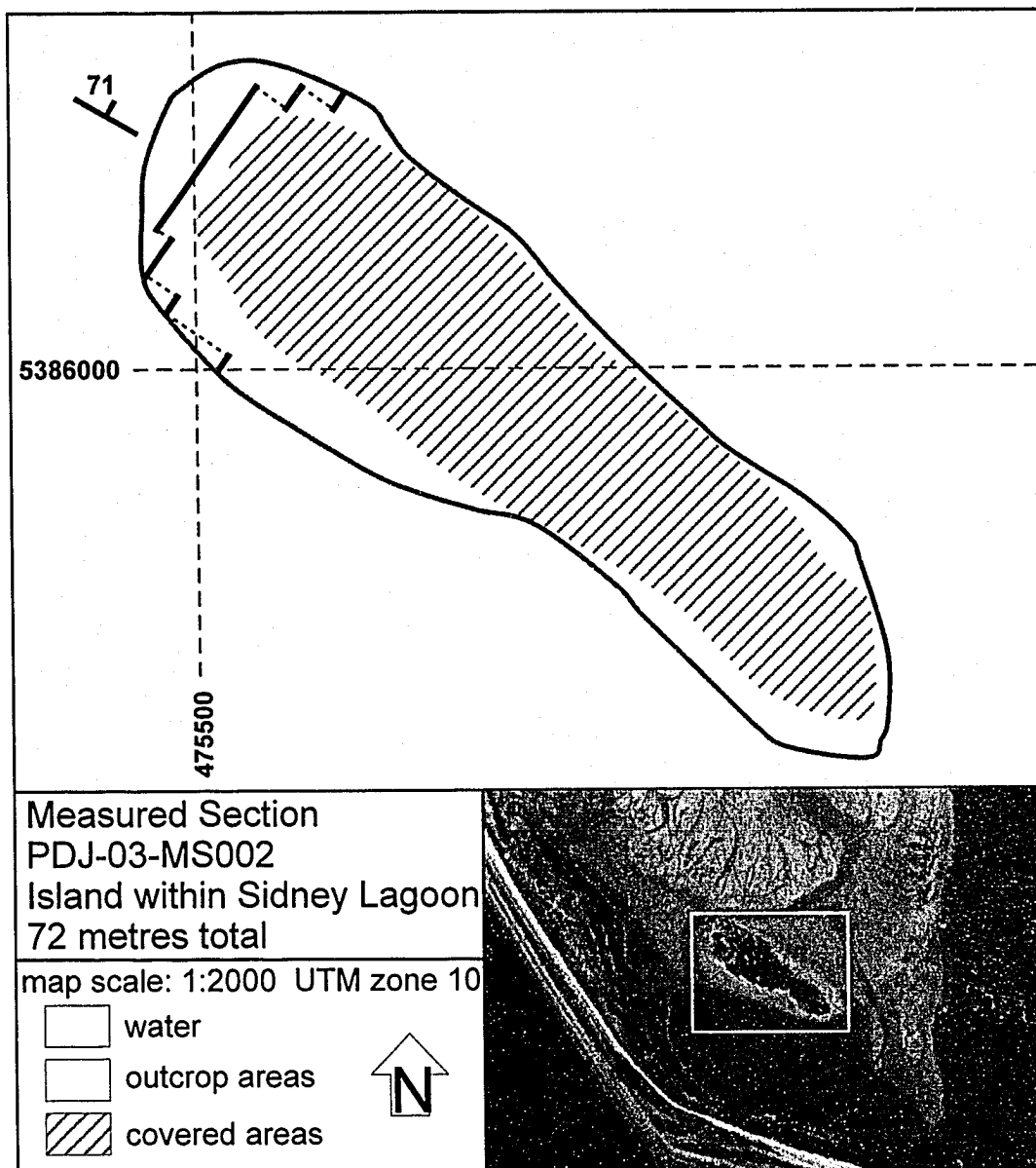
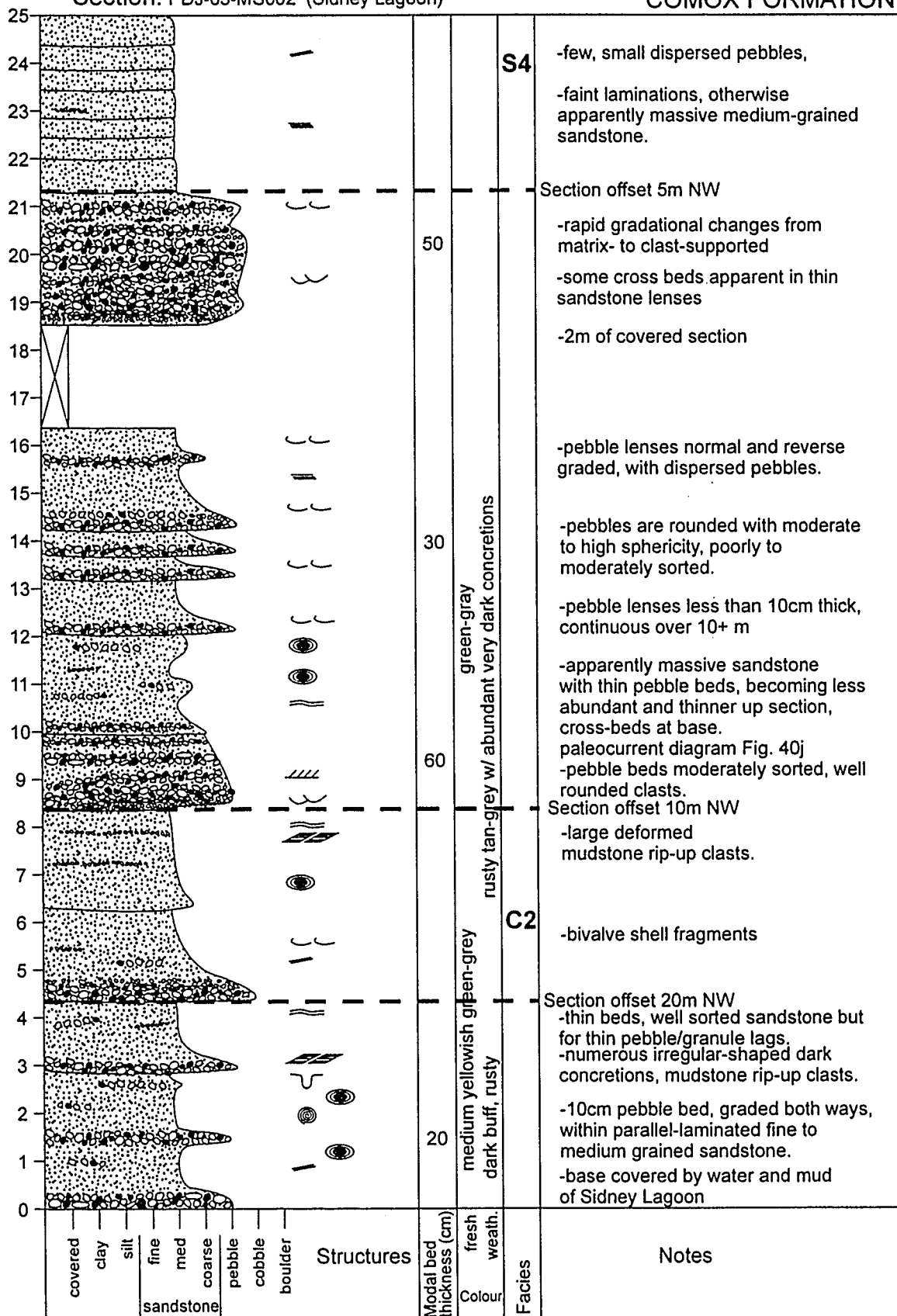


Figure A 4: Location Map, measured section MS002.

## Section: PDJ-03-MS002 (Sidney Lagoon)

## COMOX FORMATION

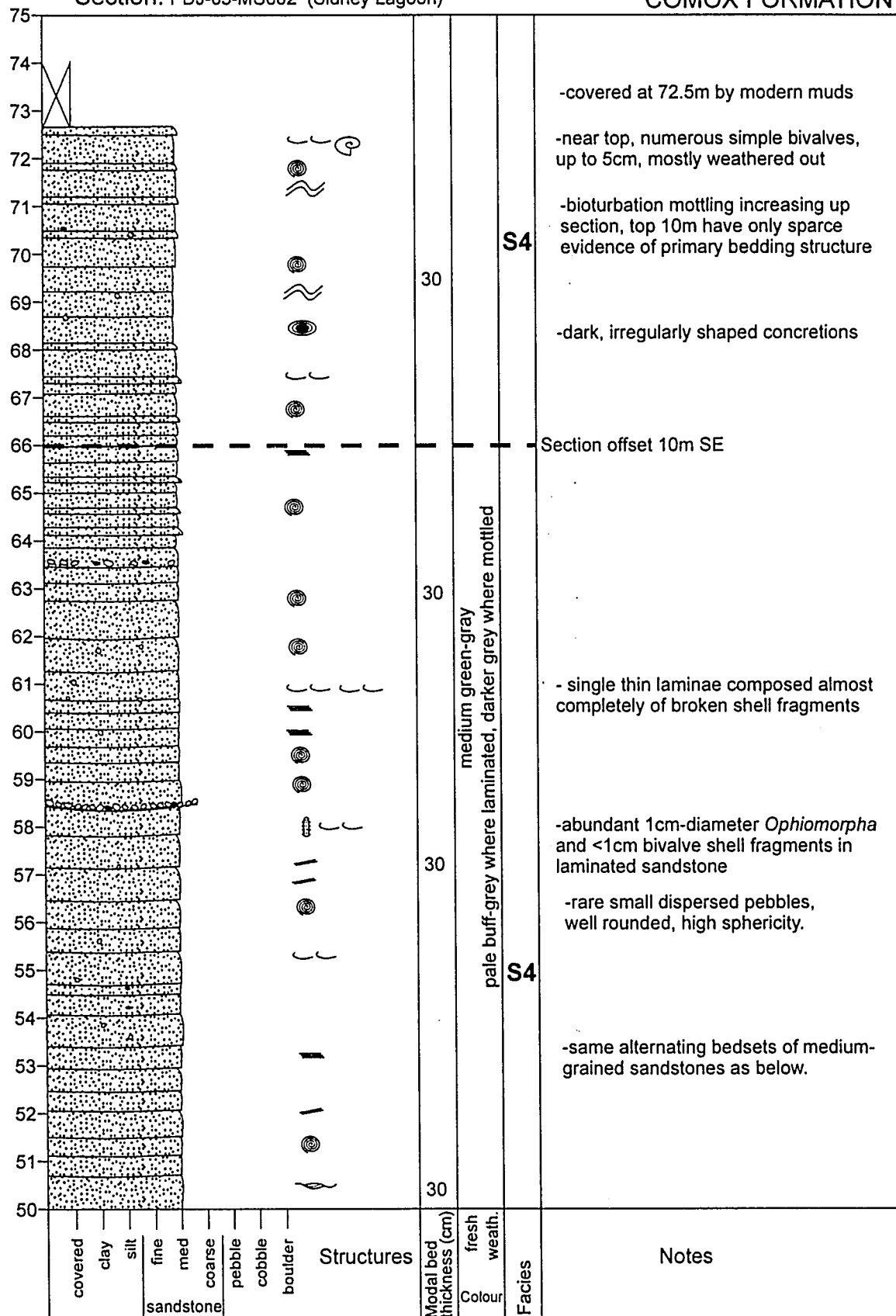


## COMOX FORMATION



## Section: PDJ-03-MS002 (Sidney Lagoon)

## COMOX FORMATION



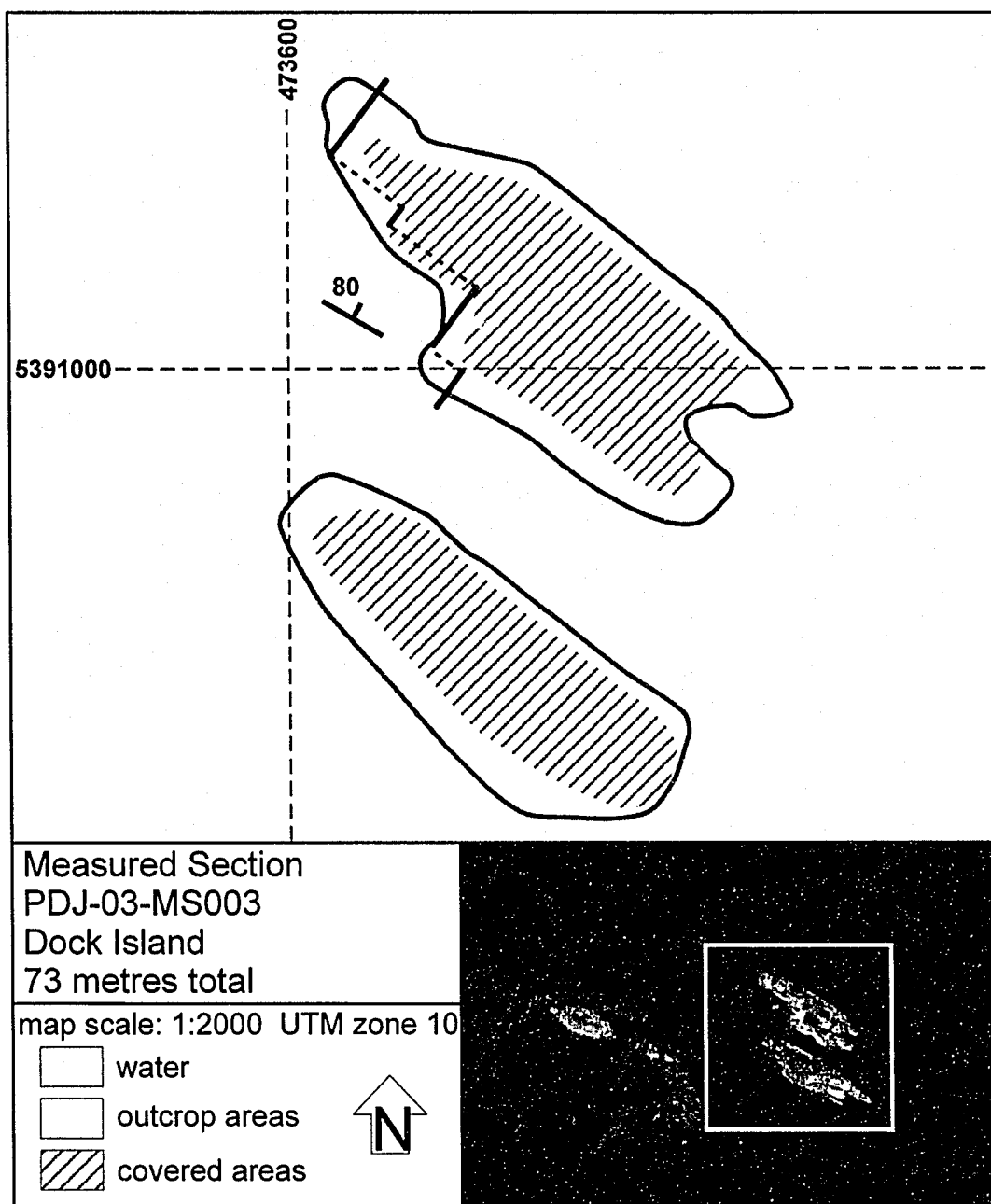
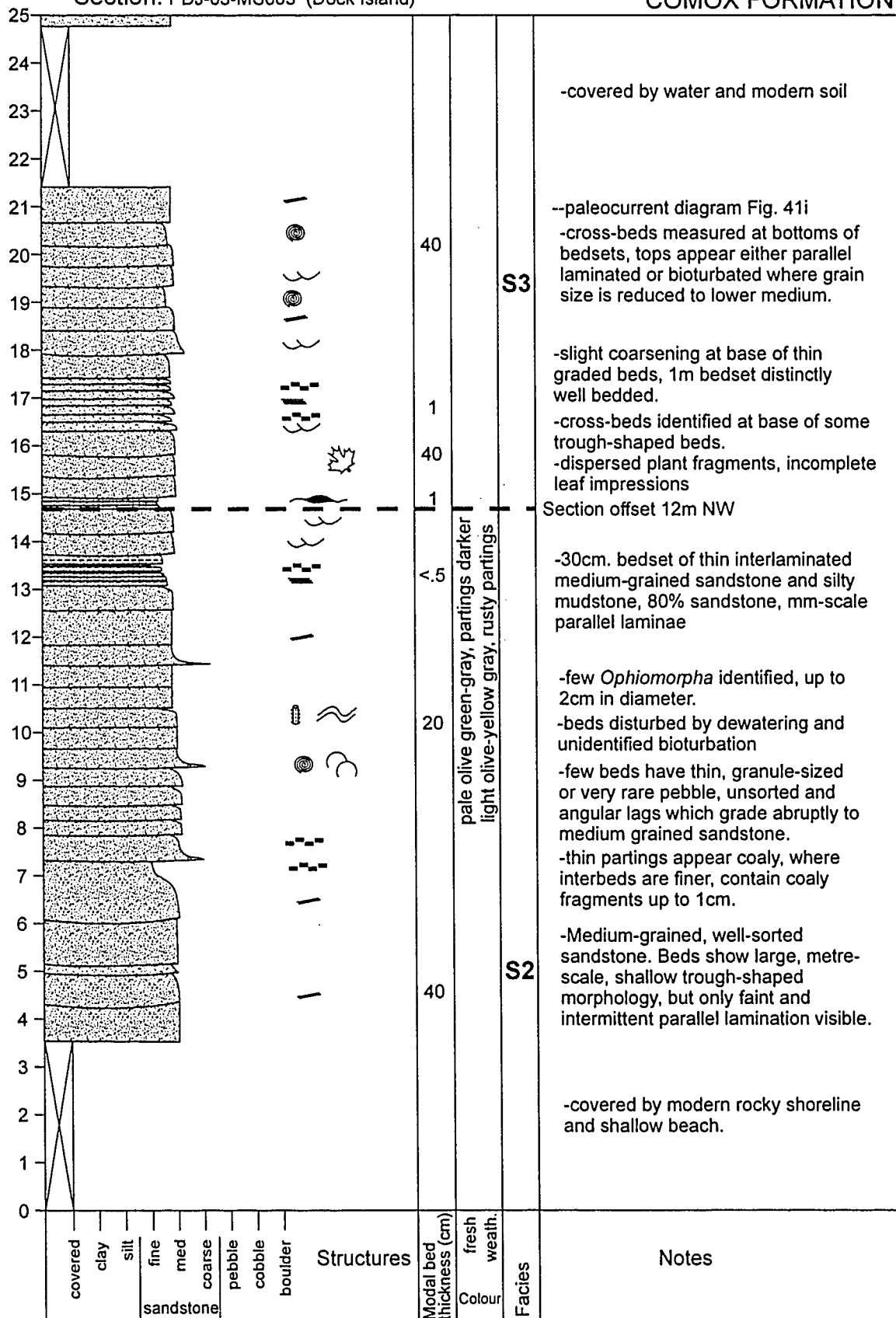


Figure A 5: Location Map, measured section MS003.

## Section: PDJ-03-MS003 (Dock Island)

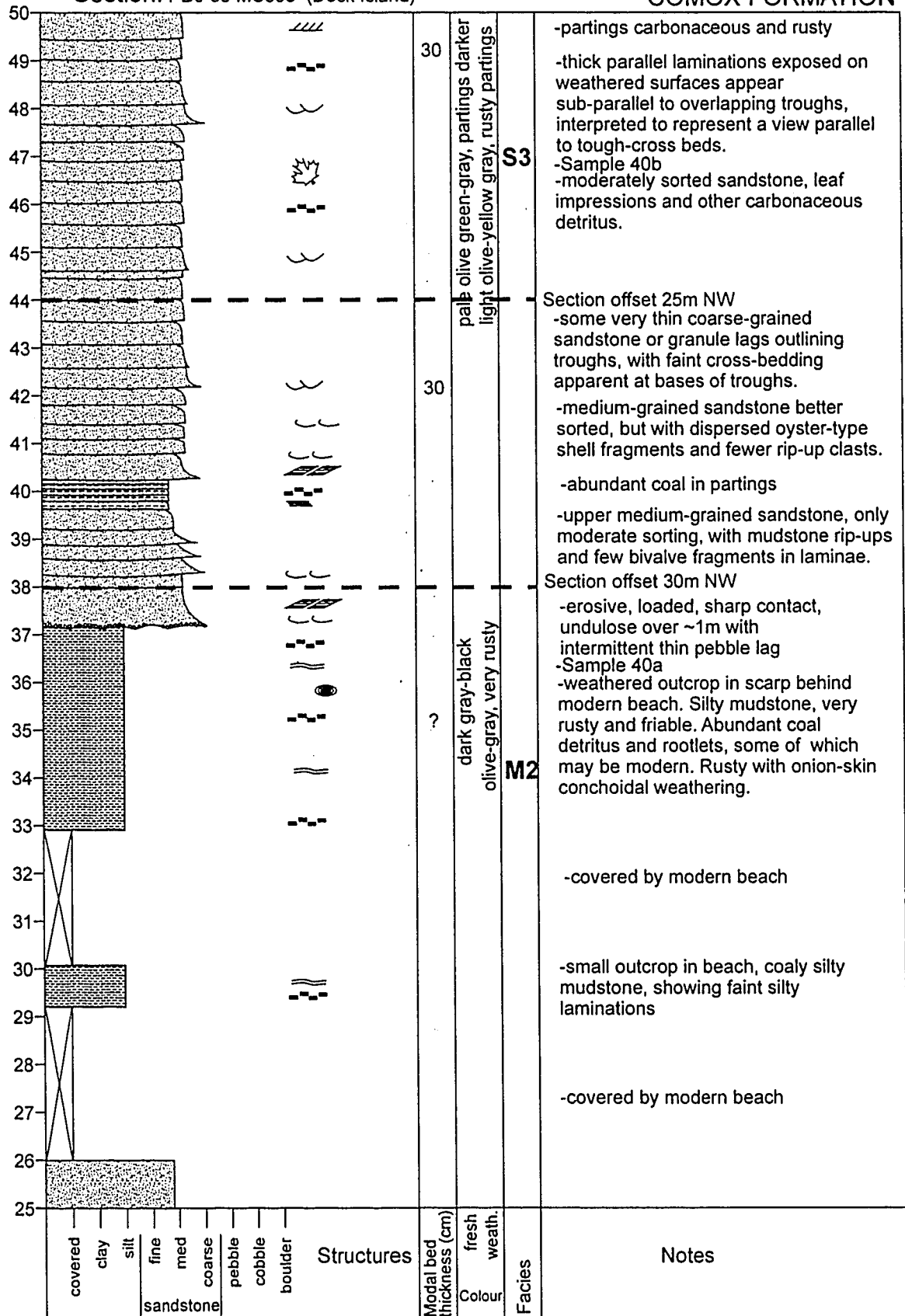
## COMOX FORMATION





## Section: PDJ-03-MS003 (Dock Island)

## COMOX FORMATION

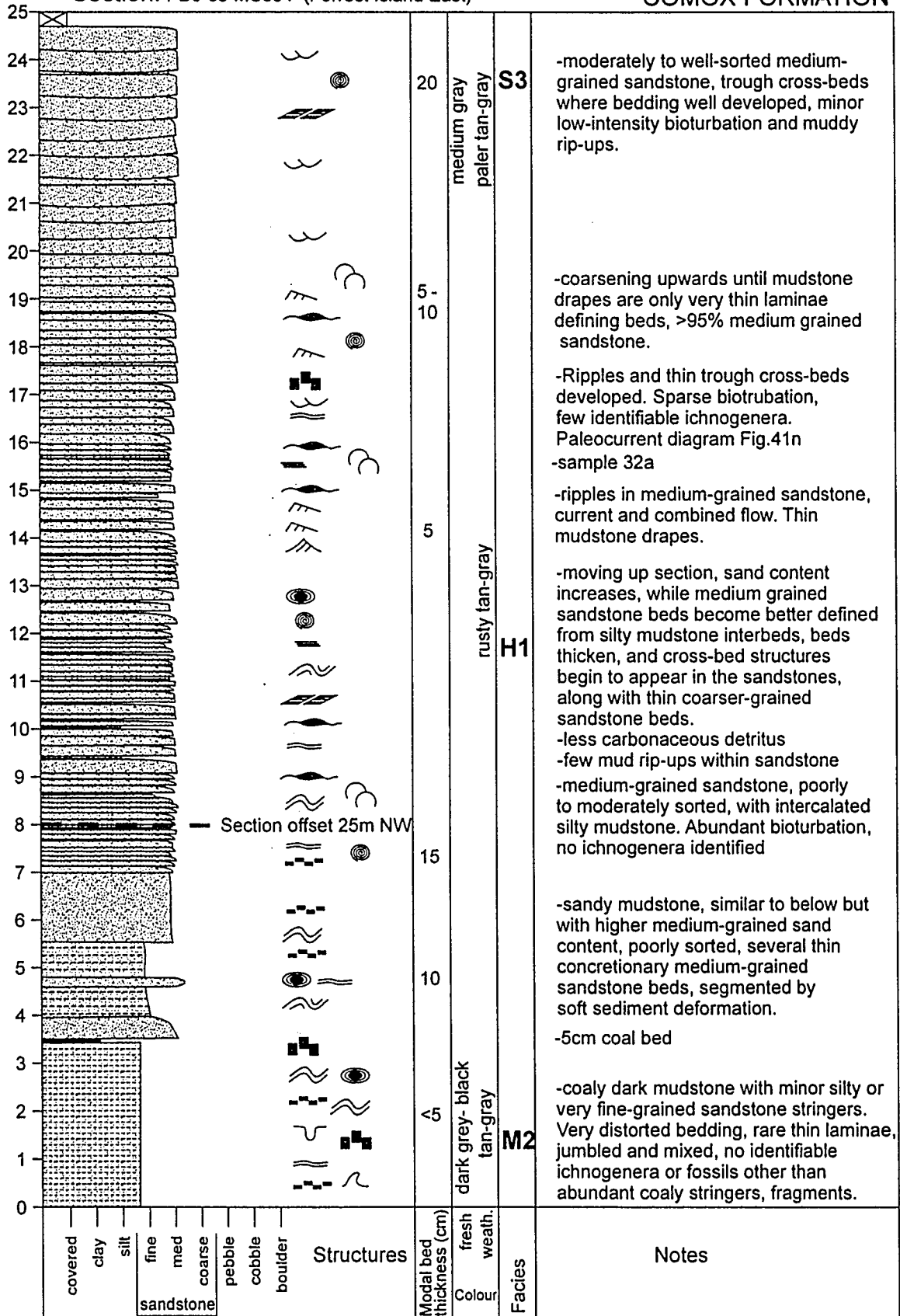


## COMOX FORMATION



## Section: PDJ-03-MS004 (Forrest Island East)

## COMOX FORMATION



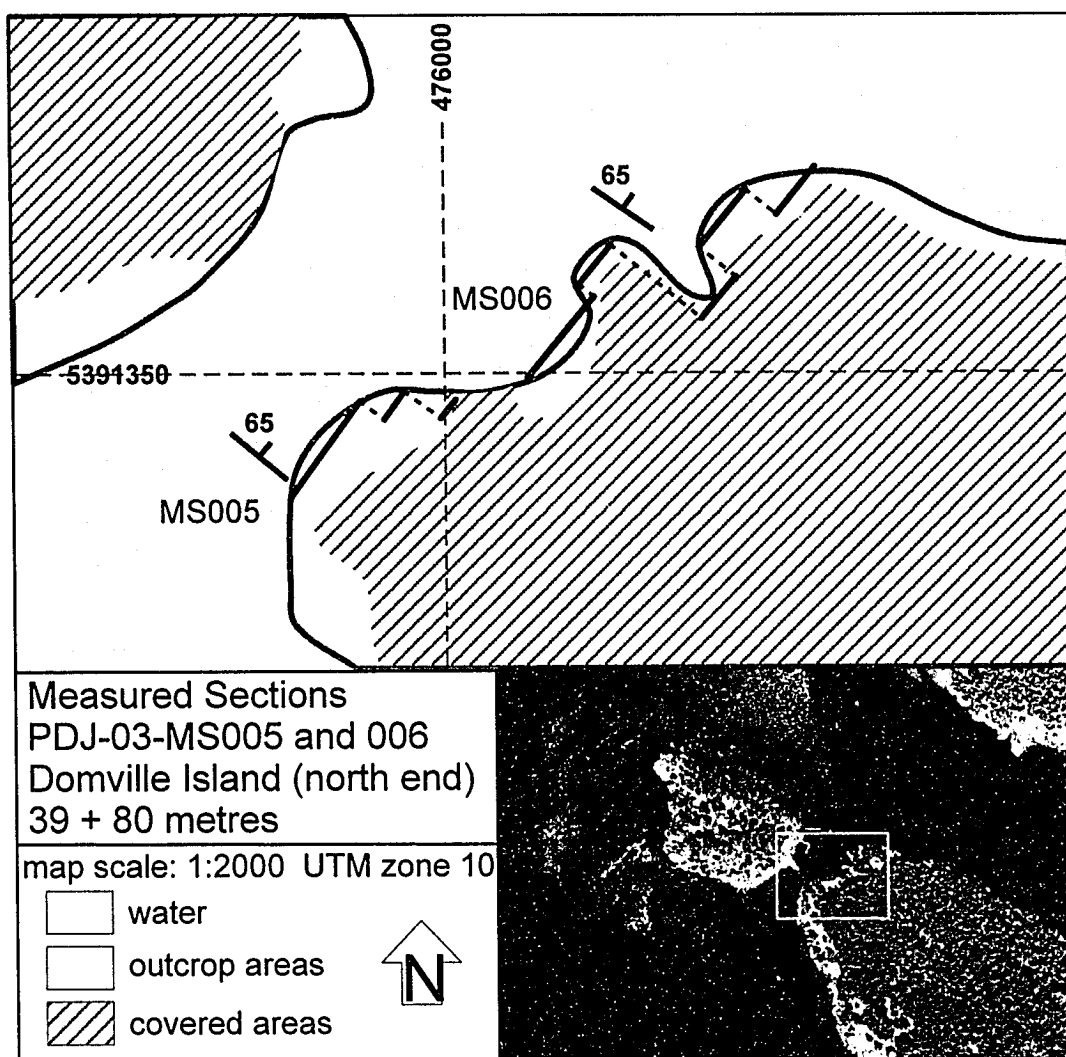
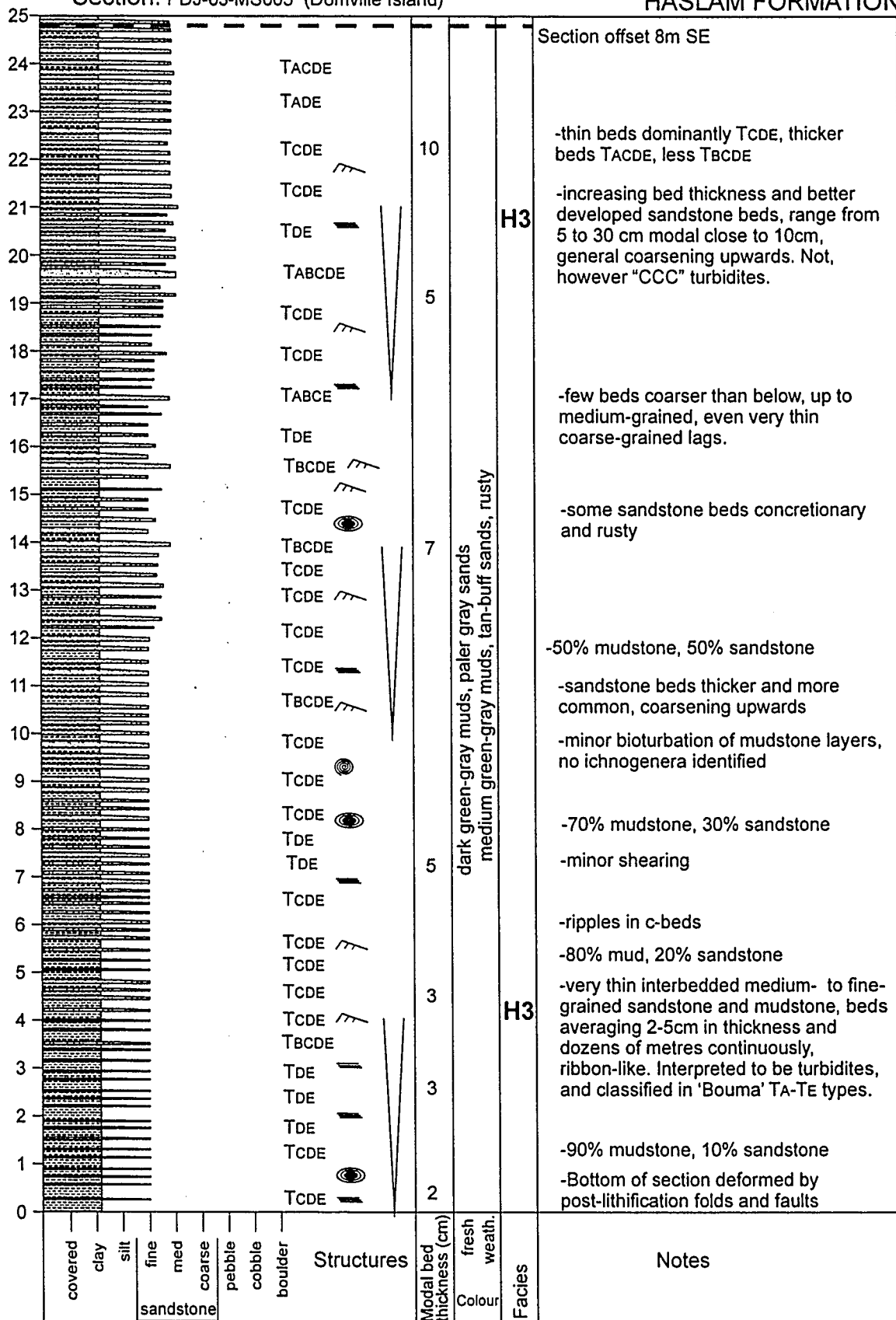


Figure A 6: Location Map, measured sections Ms005 and MS006.

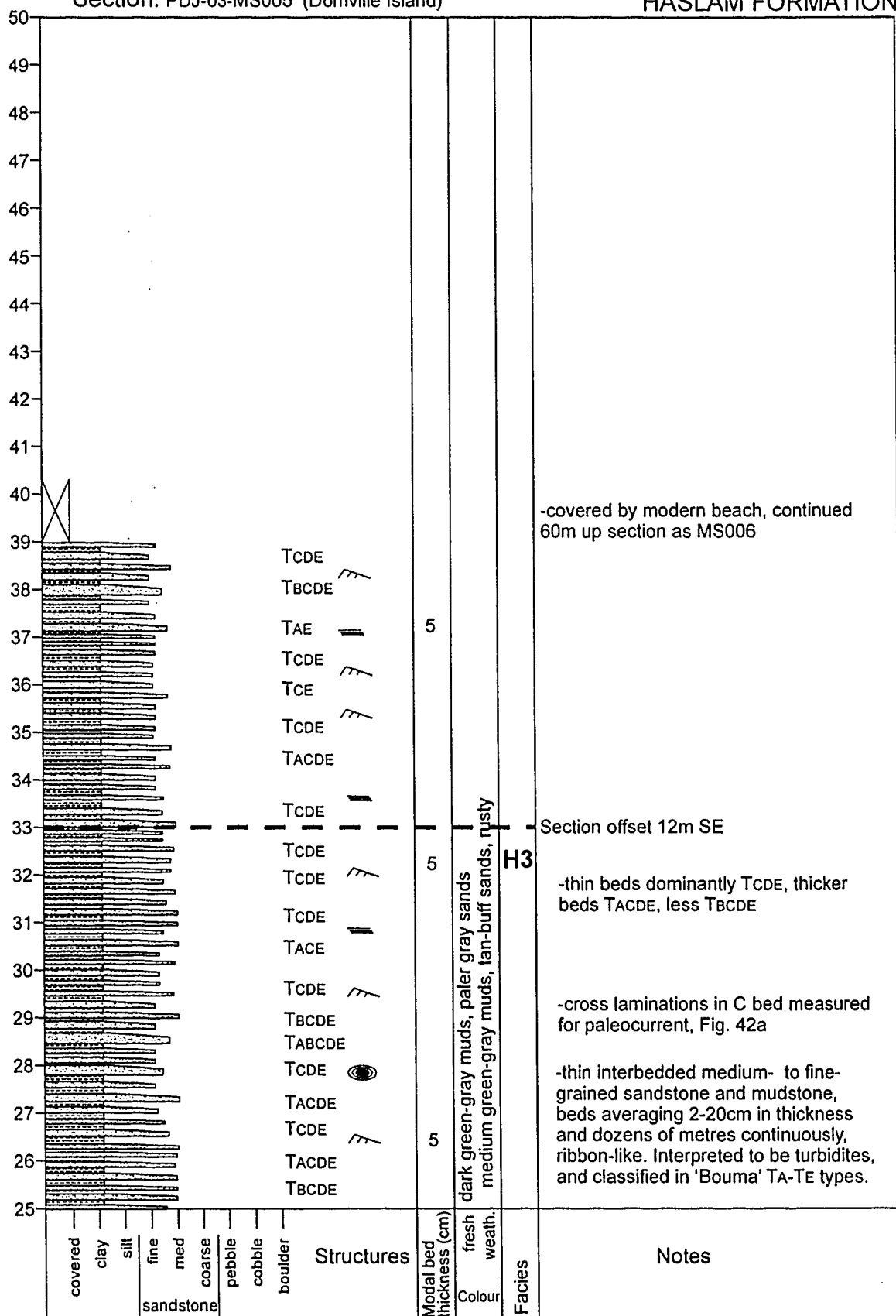
## Section: PDJ-03-MS005 (Domville Island)

HASLAM FORMATION



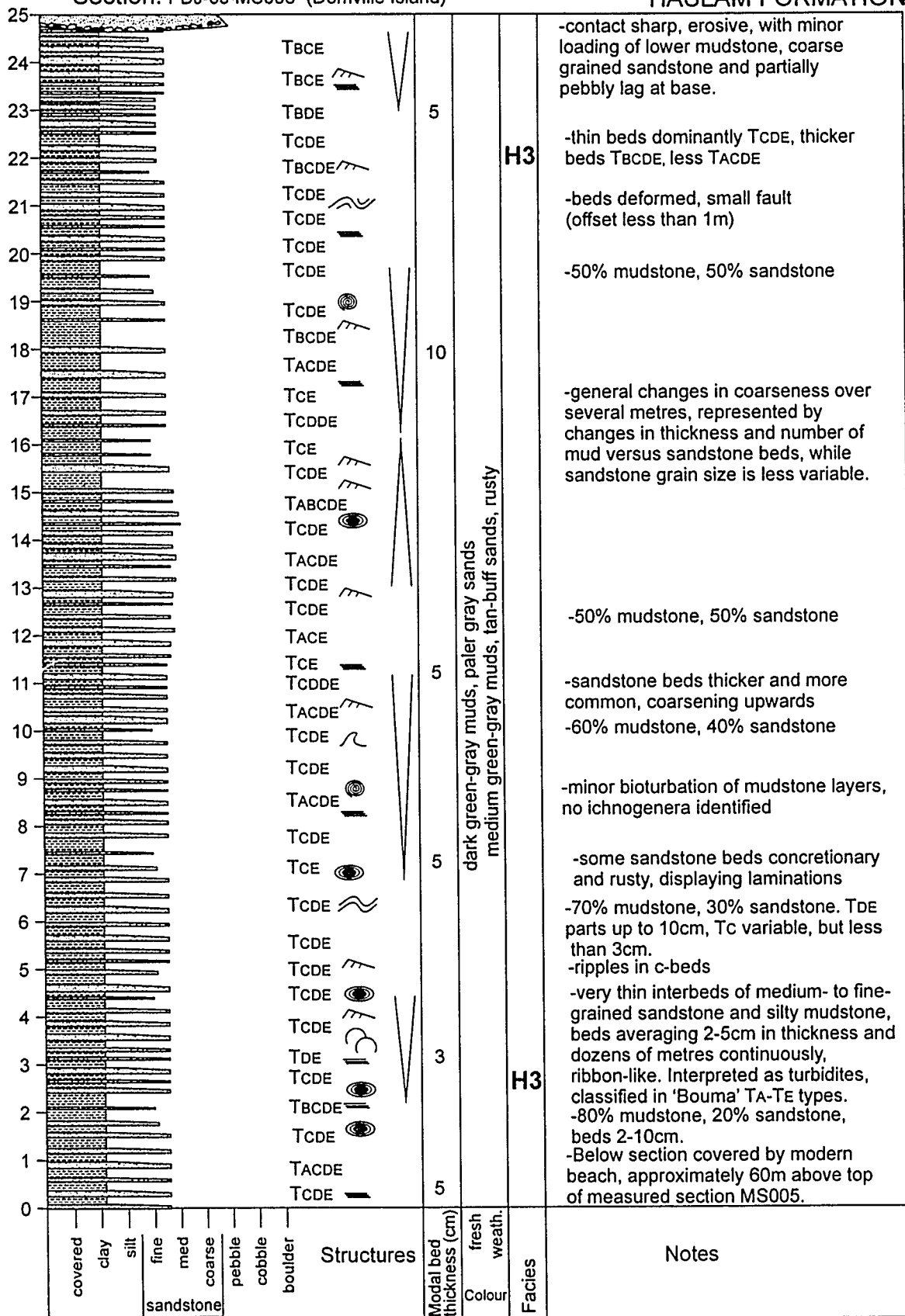
## Section: PDJ-03-MS005 (Domville Island)

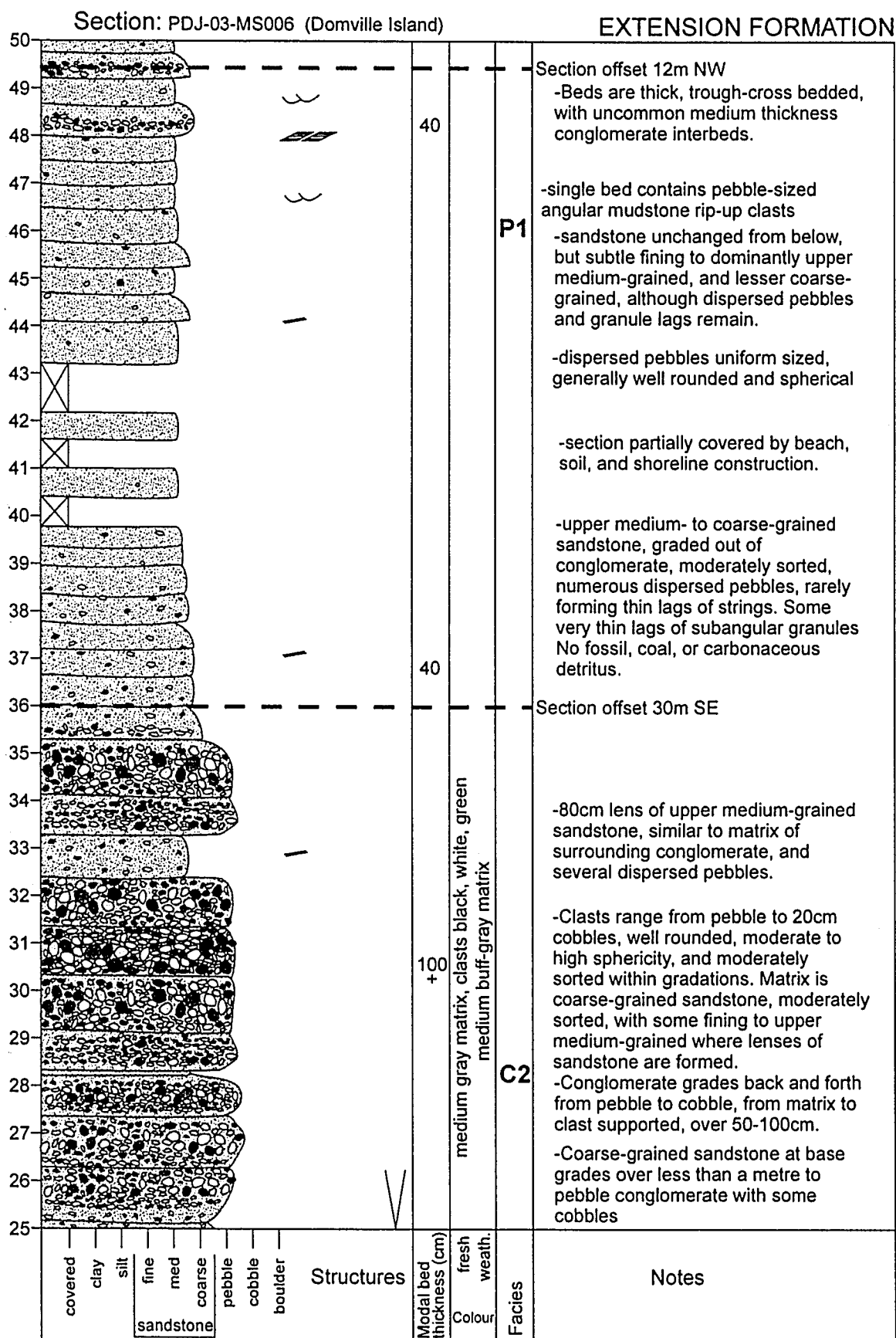
## HASLAM FORMATION



## Section: PDJ-03-MS006 (Domville Island)

## HASLAM FORMATION







## EXTENSION FORMATION



## EXTENSION FORMATION



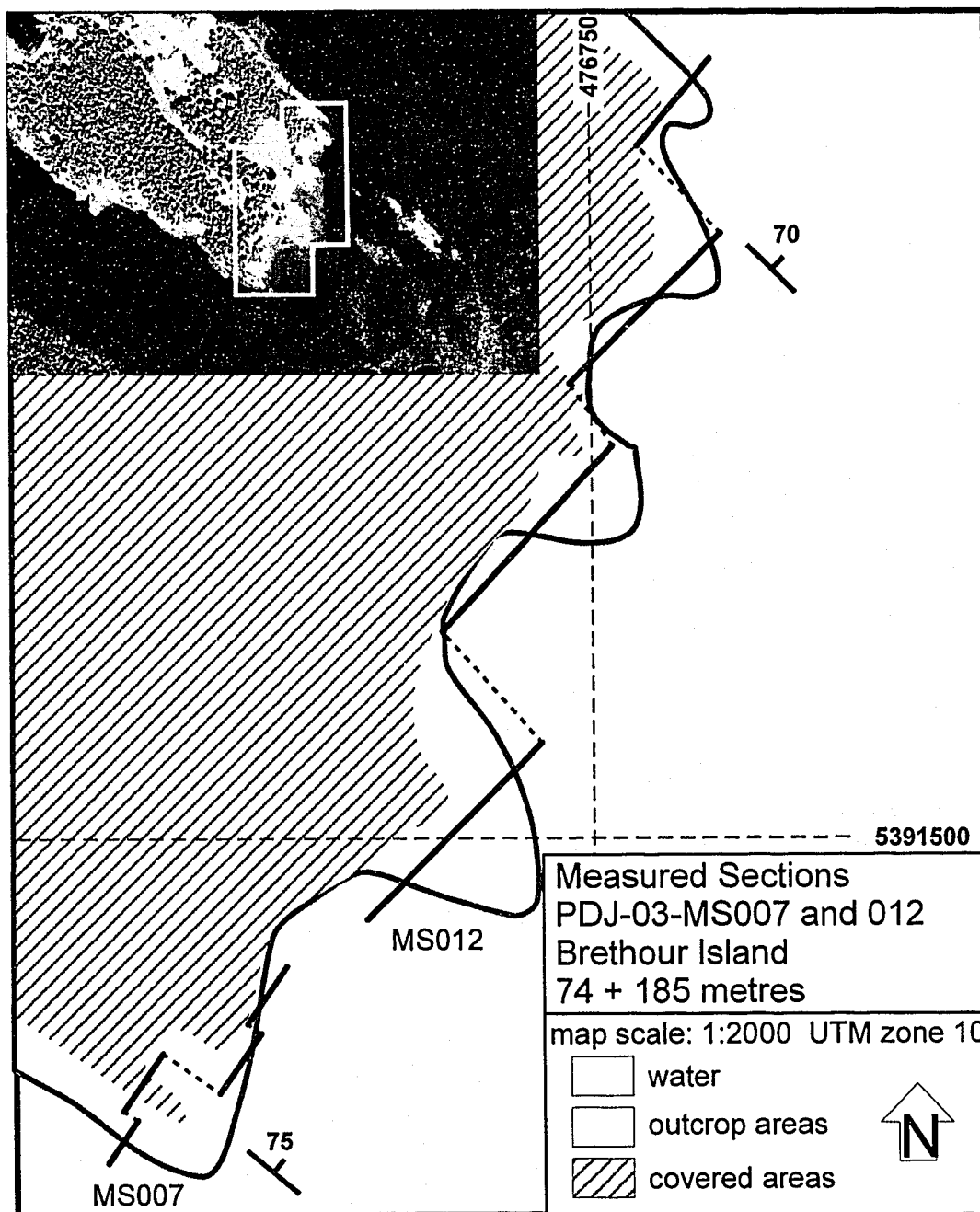


Figure A 7: Location Map, measured sections MS007 and MS012.

## COMOX FORMATION

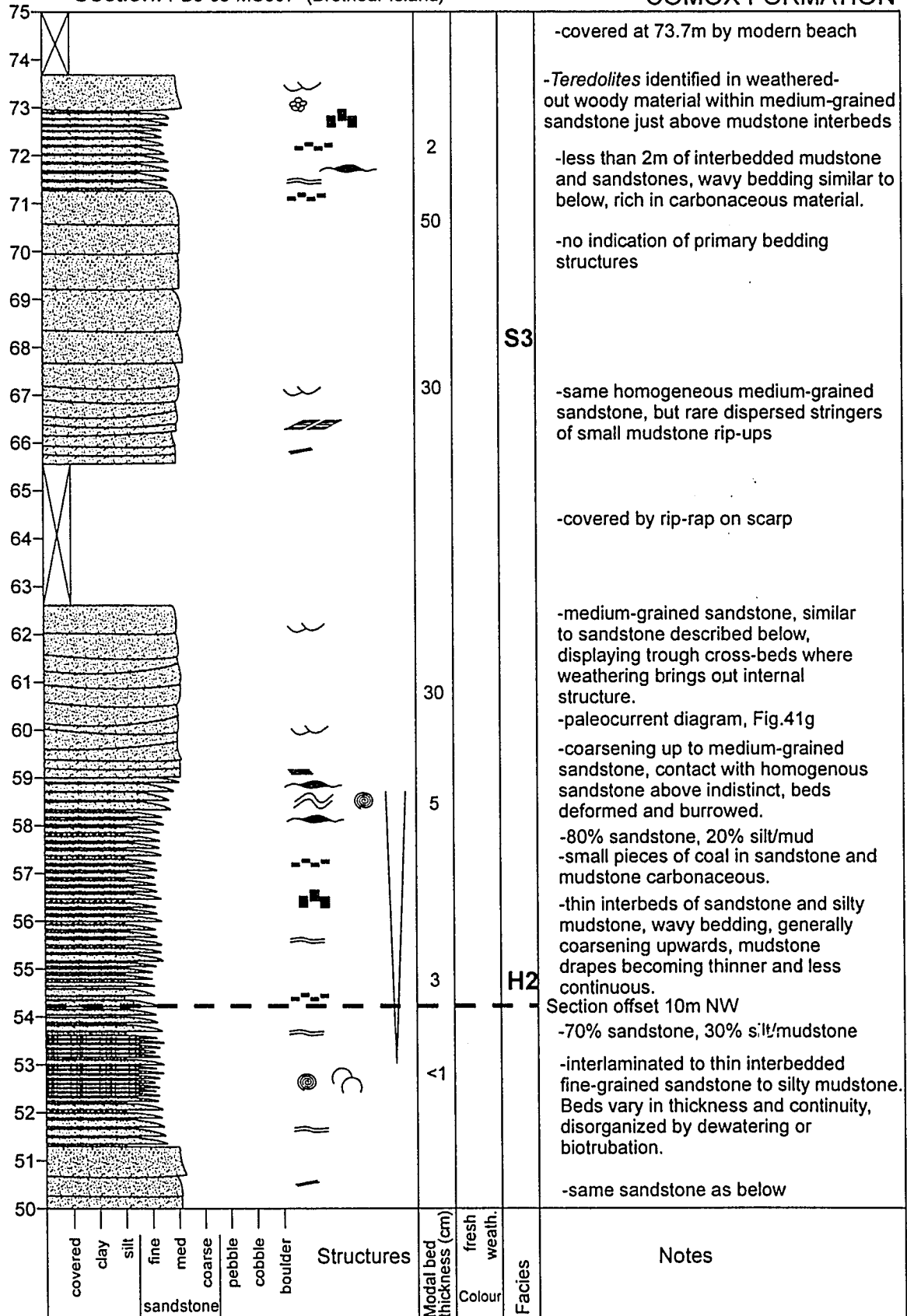


## COMOX FORMATION



## Section: PDJ-03-MS007 (Brethour Island)

## COMOX FORMATION



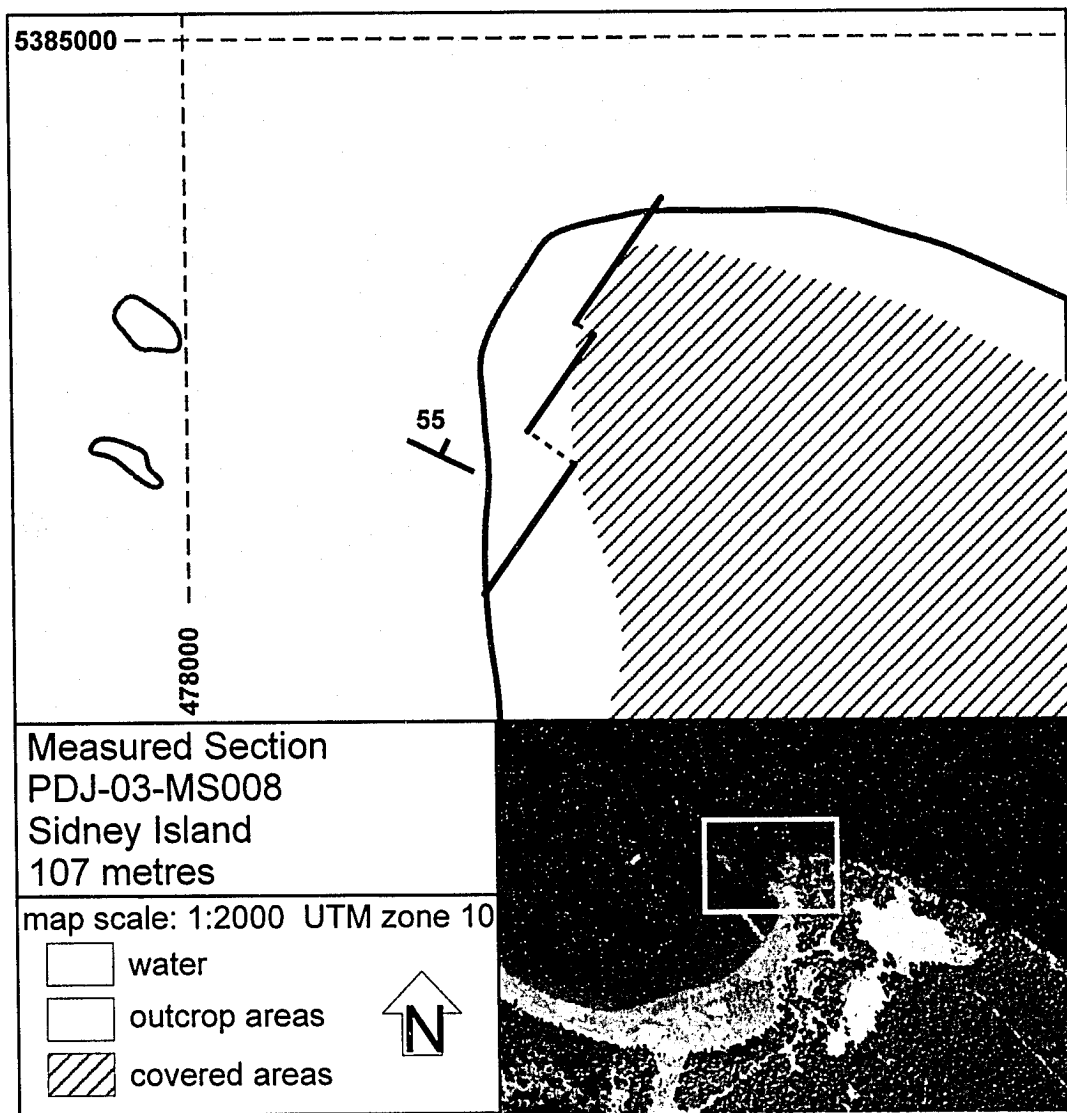


Figure A 8: Location Map, measured section MS008.

## COMOX FORMATION





## COMOX FORMATION



## COMOX FORMATION

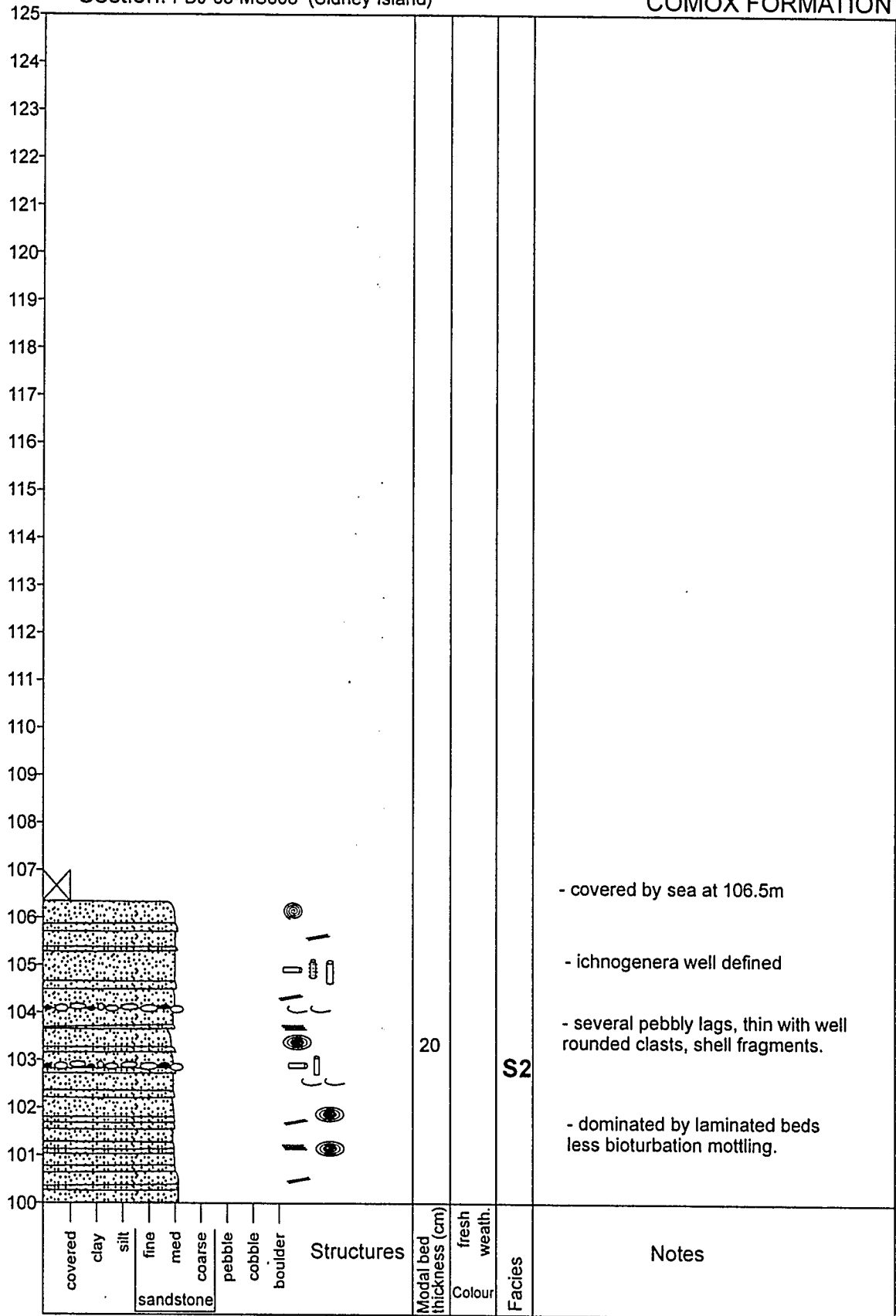


## COMOX FORMATION



## Section: PDJ-03-MS008 (Sidney Island)

## COMOX FORMATION



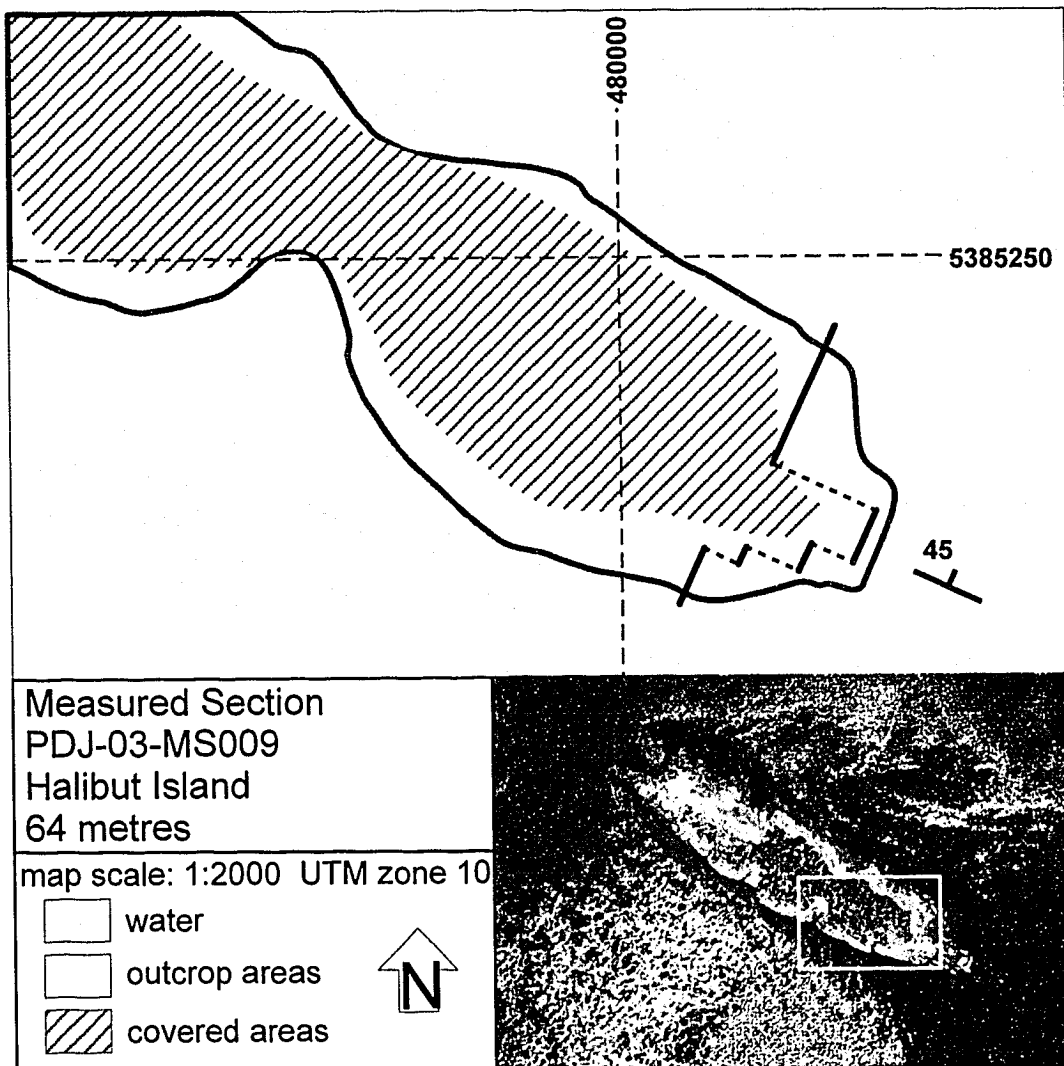


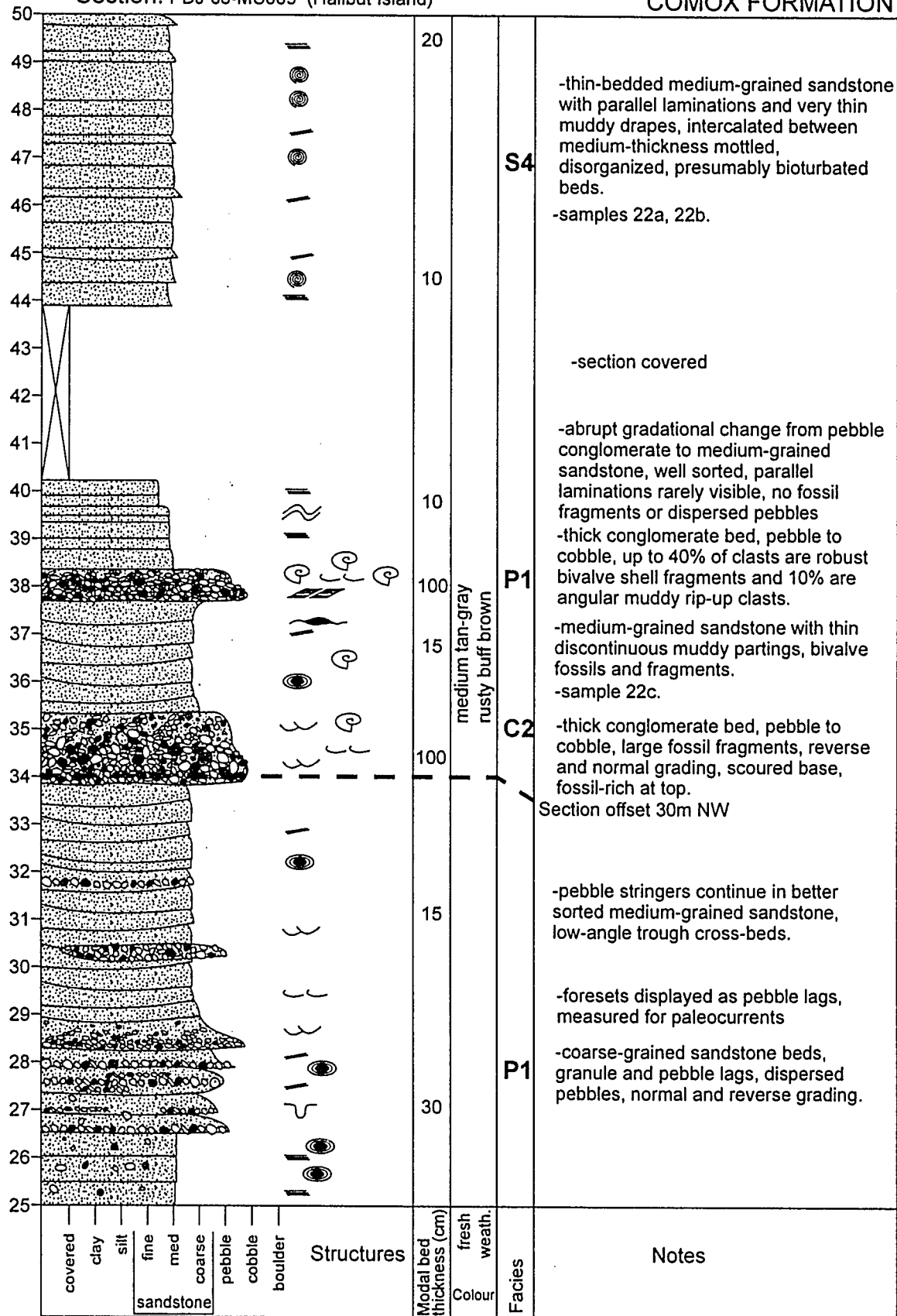
Figure A 9: Location Map, measured section MS009.

## COMOX FORMATION



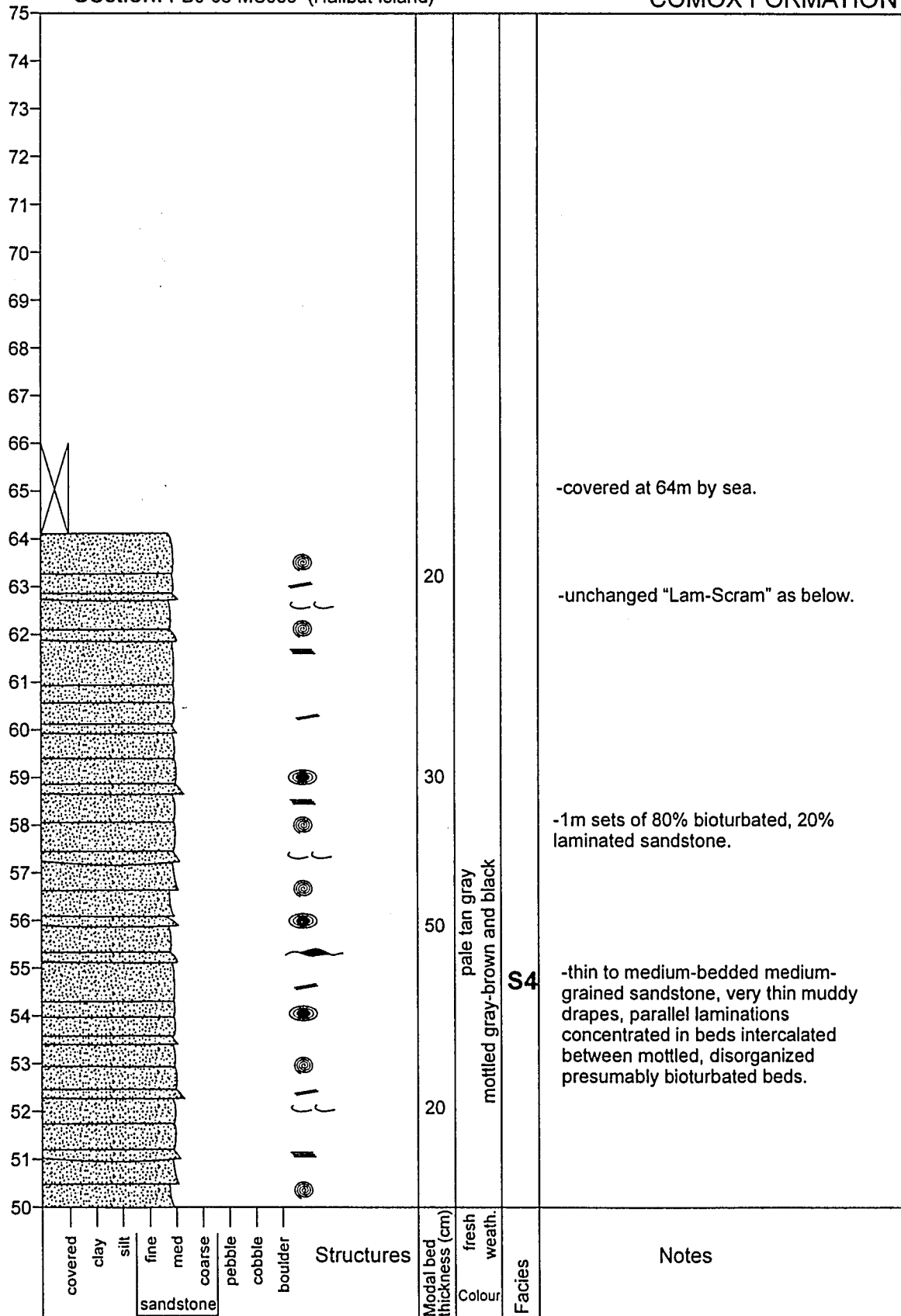
## Section: PDJ-03-MS009 (Halibut Island)

## COMOX FORMATION



## Section: PDJ-03-MS009 (Halibut Island)

## COMOX FORMATION





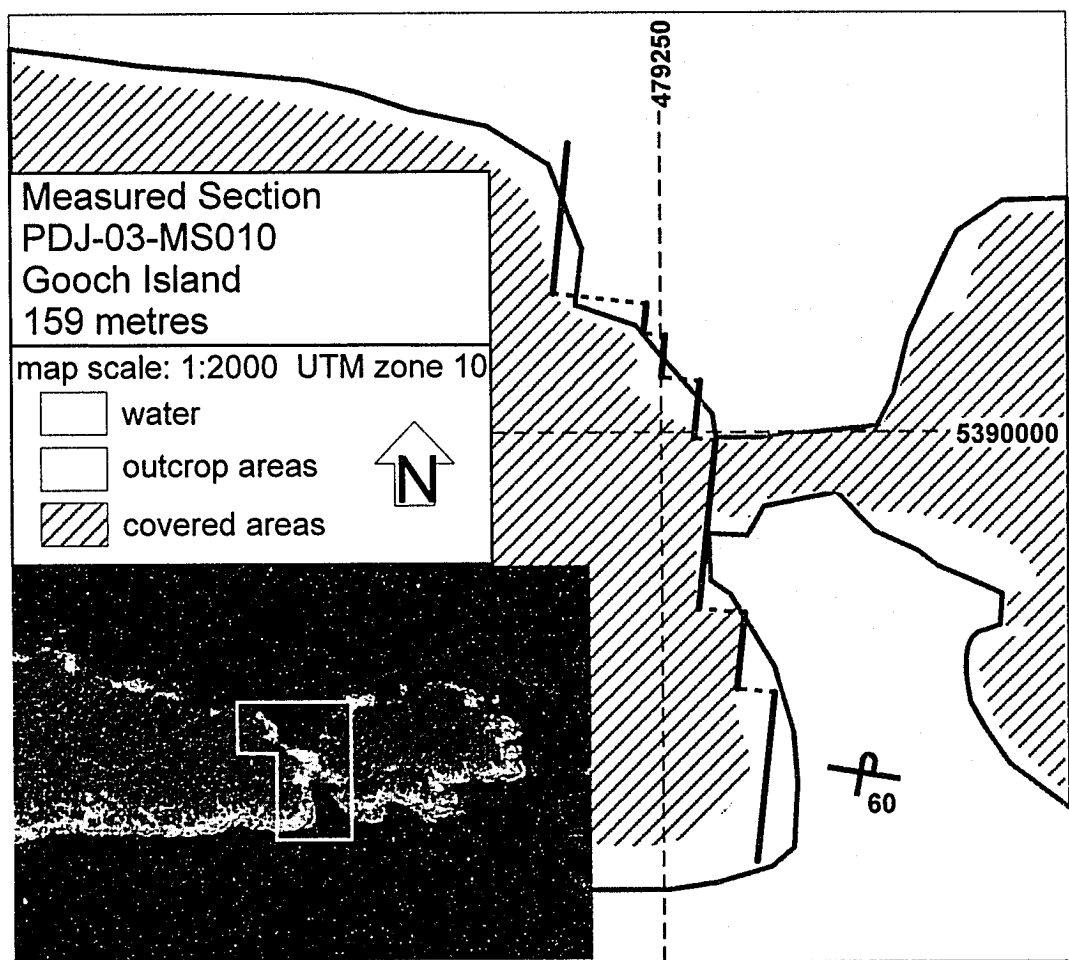


Figure A 10: Location Map, measured section MS010.

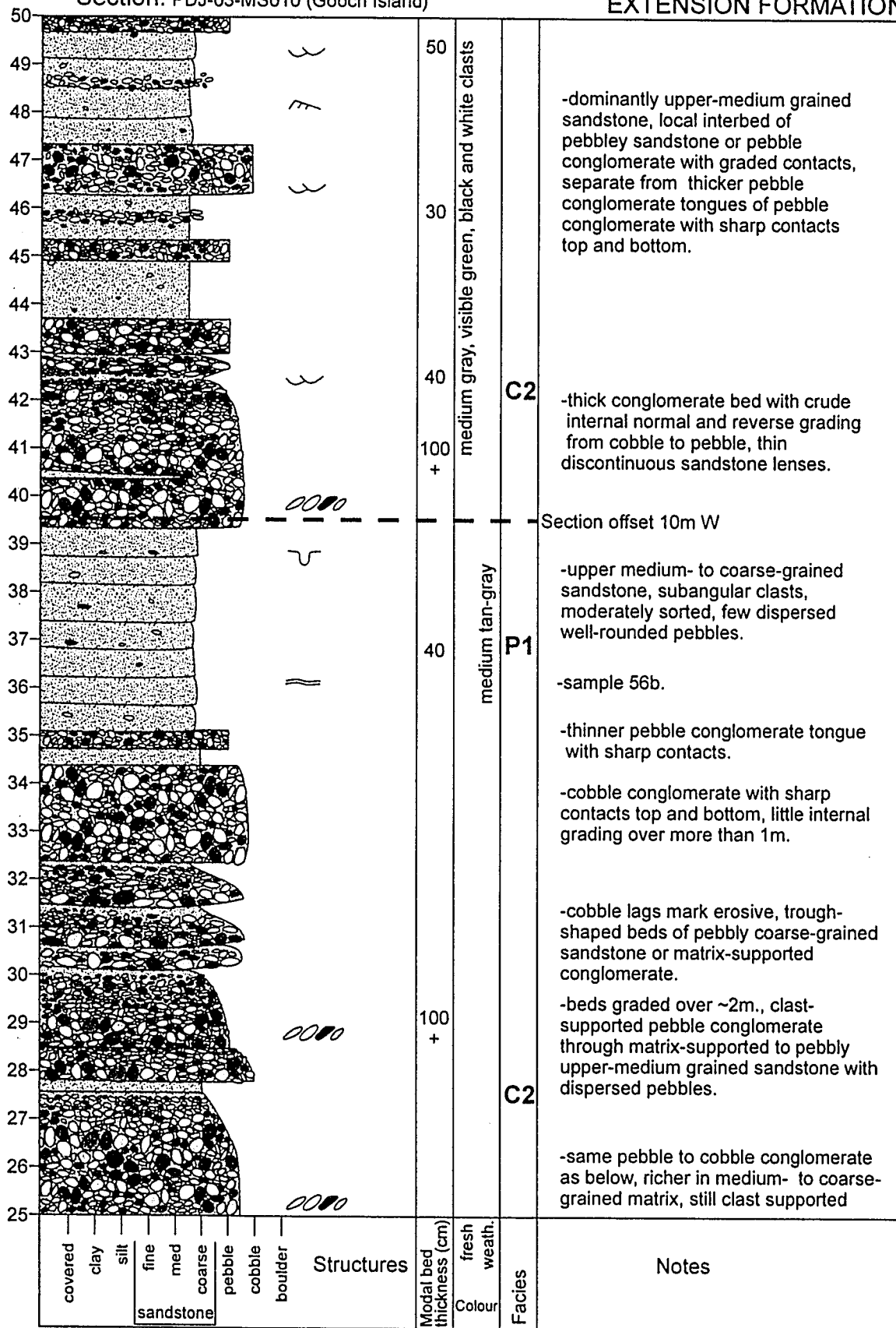
\* Stratigraphy at this locality is overturned towards the south. Vertical stratigraphic section was measured from the stratigraphic base (south to north)

## EXTENSION FORMATION



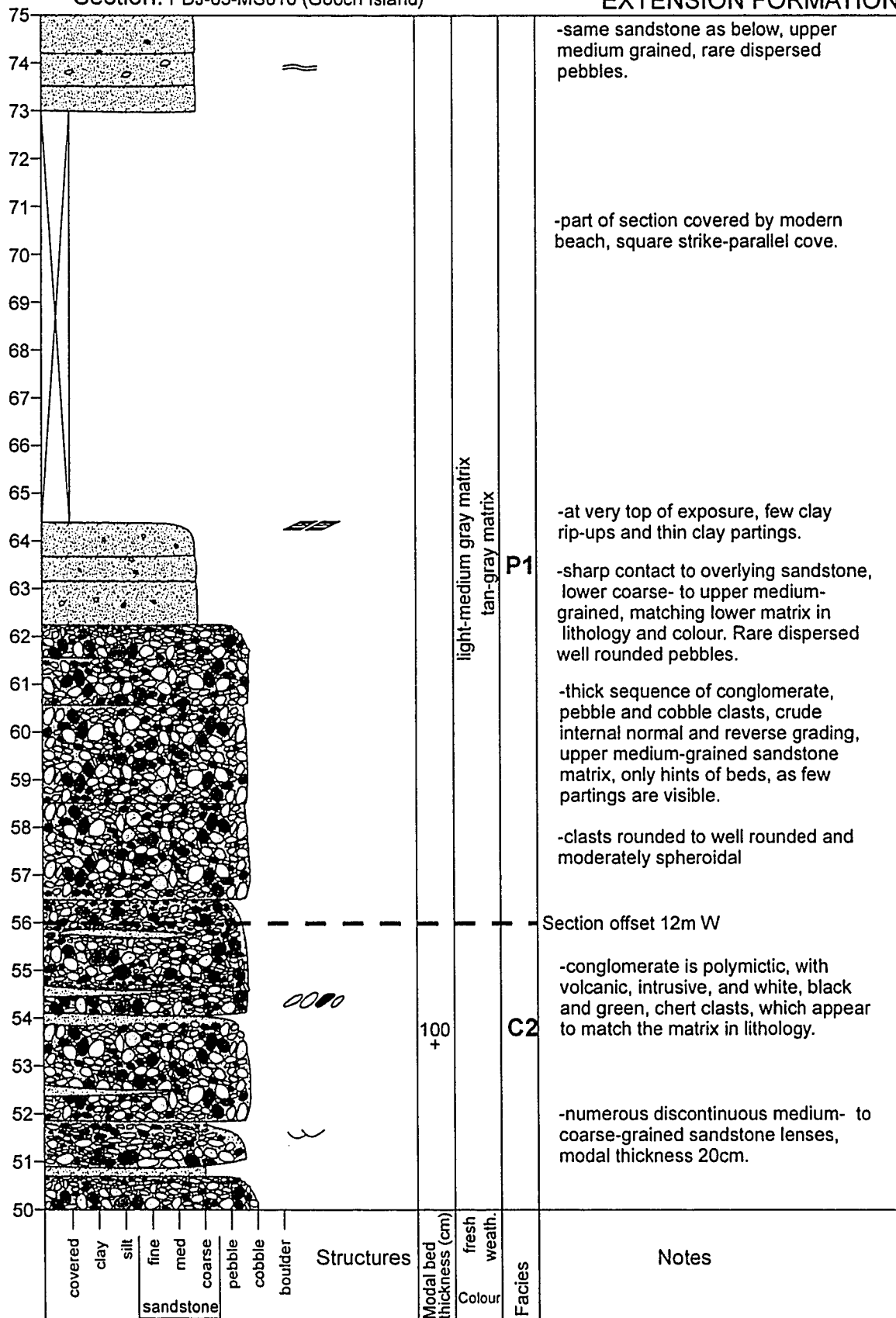
## Section: PDJ-03-MS010 (Gooch Island)

## EXTENSION FORMATION



## Section: PDJ-03-MS010 (Gooch Island)

## EXTENSION FORMATION

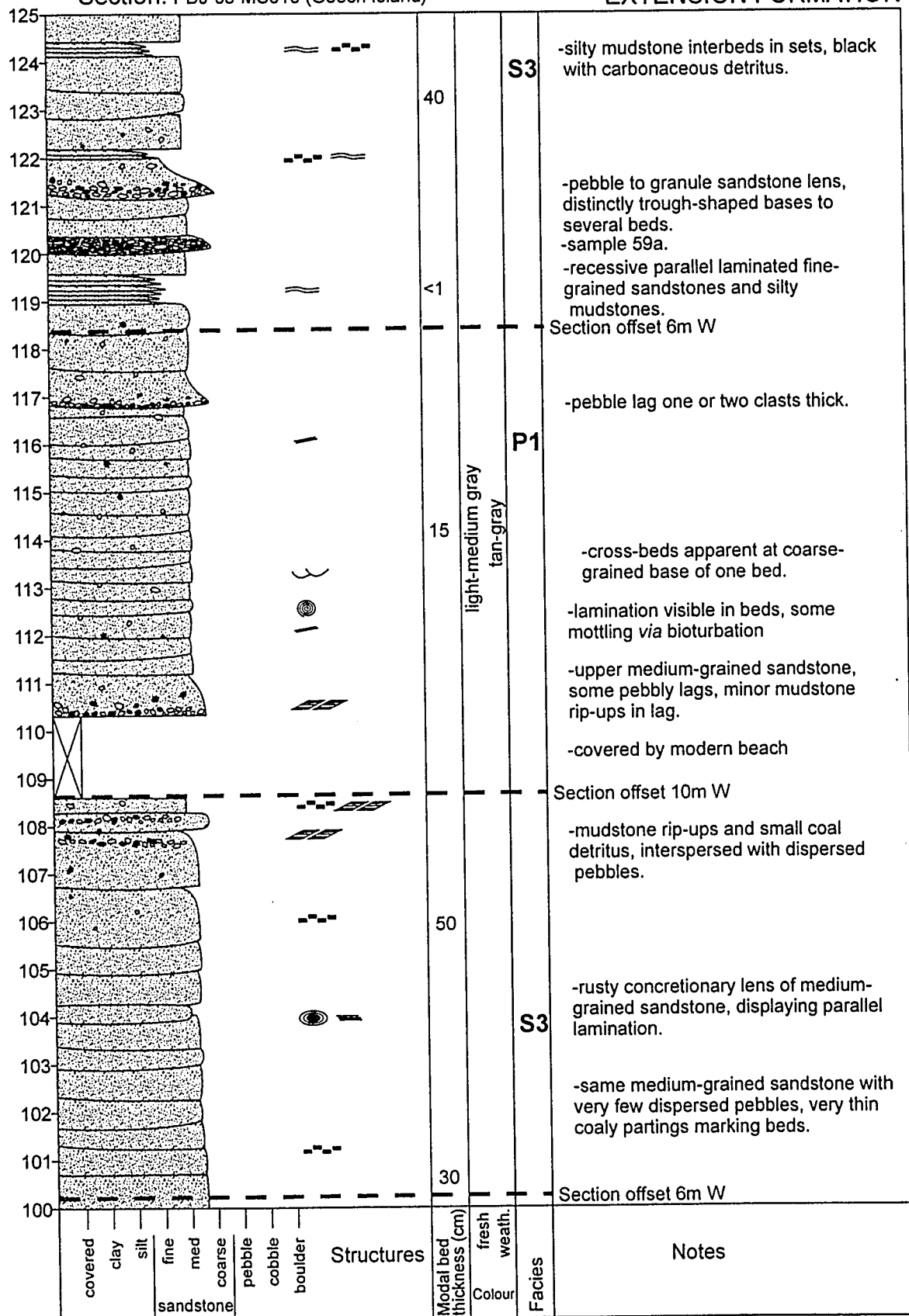


## EXTENSION FORMATION



## Section: PDJ-03-MS010 (Gooch Island)

## EXTENSION FORMATION

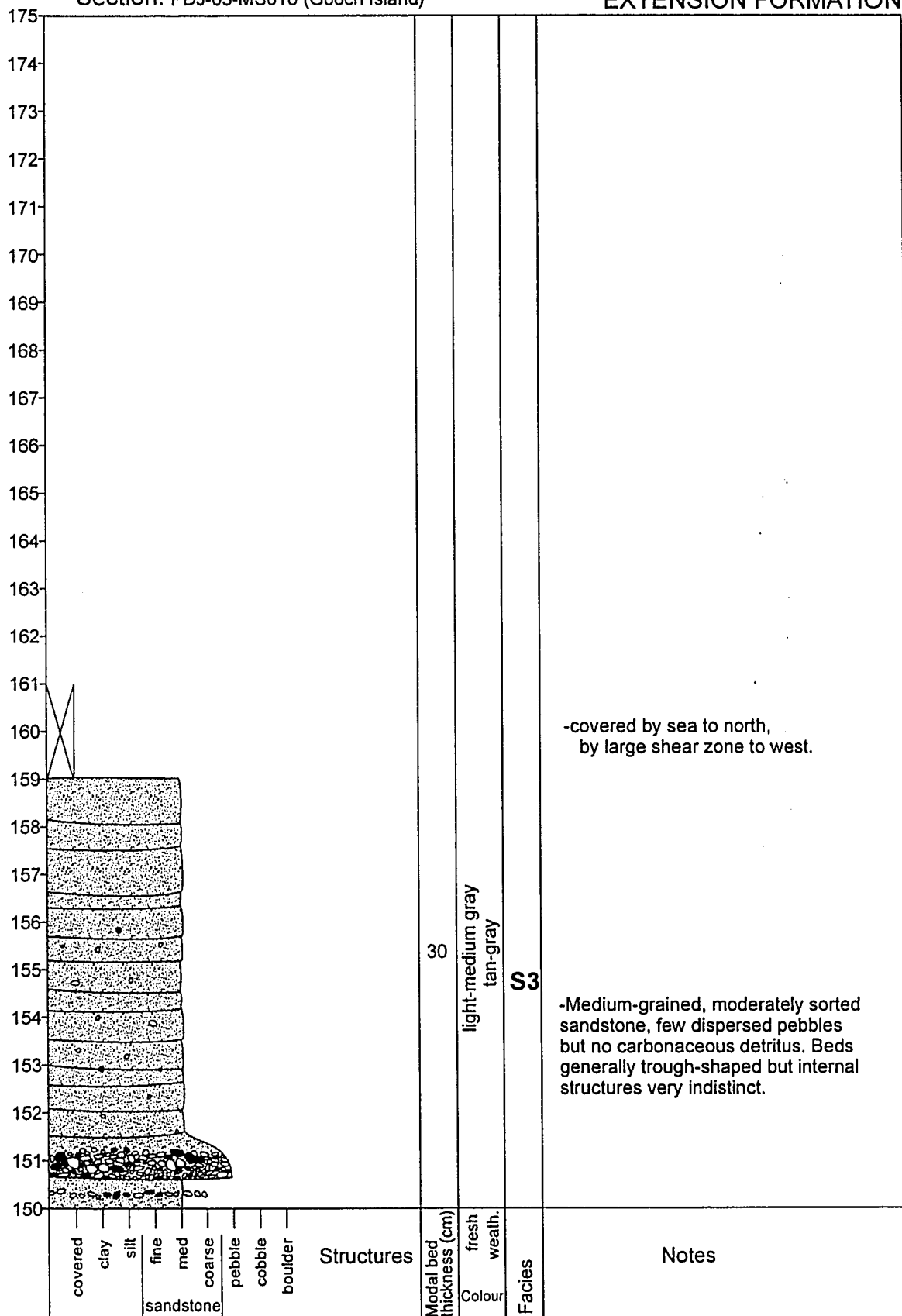


## EXTENSION FORMATION



## Section: PDJ-03-MS010 (Gooch Island)

## EXTENSION FORMATION





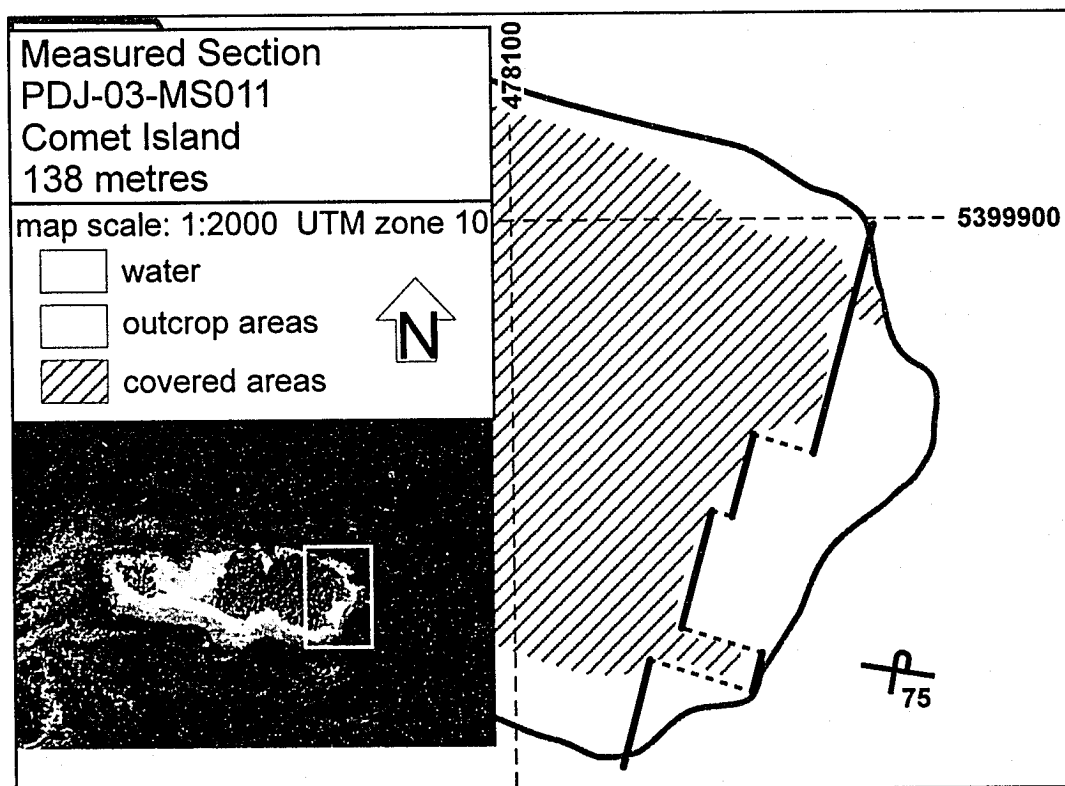


Figure A 11: Location Map, measured section MS011.

\* Stratigraphy at this locality is overturned towards the south. Vertical stratigraphic section was measured from the stratigraphic base (south to north)

## COMOX FORMATION

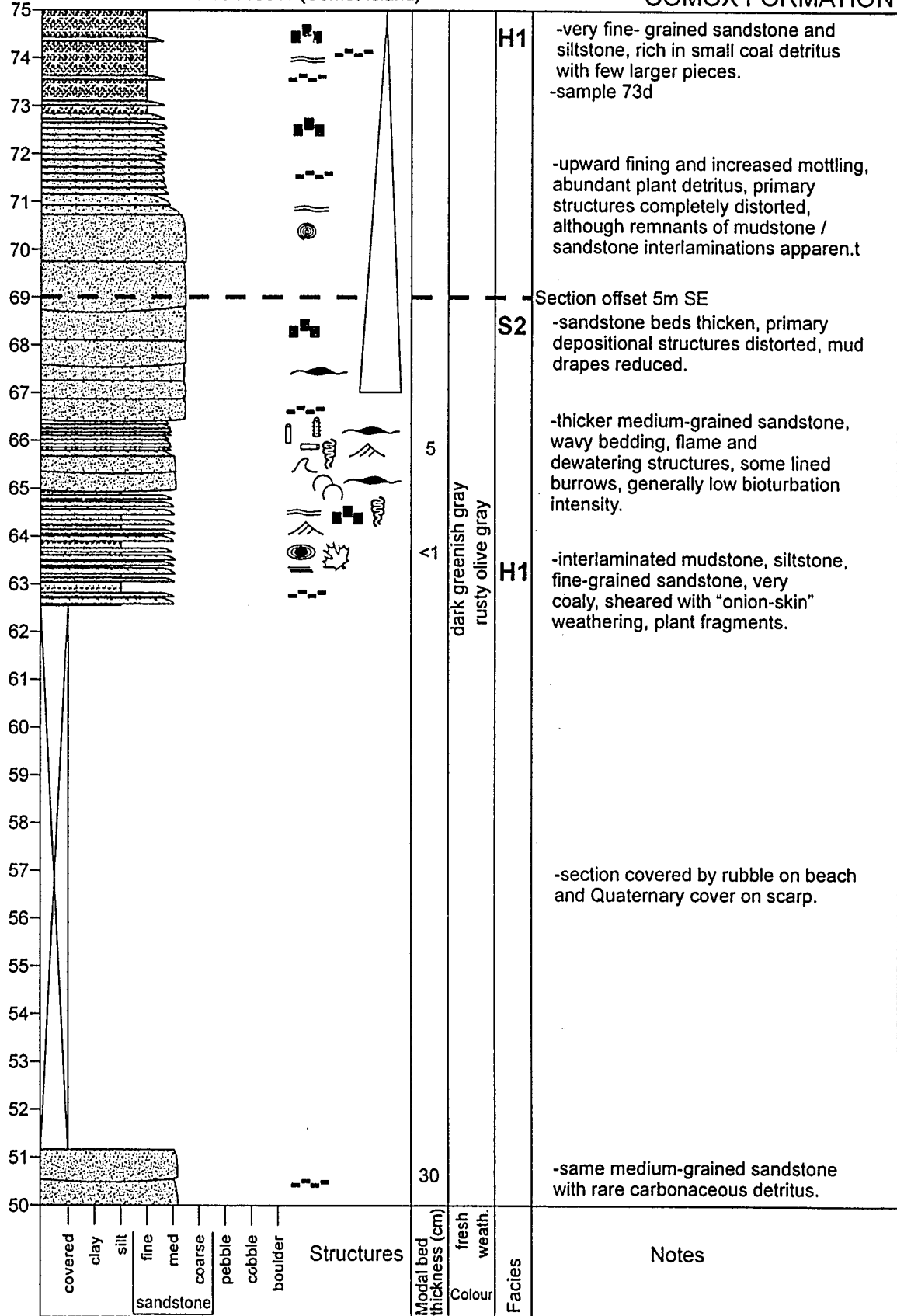


## COMOX FORMATION



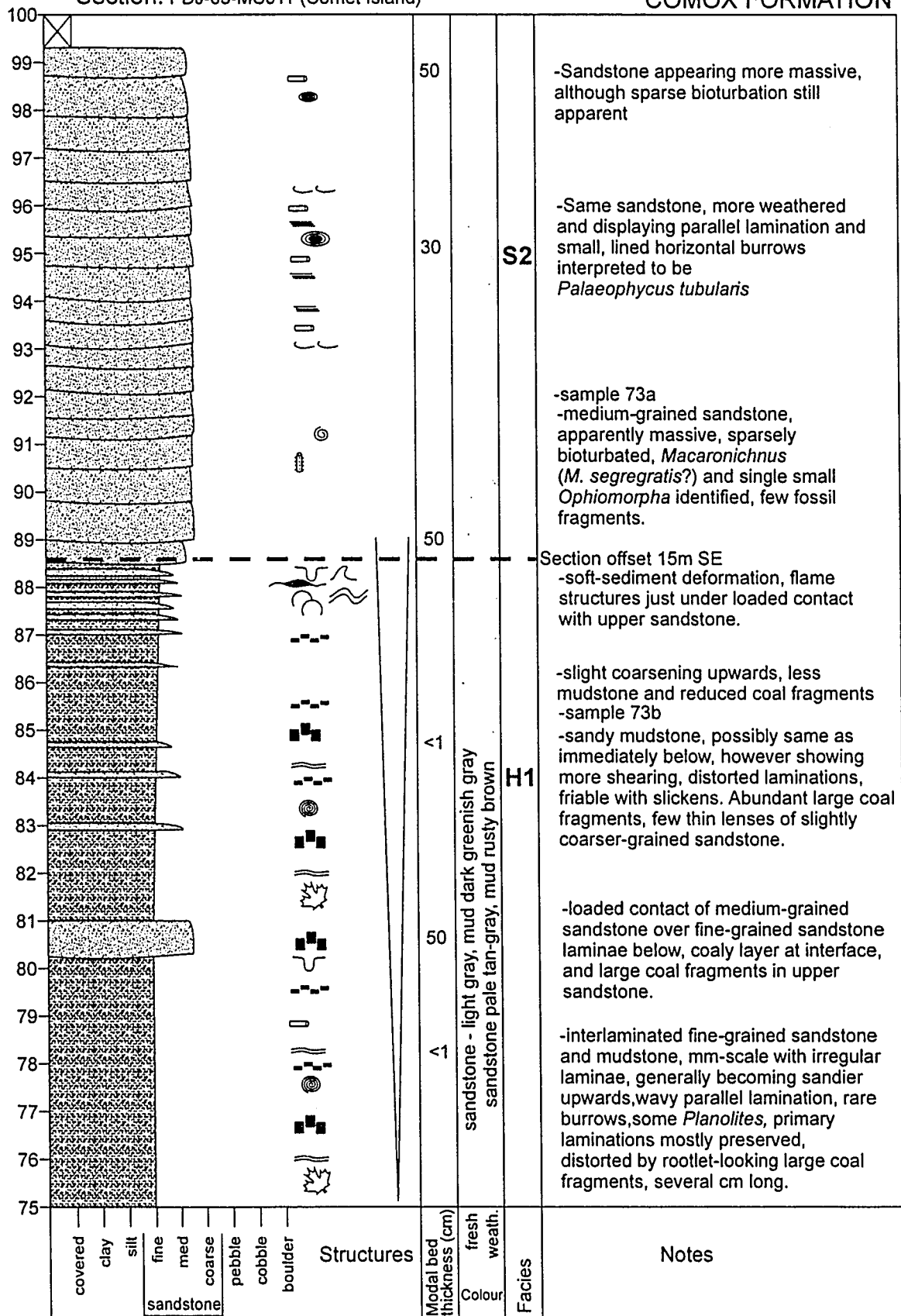
## Section: PDJ-03-MS011 (Comet Island)

## COMOX FORMATION



## Section: PDJ-03-MS011 (Comet Island)

## COMOX FORMATION



## COMOX FORMATION

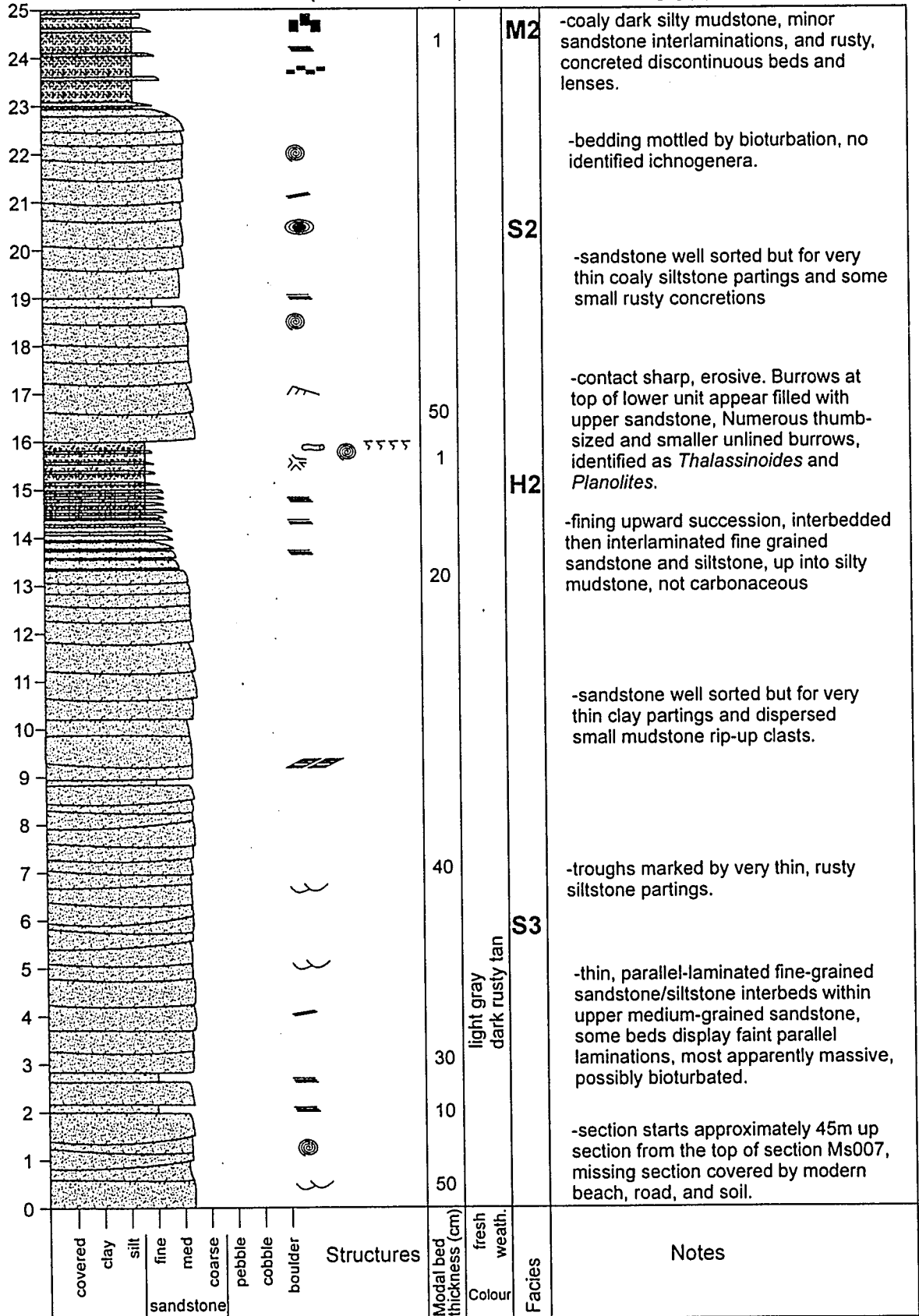
	covered	clay	silt	fine sandstone	med coarse	pebble	cobble	boulder	Structures	Modal bed thickness (cm)	fresh weath.	Colour	Facies	Notes
100-101	X													- covered by rubble
102									(O) -	50				
103									- - - -					
104									(S) -					
105									(O) -					
106									// // //					-medium-grained sandstone, very homogeneous, some parallel laminations apparent where well weathered, some mottling but no identifiable traces. Rare small concretions may be traces, fossil fragments or rip-ups. Partings are thin and dark, possibly coaly.
107									(O) - - - (O)	5				
108														
109									(S) -					
110									- - -					
111									(S) - - - (O)					
112									(O) - - - (O)				S4	-medium-grained sandstone, some beds more mottled than others, rare rusty mudstone rip-up clasts. Beds are for the most part apparently massive and 50cm thick with a few approximately 5cm thick, parallel laminated, fine-grained sandstone to mudstone partings, very coaly, local spheroidal weathering.
113									- - -	30				
114									(S) -					
115														
116									(S) -					
117														
118									(S) -					
119														-same homogeneous medium-grained sandstone, very little visible bedding structures other than partings defined by weathering. Some parallel lamination intermittently visible, and some mottling by bioturbation, suggestive of "Lam-Scram".
120									- - - -					
121									- - -					
122														
123									- - - -					-sample 73e
124										30				-medium-grained sandstone unchanged from below.

## COMOX FORMATION



## Section: PDJ-03-MS012 (Brethour Island 2)

## COMOX FORMATION





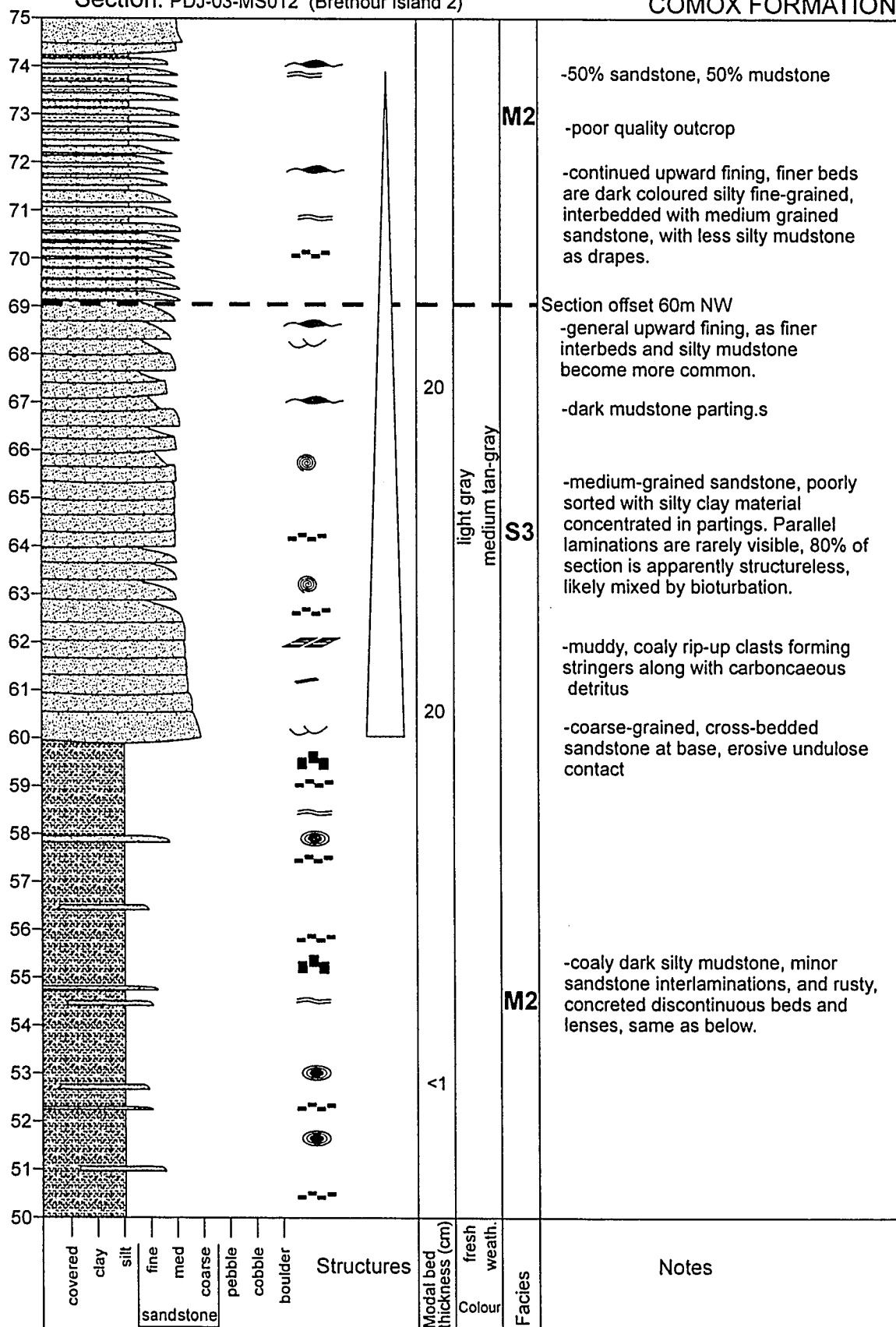
## Section: PDJ-03-MS012 (Brethour Island 2)

## COMOX FORMATION

50	covered clay silt fine med coarse pebble cobble boulder sandstone	Structures	Modal bed thickness (cm) fresh weath. Colour	Facies	Notes
25					
26			<1	M2	-dark silty mudstone, some thin, concreted rusty sandstone beds and lenses, discontinuous. Abundant coaly material, fragments and rootlets.
27					
28				M2	-hints of thin laminations, but marker beds show bedding disturbed by dewatering, bioturbation, and loading.
29					
30				dark gray, black coal peices medium brown-gray, rusty tan concretions	-nature of contact unclear, lowest medium-grained sandstone is concreted and bioturbated.
31					
32					
33					
34				light gray medium tan-gray	-sample 74a -well sorted, medium-grained sandstone, abundant leaf fossils in several beds, along with coaly detritus and muddy rip-up clasts
35					
36			40		-sample 74c -same dark silty mudstone as below, including abundant coaly material, root masses and several small stumps in apparent life position.
37					
38				light gray medium tan-gray	-sample 74c
39					
40				medium brown-gray, rusty tan concretions	-coaly dark silty mudstone, minor sandstone interlamations, and rusty, concreted discontinuous beds and lenses, same as below.
41					
42				medium brown-gray, rusty tan concretions	M2
43					
44				dark gray, black coal peices medium brown-gray, rusty tan concretions	M2
45					
46				1	
47					
48					
49					
50					

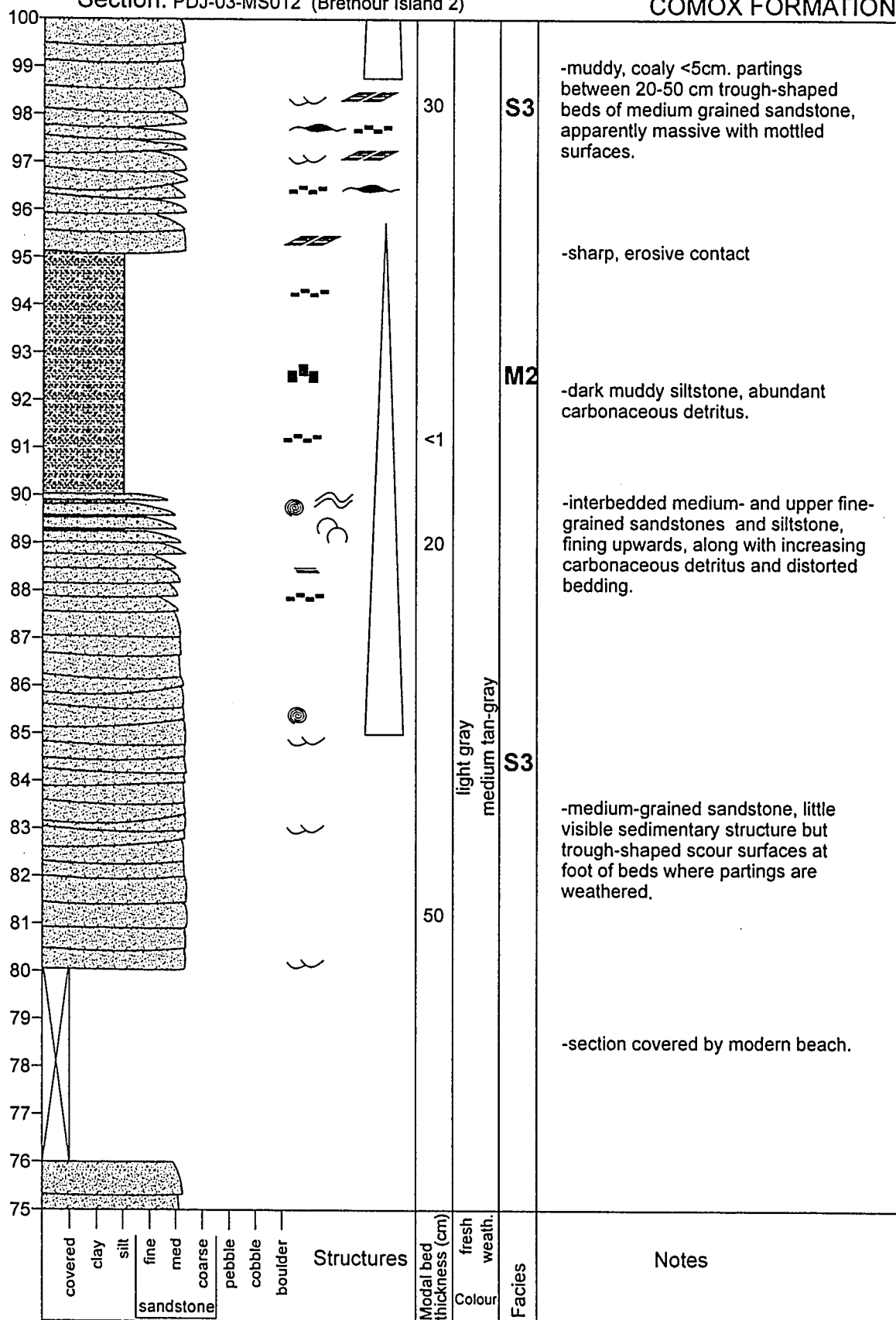
## Section: PDJ-03-MS012 (Brethour Island 2)

## COMOX FORMATION



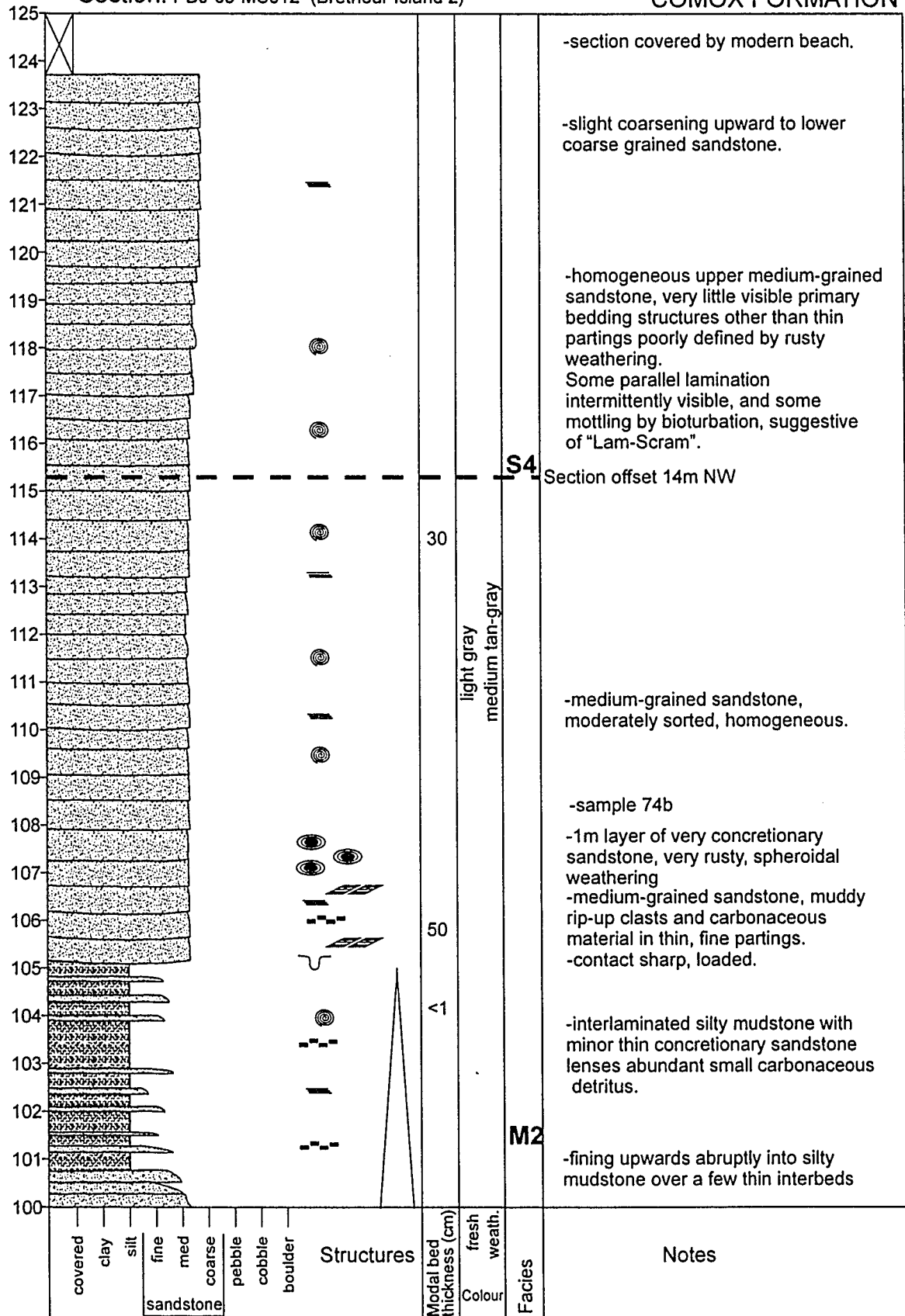
## Section: PDJ-03-MS012 (Brethour Island 2)

## COMOX FORMATION



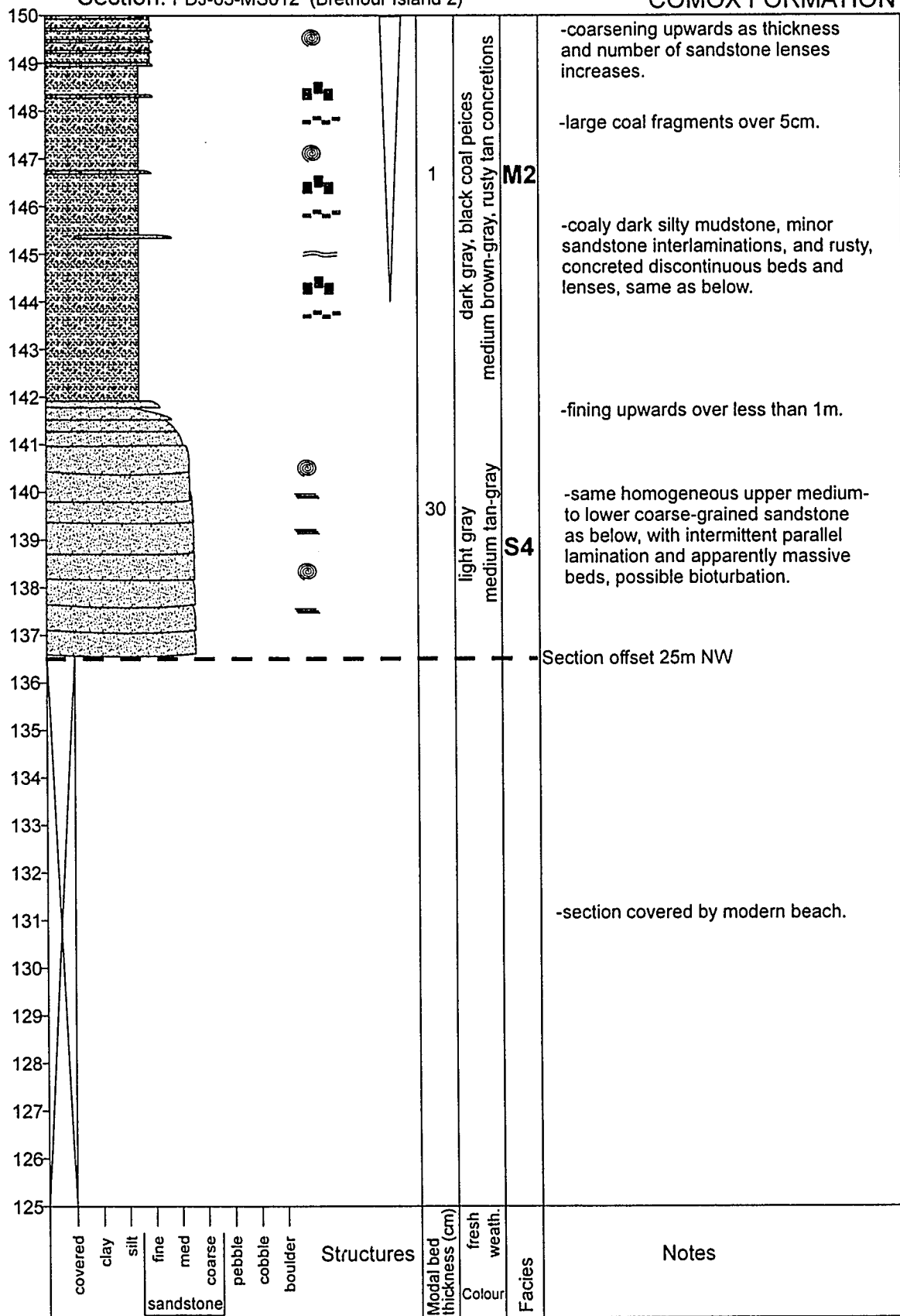
## Section: PDJ-03-MS012 (Brethour Island 2)

## COMOX FORMATION



## Section: PDJ-03-MS012 (Brethour Island 2)

## COMOX FORMATION



## COMOX FORMATION



## Appendix B: Structural Data.

A total of 3130 structural measurements were collected from the field area. The data were collected using a Brunton compass, with planar data recorded as strike and dip. Right hand rule was used where strike azimuth is 90 degrees counter clockwise from dip direction. Location coordinates were digitized at stations, with station locations recorded from GPS data. Actual measurement locations were then adjusted relative to stations using GIS software, field and digital maps, and UTM locations assigned to structural data.

Stereonets were produced digitally for various populations of data, separated by data type and structural domain. Data density was contoured using a Gaussian counting method with  $K=100$ , with contours drawn at values of  $2^2 \times$  the standard deviation ( $\sigma$ ) from the expected value ( $E$ ). Trends were further identified by principal direction analysis and production of eigenvalues (Cheeney, 1983). The relationship of the three eigenvalues to the interpreted trend is described in Table B1.

**Table B 1: Trends observed as eigenvalues.**

<b>Population Trend</b>	<b>Eigenvalues</b>
uniform	$\tau_1 = \tau_2 = \tau_3$
cluster	$\tau_1 = \tau_2 < \tau_3$
girdle	$\tau_1 < \tau_2 = \tau_3$

**Table B 2: Bedding measurements by domain, with eigenvalues.**

Bedding		Principal Plane		Eigenvalues			Eigenvalues / N		
Domain	N	Strike	Dip	$\tau_3$	$\tau_2$	$\tau_1$	$\tau_3/N$	$\tau_2/N$	$\tau_1/N$
All Data	1482	290	53	1000	344	133	0.67	0.23	0.09
Domville	174	310	65	149	19.0	5.93	0.86	0.11	0.03
Forrest	78	304	73	75.3	1.84	0.816	0.97	0.02	0.01
Gooch	104	97	64	99.1	3.90	1.04	0.95	0.04	0.01
Moresby	54	288	17	52.3	1.22	0.475	0.97	0.02	0.01
N Coal	85	282	70	76.7	5.69	2.64	0.90	0.07	0.03
Piers	127	290	65	94.5	24.9	7.67	0.74	0.20	0.06
Portland	217	340	10	161	50.2	5.20	0.74	0.23	0.02
Russell	21	278	15	20.7	0.285	0.0476	0.99	0.01	0.00
Sidney	118	305	55	113	3.60	1.67	0.96	0.03	0.01
Tsehum	276	272	53	231	31.2	13.7	0.84	0.11	0.05
W Saanich	228	268	44	171	34.3	22.5	0.75	0.15	0.10

**Table B 3: Brittle structure measurements by domain, with eigenvalues.**

Brittle Structure		Principal Plane		Eigenvalues			Eigenvalues / N		
Domain	N	Strike	Dip	$\tau_3$	$\tau_2$	$\tau_1$	$\tau_3/N$	$\tau_2/N$	$\tau_1/N$
All Data	1082	31	89	691	217	175	0.64	0.20	0.16
Domville	125	224	77	77.1	28.6	19.3	0.62	0.23	0.15
Forrest	202	37	82	143	43.3	15.6	0.71	0.21	0.08
Gooch	62	353	82	31.2	21.1	9.57	0.50	0.34	0.15
Moresby	35	215	86	24.0	8.41	2.60	0.69	0.24	0.07
N Coal	84	22	87	52.9	17.7	13.4	0.63	0.21	0.16
Piers	69	205	81	31.1	23.8	14.1	0.45	0.34	0.20
Portland	87	237	85	58.7	19.3	9.01	0.67	0.22	0.10
Russell	47	23	86	36.0	7.97	3.04	0.77	0.17	0.06
Sidney	136	222	86	99.1	23.2	13.7	0.73	0.17	0.10
Tsehum	174	17	83	139	21.3	13.2	0.80	0.12	0.08
W Saanich	61	13	76	37.4	17.1	6.49	0.61	0.28	0.11



Table B 4 : Bedding Data.

Domain	Northing	Easting	OT?	Strike	Dip		Domain	Northing	Easting	OT?	Strike	Dip
Domville	5391761	475023		280	29		Domville	5391325	475981		101	90
Domville	5391761	475023		305	36		Domville	5391330	475983		090	75
Domville	5391761	475023		290	38		Domville	5391335	476000		300	71
Domville	5391761	475023		291	45		Domville	5391335	476000		308	74
Domville	5391761	475023		280	46		Domville	5391335	476000		300	76
Domville	5391761	475023		284	47		Domville	5391333	476029		311	68
Domville	5391761	475023		265	51		Domville	5391333	476029		311	68
Domville	5391761	475023		282	51		Domville	5391341	476035		303	69
Domville	5393584	475523		280	81		Domville	5391341	476035		302	72
Domville	5393584	475523		277	83		Domville	5391341	476035		304	72
Domville	5393584	475523	OT	095	89		Domville	5391341	476035		306	75
Domville	5392451	475725		315	35		Domville	5391341	476035		299	77
Domville	5392451	475725		322	41		Domville	5391358	476042		300	64
Domville	5391572	475746		305	49		Domville	5391358	476042		299	67
Domville	5391572	475746		303	59		Domville	5391358	476042		301	67
Domville	5391491	475765		291	51		Domville	5391358	476042		298	76
Domville	5391491	475765		298	53		Domville	5391365	476043		305	75
Domville	5391491	475765		293	58		Domville	5390995	476129		320	62
Domville	5391491	475765		287	63		Domville	5390995	476129		320	66
Domville	5391491	475765		285	65		Domville	5390995	476129		309	71
Domville	5391491	475765		287	68		Domville	5391855	476150		318	64
Domville	5392251	475766		001	35		Domville	5391906	476175		317	58
Domville	5392251	475766		344	36		Domville	5391906	476175		318	60
Domville	5392251	475766		335	40		Domville	5391857	476182		311	60
Domville	5392251	475766		340	50		Domville	5391857	476182		304	64
Domville	5392251	475766		350	50		Domville	5390984	476194		334	48
Domville	5391352	475851		340	85		Domville	5390984	476194		330	50
Domville	5391353	475854		284	68		Domville	5390984	476194		328	58
Domville	5391353	475854		284	68		Domville	5391883	476198		312	66
Domville	5391353	475854		291	70		Domville	5391883	476198		312	67
Domville	5391353	475854		289	74		Domville	5391883	476198		309	74
Domville	5391350	475868		315	25		Domville	5391666	476256		305	74
Domville	5391350	475868		036	28		Domville	5391666	476256		305	79
Domville	5391350	475868		040	29		Domville	5391623	476274		291	70
Domville	5391350	475868		326	42		Domville	5391582	476320		308	70
Domville	5391350	475868		344	60		Domville	5391582	476320		308	71
Domville	5391342	475883		310	84		Domville	5391582	476320		305	73
Domville	5391342	475883		311	84		Domville	5390816	476341		330	60
Domville	5391342	475883		315	84		Domville	5390816	476341		334	60
Domville	5391342	475883		310	85		Domville	5390816	476341		328	62
Domville	5391342	475883		295	90		Domville	5391562	476416		310	69
Domville	5391342	475883	OT	125	88		Domville	5391198	476438		311	56
Domville	5391342	475883	OT	131	86		Domville	5391198	476438		308	62
Domville	5391342	475883	OT	131	85		Domville	5391198	476438		320	65
Domville	5391342	475884		304	85		Domville	5391198	476438		321	69
Domville	5391501	475907		318	51		Domville	5391198	476438		340	72
Domville	5391501	475907		310	58		Domville	5391198	476438		310	74
Domville	5391501	475907		302	68		Domville	5391198	476438		324	77
Domville	5391501	475907		308	80		Domville	5391198	476438		334	83
Domville	5391310	475958		101	79		Domville	5391198	476438		318	84

Table B 4 : Bedding Data.

Domain	Northing	Easting	OT?	Strike	Dip		Domain	Northing	Easting	OT?	Strike	Dip
Domville	5391310	475958		102	81		Domville	5390649	476439		332	49
Domville	5391310	475958		099	86		Domville	5390649	476439		329	54
Domville	5391310	475958		100	86		Domville	5390649	476439		320	59
Domville	5391310	475958		286	90		Domville	5391506	476495		314	72
Domville	5391288	475959		101	76		Domville	5391409	476631		310	75
Domville	5391288	475959		090	77		Domville	5391414	476634		310	75
Domville	5391288	475959		093	82		Domville	5390535	476635		335	39
Domville	5391331	475976		294	77		Domville	5390535	476635		340	41
Domville	5391331	475976		291	79		Domville	5390535	476635		331	44
Domville	5391331	475976		296	83		Domville	5390535	476635		321	55
Domville	5391331	475976		104	84		Domville	5390535	476635		324	56
Domville	5391331	475976		102	87		Domville	5390535	476635		320	57
Domville	5391331	475976		105	89		Domville	5390535	476635		316	58
Domville	5391318	475977	OT	104	85		Domville	5390535	476635		329	58
Domville	5390535	476635		323	59		Forrest	5391058	473670		292	74
Domville	5390535	476635		326	59		Forrest	5391058	473670		292	81
Domville	5390535	476635		320	61		Forrest	5390875	473703		309	48
Domville	5390535	476635		324	61		Forrest	5390875	473703		308	58
Domville	5390535	476635		320	63		Forrest	5390875	473703		305	59
Domville	5390535	476635		323	63		Forrest	5390977	473717		300	78
Domville	5390535	476635		318	65		Forrest	5390990	473720		305	89
Domville	5391404	476637		300	75		Forrest	5390066	474925		318	85
Domville	5391404	476637		305	80		Forrest	5389928	474978		306	84
Domville	5391411	476642		305	80		Forrest	5390012	474992		305	70
Domville	5390526	476668		320	60		Forrest	5390012	474992		304	75
Domville	5391773	476707		320	64		Forrest	5390012	474992		311	77
Domville	5391773	476707		310	66		Forrest	5390003	475039		309	74
Domville	5391773	476707		322	66		Forrest	5390003	475039		299	86
Domville	5391773	476707		319	72		Forrest	5390358	475084		305	85
Domville	5391484	476729		308	60		Forrest	5390352	475090		305	85
Domville	5391484	476729		306	66		Forrest	5390324	475099		305	85
Domville	5391484	476729		306	66		Forrest	5389977	475133		312	65
Domville	5391484	476729		314	69		Forrest	5389977	475133		315	72
Domville	5391484	476729		308	70		Forrest	5389940	475228		310	78
Domville	5391503	476731		315	65		Forrest	5390237	475237		306	83
Domville	5391503	476731		315	70		Forrest	5390237	475237		304	85
Domville	5391588	476745		310	68		Forrest	5390237	475237		305	85
Domville	5391588	476745		314	68		Forrest	5390237	475237		306	86
Domville	5391588	476745		318	69		Forrest	5390118	475339		310	89
Domville	5391588	476745		311	70		Forrest	5390118	475339		315	89
Domville	5390449	476758		304	55		Forrest	5390147	475352		315	89
Domville	5390449	476758		304	60		Forrest	5389915	475490		319	67
Domville	5390449	476758		308	61		Forrest	5389915	475490		310	70
Domville	5390557	476806		340	47		Forrest	5389915	475490		311	71
Domville	5390557	476806		348	54		Forrest	5390100	475611		313	67
Domville	5390557	476806		335	56		Forrest	5390025	475661		304	73
Domville	5390557	476806		345	62		Forrest	5390025	475661		305	76
Domville	5390357	476833		322	51		Forrest	5390025	475661		310	85
Domville	5390357	476833		325	55		Forrest	5389564	475728		305	65
Domville	5390357	476833		324	56		Forrest	5389564	475728		307	68

Table B 4 : Bedding Data.

Domain	Northing	Easting	OT?	Strike	Dip		Domain	Northing	Easting	OT?	Strike	Dip
Domville	5390308	476892		320	50		Forrest	5389564	475728		310	69
Domville	5390308	476892		304	60		Forrest	5389564	475728		305	70
Domville	5390308	476892		319	62		Forrest	5389564	475728		305	72
Domville	5391510	476940		316	61		Forrest	5389564	475728		304	73
Domville	5391510	476940		313	66		Forrest	5389564	475728		304	73
Domville	5391510	476940		320	66		Forrest	5389640	475788		306	73
Domville	5390423	476969		330	55		Forrest	5389640	475788		305	76
Domville	5390423	476969		312	62		Forrest	5389640	475788		304	79
Domville	5390423	476969		315	66		Forrest	5389640	475788		300	80
Domville	5390298	477033		330	65		Forrest	5389361	475849		306	74
Forrest	5391474	473232		310	60		Forrest	5389400	475889		296	74
Forrest	5391474	473232		315	60		Forrest	5389300	476010		290	70
Forrest	5391474	473232		290	75		Forrest	5389300	476010		295	59
Forrest	5391009	473234		295	74		Forrest	5389300	476010		316	62
Forrest	5391009	473234		296	74		Forrest	5389300	476010		301	69
Forrest	5391009	473234		299	74		Forrest	5389300	476010		305	69
Forrest	5391009	473234		301	76		Forrest	5389300	476010		301	70
Forrest	5391009	473234		301	78		Forrest	5389300	476010		300	72
Forrest	5390999	473268		304	64		Forrest	5389156	476175		301	59
Forrest	5390999	473268		295	70		Forrest	5389156	476175		302	59
Forrest	5391081	473620		300	80		Forrest	5389156	476175		302	59
Forrest	5391073	473633		299	80		Forrest	5389156	476175		306	59
Forrest	5391014	473640		299	74		Forrest	5389156	476175		303	64
Forrest	5391014	473640		298	76		Forrest	5389156	476175		303	64
Forrest	5391014	473640		298	78		Gooch	5390842	477815	OT	100	76
Forrest	5391018	473646		298	80		Gooch	5390842	477815	OT	110	75
Forrest	5391003	473646		300	80		Gooch	5389407	477829	OT	104	77
Forrest	5391058	473670		306	68		Gooch	5389407	477829	OT	094	58
Gooch	5389953	477834	OT	096	46		Gooch	5389889	479345	OT	100	60
Gooch	5390042	477859	OT	090	60		Gooch	5389889	479345	OT	100	60
Gooch	5390042	477859	OT	079	52		Gooch	5389889	479345	OT	100	60
Gooch	5390789	477912	OT	099	78		Gooch	5389889	479345	OT	100	60
Gooch	5390789	477912	OT	103	77		Gooch	5389889	479345	OT	100	60
Gooch	5390789	477912	OT	099	75		Gooch	5389889	479345	OT	100	60
Gooch	5390789	477912	OT	094	74		Gooch	5389889	479345	OT	100	60
Gooch	5390789	477912	OT	093	72		Gooch	5389889	479345	OT	100	60
Gooch	5390789	477912	OT	105	70		Gooch	5389889	479345	OT	100	60
Gooch	5390789	477912	OT	102	69		Gooch	5389889	479345	OT	100	60
Gooch	5390225	477964	OT	096	60		Gooch	5389889	479345	OT	100	60
Gooch	5390225	477964	OT	095	50		Gooch	5389889	479345	OT	100	60
Gooch	5390299	478028	OT	094	63		Gooch	5389889	479345	OT	100	60
Gooch	5390299	478028	OT	092	62		Gooch	5389889	479345	OT	100	60
Gooch	5390696	478084	OT	094	70		Gooch	5389889	479345	OT	100	60
Gooch	5390696	478084	OT	099	70		Gooch	5389889	479345	OT	100	60
Gooch	5390696	478084	OT	100	65		Gooch	5389889	479345	OT	100	60
Gooch	5390866	478085		284	86		Gooch	5389889	479345	OT	100	60
Gooch	5390866	478085		283	89		Gooch	5389889	479345	OT	100	60
Gooch	5390866	478085		281	90		Gooch	5389889	479345	OT	100	60
Gooch	5390866	478085	OT	102	85		Gooch	5389889	479345	OT	100	60
Gooch	5390866	478085	OT	090	76		Gooch	5389889	479345	OT	100	60

Table B 4 : Bedding Data.

Domain	Northing	Easting	OT?	Strike	Dip		Domain	Northing	Easting	OT?	Strike	Dip
Gooch	5390837	478117	OT	100	70		Gooch	5389889	479345	OT	100	60
Gooch	5390263	478170	OT	091	54		Gooch	5389889	479345	OT	100	60
Gooch	5390263	478170	OT	086	52		Gooch	5389889	479345	OT	100	60
Gooch	5390263	478170	OT	091	49		Gooch	5389889	479345	OT	100	60
Gooch	5389920	478188	OT	098	78		Gooch	5389889	479345	OT	100	60
Gooch	5389920	478188	OT	085	75		Gooch	5389889	479345	OT	100	60
Gooch	5389920	478188	OT	094	63		Gooch	5389889	479345	OT	100	60
Gooch	5389920	478188	OT	089	58		Gooch	5389889	479345	OT	100	60
Gooch	5389921	478189	OT	093	62		Gooch	5389889	479345	OT	100	60
Gooch	5390662	478231	OT	105	75		Gooch	5389889	479345	OT	100	60
Gooch	5390707	478283	OT	110	77		Gooch	5389889	479345	OT	100	60
Gooch	5390707	478283	OT	114	75		Gooch	5389889	479345	OT	100	60
Gooch	5390707	478283	OT	112	74		Gooch	5389889	479345	OT	100	60
Gooch	5390707	478283	OT	111	71		Gooch	5389889	479345	OT	100	60
Gooch	5390707	478283	OT	113	67		Gooch	5389889	479345	OT	100	60
Gooch	5390810	478289	OT	105	71		Gooch	5389889	479345	OT	100	60
Gooch	5390810	478289	OT	106	70		Gooch	5389889	479345	OT	100	60
Gooch	5390810	478289	OT	105	65		Gooch	5389889	479345	OT	100	60
Gooch	5390240	478357	OT	092	81		Gooch	5389889	479345	OT	100	60
Gooch	5390240	478357	OT	105	60		Gooch	5389889	479345	OT	100	60
Gooch	5390240	478357	OT	110	58		Gooch	5389889	479345	OT	100	60
Gooch	5389927	478491	OT	096	69		Gooch	5389889	479345	OT	100	60
Gooch	5389927	478491	OT	092	66		Gooch	5389889	479345	OT	100	60
Gooch	5389927	478491	OT	094	65		Gooch	5389889	479345	OT	100	60
Gooch	5389927	478491	OT	101	61		Gooch	5389889	479345	OT	100	60
Gooch	5390255	478674	OT	091	74		Gooch	5389889	479345	OT	100	60
Gooch	5390255	478674	OT	098	65		Gooch	5389889	479345	OT	100	60
Gooch	5390255	478674	OT	090	62		Gooch	5389889	479345	OT	100	60
Gooch	5390297	478680	OT	101	64		Gooch	5389889	479345	OT	100	60
Gooch	5390297	478680	OT	089	50		Gooch	5389889	479345	OT	100	60
Gooch	5389897	478916	OT	102	71		Gooch	5389889	479345	OT	100	60
Gooch	5389897	478916	OT	100	65		Gooch	5389889	479345	OT	100	60
Gooch	5390162	478946	OT	104	68		Gooch	5389889	479345	OT	100	60
Gooch	5390107	479117	OT	095	65		Gooch	5389889	479345	OT	100	60
Gooch	5390107	479117	OT	091	56		Gooch	5389889	479345	OT	100	60
Gooch	5390107	479117	OT	094	56		Gooch	5389889	479345	OT	100	60
Gooch	5390107	479117	OT	098	55		Gooch	5389889	479345	OT	100	60
Gooch	5390033	479289	OT	085	40		Gooch	5389889	479345	OT	100	60
Gooch	5390007	479309	OT	091	61		Gooch	5389889	479345	OT	100	60
Gooch	5390007	479309	OT	092	60		Gooch	5389889	479345	OT	100	60
Gooch	5390007	479309	OT	094	60		Gooch	5389889	479345	OT	100	60
Gooch	5389928	479333	OT	100	60		Gooch	5389889	479345	OT	100	60
Moresby	5397675	476538		278	21		N Coal	5393051	472038		270	80
Moresby	5397675	476538		265	24		N Coal	5393041	472218		270	82
Moresby	5397675	476538		281	24		N Coal	5393041	472218		269	86
Moresby	5397675	476538		275	26		N Coal	5393041	472218		273	86
Moresby	5397675	476538		280	28		N Coal	5391884	472560		280	80
Moresby	5397675	476538		277	34		N Coal	5392922	472567		286	76
Moresby	5397684	476768		284	22		N Coal	5392922	472567		288	77
Moresby	5397684	476768		299	28		N Coal	5392922	472567		292	80

Table B 4 : Bedding Data.

Domain	Northing	Easting	OT?	Strike	Dip		Domain	Northing	Easting	OT?	Strike	Dip
Moresby	5397232	477461		329	17		N Coal	5392891	472604		282	71
Moresby	5397232	477461		350	17		N Coal	5392891	472604		284	72
Moresby	5397232	477461		330	18		N Coal	5392891	472604		282	73
Moresby	5397141	477498		010	18		N Coal	5392891	472604		285	75
Moresby	5397110	477546		005	21		N Coal	5392891	472604		287	83
Moresby	5397078	477563		355	14		N Coal	5392125	472639		128	46
Moresby	5396760	477578		298	13		N Coal	5392125	472639		122	53
Moresby	5396760	477578		301	13		N Coal	5392130	472643		235	14
Moresby	5396760	477578		319	13		N Coal	5392130	472643		221	19
Moresby	5396760	477578		312	15		N Coal	5392130	472643		281	21
Moresby	5396702	477733		310	14		N Coal	5392137	472644		325	45
Moresby	5396702	477733		318	17		N Coal	5392146	472646		285	45
Moresby	5396702	477733		340	20		N Coal	5392146	472646		303	56
Moresby	5396631	477795		295	17		N Coal	5392146	472646		315	65
Moresby	5396631	477795		300	19		N Coal	5392253	472730		290	58
Moresby	5396397	477866		300	28		N Coal	5392253	472730		291	59
Moresby	5396501	477931		310	14		N Coal	5392253	472730		285	60
Moresby	5396501	477931		288	20		N Coal	5392253	472730		288	62
N Coal	5393135	471457		274	60		N Coal	5392766	472903		284	76
N Coal	5393135	471457		264	61		N Coal	5392764	472905		293	69
N Coal	5393135	471457		262	68		N Coal	5392766	472905		300	72
N Coal	5393135	471457		266	70		N Coal	5392750	472926		273	82
N Coal	5393196	471476		273	70		N Coal	5392750	472927		278	84
N Coal	5393196	471476		270	73		N Coal	5392749	472927		282	85
N Coal	5393196	471476		275	74		N Coal	5392290	472941		293	61
N Coal	5393196	471476		270	75		N Coal	5392290	472941		292	62
N Coal	5393189	471535		282	71		N Coal	5392290	472941		292	66
N Coal	5393189	471535		275	75		N Coal	5392739	472955		285	71
N Coal	5393189	471535		283	75		N Coal	5392394	472993		310	47
N Coal	5393189	471535		284	75		N Coal	5392394	472993		307	48
N Coal	5393189	471535		275	76		N Coal	5392394	472993		296	56
N Coal	5393189	471535		275	78		N Coal	5392662	473047		288	66
N Coal	5393189	471535		276	78		N Coal	5392662	473047		285	67
N Coal	5393189	471535		277	79		N Coal	5392662	473047		285	70
N Coal	5393189	471535		274	80		N Coal	5392662	473047		285	71
N Coal	5392949	471698		270	58		N Coal	5392662	473047		285	82
N Coal	5392949	471698		262	60		N Coal	5392452	473084		290	65
N Coal	5392949	471698		272	62		N Coal	5392452	473084		286	69
N Coal	5392949	471698		270	74		N Coal	5392611	473159		284	72
N Coal	5393108	471808		302	54		Piers	5394880	467991		250	80
N Coal	5393108	471808		280	69		Piers	5394444	468676		291	57
N Coal	5393108	471808		298	69		Piers	5394444	468676		290	59
N Coal	5393108	471808		296	70		Piers	5394444	468676		290	64
N Coal	5393108	471808		295	73		Piers	5394770	468737		106	80
N Coal	5393108	471808		279	81		Piers	5394486	468750		295	60
N Coal	5393108	471808		279	84		Piers	5394486	468750		295	60
N Coal	5393107	471823		281	69		Piers	5394486	468750		295	62
N Coal	5393107	471823		282	70		Piers	5394698	468762		331	45
N Coal	5393108	471853		275	74		Piers	5394698	468762		334	46
N Coal	5393108	471853		275	75		Piers	5394698	468762		325	49

Table B 4 : Bedding Data.

Domain	Northing	Easting	OT?	Strike	Dip		Domain	Northing	Easting	OT?	Strike	Dip
N Coal	5393108	471853		273	76		Piers	5394698	468762		331	49
N Coal	5393107	471884		276	71		Piers	5394698	468762		052	71
N Coal	5393107	471884		274	74		Piers	5394698	468762		060	72
N Coal	5393107	471884		273	75		Piers	5394698	468762		051	73
N Coal	5393107	471884		275	77		Piers	5394698	468762		054	75
N Coal	5393051	472038		272	77		Piers	5394987	468815		324	75
Piers	5395077	468981		335	39		Piers	5394517	470030		308	70
Piers	5395077	468981		334	50		Piers	5394517	470030		315	80
Piers	5394273	469029		293	52		Piers	5394884	470087		110	25
Piers	5394273	469029		295	55		Piers	5394884	470087		093	26
Piers	5394273	469029		296	58		Piers	5394884	470087		102	36
Piers	5395259	469316		265	75		Piers	5394324	470141		301	85
Piers	5395259	469316		264	78		Piers	5394324	470141		299	86
Piers	5394200	469332		275	53		Piers	5394324	470141		120	90
Piers	5394200	469332		279	55		Piers	5394379	470162		310	75
Piers	5394200	469332		281	55		Piers	5394379	470162		305	85
Piers	5394200	469332		280	57		Piers	5394153	470523		045	55
Piers	5395267	469397		274	73		Piers	5394178	470524		302	51
Piers	5395267	469397		275	78		Piers	5394162	470524		288	63
Piers	5394213	469502		284	50		Piers	5394162	470524		290	74
Piers	5394213	469502		290	50		Piers	5394162	470524		288	75
Piers	5394213	469502		286	51		Piers	5394178	470524		005	87
Piers	5394213	469502		301	53		Piers	5394138	470543		289	71
Piers	5394264	469548		296	53		Piers	5394138	470543		287	76
Piers	5394264	469548		305	55		Piers	5394138	470543		290	76
Piers	5395263	469624		275	85		Piers	5394211	470557		035	65
Piers	5395263	469624		277	85		Piers	5394211	470557		030	73
Piers	5395263	469624		279	89		Piers	5394251	470562		290	60
Piers	5395170	469660		279	82		Piers	5394251	470562		290	68
Piers	5395170	469660		280	83		Piers	5393882	470594		284	73
Piers	5395170	469660		281	84		Piers	5393882	470594		285	75
Piers	5395170	469660		283	86		Piers	5393882	470594		285	75
Piers	5394353	469680		295	19		Piers	5393882	470594		286	75
Piers	5394353	469680		298	19		Piers	5393794	470605		282	74
Piers	5394353	469680		321	20		Piers	5394151	470762		280	45
Piers	5394353	469680		340	21		Piers	5394151	470762		280	45
Piers	5394302	469742		345	38		Piers	5394151	470762		304	45
Piers	5394302	469742		349	38		Piers	5393965	470796		281	70
Piers	5394302	469742		006	40		Piers	5393965	470796		284	75
Piers	5394302	469742		342	43		Piers	5393965	470796		280	78
Piers	5394302	469742		009	46		Piers	5394354	470798		320	68
Piers	5394302	469742		018	48		Piers	5393783	470871		282	65
Piers	5394302	469742		009	50		Piers	5393783	470871		291	75
Piers	5394302	469742		345	51		Piers	5393895	470904		280	80
Piers	5394302	469742		271	61		Piers	5394286	470908		265	68
Piers	5394302	469742		267	62		Piers	5394286	470908		278	70
Piers	5394302	469742		268	64		Piers	5394286	470908		265	73
Piers	5394302	469742		269	64		Piers	5394336	471299		289	87
Piers	5394302	469742		267	66		Piers	5394336	471299		289	88
Piers	5394302	469742		244	85		Piers	5394336	471299		290	89

Table B 4 : Bedding Data.

Domain	Northing	Easting	OT?	Strike	Dip		Domain	Northing	Easting	OT?	Strike	Dip
Piers	5394302	469742		244	85		Piers	5393988	471405		095	89
Piers	5394302	469742		246	86		Piers	5393988	471405		095	89
Piers	5394302	469742		248	88		Portland	5396248	471515		180	04
Piers	5394794	469850		310	85		Portland	5396248	471515		170	06
Piers	5394243	469894		283	57		Portland	5396248	471515		160	07
Piers	5394243	469894		280	60		Portland	5397006	471556		276	38
Piers	5394243	469894		288	65		Portland	5397006	471556		285	44
Piers	5394243	469894		280	75		Portland	5397006	471556		300	69
Piers	5394298	469927		306	52		Portland	5396469	471556		179	06
Piers	5394298	469927		296	53		Portland	5396469	471556		177	07
Piers	5394298	469927		297	54		Portland	5396469	471556		175	09
Piers	5394298	469927		297	65		Portland	5396455	471636		259	05
Piers	5394613	469981		296	49		Portland	5396455	471636		267	08
Piers	5394613	469981		295	54		Portland	5396455	471636		284	08
Piers	5394613	469981		288	57		Portland	5396373	471642		244	08
Piers	5394437	469992		315	59		Portland	5396096	471644		152	09
Piers	5394437	469992		335	78		Portland	5396096	471644		140	10
Piers	5394437	469992		330	80		Portland	5396096	471644		167	10
Piers	5394517	470030		306	50		Portland	5396096	471644		152	12
Piers	5394517	470030		300	58		Portland	5396096	471644		129	16
Portland	5396397	471647		230	10		Portland	5398068	472853		316	53
Portland	5396397	471647		229	11		Portland	5395941	472859		054	19
Portland	5396213	471667		116	06		Portland	5395941	472859		070	20
Portland	5396213	471667		124	14		Portland	5395941	472859		052	24
Portland	5396213	471667		124	15		Portland	5395941	472859		070	25
Portland	5396137	471671		137	07		Portland	5396203	472904		354	16
Portland	5396137	471671		140	12		Portland	5396203	472904		339	19
Portland	5396137	471671		156	13		Portland	5396203	472904		347	23
Portland	5397121	471739		298	53		Portland	5396469	472909		021	05
Portland	5397121	471739		302	54		Portland	5396469	472909		045	05
Portland	5397121	471739		295	55		Portland	5396469	472909		046	08
Portland	5396293	471973		125	25		Portland	5396469	472909		024	09
Portland	5398105	472279		210	20		Portland	5396275	472912		017	11
Portland	5398034	472286		221	08		Portland	5396243	472915		350	20
Portland	5398034	472286		215	10		Portland	5396317	472918		008	16
Portland	5398034	472286		215	10		Portland	5396317	472918		003	19
Portland	5398210	472331		311	29		Portland	5396317	472918		001	22
Portland	5398210	472331		314	29		Portland	5395996	472926		060	20
Portland	5398210	472331		309	31		Portland	5395996	472926		085	21
Portland	5398210	472331		304	36		Portland	5395996	472926		072	24
Portland	5398210	472331		316	36		Portland	5396181	472932		341	26
Portland	5398058	472390		211	11		Portland	5396189	472932		001	29
Portland	5398058	472390		202	12		Portland	5396195	472935		049	31
Portland	5398058	472390		212	12		Portland	5396171	472937		338	26
Portland	5398058	472390		215	12		Portland	5396366	472941		356	09
Portland	5398088	472440		270	22		Portland	5396366	472941		022	17
Portland	5398126	472487		290	10		Portland	5396217	472946		345	17
Portland	5398126	472487		252	14		Portland	5396217	472946		324	20
Portland	5398126	472487		271	19		Portland	5396217	472946		346	20
Portland	5396131	472505	OT	309	86		Portland	5396217	472946		331	22

Table B 4 : Bedding Data.

Domain	Northing	Easting	OT?	Strike	Dip		Domain	Northing	Easting	OT?	Strike	Dip
Portland	5396131	472505	OT	305	82		Portland	5398008	472969		322	53
Portland	5396131	472505	OT	306	79		Portland	5398008	472969		326	56
Portland	5395837	472511		071	12		Portland	5398008	472969		320	61
Portland	5395837	472511		081	13		Portland	5396439	472970		038	06
Portland	5395837	472511		089	13		Portland	5396439	472970		020	07
Portland	5395837	472511		060	14		Portland	5396439	472970		019	12
Portland	5395837	472511		092	14		Portland	5396439	472970		040	12
Portland	5395837	472511		081	15		Portland	5396436	472998		019	05
Portland	5398195	472516		304	40		Portland	5396436	472998		030	09
Portland	5398195	472516		301	41		Portland	5396199	473001		008	11
Portland	5398169	472524		292	35		Portland	5396276	473001		023	16
Portland	5398169	472524		305	35		Portland	5396276	473001		002	18
Portland	5395911	472531		071	17		Portland	5396276	473001		024	18
Portland	5395911	472531		076	17		Portland	5396276	473001		024	19
Portland	5395911	472531		090	18		Portland	5396276	473001		024	20
Portland	5395911	472531		060	25		Portland	5396276	473001		025	21
Portland	5395932	472561		070	15		Portland	5396199	473001		008	26
Portland	5395932	472561		074	17		Portland	5398049	473050		310	10
Portland	5395889	472654		069	20		Portland	5396354	473064		080	09
Portland	5395889	472654		066	21		Portland	5396354	473064		070	18
Portland	5395889	472654		065	23		Portland	5397895	473069		320	60
Portland	5398107	472726		313	46		Portland	5397862	473083		310	63
Portland	5398107	472726		314	46		Portland	5397862	473083		302	64
Portland	5398107	472726		316	48		Portland	5397862	473083		297	66
Portland	5398051	472750		304	41		Portland	5397862	473083		312	68
Portland	5398051	472750		315	58		Portland	5397862	473083		296	69
Portland	5398051	472750		315	60		Portland	5397862	473083		299	72
Portland	5398017	472780		285	64		Portland	5397862	473083		308	72
Portland	5397999	472786		320	60		Portland	5397862	473083		300	77
Portland	5397929	472809		295	56		Portland	5398010	473091		308	05
Portland	5397929	472809		305	59		Portland	5398010	473091		313	06
Portland	5397929	472809		305	59		Portland	5398010	473091		340	08
Portland	5397929	472809		310	69		Portland	5398061	473094		310	05
Portland	5397929	472809		314	69		Portland	5397983	473107		320	03
Portland	5397983	473107		310	05		Portland	5396960	473576		125	22
Portland	5398063	473125		305	08		Portland	5396960	473576		130	22
Portland	5398063	473125		315	10		Portland	5396960	473576		124	23
Portland	5397833	473128		312	70		Portland	5396960	473576		135	25
Portland	5397833	473128		308	74		Portland	5396960	473576		129	30
Portland	5397833	473128		300	75		Portland	5396960	473576		131	33
Portland	5397833	473128		306	76		Portland	5396917	473749		130	24
Portland	5397833	473128		306	77		Russell	5399423	469666		260	09
Portland	5397833	473128		311	79		Russell	5399423	469666		280	10
Portland	5397833	473128		310	83		Russell	5399423	469666		267	11
Portland	5397833	473128		306	87		Russell	5399423	469666		275	11
Portland	5397869	473133		341	19		Russell	5399423	469666		276	13
Portland	5397869	473133		346	20		Russell	5399423	469666		284	20
Portland	5397869	473133		330	23		Russell	5399423	469666		268	21
Portland	5397869	473133		335	23		Russell	5399423	469666		274	21
Portland	5397869	473133		321	25		Russell	5399343	469844		268	18



Table B 4 : Bedding Data.

Domain	Northing	Easting	OT?	Strike	Dip		Domain	Northing	Easting	OT?	Strike	Dip
Portland	5397869	473133		337	26		Russell	5399554	469847		270	15
Portland	5397814	473147		322	62		Russell	5399498	470000		280	14
Portland	5397814	473147		304	64		Russell	5399532	470001		265	08
Portland	5397814	473147		305	76		Russell	5399532	470001		235	10
Portland	5396758	473153		038	08		Russell	5399532	470001		250	11
Portland	5396758	473153		036	09		Russell	5399718	470230		290	07
Portland	5396758	473153		040	10		Russell	5399721	470317		295	22
Portland	5397843	473200		100	17		Russell	5399721	470317		295	25
Portland	5397843	473200		100	18		Russell	5399721	470317		290	33
Portland	5397843	473200		096	22		Russell	5399620	470536		290	13
Portland	5397840	473238		075	13		Russell	5399620	470536		293	14
Portland	5397840	473238		075	15		Russell	5399620	470536		280	15
Portland	5397840	473238		077	18		Sidney	5386030	475480		304	65
Portland	5397878	473240		084	10		Sidney	5386030	475480		301	67
Portland	5397878	473240		086	10		Sidney	5386030	475480		304	69
Portland	5397878	473240		100	14		Sidney	5386030	475480		303	74
Portland	5397878	473240		098	18		Sidney	5386030	475480		300	76
Portland	5397878	473240		075	20		Sidney	5386030	475480		305	79
Portland	5397590	473346		309	52		Sidney	5386086	475483		296	65
Portland	5397590	473346		310	68		Sidney	5386086	475483		296	65
Portland	5397590	473346		313	69		Sidney	5386086	475483		294	71
Portland	5397590	473346		316	70		Sidney	5386086	475483		295	73
Portland	5397297	473379		115	10		Sidney	5386086	475483		295	73
Portland	5397297	473379		122	10		Sidney	5386005	475494		298	69
Portland	5397297	473379		112	23		Sidney	5386005	475494		300	70
Portland	5396944	473405		056	08		Sidney	5386005	475494		310	75
Portland	5396944	473405		056	09		Sidney	5386080	475536		305	71
Portland	5397487	473438		330	65		Sidney	5386080	475536		309	73
Portland	5397130	473445		124	15		Sidney	5386080	475536		303	76
Portland	5397130	473445		102	20		Sidney	5385514	477127		304	58
Portland	5396939	473452		078	08		Sidney	5385514	477127		302	72
Portland	5396939	473452		081	10		Sidney	5384866	478073		300	47
Portland	5396939	473452		075	14		Sidney	5384866	478073		304	51
Portland	5397386	473468		321	61		Sidney	5384866	478073		295	53
Portland	5397386	473468		322	61		Sidney	5384853	478078		305	70
Portland	5397386	473468		320	62		Sidney	5387273	478081		307	54
Portland	5397386	473468		326	64		Sidney	5387273	478081		308	57
Portland	5397386	473468		316	66		Sidney	5387273	478081		310	59
Portland	5397111	473483		104	19		Sidney	5387273	478081		310	62
Portland	5397085	473511		089	14		Sidney	5384936	478101		296	58
Portland	5397085	473511		105	17		Sidney	5384936	478101		299	58
Portland	5397085	473511		098	19		Sidney	5387239	478106		311	53
Portland	5397085	473511		104	19		Sidney	5387239	478106		314	55
Portland	5397085	473511		106	24		Sidney	5387239	478106		314	66
Portland	5397814	473513		130	22		Sidney	5384878	478303		305	60
Portland	5397814	473513		130	22		Sidney	5386962	478551		304	46
Portland	5397814	473513		139	22		Sidney	5386962	478551		296	50
Portland	5396960	473576		135	19		Sidney	5386962	478551		306	53
Sidney	5386962	478551		309	60		Sidney	5386101	479978		301	66
Sidney	5384551	478755		320	52		Sidney	5385166	480011		300	38

Table B 4 : Bedding Data.

Domain	Northing	Easting	OT?	Strike	Dip		Domain	Northing	Easting	OT?	Strike	Dip
Sidney	5384567	478759		304	50		Sidney	5385166	480011		310	40
Sidney	5384505	478778		295	53		Sidney	5385166	480011		296	46
Sidney	5384455	478818		285	59		Sidney	5385171	480030		298	47
Sidney	5384427	478863		315	50		Sidney	5385179	480074		295	55
Sidney	5384417	478904		329	53		Sidney	5385163	480097		295	40
Sidney	5384405	478909		308	60		Sidney	5385163	480097		300	45
Sidney	5384333	479058		296	43		Sidney	5383140	480179		282	58
Sidney	5384333	479058		295	45		Sidney	5383140	480179		316	58
Sidney	5384333	479058		280	46		Sidney	5383140	480179		314	59
Sidney	5384333	479058		280	46		Sidney	5383140	480179		315	59
Sidney	5384333	479058		294	53		Sidney	5383140	480179		317	61
Sidney	5384316	479074		325	50		Sidney	5383140	480179		318	61
Sidney	5384316	479074		318	51		Sidney	5383148	480209		310	54
Sidney	5384316	479074		300	59		Sidney	5383148	480209		312	54
Sidney	5384316	479074		305	60		Sidney	5383148	480209		316	58
Sidney	5386588	479144		300	50		Sidney	5383148	480209		314	61
Sidney	5386588	479144		301	50		Tsehum	5392086	468693		280	55
Sidney	5386588	479144		301	51		Tsehum	5392086	468693		290	60
Sidney	5386588	479144		300	53		Tsehum	5391409	468769		070	45
Sidney	5386588	479144		305	55		Tsehum	5391409	468769		065	53
Sidney	5384268	479148		320	65		Tsehum	5391409	468769		075	54
Sidney	5384208	479224		310	60		Tsehum	5391548	468962		282	56
Sidney	5386526	479274		303	49		Tsehum	5391548	468962		280	59
Sidney	5386526	479274		300	52		Tsehum	5391548	468962		290	60
Sidney	5386544	479285		300	50		Tsehum	5392106	469338		280	49
Sidney	5386544	479285		298	51		Tsehum	5392106	469338		280	49
Sidney	5386544	479285		298	52		Tsehum	5391355	469342		295	44
Sidney	5384145	479293		315	58		Tsehum	5391355	469342		300	51
Sidney	5384145	479293		312	60		Tsehum	5392115	469353		284	50
Sidney	5386494	479300		303	50		Tsehum	5392132	469379		262	18
Sidney	5386494	479300		305	56		Tsehum	5392132	469379		263	32
Sidney	5386494	479300		304	57		Tsehum	5392132	469379		275	34
Sidney	5386477	479338		300	46		Tsehum	5392132	469379		283	38
Sidney	5386477	479338		306	46		Tsehum	5392132	469379		286	42
Sidney	5384089	479362		316	58		Tsehum	5392132	469379		285	43
Sidney	5384089	479362		315	59		Tsehum	5392146	469394		275	41
Sidney	5384089	479362		309	60		Tsehum	5392146	469394		282	43
Sidney	5384089	479362		315	60		Tsehum	5392167	469415		284	42
Sidney	5384089	479362		315	61		Tsehum	5392167	469415		285	48
Sidney	5386453	479427		295	46		Tsehum	5391490	469510		304	55
Sidney	5386453	479427		307	54		Tsehum	5392242	469606		291	51
Sidney	5383877	479601		305	61		Tsehum	5392242	469606		276	54
Sidney	5383877	479601		315	63		Tsehum	5392242	469606		285	55
Sidney	5383877	479601		312	66		Tsehum	5392314	469683		264	46
Sidney	5385390	479754		310	33		Tsehum	5392314	469683		270	46
Sidney	5385390	479754		312	36		Tsehum	5392314	469683		276	47
Sidney	5385390	479754		318	39		Tsehum	5392314	469683		272	48
Sidney	5385390	479754		311	43		Tsehum	5391311	469834		290	50
Sidney	5385318	479766		305	46		Tsehum	5392734	470016		255	49
Sidney	5385316	479813		310	35		Tsehum	5392734	470016		276	49

Table B 4 : Bedding Data.

Domain	Northing	Easting	OT?	Strike	Dip		Domain	Northing	Easting	OT?	Strike	Dip
Sidney	5385316	479813		311	35		Tsehum	5392734	470016		274	50
Sidney	5385316	479813		310	39		Tsehum	5392734	470016		276	50
Sidney	5385316	479813		307	40		Tsehum	5391484	470066		296	56
Sidney	5385236	479929		295	42		Tsehum	5391484	470066		290	59
Sidney	5385236	479929		300	43		Tsehum	5391484	470066		290	60
Sidney	5385236	479929		304	43		Tsehum	5392788	470155		246	29
Sidney	5385236	479929		311	43		Tsehum	5392788	470155		240	35
Sidney	5385236	479929		297	46		Tsehum	5392788	470155		246	43
Sidney	5383508	479941		315	60		Tsehum	5392788	470155		245	45
Sidney	5385195	479955		300	43		Tsehum	5391412	470171		290	80
Sidney	5386101	479978		305	60		Tsehum	5391412	470171		288	85
Sidney	5386101	479978		306	61		Tsehum	5391412	470171		284	86
Tsehum	5392244	470190		285	52		Tsehum	5391714	470641		262	32
Tsehum	5392244	470190		294	55		Tsehum	5391714	470641		263	35
Tsehum	5392244	470190		300	58		Tsehum	5391714	470641		265	38
Tsehum	5392244	470190		295	68		Tsehum	5391967	470660		215	34
Tsehum	5392852	470271		260	22		Tsehum	5391967	470660		210	35
Tsehum	5392852	470271		255	40		Tsehum	5391967	470660		212	36
Tsehum	5392852	470271		255	45		Tsehum	5391663	470670		250	66
Tsehum	5392852	470271		259	46		Tsehum	5391663	470670		241	69
Tsehum	5390733	470317		295	58		Tsehum	5391666	470682		260	66
Tsehum	5390733	470317		295	60		Tsehum	5391651	470700		255	51
Tsehum	5390733	470317		299	61		Tsehum	5391651	470700		249	52
Tsehum	5392330	470330		249	46		Tsehum	5391651	470700		250	55
Tsehum	5392364	470334		252	34		Tsehum	5391651	470700		250	65
Tsehum	5392364	470334		250	35		Tsehum	5392360	470710		273	37
Tsehum	5392479	470337		249	40		Tsehum	5392360	470710		263	38
Tsehum	5391345	470373		290	55		Tsehum	5392360	470710		268	38
Tsehum	5391345	470373		295	55		Tsehum	5391780	470716		151	40
Tsehum	5392887	470406		251	40		Tsehum	5391869	470724		161	30
Tsehum	5392887	470406		256	40		Tsehum	5391869	470724		172	32
Tsehum	5392887	470406		254	41		Tsehum	5391869	470724		162	38
Tsehum	5392887	470406		259	41		Tsehum	5391869	470724		162	40
Tsehum	5392887	470406		250	44		Tsehum	5391869	470724		166	42
Tsehum	5392485	470421		249	39		Tsehum	5390537	470744		295	60
Tsehum	5392485	470421		245	50		Tsehum	5390537	470744		301	61
Tsehum	5392485	470421		255	53		Tsehum	5392191	470766		260	26
Tsehum	5392756	470445		257	42		Tsehum	5392191	470766		269	27
Tsehum	5392756	470445		252	43		Tsehum	5392191	470766		255	31
Tsehum	5392756	470445		250	47		Tsehum	5392191	470766		280	31
Tsehum	5392498	470471		250	60		Tsehum	5392191	470766		263	34
Tsehum	5392619	470478		261	35		Tsehum	5392191	470766		284	36
Tsehum	5392619	470478		260	36		Tsehum	5392191	470766		296	54
Tsehum	5392619	470478		255	39		Tsehum	5390511	470770		305	60
Tsehum	5391818	470574		069	17		Tsehum	5390511	470770		308	61
Tsehum	5391818	470574		265	25		Tsehum	5391599	470773		250	60
Tsehum	5391818	470574		080	28		Tsehum	5391360	470803		265	40
Tsehum	5391818	470574		270	30		Tsehum	5391360	470803		267	42
Tsehum	5391818	470574		272	31		Tsehum	5391360	470803		264	45
Tsehum	5391818	470574		081	34		Tsehum	5391360	470803		270	50

Table B 4 : Bedding Data.

Domain	Northing	Easting	OT?	Strike	Dip		Domain	Northing	Easting	OT?	Strike	Dip
Tsehum	5391818	470574		264	58		Tsehum	5391424	470813		270	42
Tsehum	5391415	470574		215	75		Tsehum	5391424	470813		270	42
Tsehum	5391415	470574		230	80		Tsehum	5391502	470834		262	45
Tsehum	5391415	470574		240	85		Tsehum	5392825	470843		290	40
Tsehum	5391502	470574		283	63		Tsehum	5392825	470843		280	48
Tsehum	5391502	470574		284	64		Tsehum	5392720	470845		279	46
Tsehum	5392026	470581		240	27		Tsehum	5392720	470845		271	49
Tsehum	5392026	470581		222	28		Tsehum	5392600	470868		280	47
Tsehum	5392026	470581		229	32		Tsehum	5391992	470932		256	25
Tsehum	5392026	470581		214	33		Tsehum	5391992	470932		265	28
Tsehum	5392026	470581		018	34		Tsehum	5391992	470932		254	30
Tsehum	5392026	470581		193	38		Tsehum	5391992	470932		260	33
Tsehum	5391805	470597		225	33		Tsehum	5391992	470932		262	34
Tsehum	5391771	470603		271	52		Tsehum	5391992	470932		268	35
Tsehum	5391771	470603		270	55		Tsehum	5391992	470932		270	36
Tsehum	5391771	470603		270	55		Tsehum	5392775	470981		276	55
Tsehum	5391409	470615		280	60		Tsehum	5392775	470981		277	56
Tsehum	5391409	470615		284	65		Tsehum	5392775	470981		280	58
Tsehum	5391409	470615		280	72		Tsehum	5392775	470981		276	59
Tsehum	5391471	470618		279	50		Tsehum	5392124	471028		276	46
Tsehum	5391471	470618		276	53		Tsehum	5392124	471028		264	54
Tsehum	5391471	470618		283	57		Tsehum	5391782	471059		265	51
Tsehum	5391471	470618		285	58		Tsehum	5391782	471059		264	52
Tsehum	5392120	470623		233	25		Tsehum	5391782	471059		266	55
Tsehum	5392120	470623		221	32		Tsehum	5392224	471113		270	54
Tsehum	5392120	470623		235	33		Tsehum	5392224	471113		275	61
Tsehum	5392224	471113		278	62		Tsehum	5391810	471690		260	60
Tsehum	5391817	471163		274	53		Tsehum	5391810	471690		257	69
Tsehum	5391817	471163		260	58		Tsehum	5391810	471690		254	70
Tsehum	5391817	471163		271	60		Tsehum	5391810	471690		275	74
Tsehum	5391817	471163		264	61		Tsehum	5391810	471690		254	76
Tsehum	5391817	471163		262	64		Tsehum	5391810	471690		270	76
Tsehum	5391817	471163		262	64		Tsehum	5391814	471728		260	66
Tsehum	5391817	471163		263	64		Tsehum	5391814	471728		259	69
Tsehum	5391817	471163		269	64		Tsehum	5391814	471728		266	71
Tsehum	5391817	471163		269	66		Tsehum	5391814	471728		268	80
Tsehum	5391817	471163		260	67		Tsehum	5391654	471735		264	32
Tsehum	5392175	471172		266	55		Tsehum	5391654	471735		256	43
Tsehum	5392175	471172		274	60		Tsehum	5391654	471735		279	46
Tsehum	5392522	471180		286	59		Tsehum	5391654	471735		295	50
Tsehum	5392522	471180		289	59		Tsehum	5391865	471750		274	69
Tsehum	5392522	471180		283	60		Tsehum	5391865	471750		269	71
Tsehum	5392522	471180		284	60		Tsehum	5391865	471750		265	72
Tsehum	5392522	471180		294	60		Tsehum	5391865	471750		270	73
Tsehum	5392674	471186		284	55		Tsehum	5391865	471750		270	75
Tsehum	5392674	471186		288	57		Tsehum	5391865	471750		265	76
Tsehum	5392674	471186		286	59		Tsehum	5391865	471750		266	78
Tsehum	5392221	471220		273	54		Tsehum	5391597	471775		256	38
Tsehum	5392377	471248		284	57		Tsehum	5391529	471850		268	36
Tsehum	5392377	471248		285	58		Tsehum	5391529	471850		270	48

Table B 4 : Bedding Data.

Domain	Northing	Easting	OT?	Strike	Dip		Domain	Northing	Easting	OT?	Strike	Dip
Tsehum	5392377	471248		285	66		Tsehum	5391529	471850		260	58
Tsehum	5392266	471295		281	48		Tsehum	5391529	471850		276	58
Tsehum	5392266	471295		286	51		Tsehum	5392016	472168		082	90
Tsehum	5392266	471295		289	54		Tsehum	5392016	472168		085	90
Tsehum	5392266	471295		286	56		Tsehum	5391863	472192	OT	100	82
Tsehum	5392266	471295		278	60		Tsehum	5391863	472192	OT	100	78
Tsehum	5392266	471295		281	64		Tsehum	5391859	472243		280	88
Tsehum	5392266	471295		280	65		Tsehum	5391859	472243		094	90
Tsehum	5392229	471299		285	60		Tsehum	5391859	472243	OT	096	85
Tsehum	5392229	471299		275	61		Tsehum	5391859	472243	OT	091	83
Tsehum	5392229	471299		282	67		Tsehum	5391705	472422		283	31
Tsehum	5392229	471299		272	77		Tsehum	5391705	472422		284	32
Tsehum	5392446	471460		276	72		Tsehum	5391705	472422		286	39
Tsehum	5392446	471460		274	74		Tsehum	5391705	472422		285	43
Tsehum	5392446	471460		280	74		W Saanich	5391686	464012		270	25
Tsehum	5392603	471472		298	54		W Saanich	5391694	464028		225	25
Tsehum	5392603	471472		298	56		W Saanich	5391693	464042		237	35
Tsehum	5392603	471472		297	57		W Saanich	5391657	464060		238	31
Tsehum	5392603	471472		294	58		W Saanich	5391655	464082		199	26
Tsehum	5392603	471472		295	60		W Saanich	5391654	464088		264	31
Tsehum	5392603	471472		276	82		W Saanich	5391649	464108		240	16
Tsehum	5392646	471505		282	72		W Saanich	5391645	464112		240	26
Tsehum	5392646	471505		290	78		W Saanich	5391743	464199		210	22
Tsehum	5392197	471523		292	72		W Saanich	5391608	464210		221	26
Tsehum	5392197	471523		256	76		W Saanich	5391608	464210		256	32
Tsehum	5392197	471523		290	76		W Saanich	5391595	464220		220	20
Tsehum	5392197	471523		260	78		W Saanich	5391576	464234		218	18
Tsehum	5392197	471523		276	80		W Saanich	5391576	464234		230	18
Tsehum	5392197	471523		275	84		W Saanich	5391576	464234		220	21
Tsehum	5391819	471570		265	64		W Saanich	5391754	464236		225	24
Tsehum	5391819	471570		260	69		W Saanich	5393038	464300		240	44
Tsehum	5391819	471570		264	74		W Saanich	5393038	464300		240	45
Tsehum	5391819	471570		266	74		W Saanich	5391857	464330		213	29
Tsehum	5392001	471572		266	78		W Saanich	5393211	464394		255	50
Tsehum	5392001	471572		270	80		W Saanich	5393211	464394		260	63
Tsehum	5392001	471572		276	82		W Saanich	5391455	464397		220	48
Tsehum	5392001	471572		274	84		W Saanich	5391455	464397		230	60
Tsehum	5391850	471591		265	59		W Saanich	5393268	464412		240	58
Tsehum	5391850	471591		264	66		W Saanich	5393377	464424		249	58
Tsehum	5391850	471591		256	67		W Saanich	5391088	464482	OT	096	88
W Saanich	5392059	464546		220	25		W Saanich	5392336	464997		220	42
W Saanich	5391002	464608		279	77		W Saanich	5392336	464997		220	50
W Saanich	5391002	464608		276	86		W Saanich	5393715	465020		250	60
W Saanich	5392078	464619		219	16		W Saanich	5392177	465029		188	52
W Saanich	5393032	464620		240	50		W Saanich	5392177	465029		176	54
W Saanich	5393032	464620		236	55		W Saanich	5392426	465102		235	41
W Saanich	5390959	464673		266	70		W Saanich	5392426	465102		235	43
W Saanich	5390959	464673		270	73		W Saanich	5392039	465102		180	46
W Saanich	5392996	464675		226	46		W Saanich	5392039	465102		180	60
W Saanich	5392996	464675		230	47		W Saanich	5392138	465117		155	49

Table B 4 : Bedding Data.

Domain	Northing	Easting	OT?	Strike	Dip		Domain	Northing	Easting	OT?	Strike	Dip
W Saanich	5392996	464675		230	48		W Saanich	5392138	465117		155	49
W Saanich	5392996	464675		234	48		W Saanich	5392138	465117		172	49
W Saanich	5392996	464675		236	51		W Saanich	5393736	465158		246	60
W Saanich	5393567	464693		250	64		W Saanich	5392543	465171		270	35
W Saanich	5393567	464693		244	66		W Saanich	5392543	465171		270	43
W Saanich	5390928	464718		280	60		W Saanich	5393753	465276		241	61
W Saanich	5390928	464718		266	79		W Saanich	5393849	465901		244	58
W Saanich	5390928	464718		270	83		W Saanich	5393861	465907		239	62
W Saanich	5391955	464767		254	44		W Saanich	5393861	465907		240	62
W Saanich	5391955	464767		242	45		W Saanich	5393861	465907		241	63
W Saanich	5391955	464767		270	51		W Saanich	5393831	466018		230	58
W Saanich	5391955	464767		260	53		W Saanich	5393845	466119		239	61
W Saanich	5391955	464767		261	61		W Saanich	5393845	466119		241	64
W Saanich	5390742	464767		085	90		W Saanich	5393891	466584		251	65
W Saanich	5390742	464767		090	90		W Saanich	5393891	466584		250	66
W Saanich	5390711	464770	OT	095	90		W Saanich	5393891	466584		254	69
W Saanich	5390711	464770	OT	095	87		W Saanich	5393743	466717		254	68
W Saanich	5390711	464770	OT	099	84		W Saanich	5393743	466717		250	70
W Saanich	5390711	464770	OT	101	81		W Saanich	5393918	466781		241	65
W Saanich	5390711	464770	OT	090	90		W Saanich	5393918	466781		244	68
W Saanich	5390778	464775	OT	094	51		W Saanich	5393927	466855		285	45
W Saanich	5390778	464775	OT	088	49		W Saanich	5393927	466855		260	54
W Saanich	5390778	464775	OT	096	41		W Saanich	5393927	466855		270	60
W Saanich	5390778	464775	OT	103	37		W Saanich	5393222	466901		278	46
W Saanich	5393611	464789		250	49		W Saanich	5393222	466901		266	47
W Saanich	5393611	464789		255	60		W Saanich	5393222	466901		272	48
W Saanich	5390794	464797	OT	101	39		W Saanich	5393222	466901		282	48
W Saanich	5390794	464797	OT	101	38		W Saanich	5393639	466905		279	55
W Saanich	5390794	464797	OT	100	35		W Saanich	5393639	466905		279	59
W Saanich	5393623	464808		246	62		W Saanich	5393639	466905		284	59
W Saanich	5393623	464808		244	64		W Saanich	5394105	467050		280	55
W Saanich	5390687	464819		224	30		W Saanich	5394105	467050		285	62
W Saanich	5390687	464819		260	32		W Saanich	5394105	467050		281	65
W Saanich	5390687	464819		255	42		W Saanich	5393887	467077		275	53
W Saanich	5390671	464819		278	68		W Saanich	5394138	467151		270	48
W Saanich	5390671	464819		275	73		W Saanich	5394138	467151		280	55
W Saanich	5390671	464819		270	75		W Saanich	5394138	467151		275	56
W Saanich	5390711	464824		270	90		W Saanich	5393547	467297		271	50
W Saanich	5390681	464825		124	15		W Saanich	5393547	467297		276	51
W Saanich	5390681	464825		135	17		W Saanich	5393547	467297		274	54
W Saanich	5390681	464825		130	22		W Saanich	5392425	467402		328	38
W Saanich	5390681	464825		256	38		W Saanich	5392425	467402		330	40
W Saanich	5390681	464825		251	40		W Saanich	5392425	467402		326	45
W Saanich	5390701	464864		224	38		W Saanich	5394110	467512		281	56
W Saanich	5390701	464864		106	66		W Saanich	5394110	467512		285	56
W Saanich	5390701	464864		113	70		W Saanich	5394110	467512		285	60
W Saanich	5391960	464919		230	54		W Saanich	5393100	467543		291	39
W Saanich	5391960	464919		235	54		W Saanich	5393100	467543		294	39
W Saanich	5391948	464934		268	76		W Saanich	5394105	467597		274	56
W Saanich	5391948	464934		270	78		W Saanich	5394105	467597		280	60

Table B 4 : Bedding Data.

Domain	Northing	Easting	OT?	Strike	Dip		Domain	Northing	Easting	OT?	Strike	Dip
W Saanich	5391948	464934		269	89		W Saanich	5392859	467646		286	47
W Saanich	5392287	464983		205	61		W Saanich	5392859	467646		294	50
W Saanich	5392287	464983		206	71		W Saanich	5392859	467646		296	50
W Saanich	5392929	464985		156	20		W Saanich	5392621	467807		324	36
W Saanich	5392621	467807		307	41		W Saanich	5393133	469132		288	38
W Saanich	5392621	467807		315	41		W Saanich	5393133	469132		280	40
W Saanich	5392621	467807		320	42		W Saanich	5393120	469180		270	34
W Saanich	5392849	467825		340	43		W Saanich	5393120	469180		278	37
W Saanich	5392849	467825		356	60		W Saanich	5393120	469180		268	38
W Saanich	5393048	467944		329	37		W Saanich	5393097	469324		286	46
W Saanich	5393558	468027		282	42		W Saanich	5393097	469324		292	46
W Saanich	5393872	468081		274	45		W Saanich	5393097	469324		280	50
W Saanich	5393872	468081		276	56		W Saanich	5393097	469324		290	52
W Saanich	5393872	468081		280	60		W Saanich	5393066	469477		290	43
W Saanich	5392374	468151		293	39		W Saanich	5393340	468797		314	28
W Saanich	5392374	468151		295	40		W Saanich	5393340	468797		315	28
W Saanich	5392374	468151		287	42		W Saanich	5393340	468797		320	28
W Saanich	5392374	468151		295	43		W Saanich	5393329	468873		290	12
W Saanich	5393605	468316		282	47		W Saanich	5393329	468873		276	15
W Saanich	5393605	468316		279	54		W Saanich	5393329	468873		285	24
W Saanich	5393594	468333		290	43		W Saanich	5393329	468873		284	26
W Saanich	5393594	468333		297	46		W Saanich	5393421	468965		276	35
W Saanich	5393594	468333		300	50		W Saanich	5393421	468965		271	36
W Saanich	5393732	468396		280	50		W Saanich	5393421	468965		277	45
W Saanich	5393732	468396		282	50		W Saanich	5393290	469065		024	18
W Saanich	5393732	468396		280	55		W Saanich	5393290	469065		039	19
W Saanich	5393712	468421		310	62		W Saanich	5393290	469065		286	20
W Saanich	5393712	468421		298	65		W Saanich	5393290	469065		027	24
W Saanich	5393714	468440		260	43		W Saanich	5393290	469065		279	27
W Saanich	5393714	468440		258	48		W Saanich	5393290	469065		286	27
W Saanich	5393338	468479		298	31		W Saanich	5393290	469065		270	28
W Saanich	5393338	468479		298	36		W Saanich	5393290	469065		296	28
W Saanich	5393338	468479		296	38		W Saanich	5393290	469065		270	29
W Saanich	5393338	468479		297	45		W Saanich	5393290	469065		274	31
W Saanich	5393677	468501		285	43		W Saanich	5393290	469065		288	36
W Saanich	5393351	468542		286	41		W Saanich	5393183	469102		329	29
W Saanich	5393644	468546		285	43		W Saanich	5393183	469102		325	34
W Saanich	5393637	468589		295	48		W Saanich	5393133	469132		286	35
W Saanich	5393637	468589		315	55							
W Saanich	5393630	468620		296	44							
W Saanich	5393630	468620		295	48							
W Saanich	5393520	468722		285	43							
W Saanich	5393520	468722		285	43							
W Saanich	5393520	468722		285	43							

Figure B 5: Brittle Fracture Measures

Domain	Northing	Easting	Type	Strike	Dip	Domain	Northing	Easting	Type	Strike	Dip
Domville	5392451	475725	fracture	215	20	Domville	5390553	476771	fracture	202	85
Domville	5392451	475725	fracture	220	70	Domville	5390553	476771	fracture	229	90
Domville	5391418	475748	fracture	100	90	Domville	5390526	476795	fracture	202	67
Domville	5391469	475759	fracture	277	83	Domville	5390526	476795	fracture	206	84
Domville	5391351	475858	fracture	200	40	Domville	5390526	476795	fracture	202	90
Domville	5391352	475863	fracture	340	85	Domville	5390546	476817	fracture	222	54
Domville	5391352	475866	fracture	170	55	Domville	5390546	476817	fracture	218	62
Domville	5391352	475871	fracture	120	55	Domville	5390546	476817	fracture	200	72
Domville	5391354	475891	fracture	275	84	Domville	5390546	476817	fracture	205	85
Domville	5392038	476069	fracture	224	74	Domville	5390546	476817	fracture	202	89
Domville	5392038	476069	fracture	221	75	Domville	5390357	476833	fracture	040	82
Domville	5391965	476125	fracture	223	69	Domville	5390357	476833	fracture	052	90
Domville	5391965	476125	fracture	228	70	Domville	5390308	476892	fracture	209	54
Domville	5391965	476125	fracture	226	74	Domville	5390308	476892	fracture	229	59
Domville	5391965	476125	fracture	223	83	Domville	5390308	476892	fracture	050	90
Domville	5391681	476254	fracture	204	64	Domville	5390195	476996	fracture	204	25
Domville	5391681	476254	fracture	196	65	Domville	5390195	476996	fracture	220	38
Domville	5391681	476254	fracture	204	65	Domville	5390195	476996	fracture	214	49
Domville	5391681	476254	fracture	200	66	Domville	5390195	476996	fracture	204	54
Domville	5391681	476254	fracture	204	66	Domville	5390195	476996	fracture	218	55
Domville	5391681	476254	fracture	200	67	Domville	5390195	476996	fracture	330	63
Domville	5391681	476254	fracture	200	80	Domville	5390195	476996	fracture	226	65
Domville	5391035	476515	fracture	235	30	Domville	5390195	476996	fracture	334	60
Domville	5391035	476515	fracture	250	64	Domville	5390195	476996	fracture	200	74
Domville	5391035	476515	fracture	063	65	Domville	5390195	476996	fracture	355	74
Domville	5391035	476515	fracture	278	68	Domville	5390195	476996	fracture	120	78
Domville	5391035	476515	fracture	040	75	Domville	5390195	476996	fracture	000	90
Domville	5391035	476515	fracture	140	75	Domville	5390195	476996	fracture	120	90
Domville	5391035	476515	fracture	144	75	Domville	5390195	476996	fracture	125	90
Domville	5391035	476515	fracture	308	76	Domville	5390195	476996	fracture	012	25
Domville	5391035	476515	fracture	231	78	Domville	5390195	476996	fracture	003	45
Domville	5391035	476515	fracture	229	80	Domville	5390412	477004	fracture	200	59
Domville	5391035	476515	fracture	230	80	Domville	5390412	477004	fracture	192	63
Domville	5391035	476515	fracture	040	81	Domville	5390326	477033	fracture	085	86
Domville	5391035	476515	fracture	075	85	Domville	5390326	477033	fracture	068	66
Domville	5391035	476515	fracture	043	90	Domville	5390326	477033	fracture	058	68
Domville	5391035	476515	fracture	077	90	Domville	5390326	477033	fracture	055	71
Domville	5391035	476515	fracture	320	90	Domville	5390326	477033	fracture	006	72
Domville	5391000	476526	fracture	076	65	Domville	5390326	477033	fracture	061	75
Domville	5391000	476526	fracture	078	68	Domville	5390326	477033	fracture	055	76
Domville	5391000	476526	fracture	084	68	Forrest	5390749	472925	fracture	191	70
Domville	5391000	476526	fracture	088	73	Forrest	5390749	472925	fracture	005	80
Domville	5390996	476530	fracture	207	56	Forrest	5390749	472925	fracture	006	83
Domville	5390914	476574	fracture	242	46	Forrest	5390749	472925	fracture	358	88
Domville	5390919	476579	fracture	242	57	Forrest	5390749	472925	fracture	010	90
Domville	5390912	476579	fracture	200	60	Forrest	5391009	473235	fracture	205	79
Domville	5390914	476579	fracture	210	69	Forrest	5391009	473235	fracture	205	81
Domville	5391773	476707	fracture	065	35	Forrest	5391009	473235	fracture	204	85
Domville	5391773	476707	fracture	247	40	Forrest	5391009	473235	fracture	195	90
Domville	5391773	476707	fracture	243	41	Forrest	5391051	473236	fracture	070	67
Domville	5391773	476707	fracture	046	44	Forrest	5391051	473236	fracture	070	79
Domville	5391773	476707	fracture	245	47	Forrest	5391051	473236	fracture	055	84
Domville	5391773	476707	fracture	203	64	Forrest	5390999	473268	fracture	194	65
Domville	5390449	476758	fracture	070	64	Forrest	5390999	473268	fracture	190	71
Domville	5390449	476758	fracture	047	82	Forrest	5390999	473268	fracture	196	76
Domville	5390449	476758	fracture	049	83	Forrest	5391072	473619	fracture	199	64



Figure B 5: Brittle Fracture Measures

Domain	Northing	Easting	Type	Strike	Dip	Domain	Northing	Easting	Type	Strike	Dip
Domville	5390449	476758	fracture	040	90	Forrest	5391072	473619	fracture	214	64
Domville	5390577	476766	fracture	042	64	Forrest	5391072	473619	fracture	200	65
Domville	5390577	476766	fracture	040	70	Forrest	5391072	473619	fracture	020	66
Domville	5390577	476766	fracture	046	76	Forrest	5391072	473619	fracture	030	66
Domville	5390577	476766	fracture	035	85	Forrest	5391072	473619	fracture	030	75
Domville	5390577	476766	fracture	040	85	Forrest	5391072	473619	fracture	025	76
Domville	5390553	476771	fracture	204	82	Forrest	5391072	473619	fracture	035	83
Forrest	5391072	473619	fracture	035	85	Forrest	5389928	475125	fracture	194	80
Forrest	5391072	473619	fracture	210	86	Forrest	5389928	475125	fracture	180	81
Forrest	5391072	473619	fracture	229	87	Forrest	5389928	475125	fracture	212	82
Forrest	5391072	473619	fracture	218	88	Forrest	5389928	475125	fracture	010	83
Forrest	5390945	473652	fracture	222	52	Forrest	5389928	475125	fracture	176	83
Forrest	5390945	473652	fracture	240	58	Forrest	5389928	475125	fracture	190	84
Forrest	5390945	473652	fracture	229	65	Forrest	5389928	475125	fracture	216	84
Forrest	5390945	473652	fracture	230	70	Forrest	5389928	475125	fracture	005	85
Forrest	5391058	473670	fracture	216	84	Forrest	5389928	475125	fracture	180	85
Forrest	5391058	473670	fracture	222	86	Forrest	5389928	475125	fracture	004	86
Forrest	5391058	473670	fracture	203	89	Forrest	5389928	475125	fracture	018	90
Forrest	5391058	473670	fracture	208	89	Forrest	5389675	475474	fracture	086	37
Forrest	5391058	473670	fracture	200	90	Forrest	5389675	475474	fracture	040	44
Forrest	5391020	473713	fracture	135	15	Forrest	5389675	475474	fracture	062	44
Forrest	5390977	473717	fracture	200	24	Forrest	5389675	475474	fracture	204	45
Forrest	5390977	473717	fracture	185	25	Forrest	5389675	475474	fracture	080	49
Forrest	5390977	473717	fracture	205	25	Forrest	5389675	475474	fracture	040	56
Forrest	5390977	473717	fracture	185	28	Forrest	5389675	475474	fracture	054	57
Forrest	5390977	473717	fracture	046	55	Forrest	5389675	475474	fracture	061	59
Forrest	5390977	473717	fracture	041	64	Forrest	5389675	475474	fracture	049	61
Forrest	5390977	473717	fracture	030	70	Forrest	5389675	475474	fracture	052	63
Forrest	5390977	473717	fracture	212	70	Forrest	5389675	475474	fracture	040	64
Forrest	5390977	473717	fracture	040	71	Forrest	5389675	475474	fracture	195	71
Forrest	5390977	473717	fracture	230	73	Forrest	5389675	475474	fracture	219	71
Forrest	5390977	473717	fracture	214	75	Forrest	5389675	475474	fracture	080	74
Forrest	5390990	473720	fracture	140	12	Forrest	5389675	475474	fracture	034	76
Forrest	5390990	473720	fracture	115	15	Forrest	5389675	475474	fracture	221	77
Forrest	5390990	473720	fracture	120	15	Forrest	5389675	475474	fracture	226	80
Forrest	5390990	473720	fracture	145	15	Forrest	5389675	475474	fracture	230	82
Forrest	5390990	473720	fracture	155	15	Forrest	5389675	475474	fracture	061	86
Forrest	5390990	473720	fracture	038	19	Forrest	5389675	475474	fracture	231	86
Forrest	5390990	473720	fracture	228	58	Forrest	5389915	475490	fracture	230	61
Forrest	5390990	473720	fracture	226	60	Forrest	5389915	475490	fracture	228	62
Forrest	5390990	473720	fracture	205	64	Forrest	5389915	475490	fracture	233	69
Forrest	5390990	473720	fracture	230	72	Forrest	5389915	475490	fracture	208	70
Forrest	5390990	473720	fracture	205	80	Forrest	5389915	475490	fracture	203	86
Forrest	5390990	473720	fracture	210	80	Forrest	5389915	475490	fracture	225	64
Forrest	5390990	473720	fracture	221	80	Forrest	5389915	475490	fracture	232	68
Forrest	5390990	473720	fracture	221	83	Forrest	5389915	475490	fracture	237	68
Forrest	5390294	474905	fracture	308	90	Forrest	5389785	475621	fracture	204	16
Forrest	5390294	474905	fracture	308	90	Forrest	5389785	475621	fracture	209	24
Forrest	5390294	474905	fracture	309	90	Forrest	5389785	475621	fracture	199	26
Forrest	5390311	474913	fracture	057	60	Forrest	5389785	475621	fracture	041	29
Forrest	5390311	474913	fracture	069	72	Forrest	5389785	475621	fracture	063	29
Forrest	5390046	474967	fracture	043	76	Forrest	5389785	475621	fracture	050	38
Forrest	5390046	474967	fracture	032	78	Forrest	5389785	475621	fracture	046	80
Forrest	5390046	474967	fracture	041	90	Forrest	5389785	475621	fracture	027	81
Forrest	5390025	474990	fracture	046	67	Forrest	5389785	475621	fracture	022	82
Forrest	5390025	474990	fracture	046	68	Forrest	5389740	475664	fracture	033	35

Figure B 5: Brittle Fracture Measures

Domain	Northing	Easting	Type	Strike	Dip	Domain	Northing	Easting	Type	Strike	Dip
Forrest	5390025	474990	fracture	041	71	Forrest	5389740	475664	fracture	045	44
Forrest	5390025	474990	fracture	042	76	Forrest	5389740	475664	fracture	040	45
Forrest	5390025	474990	fracture	028	80	Forrest	5389740	475664	fracture	053	46
Forrest	5390025	474990	fracture	050	81	Forrest	5389740	475664	fracture	051	49
Forrest	5390025	474990	fracture	039	83	Forrest	5389740	475664	fracture	052	64
Forrest	5390025	474990	fracture	044	86	Forrest	5389740	475664	fracture	049	67
Forrest	5389928	475125	fracture	118	07	Forrest	5389740	475664	fracture	048	70
Forrest	5389928	475125	fracture	120	54	Forrest	5389740	475664	fracture	035	79
Forrest	5389928	475125	fracture	028	56	Forrest	5389740	475664	fracture	045	80
Forrest	5389928	475125	fracture	109	57	Forrest	5389740	475664	fracture	065	80
Forrest	5389928	475125	fracture	223	70	Forrest	5389740	475664	fracture	035	81
Forrest	5389928	475125	fracture	206	73	Forrest	5389740	475664	fracture	060	82
Forrest	5389928	475125	fracture	011	74	Forrest	5389740	475664	fracture	051	84
Forrest	5389928	475125	fracture	358	77	Forrest	5389740	475664	fracture	052	84
Forrest	5389740	475664	fracture	035	85	Moresby	5397232	477461	fracture	196	70
Forrest	5389740	475664	fracture	045	85	Moresby	5397232	477461	fracture	222	73
Forrest	5389740	475664	fracture	059	85	Moresby	5397232	477461	fracture	218	76
Forrest	5389740	475664	fracture	035	86	Moresby	5397232	477461	fracture	214	80
Forrest	5389709	475699	fracture	016	76	Moresby	5397671	476588	gash	060	60
Forrest	5389709	475699	fracture	020	76	Moresby	5397671	476588	gash	062	89
Forrest	5389709	475699	fracture	020	82	Moresby	5397671	476588	gash	065	90
Forrest	5389709	475699	fracture	014	84	Moresby	5397695	476672	gash	055	62
Forrest	5389709	475699	fracture	029	84	Moresby	5397695	476672	gash	062	65
Forrest	5389709	475699	fracture	024	87	Moresby	5397695	476672	gash	060	70
Forrest	5389709	475699	fracture	022	90	N Coal	5393135	471457	fracture	011	46
Forrest	5389709	475699	fracture	030	90	N Coal	5393135	471457	fracture	004	50
Forrest	5389564	475728	fracture	031	52	N Coal	5393196	471476	fracture	194	62
Forrest	5389564	475728	fracture	032	59	N Coal	5393196	471476	fracture	034	63
Forrest	5389564	475728	fracture	040	61	N Coal	5393196	471476	fracture	184	66
Forrest	5389592	475760	fracture	049	36	N Coal	5393196	471476	fracture	191	67
Forrest	5389592	475760	fracture	054	45	N Coal	5393196	471476	fracture	020	68
Forrest	5389640	475789	fracture	040	49	N Coal	5393196	471476	fracture	178	70
Forrest	5389640	475789	fracture	049	49	N Coal	5393196	471476	fracture	198	70
Forrest	5389640	475789	fracture	060	53	N Coal	5393196	471476	fracture	024	71
Forrest	5389400	475889	fracture	045	55	N Coal	5393196	471476	fracture	026	74
Forrest	5389400	475889	fracture	030	57	N Coal	5393196	471476	fracture	031	74
Forrest	5389400	475889	fracture	039	57	N Coal	5393196	471476	fracture	193	74
Forrest	5389400	475889	fracture	049	57	N Coal	5393196	471476	fracture	008	76
Forrest	5389400	475889	fracture	036	58	N Coal	5393196	471476	fracture	001	77
Forrest	5389400	475889	fracture	050	60	N Coal	5393196	471476	fracture	170	77
Forrest	5389400	475889	fracture	039	62	N Coal	5393049	471588	fracture	016	45
Forrest	5389400	475889	fracture	043	69	N Coal	5393049	471588	fracture	012	48
Forrest	5389156	476175	fracture	028	55	N Coal	5393049	471588	fracture	017	48
Forrest	5389156	476175	fracture	032	58	N Coal	5391884	472560	fracture	325	25
Forrest	5389156	476175	fracture	200	86	N Coal	5391884	472560	fracture	010	26
Forrest	5389156	476175	fracture	196	89	N Coal	5391884	472560	fracture	031	39
Forrest	5389156	476175	fracture	190	90	N Coal	5391884	472560	fracture	304	46
Gooch	5390842	477815	fracture	322	67	N Coal	5391884	472560	fracture	025	50
Gooch	5390842	477815	fracture	297	79	N Coal	5391884	472560	fracture	030	55
Gooch	5390789	477912	fracture	006	70	N Coal	5391884	472560	fracture	165	65
Gooch	5390789	477912	fracture	327	72	N Coal	5391884	472560	fracture	025	69
Gooch	5390789	477912	fracture	340	76	N Coal	5391884	472560	fracture	019	72
Gooch	5390844	478159	fracture	233	80	N Coal	5391884	472560	fracture	095	72
Gooch	5390677	478192	fracture	080	64	N Coal	5391884	472560	fracture	096	74
Gooch	5390677	478192	fracture	010	50	N Coal	5391884	472560	fracture	230	75
Gooch	5390677	478192	fracture	070	64	N Coal	5391884	472560	fracture	019	76

Figure B 5: Brittle Fracture Measures

Domain	Northing	Easting	Type	Strike	Dip	Domain	Northing	Easting	Type	Strike	Dip
Gooch	5390677	478192	fracture	200	74	N Coal	5391884	472560	fracture	027	80
Gooch	5390677	478192	fracture	214	78	N Coal	5391884	472560	fracture	226	81
Gooch	5389897	478916	fracture	319	26	N Coal	5391884	472560	fracture	290	85
Gooch	5389897	478916	fracture	330	30	N Coal	5391884	472560	fracture	299	86
Gooch	5389897	478916	fracture	350	34	N Coal	5391884	472560	fracture	290	90
Gooch	5389897	478916	fracture	340	40	N Coal	5392032	472592	fracture	035	74
Gooch	5389897	478916	fracture	185	56	N Coal	5392032	472592	fracture	026	86
Gooch	5389897	478916	fracture	180	80	N Coal	5392253	472730	fracture	206	77
Moresby	5397468	476309	fracture	242	59	N Coal	5392253	472730	fracture	207	79
Moresby	5397468	476309	fracture	216	63	N Coal	5392253	472730	fracture	208	83
Moresby	5397468	476309	fracture	010	66	N Coal	5392253	472730	fracture	211	84
Moresby	5397468	476309	fracture	312	74	N Coal	5392253	472730	fracture	213	85
Moresby	5397468	476309	fracture	315	75	N Coal	5392253	472730	fracture	208	86
Moresby	5397468	476309	fracture	214	76	N Coal	5392253	472730	fracture	212	88
Moresby	5397468	476309	fracture	320	78	N Coal	5392253	472730	fracture	016	90
Moresby	5397468	476309	fracture	330	79	N Coal	5392123	472636	min. fill.	031	65
Moresby	5397468	476309	fracture	199	80	N Coal	5392123	472636	min. fill.	036	83
Moresby	5397468	476309	fracture	216	80	N Coal	5392123	472636	min. fill.	033	86
Moresby	5397468	476309	fracture	150	85	N Coal	5392130	472639	min. fill.	240	44
Moresby	5397232	477461	fracture	213	66	N Coal	5392130	472639	min. fill.	226	48
Moresby	5397232	477461	fracture	220	68	N Coal	5392130	472639	min. fill.	242	50
N Coal	5392130	472639	min. fill.	244	60	Portland	5398008	472969	fracture	210	54
N Coal	5392130	472639	min. fill.	215	73	Portland	5398008	472969	fracture	212	58
N Coal	5392130	472639	min. fill.	010	79	Portland	5398008	472969	fracture	215	58
N Coal	5392130	472639	min. fill.	006	80	Portland	5398008	472969	fracture	250	70
N Coal	5392130	472639	min. fill.	007	81	Portland	5398008	472969	fracture	252	74
N Coal	5392134	472640	min. fill.	302	55	Portland	5398049	473050	fracture	002	88
N Coal	5392134	472640	min. fill.	192	66	Portland	5398049	473050	fracture	192	89
N Coal	5392134	472640	min. fill.	194	72	Portland	5398049	473050	fracture	011	90
N Coal	5392134	472640	min. fill.	200	75	Portland	5397862	473083	fracture	246	70
N Coal	5392134	472640	min. fill.	298	76	Portland	5397862	473083	fracture	226	78
N Coal	5392134	472640	min. fill.	205	85	Portland	5397862	473083	fracture	203	80
N Coal	5392142	472642	min. fill.	212	66	Portland	5397862	473083	fracture	206	86
N Coal	5392142	472642	min. fill.	216	72	Portland	5398010	473091	fracture	046	60
N Coal	5392142	472642	min. fill.	215	75	Portland	5398010	473091	fracture	040	68
N Coal	5392142	472642	min. fill.	211	76	Portland	5398010	473091	fracture	186	77
N Coal	5392142	472642	min. fill.	205	78	Portland	5398010	473091	fracture	004	84
N Coal	5392219	472701	min. fill.	285	72	Portland	5397833	473128	fracture	219	75
N Coal	5392219	472701	min. fill.	250	78	Portland	5397833	473128	fracture	042	80
Piers	5395314	469206	fracture	151	52	Portland	5397833	473128	fracture	220	82
Piers	5395314	469206	fracture	156	55	Portland	5397833	473128	fracture	048	85
Piers	5395314	469206	fracture	159	63	Portland	5397833	473128	fracture	030	86
Piers	5394354	470798	fracture	222	25	Portland	5397833	473128	fracture	237	88
Piers	5394354	470798	fracture	225	27	Portland	5395869	472503	gash	235	76
Piers	5394328	470955	fracture	047	79	Portland	5395869	472503	gash	230	90
Piers	5394328	470955	fracture	227	85	Portland	5395869	472503	gash	250	90
Piers	5394328	470955	fracture	044	86	Portland	5395837	472511	gash	060	82
Piers	5394328	470955	fracture	220	86	Portland	5395837	472511	gash	064	86
Piers	5394328	470955	fracture	051	88	Portland	5395837	472511	gash	065	89
Piers	5394328	470955	fracture	055	89	Portland	5395837	472511	gash	065	90
Piers	5394668	469930	gash	026	88	Portland	5395837	472511	gash	075	90
Piers	5394668	469930	gash	020	90	Portland	5395837	472511	gash	079	90
Piers	5394668	469930	gash	030	90	Portland	5395837	472511	gash	082	90
Piers	5394375	468911	min. fill.	075	29	Portland	5395837	472511	gash	094	90
Piers	5394375	468911	min. fill.	068	30	Portland	5395900	472518	gash	050	87
Piers	5394375	468911	min. fill.	081	30	Portland	5395900	472518	gash	040	90

Figure B 5: Brittle Fracture Measures

Domain	Northing	Easting	Type	Strike	Dip	Domain	Northing	Easting	Type	Strike	Dip
Piers	5394273	469029	min. fill.	060	52	Portland	5395900	472518	gash	050	90
Piers	5394273	469029	min. fill.	061	52	Portland	5395900	472518	gash	052	90
Piers	5394273	469029	min. fill.	064	56	Portland	5395900	472518	gash	055	90
Piers	5395170	469660	min. fill.	204	34	Russell	5399498	470000	fracture	031	65
Piers	5395170	469660	min. fill.	202	39	Russell	5399498	470000	fracture	016	68
Piers	5395170	469660	min. fill.	200	41	Russell	5399498	470000	fracture	009	69
Piers	5395170	469660	min. fill.	204	45	Russell	5399498	470000	fracture	015	69
Piers	5394029	471419	min. fill.	201	18	Russell	5399498	470000	fracture	020	73
Piers	5394029	471419	min. fill.	189	20	Russell	5399498	470000	fracture	016	75
Piers	5394029	471419	min. fill.	191	26	Russell	5399498	470000	fracture	019	77
Piers	5394029	471419	min. fill.	200	30	Russell	5399498	470000	fracture	026	78
Portland	5396469	471556	fracture	274	76	Russell	5399498	470000	fracture	024	84
Portland	5396469	471556	fracture	274	78	Russell	5399498	470000	fracture	039	85
Portland	5396469	471556	fracture	270	80	Russell	5399498	470000	fracture	210	88
Portland	5396469	471556	fracture	085	86	Russell	5399498	470000	fracture	020	90
Portland	5396469	471556	fracture	086	88	Russell	5399546	470009	fracture	220	80
Portland	5396096	471644	fracture	285	75	Russell	5399600	470077	fracture	021	86
Portland	5396096	471644	fracture	055	80	Russell	5399600	470077	fracture	221	88
Portland	5396096	471644	fracture	206	80	Russell	5399600	470077	fracture	035	90
Portland	5396096	471644	fracture	086	84	Russell	5399747	470128	fracture	276	85
Portland	5396096	471644	fracture	289	87	Russell	5399747	470128	fracture	255	86
Portland	5396096	471644	fracture	210	88	Russell	5399747	470128	fracture	272	90
Portland	5396096	471644	fracture	245	89	Russell	5399747	470128	fracture	275	90
Portland	5396096	471644	fracture	040	90	Russell	5399719	470363	fracture	021	84
Portland	5396096	471644	fracture	069	90	Russell	5399718	470392	fracture	178	84
Portland	5396096	471644	fracture	075	90	Russell	5399713	470419	fracture	005	90
Portland	5398008	472969	fracture	235	50	Russell	5399713	470419	fracture	066	90
Portland	5398008	472969	fracture	090	52	Russell	5399703	470437	fracture	184	75
Russell	5399703	470437	fracture	252	82	Sidney	5384089	479362	fracture	258	83
Russell	5399703	470437	fracture	346	82	Sidney	5384089	479362	fracture	259	86
Russell	5399703	470437	fracture	254	86	Sidney	5384089	479362	fracture	259	86
Russell	5399703	470437	fracture	190	90	Sidney	5384089	479362	fracture	260	86
Russell	5399699	470460	fracture	186	62	Sidney	5384089	479362	fracture	238	88
Russell	5399699	470460	fracture	008	68	Sidney	5386453	479427	fracture	200	79
Russell	5399699	470460	fracture	202	70	Sidney	5386453	479427	fracture	215	81
Russell	5399480	469679	gash	025	85	Sidney	5386453	479427	fracture	024	88
Russell	5399480	469679	gash	025	85	Sidney	5386453	479427	fracture	029	90
Russell	5399480	469679	gash	030	85	Sidney	5383877	479601	fracture	279	42
Russell	5399480	469679	gash	003	90	Sidney	5383877	479601	fracture	251	44
Sidney	5385514	477127	fracture	010	87	Sidney	5385318	479766	fracture	227	69
Sidney	5385514	477127	fracture	035	80	Sidney	5385318	479766	fracture	220	75
Sidney	5385514	477127	fracture	024	90	Sidney	5385318	479766	fracture	226	85
Sidney	5387289	478056	fracture	042	73	Sidney	5385318	479766	fracture	221	86
Sidney	5387289	478056	fracture	060	75	Sidney	5385317	479793	fracture	229	76
Sidney	5387289	478056	fracture	064	75	Sidney	5385317	479793	fracture	224	85
Sidney	5387289	478056	fracture	064	77	Sidney	5385317	479793	fracture	234	90
Sidney	5387306	478080	fracture	061	74	Sidney	5385298	479818	fracture	220	76
Sidney	5387306	478080	fracture	061	76	Sidney	5385298	479818	fracture	036	80
Sidney	5387306	478080	fracture	064	76	Sidney	5385298	479818	fracture	040	85
Sidney	5387306	478080	fracture	064	77	Sidney	5385258	479822	fracture	252	79
Sidney	5387239	478106	fracture	038	73	Sidney	5385258	479822	fracture	045	80
Sidney	5387239	478106	fracture	056	79	Sidney	5385258	479822	fracture	245	80
Sidney	5387239	478106	fracture	041	83	Sidney	5385258	479822	fracture	046	82
Sidney	5387239	478106	fracture	050	85	Sidney	5385258	479822	fracture	245	86
Sidney	5387239	478106	fracture	054	85	Sidney	5385258	479822	fracture	050	90
Sidney	5384951	478141	fracture	028	85	Sidney	5385186	479966	fracture	230	81

Figure B 5: Brittle Fracture Measures

Domain	Northing	Easting	Type	Strike	Dip	Domain	Northing	Easting	Type	Strike	Dip
Sidney	5384937	478195	fracture	201	63	Sidney	5385185	480089	fracture	185	58
Sidney	5384937	478195	fracture	195	79	Sidney	5385185	480089	fracture	185	60
Sidney	5384937	478195	fracture	008	90	Sidney	5385163	480097	fracture	200	63
Sidney	5384937	478195	fracture	009	90	Sidney	5385163	480097	fracture	034	65
Sidney	5384878	478303	fracture	210	39	Sidney	5385163	480097	fracture	195	65
Sidney	5384878	478303	fracture	212	44	Sidney	5385163	480097	fracture	207	68
Sidney	5384878	478303	fracture	190	55	Tsehum	5392106	469338	fracture	000	83
Sidney	5384878	478303	fracture	186	66	Tsehum	5392106	469338	fracture	004	84
Sidney	5384878	478303	fracture	183	69	Tsehum	5392106	469338	fracture	355	85
Sidney	5384878	478303	fracture	004	84	Tsehum	5392106	469338	fracture	004	90
Sidney	5384878	478303	fracture	184	86	Tsehum	5392115	469353	fracture	044	65
Sidney	5384505	478777	fracture	340	83	Tsehum	5392115	469353	fracture	039	70
Sidney	5384417	478904	fracture	218	85	Tsehum	5392115	469353	fracture	023	75
Sidney	5384405	478909	fracture	229	85	Tsehum	5392115	469353	fracture	020	85
Sidney	5384407	478925	fracture	246	38	Tsehum	5392132	469379	fracture	184	81
Sidney	5384407	478925	fracture	218	74	Tsehum	5392132	469379	fracture	184	81
Sidney	5384333	479058	fracture	157	74	Tsehum	5392132	469379	fracture	180	82
Sidney	5384333	479058	fracture	145	77	Tsehum	5392132	469379	fracture	070	85
Sidney	5384333	479058	fracture	146	80	Tsehum	5392132	469379	fracture	010	90
Sidney	5384333	479058	fracture	320	74	Tsehum	5392132	469379	fracture	016	90
Sidney	5384333	479058	fracture	355	76	Tsehum	5392146	469394	fracture	024	85
Sidney	5384333	479058	fracture	004	86	Tsehum	5392314	469683	fracture	019	90
Sidney	5384268	479148	fracture	074	79	Tsehum	5392314	469683	fracture	190	48
Sidney	5384268	479148	fracture	093	82	Tsehum	5392314	469683	fracture	195	65
Sidney	5384268	479148	fracture	258	83	Tsehum	5392314	469683	fracture	024	80
Sidney	5384268	479148	fracture	069	87	Tsehum	5392314	469683	fracture	206	84
Sidney	5384268	479148	fracture	096	87	Tsehum	5392314	469683	fracture	021	85
Sidney	5384268	479148	fracture	190	81	Tsehum	5392314	469683	fracture	024	86
Sidney	5384268	479148	fracture	000	84	Tsehum	5392244	470190	fracture	052	75
Sidney	5384268	479148	fracture	197	84	Tsehum	5392244	470190	fracture	046	77
Sidney	5384268	479148	fracture	186	86	Tsehum	5392244	470190	fracture	044	80
Sidney	5384268	479148	fracture	003	90	Tsehum	5392244	470190	fracture	044	83
Sidney	5384089	479362	fracture	050	63	Tsehum	5392244	470190	fracture	049	85
Sidney	5384089	479362	fracture	055	66	Tsehum	5392244	470190	fracture	211	86
Sidney	5384089	479362	fracture	048	79	Tsehum	5392244	470190	fracture	040	87
Tsehum	5392244	470190	fracture	221	88	Tsehum	5392682	471655	fracture	021	19
Tsehum	5392244	470190	fracture	224	89	Tsehum	5392682	471655	fracture	011	21
Tsehum	5392244	470190	fracture	020	90	Tsehum	5392682	471655	fracture	201	60
Tsehum	5392244	470190	fracture	025	90	Tsehum	5392682	471655	fracture	200	80
Tsehum	5392852	470271	fracture	005	86	Tsehum	5392682	471655	fracture	201	82
Tsehum	5392852	470271	fracture	195	86	Tsehum	5392682	471655	fracture	190	90
Tsehum	5392852	470271	fracture	014	88	Tsehum	5391814	471728	fracture	358	80
Tsehum	5392852	470271	fracture	190	88	Tsehum	5391814	471728	fracture	002	88
Tsehum	5392852	470271	fracture	190	89	Tsehum	5391814	471728	fracture	357	89
Tsehum	5392852	470271	fracture	194	90	Tsehum	5391654	471735	fracture	020	67
Tsehum	5392357	470314	fracture	005	63	Tsehum	5391654	471735	fracture	035	69
Tsehum	5392357	470314	fracture	355	75	Tsehum	5391654	471735	fracture	024	71
Tsehum	5392357	470314	fracture	000	80	Tsehum	5391654	471735	fracture	030	71
Tsehum	5392357	470314	fracture	010	90	Tsehum	5391654	471735	fracture	024	74
Tsehum	5392357	470314	fracture	358	87	Tsehum	5391654	471735	fracture	029	74
Tsehum	5392540	470489	fracture	011	78	Tsehum	5391654	471735	fracture	031	74
Tsehum	5392540	470489	fracture	194	80	Tsehum	5391654	471735	fracture	025	81
Tsehum	5392540	470489	fracture	192	82	Tsehum	5391654	471735	fracture	044	84
Tsehum	5392540	470489	fracture	190	84	Tsehum	5391654	471735	fracture	040	89
Tsehum	5392540	470489	fracture	009	86	Tsehum	5391654	471735	fracture	038	90
Tsehum	5391805	470597	fracture	195	75	Tsehum	5391865	471750	fracture	356	78

Figure B 5: Brittle Fracture Measures

Domain	Northing	Easting	Type	Strike	Dip	Domain	Northing	Easting	Type	Strike	Dip
Tsehum	5391805	470597	fracture	195	82	Tsehum	5391865	471750	fracture	355	83
Tsehum	5391805	470597	fracture	201	87	Tsehum	5391865	471750	fracture	355	85
Tsehum	5392360	470710	fracture	315	64	Tsehum	5391865	471750	fracture	346	86
Tsehum	5392360	470710	fracture	001	65	Tsehum	5391865	471750	fracture	347	86
Tsehum	5392360	470710	fracture	315	65	Tsehum	5391865	471750	fracture	359	88
Tsehum	5392360	470710	fracture	310	77	Tsehum	5391865	471750	fracture	356	89
Tsehum	5391360	470803	fracture	210	80	Tsehum	5391865	471750	fracture	009	90
Tsehum	5391360	470803	fracture	215	85	Tsehum	5391865	471750	fracture	019	90
Tsehum	5391360	470803	fracture	040	90	Tsehum	5391597	471775	fracture	034	75
Tsehum	5392825	470843	fracture	011	81	Tsehum	5391597	471775	fracture	030	76
Tsehum	5392720	470845	fracture	022	74	Tsehum	5391597	471775	fracture	160	87
Tsehum	5392720	470845	fracture	015	84	Tsehum	5391597	471775	fracture	160	90
Tsehum	5392720	470845	fracture	019	86	Tsehum	5391529	471850	fracture	037	60
Tsehum	5392124	471028	fracture	006	73	Tsehum	5391529	471850	fracture	034	87
Tsehum	5392124	471028	fracture	020	73	Tsehum	5391529	471850	fracture	039	90
Tsehum	5392124	471028	fracture	023	76	Tsehum	5392016	472168	fracture	009	72
Tsehum	5392124	471028	fracture	011	77	Tsehum	5392016	472168	fracture	013	73
Tsehum	5392124	471028	fracture	023	78	Tsehum	5392016	472168	fracture	014	74
Tsehum	5392124	471028	fracture	028	80	Tsehum	5392016	472168	fracture	019	74
Tsehum	5392124	471028	fracture	026	84	Tsehum	5392016	472168	fracture	012	75
Tsehum	5392280	471100	fracture	340	76	Tsehum	5392016	472168	fracture	007	78
Tsehum	5392280	471100	fracture	335	77	Tsehum	5392016	472168	fracture	004	80
Tsehum	5392280	471100	fracture	341	83	Tsehum	5392016	472168	fracture	011	82
Tsehum	5391817	471163	fracture	026	84	Tsehum	5391863	472209	fracture	007	59
Tsehum	5391817	471163	fracture	019	90	Tsehum	5391863	472209	fracture	006	63
Tsehum	5391817	471163	fracture	025	90	Tsehum	5391863	472209	fracture	005	64
Tsehum	5392674	471186	fracture	034	73	Tsehum	5391863	472209	fracture	010	64
Tsehum	5392674	471186	fracture	035	83	Tsehum	5391863	472209	fracture	009	66
Tsehum	5392674	471186	fracture	035	85	Tsehum	5391863	472209	fracture	008	67
Tsehum	5392321	471232	fracture	008	88	Tsehum	5391863	472209	fracture	210	68
Tsehum	5392321	471234	fracture	024	67	Tsehum	5391863	472209	fracture	204	73
Tsehum	5392313	471238	fracture	221	71	Tsehum	5391863	472209	fracture	007	75
Tsehum	5392313	471245	fracture	021	90	Tsehum	5391863	472209	fracture	199	75
Tsehum	5392309	471256	fracture	175	54	Tsehum	5391863	472209	fracture	200	78
Tsehum	5392307	471265	fracture	160	71	Tsehum	5391863	472209	fracture	030	90
Tsehum	5392446	471458	fracture	017	61	Tsehum	5391863	472209	fracture	240	74
Tsehum	5392446	471460	fracture	029	67	Tsehum	5391863	472209	fracture	240	77
Tsehum	5392446	471460	fracture	036	79	Tsehum	5391863	472209	fracture	244	85
Tsehum	5392603	471472	fracture	344	42	Tsehum	5391863	472209	fracture	256	88
Tsehum	5392603	471472	fracture	348	44	Tsehum	5392280	471100	gash	015	68
Tsehum	5392682	471655	fracture	035	12	Tsehum	5392280	471100	gash	010	80
Tsehum	5392682	471655	fracture	020	17	Tsehum	5392115	469353	fracture	273	58
Tsehum	5392115	469353	min. fill.	273	58	W Saanich	5393047	464564	fracture	240	58
Tsehum	5392314	469683	min. fill.	008	90	W Saanich	5393049	464589	fracture	240	45
Tsehum	5392314	469683	min. fill.	020	76	W Saanich	5393049	464589	fracture	140	70
Tsehum	5392314	469683	min. fill.	020	89	W Saanich	5393049	464589	fracture	135	74
W Saanich	5391680	464010	fracture	034	74	W Saanich	5393049	464589	fracture	043	59
W Saanich	5391670	464031	fracture	040	80	W Saanich	5393049	464589	fracture	045	66
W Saanich	5391655	464082	fracture	026	80	W Saanich	5393049	464589	fracture	025	68
W Saanich	5391654	464088	fracture	018	80	W Saanich	5390794	464797	fracture	355	75
W Saanich	5391654	464096	fracture	026	76	W Saanich	5391948	464934	fracture	024	51
W Saanich	5391747	464213	fracture	022	67	W Saanich	5391948	464934	fracture	010	65
W Saanich	5391774	464267	fracture	324	79	W Saanich	5391948	464934	fracture	005	72
W Saanich	5391793	464285	fracture	320	79	W Saanich	5393824	466018	fracture	010	78
W Saanich	5393038	464300	fracture	345	66	W Saanich	5393831	466018	fracture	010	80
W Saanich	5393038	464300	fracture	346	88	W Saanich	5393831	466018	fracture	010	80

Figure B 5: Brittle Fracture Measures

Domain	Northing	Easting	Type	Strike	Dip	Domain	Northing	Easting	Type	Strike	Dip
W Saanich	5393038	464300	fracture	340	90	W Saanich	5393845	466119	fracture	341	36
W Saanich	5391835	464313	fracture	145	69	W Saanich	5393845	466119	fracture	344	43
W Saanich	5391835	464313	fracture	150	84	W Saanich	5393845	466119	fracture	342	58
W Saanich	5393138	464330	fracture	080	44	W Saanich	5393845	466119	fracture	328	80
W Saanich	5393138	464330	fracture	095	70	W Saanich	5394110	467512	fracture	310	90
W Saanich	5391899	464358	fracture	051	71	W Saanich	5394110	467512	fracture	030	78
W Saanich	5391934	464390	fracture	030	68	W Saanich	5394110	467512	fracture	036	80
W Saanich	5391111	464477	fracture	080	65	W Saanich	5394110	467512	fracture	040	80
W Saanich	5391111	464477	fracture	066	74	W Saanich	5393630	468620	fracture	213	84
W Saanich	5391111	464477	fracture	050	76	W Saanich	5393630	468620	fracture	212	89
W Saanich	5392039	464499	fracture	040	71	W Saanich	5393630	468620	fracture	215	90
W Saanich	5393047	464564	fracture	245	54	N Coal	5392123	472636	Ca.vein	036	83
W Saanich	5393047	464564	fracture	250	54	N Coal	5392123	472636	Ca.vein	031	65
N Coal	5393041	472218	joint	081	11	N Coal	5392123	472636	Ca.vein	033	86
N Coal	5393041	472218	joint	010	12	N Coal	5392130	472639	Ca.vein	240	44
N Coal	5393041	472218	joint	046	17	N Coal	5392130	472639	Ca.vein	226	48
Piers	5395314	469206	joint	020	45	N Coal	5392130	472639	Ca.vein	242	50
Piers	5395314	469206	joint	023	49	N Coal	5392130	472639	Ca.vein	244	60
Piers	5395314	469206	joint	023	49	N Coal	5392130	472639	Ca.vein	215	73
Piers	5395314	469206	joint	024	51	N Coal	5392130	472639	Ca.vein	010	79
Piers	5395314	469206	joint	025	51	N Coal	5392130	472639	Ca.vein	006	80
Piers	5395314	469206	joint	027	51	N Coal	5392130	472639	Ca.vein	007	81
Portland	5395832	472514	joint	256	80	N Coal	5392134	472640	Ca.vein	302	55
Portland	5395832	472514	joint	260	80	N Coal	5392134	472640	Ca.vein	192	66
Portland	5398010	473091	joint	050	53	N Coal	5392134	472640	Ca.vein	194	72
Portland	5398010	473091	joint	190	71	N Coal	5392134	472640	Ca.vein	200	75
Portland	5396944	473405	joint	120	84	N Coal	5392134	472640	Ca.vein	298	76
Portland	5396944	473405	joint	117	87	N Coal	5392134	472640	Ca.vein	205	85
Portland	5396944	473405	joint	110	90	N Coal	5392142	472642	Ca.vein	212	66
Sidney	5383508	479941	joint	080	40	N Coal	5392142	472642	Ca.vein	216	72
Sidney	5385166	480011	joint	180	85	N Coal	5392142	472642	Ca.vein	215	75
Tsehum	5392146	469394	joint	206	80	N Coal	5392142	472642	Ca.vein	211	76
Piers	5394273	469029	Ca.vein	061	52	N Coal	5392142	472642	Ca.vein	205	78
Piers	5394273	469029	Ca.vein	064	56	Piers	5394444	468676	Ca.vein	063	66
Piers	5394273	469029	Ca.vein	065	50	Piers	5394444	468676	Ca.vein	055	64
Piers	5395170	469660	Ca.vein	204	34	Piers	5394444	468676	Ca.vein	053	61
Piers	5395170	469660	Ca.vein	202	39	Piers	5394444	468676	Ca.vein	060	66
Piers	5395170	469660	Ca.vein	200	41	Piers	5394375	468911	Ca.vein	075	29
Piers	5395170	469660	Ca.vein	204	45	Piers	5394375	468911	Ca.vein	075	35
Piers	5394029	471419	Ca.vein	201	18	Piers	5394375	468911	Ca.vein	068	30
Piers	5394029	471419	Ca.vein	189	20	Piers	5394375	468911	Ca.vein	081	30
Piers	5394029	471419	Ca.vein	191	26	Piers	5394273	469029	Ca.vein	060	52
Piers	5394029	471419	Ca.vein	200	30						
Piers	5394029	471419	Ca.vein	194	25						



Table B6: Foliation Measures

Domain	Northing	Easting	Type	Strike	Dip
Moresby	5397479	476205	foliation	269	34
Moresby	5397479	476205	foliation	274	36
Moresby	5397479	476205	foliation	272	37
Moresby	5397479	476205	foliation	030	42
Moresby	5397479	476205	foliation	280	42
Moresby	5397479	476205	foliation	279	45
Moresby	5397479	476205	foliation	310	49
Moresby	5397479	476205	foliation	349	50
Moresby	5397479	476205	foliation	283	54
Moresby	5397479	476205	foliation	296	60
Moresby	5397479	476205	foliation	070	64
Moresby	5397479	476205	foliation	055	70
Moresby	5397479	476205	foliation	352	73
Moresby	5397479	476205	foliation	005	75
Tsehum	5392221	471220	foliation	144	05
Tsehum	5392221	471220	foliation	100	06
Tsehum	5392221	471220	foliation	098	11
Tsehum	5392221	471220	foliation	182	11
Tsehum	5392221	471220	foliation	070	12
Tsehum	5392221	471220	foliation	134	16
Tsehum	5392221	471220	foliation	026	18
Tsehum	5392221	471220	foliation	038	20
Tsehum	5392224	471113	foliation	185	20
Tsehum	5392221	471220	foliation	128	21
Tsehum	5392224	471113	foliation	322	27
Tsehum	5392175	471172	foliation	110	30
Tsehum	5392221	471220	foliation	281	31
Tsehum	5392221	471220	foliation	100	33
Tsehum	5392221	471220	foliation	082	34
Tsehum	5392221	471220	foliation	116	34
Tsehum	5392224	471113	foliation	054	35
Tsehum	5392175	471172	foliation	119	36
Tsehum	5392175	471172	foliation	100	38
Tsehum	5392221	471220	foliation	105	38
Tsehum	5392229	471299	foliation	005	84
Tsehum	5392229	471299	foliation	002	86
Tsehum	5392229	471299	foliation	005	87
Domville	5391835	476238	foliation	070	29
Domville	5391835	476238	foliation	068	32
Domville	5391835	476238	foliation	068	35
Domville	5391835	476238	foliation	076	36
Domville	5391835	476238	foliation	067	38
Domville	5391666	476256	foliation	050	18
Domville	5391666	476256	foliation	196	21
Domville	5391676	476244	foliation	341	22
Domville	5391666	476256	foliation	146	32
Domville	5391676	476244	foliation	336	40
Domville	5391666	476256	foliation	122	45
Domville	5391666	476256	foliation	124	54
Domville	5391666	476256	foliation	024	63
Domville	5391666	476256	foliation	004	68
Domville	5391666	476256	foliation	325	68
Domville	5391666	476256	foliation	310	70
Domville	5391666	476256	foliation	202	74
Domville	5391666	476256	foliation	125	80
Domville	5391666	476256	foliation	024	85
NCoal	5392211	472688	foliation	305	68

Domain	Northing	Easting	Type	Strike	Dip
Moresby	5397479	476205	foliation	354	75
Moresby	5397479	476205	foliation	000	76
Moresby	5397479	476205	foliation	004	76
Moresby	5397479	476205	foliation	358	76
Moresby	5397479	476205	foliation	084	77
Moresby	5397479	476205	foliation	089	77
Moresby	5397479	476205	foliation	000	79
Moresby	5397479	476205	foliation	248	79
Moresby	5397479	476205	foliation	354	79
Moresby	5397479	476205	foliation	340	81
Moresby	5397479	476205	foliation	354	81
Moresby	5397479	476205	foliation	250	84
Moresby	5397479	476205	foliation	049	85
Moresby	5397479	476205	foliation	001	88
Tsehum	5392221	471220	foliation	284	41
Tsehum	5392221	471220	foliation	270	44
Tsehum	5392221	471220	foliation	070	45
Tsehum	5392224	471113	foliation	038	46
Tsehum	5392224	471113	foliation	029	54
Tsehum	5392221	471220	foliation	126	56
Tsehum	5392175	471172	foliation	088	60
Tsehum	5392175	471172	foliation	104	60
Tsehum	5392224	471113	foliation	205	60
Tsehum	5392224	471113	foliation	204	64
Tsehum	5392221	471220	foliation	266	64
Tsehum	5392224	471113	foliation	355	64
Tsehum	5392175	471172	foliation	086	65
Tsehum	5392221	471220	foliation	270	67
Tsehum	5392175	471172	foliation	094	69
Tsehum	5392224	471113	foliation	021	70
Tsehum	5392229	471299	foliation	180	70
Tsehum	5392224	471113	foliation	181	71
Tsehum	5392175	471172	foliation	086	72
Tsehum	5392221	471220	foliation	100	72
Tsehum	5392221	471220	foliation	270	72
Tsehum	5392221	471220	foliation	285	75
Tsehum	5392221	471220	foliation	005	80
Tsehum	5392224	471113	foliation	188	81
Tsehum	5392221	471220	foliation	045	90
Tsehum	5392221	471220	foliation	107	90
Tsehum	5392224	471113	foliation	165	90
Domville	5393491	475505	foliation	246	41
Domville	5393491	475505	foliation	255	54
Domville	5393491	475505	foliation	250	56
Domville	5393491	475505	foliation	245	58
Domville	5393491	475505	foliation	250	60
Domville	5393491	475505	foliation	242	65
Domville	5393491	475505	foliation	241	70
Domville	5393491	475505	foliation	252	74
Domville	5393491	475505	foliation	214	76
Domville	5393491	475505	foliation	238	77
Domville	5393491	475505	foliation	226	78
Domville	5393491	475505	foliation	240	78
Domville	5393491	475505	foliation	228	87
Domville	5393491	475505	foliation	245	89
NCoal	5392176	472657	foliation	335	10
NCoal	5392203	472675	foliation	330	28



Table B6: Foliation Measures

Domain	Northing	Easting	Type	Strike	Dip
NCoal	5392176	472657	foliation	284	70
NCoal	5392155	472646	foliation	290	75
NCoal	5392211	472688	foliation	242	76
NCoal	5392211	472688	foliation	324	77
NCoal	5392176	472657	foliation	305	80
NCoal	5392190	472667	foliation	280	84
NCoal	5392190	472667	foliation	114	85
NCoal	5392176	472657	foliation	298	85
NCoal	5392190	472667	foliation	322	86
NCoal	5392190	472667	foliation	282	90
Piers	5394437	469992	foliation	008	79
Piers	5394437	469992	foliation	016	80
Piers	5394437	469992	foliation	008	82
Piers	5395263	469624	foliation	120	83
Piers	5395263	469624	foliation	127	85
Piers	5395263	469624	foliation	112	90
Piers	5395263	469624	foliation	119	90
Piers	5394273	469029	foliation	318	54
Piers	5394273	469029	foliation	322	64
Piers	5394273	469029	foliation	322	70
Piers	5394444	468676	foliation	053	61
Piers	5394444	468676	foliation	055	64
Piers	5394444	468676	foliation	063	66
Piers	5394444	468676	foliation	042	72
Piers	5394031	471421	foliation	120	65
Piers	5394031	471421	foliation	128	66
Piers	5394031	471421	foliation	124	68
Piers	5394073	471427	foliation	299	70
Piers	5394221	471397	foliation	302	72
Piers	5394221	471397	foliation	310	74
Piers	5394073	471427	foliation	298	78
Piers	5394073	471427	foliation	290	80
Piers	5394221	471397	foliation	298	80
Piers	5393783	470871	foliation	125	53
Piers	5393965	470796	foliation	313	65
Piers	5393965	470796	foliation	315	65
Piers	5393783	470871	foliation	130	68
Piers	5393783	470871	foliation	140	68
Piers	5393965	470796	foliation	310	70
Piers	5393783	470871	foliation	120	73
Piers	5394286	470908	foliation	302	69
Piers	5394286	470908	foliation	302	70
Piers	5394286	470908	foliation	310	73
Piers	5394286	470908	foliation	308	75
Piers	5394286	470908	foliation	305	80
Saanich	5390701	464864	AP clev	262	54
Saanich	5390701	464864	AP clev	260	55
Saanich	5390701	464864	AP clev	258	58
Saanich	5390701	464864	AP clev	255	63
Saanich	5390681	464825	AP clev	295	64
Saanich	5390722	464766	AP clev	291	78
Saanich	5390681	464825	AP clev	291	79
Saanich	5390722	464766	AP clev	294	79
Saanich	5390722	464766	AP clev	281	81
Saanich	5390681	464825	AP clev	293	82
Saanich	5390722	464766	AP clev	110	84
Saanich	5390778	464768	AP clev	010	85

Domain	Northing	Easting	Type	Strike	Dip
NCoal	5392155	472646	foliation	348	35
NCoal	5392203	472675	foliation	315	38
NCoal	5392190	472667	foliation	342	44
NCoal	5392176	472657	foliation	320	55
NCoal	5392176	472657	foliation	314	58
NCoal	5392155	472646	foliation	300	60
NCoal	5392176	472657	foliation	311	60
NCoal	5392211	472688	foliation	255	64
NCoal	5392203	472675	foliation	296	64
NCoal	5392176	472657	foliation	295	65
NCoal	5392211	472688	foliation	274	66
NCoal	5392176	472657	foliation	332	66
NCoal	5392211	472688	foliation	245	68
Domville	5391355	476045	foliation	282	67
Domville	5391355	476045	foliation	279	71
Domville	5391355	476045	foliation	283	72
Domville	5391355	476045	foliation	287	72
Portland	5397895	473069	foliation	115	58
Portland	5397895	473069	foliation	111	62
Portland	5397895	473069	foliation	113	65
Portland	5397895	473069	foliation	115	65
Portland	5397895	473069	foliation	110	69
Moresby	5397425	475983	foliation	261	17
Moresby	5397425	475983	foliation	020	19
Moresby	5397425	475983	foliation	265	19
Moresby	5397425	475983	foliation	225	25
Moresby	5397425	475983	foliation	254	27
Moresby	5397425	475983	foliation	270	32
Moresby	5397425	475983	foliation	260	51
Moresby	5397425	475983	foliation	260	64
Moresby	5397425	475983	foliation	263	64
Moresby	5397425	475983	foliation	074	70
Moresby	5397425	475983	foliation	252	70
Moresby	5397425	475983	foliation	110	80
Moresby	5397425	475983	foliation	126	81
Moresby	5397425	475983	foliation	045	83
Domville	5391318	475977	foliation	092	72
Domville	5391318	475977	foliation	094	78
Domville	5391318	475977	foliation	094	80
Domville	5391318	475977	foliation	080	85
Tsehum	5392314	469683	foliation	228	40
Tsehum	5392314	469683	foliation	010	55
Tsehum	5392314	469683	foliation	280	62
Tsehum	5392314	469683	foliation	270	65
Tsehum	5392314	469683	foliation	275	65
Tsehum	5392132	469379	foliation	000	84
Tsehum	5392132	469379	foliation	005	86
Tsehum	5392132	469379	foliation	355	86
Tsehum	5391486	469422	foliation	315	50
Tsehum	5391486	469422	foliation	325	50
Tsehum	5391486	469422	foliation	312	55
Tsehum	5391486	469422	foliation	310	56
Tsehum	5391461	469485	foliation	309	75
Tsehum	5391461	469485	foliation	310	78
Tsehum	5391461	469485	foliation	305	80
Tsehum	5391461	469485	foliation	300	81
Saanich	5390722	464766	AP clev	110	86

Table B7: Fault Measures

Domain	Northing	Eastng	Type	Strike	Dip
Domville	5390270	476916	dextral	268	56
Domville	5390449	476758	dextral	235	26
Domville	5390449	476758	dextral	105	28
Domville	5390513	476679	dextral	235	85
Domville	5390535	476635	dextral	050	85
Domville	5391761	475023	dextral	345	85
Domville	5391773	476707	dextral	215	65
Domville	5390816	476341	reverse	177	38
Domville	5391354	476041	reverse	312	62
Domville	5390816	476341	sinstral	105	70
Domville	5391350	475868	sinstral	275	89
Forrest	5390352	475100	sinstral	235	76
Forrest	5390352	475100	sinstral	226	82
Forrest	5390352	475100	sinstral	250	74
Forrest	5389400	475889	unknown	029	85
Forrest	5389665	475477	unknown	212	79
Forrest	5389680	475461	unknown	220	77
Forrest	5389928	475125	unknown	209	77
Forrest	5389991	475429	unknown	063	54
Forrest	5389991	475429	unknown	046	59
Forrest	5389991	475429	unknown	049	64
Forrest	5389991	475429	unknown	065	71
Forrest	5389991	475429	unknown	074	71
Forrest	5389991	475429	unknown	071	74
Forrest	5390025	474990	unknown	108	29
Forrest	5390340	474910	unknown	090	66
Forrest	5390340	474910	unknown	035	76
Forrest	5390986	473677	unknown	120	14
Forrest	5390986	473677	unknown	155	20
Forrest	5390986	473677	unknown	219	87
Forrest	5390986	473677	unknown	034	89
Gooch	5389882	479271	dextral	191	71
Gooch	5389882	479271	dextral	198	73
Gooch	5389882	479271	dextral	196	61
Gooch	5389887	479076	dextral	180	85
Gooch	5389897	478916	dextral	330	29
Gooch	5389918	478207	dextral	250	57
Gooch	5389922	478119	dextral	166	85
Gooch	5389922	478119	dextral	160	88
Gooch	5389923	479461	dextral	330	85
Gooch	5389928	478092	dextral	164	90
Gooch	5389928	478092	dextral	163	85
Gooch	5389943	479388	dextral	320	80
Gooch	5389953	479637	dextral	327	83
Gooch	5389953	479638	dextral	330	60
Gooch	5390098	479531	dextral	335	80
Gooch	5390098	479531	dextral	340	80
Gooch	5390098	479531	dextral	355	75
Gooch	5390104	479540	dextral	232	72
Domain	Northing	Eastng	Type	Strike	Dip

Domain	Northing	Eastng	Type	Strike	Dip
Gooch	5390789	477912	unknown	309	60
Gooch	5390789	477912	unknown	331	64
Gooch	5390789	477912	unknown	319	67
Gooch	5390789	477912	unknown	325	71
Moresby	5397675	476620	reverse	225	79
Moresby	5397675	476794	reverse	250	70
Moresby	5397232	477461	unknown	228	86
Moresby	5397442	475964	unknown	345	57
Moresby	5397463	475943	unknown	345	64
Moresby	5397479	476205	unknown	033	90
Moresby	5397479	476205	unknown	028	90
Moresby	5397573	475716	unknown	030	90
Moresby	5397573	475740	unknown	325	67
Moresby	5397671	476588	unknown	220	80
Moresby	5397675	476620	unknown	217	80
Moresby	5397695	476672	unknown	205	90
N Coal	5392662	473047	dextral	340	90
N Coal	5392891	472604	dextral	170	90
N Coal	5392155	472646	unknown	310	75
N Coal	5392190	472667	unknown	294	90
N Coal	5393107	471823	unknown	175	90
N Coal	5393107	471823	unknown	045	90
N Coal	5393108	471853	unknown	355	82
N Coal	5393189	471535	unknown	156	21
N Coal	5393189	471535	unknown	314	09
N Coal	5393189	471535	unknown	144	30
Piers	5394140	470541	dextral	340	75
Piers	5394140	470541	dextral	340	75
Piers	5394156	470521	dextral	080	88
Piers	5394156	470521	dextral	080	88
Piers	5394379	470162	dextral	190	85
Piers	5394379	470162	dextral	190	85
Piers	5394302	469742	dextral	260	65
Piers	5394302	469742	dextral	260	65
Piers	5394273	469029	sinstral	345	75
Piers	5394273	469029	sinstral	345	75
Piers	5394668	469930	sinstral	045	90
Piers	5394668	469930	sinstral	045	90
Piers	5394770	468737	sinstral	000	90
Piers	5395076	468857	sinstral	123	48
Piers	5395076	468857	sinstral	123	48
Piers	5394151	470527	unknown	122	71
Piers	5394151	470527	unknown	122	71
Piers	5394221	471397	unknown	145	85
Piers	5394256	470575	unknown	180	65
Piers	5394256	470575	unknown	180	65
Piers	5394354	470798	unknown	021	51
Piers	5394354	470798	unknown	021	51
Piers	5394379	470162	unknown	185	14
Domain	Northing	Eastng	Type	Strike	Dip

Table B7: Fault Measures

Gooch	5390104	479540	dextral	235	72
Gooch	5390104	479540	dextral	230	70
Gooch	5390677	478192	dextral	080	57
Gooch	5390702	478156	dextral	181	25
Gooch	5390702	478156	dextral	185	44
Gooch	5390702	478156	dextral	216	78
Gooch	5390032	477851	normal	280	50
Gooch	5390060	477862	normal	070	40
Gooch	5389887	479076	sinstral	335	30
Gooch	5389920	478390	sinstral	080	29
Gooch	5389922	478077	sinstral	307	41
Gooch	5389927	478491	sinstral	199	69
Gooch	5389927	478491	sinstral	211	70
Gooch	5389927	478491	sinstral	204	75
Gooch	5389927	478491	sinstral	210	84
Gooch	5389932	477848	sinstral	320	40
Gooch	5389932	477848	sinstral	302	38
Gooch	5390046	477855	sinstral	299	40
Gooch	5389882	479271	unknown	210	68
Gooch	5389882	479271	unknown	198	71
Gooch	5389918	478207	unknown	260	66
Gooch	5389949	479684	unknown	191	38
Gooch	5389964	479684	unknown	155	32
Portland	5397386	473468	sinstral	275	67
Portland	5398040	472758	sinstral	068	80
Portland	5398087	472723	sinstral	241	87
Portland	5398111	472767	sinstral	264	76
Portland	5398111	472767	sinstral	240	89
Portland	5395837	472511	unknown	025	90
Portland	5395869	472503	unknown	030	90
Portland	5395900	472518	unknown	025	90
Portland	5396096	471644	unknown	001	90
Portland	5396685	473139	unknown	230	80
Portland	5397653	473302	unknown	227	45
Portland	5397653	473302	unknown	090	90
Portland	5398010	473091	unknown	222	85
Portland	5398068	472853	unknown	172	64
Russell	5399343	469844	dextral	048	69
Russell	5399423	469666	dextral	356	64
Russell	5399617	470164	normal	175	65
Russell	5399617	470164	normal	170	71
Russell	5399617	470164	reverse	185	54
Russell	5399343	469844	unknown	055	82
Russell	5399480	469679	unknown	180	80
Russell	5399546	470009	unknown	010	70
Russell	5399546	470009	unknown	015	90
Russell	5399600	470077	unknown	356	46
Russell	5399718	470230	unknown	047	70
Domain	Northing	Easting	Type	Strike	Dip

Piers	5394379	470162	unknown	185	14
Piers	5394770	468737	unknown	113	82
Piers	5394770	468737	unknown	000	90
Piers	5394770	468737	unknown	113	82
Piers	5395001	469707	unknown	290	80
Piers	5395001	469707	unknown	290	80
Piers	5395076	468857	unknown	200	11
Piers	5395076	468857	unknown	200	46
Piers	5395076	468857	unknown	200	11
Piers	5395076	468857	unknown	200	46
Piers	5395076	468857	unknown	225	90
Piers	5395076	468857	unknown	225	90
Portland	5397818	473136	dextral	145	50
Portland	5396358	471642	normal	045	40
Portland	5396484	471583	normal	355	48
Portland	5397386	473468	normal	095	23
Portland	5398058	472390	normal	140	90
Portland	5398058	472390	normal	320	44
Portland	5398058	472390	normal	131	88
Portland	5396455	471636	reverse	206	54
Portland	5396455	471636	reverse	218	39
Portland	5396455	471636	reverse	226	21
Portland	5397386	473468	sinstral	278	60
Sidney	5386494	479300	unknown	043	66
Sidney	5386494	479300	unknown	045	69
Tsehum	5391930	472019	dextral	024	62
Tsehum	5392229	471299	dextral	354	86
Tsehum	5392229	471299	dextral	358	40
Tsehum	5392229	471299	dextral	359	90
Tsehum	5392229	471299	dextral	359	33
Tsehum	5392280	471100	dextral	340	75
Tsehum	5390569	470715	sinstral	310	80
Tsehum	5391908	471952	sinstral	012	80
Tsehum	5391461	469485	unknown	305	40
Tsehum	5391461	469485	unknown	310	48
Tsehum	5391502	470574	unknown	200	74
Tsehum	5391810	471690	unknown	086	84
Tsehum	5392123	469367	unknown	023	72
Tsehum	5392123	469367	unknown	023	72
W Saanich	5393079	469403	dextral	030	90
W Saanich	5393087	469384	dextral	025	80
W Saanich	5393861	465907	dextral	355	80
W Saanich	5393012	464672	reverse	155	80
W Saanich	5393012	464672	reverse	325	80
W Saanich	5393012	464672	reverse	298	87
W Saanich	5393012	464672	reverse	319	90
W Saanich	5390721	464785	sinstral	044	35
W Saanich	5390764	464774	sinstral	038	40
Domain	Northing	Easting	Type	Strike	Dip

Table B7: Fault Measures

Sidney	5383144	480193	dextral	210	72
Sidney	5383144	480193	dextral	210	74
Sidney	5384333	479058	reverse	191	81
Sidney	5385211	479935	sinstral	215	78
Sidney	5385211	479935	sinstral	220	80
Sidney	5385211	479935	sinstral	221	84
Sidney	5385211	479935	sinstral	200	80
Sidney	5385211	479935	sinstral	196	86
Sidney	5385211	479935	sinstral	217	88
Sidney	5385242	479868	sinstral	054	63
Sidney	5385242	479868	sinstral	046	69
Sidney	5385242	479868	sinstral	061	72
Sidney	5385242	479868	sinstral	055	80
Sidney	5385330	479739	sinstral	254	73
Sidney	5385330	479739	sinstral	040	75
Sidney	5385330	479739	sinstral	040	76
Sidney	5385330	479739	sinstral	043	85
Sidney	5385379	479745	sinstral	248	70
Sidney	5385379	479745	sinstral	240	76
Sidney	5386588	479144	sinstral	057	65
Sidney	5386588	479144	sinstral	060	84
Sidney	5387289	478056	sinstral	060	75
Sidney	5387306	478080	sinstral	061	74
Sidney	5383140	480179	unknown	076	43

W Saanich	5391823	464303	unknown	016	84
W Saanich	5392985	464506	unknown	140	50
W Saanich	5393307	464420	unknown	151	79
W Saanich	5393567	464693	unknown	321	84
Sidney	5384539	478762	unknown	051	90
Sidney	5384751	478520	unknown	215	37
Sidney	5384812	478441	unknown	205	45
Sidney	5384812	478441	unknown	185	50
Sidney	5384852	478378	unknown	255	52
Sidney	5384852	478378	unknown	262	52
Sidney	5384852	478378	unknown	256	58
Sidney	5385199	480050	unknown	200	45
Sidney	5385199	480050	unknown	210	56
Sidney	5385199	480050	unknown	180	72
Sidney	5385199	480050	unknown	190	72
Sidney	5385368	479760	unknown	220	71
Sidney	5385368	479760	unknown	229	81
Sidney	5385368	479760	unknown	236	84
Sidney	5385368	479760	unknown	239	85
Sidney	5385392	479694	unknown	256	66
Sidney	5385392	479694	unknown	254	69
Sidney	5385392	479694	unknown	250	73
Sidney	5386492	479334	unknown	078	78
Sidney	5386494	479300	unknown	055	54
Sidney	5386494	479300	unknown	046	57
Sidney	5386494	479300	unknown	045	63

Table B8: Fold measurements from Domville Island

UTM		fold #	Axial Plane		Hinge Line	
Northing	Easting		Strike	Dip	Trend	Plunge
5391277	475966	1	280	34	090	07
		1			092	15
		1			090	10
5391167	476018	2	330	61	132	31
		2			135	33
		2			134	30
		2			128	30
5391155	476022	3	330	55	125	27
		3			126	29
		3			130	30
5391104	476025	4	336	74	145	40
		4			143	39
		4			140	39
5391104	476025	5	330	58	115	50
		5			110	45
		5			112	45
		5			110	44
5391104	476025	6	359	48	145	35
		6			140	34
		6			143	35
5391104	476025	7	040	50	144	47
		7			145	48
		7			144	50
5391104	476025	8	030	55	140	44
		8			135	50
		8			136	45
		8			135	44
5391104	476025	9	340	57	120	40
		9			125	42
		9			130	42
		9			122	48
5391104	476025	10	330	43	099	32
		10			110	30
		10			092	34
		10			095	36
5391104	476025	11	355	50	145	31
		11			150	28
		11			145	33
5390856	476307	12	344	70	140	50
		12			136	52
		12			140	55
		12			130	50
		12			135	55
5390856	476307	13	335	65	115	50
		13			119	50
		13			120	48
		13			124	51
		13			119	52
5390856	476307	14	350	65	126	56
		14			130	55
		14			120	50
		14			120	50
		mean			344	55

Table B9: Fold measures from Piers Island

Fold 1	Fold Limbs			
UTM:	Strike	Dip		
5394302	244	85	beta axis	
469742	244	85	Trend Plunge	
	246	86	152	47
	248	88		
	345	38	bisecting surface	
	349	38	strike dip	
	342	43	034	64
	345	51		

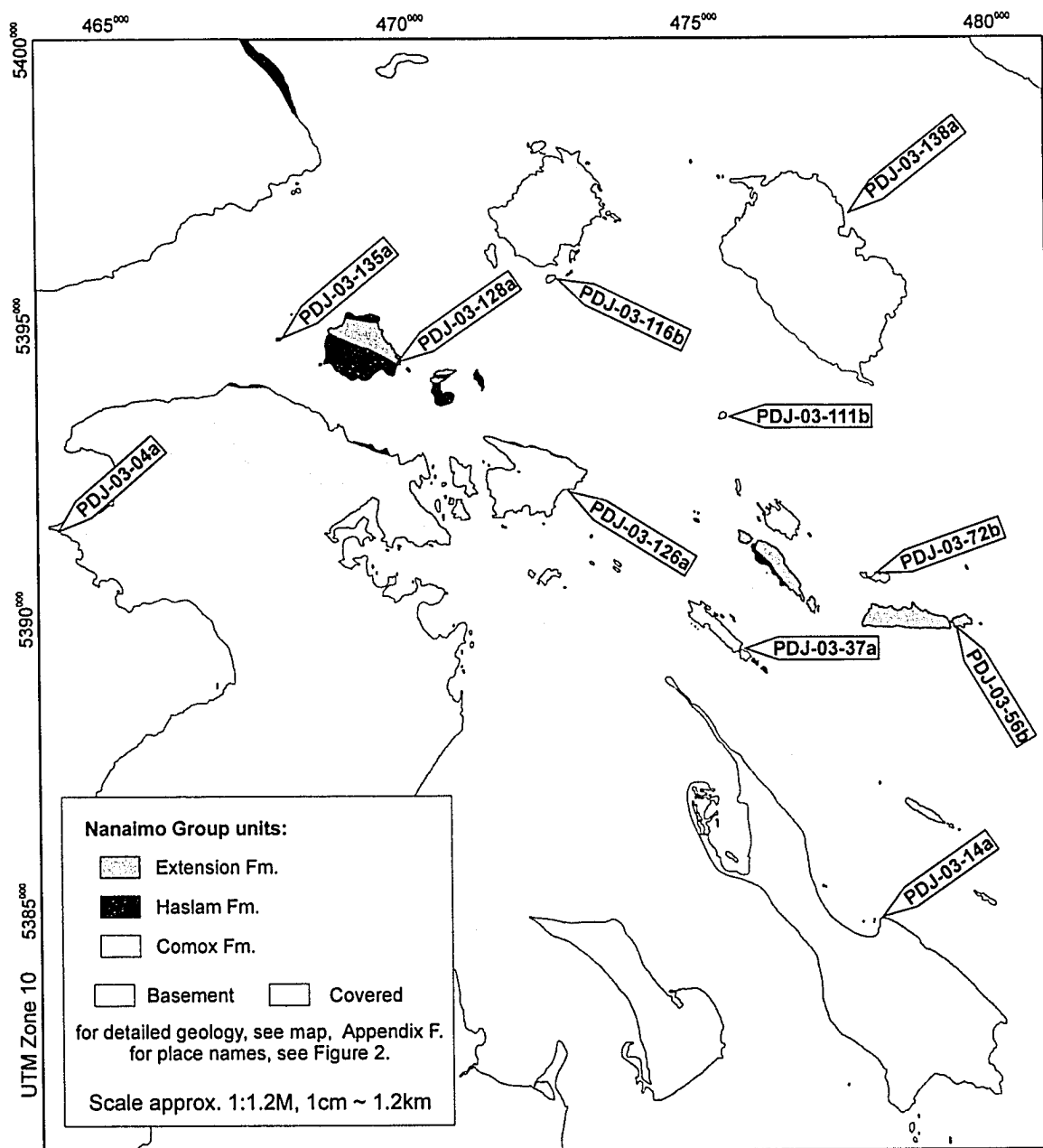
Fold 2	Fold Limbs			
UTM:	Strike	Dip		
5394302	006	40	beta axis	
469742	009	46	Trend Plunge	
	018	48	154	50
	009	50		
	267	62	bisecting surface	
	268	64	strike dip	
	269	64	055	79
	267	66		

Fold 3	Fold Limbs			
UTM:	Strike	Dip		
5394698	052	71	beta axis	
468762	060	72	Trend Plunge	
	051	73	164	44
	054	75		
	331	45	bisecting surface	
	334	46	strike dip	
	325	49	274	72
	331	49		

## **Appendix C: Thin Section Petrography.**

Twenty one sandstone hand samples were cut for thin sections, representing all three of the Nanaimo Group formations mapped in the field area. Thin sections were prepared by Vancouver Petrographics and stained with sodium cobaltinitrite to aid in the identification of K-feldspars. Thin sections allowed improved description of lithology by qualitative analysis of clast composition, cement types and diagenesis, and textures. Eleven thin sections were selected for modal grain analysis on the basis of grain size, "freshness" of samples, and geographic and stratigraphic dispersal throughout the field area (Diagram C1). Modal analysis used a random search pattern, and counts were performed until 100 grains had been counted (stops on matrix, pore space, or cement were counted in order to estimate proportions of each, but were not included in the minimum 100 points required for framework modal analysis). Counts were performed to allow plotting framework grain distribution on both Folk (1974) and Dickinson *et al.* (1983; as described in Dickinson, 1985) ternary diagrams. It should be noted that some controls suggested by Dickinson (1985), including strict framework grain size limits and staining for both potassium feldspars and plagioclase, were not followed.

Following are detailed descriptions of the eleven thin sections selected for modal grain analysis.

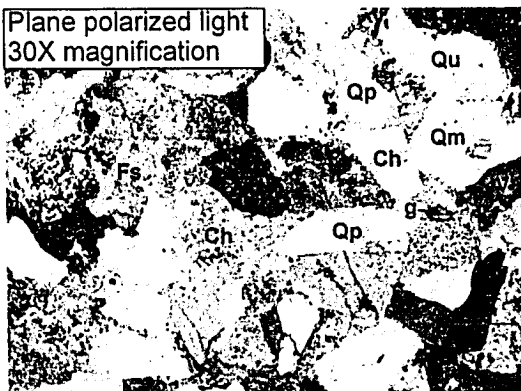


**Figure C 1: Geographic distribution of then section sample sites.**

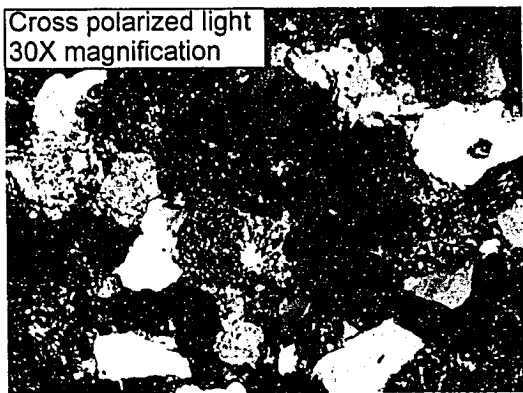


## Sample PDJ-03-04a

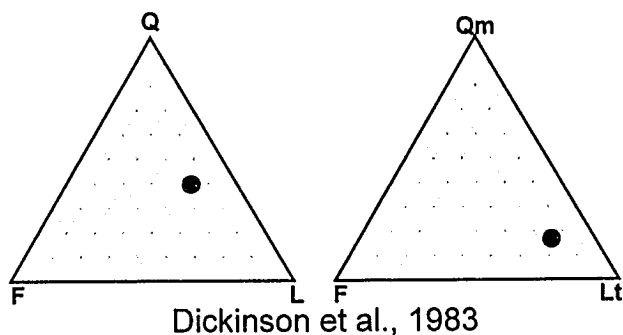
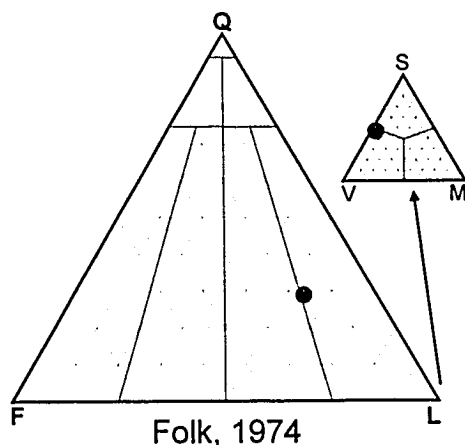
Plane polarized light  
30X magnification



Cross polarized light  
30X magnification



This sample is a volcanic litharenite which displays a variety of quartz types, including monocrystalline with straight extinction (Qm), monocrystalline with undulose extinction (Qu), polycrystalline with sutured contacts (Qp) and chert (Ch). Lithic fragments are dominated by volcanics (V) and the cement is mostly clay (cc) with some calcite. Feldspar grains are sericitized (Fs), and rare glauconite (g) and detrital mica grains (m) are present.



Comox Formation, Saanich Member.  
Coal Point, Saanich Peninsula,  
UTM 464096 5391654

### Texture

**Modal grain size:** 0.40 mm (medium grained)

**Roundness:** subangular

**Sorting:** moderate to well

### Composition:

**Folk (1974): Volcanic Litharenite**

**Matrix:** 5%

**Quartz:** 40%. Both mono- and poly-crystalline. Crystals with straight and undulose extinction. Polycrystalline fragments are generally well sutured.

**Feldspar:** 16%. Most plagioclase with simple twinning, minor amounts of microcline and orthoclase.

**Lithics:** 44%. Dominantly aphanitic dark volcanics, with significant chert and mudstones.

**Accessory Minerals:** Detrital mica grains (<5%), some hematite, chlorite and opaques.

### Cement/Diagenesis

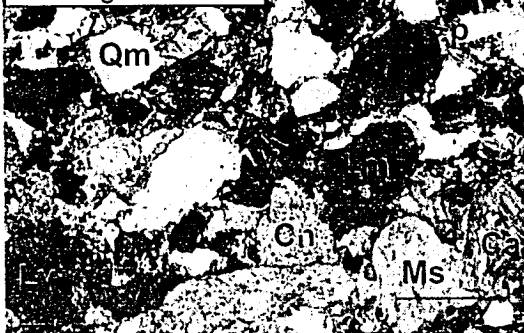
**Cement Types:** clay with minor calcite, rare hematite staining, trace glauconite.

**Grain contacts:** straight and point contacts, some deformation of softer lithic grains, no penetrative contacts.

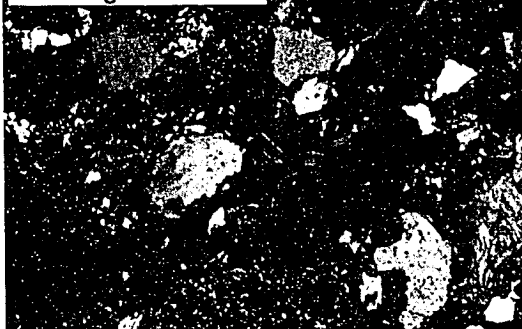
**Alteration:** sericitization of feldspars, some glauconite and chlorite..

## Sample PDJ-03-14a

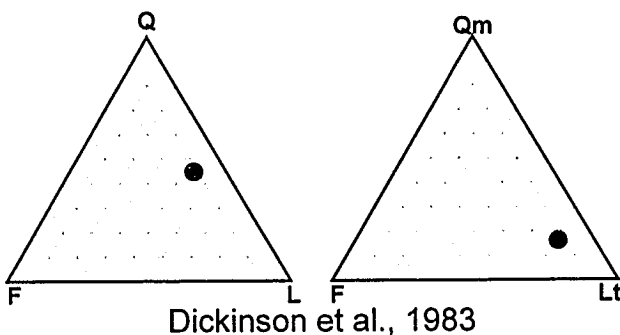
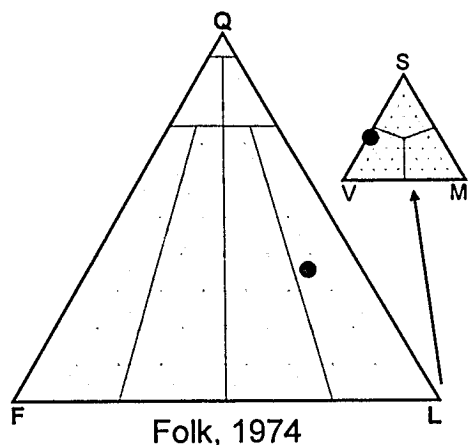
Plane polarized light  
30X magnification



Cross polarized light  
30X magnification



This volcanic litharenite shows numerous lithic fragments, including volcanics with visible feldspar lathes (V), or aphanitic (Lv), along with subangular monocrystalline quartz grains (Qm), fine-grained sedimentary lithics (Lm), including calcite fragments (Ca) and chert grains (Ch), and several potassium feldspar grains (stained yellow), at least one with sericitization accenting microcline twinning (Ms). Generally matrix-rich, with abundant opaque accessory minerals. Grain contacts only interpenetrate where large hardness contrasts exist, like an angular quartz grain penetrating a weathered mica grain (p).



Comox Formation, Saanich Member  
Bay on east side of Sidney Island,  
UTM 478073 5384866

### Texture

**Modal grain size:** 0.30 mm,  
(range 0.25 - 0.75mm)

**Roundness:** subangular to subrounded

**Sorting:** moderate to poor

### Composition

**Folk (1974):** Volcanic Litharenite

**Matrix:** 10%

**Quartz:** 36%. mostly monocrystalline with straight extinction, polycrystalline examples are both sutured and unsutured, few stretched

**Feldspar:** 12%. dominated by untwinned plagioclase, few albite twins and rare microcline.

**Lithics:** 52%. aphanitic volcanics dominate, with some chert and fine-grained sedimentary clasts, including calcite shell fragments, no identified metamorphic fragments.

**Accessory Minerals:** mica, biotite grains commonly deformed by harder grains, chlorite in mud matrix, some opaques, hematite.

### Cement/Diagenesis

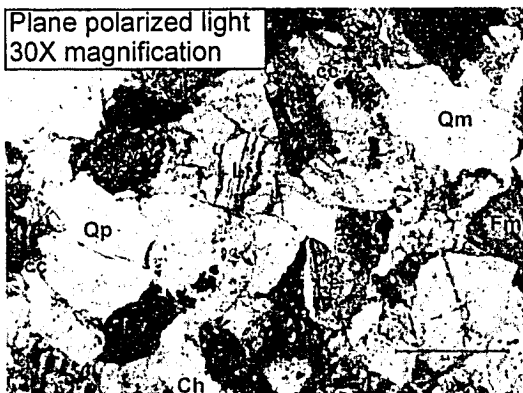
**Cement Types:** Cement up to 5%. Mostly hematite stained or chlorite altered clay. No overgrowths

**Grain contacts:** point, concave-convex. Some interpenetration of harder grains into softer grains.

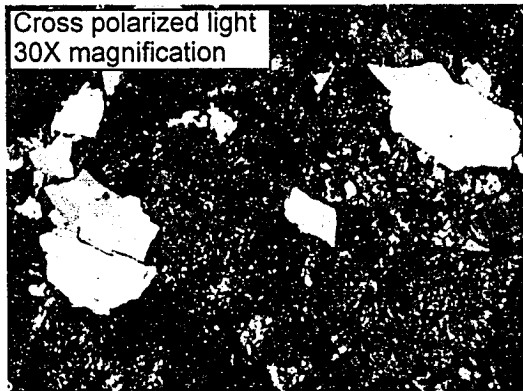
**Alteration:** Sericite after feldspars, chlorite after micas in matrix and lesser in mudstone clasts.

## Sample PDJ-03-37a

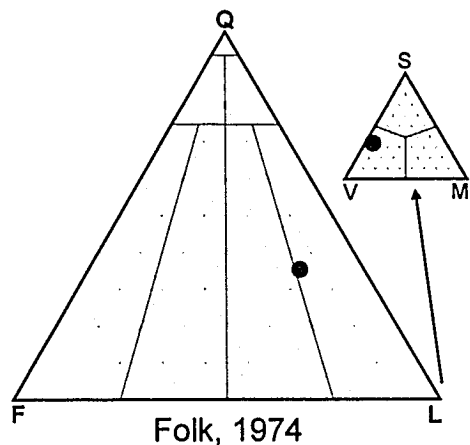
Plane polarized light  
30X magnification



Cross polarized light  
30X magnification



This sample of litharenite shows quartz both monocrystalline (Qm) and polycrystalline (Qp) along with Chert (Ch). Lithic fragments are mostly volcanic (Lv), with some foliated grains (Lf) and a single fragment comprising large quartz and feldspar crystals, likely of an extrusive source (Le). A large microcline grain (Fm) shows tartan twinning. muddy matrix is chloritized, and there is some calcite cement visible (cc).



Comox Formation, Saanich Member  
Forrest Island, south end.  
UTM 475728 5389564

### Texture

**Modal grain size:** 0.6 mm  
(lower coarse grained)

**Roundness:** subangular to subrounded

**Sorting:** moderate to well

### Composition

**Folk (1974): Volcanic Litharenite**

**Matrix:** <10%

**Quartz:** 35%. Quartz grains are almost evenly distributed between monocrystalline types with straight extinction and polycrystalline samples, the majority of which have very small, sutured crystals.

**Feldspar:** 17%. Simple and albite twinned plagioclase types are equally distributed with K-feldspars, with rare microcline twinning.

**Lithics:** 48%. Many dark-coloured aphanitic grains, some with feldspar lathes in dark groundmass (volcanics). Polycrystalline quartz at all scales, from abundant chert to quartzite. Few foliated grains, no large micas or other accessory grains.

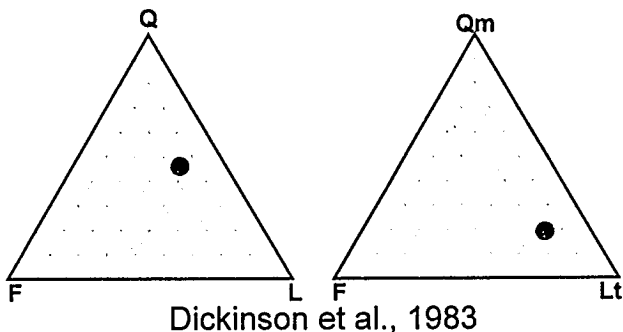
**Accessory Minerals:** few opaques, chlorite in matrix.

### Cement/Diagenesis

**Cement Types:** calcite and chloritized mud.

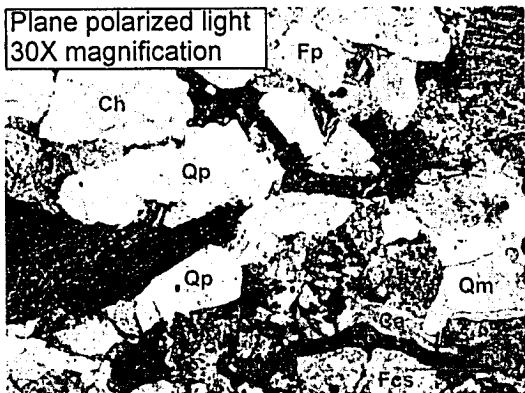
**Grain contacts:** point contacts, some concave/convex, little interpenetration

**Alteration:** Mud matrix is chloritized, some sericitization of feldspars.

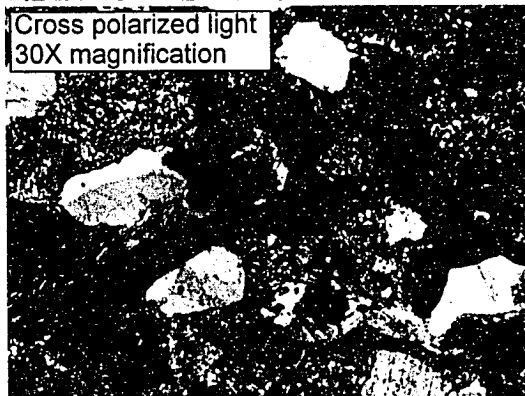


## Sample PDJ-03-56b

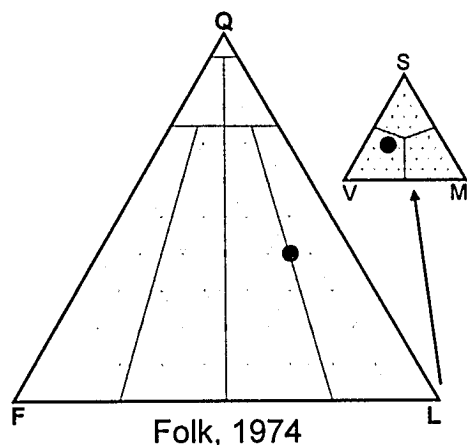
Plane polarized light  
30X magnification



Cross polarized light  
30X magnification



This coarse-grained volcanic litharenite shows both polycrystalline (Qp) and monocrystalline (Qm) quartz grains, and several generally angular lithic fragments, including a weathered mudstone (Lm) and a volcanic fragment with abundant feldspar lathes (Lv). Generally rare large feldspar grains are slightly sericitized (Fp), and soft biotite grains are deformed (Lb), rust. The large polycrystalline calcite area (Ca) is interpreted to represent a deformed fossil fragment, as there is little evidence elsewhere of large volumes of pore-filling calcite cement.



Extension Formation,  
Gooch Island,  
UTM 479418 5389907

### Texture

**Modal grain size:** 0.5 - 0.6 mm  
(coarse grained)

**Roundness:** subrounded

**Sorting:** moderate

### Composition

**Folk (1974): Volcanic Litharenite**

**Matrix:** 5%

**Quartz:** 40%. both mono and polycrystalline quartz, mostly straight extinction, some with sutures, few showing stretching.

**Feldspar:** 14%. Mostly plagioclase, abundant albite twining, some carlsbad, little microcline.

**Lithics:** 45%. dominated by fine-grained volcanics, many with visible feldspar lathes, rarely aligned, some foliated clasts, and some mudstones. Abundant chert, several calcite shell fragments, large biotite grains.

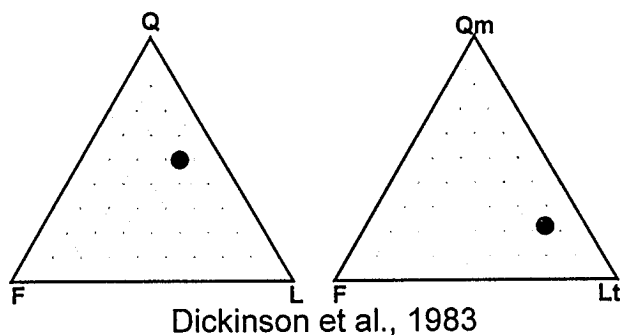
**Accessory Minerals:** Many large biotite mica grains, some very small opaque mineral grains, chlorite, minor sericite.

### Cement/Diagenesis

**Cement Types:** Hematite, clay.

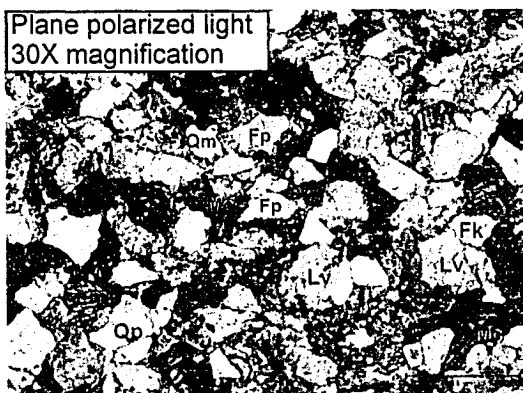
**Grain contacts:** dominantly straight, some convex-concave, soft minerals deformed.

**Alteration:** chloritization of clays, minor sericitization.

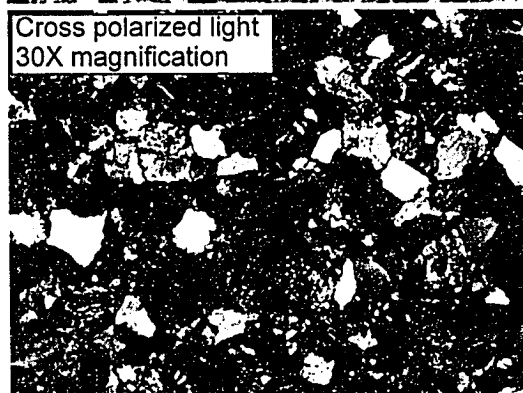


## Sample PDJ-03-72b

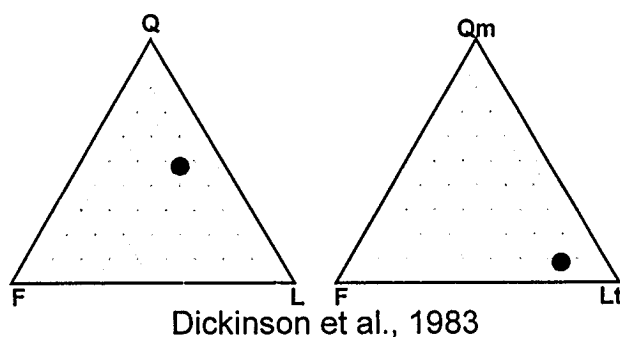
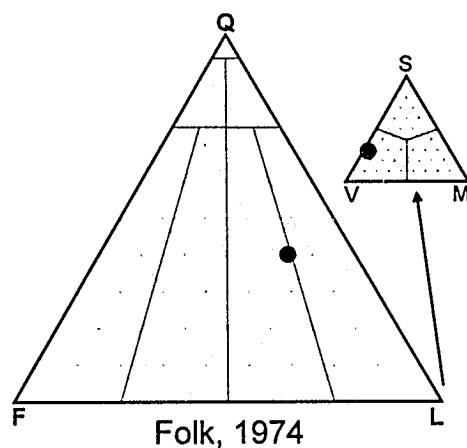
Plane polarized light  
30X magnification



Cross polarized light  
30X magnification



This sample of medium-grained arenite is rich in sercitized plagioclase grains (Fp), some displaying simple or albite twins (Pt), and a single stained potassium feldspar (Pk). The quartz grains are dominantly small, straight-extinction monocrystalline types (Qm), with some polycrystalline grains (Qp). Volcanic fragments (Lv) have visible feldspar lathes in an aphanitic groundmass. One lithic fragment displays phyllitic texture Lm). Detrital mica grains are partially altered to chlorite (Mc).



Comox Formation, Saanich Member  
north coast, Comet Island.  
UTM 478180 5390810

### Texture

**Modal grain size:** 0.25 mm (medium grained)

**Roundness:** subangular

**Sorting:** moderate to good

### Composition

**Folk (1974):** Feldspathic Litharenite

**Matrix:** 10%

**Quartz:** 40%. Monocrystalline most common in smaller grains, dominantly straight extinction. Polycrystalline, some with weathered sutures. No stretched.

**Feldspar:** 17%. Plagioclase with simple or albite twinning more common than potassium -feldspars. Most plagioclase are moderately altered to sericite.

**Lithics:** 44%. Volcanic fragments, lesser sedimentary (siltstone/mudstone) and chert. rare phyllitic clasts, detrital mica grains

**Accessory Minerals:** Sericite, glauconite, chlorite, abundant opaques

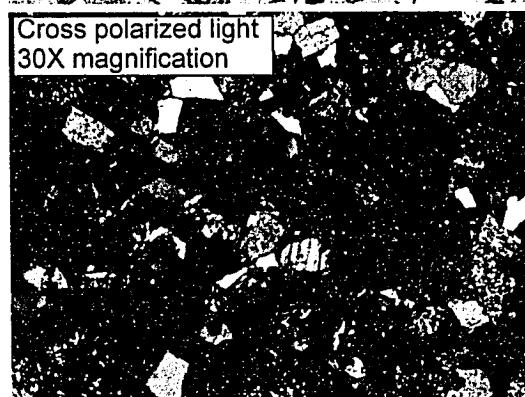
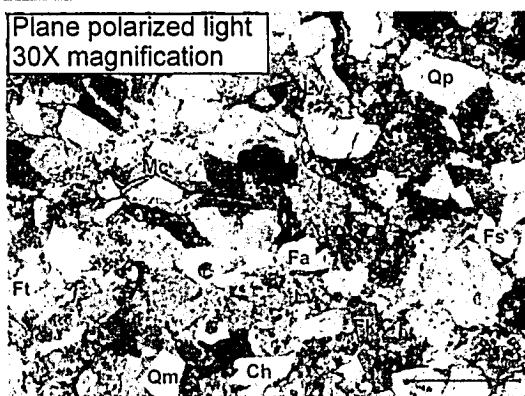
### Cement/Diagenesis

**Cement Types:** Hematite, clay.

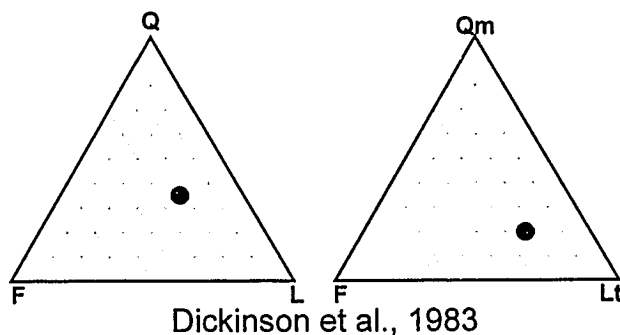
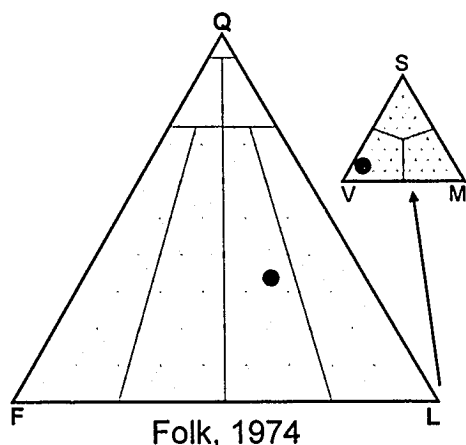
**Grain contacts:** point, concave/convex, few penetrative, some deformation of soft grains

**Alteration:** sericite-after feldspars, chlorite after biotite,

## Sample PDJ-03-111b



This feldspathic litharenite displays a wide range of feldspar grain types, including those with simple twinning (Ft), and albite twinning (Fa), some (stained) K-spars (Fk), and sericitized plagioclase (Fs). The quartz grains are mono and poly crystalline (Qm, Qp), along with abundant chert (Ch) and volcanic rock fragments (Lv). A large, deformed mica grain has been completely replaced with chlorite (Mc), and there is an abundance of dark and opaque minerals in the clay cement surrounding most grains.



Comox Formation,  
Imrie island,  
UTM 475455 5393542

### Texture

**Modal grain size:** 0.3 mm (medium grained)

**Roundness:** subangular

**Sorting:** moderate to good

### Composition

**Folk (1974): Feldspathic Litharenite**

**Matrix:** 15%

**Quartz:** 34%. Small, monocrystalline grains, few with undulose extinction. Polycrystalline grains usually only a few sutured crystals.

**Feldspar:** 22%. Potassium feldspars are commonly polycrystalline, plagioclase display albite and carlsbad twins, all sericitized.

**Lithics:** 44%. many aphanitic volcanics, some aligned grains in metamorphic grains, some chert and some brown mudstones

**Accessory Minerals:** Sericite, chlorite, hematite, some opaques and deformed mica grains.

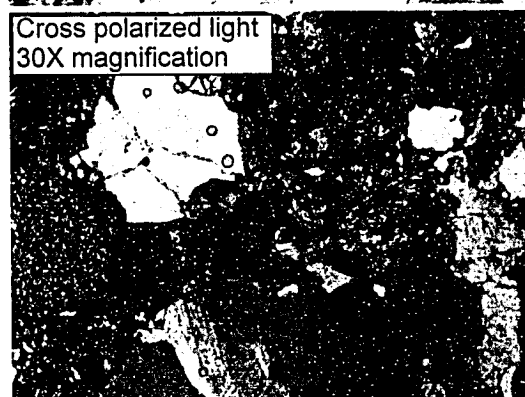
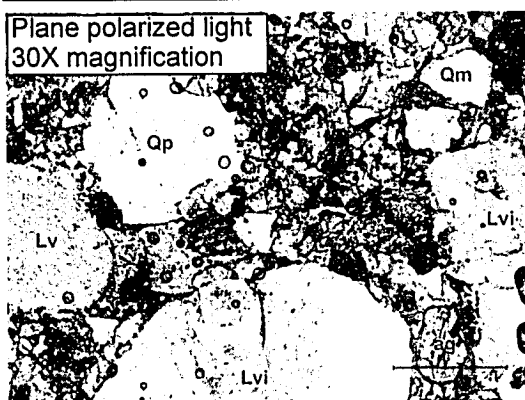
### Cement/Diagenesis

**Cement Types:** Clay, minor hematite staining around grains.

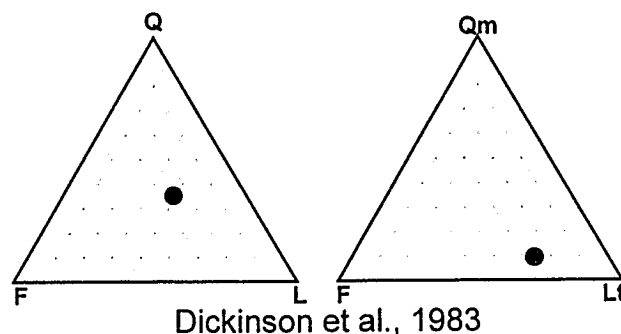
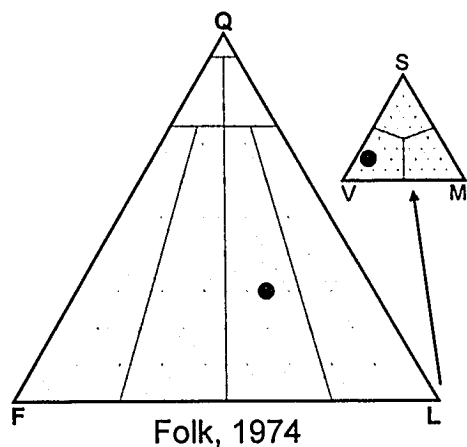
**Grain contacts:** point, straight, convex-concave, few interpenetrating, only softest grains are deformed.

**Alteration:** Sericite after feldspars, chlorite after micas.

## Sample PDJ-03-116b



This coarse-grained (but poorly sorted) litharenite has several large lithic fragments, including a volcanic rock (Lv) with chloritized matrix between interlocked microcrystalline quartz or feldspar, and two intrusive feldspar-quartz agglomerations (Lvi). Quartz grains are monocrystalline (Qm) and polycrystalline (Qp), most with straight extinction, and accessory minerals include a large detrital augite grain (ag) and opaques.



Comox Formation, Saanich Member  
Hood Island, Princess Bay,  
UTM 472497 5395963

### Texture

**Modal grain size:** 0.5 -2.0 mm (coarse grained)

**Roundness:** subrounded to subangular

**Sorting:** poor

### Composition

**Folk (1974): Fledspathic Litharenite**

**Matrix:** 15%

**Quartz:** 30%. few monocrystalline grains, only smallest grain size. Most polycrystalline and well sutured, none stretched.

**Feldspar:** 26%. Dominantly simple and albite twinned plagioclase. Some potassium feldspars and rare microcline. Numerous polycrystalline grains present.

**Lithics:** 44%. Some large grained quartz and feldspar agglomerate, interpreted to be intrusive volcanics. Dominantly microcrystalline and aphanitic volcanic fragments. Many fossil fragments.

**Accessory Minerals:** sericite, chlorite, deformed mica grains, augite, opaques, hematite.

### Cement/Diagenesis

**Cement Types:** clay, some calcite, hematite.

**Grain contacts:** smooth, convex/concave, only very soft grains are deformed, no interpenetration.

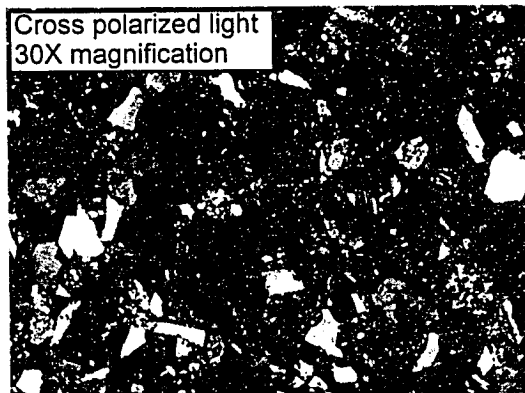
**Alteration:** sericite after feldspars. chlorite in detrital micas.

## Sample PDJ-03-126a

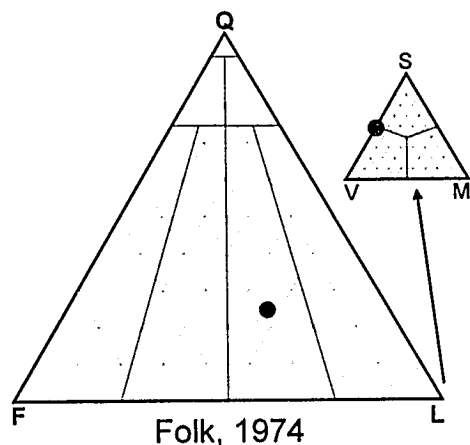
Plane polarized light  
30X magnification



Cross polarized light  
30X magnification



This lower-medium grained feldspathic litharenite has a framework of relatively angular grains, and a clay cement heavily stained with hematite. There are several penetrative contacts between harder quartz grains and softer detrital fragments (ps). The feldspars are generally highly sericitized (Fs), although some still display calrsbad twins (Fc). Deformed dark-coloured sedimentary clasts are soft mudstones (Ls). There are also small detrital carbonate (Ca) and coal fragments (c).



Comox Formation, Saanich Member  
Shear zone, southern Coal Island,  
UTM 472738 5392232

### Texture

**Modal grain size:** 0.25 mm (lower medium)

**Roundness:** subangular

**Sorting:** moderate to well sorted

### Composition

**Matrix:** 8%

**Folk (1974):** Feldspathic Litharenite

**Quartz:** 25%. Dominantly monocrystalline with straight extinction. Undulose extinction rare, some sutured fine polycrystalline grains.

**Feldspar:** 28%. Plagioclase with albite and carlsbad twins, very sericitized. No potassium feldspars or microcline recognized.

**Lithics:** 4%. Very fine and aphanitic volcanic fragments, mostly soft, brown clay-dominated fragments interpreted be mudstones. Detrital carbonaceous fragments (coal?) and small calcite (fossil?) fragments.

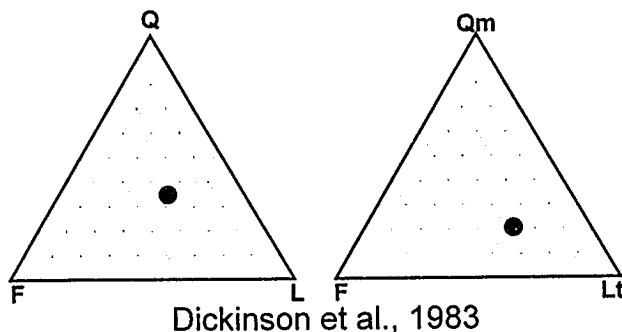
**Accessory Minerals:** calcite, carbonaceous fragments, hematite, opaques, few larger deformed mica grains.

### Cement/Diagenesis

**Cement Types:** clay, abundant hematite

**Grain contacts:** straight and point contacts, some pressure solution and interpenetration of hard grains into softer fragments. No quartz overgrowths.

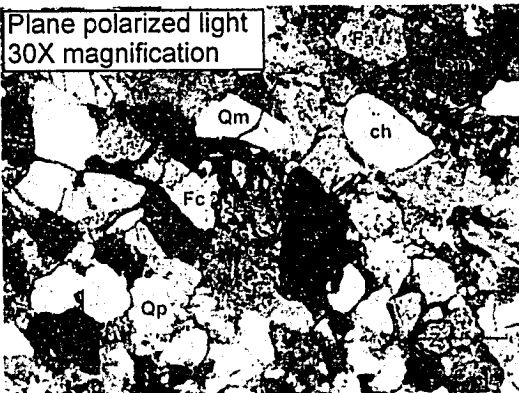
**Alteration:** sericitization of feldspars, slight chloritization of micas, but abundant unaltered mica also present.



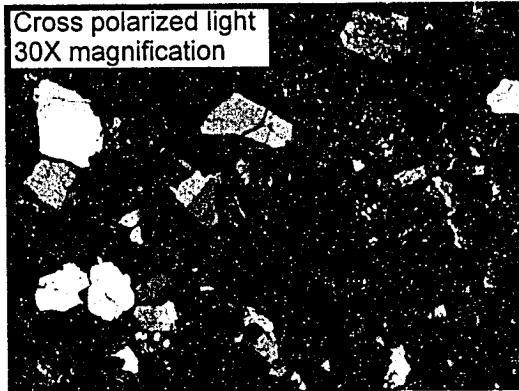


## Sample PDJ-03-128a

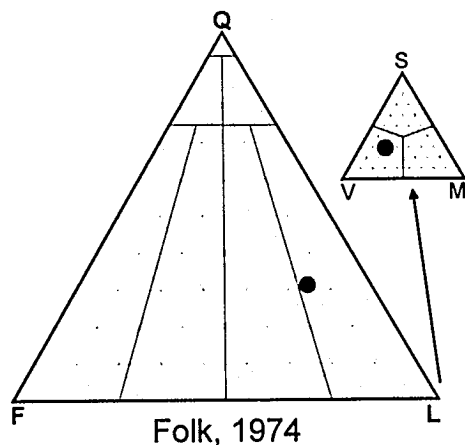
Plane polarized light  
30X magnification



Cross polarized light  
30X magnification



This image is a finer-grained portion of the sample, which grades across the slide. Several rock fragments are visible, including volcanics (Lv) and sedimentary clasts of varying grain size (Lsm, Lss). Quartz grains are monocrystalline (Qm), polycrystalline (Qp) and chert (ch). Feldspar grains display albite (Fa) and carlsbad twins (Fc), and are variously sericitized. The bottom right corner of the slide has an area of completely chloritized mica (cl) and a high-relief angular prism inferred to be a zircon (z).



**Extension Formation,**  
**SE coast, Piers Island,**  
**UTM 469992 5394437**

### Texture

**Modal grain size:** 0.2-1.0 mm (fine to coarse gained, grades across slide)

**Roundness:** subrounded

**Sorting:** moderate

### Composition

**Folk (1974):** Volcanic Litharenite

**Matrix:** 5%

**Quartz:** 31%. Monocrystalline grains have straight extinction, polycrystalline grains have a wide range of crystal sizes, some sutured, some straight contacts between crystals.

**Feldspar:** 15%. Plagioclase grains display albite and carlsbad twins. Very few K-spar grains, microcline very rare. Varying levels of sericitization.

**Lithics:** 54%. Mostly volcanics appearing as microcrystalline feldspars in aphanitic groundmass. Sedimentary clasts of varying grain sizes. Few clasts showing metamorphic textures.

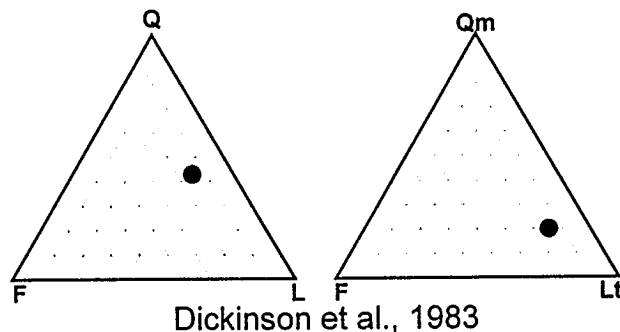
**Accessory Minerals:** considerable opaques, detrital micas. possible zircon identified.

### Cement/Diagenesis

**Cement Types:** hematite, chloritized muds, minor calcite.

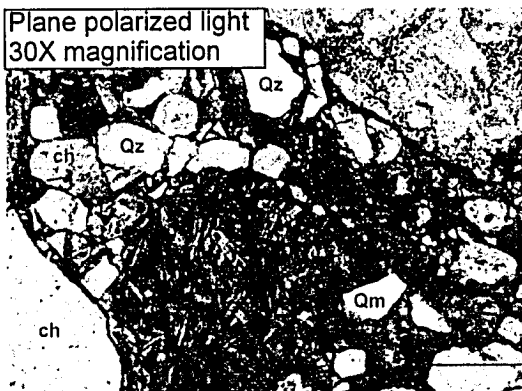
**Grain contacts:** straight, some point, some penetration of soft rock fragments by harder crystalline grains.

**Alteration:** abundant sericitization of feldspar, abundant chloritization clays in cement and framework grains.

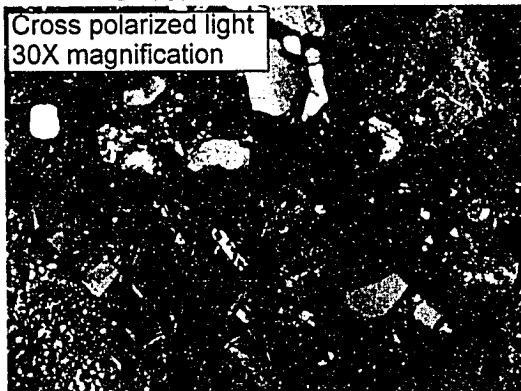


## Sample PDJ-03-135a

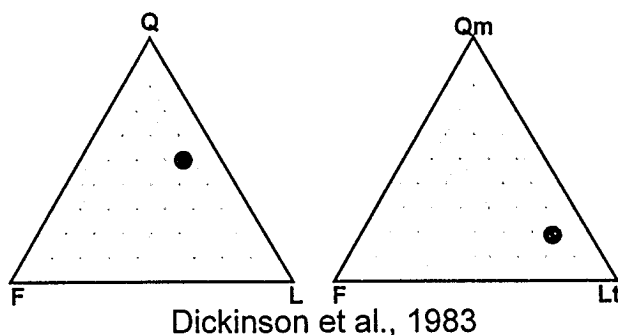
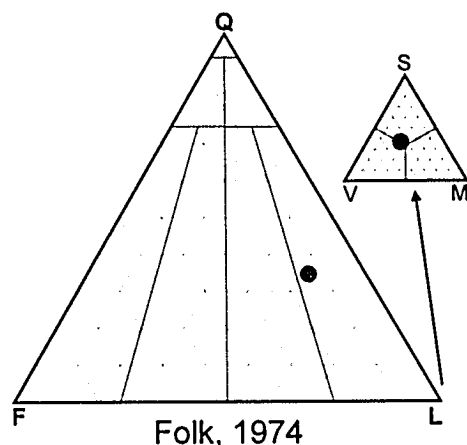
Plane polarized light  
30X magnification



Cross polarized light  
30X magnification



This sample displays several large lithic fragments, including a volcanic fragment with well developed plagioclase lathes (Lv), a calcite-cemented and well compacted sandstone fragment (Ls) and examples of chert (ch) and quartzite (Qz). Few monocrystalline quartz grains (Qm), are seen in the finer-grained portions which are dominated by a hematite-stained mud/clay matrix and small fragments of weathered lithic fragments.



Extension Formation,  
Arbutus Island,  
UTM 467991 5394880

### Texture

**Modal grain size:** 30 mm (granule)

**Roundness:** subrounded

**Sorting:** moderate to poor

### Composition

**Folk (1974): Volcanic Litharenite**

**Matrix:** 20%

**Quartz:** 35%. Few monocrystalline examples, all straight extinction. Polycrystalline grains of all sizes and types, from sutured large-crystal to chert.

**Feldspar:** 13%. Few single crystals, most in larger agglomerates. Plagioclase with simple twins and untwinned K-feldspars most common. No microcline identified.

**Lithics:** 52%. Several volcanic styles, some porphyritic. Sedimentary clasts include mudstones and calcite-cemented sandstones, Chert and quartzite common.

**Accessory Minerals:** Abundant hematite and opaques in matrix.

### Cement/Diagenesis

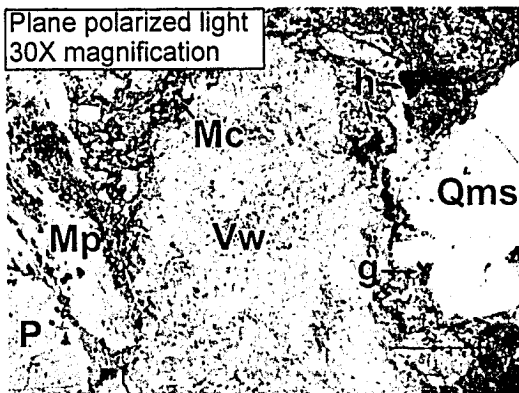
**Cement Types:** hematite, clay

**Grain contacts:** point, concave/convex. No interpenetration.

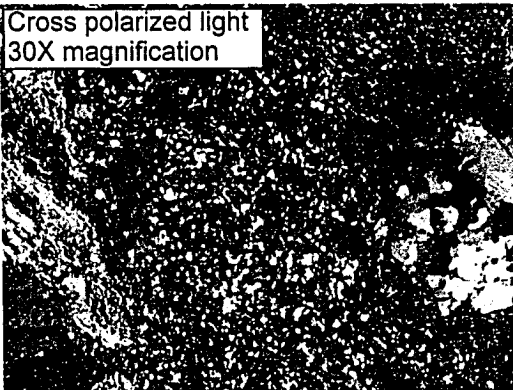
**Alteration:** Sericitization of feldspars. No chloritization except in re-mobilized clasts.

## Sample PDJ-03-138a

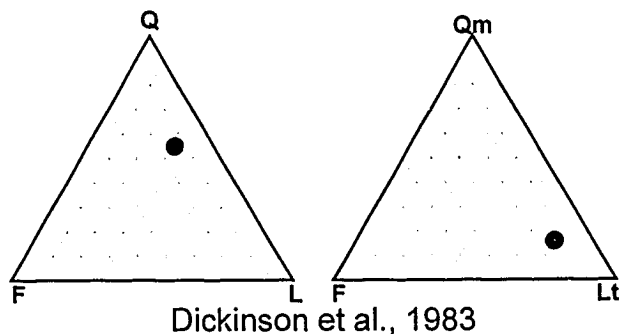
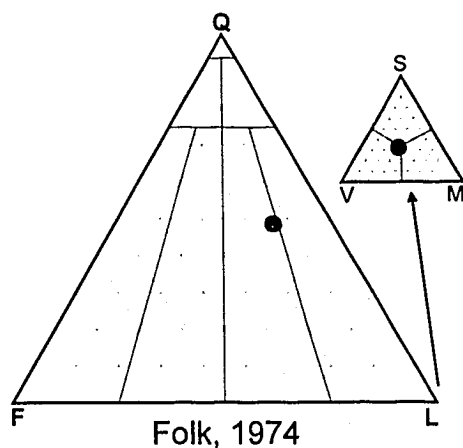
Plane polarized light  
30X magnification



Cross polarized light  
30X magnification



This example of coarse-grained litharenite shows a large volcanic clast (Vw) with chloritized heavy minerals within a matrix of interlocked quarts and feldspar grains, another large sutured polycrystalline quartz grain (Qms), a grain of phyllite (Mp) with strong alignment of micas and quartz grains, and one of Plagioclase (P) displaying simple twinning. Glaucinite (g) and hematite (h) are accessory minerals in the matrix, while large mica grains deformed by harder grains are partially chloritized (Mc).



Comox Formation, Benson Member  
East coast, Moresby Island,  
UTM 477866 5396397

### Texture

**Modal grain size:** 3 mm  
(very coarse grained sand)  
**Roundness:** subangular to subrounded  
**Sorting:** poor to moderate

### Composition

Folk (1974): Feldspathic Litharenite

**Matrix:** 15%

**Quartz:** 48%. mostly sutured polycrystalline grains, some single crystals with straight extinction (in smaller grains)

**Feldspar:** 14%. Only plagioclase identified, pericline twins.

**Lithics:** 38%. Dominantly large, weathered volcanic clasts, some clasts with aligned lathes and mica, interpreted to be metamorphic, and some chert and dark coloured mudstones.

**Accessory Minerals:** Hematite and glauconite in matrix, few larger deformed mica grains.

### Cement/Diagenesis

**Cement Types:** chloritized clay is dominant cement, although some microcrystalline calcite is also present in matrix, matrix/cement accounts for ~10% of volume.

**Grain contacts:** smooth and straight, some very minor penetration of soft grains at point contacts

**Alteration:** Sericite after plagioclase feldspars, chlorite after accessory minerals in volcanic grains (possibly pre-depositional?)

## Appendix D: Conglomerate Clast Lithologies.

Clast counts were performed at 5 locations where conglomerates outcropped. Sampling was randomized by stretching a string across the outcrop at various angles relative to bedding, and identifying the first 20-30 clasts of a size large enough to macroscopically identify with aid of a 10x hand lens (1.5 – 2 cm. minimum). The process was repeated with a new string orientation until 100 clasts were counted at each station. Clasts were characterized by gross lithologic character (Chapter 4).

Below are tables with the complete clast count data, by location, then grouped by formation. Confidence intervals at 95% are included for comparison purposes. Confidence Intervals were estimated by graphical means as outlined in Cheeney (1983).

**Table D 1: Conglomerate clast lithologies, Comox Formation.**

<b>Lithology of clast</b>	<b>Sidney Lagoon</b>		<b>Halibut Island</b>	
	count	95% c.i.	count	95% c.i.
Felsic Intrusive	15	8-22	12	5-19
Mafic Intrusive	2	1-3	0	0-1
Volcanic	36	26-46	38	28-48
Sed	7	2-12	10	4-16
Chert/Quartzite	32	22-44	37	27-47
Foliated metamorphic	8	3-13	3	2-5
total:	100		100	

**Table D 2: Conglomerate Clast Lithologies, Extension Formation.**

<b>Lithology of clast</b>	<b>Clive Islet</b>		<b>Rum Island</b>		<b>Rubly Island</b>	
	count	95% c.i.	count	95% c.i.	count	95% c.i.
Felsic Intrusive	10	4-16	20	12-28	9	3-15
Mafic Intrusive	1	0-2	0	0-1	0	0-1
Volcanic	18	10-26	31	21-41	43	33-53
Sed	18	10-26	18	10-26	21	12-30
Chert/Quartzite	53	43-63	31	21-41	25	16-34
Foliated metamorphic	0	0-1	0	0-1	2	1-3
total:	100		100		100	

**Table D 3: Conglomerate Clast Lithologies, all data.**

<b>Lithology of clast</b>	<b>Extension</b>			<b>Comox</b>			<b>overall %</b>
	count	%	95% c.i.	count	%	95% c.i.	
Felsic Intrusive	39	13	9-17	27	14	9-19	13
Mafic Intrusive	1	0	0-1	2	1	0-2	1
Volcanic	92	31	25-37	74	37	30-44	33
Sed	57	19	14-24	17	9	4-14	15
Chert/quartzite	109	36	30-42	69	35	28-42	36
Foliated metamorphic.	2	1	0-2	11	6	3-9	3
total:	300			200			100

## Appendix E: Paleocurrent data.

Paleocurrent data is presented in Chapter 4, including statistical analysis and rose diagrams. Raw paleocurrent data is listed here by station location, with representative bedding data that was utilized for paleocurrent rotation. A legend to the table format is included here:

Legend:	Station	Azimuth	Dip
	UTM_northing		
	UTM_easting		
	Measure type		
	Bedding strike/dip		
	Rose Diagram Figure #		

Table D4: Paleocurrent data.

Facies Association 1					
Comox Formation from Moresby Domain					
PDJ-03-96	030	24			
5397068	042	27			
475924	020	30			
cross bedding	024	34			
290/12	032	25			
Fig. 39a	050	25			
	021	27			
	024	34			

Facies Association 2								
Comox Formation from Moresby Domain								
PDJ-03-98	248	30	PDJ-03-98	326	31	PDJ-03-97	250	34
5397550	245	31	5397550	312	32	5397480	248	38
475666	244	34	475666	332	34	475918	255	40
cross bedding	239	35	cross bedding	320	36	cross bedding	250	34
260/13	248	30	260/13	326	31	280/12	261	34
Fig. 40a	245	31	Fig. 40a	312	32	Fig. 40a	248	38
	244	38		332	34		250	40
	237	32		320	36		255	38
	239	29		325	38		260	39
	250	32					265	30

Comox Formation from Sidney Domain								
PDJ-03-137	312	56	PDJ-03-MS009	304	25	PDJ-03-MS009	262	40
5386588	315	60	5385171	298	26	5385179	268	40
479144	318	60	480030	310	28	480074	264	45
cross bedding	312	66	cross bedding	305	30	cross bedding	272	50
300/50	313	67	298/47	318	32	295/55	272	55
Fig. 40i	314	68	Fig. 40h	316	35	Fig. 40h	276	43
	311	69		326	35		266	42
	319	70		325	36		265	45
	321	70	PDJ-03-26	285	60		274	48
	311	73	5386030	276	76		272	49
PDJ-03-23	270	35	475480	280	65			
5385163	255	40	cross bedding	272	75			
480097	262	46	302/72	288	62			
cross bedding	266	42	Fig. 40j	282	76			
300/45	269	43						
Fig. 40h	260	42						

Comox Formation from Coal North Domain								
PDJ-03-48	293	55	PDJ-03-50	030	78	PDJ-03-51	278	80
5393189	292	56	5392891	030	68	5392739	086	87
471535	291	51	472604	040	73	472955	096	89
current ripples	285	52	current ripples	038	74	cross bedding	096	90
275/78	285	48	286/81 / Fig 40l	035	76	285/71	278	80
Fig. 40k	284	45	PDJ-03-49	285	48	Fig. 40m	272	87
	275	43	5393051	276	47		096	88
	278	38	472038	272	37		089	90
			current ripples	272	36			
			271/79 / Fig. 40k	279	51			

Table D4: Paleocurrent data.

Comox Formation from Coal North Domain (cont'd)							
PDJ-03-94	269	65	PDJ-03-94	266	65	PDJ-03-94	075 36
5392611	266	67	5392662	267	68	5392662	075 36
473159	264	68	473047	269	69	473047	075 36
cross bedding	264	70	cross bedding	270	75	current ripples	
284/72	269	65	285/70	274	70	285/67	
Fig. 40n	264	65	Fig. 40n	265	66	Fig. 40o	
	265	67		268	68		
	272	70		265	75		
Comox Formation from Portland Domain							
PDJ-03-78	093	21	PDJ-03-80	052	23	PDJ-03-80	048 20
5396617	034	24	5397111	050	24	5397130	059 24
473123	083	24	473483	054	24	473445	068 29
cross bedding	088	26	cross bedding	064	24	cross bedding	051 34
040/19	080	28	104/19	018	25	102/20	049 30
Fig. 40b	040	29	Fig. 40d	015	26	Fig. 40d	059 24
	074	30		029	29		080 28
	079	33		054	29		069 29
	032	34	PDJ-03-80	312	08		070 33
	060	35	5397130	309	06		051 35
	042	38	473445	318	02	PDJ-03-85	275 29
	055	38	cross bedding	305	05	5398034	264 30
	072	40	124/15	307	03	472286	255 39
	081	40	Fig. 40d	315	02	cross bedding	275 40
	074	48	PDJ-03-80	165	24	215/10	272 28
PDJ-03-85	292	16	5397085	163	28	Fig. 40e	265 35
5398126	295	23	473511	158	29		258 31
472487	295	25	cross bedding	150	30		271 40
cross bedding	292	26	106/24	150	24	PDJ-03-86	165 40
252/14	275	32	Fig. 40c	145	26	5396917	168 42
Fig. 40e	285	24		151	28	473749	174 44
	288	33		157	33	cross bedding	170 48
	295	19		152	30	130/24	175 51
	292	26		155	30	Fig. 40f	172 38
				145	25		162 44
PDJ-03-85	300	20	PDJ-03-85	319	48	PDJ-03-86	160 18
5398126	304	24	5398210	325	51	5396960	150 22
472487	305	30	472331	320	52	473576	165 22
cross bedding	310	30	cross bedding	340	55	cross bedding	158 29
290/10	295	31	311/29	331	48	135/25	145 38
Fig. 40e	293	32	Fig. 40e	327	50	Fig. 40f	155 24
	308	35		322	50		152 25
	290	37		320	53		159 22
PDJ-03-83	355	41		336	61		152 27
5398008	355	41					145 31
472969	355	41					
current ripples							
322/53 / Fig. 40g							
Comox Formation from Saanich West Domain							
PDJ-04-015	281	37	PDJ-03-2	105	79	PDJ-03-5	008 10
5392374	268	38	5391088	102	80	5391743	020 10
468151	285	42	464482	105	80	464199	010 09
cross bedding	264	44	current ripples			current ripples	
290/42	289	44	096/88			210/22	
Fig. 40p	264	45	Fig. 40q			Fig. 40q	
	268	47					
	283	48					



Table D4: Paleocurrent data.

Facies Association 3								
Comox Formation from Tsehum Domain								
PDJ-03-105	250	48	PDJ-03-105	241	49	PDJ-03-119	265	14
5392221	265	49	5392175	251	52	5392191	294	15
471220	251	50	471172	242	55	470766	279	16
cross bedding	264	50	cross bedding	245	55	cross bedding	281	17
273/54	258	50	274/60	238	49	296/54	280	23
Fig. 41b	249	52	Fig. 41b	242	53	Fig. 41c	275	26
	265	49		247	55		266	15
	252	49		253	56		293	18
	254	50	PDJ-03-117	270	49		283	16
	260	50	5392266	276	51		278	20
PDJ-04-017	269	65	471295	280	53		275	22
5392330	257	67	cross bedding	270	54	PDJ-03-122	244	42
470330	265	67	281/48	268	50	5391817	249	42
cross bedding	262	69	Fig. 41a	278	54	471163	245	45
249/46	260	70		279	52	cross bedding	251	40
Fig. 41d	267	65		271	51	260/67	247	49
	260	67	PDJ-03-117	311	48	Fig. 41c	249	42
	264	69	5392266	320	52		243	45
	256	73	471295	309	54		241	46
	257	73	cross bedding	311	56		244	48
			278/60	315	46		247	50
			Fig. 41a	307	50			
				319	53			
				310	53			
				311	56			
Comox Formation from Domville Domain								
PDJ-03-107	315	33	PDJ-03-108	332	50	PDJ-03-108	285	75
5391906	320	35	5391582	325	54	5391562	285	76
476175	309	38	476320	320	56	476416	285	77
cross bedding	309	42	cross bedding	323	60	cross bedding	290	81
317/58	311	45	308/71	327	55	310/69	285	75
Fig. 41e	320	35	Fig. 41f	323	54	Fig. 41f	292	79
	319	40		325	60		282	77
	315	39		330	54		284	74
	309	42	PDJ-03-MS007	307	55		290	77
	319	44	5391414	310	56	PDJ-03-MS007	320	58
	309	45	476634	311	57	5391411	321	63
PDJ-03-74	300	61	cross bedding	310	60	476642	315	68
5391484	301	61	310/75	307	55	cross bedding	316	71
476729	301	62	Fig. 41g	310	56	305/80	320	73
cross bedding	302	64		310	55	Fig. 41g	322	59
308/70	304	64		309	62		321	63
Fig. 41h	305	65		313	60		313	67
	300	66	PDJ-03-MS007	300	66		317	70
	301	61	5391409	307	66		319	74
	301	62	476631	306	67			
	304	64	cross bedding	303	73			
	303	63	310/75	299	65			
	299	70	Fig. 41g	306	66			
	300	68		305	67			
				301	70			

Table D4: Paleocurrent data.

Comox Formation from Gooch Domain								
PDJ-03-72	294	65						
5390837	281	69						
478117	285	70						
cross bedding	295	72						
100/70	294	71						
overturned	282	73						
Fig. 41o	285	75						
	290	72						
	273	74						
Comox Formation from Forrest Domain								
PDJ-03-37	299	79	PDJ-03-38	286	51	PDJ-03-MS001	117	78
5389400	309	80	5389156	284	52	5390066	111	80
475889	309	85	476175	285	54	474925	120	80
cross bedding	284	86	cross bedding	290	55	cross bedding	118	81
288/86	288	86	302/59	288	50	318/85	106	84
Fig. 41k	289	79	Fig. 41k	283	53	Fig. 41l	111	85
	304	80		283	56		115	86
	309	85		292	55		108	84
	299	84	PDJ-03-MS001	115	76		112	86
	292	82	5390162	110	78		110	88
PDJ-03-MS001	291	71	474878	114	79	PDJ-03-MS003	320	58
5390083	288	78	cross bedding	117	76	5391081	310	69
474921	285	81	125/90	108	78	473620	309	70
cross bedding	115	88	Fig. 41m	114	79	cross bedding	314	72
122/90	286	76		115	80	300/80	314	73
Fig. 41m	285	81		113	80	Fig. 41j	315	74
	294	84	PDJ-03-MS003	321	56		315	74
	298	84	5391018	326	55		311	75
	114	89	473646	319	58		315	75
	116	90	cross bedding	320	61		311	76
PDJ-03-MS003	276	75	298/80	330	56		314	76
5391073	278	75	Fig. 41j	319	58		309	81
473633	280	75		315	61		319	83
cross bedding	272	76		316	64	PDJ-03-MS004	114	67
299/80	275	80	PDJ-03-MS004	290	85	5390352	117	73
Fig. 41i	276	76	5390358	109	88	475090	108	74
	276	77	475084	284	88	cross bedding	112	74
	282	78	cross bedding	285	88	305/85	114	81
	285	82	305/85	105	89	Fig. 41n	106	82
			Fig. 41n	286	89		117	73
				103	90		115	81
				110	90		104	82
							116	86
Facies Association 4a								
Haslam Formation from Domville Domain								
PDJ-03-MS005	074	75	PDJ-03-MS005	268	79	PDJ-03-52	287	70
5391330	080	82	5391325	264	80	5391341	290	71
475983	075	90	475981	270	80	475884	290	72
cross bedding	074	75	cross bedding	271	84	cross bedding	290	72
090/75	075	78	101/90	266	81	304/85	285	74
Fig. 42a	081	82	Fig. 42a	269	82	Fig. 42a	293	74
	065	85		270	70			
	077	85		273	83			
	076	89						

Table D4: Paleocurrent data.

Haslam Formation from Piers Domain						
PDJ-03-91	268	69	PDJ-03-128	290	55	
5393794	265	70	5394517	281	57	
470605	270	70	470030	280	58	
cross bedding	260	71	cross bedding	286	60	
282/74	263	73	306/50	287	56	
Fig. 42c	266	68	Fig. 42b	292	60	
	275	74		288	54	
	260	70		286	53	
	263	72				

Facies Association 4b								
Extension Formation from Domville Domain								
PDJ-03-66	336	60	PDJ-03-67	318	44	PDJ-03-69	276	41
5390357	335	62	5390557	335	45	5390298	281	43
476833	326	63	476806	325	45	477033	272	45
cross bedding	330	66	cross bedding	315	46	cross bedding	286	48
322/51	335	74	344/50	314	54	330/65	269	49
Fig. 43a	325	62	Fig. 43b	325	51	Fig. 43c	279	50
	331	66		324	53		280	50
	325	75		327	56		276	41
	336	75	PDJ-03-69	284	60		272	51
PDJ-03-69	297	57	5390423	280	62		267	49
5390423	299	58	476969	282	64		282	50
476969	310	59	cross bedding	282	64		265	47
cross bedding	310	60	312/62	284	64	PDJ-03-69	304	49
330/55	304	57	Fig. 43c	286	64	5390423	300	52
Fig. 43c	298	58		280	62	476969	308	53
	311	61		282	65	cross bedding	304	49
	303	58		284	65	315/66	298	51
	308	65		288	67	Fig. 43c	305	53
							302	54
							302	54
Extension Formation from Gooch Domain								
PDJ-03-MS010	079	46	PDJ-03-64	055	64	PDJ-03-60	081	72
5389928	078	50	5389897	071	61	5390263	080	71
479333	080	50	478916	074	48	478170	070	68
cross bedding	081	50	cross bedding	059	60	cross bedding	070	66
100/60	084	46	100/65	081	63	090/50	078	60
(overturned)	085	42	(overturned)	073	62	(overturned)	073	72
Fig. 43j	081	44	Fig. 43g	076	57	Fig. 43e	080	71
	076	45		064	48		072	71
PDJ-03-59	079	82	PDJ-03-58	065	62		074	68
5390162	085	77	5390033	065	62		078	66
478946	079	75	479289	075	69	PDJ-03-57	105	73
cross bedding	080	72	cross bedding	073	70	5389990	105	69
104/68	079	80	085/40	078	60	479690	096	66
(overturned)	087	80	(overturned)	066	62	cross bedding	100	66
Fig. 43f	085	77	Fig. 43i	057	65	090/44	102	72
	075	79		075	70	(overturned)	105	70
	082	78		064	70	Fig. 43i	099	66
	076	72		073	70		098	67
				072	73	PDJ-03-56	090	84
PDJ-03-56	082	51	PDJ-03-56	070	58	5389907	088	79
5389925	085	51	5389907	085	54	479418	091	76
479481	084	41	479418	092	50	cross bedding	093	71
cross bedding	085	51	cross bedding	080	45	100/64	085	78
109/50	083	50	094/50	075	58	(overturned)	095	80
(overturned)	075	48	(overturned)	080	55	Fig. 43h	089	77
Fig. 43h	087	41	Fig. 43h	095	48		090	72
	074	53		089	49			

Table D4: Paleocurrent Data Cont'd

Clive Island (Piers Domain)			
UTM N		5394379	
UTM E		470145	
Bedding:		305/85	
Orientation of A-B-plane of non-equant clasts (n=100):			
Dip Direction	Dip	Dip Direction	Dip
003 88		064 72	
012 81		064 86	
014 89		090 56	
014 89		110 28	
023 81		118 03	
043 80		120 69	
043 80		120 79	
054 71		122 27	
054 81		124 49	
057 68		128 22	
057 68		141 13	
058 71		142 67	
204 64		156 76	
207 69		164 48	
219 86		198 83	
221 82		201 82	
224 81		287 47	
229 85		302 15	
229 81		314 49	
243 80		317 67	
250 80		237 85	
253 43		319 38	
280 69		328 51	
326 85		355 60	
238 90		229 86	
Dip Direction	Dip	Dip Direction	Dip
009 82		005 82	
009 82		009 82	
045 77		028 27	
054 81		052 48	
056 78		054 24	
060 87		069 24	
060 69		073 40	
107 36		085 33	
111 20		118 00	
114 49		132 09	
121 28		194 67	
194 72		227 83	
194 67		228 89	
198 83		233 83	
220 83		243 86	
227 80		283 27	
227 83		283 71	
229 81		285 83	
243 86		291 09	
243 86		292 28	
250 80		292 44	
254 88		295 22	
272 79		297 58	
285 83		312 71	
340 90		353 28	

Table D4: Paleocurrent Data Cont'd

Rum Island (Gooch Domain)				Rotated about hinge of big fold, 34-116, -120 degrees, then to make bedding flat, 308/65			
UTM N		5389950					
UTM E		479579					
Bedding:		100/60 (overturned)		Rose Diagram Fig. 43k			
Orientation of A-B-plane of non-equant clasts (n=100):							
Dip Direction	Dip	Dip Direction	Dip	Dip Direction	Dip	Dip Direction	Dip
134	38	103	47	50	57	31	84
160	55	113	29	144	51	128	54
175	68	122	59	153	60	145	69
175	60	135	32	156	41	146	48
175	68	143	27	161	79	167	69
180	71	147	41	162	65	175	60
186	69	163	49	168	58	176	89
186	71	167	61	175	45	181	68
190	70	170	81	180	64	183	63
190	64	174	68	184	69	183	60
190	55	175	34	188	40	185	81
195	55	184	71	190	61	188	65
195	65	190	60	190	50	188	63
198	65	190	26	190	82	189	76
200	58	190	77	191	72	189	81
203	61	194	43	194	68	190	70
205	50	202	73	195	63	191	63
215	68	214	51	196	63	191	59
220	44	216	63	197	69	193	54
227	51	257	47	200	70	194	74
230	50	258	58	206	54	214	79
230	80	261	56	229	68	214	84
233	65	288	51	230	46	214	84
238	70	289	46	278	41	219	78
260	80	295	63	320	84	252	69

Rubly Island (Domville Domain)							
UTM N		5390195		Rose diagram Fig. 43d			
UTM E		4796996					
Bedding:		310/60					
Orientation of A-B-plane of non-equant clasts (n=55):							
Dip Direction	Dip	Dip Direction	Dip	Dip Direction	Dip	Dip Direction	Dip
334	51	293	83	314	68	333	36
325	44	300	55	319	58	316	29
314	57	301	49	154	2	292	21
138	35	16	78	349	71	337	48
318	44	306	52	331	62	339	41
297	37	310	58	315	38	320	53
301	38	311	53	72	18	310	64
63	39	307	49	287	50	342	60
317	54	168	41	265	51	310	60
359	59	307	86	289	78	327	55
74	23	335	45	324	57		
321	33	162	32	320	66		
307	32	301	59	325	52		
305	73	326	38	328	47		
300	55	326	40	154	35		

## **Appendix F: GIS Techniques.**

A Geographic Information System (GIS) was utilized for data management and map production. Several geospatial data sets were generated, and are presented on the Backpocket Map. Techniques used to generate these datasets are outlined here.

A shaded relief map of surficial and bathymetric topography was created. Land surface elevation data was acquired from 1:20,000 scale British Columbia Terrain Resources Inventory and Management (TRIM) digital data. Coastline and surface water data from (1:20,000) from BC TRIM datasets was used to constrain modelling. Bathymetric data was digitized using a tablet from paper Canadian Hydrographic Service nautical charts numbered 3476 (1:10,000) and 3462 (1:40,000). Data was digitally re-projected to match the TRIM data, and elevation was adjusted from the Chart datum (median low tide) to that of the TRIM data (mean tide). A 5-m topographic GRID was generated using an inverse distance weighted modelling technique, with stream direction enforcement. A shaded relief GRID was generated from this topographic GRID, with virtual lighting from the northwest (azimuth 300), with 45° of inclination.

Structural data was also managed using a GIS. Structural data was collected manually in the field using a hand compass and locational data was collected digitally using a hand-held GPS unit. Structure and locational data was integrated in a database, and representative data was selected for display on the

geology map. Integration of locational information and manually collected structural data in a database also facilitated selection of data and entry of data into stereonet-generating software.

All other geological data (outlines of geologic units, contacts, etc.) was digitized on screen, based on TRIM coastline and cultural data, the shaded relief map, and geologic data collected in the field. Map layout and legend production was also performed utilizing GIS software.

## **NOTE TO USERS**

**Oversize maps and charts are microfilmed in sections in the following manner:**

**LEFT TO RIGHT, TOP TO BOTTOM, WITH SMALL OVERLAPS**

**This reproduction is the best copy available.**

UMI





**Location**

**British  
Columbia**

**SALTSPR  
ISLAND**

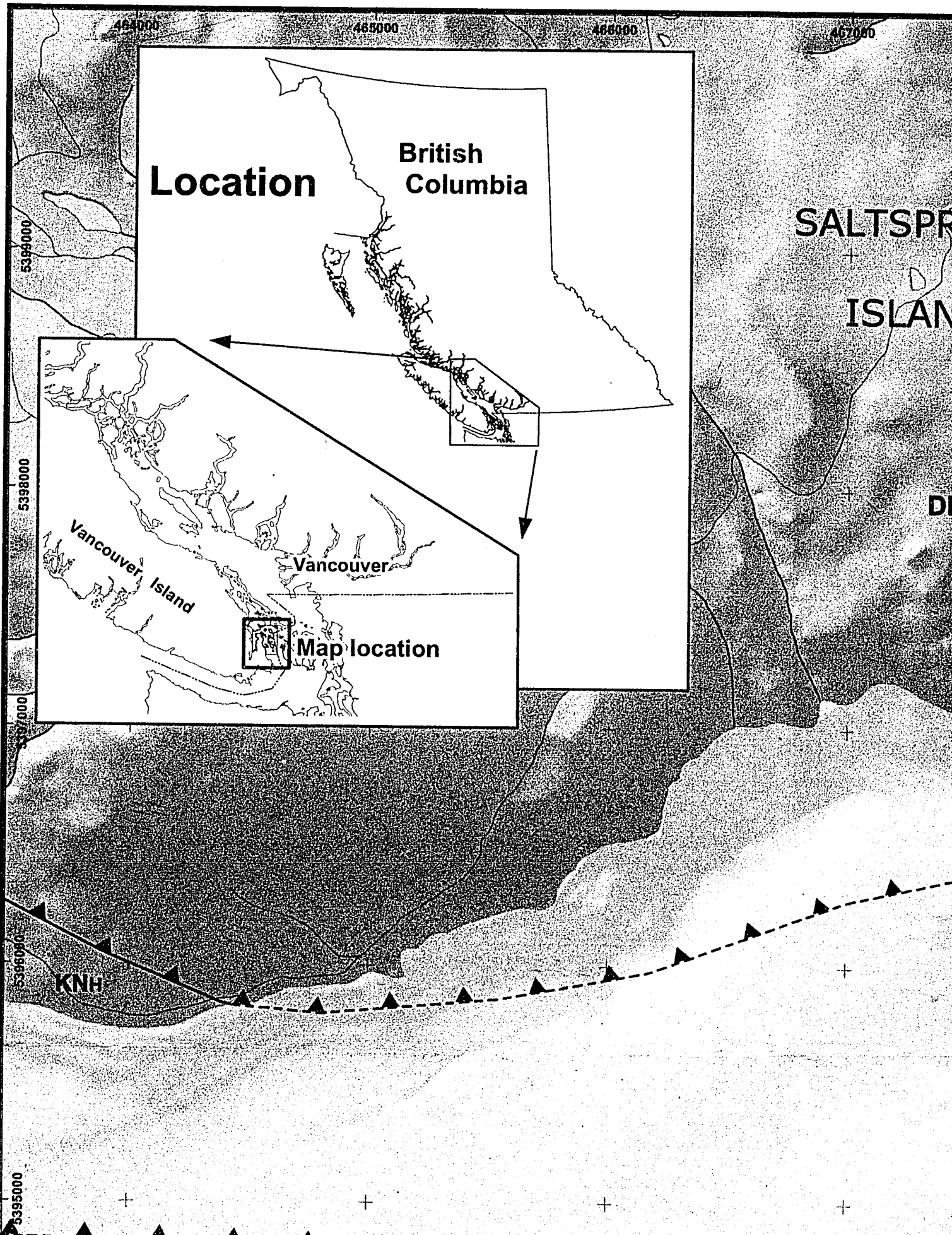
**DI**

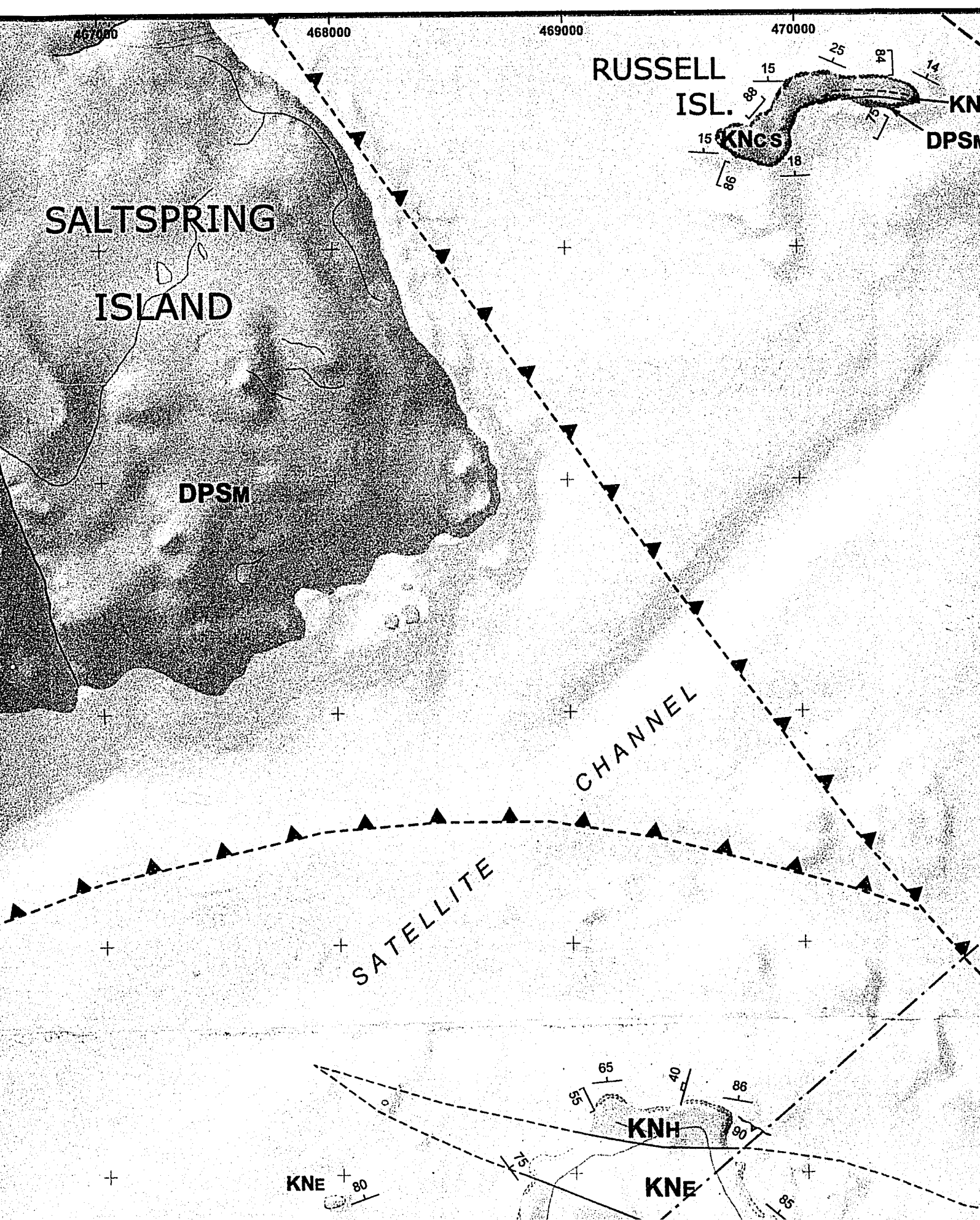
**Vancouver Island**

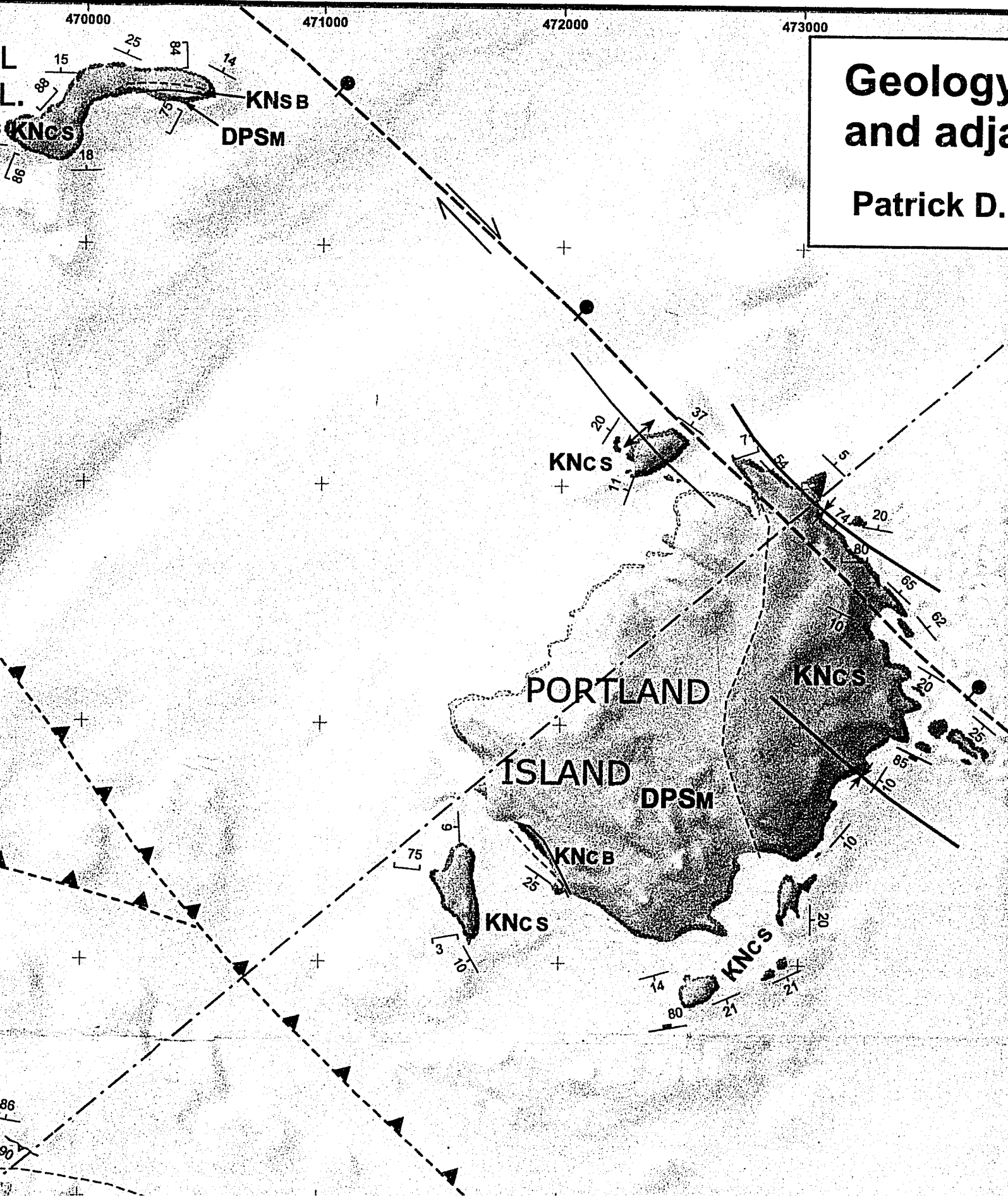
**Vancouver**

**Map location**

**KNH**







# Geology and adjacent areas

Patrick D.

473000

474000

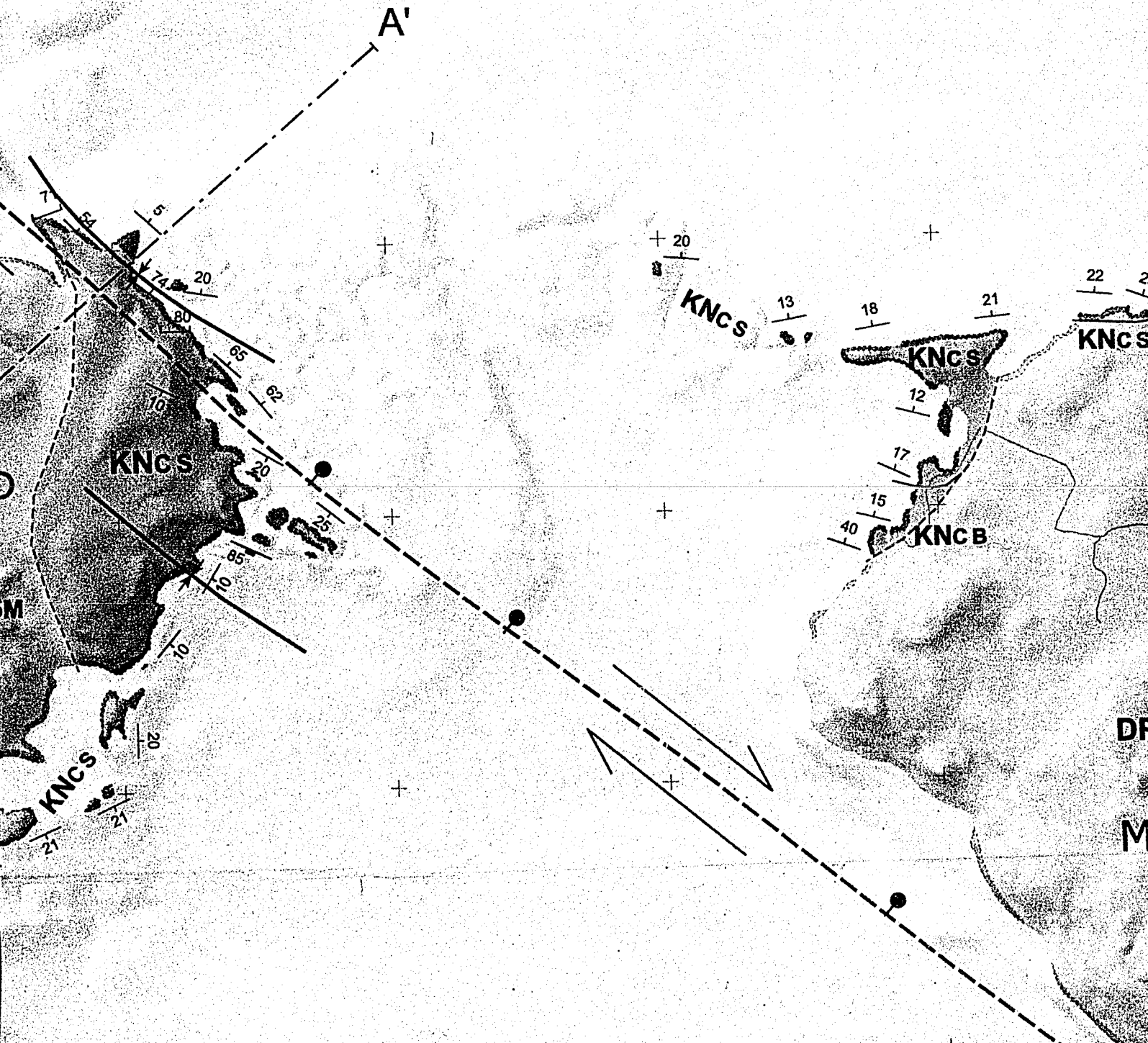
475000

476000

# Geology of the Upper Cretaceous Nanaimo and adjacent Saanich Peninsula, Southwest

Patrick D. Johnstone.

Backpocket Map: GEOLOGY OF THE UPPER CRET  
SAANICH PENINSULA, SW BRITISH COLUMBIA. Un





477000

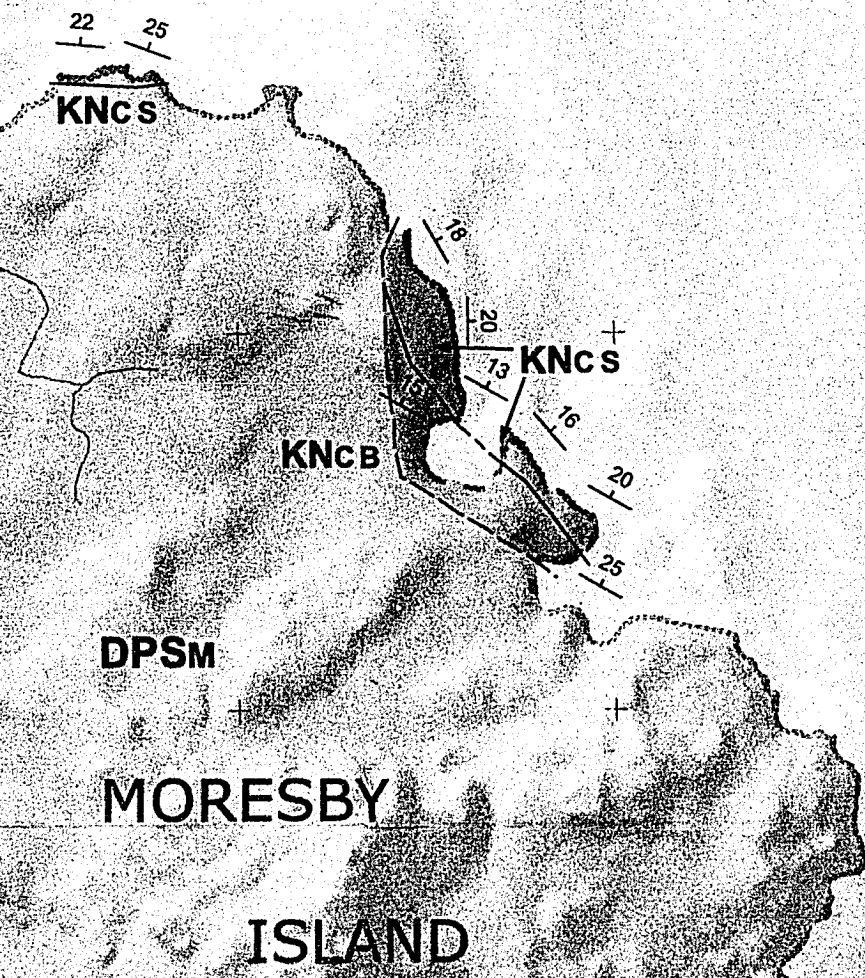
478000

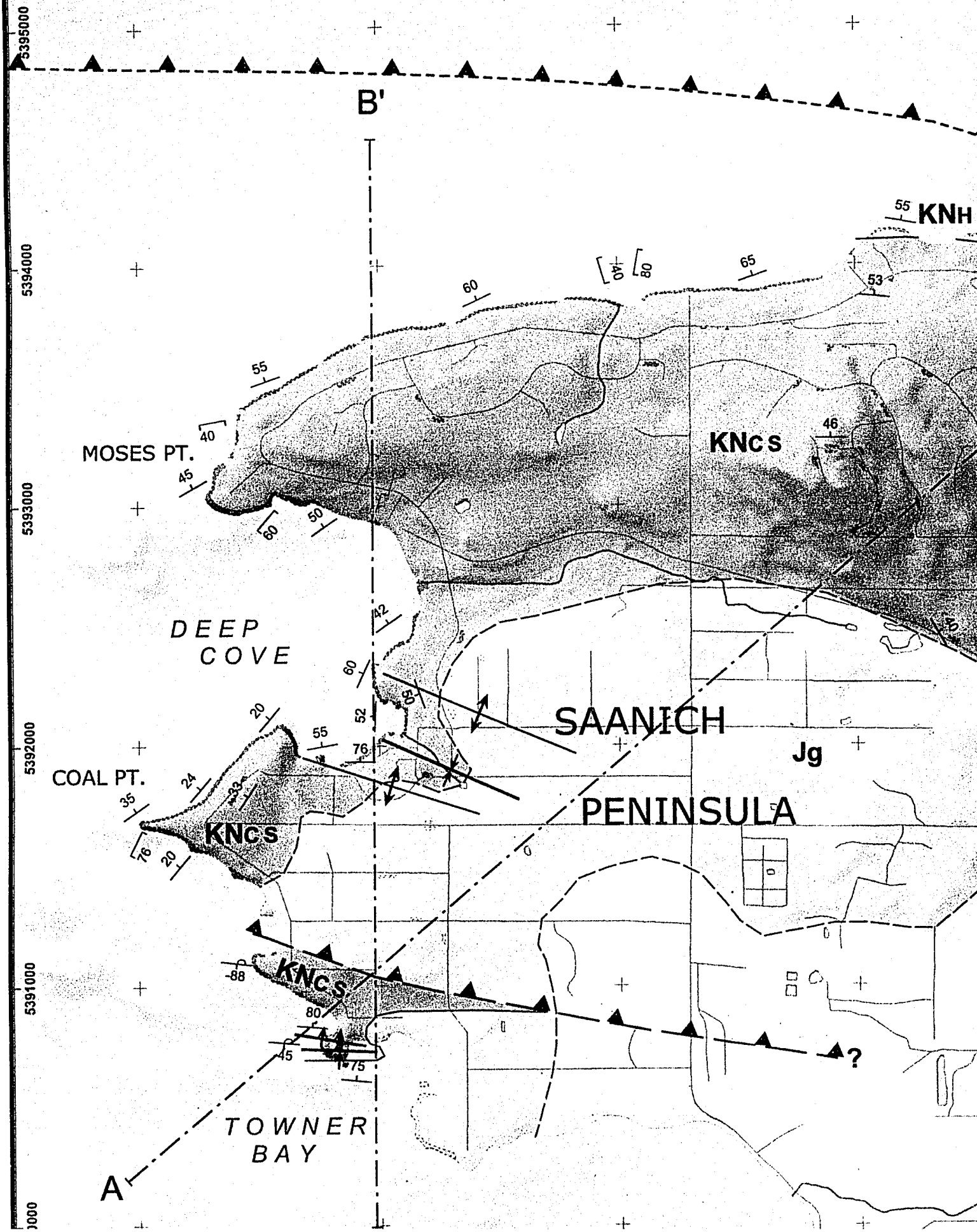
479000

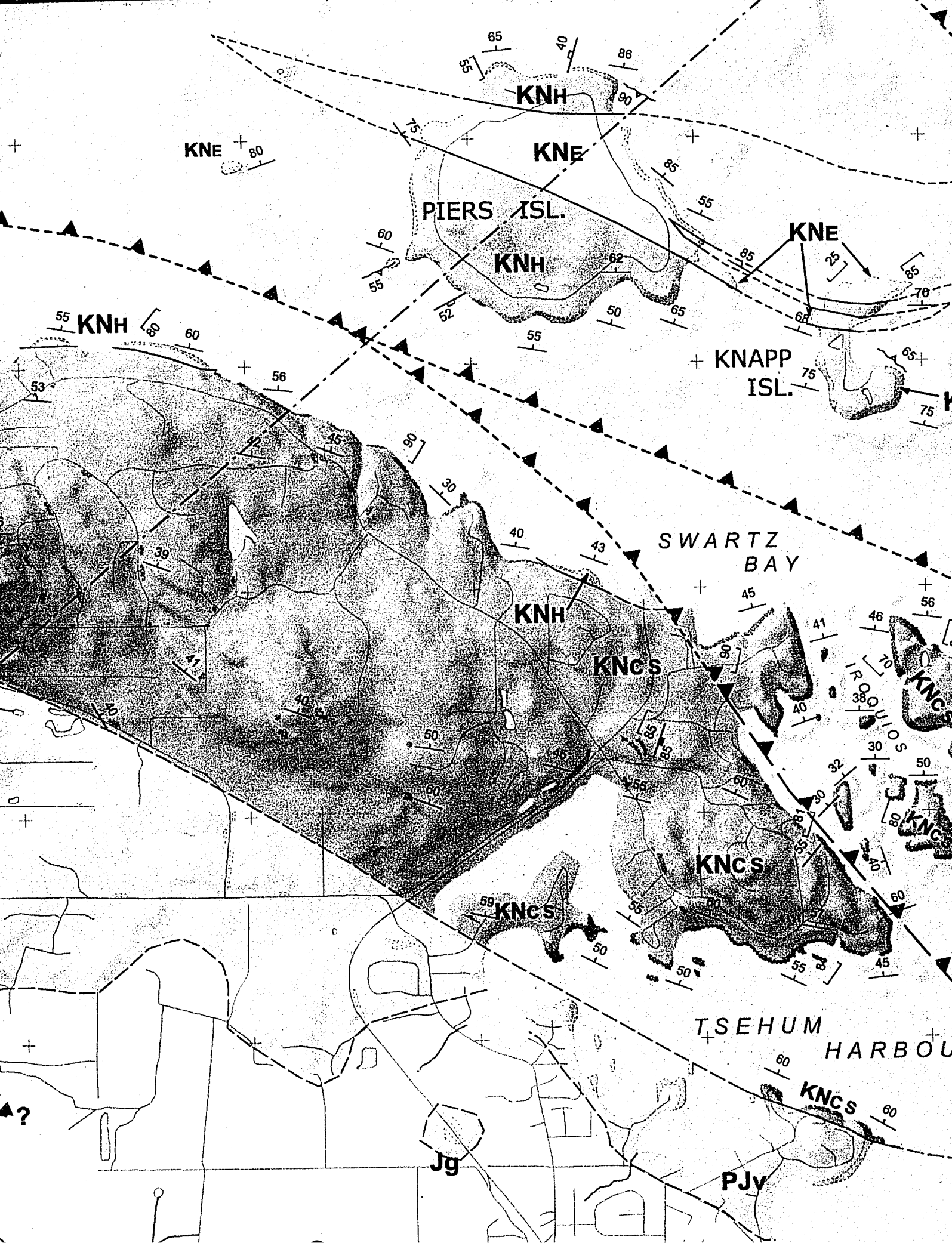
480000

# Nanaimo Group, Southernmost Gulf Islands Northwestern British Columbia.

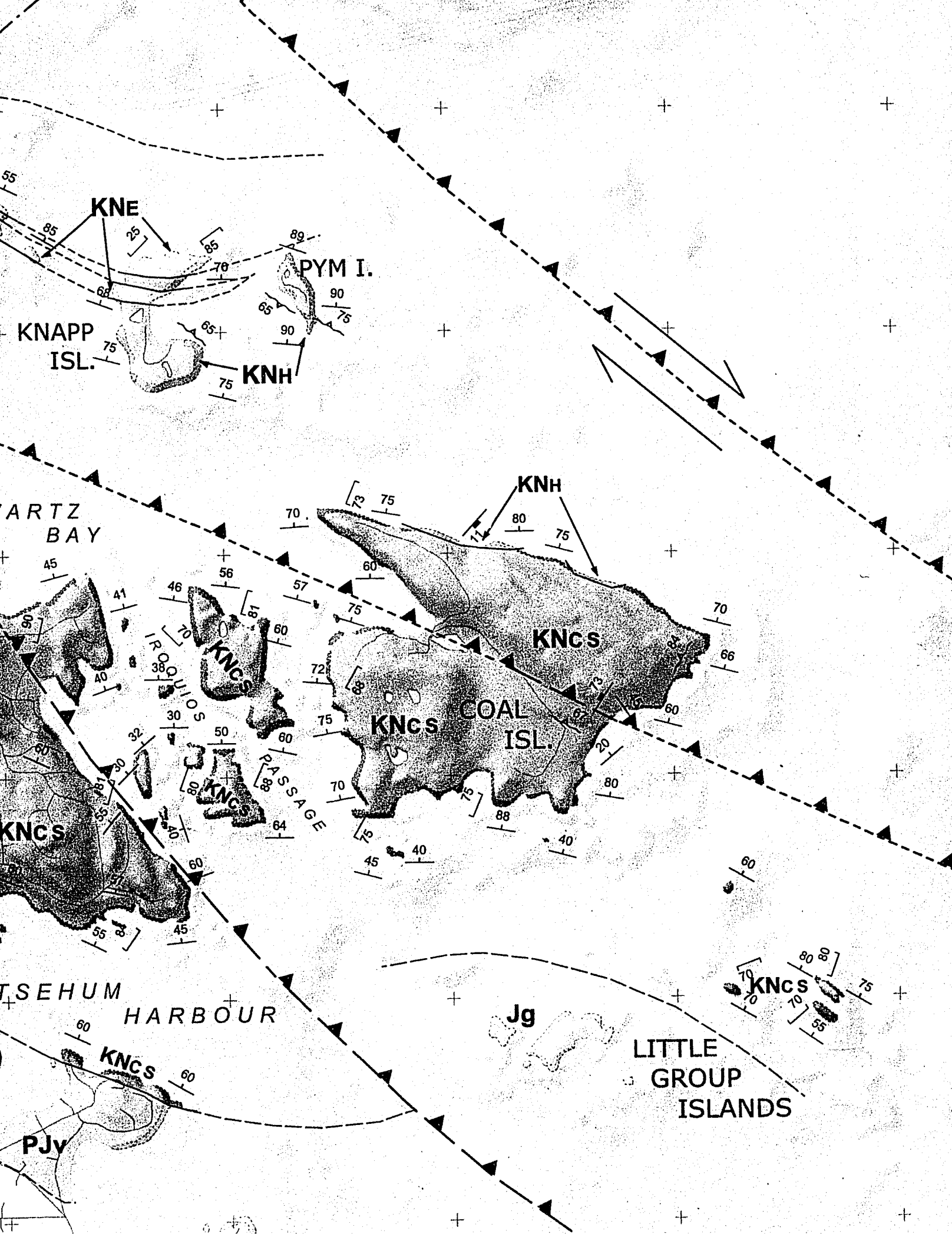
UPPER CRETACEOUS NANAIMO GROUP, SOUTHERNMOST GULF ISLANDS AND ADJACENT  
COLUMBIA. Unpublished M.Sc. Thesis, Department of Earth Sciences, Simon Fraser University. 2006.

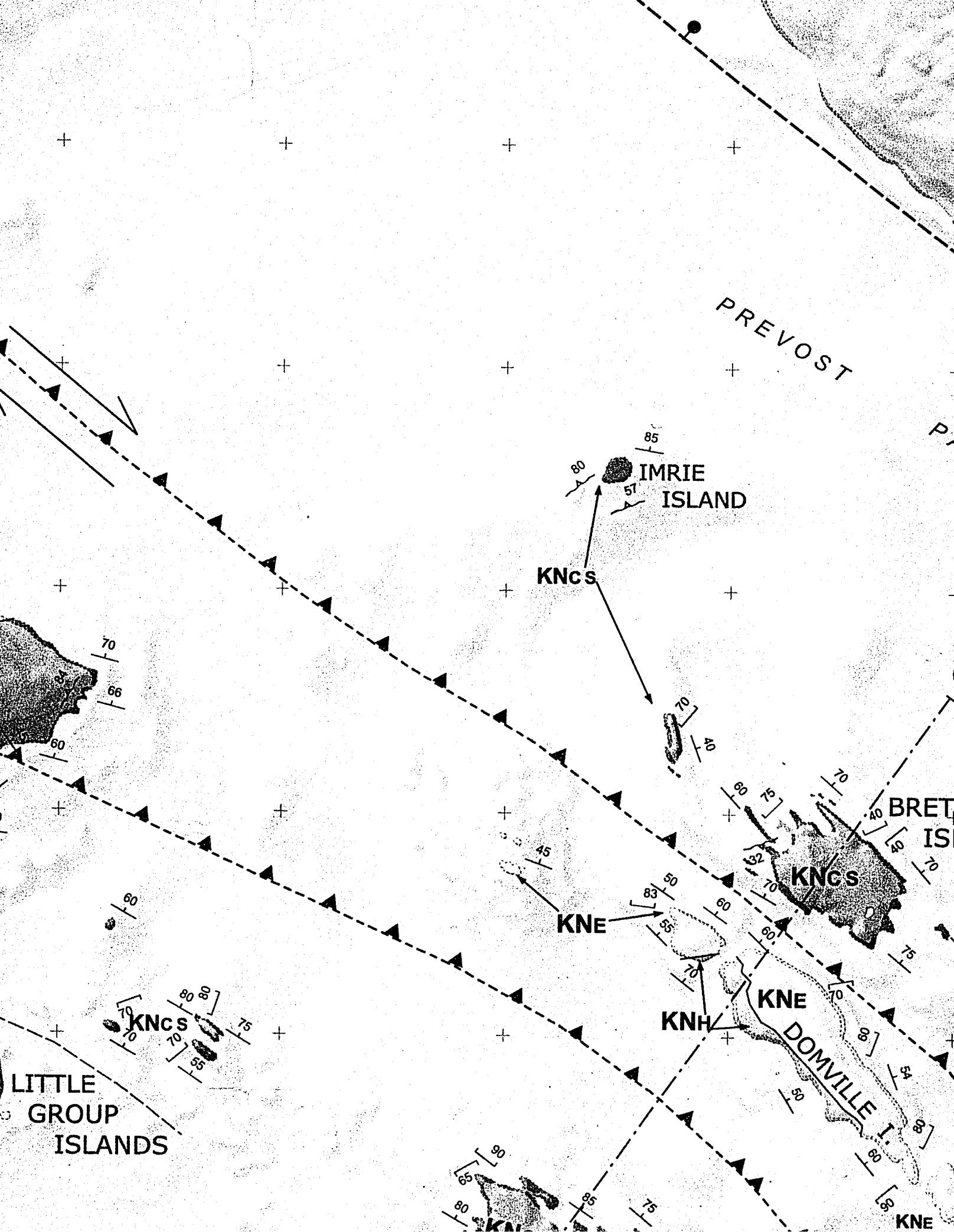












ISLAND

ST

PASSAGE

C'

BRETHOUR  
ISLAND

NCS

COMET I.

KNCs

KNCs

OMVILLE I.

KNE

KNE

RUM I.

5395000

5394000

5393000

5392000

5391000

TOWNER  
BAY

A

B

## LEGEND

### QUATERNARY

**Q** Glacial till, Glacio-fluvial sands.

### LATE CRETACEOUS

#### NANAIMO GROUP

**KNE**

covered | exposed

#### Extension Formation:

Conglomerate, pebbly sandstone and sandstone. Polymictic, moderately to poorly sorted pebble- to boulder-sized clasts, subangular to rounded. Well sorted coarse-grained litharenite matrix. Bedding is thick, and locally poorly defined or erosive-based. Planar stratified or trough cross bedded. Conglomerates are commonly graded, normal and reverse, with thick sandstone lenses. Clasts are locally imbricated. Very few dispersed robust shell fragments and shells, locally abundant carbonaceous detritus.

**KNH**

covered | exposed

#### Haslam Formation:

Interbedded sandstone and silty shale. Sandstone is well sorted, medium- to fine-grained, with thin beds that grade into silty shale. Waning flow matching Bouma-type sequences, most commonly TCDE, and TCD, with rare TABCDE. Graded sequences range from 5 to 50 cm. (average 15 cm.) and are contiguous over tens of metres. Unit grades over 10s of metres from 75% sandstone to 75% shale by thickness. Few dispersed shells. Bioturbation is low intensity (BI 0-2), ichnogenes are diminutive with a distinct paucity of vertical structures.

**KN**

covered | exposed

#### Comox Formation:

Sandstone, conglomerate and shale.

**KNcs: SAANICH MEMBER:** Sandstone and shale with minor pebble conglomerates. Sandstone is coarse- to medium-grained, generally becoming finer up section, moderately to well sorted, and thick to thin bedded. Planar stratification, trough cross bedding, and locally well developed swale cross stratification and hummocky cross stratification. Shales are silty and commonly interlaminated or interbedded with medium-grained sandstone. Lenticular, wavy and flaser bedding locally developed, with current and combined flow ripples in interstitial sandstone. Bivalves, gastropods and rare cephalopods occur in coquina-like lags, and dispersed in sandstones. Shales are carbonaceous, with abundant large coal fragments, leaf impressions, and *Teredolites*-bored logs. Ichnology varies from sparse to abundant, with *Ophiomorpha*, *Thalassinoides*, *Skolithos*, *Palaeophycus*, and *Diplocraterion* well represented.

**KNcB: BENSON MEMBER:** Conglomerate deposited on the basal unconformity. Varies from a thin, bimodal, boulder to pebble conglomerate with angular to rounded clasts of local basement lithology, with a well sorted, coarse-grained sandstone matrix, to a thick, poorly sorted, cobble to pebble conglomerate with a poorly sorted muddy sandstone matrix. Planar stratification, trough cross bedding, and crude grading are common. Dispersed robust shells, shell fragments and carbonaceous detritus are locally common, bioturbation is sparse. Conglomerate invariably fines upward into the Saanich Member.

Geo  
symbol

Sca

Sha  
Briti  
Hyd  
(bat

5390000

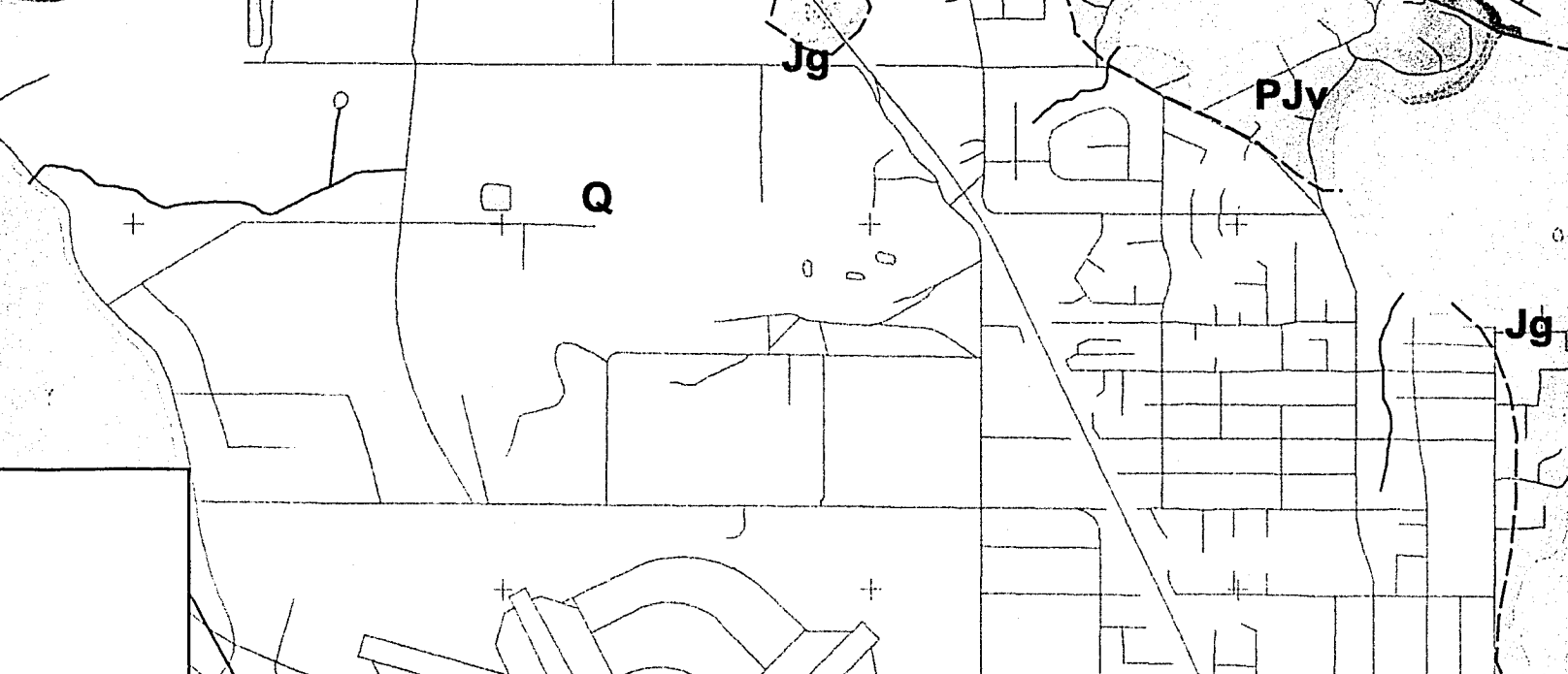
5389000

5388000

5387000

5386000

100



## Geologic Symbols

symbols aligned to strike, dip value given where known



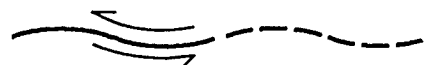
Contact: mapped, estimated, inferred



Reverse fault: mapped, estimated, inferred.  
(teeth on hanging wall)



Normal fault: mapped, inferred  
(Teeth on hanging wall)



Strike-slip fault: mapped, inferred  
(arrows also used to indicate oblique offset on other fault types)

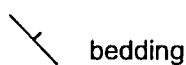
## Structures



Anticline, overturned



Syncline, overturned.



bedding



overturned bedding



mineral vein



foliation



joint  
(with plumose or systematic)



fracture  
(undetermined offset)

## Other Features

Roads



Streams



Surface Water



0

0.5

1

2

3

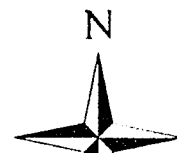
Scale 1 : 20,000.

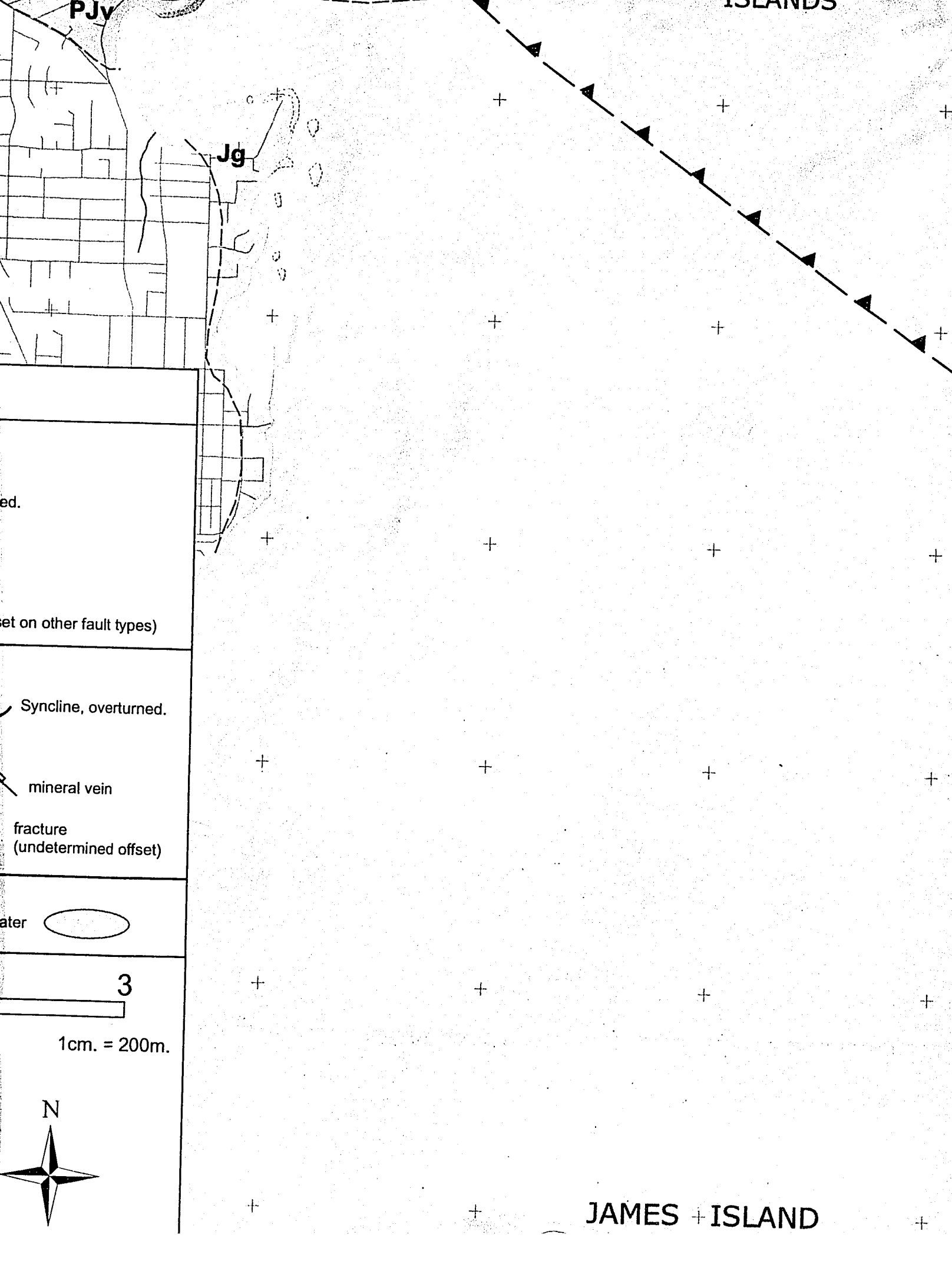
Kilometres

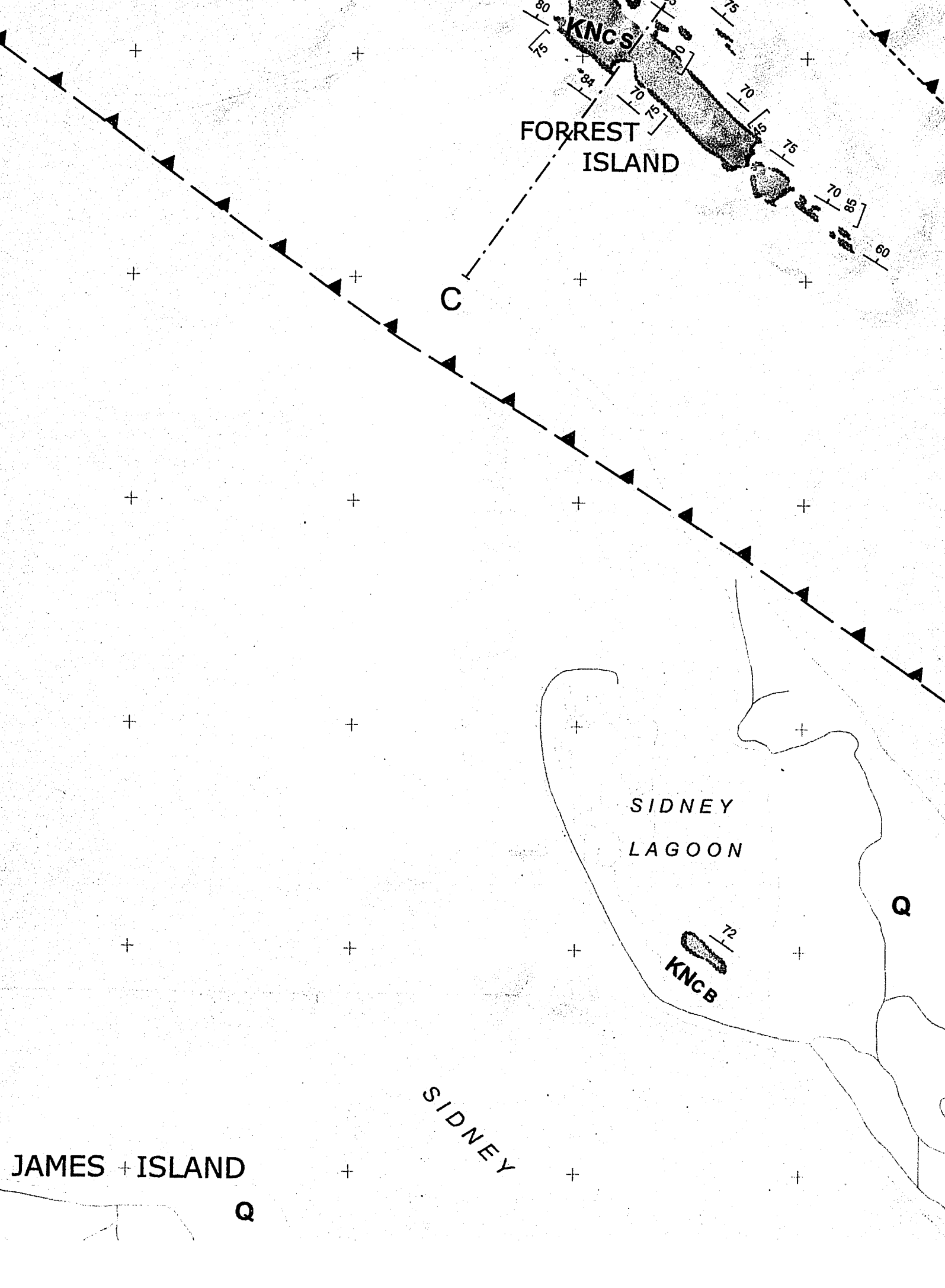
1cm. = 200m.

Universal Transverse Mercator Projection  
UTM Zone 10. NAD 83.

Shaded relief topography based on 5m elevation grid generated from British Columbia TRIM digital data (land elevations) and Canadian Hydrographic Service Marine charts 3476 (2001) and 3462 (1990) (bathymetric contours and shoreline profiles).







FORREST  
ISLAND

KNCS

C

SIDNEY  
LAGOON

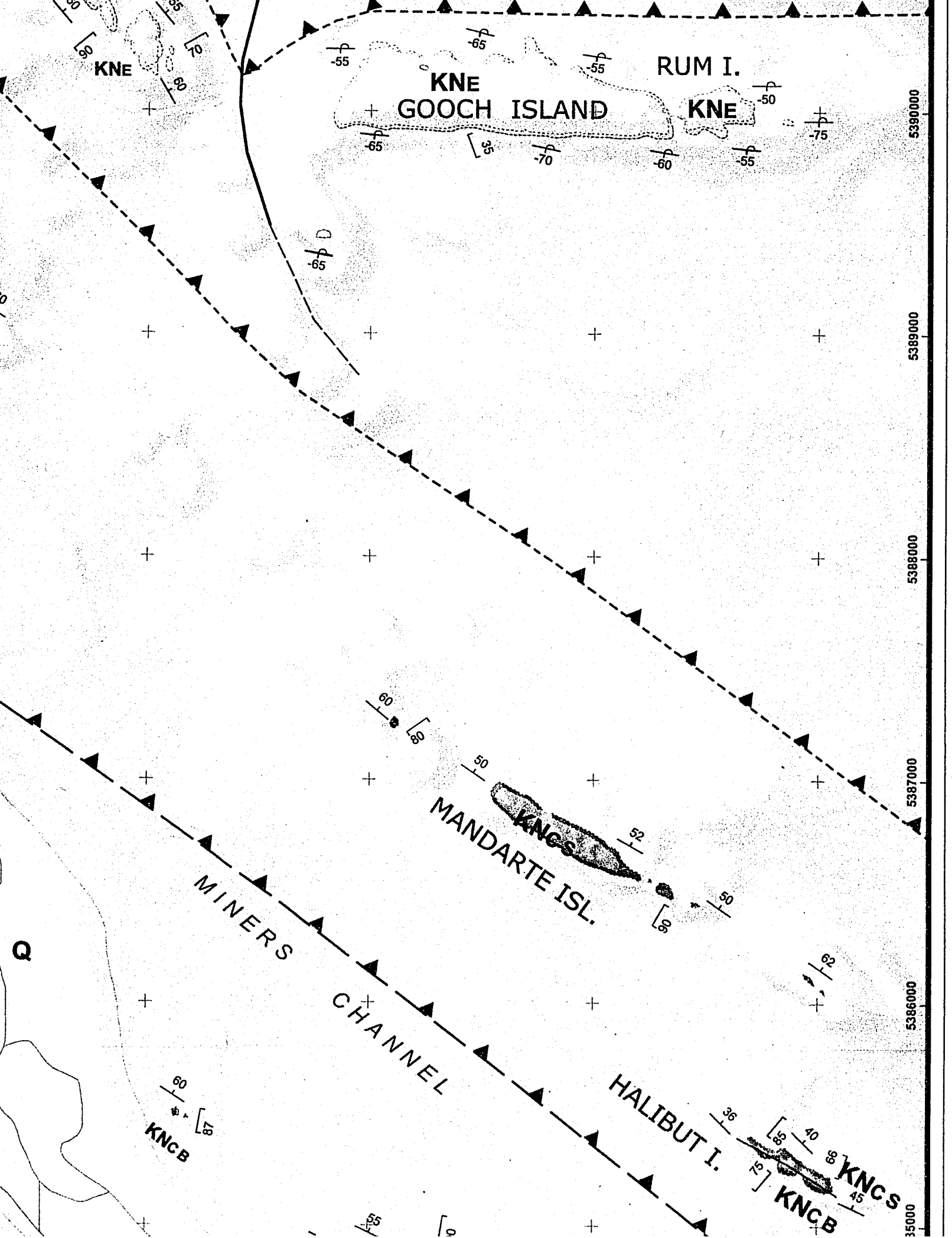
KNCB

SIDNEY

JAMES ISLAND

Q

Q





to well sorted, and thick to thin bedded. Planar stratification, trough cross bedding, and locally well developed swale cross stratification and hummocky cross stratification. Shales are silty and commonly interlaminated or interbedded with medium-grained sandstone. Lenticular, wavy and flaser bedding locally developed, with current and combined flow ripples in interstitial sandstone. Bivalves, gastropods and rare cephalopods occur in coquina-like lags, and dispersed in sandstones. Shales are carbonaceous, with abundant large coal fragments, leaf impressions, and *Teredolites*-bored logs. Ichnology varies from sparse to abundant, with *Ophiomorpha*, *Thalassinoides*, *Skolithos*, *Palaeophycus*, and *Diplocraterion* well represented.

**KNc5: BENSON MEMBER:** Conglomerate deposited on the basal unconformity. Varies from a thin, bimodal, boulder to pebble conglomerate with angular to rounded clasts of local basement lithology, with a well sorted, coarse-grained sandstone matrix, to a thick, poorly sorted, cobble to pebble conglomerate with a poorly sorted muddy sandstone matrix. Planar stratification, trough cross bedding, and crude grading are common. Dispersed robust shells, shell fragments and carbonaceous detritus are locally common, bioturbation is sparse. Conglomerate invariably fines upward into the Saanich Member.

## LATE JURASSIC

### Island Intrusions:

covered | exposed

Distinctly salt-and pepper coloured, medium-grained granodiorite. Locally rusty weathering and commonly cross-cut by quartz and epidote veins.

## PERMIAN - EARLY JURASSIC

**PJv**  
covered | exposed

### undefined volcanics:

Dark green basaltic volcanic rocks, locally with well developed pillow structures and hyaloclastites. Generally poorly exposed, weathered, and intruded by Jurassic intrusives. May correlate with upper Triassic Vancouver Group or Lower Jurassic Bonanza Group rocks of Vancouver Island. Differentiated from Sicker Group volcanics by lack of phyllitic metamorphism, primary volcanic textures, and darker colour.

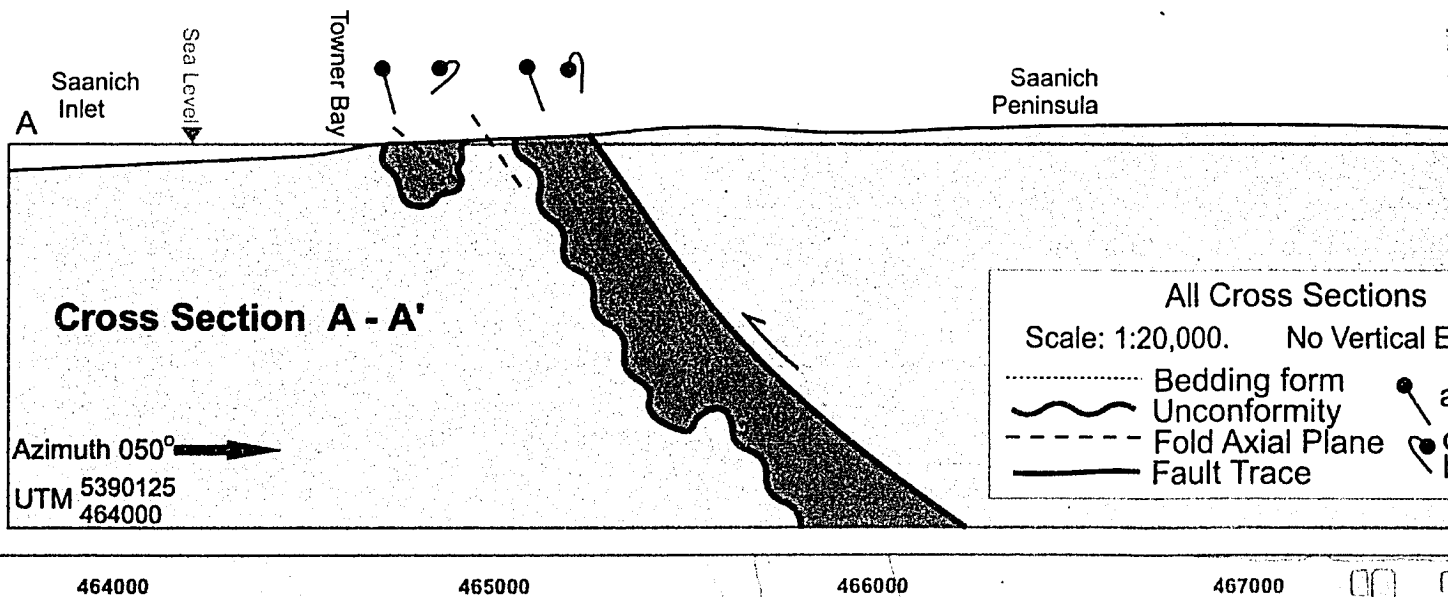
## DEVONIAN - PERMIAN

### SICKER GROUP

**DPSM**

### Myra Formation:

Phyllitic volcanic and volcanoclastic rocks. Dark green and moderately deformed, cross-cut by quartz and epidote veins.

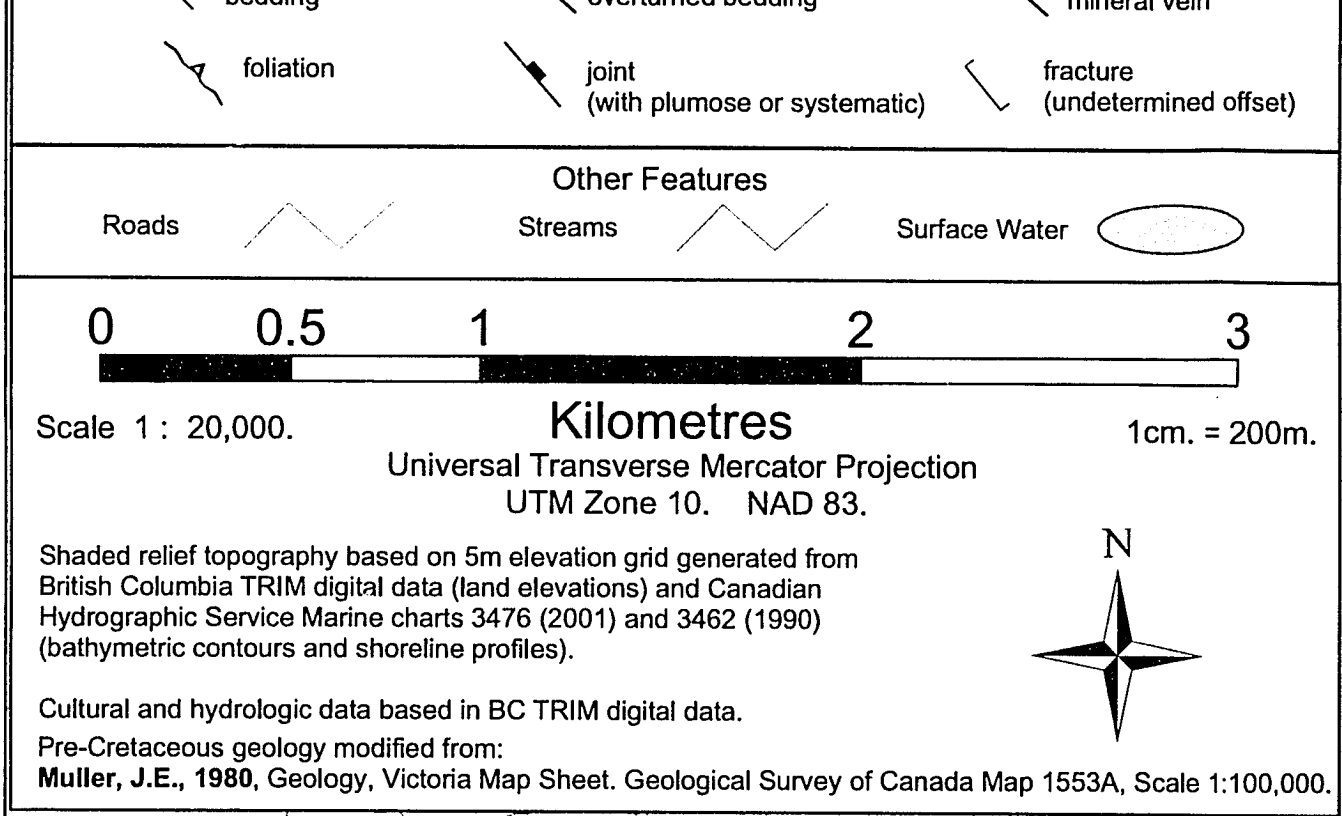


erates.  
 , moderately  
 ding, and  
 tion. Shales  
 ndstone.  
 ned flow  
 occur in  
 th abundant  
 varies  
 ophyucus,  
 ity. Varies  
 clasts of  
 o a thick,  
 dstone  
 mon.  
 y common,  
 Member.

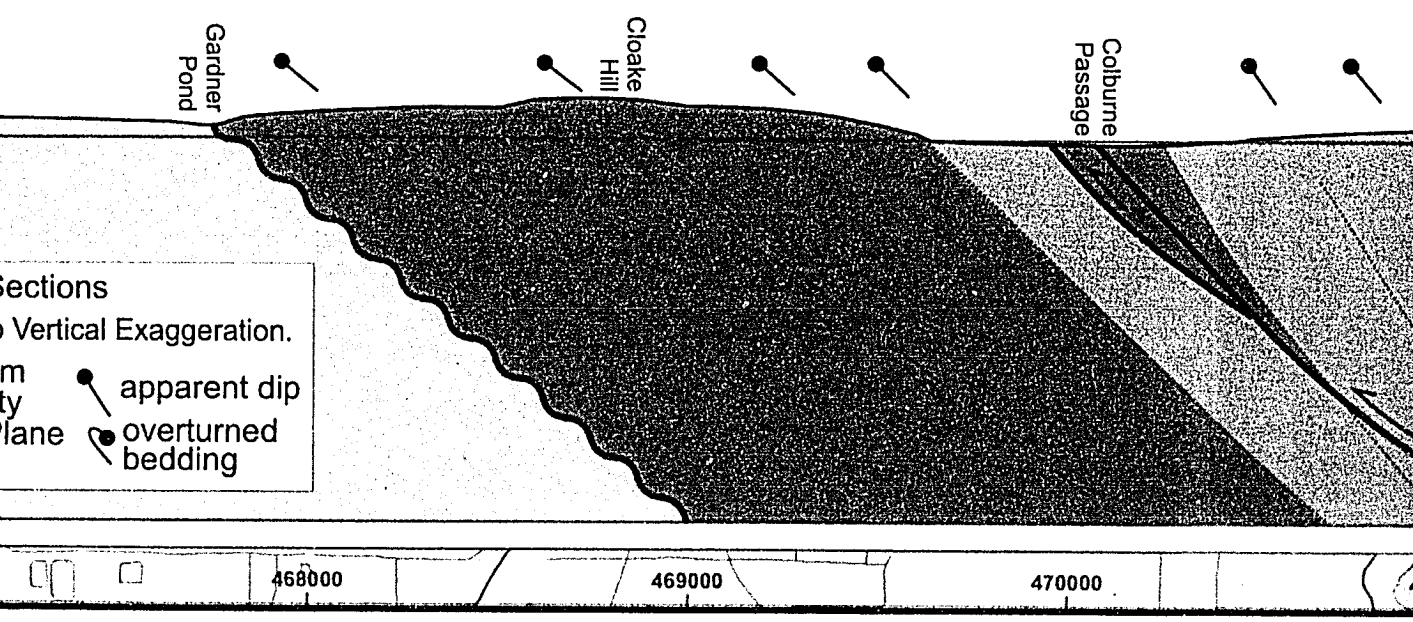
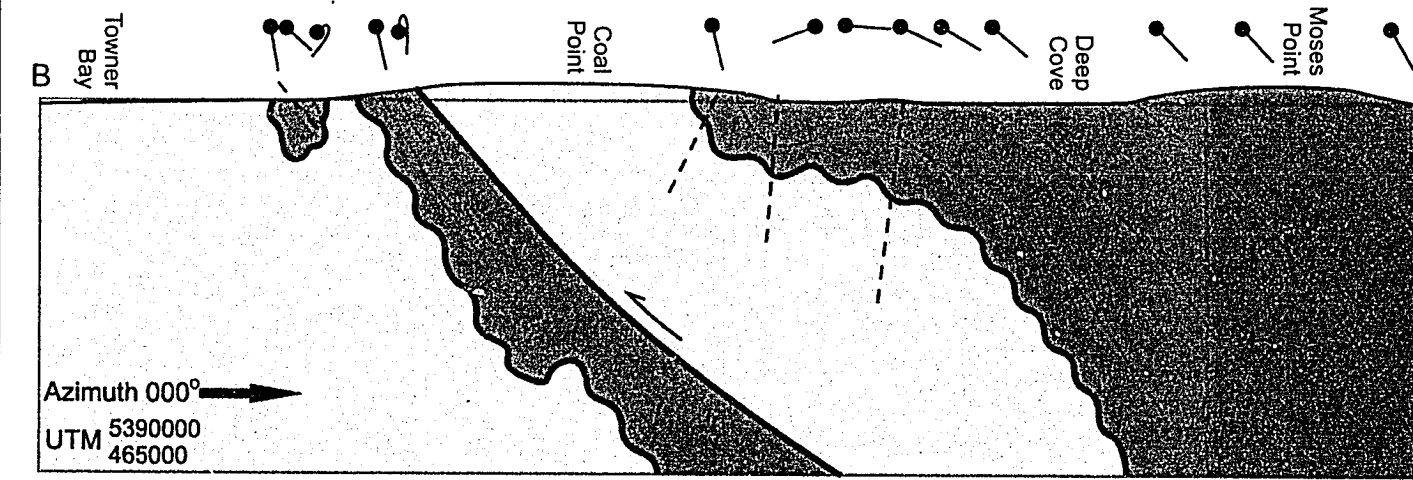
y weather-

s and  
 intrusives.  
 a Group  
 of phyllitic

ed,



### Cross Section B - B'



**All Cross Sections**  
 1:20,000. No Vertical Exaggeration.

Bedding form      ● apparent dip  
 Unconformity      ● overturned bedding  
 Fold Axial Plane  
 Fault Trace

467000

468000

469000

470000

fracture  
(undetermined offset)

Surface Water

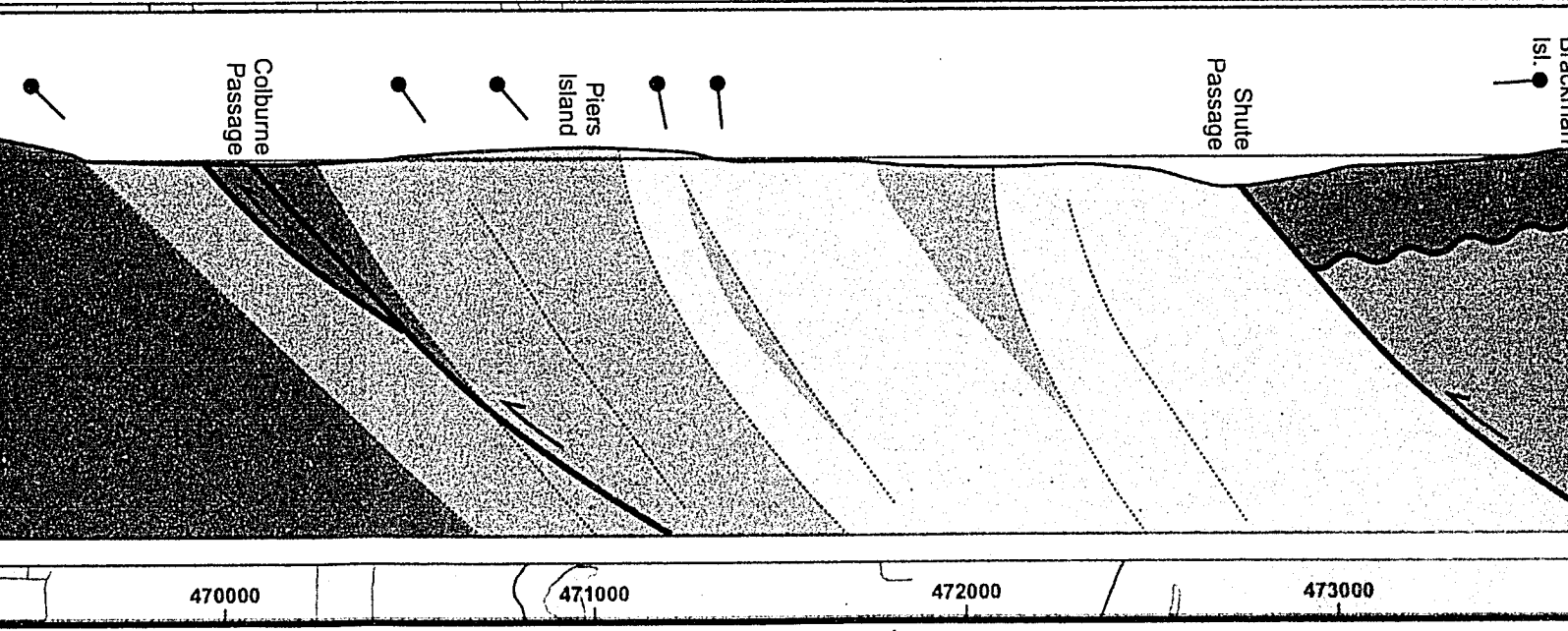
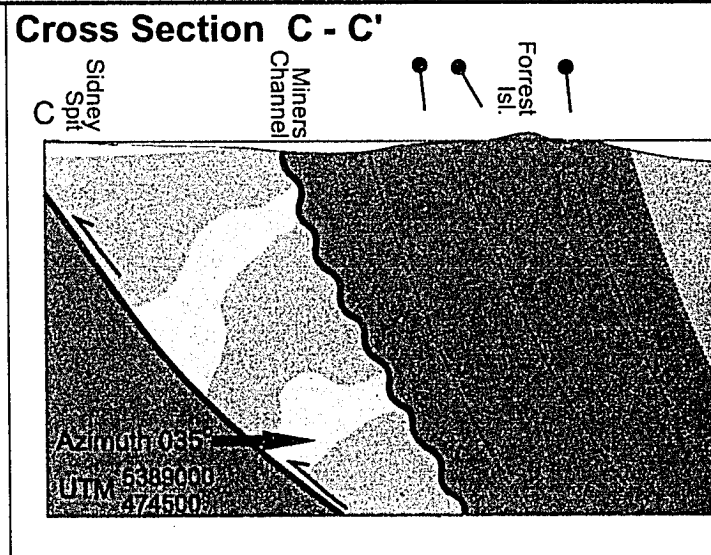
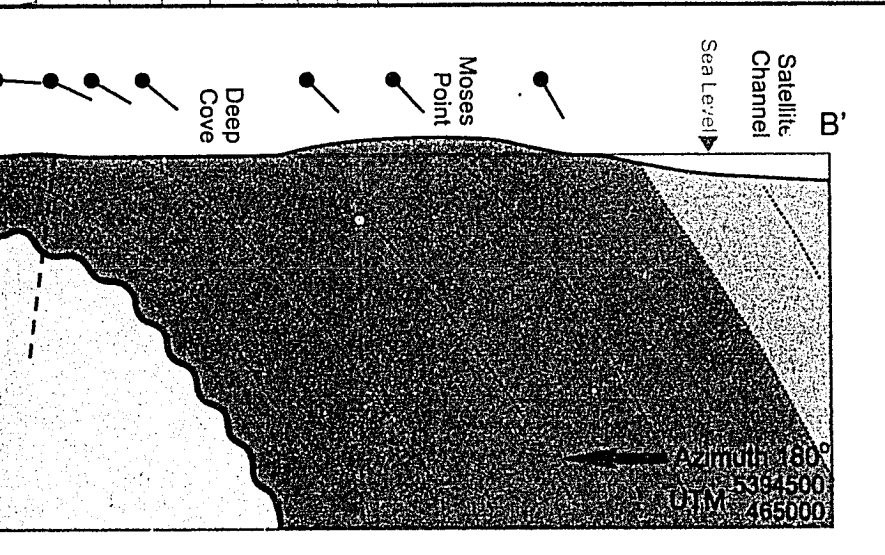
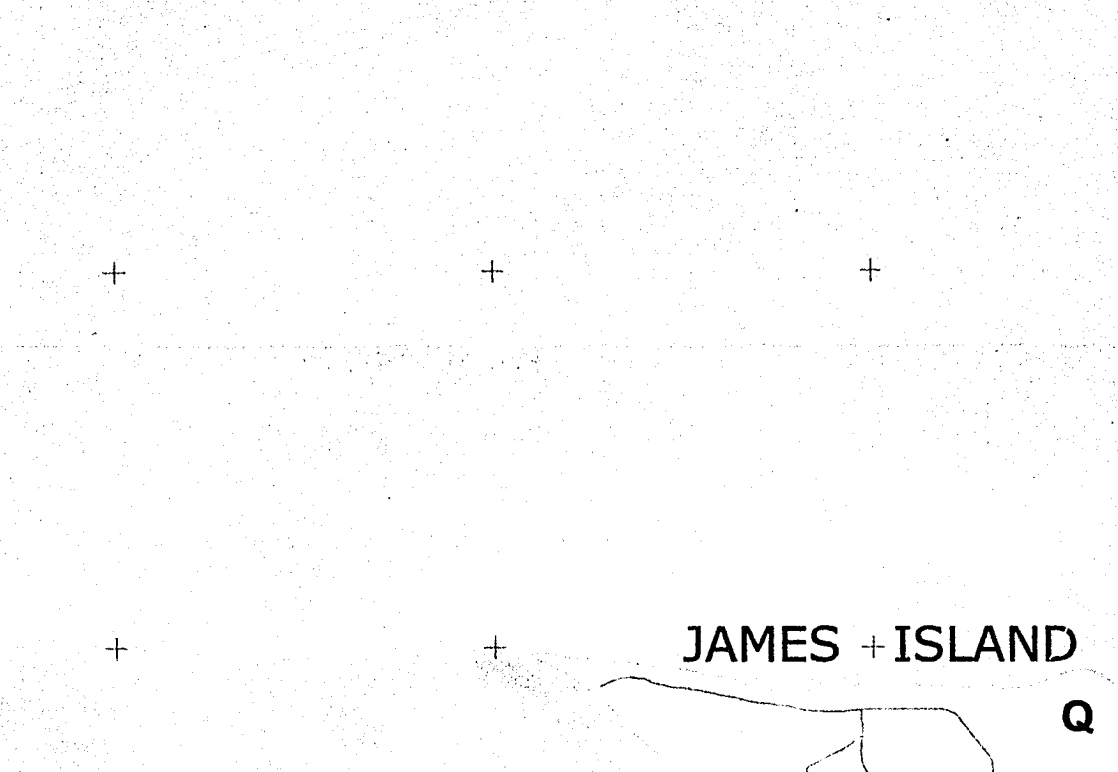
3

1cm. = 200m.

projection

N

f Canada Map 1553A, Scale 1:100,000.



SIDNEY  
LAGOON

72  
KNCB

JAMES ISLAND

SIDNEY

Section C - C'

Miners  
Channel

Forrest  
Isl.

Sea Level

Donville  
Island

Breithour  
Island

Prevost  
Passage

C'

Azimuth 215°  
UTM 5392500  
UTM 477000

Shute  
Passage

Brackman  
Isl.

Portland  
Island

Azimuth  
UTM 5

473000

474000

475000

476000

SIDNEY  
LAGOON

72  
KNCB

Q

60  
KNCB

MINERS

CHANNEL

ANDARTE ISL.

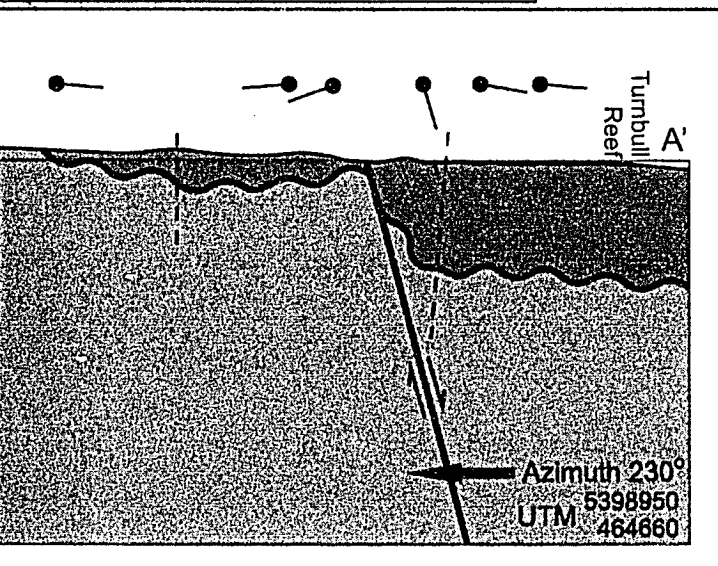
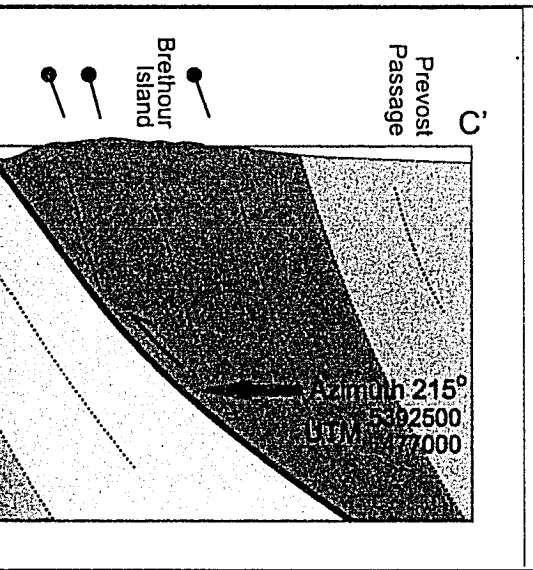
KNCB

KNCS

SIDNEY

ISLAND

CHANNEL



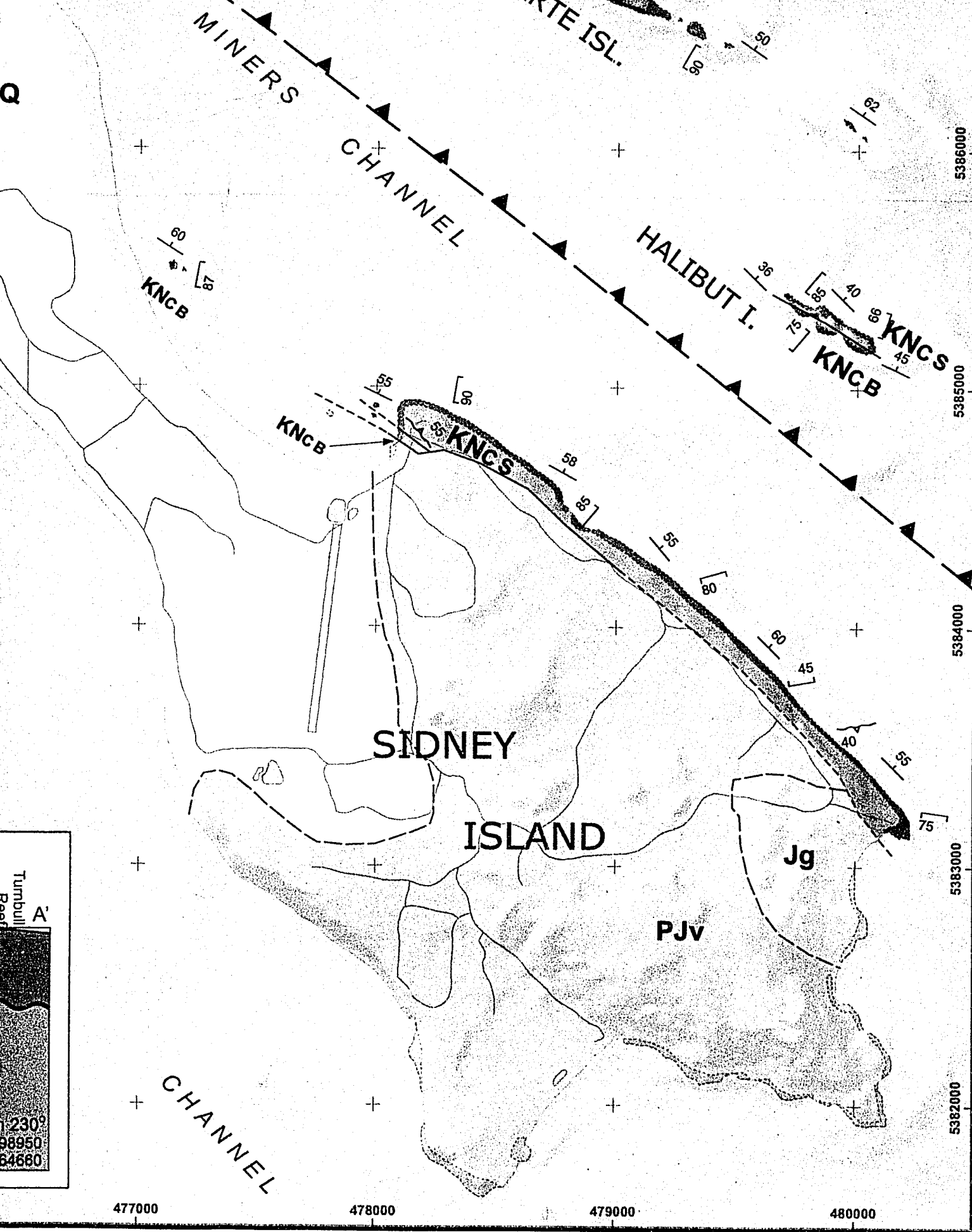
475000

476000

477000

478000

479000



Turnbull Reef

A'

230'

98950

64660